# ANNUAL REVIEW

# INSTITUTE FOR MOLECULAR SCIENCE

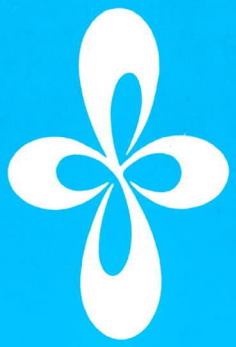

1993

# ANNUAL REVIEW

## INSTITUTE FOR MOLECULAR SCIENCE

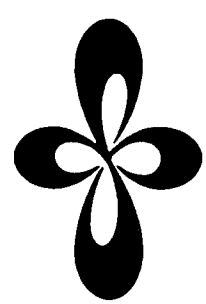

1993

*Published by*
Institute for Molecular Science
Okazaki National Research Institutes
Myodaiji, Okazaki 444, Japan
Phone 0564-55-7418 (Secretary room)
Telex 4537-475 KOKKEN J
Fax 0564-54-2254

# IMS 1993

This is the Annual Review for 1993 reporting the research activities of IMS scientists during the past year. As can be seen, the research at IMS maintains a high level. Recently, *Science* (**258**, 1992) has reported an average citation index for a scientific paper delivered by a Japanese university or research institute over the last 10 years, and according to that report, IMS achieves the highest index among universities and research institutes having comparable numbers of papers. This shows that past papers from IMS have enjoyed a high reputation in the scientific community and made significant contributions to scientific understanding. We are very pleased with the achievements of IMS researchers in the last decade. It is my hope that this high quality of research work will be maintained and enhanced further in the years to come.

Professor Inokuchi retired as Director-General of IMS at the end of March 1993, and took a new position of the President of the three National Research Institutes in Okazaki which includes IMS. Professor Inokuchi has been the Director-General of IMS for six years and has contributed a great deal to the development of IMS in both its science and administration. We would like to express our hearty thanks for his efforts and achievements and look forward to his continued support for IMS from his new position.

I was appointed as Professor Inokuchi's successor at IMS at the beginning of April. I feel a great responsibility for this important position. It is my concern that IMS continues to serve as a center of excellence in the field of molecular science and at the same time to function as an inter-university national research institute. 18 years have passed since the establishment of IMS in 1975, and I think now is the time for change and renewal. It is my desire that IMS becomes more dynamic in its research activity, more brave in exploring new fields, more tolerant in accepting new ideas and more open in its discussions. Every effort must be made with these goals in mind.

As usual, there has been a high turnover of personnel during the last year, 19 scientists moved from IMS to universities and other research institutes and 31 scientists have joined IMS. Among them Professor K. Morokuma moved to Emory University, USA, and Professor H. Ohtaki retired from IMS and was appointed to a chair at Ritsumeikan University. Three associate professors, Drs. K. Nasu, T. Mitani and K. Kitaura moved as full professors to the National Laboratory for High Energy, the Japan Advanced Institute of Science and Technology, Hokuriku and the Osaka Prefecture University, respectively. Professor A. Nakamura of Osaka University was appointed to the Director of the Coordination Chemistry Laboratories to succeed Professor Ohtaki. We have also appointed Dr. K. Kosugi of Kyoto University as Professor of the Laboratory for Photochemistry. Drs. T. Suzuki, S. Miyajima and M. Aoyagi were appointed as Associate Professors of the Laboratory of Excited State Dynamics, the Laboratory of Molecular Assemblies Dynamics and of the Computer center, respectively. Associate Professors N. Nemoto and Y. Naruta took positions in the Laboratory of Physical Organic Chemistry by transferring from their positions at Tohoku University and Kyoto University, respectively. Smilar transfers brought Professor H. Kawazoe and Associate Professor M. Nishio to the Laboratory of Interface Molecular Science from the Tokyo Institute of Technology and Saga University, respectively.

We are very pleased that Professor Ikuzo Tanaka, who has been the Chairperson of the Council of IMS for a long time, has agreed to serve as a Distinguished Research Consultant.

Finally, I would also like to congratulate Professor Emeritus Eizi Hirota, the Vice President of the Graduate University for Advanced Studies, for his Japan Academy Prize and Dr. Naoshi Ogura in the Laboratory of Molecular Structure II for his Chemical Society of Japan Award for a Young Scientist.

September, 1993

Mitsuo Ito

Mitsuo Ito
Director-General

# CONTENTS

# ORGANIZATION AND STAFF

## Organization

The Institute for Molecular Science comprises twenty two research laboratories-each staffed by a professor, an associate professor, two research associates and several technical associates-, two research laboratories with foreign visiting professors, and six research facilities. The laboratories are grouped into six departments and one facility for coordination chemistry:

| | |
|---|---|
| Department of Theoretical Sciences | Theoretical Studies I |
| | Theoretical Studies II |
| | Theoretical Studies III[1)] |
| Department of Molecular Structure | Molecular Structure I |
| | Molecular Structure II[1)] |
| | Molecular Dynamics |
| Department of Electronic Structure | Excited State Chemistry |
| | Excited State Dynamics |
| | Electronic Structure[1)] |
| | Molecular Energy Conversion[2)] |
| Department of Molecular Assemblies | Solid State Chemistry |
| | Molecular Assemblies Dynamics |
| | Molecular Assemblies[1)] |
| Department of Applied Molecular Science | Applied Molecular Science I |
| | Applied Molecular Science II[1)] |
| | Physical Organic Chemistry[3)] |
| Department of Vacuum UV Photoscience | Photochemistry |
| | Chemical Dynamics |
| | Interface Molecular Science[3)] |
| | Synchrotron Radiation Research[2)] |
| Coordination Chemistry Laboratories | Synthetic Coordination Chemistry[3)] |
| | Complex Catalysis |
| | Fundamental Coordination Chemistry |
| | Coordination Bond[1)] |
| Research Facilities are: | Computer Center |
| | Chemical Materials Center |
| | Instrument Center |
| | Low-Temperature Center |
| | Equipment Development Center |
| | Ultraviolet Synchrotron Orbital Radiation (UVSOR) Facility |

1) Professors and associate professors are adjunct professors from other universities.
2) Research Laboratories with foreign visiting professors.
3) Professors, associate professors, and research associates, along with their positions, are transferred from other universities.

# Scientific Staff

| | |
|---|---|
| **Hiroo INOKUCHI** | **Professor, Director-General (-March '93)** |
| **Mitsuo ITO** | **Professor, Director-General (April '93-)** |

## Emeritus Professors

| | |
|---|---|
| Saburo NAGAKURA | President, The Graduate University for Advanced Studies |
| Eizi HIROTA | Vice-President, The Graduate University for Advanced Studies |
| Katsumi KIMURA | Professor, Japan Advanced Institute of Science and Technology |
| Keiji MOROKUMA | Professor, Emory University (USA) |

### *Department of Theoretical Studies*

#### *Theoretical Studies I*

| | |
|---|---|
| Keiji MOROKUMA | Professor(-March '93)[1] |
| Iwao OHMINE | Associate Professor |
| Nobuaki KOGA | Research Associate (-March '93)[2] |
| Norihiro SHIDA | Research Associate (-March '93)[3] |
| Akira SHUDO | Research Associate |
| Shinji SAITO | Technical Associate |
| Jerzy MOC | JSPS Post-Doctoral Fellow (-January '93)[4] |
| Djamaladdin G. MUSAEV | JSPS Post-Doctoral Fellow (-January '93)[1] |
| Jean -F. RIEHL | JSPS Post-Doctoral Fellow |
| Feliu MASERAS | Research Fellow |
| Alexander MEBEL | Research Fellow |
| Fujiko HASHIMOTO | Research Fellow (-March '93) |
| Satoru YOSHIDA | Visiting Research Fellow |
| Tamiki KOMATSUZAKI | Graduate Student |
| Toshiaki FUJII | Graduate Student |
| Chizuru MUGURUMA | Graduate Student |
| Masakatsu ITO | Graduate Student |
| Masakazu MATSUMOTO | Graduate Student |
| Young Kee KANG | Visiting Scientist from Chungbuk National University (July '93-) |

#### *Theoretical Studies II*

| | |
|---|---|
| Hiroki NAKAMURA | Professor |
| Keiichiro NASU | Associate Professor (-November '92)[5] |
| Kaoru IWANO | Research Associate (-July '93)[5] |
| Shoji TAKADA | Technical Associate |
| Itsuki BANNO | Technical Associate (-April '93), Research Fellow (May '93-) |
| Kengo MORIBAYASHI | JSPS Post-Doctoral Fellow (April '93-) |
| Yasuji INADA | JSPS Post-Doctral Fellow (-March '92)[5] |
| Chayugan ZHU | Graduate Student |
| Kenichiro TSUDA | Graduate Student |
| Tomiyuki TSUBO | Graduate Student (-December '92)[5] |
| Yuji MICHIHIRO | Graduate Student (April '93-) |
| Miyabi HIYAMA | Graduate Student (April '93-) |
| Krzysztof STEFANSKI | Visiting Professor from Nicholas Copernics University (September '92-August '93) |

#### *Theoretical Studeis III*

| | |
|---|---|
| Shigeki KATO | Adjunct Professor from Kyoto University (-March '93) |
| Kazuo KITAURA | Adjunct Professor from University of Osaka Prefecture (April '93-) |
| Koichi YAMASHITA | Adjunct Associate Professor from Institute for Fundamental Chemistry (-March '93) |
| Masayasu KAMIMURA | Adjunct Associate Professor from Kyushu University (April '93-) |
| Kenro HASHIMOTO | Research Associate (-March '93)[6] |
| Kiyohiko SOMEDA | Research Associate |

## *Departmemt of Molecular Struture*

### *Molecular Structure I*

| | |
|---|---|
| Shuji SAITO | Professor |
| Norio MORITA | Associate Professor |
| Shuro TAKANO | Research Associate |
| Asuka FUJII | Research Associate (-August'93)[7] |
| Mitsutaka KUMAKURA | Technical Associate |
| Andrej M. SOBOLEV | Research Student (October'92-) |
| Jian TANG | Graduate Student (April'93-) |
| Masahiro GOTO | Graduate Student from Nagoya Univ.* |
| Timothy C. STEIMLE | Visiting Scientist (November'92-February'93) |
| Sang K. LEE | Visiting Scientist (July'93-September'93) |

### *Molecular Structure II*

| | |
|---|---|
| Hiroatu MATSUURA | Adjunct Professor from Hiroshima University (-March'93) |
| Tadaoki MITANI | Adjunct Professor from Japan Advanced Institute of Science and Technology (April'93-) |
| Kentaro KAWAGUCHI | Adjunct Associate Professor from National Astronomy Observatory |
| Takashi OGURA | Research Associate |
| Hiroyuki OZEKI | Research Associate (January'93-) |

### *Molecualr Dynamics*

| | |
|---|---|
| Teizo KITAGAWA | Professor |
| Tatsuhisa KATO | Associate Professor |
| Keiji KAMOGAWA | Research Associate (-March'93)[8] |
| Michio MATSUSHITA | Research Associate (April'93-) |
| Shin-ichiro SATO | Technical Associate |
| Satoru NAKASHIMA | IMS Fellow |
| Shoji KAMINAKA | JSPS Post-Doctoral Fellow (-March'93)[9] |
| Yasuhisa MIZUTANI | JSPS Post-Doctoral Fellow |
| Satoshi TAKAHASHI | JSPS Post-Doctoral Fellow (-January'93)[10] |
| Philip J. JEWSBURY | JSPS POST-Doctoral Fellow |
| Yoshinao SAKAN | Graduate Student (-September'92), Research Fellow (October'92-March'93)[11] |
| Shun HIROTA | Graduate Student |
| Denis A. PROSHLYAKOV | Graduate Student (October'92-) |
| Takeshi KODAMA | Graduate Student (April'93-) |
| Paul STEIN | Visiting Scientist (May'93-August'93) |

## *Department of Electronic Structure*

### *Excited State Chemistry*

| | |
|---|---|
| Keitaro YOSHIHARA | Professor |
| Yoshiyasu MATSUMOTO | Associate Professor |
| Hrvoje PETEK | Research Associate (-January '93)[12] |
| Kyoichi SAWABE | Research Associate |
| Keisuke TOMINAGA | Research Associate |
| Shigeichi KUMAZAKI | Technical Associate |
| Kazuo WATANABE | Technical Associate (April'93-) |
| Hideki KANDORI | IMS Fellow (-October '92)[13] |
| Bongsoo KIM | JSPS Post-Doctoral Fellow |
| Arkady P. YARTSEV | JSPS Post-Doctoral Fellow (-April '93)[14] |
| Prem B. BISHT | Post-Doctoral Fellow (-April '93)[15] |
| Yukito NAITO | JSPS Post-Doctoral Fellow (April '93-) |
| Ryoji INABA | Graduate Student from the Univ. of Tokyo* (-March '93)[16] |
| Yutaka NAGASAWA | Graduate Student |
| Hiroyuki KATO | Graduate Student (April' 93-) |
| Jihwa LEE | Visiting Scientist from Seoul National Univ., Korea (September '92-August '93) |

| | |
|---|---|
| Alan E. JOHNSON | Visiting Graduate Student from Univ. of Minnesota, USA (September '92-December '92) |
| Stephen R. MEECH | Visiting Scientist from Heroit-Watt University, UK (December '92-January '93) |
| Young S. CHOI | Visiting Scientist from Inha Univ., Korea (January '93-March '93, June '93-August '93) |
| Taek Soo KIM | Visiting Graduate Student from Inha Univ., Korea (January '93-March '93, June '93-August '93) |
| Jung Chul SEO | Visiting Scientist from Korea Research Institute of Standards and Science, Korea (January '93-Febrary '93) |
| Young Sei PARK | Visiting Graduate Student from Seoul National Univ., Korea (March '93-April '93) |
| Ronald L. CHRISTENSEN | Visiting Scientist from Bowdoin College, USA (May '93-June '93) |
| Tai Jong KANG | Visiting Scientist from Taegu Univ., Korea (June '93-August '93)) |
| Julie REHM | Visiting Graduate Student from Univ. of Rochester, USA (July '93-August '93) |
| Jae-Young KIM | Visiting Graduate Student from Seoul National Univ., Korea (July '93) |

*Excited State Dynamics*

| | |
|---|---|
| Ichiro HANAZAKI | Professor |
| Toshinori SUZUKI | Associate Professor |
| Masao TAKAYANAGI | Research Associate |
| Kenichi TONOKURA | Research Associate (January'93-) |
| Teruhiko NISHIYA | Technical Associate (-March '93)[17] |
| Kazuhiro HONDA | Graduate Student (-September '92), Visiting Research Fellow (October '92-August '93)[18] |
| Takumi KONO | Graduate Student |
| Tetsuo SEKIGUCHI | Graduate Student |
| Tatsuo GEJO | Graduate Student |
| Noriaki OKAZAKI | Graduate Student |
| Nobuhisa HASHIMOTO | Graduate Student (April' 93-) |
| Yoshihiro NAKAMICHI | Graduate Student from Nara Univ. of Education* (April '93-) |
| Yehuda HAAS | Visiting Scientist from the Hebrew Univ., Israel (September '92-October '92) |
| Hong-Lae KIM | Visiting Scientist from Kangweon National Univ., Korea (January '93-March '93, May '93) |
| Minoru YOSHIMOTO | Visiting Research Fellow (April '93-May '93) |

*Electronic Structure*

| | |
|---|---|
| Toru AZUMI | Adjunct Professor from Tohoku University |
| Minoru SUMITANI | Adjunct Associate Professor from Shizuoka Institute of Science and Technology (-March '93) |
| Ryoichi NAKAGAKI | Adjunct Associate Professor from Kanazawa University (April '93-) |
| Kaoru SUZUKI | Research Associate (-March '93)[19] |
| Yoshihito MORI | Research Associate |
| Takamichi KOBAYASHI | Research Associate (August '93-) |

*Molecular Energy Conversion*

| | |
|---|---|
| Eugene L. FRANKEVICH | Visiting Professor from Institute of Chemical Physics, Russian Academy of Science, Russia (September '93-June '93) |
| Leonid S. GRIGORYAN | Visiting Associate Professor from Institute for Physical Research, Armenia (September '92-August '93) |

***Department of Molecular Assemblies***

*Solid State Chemistry*

| | |
|---|---|
| Kyuya YAKUSHI | Professor |
| Kazushi KANODA | Associate Professor |
| Akito UGAWA | Research Associate |

| | |
|---|---|
| Yasuhiro NAKAZAWA | Research Associate |
| Ken-ichi IMAEDA | Technical Associate |
| Kazuya MIYAGAWA | Technical Associate (April '93-) |
| Mikihiro URUICHI | Technical Associate (April '93-) |
| Hirohiko SATO | IMS Fellow (April '93-) |
| Ilias I. KHAIRULLIN | JSPS Post-Doctoral Fellow (October '92-) |
| Kentaro IWASAKI | Graduate Student (-March '93)[20] |
| Toshihiro HIEJIMA | Graduate Student (April '93-) |
| Jian DONG | Graduate Student (April '93-) |
| Anvar A. ZAKHIDOV | Visiting Scientist (August '93-) |
| Atsushi KAWAMOTO | Visiting Research Fellow (-March '93)[21] |
| Takefumi MIYAZAKI | Visiting Research Fellow (April '93-) |

*Molecular Assemblies Dynamics*

| | |
|---|---|
| Yusei MARUYAMA | Professor |
| Seiichi MIYAJIMA | Associate Professor |
| Shinji HASEGAWA | Research Associate (-March '93) |
| Toshiyasu SUZUKI | Visiting research Fellow (August-September '92), Research Associate (October '92-) |
| Hironori OGATA | Graduate Student (-March '93), Research Associate (April '93-) |
| Hajime HOSHI | Technical Associate (-March '93)[22] |
| Noriko YAMAMURO | IMS Fellow (January '93-) |
| Roger WHITEHEAD | JSPS Post-Doctoral Fellow |
| Toshifumi TERUI | Graduate Student (-March '93), Visiting Research Fellow (April '93-) |
| Yoshihisa MORI | Graduate Student (-March '93)[23] |
| Shaoli FANG | Graduate Student |
| Atsushi SUZUKI | Graduate Student |
| Chikako NAKANO | Visiting Research Fellow |
| Keiichi KOHAMA | Visiting Research Fellow from Toyota Motor Corp. |
| Zhong fang LIU | Visiting Research Fellow (-May '93) |
| Shuqin ZHOU | Visiting Research Fellow (October '92) |
| Masatsugu SUZUKI | Visiting Research Fellow (September-December '92) |
| Itsuko SUZUKI | Visiting Research Fellow (September-December '92) |
| Ping WANG | Visiting Research Fellow (October-November '92) |
| Yang fang LI | Visiting Research Fellow (November-December '92) |
| Jim MCMURDO | Visiting Research Fellow (November-December '92) |

*Molecular Assemblies*

| | |
|---|---|
| Satoshi HIRAYAMA | Adjunct Professor from Kyoto Institute of Technology (-March '93) |
| Akira YOSHIDA | Adjunct Professor from Toyohashi University of Technology (April '93-) |
| Kokichi OSHIMA | Adjunct Associate Professor from Okayama University (-March '93) |
| Yukio OUCHI | Adjunct Associate Professor from Nagoya University (April '93-) |
| Takehiko MORI | Research Associate |
| Shinji HASEGAWA | Research Associate (April '93-) |

***Department of Applied Molecular Science***

*Applied Molecular Science I*

| | |
|---|---|
| Kazuhiro NAKASUJI | Professor |
| Kiyoshi ISOBE | Associate Professor |
| Yasushi MORITA | Research Associate |
| Makoto TADOKORO | Research Associate |
| Masaaki ABE | Research Associate (April '93-) |
| Takanori NISHIOKA | Technical Associate |
| Hiroshi SHIMOMURA | IMS Fellow (April '93-) |
| Ken-ichi SUGIURA | Graduate Student (-September '92)[24] |
| Rimo XI | Graduate Student |

| | |
|---|---|
| Tetsuji ITOH | Graduate Student |
| Kunio HATANAKA | Graduate Student |
| Md. Badruz ZAMAN | Graduate Student (January '93-) |
| Minoru MITSUMI | Graduate Student (April '93-) |
| Koichi TAMAKI | Graduate Student (April '93-) |
| Seiji OGO | Graduate Student (April '93-) |
| Joon T. PARK | Visiting Professor from Korea Advanced Institute of Science and Technology, Korea (December '92-February '93) |
| Vadim Y. KUKUSHKIN | Visiting Professor from St. Petersburg Univ., Russia (December '92-April '93) |

*Applied Molecular Science II*

| | |
|---|---|
| Yumihiko YANO | Adjunct Professor from Gunma University (-March '93)[25] |
| Hiyoshizo KOTSUKI | Adjunct Associate Professor from Kochi University (-March '93)[26] |
| Yasuhiro AOYAMA | Adjunct Professor from Nagaoka University of Technology (April '93-) |
| Motokazu UEMURA | Adjunct Associate Professor from Osaka City University (April '93-) |
| Jiro TOYODA | Research Associate |
| Takayoshi SUZUKI | Rsearch Associate |

*Physical Organic Chemistry*

| | |
|---|---|
| Junji INANAGA | Associate Professor (-March '93)[27] |
| Teruo SHINMYOZU | Associate Professor (-March '93)[27] |
| Masaaki MISHIMA | Research Associate (-March '93)[27] |
| Takeshi HANAMOTO | Research Associate (-March '93)[27] |
| Yoshinori NARUTA | Associate Professor (April '93-) |
| Hisao NEMOTO | Associate Professor (April '93-) |
| Satoshi USUI | Research Associate (April '93-) |
| Naoki ASAO | Research Associate (April '93-) |
| Yasuo YOKOYAMA | Graduate Student from Kyushu Univ.* (-March '93)[27] |
| Yuichi SUGIMOTO | Graduate Student from Kyushu Univ.* (-March '93)[27] |
| Satoshi OSADA | Graduate Student from Kyushu Univ.* (-March '93)[27] |
| Masa-aki SASAYAMA | Graduate Student from Kyoto Univ.* (April '93-) |
| Mari ICHIMURA | Graduate Student from Kyoto Univ.* (April '93-) |
| Nobuyuki SAWADA | Graduate Student from Kyoto Univ.* (April '93-) |
| Hideki TANAKA | Graduate Student from Kyoto Univ.* (April '93-) |
| Yukiyasu CHONAN | Graduate Student from Tohoku Univ.* (April '93-) |
| Satoshi IWAMOTO | Graduate Student from Tohoku Univ.* (April '93-) |

## *Department of Vacuum UV Photoscience*

*Photochemistry*

| | |
|---|---|
| Nobuhiro KOSUGI | Professor (January '93-) |
| Kosuke SHOBATAKE | Associate Professor |
| Kiyohiko TABAYASHI | Research Associate (-March '93)[28] |
| Katsuhiko OKUYAMA | Research Associate |
| Haruhiko OHASHI | Technical Associate |
| Martin COCKETT | JSPS Post-Doctoral Fellow (-January '93)[29] |
| Hiroyuki OZEKI | JSPS Post-Doctoral Fellow (-December '92) |
| Hiroshi YOSHIKAWA | Graduate Student |
| Mitsuhiko KONO | Graduate Student |
| Koji ITO | Graduate Student from Nagoya Univ.* (-March '93), Visiting Research Fellow (April '93-) |

*Chemical Dynamics*

| | |
|---|---|
| Tsuneo URISU | Professor |
| Koichiro MITSUKE | Associate Professor |
| Kazuhiko MASE | Research Associate |
| Hiroaki YOSHIDA | Research Associate |
| Yuji UKISU | Technical Associate (April '93-June '93)[30] |

| | |
|---|---|
| Hideo HATTORI | Technical Associate |
| Mitsuru NAGASONO | Technical Associate (April '93-) |
| Yanping ZHANG | JSPS Post-Doctoral Fellow (November '92-) |
| Hiroaki YOSHIGOE | Graduate Student (April '93-) |
| Minoru KANNO | Graduate Student (April '93-) |
| Satoshi MINOURA | Graduate Student from Shinshu Univ.* (April '93-) |

*Interface Molecular Science*

| | |
|---|---|
| Akira YOSHIDA | Professor (-March '93)[31] |
| Hiroshi KAWAZOE | Professor (April '93-) |
| Shinri SATO | Associate Professor (-March '93)[32] |
| Mitsuhiro NISHIO | Associate Professor (April '93-) |
| Yuichi OHNO | Research Associate (-March '93)[32] |
| Seigi MIZUNO | Research Associate (-March '93)[32] |
| Takuya HASHIMOTO | Research Associate (April '93-) |
| Koji HAYASHI | Research Associate (April '93-) |
| Yuji UKISU | Technical Associate (-March '93)[30] |
| Masahiro TOMIDA | Graduate Student from Toyohashi Univ. of Technology* (-March '93) |
| Hisashi OGAWA | Graduate Student from Shinshu Univ.* (-March '93) |
| Makoto IKEJIRI | Graduate Student from Saga Univ.* |
| Toshihiro OGATA | Graduate Student from Saga Univ.* |
| Gheyas S. IRFAN | Graduate Student from Saga Univ.* (April '93-) |
| Koichi NAKANOSE | Graduate Student from Saga Univ.* (April '93-) |

*Synchrotron Radiation Research*

| | |
|---|---|
| Jerzy GORECKI | Visiting Associate Professor from Polish Academy of Science, Warsaw, Poland (-October '92) |
| Krzysztof STEFANSKI | Visiting Associate Professor from Institute for Physics, Nicholas Copernicus Univ., Poland (November '92-August '93) |

***Coordination Chemistry Laboratories***

| | |
|---|---|
| Hitoshi OHTAKI | Director (-March '93)[33] |
| Akira NAKAMURA | Director (April '93-) |

*Synthetic Coordination Chemistry*

| | |
|---|---|
| Yutaka FUKUDA | Professor |
| Kiyoshi SAWADA | Associate Professor |
| Hikaru ICHIDA | Research Associate |
| Keiichi SATOH | Research Associate |
| Hiroyuki YOKOYAMA | Graduate Student from Niigata Univ.* (-March '93) |
| Kayoko KASAI | Graduate Student from Ochanomizu Univ.* (-March '93) |
| Tomohide ICHIKAWA | Graduate Student from Niigata Univ.* (April '93-) |
| Haruko HOSOI | Graduate Student from Ochanomizu Univ.* (April '93-) |

*Complex Catalysis*

| | |
|---|---|
| Hitoshi OHTAKI | Professor (-March '93)[33] |
| Akira NAKAMURA | Professor (April '93-) |
| Hisanobu OGOSHI | Adjunct Professor from Kyoto Univ. |
| Fumio KAWAIZUMI | Adjunct Associate Professor from Nagoya Univ. |
| Thomas DANIEL | Research Associate (April '93-) |
| Kenji WAIZUMI | Technical Associate |
| Hiroshi SHIMOMURA | Graduate Student from Osaka Univ.* (-September '92) |
| Masahiro TANIO | Graduate Student from Kochi Univ.* (-September '92) |

*Functional Coordination Chemistry*

| | |
|---|---|
| Koji TANAKA | Professor |
| Tamotsu TAKAHASHI | Associate Professor |
| Hirotaka NAGAO | Research Associate |
| Noriyuki SUZUKI | Research Associate |

| | |
|---|---|
| Tetsunori MIZUKAWA | Technical Associate |
| Ryo MIYAMOTO | IMS Fellow (-March '92)[34] |
| Denis Y. KONDAKOV | JSPS Post-doctoral Fellow (-June '93)Visiting Research Fellow (June '93-) |
| Martin KOTORA | JSPS Post-doctoral Fellow (March '93-) |
| Victor DENISOV | CIBA-GEIGY Exchange Scientist (-May '93) |
| Zhenfeng XI | Visiting Reserch Fellow (February '93-) |
| Marina KONDAKOVA | Visiting Research Fellow (April '93-) |
| Douman JIN | Visiting Research Fellow (September '93-) |
| Nobutoshi KOMEDA | Graduate Student from Osaka Univ.* |
| Hiroaki TANAKA | Graduate Student (-March '93) |
| Hide KAMBAYASHI | Graduate Student |
| Koichiro AOYAGI | Graduate Student |
| Motohiro KAGEYAMA | Graduate Student from Tokyo Univ.* (-March '93) |
| Ryuichiro HARA | Visiting Research Fellow (-March '93) Graduate Student (April '93-) |
| Yoshinori KUSHI | Graduate Student (October '93-) |
| Hiroshi NAKAJIMA | Graduate Student (April '93-) |
| Kiyotsuna TOYOHARA | Graduate Student (April '93-) |
| Kayoko KASAI | Graduate Student (April '93-) |
| Hideyuki MORI | Visiting Research Fellow (-March '93) |
| Fidefumi UCHINO | Visiting Research Fellow (-March '93) |

*Coordination Bond*

| | |
|---|---|
| Tasuku ITOH | Adjunct Professor from Tohoku Univ. (-March '93)[35] |
| Kazuko MATSUMOTO | Adjunct Professor from Waseda Univ. (April '93-) |
| Masatatsu SUZUKI | Adjunct Associate Professor from Kanazawa Univ. (-March '93)[36] |
| Akira NAGASAWA | Adjunct Associate Professor from Saitama Univ. (April'93-) |

## *Research Facilities*

*Computer Center*

| | |
|---|---|
| Keiji MOROKUMA | Director (-March '93)[1] |
| Hiroki NAKAMURA | Director (April '93-) |
| Kazuo KITAURA | Associate Professor (-March '93)[37] |
| Umpei NAGASHIMA | Associate Professor (April '93-September '93)[38] |
| Mutsumi AOYAGI | Associate Professor (May '93-) |
| Shinkoh NANBU | Research Associate |
| Satoshi MINAMINO | Technical Associate |

*Chemical Materials Center*

| | |
|---|---|
| Kazuhiro NAKASUJI | Director (-May '93) |
| Ichiro HANAZAKI | Director (June '93-) |
| Yoshiro YAMASHITA | Associate Professor |
| Shoji TANAKA | Research Associate |
| Masaaki TOMURA | Technical Associate |
| Masatoshi KOZAKI | Graduate Student |
| Katsuhiko ONO | Graduate Student |
| Chitoshi KITAMURA | Graduate Student (April '93-) |
| Akira OHTA | Graduate Student (April '93-) |

*Instrument Center*

| | |
|---|---|
| Shuji SAITO | Director |
| Kiyokazu FUKE | Associate Professor |
| Shunji BANDOW | Research Associate |
| Fuminori MISAIZU | Research Associate |
| Keizo TSUKAMOTO | Graduate Student (-September '92) |
| Masaomi SANEKATA | Graduate Student |

*Low-Temperature Center*

| | |
|---|---|
| Yusei MARUYAMA | Director |

*Equipment Development Center*

| | |
|---|---|
| Teizo KITAGAWA | Director |
| Tadaoki MITANI | Associate Professor (-March '93)[39] |
| Shuji ASAKA | Research Associate |
| Hiroshi KITAGAWA | Research Associate |
| Jeung Sun AHN | Research Associate |
| Taro SEKIKAWA | Graduate Student from University of Tokyo* |

*Ultraviolet Synchrotron Orbital Radiation Facility*

| | |
|---|---|
| Kyuya YAKUSHI | Director |
| Makoto WATANABE | Associate Professor |
| Goro ISOYAMA | Associate Professor |
| Masao KAMADA | Associate Professor |
| Eiji ISHIGURO | Adjunct Associate Professor from Osaka City Univ. (-March '93) |
| Kazumichi NAKAGAWA | Adjunct Associate Professor from Kobe Univ. (April '93-) |
| Atsunari HIRAYA | Research Associate |
| Shin-ichiro TANAKA | Research Associate |
| Hiroyuki HAMA | Research Associate |
| Shigeo OHARA | IMS Fellow |
| Sayumi HIROSE | Graduate Student |

# Technical Staff

| | |
|---|---|
| Akira UCHIDA | Technical Division Head |
| Keiichi HAYASAKA | Technical Section Chief |
| Kusuo SAKAI | Technical Section Chief |
| Fumio NISHIMOTO | Computer Center (Unit Chief) |
| Fumitsuna TESHIMA | Computer Center |
| Kunihiko TANAKA | Computer Center |
| Sachiyo NOMURA | Chemical Materials Center |
| Takaya YAMANAKA | Instrument Center |
| Masahiro SAKAI | Instrument Center |
| Kiyonori KATO | Low-Temperature Center (Unit Chief) |
| Takashi TAKAYAMA | Low-Temperature Center |
| Toshio HORIGOME | Equipment Development Center (Unit Chief) |
| Norio OKADA | Equipment Development Center |
| Mitsukazu SUZUI | Equipment Development Center |
| Masaaki NAGATA | Equipment Development Center |
| Hisashi YOSHIDA | Equipment Development Center |
| Shinji KATO | Equipment Development Center |
| Nobuo MIZUTANI | Equipment Development Center |
| Kouichi UCHIYAMA | Equipment Development Center |
| Osamu MATSUDO | UVSOR Facility (Unit Chief) |
| Toshio KINOSHITA | UVSOR Facility |
| Masami HASUMOTO | UVSOR Facility |
| Jun-ichiro YAMAZAKI | UVSOR Facility |
| Eiken NAKAMURA | UVSOR Facility |

* Carries out gradurate research of IMS on the Cooporative Education Program of IMS with graduate schools.

1) Present Address: Emory University, Cherry L. Emerson Center for Scientific Comp., Atwood Hall, 1515 Pierce Drive, Atlanta, Georgia 30322, U.S.A.
2) Present Address: College of General Education, Nagoya Univ., Furo-cho, Chikusa-ku, Nagoya 464.
3) Present Address: Dept. of Chemistry, Nagoya Institute of Technology, Gokisho-cho, Showa-ku, Nagoya 466.
4) Present Address: Dept. of Chemisty, Iowa State University of Science and Technology, Gilman Hall, Ames, Iowa 50011, U.S.A.
5) Present Address: Instrumentation Division, National Laboratory for High Energy Physics, Ooho 1-1, Tsukuba-shi, Ibaragi 305
6) Present Address: Dept. of General Education, Tokyo Metropolitan Univ., Minami-Osawa 1-1, Hachioji-shi, Tokyo 192-03

7) Present Address:Dept. of Chemistry, Faculty of Science, Tohoku Univ., Aramaki, Aoba-ku, Sendai 980
8) Present Address:The Ministry of Education, Culture and Science, Kasumigaseki, Chiyoda-ku, Tokyo 100
9) Present Address:School of Medicine, Kurume Univ., Asahi-cho, Kurume 830
10) Present Address:AT&T Bell Laboratories, Murray Hill, N.J. 07974-2070 USA
11) Present Address:Toshiba Co. Komukaitoshiba-cho, Saiwai-ku, Kawasaki 210
12) Present Address:Advanced Research Laboratory, Hitachi Ltd., Hatoyama, Saitama 350-03
13) Present Address:The Institute of Physical and Chemical Research, Wako, Saitama 351-01
14) Present Address:Hitachi Research Laboratory, Hitachi Ltd., Ohmika, Hitachi, Ibaraki 319-12
15) Present Address:Institute of Spectroscopy, Russian Academy of Science, 142092 Troitzk, Moscow Region, Russian Federation
16) Present Address:Department of Physics, Kumaon University, Naini Tal 263001, India
17) Present Address:NTT Co. Ltd., 3-1, Wakamiya, Morinosato, Atsugi, Kanagawa 243-01
18) Present Address:Department of Chemical Technology, Kanagawa Institute of Technology, 1030, Shimo-ogino, Atsugi, Kanagawa 243-02
19) Present Address:Tokoha-gakuen Univ., 1000 Sena, Shizuoka 420
20) Present Address:Department of Image Science, Faculty of Engineering, Chiba University, Yayoi-cho, Inage-ku, Chiba 263
21) Present Address:Department of Physics, Faculty of Science, Ochanomizu University, Otsuka, Bunkyo-ku, Tokyo 112
22) Present Address:Department of Organic and Polymeric Materials, Tokyo Institute of Technology, O-okayama, Meguro-ku, Tokyo 152
23) Present Address:Department of Physics, Okayama University of Science, Ridai-cho, Okayama 700
24) Present Address:The Institute of Scientific and Industrial Research, Osaka Univ., 8-1 Mihogaoka, Ibaraki, Osaka 567
25) Present Address:Dept. of Applied Chemistry, Faculty of Engineering, Gunma Univ., Kiryu, Gunma 376
26) Present Address:Dept. of Chemistry, Faculty of Science, Kochi Univ., Akebono-Cho, Kochi 780
27) Present Address:Institute for Fundamental Research of Organic Chemistry, Kyusyu Univ., 6-10-1 Hakozaki, Higashi-ku, Fukuoka 812
28) Present Address:Dept. of Chemistry, Faculty of Science, Hiroshima Univ., 1-3 Kagamiyama, Higashihiroshima 724
29) Present Address:Dept. of Chemistry, The Univ. of Edinburgh, Kings Buildings West Mains Road, Edinburgh EH9 3JJ, U.K.
30) Present Address:Ebara Research Corp., Center for Environmental Engineering, 4-2-1 Honfujisawa, Fujisawa 251
31) Present Address: Dept. of Electrical and Electronic Engineering, Toyohashi Univ. of Technology, 1-1 Hibarigaoka, Tempaku, Toyohashi 441
32) Present Address: Catalysis Research Center, Hokkaido Univ., N11, W10, Kita-ku, Sapporo 060
33) Present Address: Dept. of Sci. and Tech. Ritsumeikan Univ. 56-1 Toujiin-kitamachi, Kita-ku, Kyoto 603.
34) Present Address: Dept. of Chem. Hirosaki Univ. 3 Bunkyo-cho, Hirosaki, Aomori 036.
35) Present Address:Tohoku Univ. Aoba, Aramaki, Aoba-ku, Sendai, Miyagi 980
36) Present Address:Dept. of Chem. Kanazawa Univ. 1-1 Marunouchi, Kanazawa, Ishikawa 920
37) Present Address:Colledge of Integrated Art and Science, University of Osaka Prefecture, Gakuen-cho 1-1, Sakai, Osaka 591
38) Present Address:Faculty of Science, Ochanomize Univ., 2-1-1 Ohtsuka, Bunkyo-ku, Tokyo 153
39) Present Address:Dept. of Material Science, Japan Advanced Institute of Science and Technology, Tatsunokuchi, Ishikawa 923-12

# COUNCIL

| | |
|---|---|
| **Hiroo INOKUCHI** | **Director-General (- March '93)** |
| **Mitsuo ITO** | **Director-General (April '93-)** |

# Councilors

| | | |
|---|---|---|
| *Chairman* | Ikuzo TANAKA | President, National Institute for Academic Degrees (- May '93) |
| *Chairman* | Teijiro YONEZAWA | Professor, Kinki University (May '93 -) |
| *Vice-Chairman* | Yutaka TOYOZAWA | Professor, Chuo University (- May '93) |
| *Vice-Chairman* | Yukio HORI | Executive Director, Japan Society for the Promotion of Science (June '93 -) |
| | Hirotsugu AKAIKE | President, The Institute of Statistical Mathematics |
| | Schunichi AKIMOTO | Professor Emeritus, The University of Tokyo (June '93 -) |
| | Hideaki CHIHARA | Executive Director, Japan Association for International Chemical Information |
| | Eiichi FUJITA | Professor Emeritus, Kyoto University (- May '93) |
| | Kenichi FUKUI | President, Institute for Fundamental Chemistry (- May '93) |
| | Yoshikazu ITO | Chairman of The Board, Toray Industries, Inc. |
| | Hiizu IWAMURA | Professor, The University of Tokyo (June '93 -) |
| | Nobuo KATO | President, Nagoya University (June '93 -) |
| | Kozo KUCHITSU | Professor, Josai University |
| | Haruo KURODA | Professor, Science University of Tokyo (June '93 -) |
| | Yoshio MATSUNAGA | Professor, Kanagawa University |
| | Akira MIKAZUKI | Professor Emeritus, The University of Tokyo (- May '93) |
| | Hidetaka MORIMOTO | Adviser, Toyota Central Research & Development Loboratories, Inc. (June '93 -) |
| | Toru MORIYA | Professor, Science University of Tokyo (June '93 -) |
| | Kazuo SAITO | Professor, International Christian University |
| | Hideki SAKURAI | Dean of The Faculty of Science, Tohoku University |
| | Hirotoshi SANO | President, Tokyo Metropolitan University (- May '93) |
| | Shinichi SASAKI | President, Toyohashi University of Technology |
| | Hiroshi SHIONO | Professor, Seikei University (June '93 -) |
| | Kenji TAMARU | Professor, Science University of Tokyo (- May '93) |
| | Hisashi TANAKA | Former President, Kyoto Pharmaceutical University (June '93 -) |
| | Peter DAY | Director, The Royal Institution of Great Britain |
| | John C. POLANYI | Professor, University of Toronto |

The Council is the advisory board for the Director-General. Two of the councilors are selected among distinguished foreign scientists.

# Distinguished Research Consultants

| | |
|---|---|
| Kenichi FUKUI | President, Institute for Fundamental Chemistry |
| Saburo NAGAKURA | President, The Graduate University of Advanced Studies |
| Kenji TAMARU | Professor, Science University of Tokyo |
| Ikuzo TANAKA | President, National Institute for Academic Degrees |
| Yasutada UEMURA | Chancellor, Musashi Gakuen |

# Administration Bureau

| | |
|---|---|
| Jiro SATO | Director-General, Administration Bureau (July '92 -) |
| Shozo IMAKAWA | Director, General Affairs Department (- June '93) |
| Nobuaki SHIMIZU | Director, General Affairs Department (July '93 -) |
| Yasuyoshi NONAKA | Director, Finance and Facilities Department (- March '93) |
| Mutsuo MIYAZAKI | Director, Finance and Facilities Department (April '93 -) |
| Ryoichi ASANO | Head, General Affairs Division |
| Makoto SUZUKI | Head, Personnel Division (- March '93) |
| Isao FUJII | Head, Personnel Division (April '93 -) |
| Satoru TAMURA | Head, Research Cooperation and International Affairs Division |
| Masaaki TSUJITA | Head, Budget Division (- March '93) |
| Yoshiji SHIMA | Head, Budget Division (April '93 -) |
| Saigyo KAMIYAMA | Head, Accounts Division (- June '93) |
| Masayuki JINNO | Head, Accounts Division (July '93 -) |
| Hiromu KITAJIMA | Head, Construction Division |
| Kunikatsu SHOJI | Head, Equipment Division (- October '92) |
| Hiroaki KAMACHI | Head, Equipment Division (November '92 -) |

# BUILDINGS AND CAMPUS

The IMS campus covering 62,343 $m^2$ is located on a low hill in the middle of Okazaki City. The inequality in the surface of the hill and growing trees are preserved as much as possible, and low-storied buildings are adopted for conservation of the environment. The buildings of IMS are separated according to their functions as shown in the map. The Research Office Building and all Research Facilities except for the Computer Center are linked organically to the Main Laboratory Building by corridors. Computer Center, Library and Administration Buildings are situated between IMS and the neighboring National Institute for Basic Biology and National Institute for Physiological Sciences, because the latter two facilities are common to these three institutes.

The lodging facility of IMS called Yamate Lodge, located within ten minutes' walk, has sleeping accommodations for 19 guests and two families. Mishima Lodge, located within four minutes' walk east of IMS can accommodate 68 guests and ten families. Scientists who visit IMS as well as the two other institutes can make use of these facilities. Foreign visiting scientists can also live at these lodgings with their families during their stays.

The Institute for Molecular Science

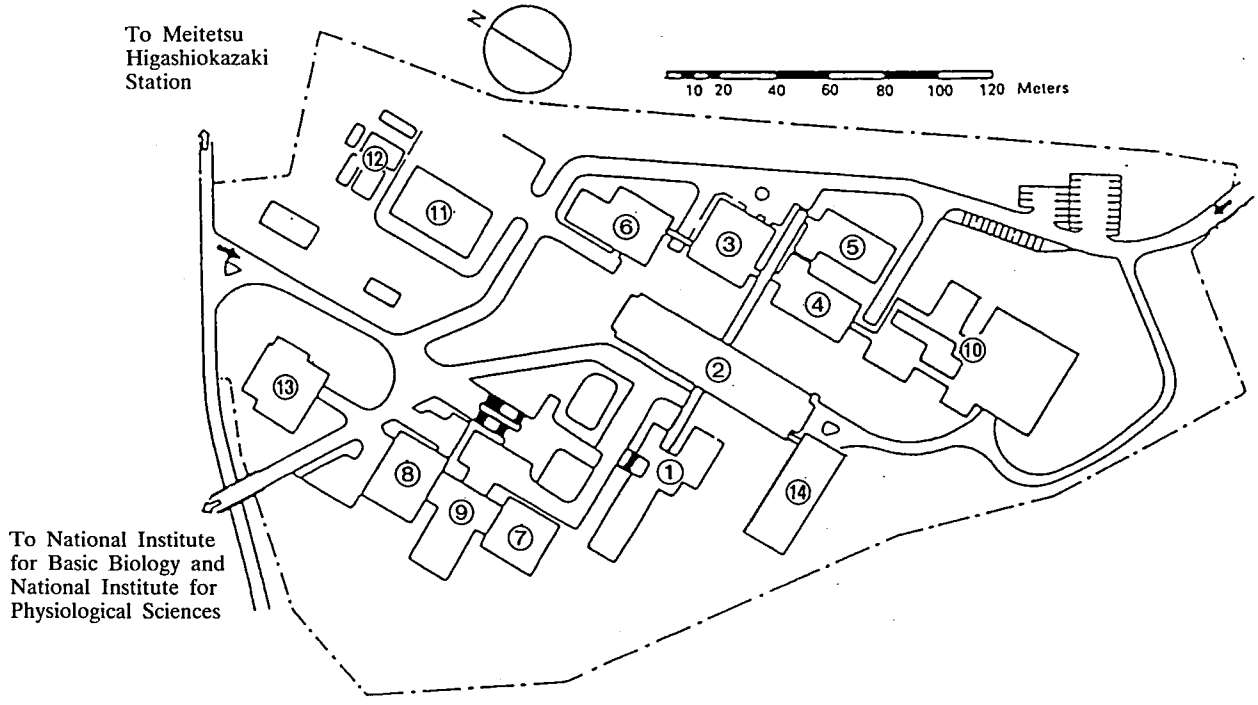


1. Research Office Building
2. Main Laboratory Building
3. Equipment Development Center
4. Instrument Center
5. Chemical Materials Center
6. Low-Temperature Center
7. Computer Center
8. Library
9. Central Administration
10. UVSOR Facility
11. Power Station
12. Waste-Water Disposition Facilities
13. Faculty Club
14. South Laboratory Building


Okazaki (population 300,000) is 260 km southwest of Tokyo, and can be reached by train in about 3 hours from Tokyo via New Tokaido Line (Shinkansen) and Meitetsu Line.
The nearest large city is Nagoya, about 40 km west of Okazaki.

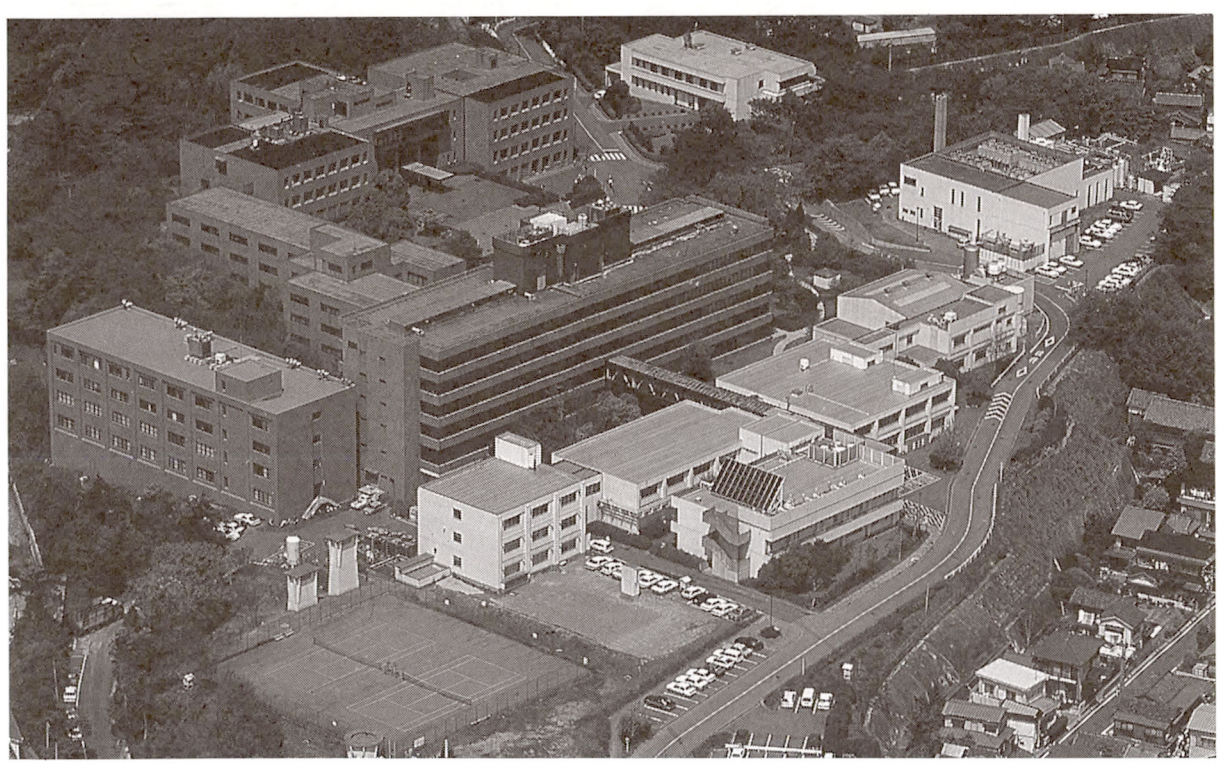

# RESEARCH ACTIVITIES I
# Department of Theoretical Studies

## I—A Potential Energy Surfaces and Dynamics of Elementary Chemical Reactions

This will be the last full activity report from the Morokuma's group, who left IMS at the end of March 1993. We had relatively light activity in this field of elementary reactions of simple molecules. Dr. Hashimoto became Associate Professor at Tokyo Metropolitan University in April 1993.

### I-A-1 Theoretical Study of the Highly Vibrationally Excited States of $FHF^-$: *Ab initio* Potential Energy Surface and Hyperspherical Formulation

**Koichi YAMASHITA** *(Inst. Fund. Chem.)*, **Keiji MOROKUMA, and Claude LEFORESTIER** *(Univ. Paris-Sud)*

[*J. Chem. Phys.*, in press]

A three-dimensional description of vibrationally highly excited linear molecules is formulated in hyperspherical coordinates, based on a Successive Adiabatic Reduction scheme. The method is applied to the low-lying and highly excited vibrational states of $FHF^-$, a prototype of symmetric bihalide anions, which has attracted spectroscopic interest due to its peculiar vibrational anharmonicity. *Ab initio* potential energy surfaces (PESs) which cover the ground-state potential well of $FHF^-$ and/or its dissociation to the $F^-$+HF channel have been obtained by using the CEPA (coupled electron pair approach) method. A hyperspherical calculation using the *ab initio* PES of the sixth-order Simons-Parr-Finlan analytical form has correctly reproduced the experimental fundamental frequencies. Specifically, the vibrationally highly excited $FHF^-$ above the dissociation threshold is proposed as a candidate for transition state spectroscopy (TSS) of unimolecular dissociation reactions without barrier.

### I-A-2 Theoretical Study of the Photodissociation of $HgI_2$

**Kenro HASHIMOTO and Keiji MOROKUMA**

In connection to the femtosecond real-time probing experiment on the photodissociation of $HgI_2$ at 310 nm excitation, we have been calculating the potential energy surfaces for its ground and several low-lying excited states, taking the spin-orbit interaction explicitly into the CI calculation. The MOs used in the MRCI calculation are obtained by the average state SCF method in which we take the equal-weight average of all possible electronic configurations obtained by putting 12 electrons into 10 valence MOs. We have found two states, the second and the third "1" states, in the vicinity of the experimental energy which carry a substantial transition dipole between the ground state. The former gives the ground state $I(^2P_{3/2})$ product, whereas the latter gives the excited state $I^*(^2P_{1/2})$ product. The calculated energy difference between the I and I* channels at the dissociation limit is in good agreement with the experiment.

### I-A-3 An MO *ab initio* Study of Unimolecular Elimination Reactions of Vinyl Chloride

**Jean-Frédéric RIEHL and Keiji MOROKUMA** *(Emory Univ. and IMS)*

Using MP2/6-31G** optimization and QCISD(T)/6-311+G** single-point calculations, we carried out an extensive study of the unimolecular dissociation reactions in vinyl chloride (VCl): H and Cl single atom detachment, $H_2$ and HCl molecular elimination or migration reactions can take place. Despite a large number of experiments, the mechanistic details are still poorly understood, because of a large number of dissociation channels.

All possible reaction pathways on the ground state potential energy surface have been systematically determined. We have shown that the HCl three-center elimination followed by the isomerization of vinylidene is easier by 8 kcal/mol than the HCl four-center elimination, in agreement with the most recent experimental studies. $H_2$ elimination pathways are in general more difficult than HCl pathways. Among them, three-center $H_2$ elimination followed by isomerization of chlorovinylidene is the easiest. The $\alpha$-H shift gives $\alpha$-chloroethylidene with a low activation energy, but the subsequent $H_2$ elimination is very difficult. The direct $H_2$ four-center elimination from VCl does not take place. The results are also compared with our previous calculations on vinyl fluoride and our recent calculations of the $H_2$ elimination from ethylene.

### I-A-4 An MO *ab initio* study of Unimolecular Elimination Reactions in Dichloroethylene. A Comparison with Ethylene, Vinylchloride and Trichloroethylene

**Jean-Frédéric RIEHL and Keiji MOROKUMA** *(Emory Univ. and IMS)*

We extended our study of the molecular elimination processes in vinylchloride (VCl) to the other Cl substituted ethylenes, namely di- and trichloroethylene, using a similar level of theory. Compared to VCl, the overall reaction scheme for dichloroethylene (DCE) is more complicated because of the existence of three isomers of the reactant (*cis*-DCE, *trans*-DCE and 1,1-DCE) and three molecular elimination products ($H_2$, HCl and $Cl_2$). These calculations show again the preference for the HCl three-center elimination. In *trans*-DCE, the three-center elimination is easier that the four-center elimination, with an energy difference comparable to that of VCl. However, the HCl four-center elimination from 1,1-DCE, in which the three-center

reaction is impossible, is comparable in the activation energy to the three-center elimination in *trans*-DCE. In TCE, the three-center elimination is also more favorable.

The direct $H_2$ four-center elimination from *cis*-DCE does not take place, a situation similar to that for ethylene and VCl. A $H_2$ three-center elimination from 1,1-DCE is feasible, but $H_2$ elimination from *trans*-DCE can take place only after an H migration. The study of $Cl_2$ elimination and of the stability of Cl-substituted ethylidenes is in progress.

### I-A-5 Pathways for $H_2$-Elimination from Ethylene: A Theoretical Study

**Jan JENSEN*, Keiji MOROKUMA, and Mark GORDON*** *(*Iowa State Univ.)*

*Ab initio* quantum chemical methods are applied to the study of ethylene decomposition to acetylene and molecular hydrogen in the ground electronic state. Results are reported on three different pathways for ethylene decomposition: two stepwise processes involving a hydrogen transfer followed by 1,1-elimination of $H_2$, or vice versa, and a 1,2-elimination. The latter proceeds through an energy maximum with two imaginary frequencies, rather than one as for conventional transition states. Ethylidene and vinylidene are predicted to be stationary points on the $C_2H_4$ and $C_2H_2$ potential energy surfaces, respectively. Recent photochemical studies have observed rotationally hot $H_2$. It is shown that due to the excess energy available in the photochemical experiments all three mechanisms can give rise to rotationally hot $H_2$ when proper account is taken of the transverse vibrational modes along the reaction paths.

## I—B Structure and Spectroscopy of Clusters

Varieties of theoretical studies in the field of atomic and molecular clusters are in progress.

### I-B-1 Structures, Stabilities and Ionization Potentials of $Na(H_2O)_n$ and $Na(NH_3)_n$ (n=1-6) Clusters. An *ab initio* MO Study

**Kenro HASHIMOTO, Shaoren HE, and Keiji MOROKUMA** *(Emory Univ. and IMS)*

[*Chem. Phys. Lett.*, **206**, 297 (1993)]

The structures and stabilities of $Na(H_2O)_n$ and $Na(NH_3)_n$ (n=1-6) have been calculated at the HF/3-21G level. For $n \geq 4$ $Na(H_2O)_n$ is a surface complex, where Na atom tends to be situated on the surface of $(H_2O)_n$ cluster. $Na(NH_3)_n$ is an inclusion complex where Na is surrounded by $NH_3$ molecules. Water—water hydrogen bonds play an essential role in stabilizing $Na(H_2O)_n$, whereas stabilization by Na-N bond formation is more important for $Na(NH_3)_n$. Calculated ionization potentials as functions of n can reproduce qualitatively the experimentally found different trends between $Na(H_2O)_n$ and $Na(NH_3)_n$, which are related to the above-mentioned different structural features.

These conclusions have been confirmed to remain unchanged in our more recent calculations using larger basis sets and higher levels of theory.

### I-B-2 A Theoretical Study on Ligand Substitution Reaction of Pt(II) Complex in Water

**Chizuru MUGURUMA** *(Grad. Univ. for Adv. Studies, Emory Univ. and IMS)*, **Nobuaki KOGA, Kazuo KITAURA, and Keiji MOROKUMA** *(Emory Univ. and IMS)*

In order to investigate the solvent effect of the reaction:

$$[Pt(NH_3)_3Cl]^+ + H_2O \rightarrow [Pt(NH_3)_3(H_2O)]^{2+} + Cl^- \quad (1),$$

we fitted the *ab initio* two-body interaction energies between $[Pt(NH_3)_3]^{2+}$ and $H_2O$, between $[Pt(NH_3)_3]^{2+}$ and $Cl^-$ and between $H_2$ and $Cl^-$ to the potential functions represented by overlap integrals of localized molecular orbitals (LMOs), as proposed by Kitaura. As we reported last year, we have obtained a good fit for the two-body potential functions.

When *ab initio* calculations are carried out for the entire interacting system $[Pt(NH_3)_3]^{2+}(H_2O)Cl^-$ in the region where the reaction (1) is likely to probe, we found a considerable repulsive three-body interaction energy. This kind of repulsive interaction can be found in the literature for solvation of metal ions, and proposals have been made to fit it to exponential-type functions as an extra exchange repulsion among three molecules.

Our analysis suggests that the three-body repulsion in the present case comes mainly from $Cl^-$ to Pt makes the charge transfer from $H_2O$ to Pt more difficult. Thus in the spirit of the Kitaura two-body potential, we are trying to fit the three-body repulsive potential to a sum of $C_{abc}\, S_{ab}\, S_{bc}\, S_{ca}$ and $C_{a^*bc}\, S_{a^*b}\, S_{bc}\, S_{ca^*}$ type functions. Here, $C_{abc}$ and $C_{a^*bc}$ are parameters, and S refers to overlap integral involving both occupied (un-starred) and vacant (starred) LMOs. A double perturbation expansion of the three-body interaction energy attribute these terms to $E_0^{13}$ and $E_0^{23}$, respectively.

### I-B-3 Cluster and Solution Simulation of Formaldehyde-Water Complexes and Solvent Effect on Formaldehyde $^1(n, \pi^*)$ Transition

**Hiroo FUKUNAGA** *(Fuji Photo Film Co. and IMS)* **and Keiji MOROKUMA**

[*J. Phys. Chem.*, **97**, 58 (1993)]

On the basis of *ab initio* molecular orbital calculations, we have derived 12-1-3 potential functions for interaction between formaldehyde, in both the ground and the n-$\pi^*$ singlet excited state, and one water molecule as well as the transition dipole moment functions in the n-$\pi^*$ transition of formaldehyde interacting with a water molecule. Using these functions, we carried out simulations of vibrational

structures in the n-$\pi^*$ absorption spectrum of formaldehyde complexed with a few water molecules (n=1-3) and in water solution. Detailed analyses of structural and energetic features have been carried out. Formaldehyde in cluster interacts with the chain of hydrogen-bonding water molecules, while formaldehyde in water solution is surrounded by water molecules. Water molecules around the oxygen atom of formaldehyde interact attractively and those around the hydrogen atoms of formaldehyde interact both attractively and repulsively with formaldehyde. Though the transition energy shift in the $H_2CO$-3($H_2O$) cluster does not reach that in water solution, the band width of the simulated absorption spectrum in the $H_2CO$-3($H_2O$) cluster is nearly the same as that in water solution.

### I-B-4 *Ab initio* Study of Neutral and Cationic $B_{12}$ and $B_{13}$ Clusters

**Hiroshi KATO*, Koichi YAMASHITA* (*Inst. Fund. Chem.), and Keiji MOROKUMA**

[*Bull. Chem. Soc. Jpn.*, in press]

The geometries, electronic structures and energies of the neutral and cationic $B_{12}$ and $B_{13}$ clusters were investigated by the *ab initio* molecular orbital method. Several planar and non-planar stationary structures were optimized for neutrals and cations of each cluster size. A characteristic $C_{2v}$ cyclic form with one atom in the middle was found to be stable for each cluster. While the $D_{5d}$ icosahedral $B_{12}^+$ was found to be the most stable, the triplet $D_{5d}$ icosahedral $B_{12}$ was stable but energetically unfavorable than the $C_{2v}$ cyclic $B_{12}$. All the three-dimensional structures considered for $B_{13}$ and $B_{13}^+$ clusters were unstable.

## I—C Structure and Reactivity of Boranes

Dr. Alexander Mebel, joined Morokuma's group in 1992 and concentrated his studies on structure, stability and reactivity of boranes and related compounds. He is leaving IMS in the fall of 1993.

### I-C-1 *Ab initio* MO Study of Mechanisms of the Reaction of $B_2H_6$ with $SH_2$.

**Alexander M. MEBEL, Djamaladdin G. MUSAEV*, and Keiji MOROKUMA* (*IMS and Emory Univ.)**

[*J. Phys. Chem.*, **97**, 7543 (1993); *Chem. Phys. Lett.*, submitted]

The potential energy surface for the reaction of diborane with sulfur dihydride has been calculated by using MP4/6-31+G(2d,p)//MP2(FULL)/6-31G(d) method with zero-point energy corrections. The proposed mechanism of formation of mercaptoborane, $BH_2SH$, from the reaction includes as initial step the bimolecular addition of $SH_2$ to $B_2H_6$ to form the $B_2H_7^-$ like complex, $H_2S \cdot B_2H_6$. Then this complex can be transformed by three different ways, elimination of $BH_3$ to give $BH_3 \cdot SH_2$, rearrangement into hypervalent isomer, $SH_2(BH_3)_2$, and concerted elimination of $BH_3$ and $H_2$ to form $BH_2SH$. $SH_2(BH_3)_2$ can eliminate either $BH_3$ or $H_2$. The latter pathway with formation of $B_2H_5 \cdot SH$ complex is the most favorable thermodynamically but is forbidden by a high barrier of $H_2$ elimination. Removal of $BH_3$ also gives $BH_3 \cdot SH_2$ species, and $H_2$ elimination from $BH_3SH_2$ leads to $BH_2SH$. The pathway involving concerted elimination of $BH_3$ and $H_2$ from $H_2S \cdot B_2H_6$ complex has the highest energy 27.4 kcal/mol relative to $SH_2$+$B_2H_6$, which is lower than those for the reaction pathways involving $H_2$ elimination from $SH_2(BH_3)_2$ and $BH_3SH_2$, 41.0 and 44.8 kcal/mol, respectively. At high temperatures (>200°C) entropy factor destabilizes the transition structure for concerted $BH_3$ and $H_2$ elimination, and the mechanism with $BH_3 \cdot SH_2$ formation followed by $H_2$ elimination is more favorable according free Gibbs energy criterion.

Calculated vibrational frequencies (MP2(FULL)/6-31G(d)) are compared with experimental values for $BH_2SH$ and HBS and are predicted for $SH_2B_2H_6$, $SH_2(BH_3)_2$, and $B_2H_5SH$. Comparison of mechanisms of the reactions of diborane with $SH_2$ and $NH_3$ is performed.

### I-C-2 *Ab initio* Molecular Orbital Study of Structure and NMR $^{11}B$ Chemical Shifts of Lewis Base Adducts of CO, $NH_3$, CO, $PF_3$, and $PH_3$ with Small Nido-Boranes, $B_3H_7$ and $B_4H_8$.

**Alexander M. MEBEL*, Djamaladdin G. MUSAEV, and Keiji MOROKUMA* (*Emory Univ. and IMS)**

[*Chem. Phys. Lett.*, in press]

A typical property of electron deficient boranes is their Lewis acidity which reflects the fact that boron possesses fewer valence electrons than valence orbitals. As a result, boranes readily form donor-acceptor adducts with Lewis bases such as $NH_3$, CO and $PR_3$. The geometries, formation energies, and NMR $^{11}B$ chemical shifts of $B_3H_7CO$, $B_3H_7NH_3$, $B_4H_8CO$, $B_4H_8PH_3$, and $B_4H_8PF_3$, Lewis base adducts of the $B_3H_7$ and $B_4H_8$ nido-boranes, have been investigated by *ab initio* molecular orbital method. MP2/6-31G* optimized geometries and calculated NMR chemical shifts are in good agreement with experiment. For instance, the average deviation of $^{11}B$ chemical shifts calculated by IGLO method with the MP2/6-31G* geometries for $B_3H_7CO$, $B_4H_8CO$, and $B_4H_8PF_3$ from experimental data is 2.4 ppm. Lewis bases cause pronounced elongation of BB distances and strong upfield chemical shift for the attacked boron atoms.

### I-C-3 Metallaboranes with IIB Subgroup Transition Metals. Is Accurate *Ab initio* MO Calculation of Structure, Stability and NMR Chemical Shifts Possible?

**Alexander M. MEBEL*, Djamaladdin G. MUSAEV, Nobuaki KOGA, and Keiji MOROKUMA*** *(*Emory Univ. and IMS)*

[*Bull. Chem. Soc. Jpn.*, 66, #11 (1993), in press]

*Ab initio* MO study of structure and stability of nido-metallaboranes with Ir, Co and Fe transition metals has been performed at HF and correlational MP2 levels. Reasonable agreement with experiment has been found for optimized geometry of $[(IrB_5H_8)(CO)(PH_3)_2]$ iridaborane, and the MP2 optimization improves the agreement to the maximum error of 0.035 Å. Methods more sophisticated than MP2 would be necessary for accurate calculations of metallaboranes with first row transition metals.

Two geometric isomers, 2- with basal Ir and 1- with apical Ir are close in energy for $[(IrB_5H_8)(CO)(PH_3)_2]$. While 2-isomer has been observed experimentally, 1- is predicted to be thermodynamically more stable by 8.6 kcal/mol at MP4(SDQ) level. Ir atom in the iridaborane has octahedral stereochemistry and a large negative charge, with borane $B_5H_8$ serving as electron donor.

Calculated by the IGLO method NMR $^{11}B$ chemical shifts for 2-$[(IrB_5H_8)(CO)(PH_3)_2]$ are in qualitative agreement with experiment. However, reliability of the calculated $^{11}B$ chemical shifts is not as high as found for usual boranes and carboranes; the largest discrepancy of theoretical values from experiment reaches 10 ppm, and the average deviation is 6.6 ppm. Probably, larger basis sets are necessary for more accurate calculations, or correlation effects on geometry are more significant in chemical shift calculation for metallaboranes than for boron hydrides.

### I-C-4 *Ab initio* MO Study of Skeletal Rearrangements in Pentagonal Pyramidal Clusters, $B_6H_{10}$ Borane and $[(IrB_5H_8)(CO)(PH_3)_2]$ Metallaborane.

**Alexander M. MEBEL*, Djamaladdin G. MUSAEV, and Keiji MOROKUMA*** *(*Emory Univ. and IMS)*

Systematic *ab initio* MO study of all possible degenerate cage rearrangement mechanisms for $B_6H_{10}$ has been performed at MP2/6-31G* and HF/6-31G levels. The mechanism, which involves a diamond-square-diamond (DSD) rearrangement with formation of $B_5H_8(BH_2)$ tetragonal pyramidal cluster having a bridging $BH_2$ group, and the middle structure of $C_2$ symmetry on the pathway, has been shown to be favorable for the apical-basal rearrangement. The preferable mechanism for basal-basal reorganizations involves scrambling of the bridging $BH_2$ group from one basal edge to another in $B_5H_8(BH_2)$ and has the middle structure of nido-type with one square face. For both mechanisms the initial DSD rearrangement is the rate determining step with the barrier of 47.0 kcal/mol at MP2/6-31G* + ZPE(HF/6-31G) level. Rearrangement mechanism with low activation energy does not exist.

For $[(IrB_5H_8)(CO)(PH_3)_2]$ the isomerization process leading the Ir atom from basal to apical position is shown to occur by the mechanism similar to that of apical-basal rearrangement of $B_6H_{10}$. The calculated barrier, 38.7 kcal/mol at MP2//HF/ECP+DZ, is high enough to prevent the isomerization. Alternative synthetic attempts are encouraged to get the unknown 1-isomer with apical Ir.

## I—D Structure and Reaction of Gas Phase Transition Metal Ion Complexes

Chemistry of transition metal complexes, summarized in sections I-D to I-F, continued to be the most active research area of Morokuma's group. The topics covered ranged from gas phase ions to complexes in solution and solid state, from mononuclear to trinuclear complexes and from structure and stability to reactivities. Dr. Musaev continued his energetic studies on the gas-phase transition metal ion complexes. He moved to Emory Univ. in February 1993.

### I-D-1 *Ab initio* Molecular Orbital Study of Electronic and Geometrical Structures of $MCH_2^+$ and $MSiH_2^+$ Complexes (M=Co, Rh and Ir)

**Djamaladdin G. MUSAEV*, Keiji MOROKUMA*** *(*IMS and Emory Univ.)*, **and Nobuaki KOGA** *(IMS and Nagoya Univ.)*

[*J. Chem. Phys.*, in press]

Complete active space self-consistent field (CASSCF) and internally contracted single and double configuration interaction from the CASSCF reference functions (MR-SDCI-CASSCF) methods have been used to calculate electronic and geometrical structures of low-lying $^3A_1$, $^3A_2$, $^3B_1$, $^3B_2$ and $^1A_1$ states of methylene, $MCH_2^+$, and silylene, $MSiH_2^+$, complexes for M=$Co^+$, $Rh^+$ and $Ir^+$. The ground state of $CoCH_2^+$, $IrCH_2^+$ and all considered $MSiH_2^+$ complexes is the nearly degenerate $^3A_1$ and $^3A_2$ states. For $RhCH_2^+$ the ground state is $^1A_1$, with $^3A_1$ and $^3A_2$ states lying only 4—5 kcal/mol higher. The $M^+$=$CH_2$ bond is about 10—20 kcal/mol stronger than the $M^+$=$SiH_2$ bond. Our best calculated binding energies are 80.3 for $CoCH_2^+$, 78.3 for $RhCH_2^+$, 113.1 for $IrCH_2^+$, 61.5 for $CoSiH_2^+$, 69.3 for $RhSiH_2^+$ and 98.7 kcal/mol $IrSiH_2^+$, which are in general in good agreement with experimental values. By using MC/LMO/CI technique has been shown that all present silylene complexes have mostly Fischer-type character with donor-acceptor s and p bond. In contrary, the analogous methylene complexes are mostly Schrock-type complexes with covalent s and p bond, except $^3A_1$, $^3B_2$ and $^3B_1$ states of $RhCH_2^+$, which have mostly Fischer-type character.

### I-D-2 *Ab initio* Study of the Molecular and Electronic Structure of $CoCH_2^+$ and the Reaction Mechanism: $CoCH_2^+ + H_2$

**Djamaladdin G. MUSAEV*, Keiji MOROKUMA*** *(*IMS and Emory Univ.),* **Nobuaki KOGA, Kiet A. NGUYEN**, Mark S. GORDON**** *(**Iowa State Univ.),* **and Thomas R. CUNDARI** *(Memphis State Univ.)*

[*J. Phys. Chem.*, in press]

Both CASSCF and MR-SDCI-CASSCF methods have been used with two different effective core potentials to investigate the mechanism for the reaction $CoCH_2^+ + H_2$. A similar hydrogenolysis reaction mechanism holds for the $^3A_2$ and $^3A_1$ states of the $CoCH_2^+ + H_2$ reactants: In the first step, the reactants yield an ion-molecule complex, $(H_2)CoCH_2^+$, stabilized by 8–9 kcal/mol. Subsequently, the H-H bond is activated, leading to a four-center transition state with an energy barrier of about 31–34 kcal/mol. An intermediate complex, $HCoCH_3^+$, is predicted to be a minimum at the CASSCF level, but MR-SDCI-CASSCF single point calculations suggest that this minimum disappears at higher level of theory. Following H-H bond cleavage, a $CoCH_4^+$ ion-molecule complex is formed, with a stabilization energy of 19–22 kcal/mol. The hydrogenolysis reaction is predicted to be exothermic by 20–30 kcal/mol. The channels leading to formation $CoH^+ + CH_3$ and $CoCH_3^+ + H$ are endothermic by about 5–12 kcal/mol. The reverse reaction $Co^+ + CH_4$ may give only one product, the ion-molecule complex $CoCH_4^+$ at moderate temperatures. Hay-Wadt and Stevens-Krauss-Basch-Jasien pseudopotentials give qualitatively same results.

## I-D-3 *Ab initio* MO Study of the Electronic and Geometric Structure of $RhCH_2^+$ and the Reaction Mechanism: $RhCH_2^+ + H2 \rightarrow Rh^+ + CH_4$

**Djamaladdin G. MUSAEV*, Nobuaki KOGA, and Keiji MOROKUMA*** *(*IMS and Emory Univ.)*

[*J. Phys. Chem.*, **97**, 4064 (1993)]

By using CASSCF and MR-SDCI-CASSCF methods we have calculated electronic and geometric structures of $RhCH_2^+$, as well as the potential energy surfaces (PESs) of reaction: $RhCH_2^+ + H_2 \rightarrow Rh^+ + CH_4$. The ground state of $RhCH_2^+$ is $^1A_1$, and nearly degenerate $^3A_1$ and $^3A_2$ states lie about 4–5 kcal/mol higher. The calculated binding energy for $RhCH_2^+(^1A_1) \rightarrow Rh^+(^3F) + CH_2(^3B_1)$ is 78.3 kcal/mol vs experimental results $91 \pm 5$ kcal/mol. The PESs of the reaction, calculated for the ground $^1A_1$ and the excited $^3A_1$ states of $RhCH_2^+$, are very similar. In the first step, reactants give an ion-molecule complex, $(H_2)RhCH_2^+$, with a stabilization energy of about 7 kcal/mol. Then the H-H bond activation takes place with a 16 kcal/mol barrier. The resultant complex $HRhCH_3^+$ probably does not exist but rearranges without barrier to the product complex $RhCH_4^+(^3A')$, which is stable by about 17 kcal/mol relative to $Rh^+(^3F) + CH_4$.

## I-D-4 *Ab initio* MO Study of Electronic and Geometrical Structures of $MCH_2^+$ Complex and Its Reactivity with $H_2$, where M=Co, Rh and Ir.

**Djamaladdin G. MUSAEV* and Keiji MOROKUMA*** *(*IMS and Emory Univ.)*

[*Israel J. of Chem.*, in press]

By using CASSCF (for optimization of geometries) and MR-SD-CI-CASSCF (for energies) methods we have studied and compared the mechanism of reaction $MCH_2^+ + H_2$, as well as the electronic and geometrical structure of the $MCH_2^+$ complex, where M=Co, Rh and Ir. It has been found that the mechanisms of reaction $MCH_2^+ + H2 \rightarrow M^+ + CH_4$ **(1)** for M=Co and Rh are similar and follow the path: $MCH_2^+ + H_2 \rightarrow (H_2)MCH_2^+ \rightarrow$ [TS1, $H_2$-activation] $\rightarrow MCH4^+ \rightarrow M^+ + CH_4$. The key step is activation of the H-H bond, which has a barrier about twice as high for M=Co as for M=Rh; reaction (1) occurs more easily for M=Rh than M=Co. M=Ir completely changes the mechanism of reaction **(1)**, which now follows the path: $IrCH_2^+(^3A_2) + H_2 \rightarrow (H_2)IrCH_2^+(^3A_2) \rightarrow$ [TS1, $H_2$-activation] $\rightarrow (H)2IrCH_2^+(^1A') \rightarrow$ [TS2, H-migration] $\rightarrow HIrCH_3^+(^3A) \rightarrow$ [TS3, $CH_4$-elimination] $\rightarrow IrCH_4^+(^3A_2) \rightarrow Ir^+(^5F, s^1d^7) + CH_4$. The reaction **(1)** is exothermic for M=Co and Rh, but endothermic for M=Ir. For M=Co and Rh the reverse reaction $M^+ + CH_4$ can give only one product $MCH_4^+$ and does not proceed further easily; for M=Co, at elevated temperature $CoCH_4^+$ may give $CoH^+$ and $CoCH_3^+$. However, for M=Ir the reverse reaction can proceed further to give hydridomethyl $HIrCH_3^+$ and bishydrido $(H)_2IrCH_2^+$ complexes, as well as $IrCH_4^+$.

## I-D-5 *Ab initio* MO Study of the Mechanism of Reaction of $FeCH_2^+$ with $H_2$

**Djamaladdin G. MUSAEV* and Keiji MOROKUMA*** *(*Emory Univ. and IMS)*

CASSCF and internally contracted MR-SDCI-CASSCF methods are employed to investigate the electronic structure of $FeCH_2^+$ and its reactivity with molecule hydrogen. The ground state of $FeCH_2^+$ has been found to be nearly degenerated $^4B_1$ and $^4B_2$ states, with the $^4A_2$ state lying only 2.0 kcal/mol higher. The doublet electronic states $^2A_1$, $^2A_2$ and $^2B_2$ are about 25–45 kcal/mol higher and will not make any major contribution to its reactivity. The binding energy $D(Fe^+{=}CH_2)$ is calculated to be 67.7 kcal/mol.

The reaction $FeCH_2^+(^4B_2) + H_2 \rightarrow Fe^+ + CH_4$ **(1)** is exothermic by 27.5 kcal/mol leading to the first excited $^4F(d^7)$ state of $Fe^+$. The reactions $FeCH_2^+(^4B_2) + H_2 \rightarrow FeH^+(^5D) + CH_3$ **(2)** and $FeCH_2^+(^4B_2) + H_2 \rightarrow FeCH_3^+(^5E) + H$ **(3)** are about 6–8 kcal/mol exothermic. The reactants at first yield a dihydrogen complex, $(H_2)FeCH_2^+$, which is stable by 6.2 kcal/mol relative to $H_2 + FeCH_2^+$. However, the reactions **(1-3)** can not take place at moderate temperatures because of a high (about 30.0 kcal/mol) H-H bond activation barrier in the quartet state. Following the H-H bond cleavage, the complex $HFeCH_3^+$ does not exist and the ion-molecule complex $FeCH_4^+$ is formed directly or the dissociation processes, **(2)** and **(3)**, should take place. The ion-molecule complex $FeCH_4^+$ has a stabilization energy of about 12.5 kcal/mol relative to $Fe^+(^4F) + CH_4$.

# I—E Structure and Reactivity of Transition Metal Complexes

In connection with the structure of transition metal complexes, Dr. Maseras' very careful study led us to a prediction of the most stable structure of experimentally disputed $[Os(PR_3)_3"H_5"]^+$ complex. Very recently his prediction has been confirmed by a new neutron diffraction study. He is expected to go back to Spain in December 1993. We also continue to work on varieties of important reactions of transition metal complexes. Dr. Koga, Morokuma's long-term associate and right hand, has become Associate Professor at Nagoya Univ. as of April 1993. Dr. Yoshida, visiting scientist from Tosoh, remains at IMS until March, 1994.

## I-E-1 An *Ab initio* Molecular Orbital Study on the Structure of $[Os(PR_3)_3"H_5"]^+$ Complexes

**Feliu MASERAS, Nobuaki KOGA** *(Nagoya Univ. and IMS)*, **and Keiji MOROKUMA** *(Emory Univ. and IMS)*

[*J. Am. Chem. Soc.*, **115**, 8313 (1993)]

The problem of the structural characterization of $[Os(PR_3)_3"H_5"]^+$ complexes, which is experimentally unsolved, is considered from the theoretical point of view with a systematic study of the model system $[Os(PH_3)_3H_5]^+$ with the *ab initio* MO methodology. A fair selection of more than 20 possible isomers, including molecular hydrogen complexes of general formula $[Os(PH_3)_3H(H_2)_2]^+$, $[Os(PH_3)_3H_3(H_2)]^+$, and pure pentahydride species $[Os(PH_3)_3H_5]^+$, is considered, and geometry optimization at the correlated MP2 level is extensively used. A more accurate introduction of correlation energy is also considered through single point calculations at the more elaborated MP4 and QCISD(T) levels.

This theoretical study leads to the conclusion that the most stable form for this type of complexes is an eight-coordinate pentahydride complex $[Os(PR_3)_3H_5]^+$, the associated coordination polyhedron being a dodecahedron. Several stable isomers with this general coordination shape are found to be stable local minima in the potential hypersurface. The most stable of them is characterized by having three phosphine ligands in the 5-neighbor B coordination sites, with four hydride ligands in the 4-neighbor A positions and another one in the remaining B site. The predicted structure has been very recently confirmed by a neutral diffraction study.

## I-E-2 Pentagonal Bipyramidal Coordination in Transition Metal Complexes. An *Ab initio* Study on the $[Os(PR_3)_3H_4]$ System

**Feliu MASERAS, Xue-Kui LI, Nobuaki KOGA** *(Nagoya Univ. and IMS)*, **and Keiji MOROKUMA** *(IMS and Emory Univ.)*

[*J. Am. Chem. Soc.*, in press]

General features of seven-coordination are investigated through an *ab initio* study of the $[Os(PR_3)_3H_4]$ complex. After an assessment of the validity of different methods for the description of the generic $[Os(PR_3)_3"H_4"]$ system, the characteristics of the two different sites of the preferred coordination polyhedron, a pentagonal bipyramid, are examined. It is found that formally neutral ligands prefer axial sites, while formally negative ligands prefer equatorial sites. The Energy Decomposition Analysis (EDA) allows to trace this result down to differences in the electrostatic interactions, and explains it as a consequence of the anisotropy in electron distribution associated to the metal non-bonding d orbitals which is depicted in the Scheme.

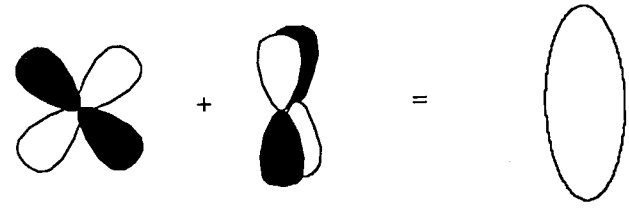

Occupied valence orbitals  Density on the metal atom

## I-E-3 *Ab initio* MO Study on the Structure of $[Ru(PPh_2(CH_2)_4PPh_2)_2"H_3"]^+$ Systems

**Feliu MASERAS and Keiji MOROKUMA** *(Emory Univ. and IMS)*

Experimental NMR data on the structure of $[Ru(PPh_2(CH_2)_4PPh_2)_2"H_3"]^+$ complexes[1] show the presence of an equilibrium between two species in solution. One of them (**1**) is clearly identified as an octahedral *trans* $(H_2,H^-)$ complex, while the nature of the other complex (**2**) is unclear. In order to clarify its nature, we have carried out calculations at the MP2 level with a valence double-zeta quality basis set on the model system $[Ru(PH_3)_4"H_3"]^+$. When no restrictions are imposed to the location of the phosphorus atoms, the octahedral species **1** is predicted to be the absolute minimum, but none of the other computed local minima can account for the spectral properties of **2**. A satisfactory structure for **2** can nevertheless be obtained when the phosphorus atoms are forced to occupy equivalent positions, as observed in the NMR spectra. The need to restrict the phosphine orientations is likely associated to steric requirements which cannot be reproduced in our simple modeling. The resulting structure predicted for **2** is a seven-coordinate trihydride species, with long H-H distances of 1.8 Å. Its most remarkable feature is the free rotation of the $(H^-)_3$ subunit, with a calculated barrier of less than 0.01 kcal/mol.

**Reference**

1) M. Saburi, K. Aoyagi, H. Takeuchi, T. Takahashi, Y. Uchida, *Chem. Lett.*, 991—994 (1990).

## I-E-4 *Ab initio* MO Study of Alkene Hydrosilation Catalyzed by Zr Complex

**Nobuaki KOGA** *(Nagoya Univ. and IMS)* **and Keiji MOROKUMA** *(Emory Univ. and IMS)*

In connection to recent experimental study of regioselec-

tive catalytic hydrosilation of 1-alkenes by $Cp_2Zr(n\text{-}Bu)_2$ by Takahashi et al., we have carried out *ab initio* MO study of the mechanism of reaction of $SiH_4$ with $X_2Zr(C_2H_4)$, (X=Cl, Cp). The structures of the stationary points were determined at the second-order perturbation (MP2) level.

The $Zr(C_2H_4)$ moiety in the reactant is a metallacyclopropane with a long CC bond and ZrC s bonds, and s-metathesis takes place between the SiH and the ZrC s bond. As we reported last year, at the first stage of reaction of $SiH_4$ with $Cl_2Zr(C_2H_4)$, an end-on complex $Cl_2Zr(C_2H_4)(SiH_4)$ is formed, and of two paths from there, path A leading to $Cl_2Zr(CH_2CH_2SiH_3)(H)$ and path B leading to $Cl_2Zr(C_2H_5)(SiH_3)$, the latter has a slightly lower barrier and a substantially larger exothermicity. In the transition state for path B, the hydrogen shift is assisted by the strong Zr-H interaction, as indicated by its short distance. The migration of spherical hydrogen, which is suitable for multi-centered interaction, is more favorable than the migration of $SiH_3$, which has more directional orbital. In the transition state for path A, the Si atom takes nearly trigonal bipyramidal structure; the hypervalency helps the $SiH_3$ migration and therefore the activation barrier for path A is only 2 kcal/mol higher than that for path B. The larger exothermicity for path B is ascribed to the fact that the newly forming bond in path B, the CH bond, is stronger than that in path A, the CSi bond. When the Cl ligands were replaced by the bulkier Cp ligands, the potential energy profile changes drastically. The $SiH_4$ complex does not exist and path B is down-hill. On the other hand, $Cp_2Zr(H)(CH_2CH_2SiH_3)$ is too unstable to exist. On path A, the structure with hypervalent Si atom, which corresponds to the TS with X=Cl, is an intermediate. These differences are ascribed to the steric effect of Cp.

## I-E-5 SiH, SiSi, and CH Bond Activation by Coordinatively Unsaturated $RhCl(PH_3)_2$. *Ab initio* MO Study

**Nobuaki KOGA and Keiji MOROKUMA**

[*J. Am. Chem. Soc.*, **115**, 6883 (1993)]

SiH bond activation, oxidative addition of SiH bond of $SiH_4$ to coordinatively unsaturated $RhCl(PH_3)_2$ was theoretically investigated with an *ab initio* MO method and its potential energy profile was compared with that for CH bond activation, oxidative addition of CH bond of $CH_4$. All the stationary points were determined at the MP2 level. While CH bond activation passes through an $\eta^2$-$CH_4$ complex and a three-centered transition state, SiH bond activation is down-hill and the $\eta^2$-$SiH_4$ complex is a transition state for intramolecular rearrangement connecting two silylhydride complexes, the products of SiH bond activation. This difference originates from the much larger exothermicity of SiH bond activation due to the weaker SiH bond and the stronger RhSi bond compared with the C counterparts. The RhSi bond is about 20 kcal/mol stronger than the RhC bond; the large electron donation from $SiH_3$ to Rh can take place in the late transition metal complex to stabilize the electropositive silyl group. However, the order in M-R bond strength depends on transition metal. In the Zr complex, a strong back-donation from Zr to $CH_3$ takes place because of the small electronegativity of Zr, resulting in the stronger ZrC bond than the ZrSi bond. For $Si_2H_6$, activation of both SiH and SiSi bond takes place easily, and $RhCl(PH_3)_2(SiH_3)_2$ and $HRhCl(PH_3)_2(Si_2H_5)$ can rearrange with each other intramolecularly. Also, the electron correlation effect on structure and energetics is discussed.

## I-E-6 Theoretical Study on Hydrozirconation

**Jun ENDO** *(IMS and Mitsubishi Petrochemical Co.)*, **Nobuaki KOGA, and Keiji MOROKUMA**

[*Organometallics*, **12**, 2777 (1993)]

An *ab initio* MO study has been carried out for hydrozirconation of ethylene and acetylene by $Cp_2Zr(H)Cl$. Of the two possible reaction paths, attack of ethylene and acetylene at Zr between the Cl and H ligands (path 1) and that from the opposite side of the Cl ligand (path 2), the former is found to be more favorable, with a very low activation energy. With an energy decomposition analysis, this difference has been attributed to the smaller distortion of the Zr complex required to reach the transition state for path 1. Hydrozirconation of acetylene is intrinsically more difficult than that of ethylene. The olefin insertion at $Cp_2Zr(R)Cl$, R=alkyl, i.e. the second insertion of olefin, is substantially more difficult than hydrozirconation (R=H) the first insertion. Its origin is also discussed. For comparison, the results of hydrozirconation by $Cl_3ZrH$ have been presented, to clarify the size effect of Cp ligand.

## I-E-7 A Theoretical Study on Ethylene Polymerization Using Silylene-Bridged Group 4 Metallocene Catalysts

**Tohru YOSHIDA** *(IMS and Tosoh Corporation)*, **Nobuaki KOGA** *(IMS and Nagoya Univ.)*, **and Keiji MOROKUMA** *(IMS and Emory Univ.)*

Cationic group 4 metal alkyl complexes are catalytically active species in the homogeneous metallocene-based Ziegler-Natta polymerization. In this study, we elucidate the mechanism of homogeneous polymerization of ethylene with a silylene-bridged group 4 metallocene model catalyst $(H_2SiCp_2M\text{-}R)^+$. We have concentrated on two important reactions in the polymerization: the repetitive insertion of ethylene to the metal-alkyl bond along Cossee's direct insertion mechanism and the $\beta$-elimination considered to be

Insertion Reaction

$[M]^+\text{-}R + CH_2CH_2 \rightarrow [M]^+\text{-}R(CH_2CH_2) \rightarrow (\mathbf{TS_1}) \rightarrow$
**(Cation Alky)** **($\pi$-Complex$_1$)**
$[M]^+\text{-}CH_2CH_2R \rightarrow [M]^+\text{-}CH_2CH_2R$
**($\gamma$-Agostic)** **($\beta$-Agostic)**

$\beta$-Elimination Reaction

$[M]^+\text{-}CH_2CH_2R \rightarrow (\mathbf{TS_2}) \rightarrow [M]^+\text{-}H(CH_2CHR) \rightarrow$
**($\beta$-Agostic)** **($\pi$-Complex$_2$)**
$[M]^+\text{-}H + CH_2CHR$
**(Metal Hydride)**

$[M]^+ = H_2SiCp_2M^+$; M = Ti, Zr, Hf; R = $CH_3$

a termination or a chain-transfer step. In the direct insertion using Ti, Zr, and Hf cation alkyls, the transition state ($TS_1$) lies in the midway between the structures of the $\pi$-complex$_1$ and the $\gamma$-agostic product. On the contrary, the transition state ($TS_2$) structure in the $\beta$-elimination is similar to that of $\pi$-complex$_2$.

The energetics at the MP2 level, based on the RHF optimized structures in the insertion reactions give the exothermicity of 31.4 kcal/mol (Ti), 40.9 kcal/mol (Zr), and 39.2 kcal/mol (Hf), with an activation energy of 13.8 kcal/mol (Ti), 6.0 kcal/mol (Zr), and 7.1 kcal/mol (Hf). These results indicate that the insertion reaction proceeds rapidly and the relative order of insertion activity is Zr ≥ Hf > Ti, being consistent with the recent experimental results.

## I-E-8 *Ab initio* and MM Study on Stereoregular Propylene Polymerization Using Homogeneous Stereorigid Group 4 ansa-Metallocene Catalysts

**Tohru YOSHIDA** *(IMS and Tosoh Corporation)*, **Nobuaki KOGA** *(Nagoya Univ. and IMS)*, **and Keiji MOROKUMA** *(Emory Univ. and IMS)*

Stereoregular propylene polymerization is an important capability in $\alpha$-olefin polymerization catalysts. In this study, ansa-metallocenes (M=Ti,Zr,Hf) having indenyl **1** or tetrahydroindenyl **2** moieties, are investigated for the isotactic stereoregulation at the transition state of propylene insertion, using a combination of molecular orbital and molecular mechanics methods, as done before by us for M=Zr.

In every case, the primary insertions ($R^1$ or $R^2$=Me) are favored over the secondary insertions ($R^3$ or $R^4$=Me), and Ti shows the highest regio- and stereoselectivities among group 4 metals due to the shorter bond distances. When R=Me, corresponding to the initial stage of insertion, MM calculation suggests that the stereoregulation (*catalyst control*) is substantial with Ti but not Zr and Hf catalysts. As the polymer chain grows, the stereoregulation (*chain-end control*) is clearly enhanced for all metals, where only the last inserted monomer unit affects the selectivity. The calculation suggests that there is no difference in the selectivity between indenyl and tetrahydroindenyl ligands.

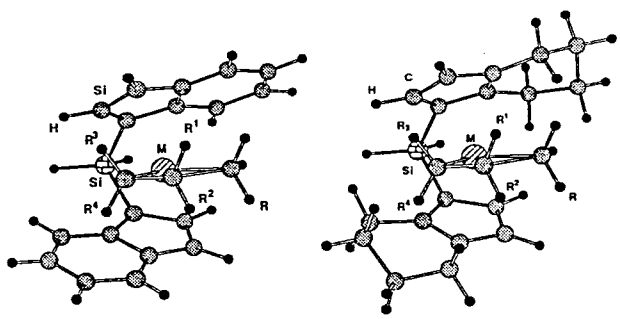


$SiH_2(Indenyl)_2M^+$ 1

$SiH_2(Tetrahydroindenyl)_2M^+$ 2

## I-E-9 An *Ab initio* MO Study on Two Possible Stereochemical Reaction Paths for Methanol Dehydrogenation with $Ru(OAc)Cl(PEtPh_2)_3$

**Hiroaki ITAGAKI*, Nobuaki KOGA, Keiji MOROKUMA, and Yasukazu SAITO*** *(*Univ. of Tokyo)*

[*Organometallics*, **12**, 1648 (1993)]

An *ab initio* MO study was carried out for two possible stereochemical reaction paths for methanol dehydrogenation with $Ru(OAc)Cl(PEtPh_2)_3$, taking into account the coordination of solvent methanol to reaction intermediates. An appreciable trans influence of the phosphine ligand was indicated from the optimized geometry of $Ru(\eta^1\text{-}OAc)Cl(PH_3)_3$, a model complex of the $Ru(OAc)Cl(PEtPh_2)_3$ catalyst, since the acetato Ru-O bond trans-disposed to phosphine was more weakened than the other. $Ru(\eta^1\text{-}OAc)Cl(MeOH)(PH_3)_3$, an assumed intermediate, was relatively stable at the coordination mode of methanol trans-disposed to phosphine. A coordinatively-unsaturated species can be formed endothermically from $RuCl(OCH_3)(MeOH)(PH_3)_3$ by methanol dissociation; the stereoisomer of $RuCl(OCH_3)(PH_3)_3$ with a vacant site trans-disposed to the Cl ligand was stabilized by the presence of an agostic interaction between CH$\beta$ and Ru. Dissociation of the methoxy C-H bond in $RuCl(OCH_3)(PH_3)_3$ was exothermic according to the MP2 method, irrespective of coordination modes of the methoxy ligand. These *ab initio* calculations on the stereochemical reaction paths are consistent with the conclusion deduced form the observed methanol dehydrogenation with the $Ru(OAc)Cl(OCH_3)(PEtPh_2)_3$ catalyst.

## I-E-10 Quantum-Chemical and Experimental Analyses on $H_2$ Elimination from $IrCl(H)_2(CO)(PR_3)_2$

**Hiroaki ITAGAKI*, Yuuichiro NAKAOKI*, Tsuyoshi OGATA*, Nobuaki KOGA, Keiji MOROKUMA, and Yasukazu SAITO*** *(*Univ. of Tokyo)*

*Ab initio* calculations were carried out for an elementary process of $H_2$ elimination from $IrCl(H_2)(CO)(PMe_3)_2$. Smaller activation enthalpy of $IrCl(D_2)(CO)(PMe_3)_2$ (22.0 kcal/mol) than its hydrogen analog (23.7 kcal/mol) indicates substantial formation of H-H bondage in the transition state, which was confirmed by rather short H-H distance (0.921 Å), as optimized in the MP2 framework.

## I-E-11 On the Transformation of 1-Alkyne to Vinylidene in the Coordination Sphere of Ruthenium(II)

**Yasuo WAKATSUKI*, Nami KUMEGAWA*** *(Inst. Phys. Chem. Res.)*, **Hiroshi YAMAZAKI** *(Chuo Univ.)*, **Nobuaki KOGA, and Keiji MOROKUMA**

The reaction of $RuX_2(PPh_3)_3$ (X=Cl, Br) with t-butylacetylene to give vinylidene complexes $RuX_2(PPh_3)_2(C{=}CH^tBu)$ has been studied in detail to clarify the mechanism. IR and NMR data have indicated that the initial product of this reaction is a mixture off two complexes each of which has a vinylidene unit, two trans-chlorides, and cis-bis(phosphine). In solution, these kinetic products gradually isomerize to the final complex with trans bis(phosphine). The structure of this five-coordinated and thermodynamically stable complex (X=Br) was determined

by X-ray crystallographic analysis to have a quasi trigonal bipyramidal conformation with the two phosphines occupying axial positions. Based on these observation, the process in which a terminal alkyne is converted to vinylidene ligand in the Ru(II) complex has been elucidated and its transition state calculated by the *ab initio* MO method. The migration reaction of an alkynyl ligand to the coordinated vinylidene carbon to form a butenynyl ligand has also been theoretically analyzed.

# I—F Structure and Reactivity of Transition Metal Cluster Complexes

Multinuclear transition metal complexes provide very rich varieties of structure and reactivity problems not encountered in mononuclear complexes. Jean-Frédéric Riehl picked up several very interesting problems and challenged them. Here are some results.

## I-F-1 *Ab initio* Study on Structure and $H_2$ Dissociation Reaction of Tetrahydride-Bridged Dinuclear Ru Complex, $(C_5H_5)Ru(\mu\text{-}H)_4Ru(C_5H_5)$

**Nobuaki KOGA and Keiji MOROKUMA** *(IMS and Emory Univ.)*

[*J. Mol. Str. (Theochem)*, in press]

The structure and bonding nature and the $H_2$ dissociation reaction of $(C_5H_5)Ru(\mu\text{-}H)_4Ru(C_5H_5)$ have been studied by using an *ab initio* molecular orbital (MO) method at the RHF and the MP2 level. Between the two Ru atoms there exist four hydride-bridged, three-center two-electron bonds (Ru-H-Ru) with an estimated bond energy of 74 kcal/mol, but without direct Ru-Ru bond. The four hydrides are almost equivalent and there is no H-H bond. The $H_2$ dissociation reaction which gives coordinatively highly unsaturated $CpRu(\mu\text{-}H)_2RuCp$ is up-hill and endothermic by 57 kcal/mol as a result of loss of strong hydride-bridged bonds.

## I-F-2 An *ab initio* MO Study of the Electronic Structure and the Rotational Barrier of Benzene in the "Helicopter" Complex $Os_3(CO)_9(C_6H_6)$

**Jean-Frédéric RIEHL, Nobuaki KOGA** *(IMS and Nogoya Univ.)*, **and Keiji MOROKUMA** *(IMS and Emory Univ.)*

A theoretical analysis is presented on the structure, the bonding nature and the rotational barrier of the $Os_3(CO)_9(C_6H_6)$ complex which has a benzene molecule in a new face-capping $\mu_3{:}\eta^2{:}\eta^2{:}\eta^2$ coordination mode. Using RHF geometry optimization and MP2 calculations, we have estimated the interaction energy between the $Os_3(CO)_9$ fragment and the benzene molecule, as well as the benzene rotational barrier with respect to the $Os_3$ triangle (15.9 kcal/mol). An analysis leads to an interpretation of the interaction between $Os_3(CO)_9$ and benzene in terms of donation and backdonation which is enhanced by CH bending and Kekule distortion of the benzene molecule. The origin of the rotational barrier is an exchange repulsion between the $\pi$ electrons of benzene and the $t_{2g}$-like electrons of metal centers. A comparison has been made among the interaction of this polymetallic compound with benzene and ethylene as well as that of a model monometallic fragment with ethylene and benzene; a monometallic fragment is also capable of forming a strong bond with benzene.

## I-F-3 An *ab initio* MO Study of Hydrogen Exchange Mechanism in the Carbonyl Triosmium Complex $Os_3(CO)_9(\mu\text{-}H)_3(\mu_3\text{-}CH)$

**Jean-Frédéric RIEHL, Nobuaki KOGA** *(IMS and Nagoya Univ.)*, **and Keiji MOROKUMA** *(IMS and Emory Univ.)*

It has been noticed in several trimetallic carbonyl polyhydrides that a hydrogen atom connected to a metal center, terminal or bridging proton, can undergo site exchange with a proton in a ligand. The example we have chosen for an MO study is the trimetallic nonacarbonyl $M_3(CO)_9(\mu\text{-}H)_3(\mu_3\text{-}CH)$, M=Ru, Os, in which the exchange between a $\mu$-H and the methylidene proton has been observed.

Many significant structures of the exchange paths have been determined by the RHF gradient optimization and the energies have been improved by the MP2 single point calculation. The calculated reaction pathway is consistent with the mechanism proposed by the experimentalists and the measured $\Delta G$ of the reaction. We have shown that the reaction takes place through an intermediate obtained by the insertion of a bridging hydrogen into the M-($\mu$)C bond. Relative to the reactant, the energy of this stable intermediate is 14.6 kcal/mol for M=Os and 12.6 kcal/mol for M=Ru. The second step of the reaction is a twist-rotation of the so formed $CH_2$ fragment. The transition state associated to this motion is a $C_s$ structure with a general formula $Os_3(CO)_9(\mu\text{-}H)_2(\mu_3{:}\eta^1\text{-}CH_2)$, the $CH_2$ plane being perpendicular to the mirror plane of the molecule. The energy of this $C_s$ transition state is 22.6 kcal/mol for M=Os and 22.9 kcal/mol for M=Ru, suggesting a similar behavior for the two metals.

## I-F-4 *Ab initio* Molecular Orbital Study of Triruthenium Complexes: Geometrical and Electronic Structure of $Ru_3Cp^*_3(\mu\text{-}H)_3$, $Ru_3Cp^*_3(\mu\text{-}H)_6^+$ and Rearrangement of $Ru_3Cp^*_3(\mu\text{-}H)_3(\mu_3{:}\eta^2\text{-}HCCR')$

**Jean-Frédéric RIEHL, Nobuaki KOGA** *(IMS and Nagoya Univ.)*, **and Keiji MOROKUMA** *(IMS and Emory Univ.)*

The structure and bonding nature of several recently synthesized cyclopentadienyl triruthenium clusters have been investigated using RHF geometry optimizations and MP2 single point calculations. Experimental Cp* ligands ($Cp^*=C_5Me_5$) were replaced by Cp ($Cp=C_5H_5$) ligands. The calculated structures of the polyhydrides $Ru_3Cp_3H_5$ and $Ru_3Cp_3H_6^+$, as well as of the alkyne cluster

$Ru_3Cp_3H_3(HCCR)$, (R=H, Me, t-Bu and Ph) are in reasonable agreement with the available experimental data. The estimation of the total cohesive energy in these systems suggested that Ru-H bonds are stronger in the pentahydride than in the hexahydride. These theoretical calculations also reproduce the conformational preference of the alkyne clusters, namely the preference for a conformation with the triple bond perpendicular to a Ru-Ru bond vs. a conformation with the triple bond parallel to a Ru-Ru bond. In these complexes, the interaction energy between the alkyne ligand and the metallic fragment is strong. We also analyzed the motion of the triple bond on the top of the metal triangle. Experimentally the Cp* ligands become equivalent at high temperatures. This study suggests that the exchange should take place through the parallel conformation, rather than through a decoordination of the alkyne from two metals to form a $\mu_1$:$\eta_2$ complex. An orbital analysis led to an interpretation of the interaction and the conformational preference in terms of donation and back donation, and suggested that, after interaction, the original triple bond becomes a double bond. We carried out molecular mechanics calculations on the real systems with bulky substituents, in order to estimate the total steric energies.

## I—G Structure and Reactivity of Hypervalent Compounds

Dr. Moc continued his systematic study on a series of hypervalent compounds to explore their periodic trends. Results have been in part published, in press, submitted and in preparation. He moved to Iowa State University in the summer of 1992.

### I-G-1 Transition Structures for $H_2$ Elimination from $XH_4$ Hypervalent Species (X=S, Se and Te). *Ab initio* MO Study

**Jerzy MOC, Andrea E. DORIGO, and Keiji MOROKUMA**

[*Chem. Phys. Lett.*, **204**, 65 (1993)]

*Ab initio* MO calculations on the fragmentation of hypervalent $XH_4$ (X=S, Se and Te) to $XH_2$ and $H_2$ show that the most favorable transition state structure is highly polarized with $C_1$ symmetry, which can be viewed as a trigonal bipyramid where one apical and one equatorial ligand are coupled. The least-motion $C_{2v}$ transition state previously obtained theoretically is much higher in energy.

### I-G-2 Transition Structures for $H_2$ Elimination from $SH_3X$ Hypervalent Species (X=F,Cl and BeH)

**Jerzy MOC and Keiji MOROKUMA**

The influence of electron acceptors and electron donors on the fragmentation of hypervalent $SH_3X$ (X=F, Cl, BeH) to SHX and $H_2$ was studied using the *ab initio* MO theory. For the halogen-substituted case, the reaction proceeds through a homopolar transition state of $C_s$ symmetry having the substituent in the *axial* position. By contrast, for the BeH-substituted case, the reaction rather proceeds through a heteropolar transition state of $C_1$ symmetry having the substituent in the *equatorial* position.

### I-G-3 *Ab initio* MO Study on the Periodic Trends in Structures and Energies of Hypervalent Compounds: Five-Coordinated $XH_5$ Species Containing a Group 15 Central Atom (X=P, As, Sb, Bi)

**Jerzy MOC and Keiji MOROKUMA**

[*Inorg. Chem.*, in press]

An *ab initio* MO study employing effective core potentials on the central atoms has been carried out for the $D_{3h}$ and $C_{4v}$ structures of the hypervalent $XH_5$ hydrides, where X=P, As, Sb, Bi. The periodic trends in the barriers to Berry pseudorotation of $XH_5$ and in their thermodynamic stabilities with respect to $XH_3 + H_2$ were explored. In rationalizing the irregular trend in the thermodynamic stabilities of $XH_5$ relative to $XH_3 + H_2$, the energy decomposition analysis of Morokuma and Kitaura was applied. The parallel all-electron *ab initio* calculations were also carried out for $XH_5$ with X=P, As, Sb in order to examine in a systematic way the electron correlation effects (MP2) on their geometries as well as for the sake of comparison with the *ab initio* ECP predictions.

### I-G-4 *Ab initio* MO Study on the Periodic Trends in Structures and Energies of Hypervalent Compounds: Five-Coordinated $XF_5$ Species Containing a Group 15 Central Atom (X=P, As, Sb and Bi)

**Jerzy MOC and Keiji MOROKUMA**

An *ab initio* MO study using effective core potentials (ECP) on the central atoms has been carried out on the $D_{3h}$ and $C_{4v}$ structures of the well known hypervalent pentafluorides $XF_5$, where X=P, As, Sb and Bi. The simultaneous all-electron (AE) *ab initio* calculations at the RHF and MP2 levels were also performed for $XF_5$ with X=P, As, Sb. The $XF_5$ Berry pseudorotation barriers were found to decrease gradually on going down the column, being 4.3, 3.0, 1.8 and 1.3 kcal/mol for X=P, As, Sb and Bi, respectively. The corresponding MP2/AE barriers for X=P, As, Sb differed at most 0.4 kcal/mol from the MP2/ECP estimates. The periodic trend in the pseudorotation barriers followed the behavior in the axial-equatorial distance differences of $XF_5(D_{3h})$. The effect of cumulative fluorine substitution on the geometries and energetics of the hypothetical pentahydrides $XH_5$ was inferred by a comparison of our *ab initio* findings for the $XH_5$ and $XF_5$ hypervalent series.

### I-G-5 *Ab initio* Study on the Periodic Trends in Structures and Energies of Hypervalent Compounds: Four-Coordinated $XH_4^-$ and $XF_4^-$ Anions Containing a Group 15 Central Atom (X=P, As, Sb, Bi)

**Jerzy MOC and Keiji MOROKUMA**

A systematic *ab initio* MO study employing effective core potentials on the central atoms has been carried out to predict $C_{2v}$, $C_{4v}$, $D_{4h}$ and $T_d$ structures, the corresponding energies and stabilities as well as the periodic trends in these molecular properties for the series of hypervalent (hypercoordinated) $XH_4^-$ and $XF_4^-$ anions, where X=P, As, Sb, Bi. The comparative all-electron calculations for the $C_{2v}$ and $C_{4v}$ structures of these species with X=P, As, Sb were also done.

The lowest energy forms for both $XH_4^-$ and $XF_4^-$ were those of $C_{2v}$ symmetry. All $XF_4^-$ ($C_{2v}$) were found to be minima on the SCF potential energy surfaces, whereas the inclusion of electron correlation (MP2) changed the nature of $PH_4^-$ ($C_{2v}$) and $AsH_4^-$ ($C_{2v}$) from unstable transition states (TS) to stable minima. $D_{4h}$ forms of $XH_4^-$ and $PF_4^-$ appeared to be TS's for inversion of the $C_{4v}$ forms; on the other hand, $XH_4^-$ ($C_{4v}$) and $XF_4^-$ ($C_{4v}$) were found themselves to be TS's connecting $C_{2v}$ minima. The energy decomposition analysis was used to clarify the periodic trends in both the $E(C_{4v})$-$E(C_{2v})$ energies for $XH_4^-$ and $XF_4^-$ and in the thermodynamic stabilities of these species relative to loss of $H^-$ or $F^-$.

# I—H Reaction Mechanisms of Organic Compounds

Close collaboration continues with Prof. Eiichi Nakamura's group at Tokyo Institute of Technology, in order to elucidate the reaction mechanism and the origin of regio and stereoselectivity in organic reactions. We have also written a paper on the electron transfer reaction carried out about four years ago by Dr. Sameshima, then a graduate student.

## I-H-1 Theoretical Studies on Carbometalation of Cyclopropene. Transition Structures of Addition of $Me^-$, MeLi, MeCu, and $Me_2Cu^-$ and Origin of the High Selectivity of the Strained Double Bond

**Eiichi NAKAMURA*, Masaharu NAKAMURA*, Yoshimitsu MIYACHI* (*Tokyo Inst. of Tech.), Nobuaki KOGA, and Keiji MOROKUMA**

[*J. Am. Chem. Soc.*, **115**, 99 (1993)]

Comparative structural and energy decomposition analyses of the reaction of the additions of $Me^-$, MeLi, MeCu, and $Me_2Cu^-$ to ethylene and cyclopropene have provided general information on the mechanism of release of the ring strain and, consequently, reasons for the high reactivities of organocopper reagents to cyclopropenes. Analyses of structural parameters of the transition structures indicated that the $Me^-$ and MeLi addition to cyclopropene involve an "earlier" transition state than the corresponding additions to ethylene, as expected form the higher exothermicity of the latter reaction. In contrast, the transition structures of the MeCu addition to cyclopropene is quite asynchronous, in that the overall nature of the TS is still early but the C=C bond cleavage is quite advanced. As a result of this advanced C=C bond cleavage, the olefinic carbons are significantly rehybridized so that the cyclopropene moiety experiences substantial orbital interaction with the vacant copper 4p orbital. Analysis of the localized molecular orbitals indicated that the filled copper 3d orbitals do not actively participate in the bond exchange in the transition state of the MeCu addition to ethylene.

## I-H-2 Theoretical Studies on the Reaction of Solvated Methyllithium Open Dimer with Aldehyde

**Masaharu NAKAMURA*, Eiichi NAKAMURA* (*Tokyo Inst. Tech.), Nobuaki KOGA, and Keiji MOROKUMA** *(IMS and Emory Univ.)*

The kinetic importance of an open dimer of an organometallic reagent in carbonyl additions, much discussed by experimentalists, has been probed by the *ab initio* molecular orbital theory by taking the reaction of an open dimer of MeLi with formaldehyde and acetaldehyde as a model reaction. The open dimer solvated by one molecule each of water and an aldehyde has been determined as a local minimum and was found to show close resemblance to a crystal structure of related open dimer of lithium amide. This open dimer leads to the product via a transition structure with a very small activation energy. The transition structure is very early for formaldehyde and later for acetaldehyde. Structural and energetic analysis of the reaction provided several important implications to the mechanism of carbonyl additions.

## I-H-3 *Ab initio* MO Calculations of Electronic Coupling Matrix Elements on Model Systems for Intramolecular Electron Transfer, Hole Transfer, and Triplet Energy Transfer: Distance Dependence and Pathway in Electron Transfer and Relationship of Triplet Energy Transfer with Electron and Hole Transfer

**Nobuaki KOGA, Keiichiro SAMESHIMA, and Keiji MOROKUMA**

[*J. Phys. Chem.*, in press]

The matrix elements for electron transfer (ET) for anions of 1,3- and 1,4-dimethylenecyclohexane and 2,7- and 2,6-dimethylenedecalin, those for anions of methylene chains, $H_2C$-$(CH_2)_n$-$CH_2$ (n=3,4,5) and those for ET, hole transfer (HT), and triplet energy transfer (TT) of anion, cation, and neutral systems of 1,4-divinylcyclohexanes have been calculated with the *ab initio* MO method by using the UHF wave functions as diabatic states. Calculations for methylene chains indicate that the observed "distance dependence" is not only determined by the number of CC bonds but also by subtle angular dependency of MO overlap. The most favorable all-trans path exists in 1,3-dimethylenecyclohexane and 2,7-dimethylenedecalin, whereas more than one unfavorable gauche pathway are available in 1,4-dimethylenecyclohexane and 2,6-di-

methylenedecalin. The calculated matrix elements for the divinyl compounds point out that HT and TT are faster in the trans-equatorial-equatorial isomer than in the trans-axial-axial isomer. Though the matrix element for ET in the trans-axial-axial isomer is larger, the torsional angle in the real compound is likely to make ET in the trans-equatorial-equatorial isomer faster. The matrix element for TT, a two-electron process, is found to be proportional to the product of those of ET and HT.

# I—I Chemical Reactions on Solid Surfaces

### I-I-1 An Electronic Structure Study of $H_2$ and $CH_4$ Interactions with MgO and Li-doped MgO Clusters

**James ANCHELL, Keiji MOROKUMA, and Anthony HESS** *(Pacific Northwestern Labs)*

[*J. Chem. Phys.*, in press]

An *ab initio* study is presented concerning the chemisorption of hydrogen on a model of the (100) surface of MgO and Li-doped MgO. The local surface environment was modeled by employing cubic and tetragonal clusters composed of eight and twelve atoms, respectively. The lattice constant for the clusters was fixed at the experimentally determined value for bulk MgO, and the geometry of the adsorbate was optimized at the UHF level of theory. Correlation energy was treated at the UMP2 level at the UHF optimized geometry. It was found that $H_2$ undergoes heterolytic dissociation at neighboring three-coordinated Mg and O sites (denoted $Mg_{3c}$ and $O_{3c}$) in MgO with an activation energy of 4.2 kcal/mol and 2.4 kcal/mol at the UHF and UMP2 levels, respectively. Li-doped MgO did not support heterolytic dissociation at neighboring Mg and O sites. Instead $H_2$ was found to homolytically dissociate without barrier at two $O_{3c}$ sites, and to undergo hydrogen atom abstraction at $O_{3c}$ and $O_{4c}$ sites. At the UHF/UMP2 level it was found that $O_{3c}$ sites that abstraction occurs with a 17.9/3.0 kcal/mol barrier, and at $O_{4c}$ sites abstraction occurs with a 15.7/0.6 kcal/mol activation energy.

# I—J Theoretical Studies of Highly Vibrationally Excited Molecules

### I-J-1 Theoretical Potential Energy Functions and Rovibronic Spectrum of Electronically Excited States of $HCO^+$

**Bernhard WEIS** *(Institute for Fundamental Chem.)* **and Koichi YAMASHITA** *(Institute for Fundamental Chem. and IMS)*

[*J. Chem. Phys.*, in press]

Three-dimensional potential energy functions (PEFs) and rovibronic spectra for several low-lying electronically excited singlet states of $HCO^+$ have been investigated based on the *ab initio* complete active space self-consistent field (CASSCF) method. The calculated electronic transition moments show that the ultraviolet (UV) absorption spectrum of the ion should be dominated by the transition $C^1P$-$X^1S^+$. Analytical representations of the PEFs for the two components of the degenerated $C^1P$ state have been used in beyond Born-Oppenheimer calculations of the rovibronic energy levels of $HCO^+$ and $DCO^+$ by a Renner-Teller variational approach which accounts for anharmonicity, rotation-vibration, and electronic angular momentum coupling effects. Since the excited states of $HCO^+$ are experimentally unknown up to now, the calculated spectroscopic constants, the vertical and adiabatic excitation energies and the absorption spectra should provide valuable information for future experimental characterization of the excited states.

### I-J-2 Theoretical Study of the Highly Vibrationally Excited States of $FHF^-$: *Ab Initio* Potential Energy Surface and Hyperspherical Formulation

**Koichi YAMASHITA** *(Institute for Fundamental Chem. and IMS)*, **Keiji MOROKUMA, and Claude LEFORESTIER** *(Univ. of Paris-Sud, France)*

[*J. Chem. Phys.*, in press]

A three-dimensional description of vibrationally highly excited linear molecules is formulated in hyperspherical coordinates, based on a Successive Adiabatic Reduction scheme. The method is applied to the low-lying and highly excited vibrational states of $FHF^-$, a prototype of symmetric bihalide anions, which has attracted spectroscopic interest due to its peculiar vibrational anharmonicity. *Ab initio* potential energy surfaces (PESs) which cover the ground-state potential well of $FHF^-$ and/or its dissociation to the $F^-$ + HF channel have been obtained by using the CEPA (coupled electron pair approach) method. A hyperspherical calculation using the *ab initio* PES of the sixth-order Simons-Parr-Finlan analytical form has correctly reproduced the experimental fundamental frequencies. Specifically, the vibrationally highly excited $FHF^-$ above the dissociation threshold is proposed as a candidate for transition state spectroscopy (TSS) of unimolecular dissociation reactions without barrier.

# I—K Structures and Reactions of Manybody Chemical Systems

Electronic structure and dynamical behavior of large systems such as liquid and polyenes are investigated theoretically. (a) Collective motion and fluctuation in liquid and clusters (b) Chemical reactions and relaxation in liquid and clusters, and (c) Electronic structure and dynamical behavior of polyenes, are analyzed.

## I-K-1 Fluctuation, Relaxations and Hydration in Liquid Water; Hydrogen Bond Rearrangement Dynamics

**Iwao OHMINE and Hideki TANAKA** *(Kyoto Univ.)*

[*Chemical Reviews*, in press]

It is surveied that the recent progress in application of these theoretical and computational techniques to analyze strongly correlated molecular motions, collective motion and fluctuation of hydrogen bond network in liquid water. As a problem bearing on the hydrogen bond network structure and dynamics, we discuss about the hydration of nonpolar solutes. It is still controversial what is the physical origin of the hydrophobic hydration and the hydrophobic interaction. Many theoretical methods such as the scaled particle theory, integral equation methods and computer simulation technique have been proposed to calculate the hydration mixing energy, excess entropy, and solvent induced solute-solute interaction. The recent development of these theoretical studies on hydration will be reviewed.

## I-K-2 Structure, Dynamics, and Thermodynamics of Model $(H_2O)_8$ and $(H_2O)_{20}$ Clusters

**David J. WALES and Iwao OHMINE** *(Cambridge Univ. and IMS)*

[*J. Chem. Phys.*, **98**, 7245 (1993)]

We present molecular dynamics simulations of $(H_2O)_8$ and $(H_2O)_{20}$, paying particular attention to the possibility of solid-like/liquid-like coexistence. Four differently parametrized rigid molecule potentials are examined for $(H_2O)_8$; only the most promising is applied to $(H_2O)_{20}$. In every case, we find evidence for time-scale coexistence in the statistics of the short-time averaged temperature. In several cases, we also observe loops in the microcanonical caloric curve [$T(E)$], indicating the formal existence of two stable states over a finite range of energy Further evidence is provided by systematic quenching, both by comparison with the dynamics and in terms of model density of states calculations of the microcanonical $T(E)$, energy distribution function $f(E)$, Helmholtz free energy $A(T)$, and hear capacity $C_v(T)$. We discuss two possible approaches to these thermodynamic functions from the distribution of local energy minima and compare the results with those for atomic clusters bound by the Lennard-Jones potential.

## I-K-3 Rearrangements of Model $(H_2O)_8$ and $(H_2O)_{20}$ Clusters

**David J. WALES and Iwao OHMINE** *(Cambridge Univ. and IMS)*

[*J. Chem. Phys.*, **98**, 7257 (1993)]

We have calculated rearrangement mechanisms for $(H_2O)_8$ and $(H_2O)_{20}$ clusters by eigenvector following. For $(H_2O)_8$, two different parametrizations of a four-site, rigid water effective pair potential were considered and found to give very similar results. Hence, only one of the potentials is applied $(H_2O)_{20}$. $6N$-6 internal coordinates are required to describe a $(H_2O)_N$ cluster in these calculations, of which $3N$-6 were chosen as center-of-mass distances, angles and dihedral angles, the other $3N$ being Euler angles. A wide variety of different rearrangements for both $(H_2O)_8$ and $(H_2O)_{20}$ are illustrated, with barrier heights ranging over three orders of magnitude. The mechanisms range from almost imperceptible changes of geometry to folding processes that result in dramatic structural transformations.

## I-K-4 Relaxation Dynamics of Model $(H_2O)_{20}$ Clusters

**Iwao OHMINE, Shinji SAITO, and David J. WALES** *(Cambridge Univ. and IMS)*

Relaxation phenomena in model $(H_2O)_{20}$ clusters are investigated by considering energy fluctuations and dielectric relaxation, making connections with the underlying hydrogen-bond rearrangement dynamics. In particular, we relate these effects to the potential energy surface, including rearrangement mechanisms, minimum energy pathways and normal mode excitations. RRKM rate constants are calculated and compared with the rates observed in molecular dynamics simulations. We find that the energy fluctuations and dielectric relaxation are non-Debye in character, but instead exhibit so-called 1/f spectra.

## I-K-5 Dynamics and Orientation Relaxation of Water Clusters

**Shinji SAITO and Iwao OHMINE**

The orientation relaxation have been analyzed to explore the intrinsic dynamics of liquid water and water clusters. Two kinds of orientation relaxations are analyzed; the single molecular orientation relaxation (SMOR), and the collective orientation relaxation (COR). In the liquid-like state of the larger cluster, both the SMOR and COR yield the Debye type relaxation except the initial oscillation arising from the libration motion. In the smaller cluster the COR is not the Debye relaxation. The relaxation time of the COR is much faster than that of the SMOR in the cluster. In liquid water, however, the COR is slower than the SMOR and the both yield the Debye relaxation except for very high frequency. In addition to this difference, the Kirkwood g-factor and its radial dependence in the clusters differs from those in liquid water. The difference between the static and dynamic factors arises from that the self and cross correlation terms in COR mutually cancel in the cluster, while the self and cross terms have the same signs in liquid water. The relation between the COR and SMOR is investigated by using the generalized Langevin equation (GLE) to understand whether the difference of their relaxations in the cluster and liquid water is universal or not. Based on the GLE, we have derived a general equation between the COR and SMOR by using the Kirkwood g-factor and 'dynamic Kirkwood g-factor'. This equation indeed predicts the COR is faster than the SMOR in the finite system, while the SMOR is faster in infinite system. We also calculated the normal mode approximated (NMA) COR and SMOR by using the normal modes at the Quenched (Q-) structures along trajectories. The initial decays of the COR and SMOR are reproduced by the NMA COR and SMOR.

The dephasing factor was introduced to express the transition between the Q-structures. These results indicate that 1) the anharmonicity in the dynamics is not large, 2) the long time behavior is ue to the transition of Q-structures, and 3) in the larger cluster the transition of Q-structures can be expressed in the single exponential function, but not in the smaller cluster.

## I-K-6 Raman Spectra in Liquid Water and Water Clusters

**Shinji SAITO and Iwao OHMINE**

In order to clarify the intrinsic dynamics of the hydrogen bond systems we analyze the Raman spectra of liquid water and water clusters by performing molecular dynamics simulations. Raman spectrum can be obtained by the time correlation function of the polarizability. Only the first order term is included into the induced polarizability in this analysis. We calculated the Raman spectra in the instantaneous, vibrationally averaged, and Quenched structures of liquid water and water cluster to separate the intrinsic contribution from various vibrational elements. In the relaxation of total dipole moments (i.e. the dielectric relaxation), it is known that its time correlation function (TCF) decays in a single exponential function in liquid water and large cluster and the contribution of the induced term is not large. In the Raman spectrum, however, the corresponding TCF yields the non-Debye relaxation in both liquid water and large water cluster. The induced term is dominant in the Raman spectrum. These difference in dielectric relaxation and Raman type relaxation implies that both time and spatial averagings are effective in the dielectric relaxation of liquid water and large cluster, while only time averaging is effective in the Raman spectrum. In the small cluster, a non-Debye relaxation takes place even in the dielectric relaxation.

## I-K-7 Energetics of Proton Transfer in Liquid Water I; *Ab initio* Study of Origin of Many Body Interaction and Potential Energy Surfaces

**Tamiki KOMATUZAKI** *(Grad. Univ. for Adv. Studies and IMS)* **and Iwao OHMINE**

Energetics of proton transfer in liquid water is investigated by using *ab initio* calculation. Molecular electronic interaction of hydrated proton clusters is classified into many body interaction elements by a new energy decomposition method. It is found that up to three-body molecular interaction is essential to describe the potential energy surface. The three-body effect mainly arises from the (non-classical) charge transfer and strongly depends on their configuration. Beyond the three body effect are small enough to be ignored. To simulate the liquid state reactions, two cluster models including all water molecules up to the second shell in the proton transfer reactions are employed. The potential energy surfaces for a single proton transfer and for a simultaneous double proton transfer are calculated for cluster model with 12 water molecules + $H_5O_2^+$ (single proton transfer) and a cluster model with 15 water molecules + $H_7O_3^+$ (double proton transfer), respectively. It is shown that these proton transfer reactions only involve small potential energy barriers of a few kcal/mol or less when adiabatic structural rearrangement of the solvent is induced along the proton movement.

## I-K-8 New Molecular Dynamics Method for Cooperative Proton Transfer Dynamics in Liquid Water

**Tamiki KOMATUZAKI** *(Grad. Univ. for Adv. Studies and IMS)* **and Iwao OHMINE**

New molecular dynamics method has been developed in order to scrutinize the proton transport dynamics in liquid water. The many body and the charge transfer interaction have been shown to play a dominant role for the potential energy surface.

This new model makes use of electronegativity equalization principle in "Atoms in Molecule" in empirical density functional theory. The charge density distribution is fully minimized on the each time step of MD calculation and the trajectory of the nucleus on the adiabatic potential surface can be estimated.

The electronic energies of the atoms constituting the total system are approximated by the Taylor expansion from the isolated equilibrium states in terms of the electronic distribution function and the external potential. The sum of the total atomic electronic energies and the nuclear repulsion energies can be regarded as the total energy of the system. The electronic distribution function is represented by the electronic "point site" on atoms/bonds and the scaled Ohno formula is used for the external potential.

Because Taylor expansion is truncated by the order of two, the minimization can be accomplished without any iterative procedures and the force can be estimated without calculating the derivatives of the charge with respect to nuclear coordinates, like energy gradient method in electronic structure theory. We have found that there are the excellent correlation of the properties, total energy, force, electronic dipole moment vector and Mulliken population between this new model and *ab initio* calculation(RHF/MIDI-4**) for 50–100 samples of each $H_2O$, $H_3O^+$, $OH^-$. The nonlinear fitting procedures to reproduce the intermolecular properties and proton transfer potential surface are now in progress.

## I-K-9 *Ab initio* MO Studies of the Photoisomerization of Octatetraene

**Masakatsu ITO** *(Grad. Univ. for Adv. Studies and IMS)* **and Iwao OHMINE**

The Potential energy surface of the lowest singlet ($2^1Ag^-$) of trans, trans- and cis, trans-1,3,5,7-octatetraene has been calculated using *ab initio* MCSCF method. The basis set used were STO-3G for geometry optimizations and DZ otherwise. Because the multicofiguration description is essentially needed for the $2^1Ag^-$ state, we have used the CAS(complete active space) type configurations where all possible configurations are generated by occupying eight electrons in eight $\pi$ orbitals [1764 configuration state functions (CSF)].

The determination of the equilibrium geometries and the

force constants shows that the both trans, trans- and cis, trans-isomer in the $2^1Ag^-$ state are planar and the difference of the vibrational frequencies of the two ones are quite small ($\sim 84$ cm$^{-1}$). It means that the cis, trans-isomer cannot be distinguished from the trans, trans one by comparing the frequency intervals observed in the one photon spectra with those in the two-photon spectra.

To establish the career of the one-photon spectra and to resolve the photoisomerization process, the calculation of the vibronically induced intensity for a symmetry fobidden transition $1^1Ag^-$ to $2^1Ag^-$ using MRSDCI method are being carried out.

# I—L Theoretical Studies of Chemical Reaction Dynamics

Clarification of the reaction mechanisms and development of illuminating good approximate theories are our ultimate purposes.

### I-L-1 Quantum Mechanical Studies of Triatomic Reaction Dynamics Based on Hypersherical Coordinate Approach.

**Kengo MORIBAYASHI, Ken-ichiro TSUDA, Shoji TAKADA, and Hiroki NAKAMURA**

The hyperspherical coordinate approach to atom-diatom reactions has been pursued and extended. The exact treatment is now possible also for $J \neq 0$, where J is the total angular momentum quantum number. Clarification of the mechanisms and development of a good approximation have been carried out. For instance, the constant centrifugal potential approximation (CCPA) is generalized so as to be applicable to the reactions of rotationally excited reactants. The method is applied to the $D+H_2$ ($v_i$=0, $j_i$) reactions and is proved to be useful.

### I-L-2 WKB Theory of Multidimensional Tunneling

**Shoji TAKADA and Hiroki NAKAMURA**

Multidimensional tunneling is one of the very basic phenomena in chemical reaction dynamics. General WKB theory of multidimensional tunneling is formulated and illuminating physical picture on the effects of multidimensionality is provided. The following two basic problems are analyzed: (1) connection of the wave functions between classically accessible and inaccessible regions, and (2) wave propagation in classically inaccessible region. It is found that there exist two distinct types of tunneling: pure tunneling and mixed tunneling. General procedure and an approximate formula for the energy splitting in double well are obtained.

### I-L-3 Decoupling Surface Analysis of Classical Irregular Scattering and Clarification of Its Icicle Structure

**Kiyohiko SOMEDA, Ramakrishna RAMASWAMY** *(Jawaharlal Nehru Univ., India and IMS)*, **and Hiroki NAKAMURA**

[*J. Chem. Phys.*, **98**, 1156 (1993)]

Irregular Scattering in molecular inelastic collision is analyzed classical mechanically by a novel method called "decoupling surface analysis." Effective Hamiltonian of this analysis provides a phase space view of collision processes analogous to the Poincaré section of coupled-oscillator systems. In this phase space view irregular scattering occurs in a stochastic layer formed around separatrix connected to resonance structure of the effective Hamiltonian. This circumstance is parallel to that in the coupled-oscillator systems, in which stochastic motion is known to be connected to nonlinear resonance. The resonance structure in collision indicates trapping of classical trajectories in a certain dynamical well. The decoupling surface analysis suggests that the dynamical well is formed by a dip of stability exponents of trajectories as a function of time. By using a prototypical model exhibiting irregular scattering, a formal theoretical treatment is developed to analyze the structure of the fractal, termed icicle structure, observed in the plot of final vibrational action against the initial vibrational phase angle.

### I-L-4 Overlapping Resonances and the Statistical Behavior

**Kiyohiko SOMEDA, Hiroki NAKAMURA, and Frederick H. MIES** *(NIST, U. S. A. and IMS)*

Systematics of the average decay rate and its connection with the RRKM theory are studies and clarified by randomly generating the Hamiltonian matrices. The distribution of the decay rates is found to bifurcate into long-lived and short-lived branches when the density of state $\rho$ is larger that a certain critical value $\rho_c$. The decay rates of the long-lived branch systematically decrease with $\rho$ at $\rho \gg \rho_c$. The rate agrees with that of RRKM theory in the region $\rho \sim \rho_c$, where the spectral profile becomes most diffuse. This observation ascertains the conventional belief that the RRKM theory holds only when resonances overlap and that it gives the upper bound.

# I—M Theory of Nonadiabatic Transition

Nonadiabatic transition is one of the very basic mechanisms of state (phase) change in various fields of physics and chemistry. Recently, we have succeeded in deriving good analytical new formulae for the Landau-Zener and nonadiabatic tunneling cases within the linear potential model. Especially, a simple and compact formula much better than the famous Landau-Zener formula was proposed. Generalizations to general curved potential and also to multi-level crossing are now in progress.

### I-M-1 The Two-State Linear Curve Crossing Problems Revisited. III. Analytical Approximations for Stokes Constant and Scattering Matrix: Nonadiabatic Tunneling Case

**Chaoyuan ZHU and Hiroki NAKAMURA**

[*J. Chem. Phys.*, **98**, 6208 (1993)]

Based on the exact solution of the linear curve crossing problems reported in the first paper of this series, approximate analytical solution is discussed here for the opposite sign of slopes of the two diabatic potentials (nonadiabatic tunneling case). Two new compact analytical formulas for reduced scattering matrix are derived for $|b^2| > 1$, where $b^2$ represents the effective collision energy. The whole range of the two parameters $a^2$ (effective coupling strength) and $b^2$ is divided into five regions, in each one of which the best recommended formulas are proposed. This analysis provides a complete picture of the nonadiabatic tunneling problem, for the first time. The new formulas proposed here are simple and explicit functions of the two parameters, and thus useful for practical applications. In the case of $|b^2| \leq 1$, certain fitting formulas are proposed for the Stokes constat on the basis of a comparison with the exactly solvable differential equation with special quartic polynomial as coefficient.

## I—N Theoretical Studies of Characteristics and Dynamics of Superexcited States of Molecules

Superexcited states show various intriguing properties and participate in a variety of dynamic processes. We believe that they will open a new challenging world of science. The ultimate purpose of our studies is to find new collective motions in these states and understand their participating dynamics.

### I-N-1 Electron Correlation in Doubly Excites States of the Hydrogen Molecule

**Masahiro Iwai, Sungyul LEE** *(Kyunghee Univ., Korea and IMS)*, **and Hiroki NAKAMURA**

[*Phys. Rev.*, **A47**, 2686 (1993)]

The electron correlation in some low-lying doubly excited states of the $H_2$ molecule is investigated by analyzing two-body correlation functions in comparison with the corresponding doubly excited states of He. Effects of increasing the internuclear distance and of avoided crossings are discussed. Some interesting features of electron-correlation patterns are found to appear because of the additional symmetries of the molecule. Autoionization widths of the doubly excited states are evaluated and the autoionization mechanisms are analyzed in connection with the electron correlation.

### I-N-2 Characteristics of Superexcited States of Molecules and MQDT Studies of $NO^+$ Dissociative Recombination

**Hosung SUN** *(Pusan Nat. Univ., Korea and IMS)*, **Keiji NAKASHIMA** *(Kyushu Univ.)*, **and Hiroki NAKAMURA**

[Dissociative Recombination: Theory, Experiment, and Applications, edited by B. R. Rowe and J. B. A. Mitchell (*Plenum, New York*), in press]

The concept and characteristics of "superexcited states", which play essential roles in dissociative recombination, are explained from a general view point of the mechanisms of molecular dynamic processes. The states are classified into (1) doubly excited states (1st kind of superexcited state) and (2) rovibrationally excited Rydberg states (2nd kind). Interplay between theory and experiment is pointed out to be very useful and important in order to reveal the properties of these states. This is demonstrated in the case of NO. The REMPI (Resonantly Enhanced Multi-Photon Ionization) experiment is analyzed by the MQDT (Multichannel Quantum Defect Theory). An analysis of the dissociative recombination of $NO^+$ is reported with use of the information thus obtained. The $B^2\Pi$ dissociative first kind of superexcited state is found to be a dominant path for the dissociative recombination of $NO^+$. An interesting interplay between two mechanisms is also found.

## I—O Electron Density, Symmetry, and Structure of Matter

The final goal of this study is to develop a phenomenological theory of structure of matter.

### I-O-1 Electron Density in a Half-Filled Shell Atom

**Itsuki BANNO**

[*Prog. Theor. Phys.*, **89**, 935 (1993)]

It is found that wave functions belonging to a certain subspace in a half-filled shell yield spherical symmetric electron density. This result comes from the well-known disappearance rule in the atomic spectroscopy together with additional considerations.

# I—P Nonlinear Excitations in Halogen-Bridged Mixed-Valence Metal Complexes

To clarify the nonlinear nature of various optical excitations in a one-dimensional charge density wave state, we study nonlinear optical spectra of this complex.

## I-P-1 Nonlinear Optical Spectra in Halogen-Bridged Mixed-Valent Platinum Complexes

**Kaoru IWANO and Keiichiro NASU** *(KEK. PF)*

Nonlinear optical properties in halogen-bridged mixed-valent platinum complexes are studied theoretically for the first time. Two types of nonlinearities are treated here. One is the electric-field modulation of the absorption spectrum, and the other is the third-harmonic generation. The spectral shapes of these nonlinearities are determined by a method in which both effects of the electron-hole correlation and the lattice fluctuations are taken into account. As for the electric-field modulation, the difference spectrum observed in the visible region for $[Pt(en)_2][Pt(en)_2Cl_2](ClO_4)_4$ is well reproduced with features such as the rigid shift of the main charge-transfer band and the newly appearing peak due to the parity-even exciton. On the other hand, in the spectrum of the frequency-dependent intensity of the third-harmonic generation, several enhancements are found: the three-photon resonance structure due to the parity-odd exciton and the free electron-hole continuum, and the two-photon resonance peak due to the parity-even exciton. In particular, the last one seems to correspond to that observed in the experiment.

# RESEARCH ACTIVITIES II
# Department of Molecular Structure

## II—A Laboratory and Astronomical Spectroscopy of Transient Interstellar Molecules

Vast, cold, and low-density space environment is a unique laboratory, whose physical and chemical conditions are rarely attained in the laboratory on Earth. The unique space laboratory is favorable to the existence of transient molecules such as molecular ions, free radicals, and unstable molecules, most of which are very exotic and non-terrestrial. These exotic transient molecules are generally difficult and challenging problems for laboratory spectroscopy. Laboratory spectroscopy may be enriched by astronomical studies on non-terrestrial transient species which represent new development in high-resolution molecular spectroscopy. On the other hand, detailed knowledge about new transient molecules obtained by laboratory spectroscopy is essential to a deeper understanding of physical and chemical processes in space. We develop a high-sensitivity submillimeter-wave and far-infrared spectrometers suitable for high-resolution spectroscopy of transient molecules of astronomical interest. We expect that our laboratory spectroscopy may accelerate the mutually beneficial aspect between laboratory spectroscopy, and astrochemistry and astrophysics.

### II-A-1 The Millimeter Wave Spectrum of Calcium Isocyanide, CaNC

**Timothy C. STEIMLE** *(Arizona State Univ. and IMS)*, **Shuji SAITO, and Shuro TAKANO**

[*Astrophys. J.* **410**, L49 (1993)]

The 28 absorption features in the 130–370 GHz spectral region have been measured and assigned as fine-structure components of 14 pure rotational transitions of Calcium isocyanide (CaNC) in its $X^2\Sigma^+$ state. The spectrum was analyzed using a standard Hamiltonian model for a linear molecule, and the resulting spectroscopic parameters were used to predict the transition frequencies and Einstein A-coefficients. The determined parameters are (in MHz) B=4040.742(14), D=4.96(3)×10$^{-3}$, H=4.1(3)×10$^{-7}$, L=−6.0(13)×10$^{-11}$, M=5.3(20)×10$^{-15}$, $\gamma$=18.03(12), $\gamma_D$=−3.2(13)×10$^{-5}$, where the numbers in parentheses are 3$\sigma$ error estimates.

### II-A-2 Laboratory Submillimeter-Wave Spectroscopy of the $CH_2(\tilde{X}^3B_1)$ Radical: $2_{12}$–$3_{03}$ Transition at 440–445 GHz

**Hiroyuki OZEKI and Shuji SAITO**

The simplest carbene, $CH_2$ radical, is one of essential intermediates in interstellar hydrocarbon chemistry from $C^+$ to $CH_4$. Another important intermediate, CH radical, was first identified in space, and then its spectral lines were measured in the laboratory and used to diagnose interstellar molecular clouds. $CH_2$ has the ground electronic state of $^3B_1$ with a dipole moment along the b axis, and has only three rotational lines below 1 THz. The lowest rotational transition of $CH_2$ is located around 70 GHz and was measured in the laboratory in 1983. However, it has not been detected in space,[1] because the transition is located near the upper edge of the atmospheric oxygen band and its excitation is rather high, 150 cm$^{-1}$ above the true ground level.

$CH_2$ has its second lowest rotational transition, $2_{12}$–$3_{03}$, at 440 GHz, which we precisely measured with submillimeter-wave spectroscopy.[2] The $CH_2$ radical was generated by discharging pure ketene in the hollow cathode absorption cell cooled at −180°C. Three fine structure components were detected at the frequencies of 440 to 445 GHz, which were predicted mainly from FIRLMR and MW data.[3] The measured frequencies are listed in Table 1 and compared with the predicted ones. If we use the predicted abundance of $CH_2$ in the diffuse molecular cloud $\zeta$Oph[4] and the excitation temperature of 100 K, the brightness temperature of the transition concerned is calculated to be about 0.6 K, which is high enough to be detected with modern submillimeter-wave telescopes.

**References**

1) J.M. Hollis, P.R. Jewell, and F.J. Lovas, *Astrophys. J.* **346**, 794 (1989).
2) S. Saito and M. Goto, *Astrophys. J.* **410**, L53 (1993).
3) T.J. Sears, A.R.W. McKellar, P.R. Bunker, K.M. Evenson, and J.M. Brown, *Astrophys. J.* **276**, 399 (1984).
4) E.F.VanDishoeck and J.H. Black, *Astrophys. J. Suppl.* **62**, 107 (1986).

**Table 1.** Observed Frequencies of the $2_{12}$–$3_{03}$ Transition of $CH_2(\tilde{X}^3B_1)$(MHz)

| J′–J | $\nu_{obs}$[a] | $\nu_{obs}-\nu_{calc}$[b] |
|---|---|---|
| 2–3 | 439960.991(10) | 0.991 |
| 3–4 | 444825.666(12) | −0.334 |
| 1–2 | 444913.930(13) | −8.070 |

[a](1$\sigma$). [b]Reference 2).

### II-A-3 Millimeter-Wave Spectrum of $C_3S$ in the Vibrationally Excited State of the Lowest Bending Mode

**Jian TANG, Shuji SAITO, and Satoshi YAMAMOTO** *(Univ. of Tokyo)*

The $C_3S$ molecule is one of the important members of the sulfur-containing carbon-chain interstellar molecules. Its spectral lines were first detected toward the dark molecular cloud TMC-1,[1] and then by laboratory microwave spectroscopy.[2] It was also detected in the envelope of the carbon star IRC+10216,[3] where several molecules were found to exist even in the vibrationally excited states. Since the $C_3S$ molecule has a low-frequency bending mode of about

150 $cm^{-1}$,[4] $C_3S$ may exist in the vibrationally excited state in the envelope of the carbon star.

We have recently detected satellite lines of $C_3S$ in the millimeter-wave region, and assigned them to the vibrationally excited state of the $v_5$=1 mode. The $C_3S$ was generated in the 2 m long free space absorption cell by discharging a mixture of $CS_2$(30 mTorr) and He(20 mTorr) at the temperature of −100°C. The discharge current was 120 mA dc. We measured 59 lines in the frequency region of 116 to 296 GHz, and analyzed them by using a conventional rotational Hamiltonian for a linear polyatomic molecule with a degenerate bending vibration. The molecular constants determined are listed in Table 1, where the molecular constants predicted by an ab initio method are given for a comparison.[4] The observed frequencies of the satellite lines of $C_3S$ are useful to identification of weaker lines detected toward the envelope of the carbon star.


**References**

1) N. Kaifu, H. Suzuki, M. Ohishi, T. Miyaji, S. Ishikawa, T. Kasuga, H. Morimoto, and S. Saito, *Astrophys. J.* **317**, L111(1987).
2) S. Yamamoto, S. Saito, K. Kawaguchi, N. Kaifu, H. Suzuki, and M. Ohishi, *Astrophys. J.* **317**, L119(1987).
3) J. Cernicharo, M. Guélin, H. Hein, and C. Kahane, *Astron. Astrophys.* **181**, L9(1987).
4) S. Seeger, P. Botschwina, J. Flügge, H. P. Reisenauer, and G. Maier, *Theochem.* preprint, (1993).


**Table 1.** Molecular Constants of $C_3S$ in the $v_5$=1 State (MHz).

| Constant | MW[a] | Ab initio[b] |
|---|---|---|
| $B_v$ | 2902.70538(63) | |
| $D_v \times 10^4$ | 2.4692(45) | |
| $H_v \times 10^{10}$ | 1.83(93) | |
| $\alpha_5$ | −12.325(1) | −12.22 |
| $q_5$ | 3.96457(53) | 3.907 |
| $q_5^J \times 10^5$ | −1.158(15) | −1.138 |

[a](3σ). [b]Reference 4) CEPA-1.

## II-A-4 Microwave Spectroscopy of Metal Hydrides: ZnH and ZnD


**Masahiro GOTO** *(Nagoya Univ. and IMS)* **and Shuji SAITO**


The metal hydrides have fundamental importance in chemistry, but microwave spectroscopy has rarely been applied to them because they are hardly produced in the laboratory, they have quite large rotational constants, they have relatively small dipole moments, and so on. Recently we have detected the lowest transitions of ZnH and ZnD with submillimeter-wave spectroscopy. The ZnH or ZnD radical was produced in the 1 m stainless steel free space cell by the reaction of dc glow discharge product of $H_2$ or $D_2$, respectively, with the Zn vapor generated from the stainless steel boat held at about 600°C in the bottom of the center of the stainless steel tube. The spectral lines of ZnH or ZnD were detected in the frequency region calculated from the molecular constants determined by infrared spectroscopy. The optimum signals were obtained at the pressure of 100 mTorr with dc current of 100mA. All the observed ZnH or ZnD lines were analyzed by using a conventional Hamiltonian describing the diatomic free radical in the doublet state. The molecular constants determined by least-squares fitting to the observed spectral lines are listed in Table 1.


**References**

1) R.-D. Urban, U. Magg, H. Birk, and H. Jones, *J. Chem. Phys.* **92**, 14 (1990).
2) H. Birk, R.-D. Urban, P. Polomsky, and H. Jones, *J. Chem. Phys.* **94**, 5435 (1991).
3) L.B. Knight and W. Weltner, *J. Chem. Phys.* **55**, 2061 (1971).


**Table 1.** Molecular Constants of the ZnH and ZnD Radicals[a]

| Constant | ZnH | ZnD |
|---|---|---|
| $B_o$ | 196292.9701(48) | 100411.2004(64) |
| $D_o$ | 14.155[b] | 3.652[b] |
| $\gamma_o$ | 7588.0537(120) | 4017.1830(170) |
| $\gamma_D$ | −2.83[b] | −0.694[b] |
| $b_F$(H,D) | 501.8705(195) | 76.110(22) |
| C(H,D) | −0.277(63) | |
| $C_l$(H,D) | 0.0656(151) | |

[a]MHz(3σ). [b]Fixed.

# II—B Development of a Mt. Fuji Submillimeter-Wave Telescope


**Shuji SAITO, Satoshi YAMAMOTO** *(Univ. of Tokyo)*, **Junji INATANI** *(National Astronomical Observatory)*, **Masatoshi OHISHI** *(National Astronomical Observatory)*, **and Norio KAIFU** *(National Astronomical Observatory)*


In these years the submillimeter-wave to far infrared region has attracted much attention in the field of astronomy, because the initial stage of star-forming activity or, in other words, the final stage of molecular cloud contraction shows various physical and chemical phenomena in the energy region of this wavelength. Several submillimeter-wave telescopes have now been developed to study astrophysics and astrochemistry of the star-forming region through atomic and molecular lines. Since atmospheric attenuation, mainly due to water vapor, becomes high in the submillimeter-wave to far infrared region, astronomical observations should be made at a high-altitude place with cold environment.

We plan to build a submillimeter-wave telescope at the summit of Mt. Fuji. The main scientific purpose of our project is (1) a survey of the neutral carbon($C_I$) line at 492 GHz, and (2) a search for new simple and fundamental molecules, especially related to dust chemistry, which will make us to understand evolutional physical and chemical processes of the molecular cloud as a whole.

Mt. Fuji is the highest mountain in Japan, and has the altitude of 3776 m above the sea level. Weather data from Japan Meteorological Agency show that precipitable water vapor at the summit is expected to be less than 1.0 mm for

about 40% of winter days (November 1990 to February 1991). This makes it possible to carry out good observations in the atmospheric window regions between 400 and 900 GHz.

The telescope planned has a 2 m diameter disk with surface accuarcy of 10 $\mu$m, enclosed with a radome transparent up to 1000 GHz. Since the weather conditions are very terrible in the winter, the temperature less than −30°C and the wind speed up to 100 m/s, and do not allow us access to the summit, the radome building has to survive against strong winds and heavy snowing and icing, and data processing and telescope operation have to be made by remote control via satellite communication.

This summer we measured atmospheric transmittance at the summit with a home made radio meter operated at 110 GHz, and found that the atmospheric optical depth was about 0.06 corresponding to about 2 mm precipitable water. This result indicates a possibility of astronomical observations even in the summer season. We plan to measure the optical depth in the coming winter under collaboration with the Mt. Fuji station of Japan Meteorological Agency.

Detailed investigations are now in progress on the design of the telescope, radome, 500 GHz receiver, back-end spectrometer, data processing, and remote control.

# II—C Laser Investigation of Superexcited States of Diatomic Molecules and Exotic Molecules

Above the first ionization threshold, there are still many neutral states. These molecular states are called superexcited states, and have been considered to make important contribution to chemical reactions because of their high state density and large oscillator strength. In this type of states, not only ionization channels but also many dissociation channels are generally open, and they are strongly competing with each other. To disentangle this complicated competition is the main subject of the study on the dynamics of superexcited states. On the other hand, a recent discovery of anomalous survival of antiprotons in helium medium strongly suggests the production of an antiprotonic helium atom consisting of $He^{2+}$, an electron and an antiproton. From a viewpoint of spectroscopy, this completely new entity is a very attractive object of study, because it has intermediate characters between atoms and diatomic molecules; in other words, it is neither an atom nor a molecule. According to theoretical calculations, the nascent population is expected to be distributed in superexcited states in a molecular picture. This prediction may allow us to study this new entity with laser spectroscopic methods by using a property peculiar to superexcited states, namely, autoionization.

## II-C-1 Laser Investigation of the Competition between Rotational Autoionization and Predissociation

**Asuka FUJII and Norio MORITA**

[*J. Chem. Phys.* **98**, 4581 (1993)]

Rotational autoionization has generally been believed to play an important role in the decay dynamics of rovibrational superexited states. However, there have been only a few experimental studies on this decay process. This may be partly because rotational superexcited states can be produced only in very high Rydberg states, which is generally difficult to distinguish this process from other decay channels, such as predissociation.
channels, such as predissociation.

In this work, rotational superexcited *np* Rydberg states ($n>22$, $v=0$) of NO have successfully been produced state-selectively with a two-color double resonance excitation method. In addition, not only $NO^+$ ions generated by autoionization but also nitrogen atoms produced by predissociation have been directly detected. As a result, three decay processes (rotational autoionization and two predissociation processes) have been separately observed and their competing feature has been successfully observed. One of the important results of this work is that the predissociation efficiency of the *np* Rydberg states hardly depends on whether the rotational autoionization channels are open or not. This fact clearly demonstrates that the decay dynamics of these states is governed by predissociation, not by rotational autoionization.

## II-C-2 Three-Color Triple Resonance Spectroscopy of Highly Excited *ng* Rydberg States of NO: Studies on the Decay Dynamics of High Orbital-Angular-Momentum States

**Asuka FUJII and Norio MORITA**

By means of a three-color triple resonance technique, we have observed rotational-state-resolved photoionization spectra of $ng \leftarrow 4f$ transition of NO. A typical example of the observed spectra is shown in Figure 1. Highly excited *ng* Rydberg states up to $n=70$ have been observed, and their term energies and quantum defects have been determined. We have also performed a theoretical calculation of the term energies based on the long range force model, and the results have well reproduced the observed ones within the experimental error, showing that there is no appreciable perturbation in the *ng* Rydberg states. Regarding autoionization rates, our measurement has shown that they are in good agreement with those predicted by previous theoretical calculations. This is the first experimental evidence for the existence of efficient rotational and vibrational autoionization in $l>3$ Rydberg states. In addition to autoionization, predissociation decay has also been found to exist appreciably even in such high orbital-angular-momoentum states. However, from the investigation on the competition between these two decay processes based on the principle of the continuity of oscillator strength at the ionization threshold, it has been found that the effect of predissociation is sitll rather small and the decay dynamics are mainly governed by autoionization, not by predissociation.

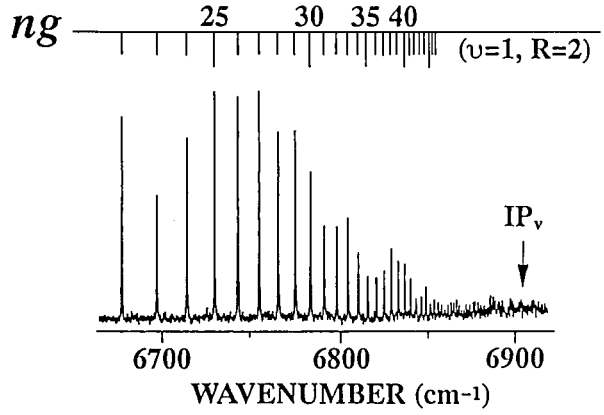


**Figure 1.** Typical example of photoionization spectra due to the $ng \leftarrow 4f$ transition of NO. In this observation, a single rotational level of the $4f$ Rydberg state ($v$=1) is pumped by using two-color double resonance excitation via the $A^2\Sigma^+$ state, and the third laser is scanned over the $ng \leftarrow 4f$ transition.

### II-C-3 Laser Spectroscopy of Metastable Antiprotonic Helium Atomcules

**Norio MORITA, Kazumasa OHTSUKI** *(Univ. of Electro-Commun.)*, **and Toshimitsu YAMAZAKI** *(INS, Tokyo univ.)*

[*Nucl. Instrum. Methods*, **A330**, 439 (1993)]

Anomalous survival of antiprotons in gaseous, liquid and solid helium has recently been found by a research group of University of Tokyo. Theoretical caluculations following this discovery have shown that production of neutral antiprotonic helium atoms ($\bar{p}He^+$, comprised of He nucleus, an electron in the ground 1s state and an antiproton in an orbital $(n, l)$) with $n \approx (M^*/m)^{1/2} \approx 38$ and large $l$ can be responsible for this long survival of antiprotons. This $\bar{p}He^+$ atom is named "atomcule" because it has characters of both atom and molecule.

To test this theoretical assumption, we have proposed a laser spectroscopic observation of this "atomcule" in this paper. Because of the very small production rate of this exotic molecule ($\approx 300$ $s^{-1}$), usual laser spectroscopic methods, such as absorption or fluorescence detection, cannot be applied to this observation. The multiphoton ionization technique is also very difficult to use, because the target is produced only in highly dense host medium (helium atoms) and also because the ionization energy is too high ($\approx 25$ eV) for laser excitation. Forunately, we expect that there are certain short-lived levels which proceed to ionization via fast Auger transition and are connected by dipole-allowed transition with long-lived states. The latter states are expected to have an appreciable population even at 1 $\mu$s following the $\bar{p}He^+$ production. A laser can resonantly move this population to the short-lived states, which are quickly autoionized. After the ionization, $\bar{p}He^{2+}$ immediately annihilates due to Stark effect to generate many high-energy elementary particles, such as pions. Detecting these particles, we can expect to observe the resonance effect of laser excitation. We start this experiment at CERN by using the low-energy antiproton beam from LEAR in September 1993.

## II—D Laser Cooling and Trapping of Neutral Atoms

When an atom absorbs or emits a photon, it is accelerated or decelerated since a photon has momentum. Using this mechanism, the translational motion of neutral atoms can be cooled to an extremely low temperature by laser radiation. As the translational temperature goes down to a nanokelvin region, the atomic de Broglie wavelength becomes a macroscopic size. A macroscopic quantum-mechanical collective motion of an atomic aseembly can then be expected to occur in a very thin gas. Mòreover, the long de Broglie wavelength enables us to realize an atomic interferometer, which is analogous to a neutron interferometer but more sensitive to the change of velocity and acceleration. On the other hand, a strong radiation field can modify the internal energy of an atom, so that an atom in an inhomogeneous radiation field receives a force from the field. This mechanism allows us to trap atoms in a laser beam, so that we can easily control the spatial position of atoms. To achieve these interesting translational states of atoms, we have been studying the laser cooling and trapping.

### II-D-1 Observation of the Diffraction of He Atomic Wave with a Transmission Grating

**Mitsutaka KUMAKURA and Norio MORITA**

We have observed the diffraction of He atoms with a transmission grating. The He atoms are decelerated with the Zeeman tuning method and cooled to 1.2 mK in the magneto-optical trap. The trapped He atoms are then released and introduced to a transmission diffraction grating (2000 lines/mm) by turning off the trapping laser and magnetic field. The grating is placed so that its grids are parallel to the gravity. This configuration makes the diffraction free from gravitational effects. The most probable horizontal velocity of the incident atoms is 2.7m/s, which is determined by the temperature of the trapped atoms and an aperture placed in front of the grating. The transmitting He atoms, which lie in the $2s^3S$ metastable state, are detected by a multichannel plate detector with a phosphor screen. Detecting the fluorescence from the screen with a CCD camera and accumulating this signal for a number of trap-release cycles, the diffraction pattern of the He atomic wave has been obtained (Figure 1). The primary peak at the center corresponds to the zeroth order diffraction. On both sides of this peak, about 3 mm apart from the center, there are two secondary maxima, which correspond to the first order diffraction. From their displacement, the diffraction angle of the He atom is estimated to be about 4.3 degree. This means that de Broglie wavelength of the incident He atom is 37 nm. These values are in good agreement with those calculated from the most probable velocity of the incident He atoms.

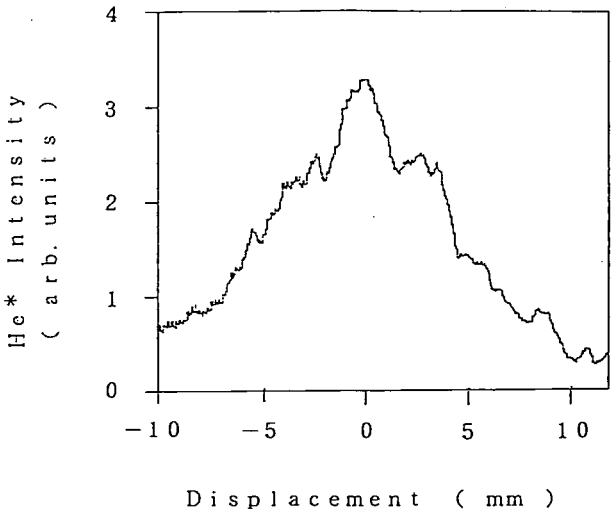


**Figure 1.** Diffraction pattern of He atomic waves.

# II—E Molecular Science of Biomolecules and Their Model Compounds

Elucidation of the structure-function relationship of proteins is a current subject of this group. The primary technique used for this project is the stationary and time-resolved resonance Raman and absorption spectroscopies. The main themes that we want to explore are 1) mechanism of oxygen activation by enzymes, 2) electron- and proton-transfers through proteins and their coupling in the energy transducing membrane, 3) the primary process of photoreceptor proteins, 4) dynamical features of higher order protein structures. In category (1), we have treated reaction intermediates of cytochrome *c* oxidase, cytochrome P-450, chloroperoxidase, and horseradish peroxidase by using the mixed-flow transient Raman apparatus and Raman/absorption simultaneous measurement system. We also examined model compounds such as $Fe^{IV}$=O porphyrin and its $\pi$ cation radical. For (2), we have investigated bacteriorhodopsin and cytochrome *c* oxidase, while for (3) we have found the structural difference between $P_r$ and $P_{fr}$ forms of phytochrome and their model compounds. For (4), we observed the UV (200—240nm)-excited time-resolved resonance Raman spectra of hemoglobin-CO in the time resolution of 10 ns, discussing a mechanism of its quaternary structure change. In order to make the UV Raman experiment more practical, we developed a novel technique based on the combined use of the first/second order dispersions of two gratings in an ordinary double-monochromator and applied it successfully to 244 nm-excited RR spectra of several proteins including phytochrome, hemoglobin and viruses. Furthermore, the pump/probe time-resolved Raman system using two 10-ns visible lasers was set up and applied to pursue recombination dynamics of photodissociated CO of myoglobin, hemoglobin and their mutants. These experiments enabled us to explore dynamical features of protein structures.

## II-E-1 Ultraviolet Resonance Raman Spectra of Pea Intact, Large, and Small Phytochromes: Differences in Molecular Topography of the Red and the Far-red Absorbing Forms

**Yasuhisa MIZUTANI, Satoru TOKUTOMI** *(NIBB)*, **Shoji KAMINAKA, and Teizo KITAGAWA**

[*Biochmistry* **32**, 6916—6922 (1993)]

Ultraviolet resonance Raman (UV RR) spectra excited at 244 nm were observed for pea intact, large and small phytochromes at pH 7.8. Raman bands assignable to Trp residues dominated the UV RR spectra. The intensity ratios of Trp W7 doublet bands, I(1358)/I(1342), of all the three phytochromes in the red-light absorbing form ($P_r$) were almost the same as that of an aqueous Trp solution, indicating that most of the 6 and 4 Trp residues in the 59-kDa chromophoric and the C-terminal 59-kDa nonchromophoric domains, respectively, reside under hydrophilic microenvironments in $P_r$. This ratio increased under red light illumination, where the photoequilibriums between $P_r$ and the far-red absorbing form ($P_{fr}$) for intact and small phytochromes and among $P_r$, a bleached intermediate ($I_{bl}$) and $P_{fr}$ for large phytochrome, respectively, are attained. The increase of the intensity ratio was most prominent for small phytochrome. These observations suggest that the microenvironments around some Trp residues become hydrophobic due to conformational changes induced by phototransformation from $P_r$ to $I_{bl}$ and that the hydrophobicity increase mainly derives from the chromophoric domain. Among six Trp residues in the chromophoric domain, $Trp^{365}$ $Trp^{567}$ are deduced to be likely candidates for those involved in this hydrophobicity increase. Intensity distribution of amide I band shows little population of the $\beta$-sheet in both $P_r$ and $P_{fr}$ of the intact, large and small phytochromes and $\alpha$-helices and non-regular structure are less populated in the chromophoric domain than in the N-terminal 6-kDa segment and the C-terminal nonchromophoric domain.

## II-E-2 Resonance Raman Characterization of Iron(III) Porphyrin N-oxide: Evidence for an Fe-O-N Bridged Structure

**Yasuhisa MIZUTANI, Yoshihito WATANABE** *(Kyoto Univ.)*, **and Teizo KITAGAWA**

Resonance Raman (RR) spectra are reported for iron(III) tetramesityl porphyrin (TMP) N-oxide and its $^{18}O$ and $^{15}N$ derivatives. The RR bands assignable to the Fe-O stretching, O-N stretching, and Fe-O-N bending vibrations were observed at 506, 1122, and 743 and 708 $cm^{-1}$, respectively. This confirms that the complex has the Fe-O-N bridged structure. The RR bands of the macrocycle such as the $C_\beta C_\beta$ and $C_\alpha N$ stretching modes were split into doublets due to lowering of symmetry. The RR band arising from the $C_m$-phenyl stretching band exhibited a downshift by 4 $cm^{-1}$ upon formation of the N-oxide, suggesting considerable distortion of the macrocycle.

## II-E-3 The Molecular Features and Catalytic Activity of $Cu_A$-Containing $aco_3$-type Cytochrome *c* Oxidase from a Facultative Alkalophilic *Bacillus*

**Isao YUMOTO** *(Tokyo Institute of Tech.)*, **Satoshi TAKAHASHI, Teizo KITAGAWA, Yoshihiro FUKUMORI** *(Tokyo Institute of Tech.)*, **and Tateo YAMANAKA** *(Tokyo Institute of Tech.)*

[*J. Biochem* (Tokyo), **114**, 88–95 (1993)]

Cytochrome $aco_3$ of *Bacillus* YN-2000 was purified by an improved procedure and its molecular features and catalytic activity were extensively studied. The enzyme molecule was composed or three subunits with $M_r$s of 50,000, 41,000 and 22,000 and contains 1 molecule each of cytochrome *a*, cytchrome *c*, and cytochrome $o_3$ in the minimal structural unit ($M_r$, 113,000). The 41,000 subunit (subunit II) contains heme C. The EPR, optical, and resonance Raman spectra of the oxidized enzyme demonstrated the presence of $Cu_A$ whose coordination environment bore close resemblance to that of the $aa_3$-type cytochrome *c* oxidase. Resonance Raman studies demonstrated that cytochrome *a* moiety was similar to that of an $aa_3$-type oxidase and also that the cytochrome $o_3$ contained a five-coordinated high-spin heme with a histidine as an axial ligand. The Fe-CO stretching mode of the cytochrome $o_3 \cdot CO$ complex was observed at 520 $cm^{-1}$, which was the same in frequency as that of cytochrome $aa_3 \cdot CO$. The oxygen consumption activity of cytochrome $aco_3$ was measured using several kinds of cytochromes *c* as the electron mediators. The reaction between cytochrome $aco_3$ and eucaryotic cytochromes *c* was completely inhibited by poly-L-lysine. On the contrary, poly-L-lysine was indispensable for the sufficient reaction between the oxidase and *Bacillus* YN-2000 cytochrome *c*-553, the physiological electron donor. The combined studies on the structure and enzymatic properties suggest that the cytochrome $aco_3$ is very similar to cytochrome $caa_3$ except that the cytochrome $aco_3$ has cytochrome $o_3$ in place of cytochrome $a_3$ and cytochrome *c* component has very low redox midpoint potential (95 mV). A possible relationship between the role of the role of the low redox potential cytochrome *c* and the bioenergetic properties of the alkalophilic bacterium was discussed.

## II-E-4 Sequential Changes of the Fe-Histidine Bond upon Ligand Binding to Hemoglobin: Resonance Raman Study of $\alpha\alpha$-Cross-linked Co-Fe Hybrid Hbs.

**Shouji KAMINAKA, Y-X. ZHOU** *(Univ. of Pennsylvania)*, **A. Tsuneshige** *(Univ. of Pennsylvania)*, **T. Yonetani** *(Univ. of Pennsylvania)*, **and Teizo KITAGAWA**

Resonance Raman spectra were observed for $\alpha\alpha$-cross-linked Co-Fe hybrid Hbs. The Fe-histidine (F8) stretching ($\nu_{Fe\text{-}His}$), Fe-CO stretching ($\nu_{Fe\text{-}CO}$), Fe-C-O bending ($\delta_{FeCO}$) and O-O stretching ($\nu_{OO}$) frequencies were determined for *mono*-, *di*-, and *tri*-Fe tetramers in a function of the number of bound ligands. The $\nu_{Fe\text{-}His}$ band center was determined with the accuracy of $\pm 0.25$ $cm^{-1}$ while uncertainties of the $\nu_{Fe\text{-}Co}$ and $\nu_{OO}$ frequencies were $\pm 1$ $cm^{-1}$. The $\nu_{Fe\text{-}His}$ band of $\alpha\alpha$-cross linked Hb appeared at 214 and 220 $cm^{-1}$ for the equilibrium deoxy and CO-photodissociated transient forms, respectively, in good agreement with those of Hb A. The $\nu_{Fe\text{-}His}$ bands of *mono* and *di*-$\alpha$(Fe) tetramers were alike and were composed of two bands irrespective of the number of bound ligands, and they were significantly lower than those of *mono*- and *di*- (deoxy) $\beta$(Fe) subunits, which gave an intense symmetric band, indicating inequivalence between $\alpha$ and $\beta$ subunits. This feature was qualitatively retained while the frequencies of two $\alpha$(Fe) hemes and their relative intensity were slightly changed in the binding process of four ligands. In contrast, the $\nu_{Fe\text{-}His}$ frequency of the $\beta$ subunits changed gradually as the number of bound ligands increased. The $\nu_{Fe\text{-}His}$ frequency of $\alpha$(Fe) in the $\alpha\alpha$-than in the $\beta\beta$-cross-linked Co-Fe hybrid Hb was lower by 4–6 $cm^{-1}$, while those of $\beta$(Fe) were alike. The $\nu_{Fe\text{-}CO}$ frequency was higher for the $\alpha$(Fe) than $\beta$(Fe) subunits by 2–4 $cm^{-1}$ for both *mono*- and *di*-Fe species, and changed a little with the number of bound ligands for the $\alpha$ subunit but not for the $\beta$ subunit. The $\nu_{OO}$ frequency of oxyCo subunit was scarcely altered between the $\alpha$ and $\beta$ subunits and also with the number of bound $O_2$ ligands. The present results about $\nu_{Fe\text{-}CO}$ and $\nu_{OO}$ bands were in agreement with the results previously obtained for the $\beta\beta$-cross linked Co-Fe hybrid Hb, suggesting that structural changes upon the increase in the numer of the bound ligands are much larger in the proximal side than in the distal side. The behavior of $\nu_{Fe\text{-}His}$ band suggests that the proximal structure little changes in the $\alpha$ subunit until binding of two ligands but that in the $\beta$ subunit starts to change from the first ligand.

## II-E-5 A Novel Tetranuclear $[\{Rh_2(\eta^5\text{-}C_5Me_5)_2(\mu\text{-}CH_2)_2\}_2(\mu\text{-}S_2)_2]^{2+}$ Cationic Complex with a Doubly Bridge of $S_2$ Ligand

**Yoshiki OZAWA, Amelio Vazquez de MIGUEL, Tian-Wei ZHU, Kiyoshi ISOBE, Kui-Ming ZHAO, Takanori NISHIOKA, Takashi OGURA, and Teizo KITAGAWA**

The oxidation reaction of $[Rh_2(\eta^5\text{-}C_5Me_5)_2(\mu\text{-}CH_2)_2(\mu\text{-}SH)]Cl$ with $O_2$ was undertaken to explore the transformation of the M($\mu$-SH)M functionality. We have isolated a novel tetranuclear complex $[\{Rh_2(\eta^5\text{-}C_5Me_5)_2(\mu\text{-}CH_2)_2\}_2(\mu\text{-}S_2)_2]Cl(OH)$ [or the $BF_4$ salt) in high yield. The

cationic moiety of the compound possesses approximately $2/m$ symmetry, and consists of two $S_2$ and $Rh_2$ ($\eta^5$-$C_5Me_5)_2(\mu$-$CH_2)_2$ groups with a Rh-Rh single bond (2.650Å(mean)). Two $S_2$ ligands with trans end-on coordination bridge two $\mu$-methylene-rhodium groups to form a $Rh_4S_4$ eight member ring of a new centrosymmetric chair like core. We have assigned the Raman bands at 579 and 260 $cm^{-1}$ to the $\nu$(S-S) and $\nu$(Rh-S) stretching modes, respectively, by using a sample enriched by $^{34}S$.

The data of X-ray diffraction and resonance Raman and XP spectroscopies as well as comparison with [{$Rh_2(\eta^5$-$C_5Me_5)_2(\mu$-$CH_2)_2$}$_2(\mu$-CN)$_2$] $(PF_6)_2$ show clearly that the $S_2$ ligand has a supersulfide character in both senses of formal and effective charges on it.

Although further experiments are needed to distinguish between various mechanistic possibilities for the formation of the tetranuclear complex, the oxidation of [$Rh_2(\eta^5$-$C_5Me_5)_2(\mu$-$CH_2)_2(\mu$-SH)] Cl probably involves a unique 3e process per molecule (eq. 1)

$$2[Rh_2(\eta^5\text{-}C_5Me_5)_2(\mu\text{-}CH_2)_2(\mu\text{-}SH)]^+ + 2H_2S + 3/2O_2 \rightarrow [[Rh_2(\eta^5\text{-}C_5Me_5)_2(\mu\text{-}CH_2)_2]_2(\mu\text{-}S_2)_2]^{2+} + 3H_2O \quad (1)$$

### II-E-6 Monomeric Carboxylate Ferrous Complexes as Models for the Dioxygen Binding Sites in Non-Heme Iron Proteins. The Reversible Formation and Characterization of $\mu$-Peroxo Diferric Complexes

**Nobumasa KITAJIMA** *(Tokyo Institute of Technology)*, **Nobuchika TAMURA** *(Tokyo Institute of Technology)*, **Hironobu AMAGAI** *(Tokyo Institute of Technology)*, **Hideno FUKUI** *(Tokyo Institute of Technology)*, **Yoshihiko MORO-OKA** *(Tokyo Institute of Technology)*, **Yasuhisa MIZUTANI, Teizo KITAGAWA, Rejeev METHUR** *(Univ. of Southern California)*, **Kristel HEERWEGH** *(Univ. of Southern California)*, **Christopher A. REED** *(Univ. of Southern California)*, **Clayton R. RANDALL** *(Univ. of Minnesota)*, **Lawrence QUE, Jr.,** *(Univ. of Minnesota)*, **and Kazuyuki TATSUMI** *(Osaka Univ.)*

A series of monomeric carboxylate ferrous complexes with a $N_3$ ligand HB(3,5-$iPr_2$pz)$_3$ has been synthesized and characterized as a model for the iron site in non-heme iron proteins which bind or activate dioxygen. The structures of Fe(OAc)(HB(3,5-$iPr_2$pz)$_3$), Fe(OBz)(MeCN)(HB(3,5-$iPr_2$pz)$_3$) and Fe(OOCtBu)(HB(3,5-$iPr_2$pz)$_3$) were determined by X-ray crystallography. The five-coordinate complex Fe(OBz)(HB(3,5-$iPr_2$pz)$_3$) was found to bind a variety of $\sigma$-donating ligand such as dimethylsulfoxide and pyridine at the open coordination site. The reaction between the ferrous complexes and dioxygen has been explored. Fe(OBz)(HB(3,5-$iPr_2$pz)$_3$) was found to bind dioxygen to form a dioxygen adduct which is reasonably stable at below −20°C. The dioxygen adduct was characterized by the dioxygen uptake measurement, and UV-vis, resonance Raman, $^1$H-NMR and X-ray absorption spectroscopy. Based on these results: the Fe:$O_2$ stoichiometry of 2:1, an intense absorption band observed at 682 nm, $\nu$(O-O) detected at 876 $cm^{-1}$, and the Fe · · Fe separation of 4.3Å estimated by EXAFS; the dioxygen adduct was identified to a $\mu$-peroxo dinuclear ferric complex. The variable temperature magnetic susceptibility measurement of the isolated $\mu$-peroxo complex indicates that the complex is antiferromagnetic with J=−33 $cm^{-1}$, which is weaker than those known for other $\mu$-peroxo dinuclear ferric complexes. This characteristic feature may be associated with the structurally unique Fe-O-O-Fe frame, which is discussed based on the Extended Hückel calculations. Above −20°C, the reaction of Fe(OBz)(HB(3,5-$iPr_2$pz)$_3$) with dioxygen causes irreversible oxidation of the complex, resulting in formation of a trimeric ferric complex (HB(3,5-$iPr_2$pz)$_3$)$(OBz)_2$(O)Fe(OH)-$(OBz)_2$Fe(HB(3,5-$iPr_2$pz)$_3$) the assignment being consistent with the magnetic property, Mössbauer spectrum and X-ray analysis.

### II-E-7 Proton Pumping Activity and Visible Absorption and Resonance Raman Spectra of a *cao*-Type Cytochrome *c* Oxidase Isolated from Thermophilic Bacterium *Bacillus* PS3

**Nobuhito SONE** *(Kyushu Inst. of Tech.)* , **Takashi OGURA, Shunsuke NOGUCHI** *(Kyushu Inst. of Tech.)*, **and Teizo KITAGAWA**

[Biochemistry in press]

Cytochrome *c* oxidase having heme O in addition to heme C and heme A (cytochrome *cao*) [Sone, N. & Fujiwara, Y. (1991) FEBS Lett. 288 154−158] was isolated from a thermophilic bacterium, *Bacillus* PS3 grown under slightly air-limited conditions. The cytochrome *cao* could oxidize yeast cytochrome *c* and N,N,N′,N′-tetramethyl p-phenylenediamine twice faster than cytochrome $caa_3$, which this organism yielded under normal growing condition, did. The cytochrome *cao* also pumped protons upon cytochrome *c* oxidation in a way similar to cytochrome $caa_3$. Binding of cyanide to cytochrome *cao* caused the spin-state conversion of heme O at the binuclear center and seriously inhibited its physiological activity. A low value of $K_i$(0.4$\mu$M) for cyanide was found to be mainly due to small "off" constnat. Resonance Raman spectra of cytochrome *cao* bore close resemblance to those of cytochrome $caa_3$ in both oxidized and reduced states, although the formyl stretching ($\nu_{CH=O}$) band was absent. The Fe-histidine stretching ($\nu_{Fe\text{-}His}$) and Fe-CO stretching ($\nu_{Fe\text{-}CO}$) frequencies of cytochrome *cao* were very close to those seen for cytochrome $caa_3$, but were distinct from those of hemoglobin and peroxidases, suggesting that the protein structure in the vicinity of heme O is close to that of the heme $a_3$ moiety of cytochrome $caa_3$.

## II—F Vibrational Spectroscopy on Short-lived Molecules

Raman spectroscopy reveals the vibrational spectrum of molecule which is sensitive to geometrical as well as electronic structures. When the wavelength of the probe beam is tuned within the absorption band of the molecule in question,

resonance enhancement of Raman intensity makes it possible to detect Raman scattering from an excited molecule or a reaction intermediate even if its life time is short and thus its population are considerably small. We take this advantage of resonance effect to explore the structures of metallo- and free-base porphyrins in the excited singlet and triplet states. We also investigated intermediates of photoreduction of iron-porphyrins. Recently we extended similar measurements to a ps time regime and succeeded in observing vibrational relaxation in a dd excited electronic state for Ni-porphyrin. In order to develop a new technique for obtaining ps time-resolved resonance Raman spectra with a smaller power density of laser, we constructed a multichannel Fourier transform Raman spectrometer and investigated its ability with benzene.

### II-F-1 Vibrationally Hot (dd) Excited State of $Ni^{II}$-Porphyrin Probed by Picosecond Time-Resolved Resonance Raman Spectroscopy

**Shin-ichiro Sato, and Teizo KITAGAWA**

The ps pump/probe time-resolved resonance Raman ($TR^3$) spectra were obtained with $Ni^{II}$ octaethylporphyrin in benzene and THF in the time range from −40 to 860 ps following the ($\pi\pi$) excitation of the macrocycle. The spectrum for $\Delta t$=0 ps was distinct from others, while the $TR^3$ spectra after $\Delta t$=60 ps are in agreement with those of the (dd) excited state and decayed with the time constant of ca. 280 ps. The $\nu_4$ band of the spectrum for $\Delta t$=0 ps exhibited broadening similar to other bands, indicating that a structural alteration from the ruffled- to planar forms is not the main event in the initial relaxation with $\tau_1$= ~ 10ps. On the other hand, anti-Stokes Raman bands were observd only for $\Delta t$=0 ps. Consequently, the rather uniform broadening and small downshifts of Raman bands at $\Delta t$=0 ps compared with those after 60 ps were ascribed to vibrationally hot ($d_{z^2}$, $d_{x^2-y^2}$) states.

### II-F-2 Multichannel Fourier Transform Spectroscopy Using Two-Dimensional Detection of Interferogram and Its Application to Raman Spectroscopy

**Satoshi TAKAHASHI, Jeung Sun AHN, Shuji ASAKA, and Teizo KITAGAWA**

[*Appl. Spectrosc.* **47**, 863–868 (1993)]

A system for multichannel Fourier transform spectroscopy was constructed by using a CCD detector and an interferometer consisting of Savart plate held between two polarizers, and practical problems associated with its application to Raman experiments were investigated. A novel idea of the present system lies in avoiding the aliasing distortion, seen in the spectrum measured with an one-dimensional multichannel detector, by arranging the principal axis of sensitized plane of the CCD detector being not coincident with the direction of the fringe pattern of interferogram. The observed interferogram suffered geometrical distortion due to incompleteness of the Savart plate. In order to circumvent this problem, algorithm for correcting this distortion by referring to the interferogram of appropriate monochromatic light was developed successfully. The resolution of a Raman spectrum obtained for indene was ca. 40 $cm^{-1}$, in agreement with the theoretical value expected for this system.

### II-F-3 Time-Resolved Resonance Raman Study on Free-base Octaethylporphyrin in the $S_0$, $S_1$, and $T_1$ States

**Shin-ichiro Sato, Katsuhiro Aoyagi** *(Fukushima National College of Tech.)*, **and Teizo Kitagawa**

Time-resolved resonance Raman spectra are reported for the free-base octaethylporphyrin ($OEPH_2$) and its meso-$d_4$ isotopomers as well as for these of imino-$d_2$ isotopomers in the ground ($S_0$) state, lowest excited singlet ($S_1$, $^1(\pi\pi)$) state and triplet ($T_1$, $^3(\pi\pi)$) state. The observed Raman bands in the excited electronic states are interpreted based on the polarization properties of each Raman bands and the reported assignments for the free-base porphine [Li et al J. Phys. Chem. 1991, 95, 4268] and NiOEP [Li et al J. Phys. Chem. 1990, 94, 47] in the ground electronic state. Both the totally symmetric and non-totally symmetric Raman bands were observed for the $S_1$ and $T_1$ states. As a common feature for the $S_1$ and $T_1$ states, the polarized Raman bands, which were sensitive to the isotopic substitution of the ethyl position, were enhanced at around 1200 $cm^{-1}$, which suggests existence of interaction between $\pi$-orbital of the macrocycle and $\sigma\pi$-orbital of the ethyl substituents in the $S_1$ and $T_1$ state. In the $S_1$ state, the $C_aC_m$ antisymmetric stretching mode, corresponding to the $\nu_{19}$ mode in the $S_0$ state, was resonance-enhanced at 1534 $cm^{-1}$ that was downshifted by 54 $cm^{-1}$ from the position (1558 $cm^{-1}$) in the ground electronic state, indicating the fact of $S_1$-$S_2$ vibronic coupling. On the other hand, in the $T_1$ state, no ap band was observed in 1600–1500 $cm^{-1}$ region. Instead not-resolved and complicated structures of the depolarized bands, which are sensitive to imino-$d_2$ and meso-$d_4$ substitutions, were noticeably enhanced at around 1440–1400 $cm^{-1}$, suggesting another vibronic mechanics, likely to be pseudo Jahn-Teller effect between $^3B_{3u}$ and $^3B_{2u}$ states, may distort the potential in the triplet states and affect a N-H tautomerization in the $T_1$ state.

## II—G Molecular and Electronic Structures of $M@C_{82}$ and the $C_{60}$ Radical Anion

The continued interest in metallofullerenes and radical ions of fullerenes has resulted from the discovery of superconductivity in the CT complexes of alkali metals with fullerenes. The electronic structure of the $C_{60}$ anion has been discussed in connection with the Jahn-Teller distortion. Spectroscopic information concerning the electronic structure of the $C_{60}$ anion has been obtained by absorption, luminescence, and ESR measurements. Considering the metallofullerene as the endohedral

(i.e. intramolecular) CT complex of a metal with the fullerene, the electronic structure of the mettalofullerne is expected to be very significant in explaining the possibility of the superconductivity or the ferromagnetism of the metallofullerene crystal. Both theoretical and experimental discussions of the electronic structure of the metallofullerene have been given.

### II-G-1 A Theoretical Approach to $C_{82}$ and La@$C_{82}$

**Shigeru NAGASE** *(Yokohama National Univ.)*, **Kaoru KOBAYASHI** *(Yokohama National Univ.)*, **Yohji ACHIBA** *(Tokyo Metropol. Univ.)*, **and Tatsuhisa KATO**

[*Chem. Phys. Lett.*, **201**, 475 (1993)]

In view of the recent experimental interest, the relative stabilities of the $C_{82}$ isomers and the electronic properties of La@$C_{82}$ are investigated by means of molecular orbital calculations. It is calculated that the most stable $C_{82}$ isomer has $C_2$ symmetry, as detected most abundantly via NMR measurement. An interesting finding is that the electronic structure of La@$C_{82}$ depends strongly on the position of the La atom. At the energetically most favorable position the electronic state is described as $La^{3+}@C_{82}^{3-}$, as suggested from the EPR measurement. It is predicted that the La atom is trapped inside the cage of $C_2$ symmetry and is strongly bound to the cage carbons; La@$C_{82}$ has strong electron-donating character.

### II-G-2 Spectroscopic Studies of the Radical Anion of $C_{60}$. Detection of the Fluorescence and Reinvestigation of the ESR Spectrum

**Tadamasa SHIDA** *(Kyoto Univ.)*, **Takeshi KODAMA, and Tatsuhisa KATO**

[*Chem. Phys. Lett.* **205**, 405 (1993)]

An emission band with a mirror image pattern to the near-IR absorption band is detected for $C_{60}^-$ produced electrolytically in a solution at room temperatures. The emission band reinforces our previous assignment of the absroption band. The lineshape of the ESR spectrum was reinvestigated to conclude that the isotropic feature at temperatures above 50 K is mainly due to the averaging of the Jahn-Teller distorted structures by pseudo-rotation. The significance of the residual angular momentum is discussed.

### II-G-3 ESR Study of the Electronic Structures of Metallofullerens: A Comparison between La@$C_{82}$ and Sc@$C_{82}$

**Shinzo SUZUKI** *(Tokyo Metropol. Univ.)*, **Koichi KIKUCHI** *(Tokyo Metropol. Univ.)*, **Yohji ACHIBA** *(Tokyo Metropol. Univ.)*, **and Tatsuhisa KATO**

The line widths of the hyperfine components of ESR spectra of La@$C_{82}$ and Sc@$C_{82}$ in $CS_2$ and toluene solutions have been measured as a function of temperature. The extent of line broadening due not only to the insufficient rotational averagning of g and hyperfine tensors but also to the spin-rotation coupling interaction have been determined. The values of anisotropy for the g and hyperfine tensors are deduced by analysis according to Kivelson's formalism for these line broadening mechanisms. Although the two spectra for La@$C_{82}$ and Sc@$C_{82}$ in solution at room temperature look similar to each other, the different electronic structure for each endohedral metal is reflected in their differing values for the anisotropy of the g and hyperfine tensors. The electronic strucutures of La@$C_{82}$ and Sc@$C_{82}$ are discussed comparatively in terms of a theoretical interpretation for the anisotropic correction of the g factor and the hyperfine coupling constant. The results exhibit different electronic structures for La@$C_{82}$ and Sc@$C_{82}$; the radical electron is assigned to a $\pi$ orbital of the $C_{82}$ cage for La@$C_{82}$, but to a d orbital of the metal for Sc@$C_{82}$.

## II—H Laboratory Spectroscopy of MgNC: The First Radioastronomical Identification of Mg-bearing Molecule

**Kentarou KAWAGUCHI*, Eriko KAGI**, and Tsuneo HIRANO**, Shuro TAKANO, and Shuji SAITO** *(*Nobeyama Radio Observatory and IMS, **Ochanomizu Univ.)*

[*Ap. J. Letters:* **406**, L39 (1993)]

The linear MgNC radical was detected, for the first time, by laboratory microwave spectroscopy, and six unidentified lines in IRC+10216 reported by Guélin et al.[1] were assigned to the transitions of this radical. The radical was produced in a free-space absorption cell by a DC discharge in a mixture of magnesium vapor, argon, and cyanogen. Observed spectral lines in the 250–370 GHz region were analyzed by using the $^2\Sigma$ energy level expression, to give the rotational, centrifugal distortion and spin-rotation constants: $B_0$=5966.8969(24) MHz, $D_0$=0.0042338(35) MHz, $H_0$=0.308(16)×$10^{-7}$ MHz, and $\gamma_0$=15.219(13) MHz, with one standard deviation in parentheses. The column density of MgNC in IRC+10216 was determined to be 1–2×$10^{13}$ $cm^{-2}$ in conditions of local thermodynamic equilibrium. The MgNC abundance is lower by three order of magnitude than the Si abundance involved in all Si-bearing molecules detected in IRC+10216, where we note that the element Mg is similar to Si in cosmic abundance.

**References**

1) M. Guélin, J. Cernicharo, C. Kahane, and J. Gomez-Gonzalez, 1986, *Astron. Astrophys.* **157**, L17.

# RESEARCH ACTIVITIES III
# Department of Electronic Structure

## III—A Ultrafast Intermolecular Electron Transfer in Electron Donating Solvent

Photo-induced intermolecular electron transfer (ET) in non-reactive solvent is usually limited by the translational diffusion rate, which determines the probability of encounter. To study the dynamics of fast ET dynamics, it is preferable to perform the experiment in a system, in which electron donor and acceptor are in direct contact, so that the diffusion process may be neglected. One example of such type of system is realized when the solvent itself acts as a donor or an acceptor. We have recently reported ultrafast fluorescence quenching of exited dye molecule (nile blue A perchlorate) in neat weakly polar electron- donating solvents: aniline and N,N-dimethylaniline, and the picosecond transient absorption of reaction products. To understand the role of solvent dynamics and intramolecular motion in ET, it is important to study the time dependence of the reaction in detail. Accurate measurements of fluorescence decay were made with xanthene and coumarin in aniline and N,N- dimethylaniline. We found ET rate in some cases determined directly by nuclear rearrangement and in the other cases by solvent relaxation dynamics. Most interestingly we found a substituent effect of ET in 7-aminocoumarins.

### III-A-1 Femtosecond Intermolecular Electron Transfer between Dyes and Electron-Donating Solvents

**Keitaro YOSHIHARA, Arkadiy YARTSEV, Yutaka NAGASAWA** *(Graduate Univ. for Advanced Studies),* **Hideki KANDORI, Abderrazzak DOUHAL, and Klaus KEMNITZ** *(Govern. Indust. Res. Inst.)*

[*Pure & Appl. Chem.* **65**, 1671 (1993)]

Ultrafast intermolecular electron transfer (ET) is discussed for the system of various xanthene dyes in diffusionless weakly polar electron donating solvents. ET was observed by fluorescence quenching dynamics. It gives a non-exponential process in case of dyes in aniline. ET rate is determined by mutual displacement of the reactants and by the solvent relaxation. In case of dyes in N,N-dimethylaniline, ET quenching gives very different dynamics and shows a single exponential decay with a rate constant as fast as $10^{13}s^{-1}$. Ultrafast ET, which is much faster than solvent relaxation process, requires a new mechanism for a cause of ET and its rate constant may be determined by nuclear motion, rather than controlled by solvent dynamics as shown with two dimensional description of potential energy surfaces in Figure 1.

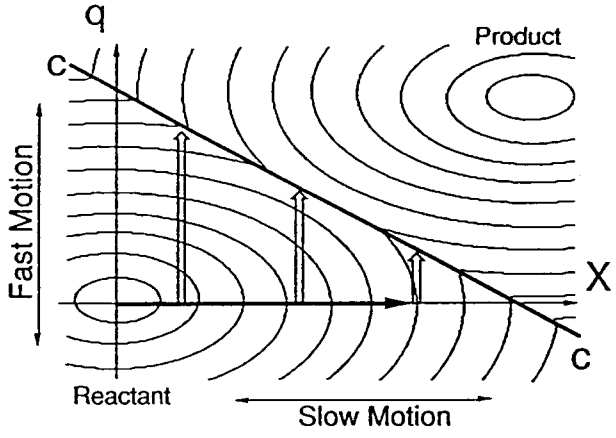


**Figure 1.** Two dimensional description of the free energy potential surface for the reaction. The reactant and product surface intersect on Curve C.

### III-A-2 Solvent and Nuclear Dynamics in Ultrafast Intermolecular Electron Transfer in a Diffusionless, Weakly Polar System

**Arkadiy YARTSEV, Yutaka NAGASAWA** *(Graduate Univ. for Advanced Studies),* **Abderrazzak DOUHAL, and Keitaro YOSHIHARA**

[*Chem. Phys. Lett.* **207**, 546 (1993)]

Femtosecond intermolecular electron (ET) transfer dynamics were studied by time-resolved fluorescence up-conversion technique in contact systems of oxazine dyes in electron-donating solvents. Clearly non-exponential ET time dependence was observed in aniline as shown in Figure 1 and explained by the effects of both solvent reo-

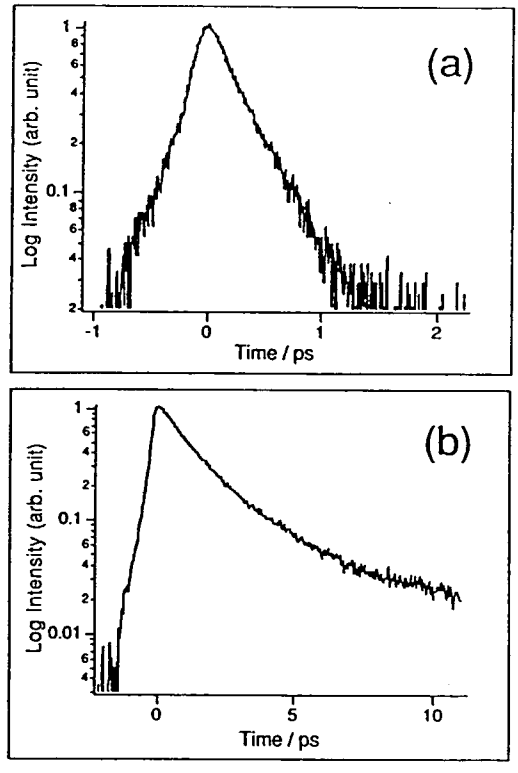


**Figure 1.** Fluorescence decays of oxazine 1 in (a) N,N-dimethylaniline and (b) aniline, pumped at 605 nm and probed at 725 nm.

rientation and nuclear motion of the reactants. Single exponential processes were measured for the nile blue (< 160 fs) and oxazine 1 (> 280 fs) in N,N-demethylaniline. The rate of ET is explained to be limited only by ultrafast nuclear relaxation.

### III-A-3 Substituent Effects on Intermolecular Electron Transfer: Coumarins in Electron Donating Solvents

**Yutaka NAGASAWA** *(Graduate Univ. for Advanced Studies)*, **Arkadiy YARTSEV, Keisuke TOMINAGA, Alan E. JOHNSON, and Keitaro YOSHIHARA**

[*J. Am. Chem. Soc.* **115**, 7922 (1993)]

Substituent effects on intermolecular electron transfer (ET) were found with the systems of 7-aminocoumarins as electron acceptors and anilines as electron donating solvents. Extending the alkyl chain on the 7-amino group and formation of a hexagonal ring with the benzene moiety reduce the rate of ET from a few hundred femtoseconds to several tens of picosecond as shown in Figure 1. This effect was explained by a change in the free energy difference of the reaction. The vibrational motion of the amino group was also considered as a possible cause of the reaction.

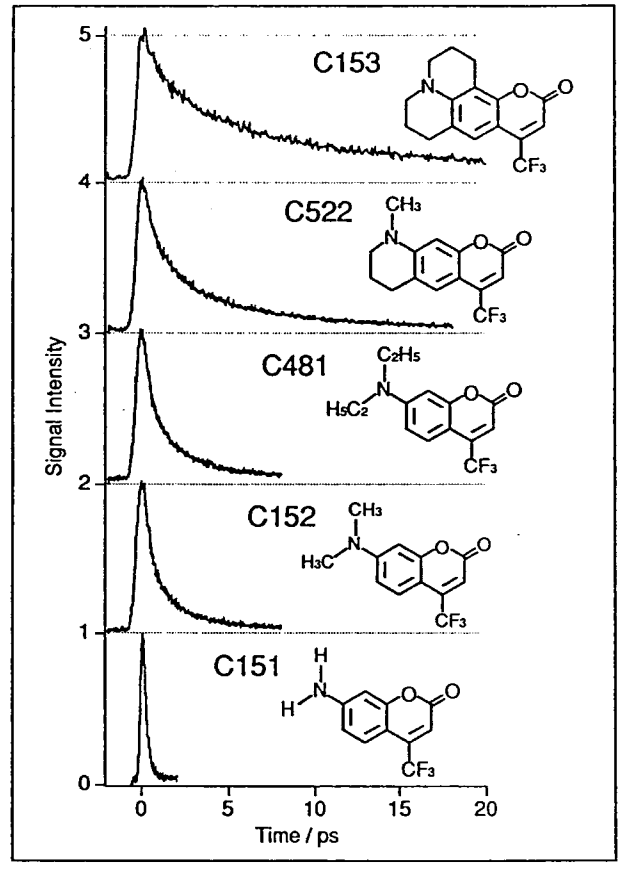


**Figure 1.** Fluorescence decays of coumarins in N,N-dimethylaniline, pumped at 390 nm and probed at 510 nm.

## III—B Applications of Femtosecond Time-Resolved Coherent Anti-Stokes Raman Scattering and Raman Echo

Vibrational phase relaxation (dephasing) is a fundamental physical process of molecular dynamics and has recently attracted considerable attention. Both experimental and theoretical studies have been performed to understand microscopic processes of vibrational dephasing. Developments in ultrafast spectroscopy enable us to obtain direct time-domain information on molecular vibrational dynamics. We have constructed a femtosecond time- resolved coherent anti-Stokes Raman scattering (CARS) measuring system, with an overall time resolution of less than 100 fs. This system has been used to study vibrational dephasing of molecules in liquids and solutions. Here we report femtosecond time- resolved CARS for C≡C stretching vibration of various alkynes ($C_nH_{2n+1}C{\equiv}C$) and dialkylacetylenes ($C_nH_{2n+1}C{\equiv}CC_mH_{2m+1}$). From the results obtained for these two series of acetylenes, we discuss intramolecular and intermolecular contributions to vibrational dephasing. We also studied alkanenitriles ($C_nH_{2n+1}C{\equiv}N$) systematically with a great variety of n(n=1 ~ 17). We have extended our work to obtain rotational correlation function with polarized CARS method. Finally we were successful in observing Raman echo signal from benzonitrile and discussed the main cause of vibrational line broadening.

### III-B-1 Femtosecond Time-Resolved Coherent Anti-Stokes Raman Scattering of the C≡C Stretching in Liquid Alkynes

**Ryoji INABA** *(Univ. of Tokyo and IMS)*, **Hiromi OKAMOTO** *(Univ. of Tokyo)*, **Keitaro YOSHIHARA, and Mitsuo TASUMI** *(Univ. of Tokyo)*

[*J. Phys Chem.* **97**, 7815 (1993)]

Femtosecond time-resolved coherent anti-Stokes Raman scattering has been observed for the C≡C stretching of alkynes (monoalkylacetylenes and dialkylacetylenes) as shown in Figure 1. The dephasing of the C≡C stretching of $C_3H_7C{\equiv}CH$ is found to be accelerated in mixtures with either proton-donors or proton-acceptors. The dephasing rates of the C≡C stretching of monoalkylacetylenes ($C_nH_{2n+1}C{\equiv}CH$) with relatively long alkyl chains ($n{\geq}4$) are nearly the same, and are accelerated in mixtures with dimethylformamide regardless of the length of the alkyl chain. On the other hand, the dephasing in dialkylacetylenes is not accelerated in mixtures with dimethylformamide, reflecting the absence of hydrogen bonding between dialkylacetylenes and dimethylformamide.

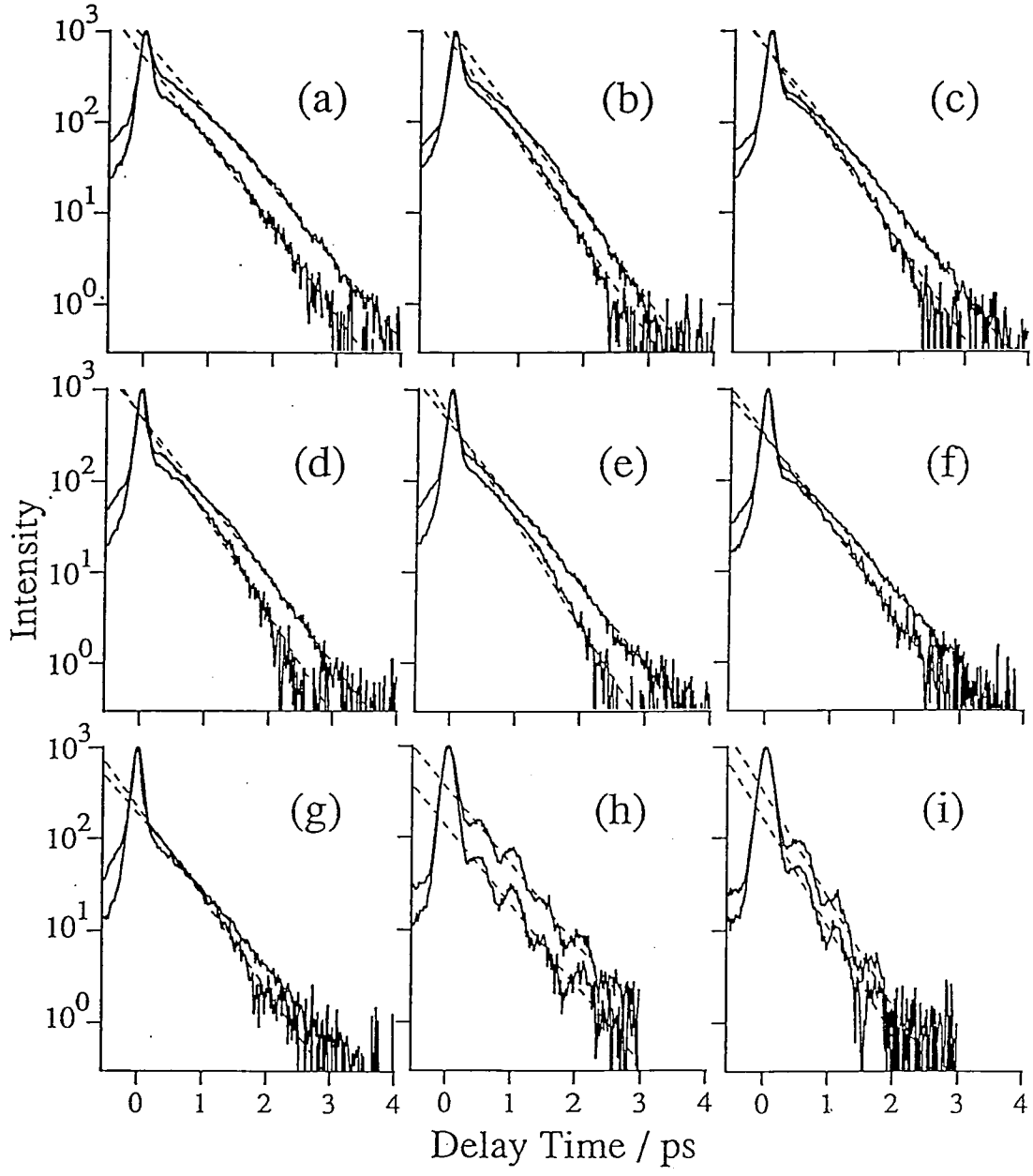


**Figure 1.** Time-resolved CARS for the C≡C stretching of alkynes in the neat state (upper trace in each panel) and in mixtures with DMF (lower trace); (a) $C_3H_7C{\equiv}CH$; (b) $C_4H_9C{\equiv}CH$; (c) $C_5H_{11}C{\equiv}CH$; (d) $C_6H_{13}C{\equiv}CH$; (e) $C_7H_{15}C{\equiv}CH$; (f) $C_8H_{17}C{\equiv}CH$; (g) $C_{10}H_{21}C{\equiv}CH$ (h) $CH_3C{\equiv}CC_2H_5$; (i) $C_3H_7C{\equiv}CC_3H_7$. The mole fraction is 50% in each mixture.

## III-B-2 Femtosecond Vibrational Dephasing of the C≡N Stretching in Alkanenitriles with Long Alkyl Chains. Dependence on the Chain Length and Hydrogen Bonding

**Hiromi OKAMOTO** *(Univ. of Tokyo)*, **Ryoji INABA** *(Univ. of Tokyo and IMS)*, **Keitaro YOSHIHARA**, and **Mitsuo TASUMI** *(Univ. of Tokyo)*

[*Chem. Phys. Lett.* **206**, 386 (1993)]

Femtosecond time-resolved coherent anti-Stokes Raman Scattering has been observed for the C≡N stretching vibration of alkanenitriles ($C_nH_{2n+1}CN$, n=1–17). The vibrational dephasing rates ($1/T_2$) observed for the neat alkanenitriles are proportional to the square root of the number of carbon atoms (n) in the alkyl chain. The dephasing rates observed for mixtures of the alkanenitriles with methanol (1:1 mole ratio) are about 30% faster than those for the corresponding neat alkanenitriles as shown in Table 1. Possible origins of this acceleration in the dephasing rate are discussed.

**Table 1.** Dephasing times ($T_2$) and frequencies ($\nu$) of the C≡N stretching of alkanenitriles

| Molecule | $T_2$/ps Neat liquid | $T_2$/ps Mixture with methanol (50 mole %) | $\nu$/cm$^{-1}$ Neat liquid |
|---|---|---|---|
| $CH_3CN$ | 2.57 | 1.69 | 2253 |
| $C_2H_5CN$ | 1.74 | 1.30 | 2246 |
| $C_5H_{11}CN$ | 1.06 | 0.72 | 2246 |
| $C_7H_{15}CN$ | 0.64 | 0.46 | 2247 |
| $C_8H_{17}CN$ | 0.64 | 0.42 | 2246 |
| $C_{10}H_{21}CN$ | 0.54 | 0.38 | 2247 |
| $C_{11}H_{23}CN$ | 0.54 | 0.36 | 2246 |
| $C_{14}H_{29}CN$ | 0.44 | 0.30 | 2247 |
| $C_{17}H_{35}CN$ | 0.34 | 0.26 | 2246 |

## III-B-3 Femtosecond Time-resolved Polarized Coherent Anti-Stokes Raman Studies on Reorientational Relaxation in Benzonitrile

**Hiromi OKAMOTO** *(Univ. of Tokyo)*, **Ryoji INABA** *(Univ. of Tokyo and IMS)*, **Keitaro YOSHIHARA**, and **Mitsuo TASUMI** *(Univ. of Tokyo)*

[*Chem. Phys. Lett.* **202**, 161 (1993)]

Femtosecond time-resolved polarized coherent anti-Stokes Raman scattering has been observed for the C≡N stretching vibration of benzonitrile in the neat liquid and in mixtures of benzonitrile and other liquid compounds. From isotropy and anisotropy measurements, rotational correlation functions has been determined directly in the time domain. In addition to a picosecond decay component, a faster decay component has been found in the case of neat benzonitrile as shown in Figure 1. This component is ascribed to non-dissipative free motion of molecule in liquid. For picosecond component, the Stokes-Einstein relation applies to low-viscosity mixtures of benzonitrile and other liquid compounds, but not to high-viscosity ones.

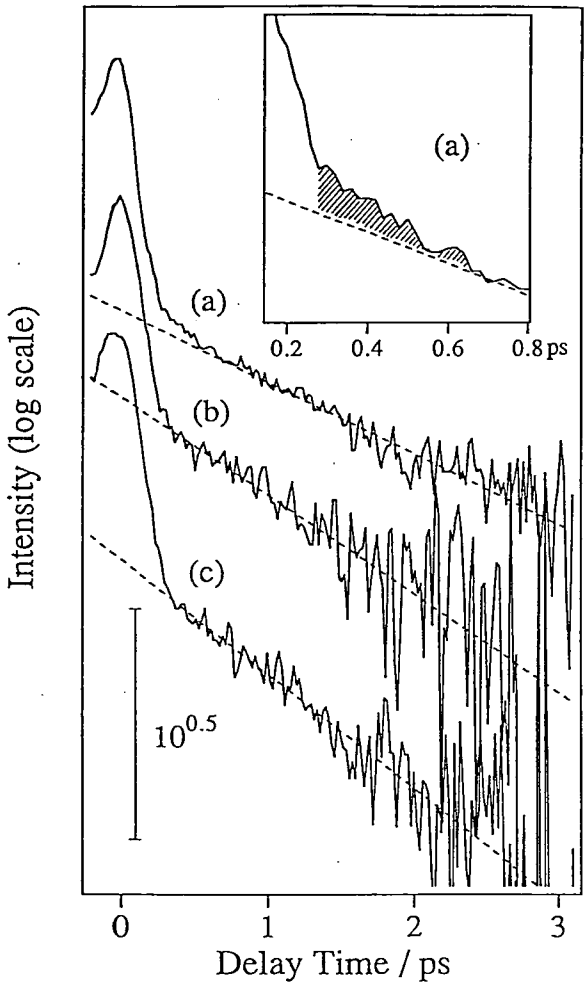


**Figure 1.** Correlation functions obtained by dividing the [90°, 0°, 90°] traces by the [0°, 54.7°, 54.7°] trace. (a)Neat benzonitrile, (b)benzonitrile + 1-pentanol (50:50 mole ratio), and (c) benzonitrile + benzene (50:50 mole ratio). The decay time constants ($=\gamma_{OR}/2$) obtained are (a)2.29 ps (b)2.00 ps, and (c)1.87 ps.

## III-B-4 Observation of Homogeneous Vibrational Dephasing in Benzonitrile by Ultrafast Raman Echoes

**Ryoji INABA** *(Univ. of Tokyo and IMS)*, **Keisuke TOMINAGA**, **Mitsuo TASUMI** *(Univ. of Tokyo)*, **Keith A. NELSON** *(MIT and IMS)*, and **Keitaro YOSHIHARA**

[*Chem. Phys. Lett.* **211**, 183 (1993)]

Raman echo is induced by exciting seventh order nonlinear susceptibility of matter, as shown in Figure 1, and is applicable to separate homogeneous in inhomoheneous contributions to the vibrational dephasing processes.[1] Raman echoes are observed for the C≡N stretching of benzonitrile in the liquid phase. It is found that the vibrational line broadening of C≡N stretching is mainly due to homogeneous effect. Experimental method involving amplified ultrafast laser pulses of two colors at high repetition rate and phase sensitive detection of echo signal is described.

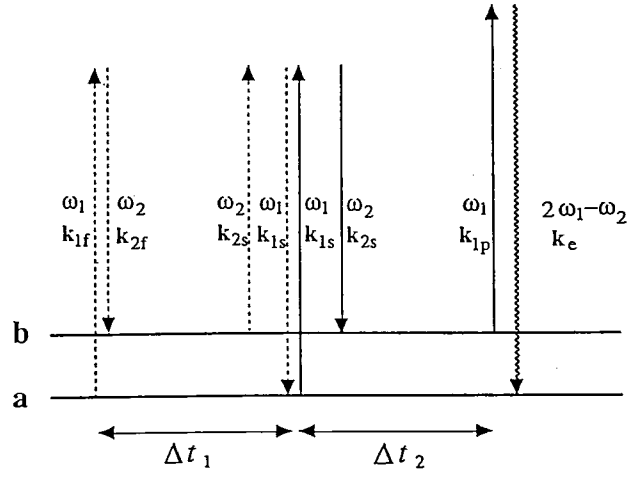


**Figure 1.** Energy and time evolution diagram of the Raman echo. Time elapses from left to right. The longitudinal solid and broken arrows represent the ket- and bra-side dipole transitions, respectively. The wavy arrow indicates the light emitting transition by the induced polarization.

**Reference**

1) R.R. Loring and S. Mukamel, *J. Chem. Phys.* **83**, 2116 (1985).

# III—C Development of Ultrafast Spectroscopic Methods

It is generally recognized that many elementary processes in chemical reactions and molecular dynamics fall into picosecond to femtosecond timescale. Development of ultrafast spectroscopic techniques enables us to observe these phenomena in real time. We have been developing suitable ultrafast measuring systems for research subjects described in section III. We have developed a spectrometer for Raman echo measurement in order to investigate liquid dynamics and structure.

## III-C-1 Femtosecond Raman Echo Spectrometer

**Ryoji INABA** *(Univ. of Tokyo and IMS)*, **Keisuke TOMINAGA, Mitsuo TASUMI** *(Univ. of Tokyo)*, **Keith A. NELSON** *(MIT and IMS)*, **and Keitaro YOSHIHARA**

[*Chem. Phys. Lett.* **211**, 183 (1993)]

A home made CW mode-locked Nd:YAG laser, picosecond and femtosecond dye lasers were used for the basic light pulses. Since the Raman echo is a seventh-order nonlinear process (III-B- 4), the light pulses are amplified with dye amplifiers which are excited by a copper-vapor laser at a repetition rate of 6kHz. The pulse energy of the red picosecond light obtained is as high as 5$\mu$J/pulse (gain ~ 10,000) and that of the orange femtosecond light is 0.7$\mu$J/pulse (gain ~1,000). All the beams are introduced to a sample to match the interacting light pulses temporally and spatially and most importantly to fulfill the momentum conservation geometry. In order to separate the Raman echo from the CARS signals (3rd. order nonlinear process), $\mathbf{K}_{1f}$ and $\mathbf{k}_{1s}$ (see III-B-4) beams are mechanically chopped with frequencies of $f_f$=840Hz and $f_s$=700Hz, respectively, by a dual chopper wheele. The Raman echo signal is modulated at 140 Hz and observed in the direction of $\mathbf{k}_{1p}+2(\mathbf{k}_{1s}-\mathbf{k}_{2s})-(\mathbf{k}_{1f}-\mathbf{k}_{2f})$. The echo signals are detected by varying $\Delta t_1$ or $\Delta t_2$ by fixing the other one with some delays. The whole experimental setup is shown in Figure 1.

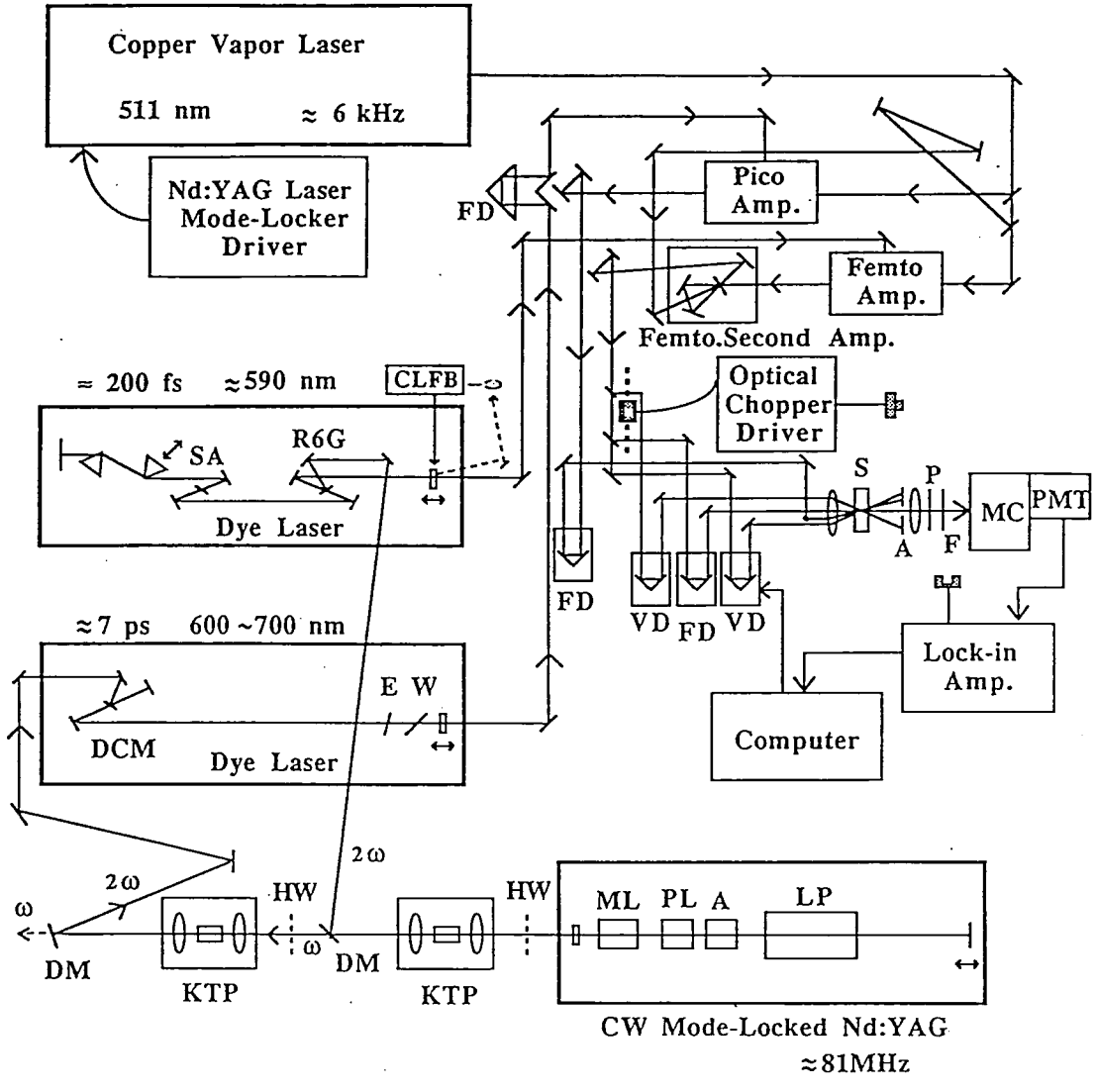


**Figure 1.** Block diagram of the ultrafast Raman-echo experiment system: ML, mode-locker; PL, polarizer; A, aperture; LP, laser pot; HW, half-wave plate; DM, dichroic mirror; R6G, rhodamine 6G; SA, saturable absorber; CLFB, cavity length feedback system; W, tuning wedge; E, ethalon; FD, fixed delay; VD, variable delay; BS, beam splitter; F, filter; S, sample; P, polarizer; MC, monochromator; PMT, photomultiplier.

# III—D Spectroscopy and Reaction Dynamics of Alkali Metal Dimers

Alkali metal dimer is one of the simplest molecules with only two valence electrons. Because of its simplicity, it has attracted much attention from the molecular spectroscopists as well as theoreticians. Theoretical treatment of alkali dimers is much simpler than those for other diatomics. Alkali dimers provide a good system to study the perturbations and photodissociation dynamics of the excited states. When sufficient energy is provided, it can dissociate into fragments that have nonzero angular momentum through many different channels. Therefore, the collision processes of open shell atoms can be investigated from the spectroscopy of alkali dimers. By applying the resonance enhanced two photon ionization (RE2PI) technique and mass spectrometry to a very cold molecular beam of alkali dimers, new information on the molecular structure and dissociation dynamics of the homonuclear and heteronuclear alkali dimers is obtained.

## III-D-1 Triplet-Triplet Transition of $Cs_2$ Studied by Multiphoton Ionization Spectroscopy in a Very Cold Pulsed Molecular Beam

**Bongsoo KIM and Keitaro YOSHIHARA**

[*Chem. Phys. Lett.* **204**, 407 (1993)]

The (2) $^3\Pi_g \leftarrow X\ ^3\Sigma_u^+$ transition of $Cs_2$ is observed in a very cold pulsed molecular beam using resonance enhanced two photon ionization method. Because of the very low temperature in the supersonic beam, the triplet ground state of $Cs_2$ is generated in high concentrations. The spectral positions and relative intensities of our observed vibrational bands show significant differences from those observed by the laser induced fluorescence experiment.[1] The term values of the substates of (2) $^3\Pi_g$ state are determined to be $T_e$ = 14121.0 ± 0.1, 14013.2 ± 0.1, 13912.9 ± 0.1, and 13909.4 ± 0.1 $cm^{-1}$ for the $2_g$, $1_g$, $0_g^+$, and $0_g^-$ state, respectively. These term values agree well with the theoretical predictions.

**Reference**

1) U. Diemer, J. Gress, and W. Demtröder, *Chem. Phys. Lett.* **178**, 330 (1991).

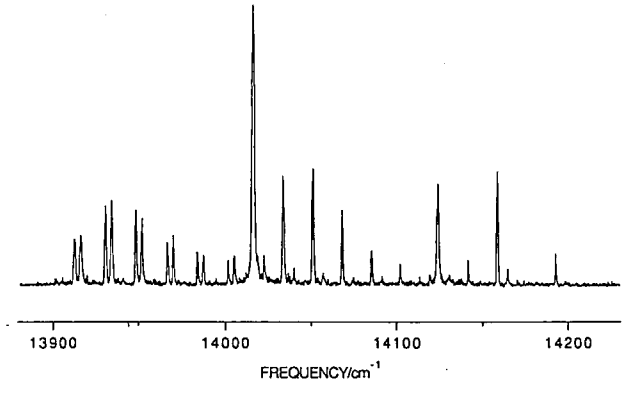


**Figure 1.** The (2) $^3\Pi_g \leftarrow$ x $^3\Sigma_u^+$ transition of $Cs_2$, obtained by RE2PI method. Cs vapor is expanded with 1.2 atm of Ar.

## III-D-2 The 480 nm System of $Cs_2$ Studied in a Very Cold Molecular Beam: Direct Observation of a New E″ and the Ion-Pair States

**Bongsoo KIM and Keitaro YOSHIHARA**

[*J. Chem. Phys.* **98**, 5990 (1993)]

The 480 nm absorption system of $Cs_2$ is studied in a molecular beam using the resonance enhanced two photon ionization method. The main goal of this experiment is to identify the ion- pair state predicted by Tellinghuisen et al.,[1] from which continuously tunable lasing at 500 − 600 nm might be obtained. By employing a very cold beam of $Cs_2$ and the RE2PI technique, the ion-pair state ($O_u^+$) is directly observed for the first time. The rotational constant is estimated to be about 0.003 $cm^-$ by the simulation of rotational contours. The avoided crossing of the E $^1\Sigma_u$ and ion pair states is observed near 20752 $cm^-$. Previously observed E′ $^1\Pi_u$ state is not detected at the expected positions. Instead, we observe another new electronic state, E″, in the range of 470 − 480 nm.

**Reference**

1) J. Tellinghuisen, G. Pichler, W. L. Snow, M. E. Hillard, and R. J. Exton, *Chem. Phys.* **50**, 313 (1980).

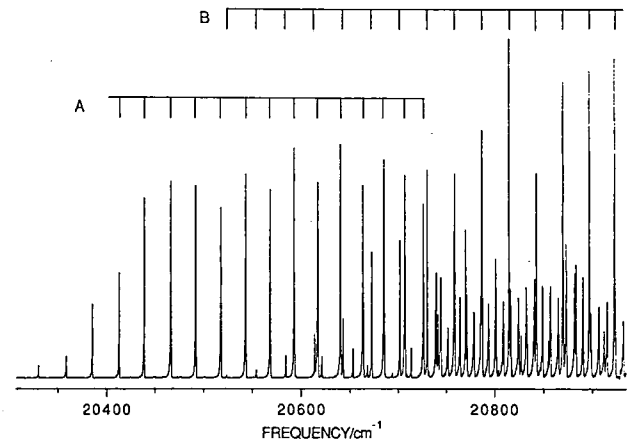


**Figure 1.** RE2PI spectrum of $Cs_2$. $Cs_2$ was expanded with 1 atm of Kr. The vibrational temperature is lower than 5 K and the rotational temperature ($T_r$) is about 0.5 K.

## III-D-3 Multichannel Quantum Interference in the Predissociation of $Cs_2$: Observation of q-Reversal in a Complex Resonance.

**Bongsoo KIM and Keitaro YOSHIHARA**

[*J. Chem. Phys.* **99**, 1433 (1993)]

State-specific photofragment yield spectrum is obtained in the 580 mm system of $Cs_2$ by monitoring Cs (6 $^2P_{3/2}$). Strongly asymmetric line shapes are observed and interpreted as being due to resonances. We observe a gradual sign change of the Fano line shape parameter, as is called "q- reversal", for the first time in predissociation. Some of other lines show complex line shapes that cannot be fitted by a usual Beutler-Fano profile. These complex line shapes may be attributed to the interfering resonances.

The rich features observed in the complex resonances of $Cs_2$ contain a wealth of dynamical information about the exact shapes of potential energy curves, curve crossings, and interchannel couplings, because the line shapes are the direct results of the quantum interference between coupled channels. They should provide a good touchstone for the theoretical studies of the resonances.

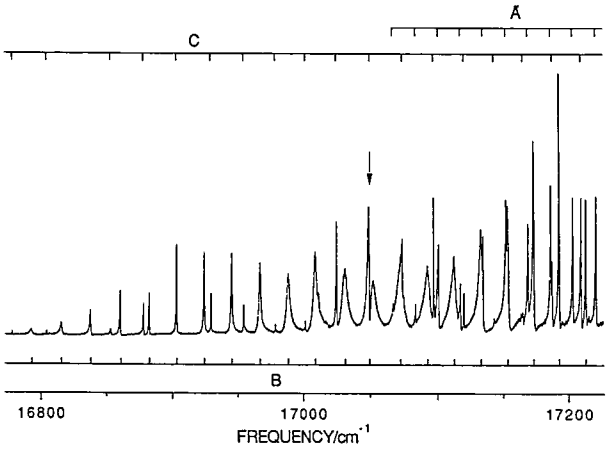


**Figure 1.** Photofragment yield (PFY) spectrum of $Cs_2$ as a function of the frequency of the photodissociating laser. Cs ($6^2P_{3/2}$) atoms are monitored by the single photon ionization and TOF mass spectrometry. The wavelength of the ionizing laser is 507 nm. The arrow shows a feature which cannot be described by a single Beutle-Fano profile.

## III-D-4 $^3\Delta - {}^1\Sigma^+$ Transition of RbCs Observed in a Very Cold Molecular Beam

**Bongsoo KIM and Keitaro YOSHIHARA**

[*Chem. Phys. Lett.* **212**, 271 (1993)]

A new excitation band of RbCs is observed near 605 nm in a very cold molecular beam using the resonance enhanced two photon ionization (RE2PI) method. From the rotational contour analysis and comparison with ab initio calculations, the new excitation band is assigned to the (1) $^3\Delta$ ($\Omega$=1) $-$ $X^1\Sigma^+$ transition. We determine the term value as $T_e$=16481.65 $\pm$ 0.15 cm$^{-1}$ and the dissociation energy as $D_e$=1862.8 $\pm$ 1.2 cm$^{-1}$.

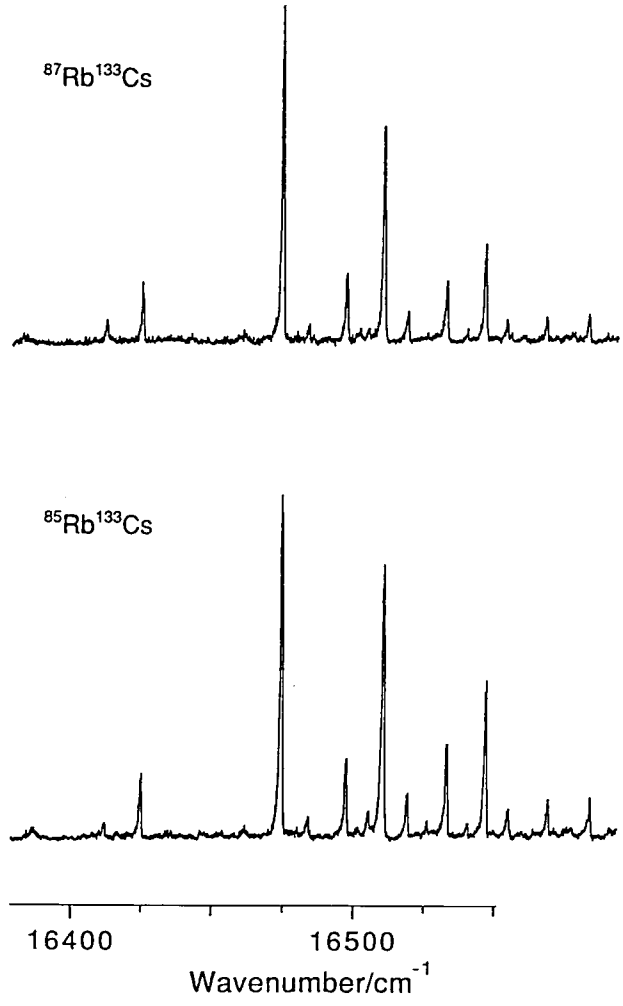


**Figure 1.** RE2PI spectrum of RbCs, which corresponds to the (2) $^1\Pi$ $-$ X $^1\Sigma^+$ transitions. The upper trace is the spectrum of $^{87}Rb^{133}Cs$ and the lower one is that of $^{85}Rb^{133}Cs$.

## III-D-5 Resonance Enhanced Two Photon Ionization Spectroscopy of RbCs in a Very Cold Molecular Beam

**Bongsoo KIM and Keitaro YOSHIHARA**

[*J. Chem. Phys.* in press]

Resonance enhanced two photon ionization spectrum of RbCs is obtained in a very cold molecular beam by using a high temperature pulsed nozzle. We observe three electronic states from the excitation spectrum in the range of 540 $-$ 590 nm. The excited electronic state that shows very long vibrational series is assigned to the (4) $^1\Sigma^+$ state. The absolute vibrational quantum numbers are determined from the isotopic shift of the vibrational energy. Rotational constants of several vibrational levels are determined in comparison with Fourier transform spectroscopic data reported previously. Another electronic state that shows a short and intense vibrational series is assigned to the (3) $^1\Pi$ state and the vibrational quantum numbers are determined. Term values and the vibrational frequencies of $^{85}$RbCs are determined as $T_e$=16628.6 $\pm$ 1cm$^{-1}$ and $\omega_e$=24.51 $\pm$ 0.2 cm$^{-1}$ for the (4) $^1\Sigma^+$ state and $T_e$=17418.9 $\pm$ 1 cm$^{-1}$ and $\omega_e$=22.53 $\pm$ 0.2 cm$^{-1}$ for the (3) $^1\Pi$ state.

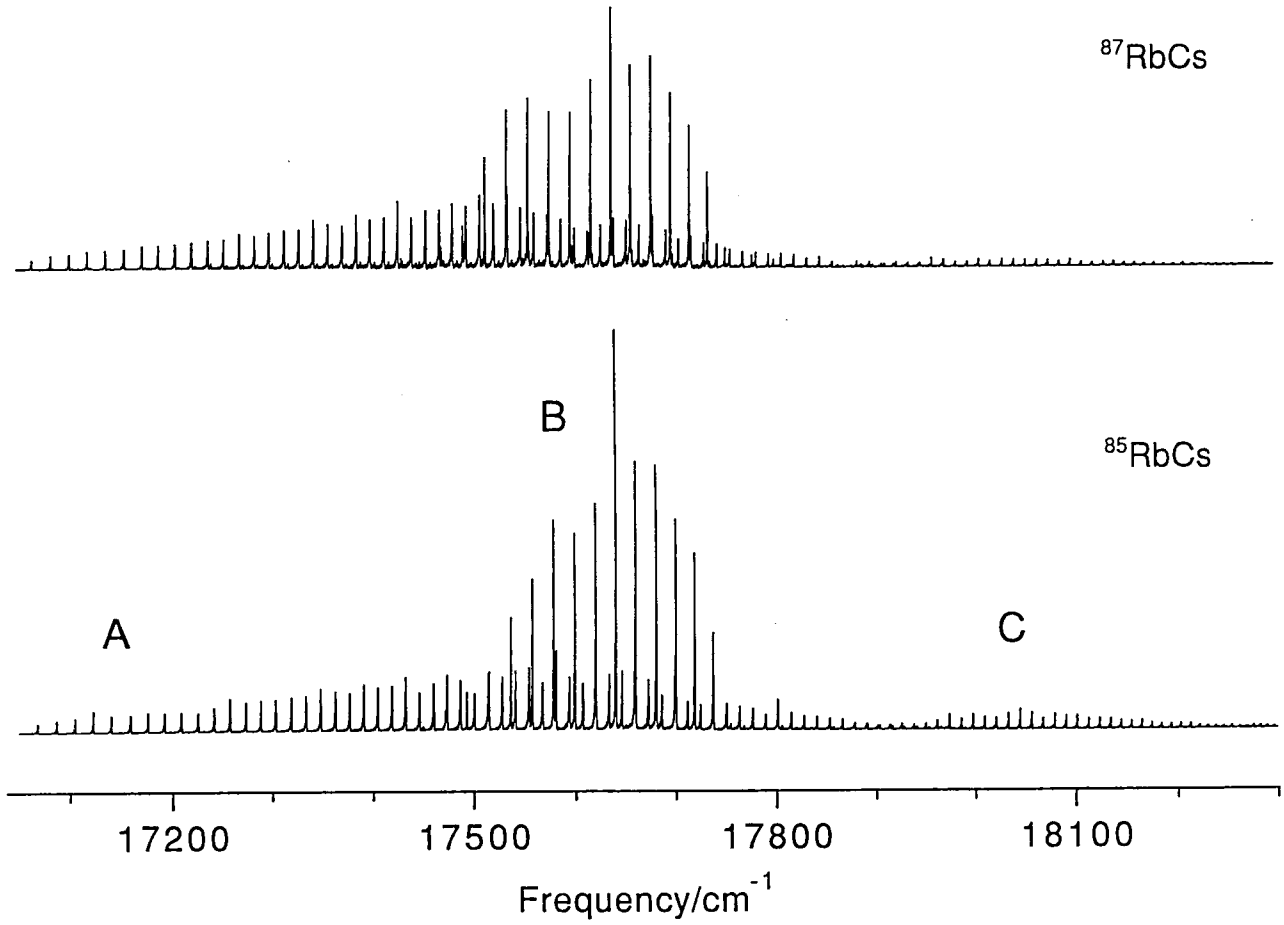


**Figure 1.** RE2PI spectrum of RbCs observed between 540 nm and 590 nm. The upper trace is the spectrum of $^{87}Rb^{133}Cs$ and the lower one is that of $^{85}Rb^{133}Cs$.

## III—E Excited-State Dynamics of Dye J-Aggregates

J-aggregate of dyes has a quasi-one dimensional molecular structure and drew a great deal of attention due to its interesting optical characteristics. A strong dipole-dipole interaction of monomeric dyes in J-aggregate, leading to formation of a sharp excitonic transition, causes delocalization of the optical excitation through many monomers. Some of the characteristics, namely, the sharp absorption spectra and high value of optical susceptibilities, are used or could be used in photographic films, nonlinear optical materials, sharp optical filters, etc. We have been studying the excited-state dynamics of J-aggregates on silver bromide crystals. This year we studied J-aggregate in solution, and clarified fluorescence spectral shift and broadening at a very low temperature and exciton dynamics at high pump intensities at room temperature.

### III-E-1 Time-Resolved Emission Spectra of BIC J-Aggregate at Low Temperature

**Valey F. KAMALOV, Irina A. STRUGANOVA, and Keitaro YOSHIHARA**

[*Chem. Phys. Lett.* **213**, 559 (1993)]

A red shift and broadening of the emission of BIC J- aggregate in glass were observed at low temperature (4.5 K) as shown in Figure 1. To explain the observation, the transformation of the excess excitation energy in the bath with disordering of the structure of molecular aggregate in proposed. The characteristic time of this energy transformation is 315 ps at 4.5 K for excess energy of 400 cm$^{-1}$. Another possible mechanism of exciton self-trapping by exciton-phonon interaction is discussed.

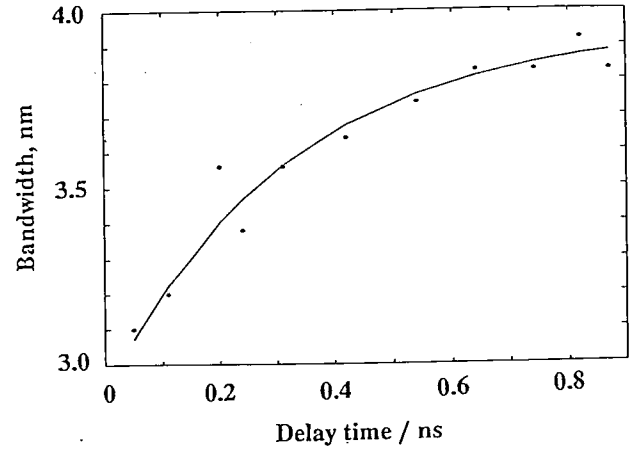


**Figure 1.** Kinetics of broadening of time-resolved emission spectra of J-aggregates at 4.5 K. Excitation wavelength is 582 nm. Solid line gives an exponential fit with time constant of 315 ps.

### III-E-2 Pump-Probe Spectroscopy and Exciton Dynamics of J-Aggregates at High Pump Intensities

**Alan E. JOHNSON** *(Univ. of Minnesota and IMS)*, **Shigeichi KUMAZAKI, and Keitaro YOSHIHARA**

[*Chem. Phys. Lett.* **211**, 511 (1993)]

We have measured the picosecond pump-probe spectra of BIC J-aggregates using a spectral continuum for the probe. The excitation pulses were intense ($10^{15} - 2 \cdot 10^{16}$ photons/cm$^2$) and created many excitons per aggregate. The observed dynamics are intensity dependent and reflect exciton-exciton annihilation processes. In addition, the zero time spectrum is also intensity dependent. In particular, the observed strength and position of the negative going signal (combination of stimulated emission and ground state bleach) and of the positive going signal (excited state absorption) both depend on excitation intensity, as shown in Figure 1. From an analysis of the intensity dependence and time dependence of the pump-probe spectra, we show that the absorption spectrum of an aggregate with multiple excitons is very similar to the ground state aggregate spectrum. A qualitative theoretical treatment indicates that an aggregate with multiple excitons should have an absorption spectrum similar to a ground state aggregate, in agreement with experiment. This has important consequences for resonant four wave mixing processes in J-aggregate, since multiple exciton states can participate.

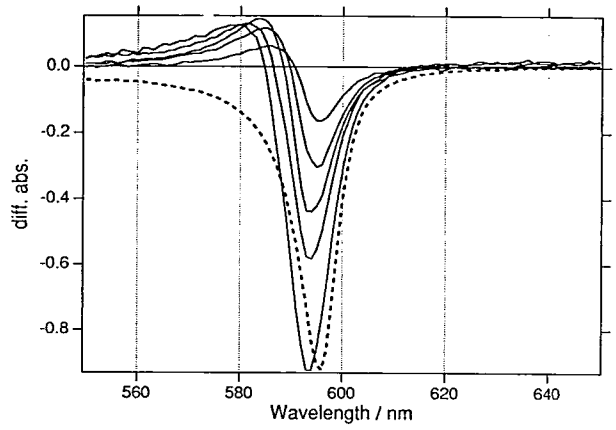


**Figure 1.** Zero time pump-probe spectra of BIC J-aggregates as a function of pump intensity. With increasing intensity, the negative going signal increases in intensity and shifts to higher energy. The dashed line in the figure is the static absorption spectrum, inverted for comparison purposes.

## III—F Primary Processes in Photosystem I Reaction Center Complex

A recent X-ray crystallographic study indicates that the arrangement of functional components in the electron transfer chain in Photosystem I (PS I) is different from that in Photosystem II or in purple bacteria, which seems to reflect the situation that the reaction center polypeptides of PS I have almost no homology to those of the other two systems. This means that detailed kinetic measurements in PS I provide a new test-bed for various electron transfer theories which have tried to describe the efficient energy conversion in photosynthetic systems.

### III-F-1 Picosecond Reduction and Oxidation Kinetics of Primary Electron Acceptor Chlorophyll ($A_0$) in Green Plant Photosystem I Reaction Center Which Contains Different Secondary Acceptor Quinones

**Shigeichi KUMAZAKI, Masayo IWAKI** *(NIBB)*, **Isamu IKEGAMI** *(Teikyo Univ.)*, **Hideki KANDORI** *(Riken and IMS)*, **Keitaro YOSHIHARA, and Shigeru ITOH** *(NIBB)*

The primary photochemical events are studied by picosecond transient absorption spectroscopy with 1 ps time resolution with the photosystem I reaction center, in which the intrinsic electron acceptor phylloquinone is depleted and replaced by different quinones. The electron transfer process from the primary electron donor chlorophyll dimer (P700) to the primary electron acceptor chlorophyll-a-686 ($A_0$), and to the secondary acceptor quinone ($Q_\phi$) was measured for the first time sequentially in the same sample under the same experimental condition. After excitation at 605 nm a depletion of ground state of P700 was observed at 696 nm within 1 ps. A bleach of $A_0$ at 685 nm rose with a time constant of 6.5 ps and remained for more than 800 ps in the absence of $Q_\phi$. Reconstitution of menaquinone-4 or phylloquinone as $Q_\phi$ induced a decay of $A_0^-$ with a time constant of 38 ps or 67 ps, respectively. When 2-methyl-1,4-naphtoquinone was reconstituted as $Q_\phi$, $A_0^-$ decay showed a time constant of 315 ps. This series of kinetic measurements with varying redox potentials of quinones will provide a unique method for studying the mechanism of highly efficient electron transfer in photosynthetic reaction center proteins.

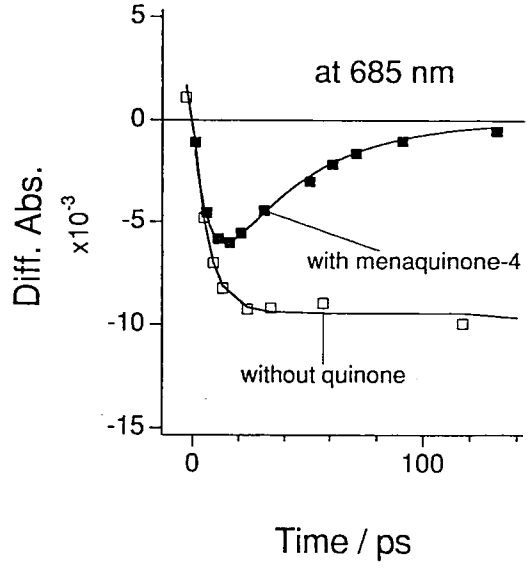


**Figure 1.** Time course of absorbance change at 685 nm proportional to the concentration of $A_0^-$ estimated in the particles with chlorophylls/P700 ratio of ~30. Closed squares, menaquinone-4-reconstituted particles; open squares, phylloquinone-depleted particles. Lines indicate fitting curves to data points.

# III—G Photochemistry on Well-defined Surfaces

Recently, it has been found that upon the irradiation of light from visible to ultraviolet, a number of adsorbed molecules on metal surfaces reveal variety of photochemical processes, including photo-stimulated desorption, rearrangement of adsorbed states, photodissociation, and photo-initiated reactions with coadsorbates. Since photo-initiated reactions can be induced without any thermal activation of reactants, various combinations of coadsorbates can be prepared at sufficiently low surface temperatures. Thus, this provides a method for studying a new class of surface reactions which may not be induced thermally. In the last year, we studied photochemistry of adsorbates on well-defined solid surfaces mainly by temperature-programmed desorption (TPD). In this year we have succeeded to measure translational energy distributions of desorbed species produced in the photochemical processes by using time-of-flight (TOF) spectroscopy. These measurements provide more detailed information on the reaction mechanisms and reaction dynamics. Furthermore, we have found that energetic atomic species produced at a surface via photodissociation of precursor molecules react with coadsorbates. The experimental results indicate that the dynamics of the photo-initiated reaction is quite different from that of the Langmuir-Hinshelwood type widely observed in thermal reactions.

## III-G-1 Photochemistry and Photodissociation Dynamics of $N_2O$ on Pt(111)

**Kyoichi SAWABE and Yoshiyasu MATSUMOTO**

[*Surf. Sci.* **283**, 126 (1993)]

Photochemistry of $N_2O$ adsorbed on a Pt(111) surface at 193 nm has been studied by temperature-programmed desorption (TPD) and time-of-flight distribution (TOF) analysis.[1] Upon the irradiation of excimer laser pulses at 193 nm, adsorbed $N_2O$ molecules are either desorbed or dissociated to produce oxygen adatoms and nitrogen molecules in the gas phase. In addition, a small amount of adsorbed NO is found after the irradiation. Polarization and angle-of-incidence dependence of oxygen adatom yields suggests that the primary step of production of oxygen adatoms is dominated by electron transfer to adsorbed $N_2O$ from the bulk surface.

TOF measurements are useful for investigating not only what species are desorbed from the surface, but also how energetic the desorbed species are. The typical TOF distributions of desorbed molecules at m/e=29 ($^{14}N^{15}N$) and 45 ($^{15}N^{14}N^{16}O$) are shown in Figure 1. It should be noted that these TOF distributions consist of multiple peaks. The $N_2O$ and $N_2$ TOF distributions were analyzed with modified Maxwell-Boltzmann distribution functions. At least three velocity components were required for a satisfactory fit. The obtained values of the average translational energy for the components in $N_2O$ TOF distribution are 0.71, 0.26, and 0.07 eV. These results clearly indicate that the photodissociation and photo-stimulated desorption processes are nonthermal in origin. The possible origins of the multi-velocity components of $N_2$ and $N_2O$ can be the following: (1) different excitation mechanisms, i.e., the direct electronic excitation vs. the electron-transfer mechanism, (2) the involvement of different electronic states of $N_2O^-$, (3) secondary process caused by photofragments.

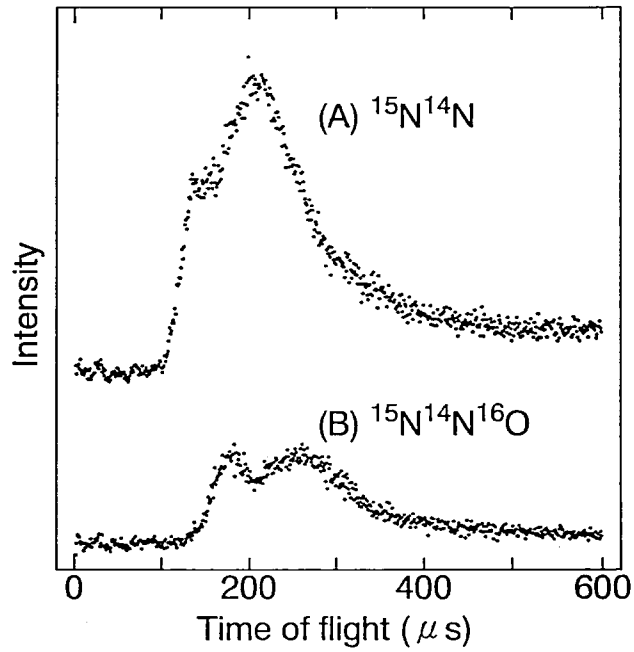


**Figure 1.** TOF distributions at (A) m/e=29 ($^{14}N^{15}N$) and (B) m/e=45 ($^{15}N^{14}N^{16}O$) obtained by 193 nm photon irradiation of Pt(111) with the saturated coverage of $^{15}N^{14}N^{16}O$.

## III-G-2 Dynamics of the Oxygen Combination Reaction on Pt(111) Initiated by Photodissociation of $N_2O$ at 193 nm: $O^*+O(ad)\rightarrow O_2(g)$

**Kyoichi SAWABE, Jihwa LEE, and Yoshiyasu MATSUMOTO**

[*J.Chem.Phys.* **99**, 3143 (1993)]

Photodissociation of molecules adsorbed on a solid surface gives rise to energetic photofragments that may further react with coadsorbed species. Hence, this provides a good opportunity for exploring the dynamics of fundamental surface reactions including radical combination and exchange reactions. We have found that an energetic oxygen atom produced via photodissociation of $N_2O$ adsorbed on Pt(111) reacts with a chemisorbed oxygen adatom before accommodating with the surface.

First, the surface was saturated with $^{18}O_2$ at 82 K and annealed to 170 K. This procedure served to make a p (2×2) lattice of $^{18}O$ adatoms. Then, the surface was saturated with $^{15}N^{14}N^{16}O$ at 82 K. Thereby the surface was covered with 0.25 ML of $^{18}O$ and 0.44 ML of $^{15}N^{14}N^{16}O$.

**Reference**

1) Y. Matsumoto, K. Sawabe, and J. Lee, *Proceedings of SPIE conference on "Laser techniques for state-selected and state-to-state chemistry"*, **1858**, 378 (1993).

After these procedures, the surface was irradiated with 193 nm photons and the desorbed species at the mass number of 34 ($^{18}O^{16}O$) along the surface normal was detected by the QMS. The coverage of $N_2O$ decreased to ~0.1 ML during the photon irradiation. Figure 1 shows a TOF distribution of $^{18}O^{16}O$ measured with a dwell time of 5 $\mu$s. This result clearly indicates that an oxygen atom produced by photodissociation of $N_2O$ reacts with a chemisorbed oxygen adatom to form an oxygen molecule; the produced $O_2$ is energetic enough to surmount the activation barrier for desorption, i.e., $O^* + O(ad) \rightarrow O_2(g)$. Here $O^*$ denotes an oxygen atom in the transition between the adsorbed and the gaseous state. The energetic oxygen atoms would travel a distance of the order of angstroms until they find pre-adsorbed oxygen to react. Thus, the dynamics of the combination reaction is closely related to that of Eley-Rideal processes rather than that of Langmuir-Hinshelwood processes.

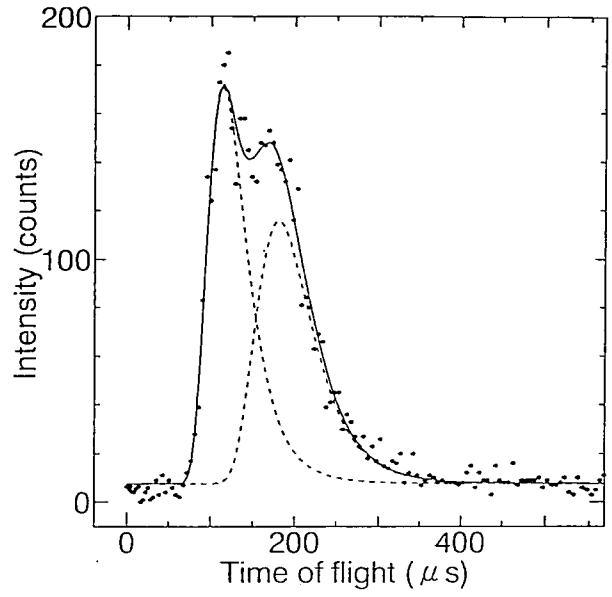


**Figure 1.** TOF distribution of $^{18}O^{16}O$ photoproduct taken at 193 nm for Pt(111) with 0.25 ML of $^{18}O$ and 0.44 ML of $^{15}N^{14}N^{16}O$. The dwell time of a multichannel scaler was 5 $\mu$s. The TOF distribution was corrected for ion drifting times in the QMS. The solid curve represents a fit by two modified Maxwell-Boltzmann distributions. The average translational energies of the fast and the slow components are 0.69 eV (4000 K) and 0.28 eV (1600 K), respectively.

## III—H Reactions of Coadsorbed Species on Well-defined Surfaces

Vast majority of surface reactions studied so far has been interpreted in terms of a Langmuir-Hinshelwood mechanism; reactants are first adsorbed on a surface and a reaction takes place between two chemisorbed species. Therefore, it is very important to investigate how reactions occur among coadsorbed species on a well-defined surface. For this purpose, coadsorbed species are prepared at sufficiently low surface temperatures and reactions are induced by annealing the surface. Here, we mainly focus on an important class of surface reactions, i.e. oxidation on metal surfaces. Although the reactivity of atomic oxygen has been thoroughly investigated, the role of molecular oxygen in oxidation reactions has been hardly known. Thus, in this year we have studied the reactivity of molecular oxygen with coadsorbed species on a platinum surface.

### III-H-1 Oxygen-exchange Reaction in $O_2$ and NO Coadsorbed on a Pt(111) Surface: Reactivity of Molecularly Adsorbed Oxygen

**Kyoichi SAWABE and Yoshiyasu MATSUMOTO**

[submitted to *Surf. Sci.*]

The oxygen-exchange reaction between $N^{16}O$ and $^{18}O_2$ coadsorbed on Pt(111) i.e., $N^{16}O + {}^{18}O_2 \rightarrow N^{18}O + {}^{16}O^{18}O$, has been studied by temperature-programmed desorption (TPD). Reaction products of $N^{18}O$ and $^{18}O^{16}O$ are desorbed from Pt(111) initially saturated with $^{18}O_2$ at 94 K followed by exposure of $N^{16}O$. Three distinct desorption peaks are observed in $N^{18}O$ TPD spectra at 145, 310, and 340 K, and two peaks in $^{18}O^{16}O$ at 155 K and between 600 and 1000 K. In contrast, the exchange reaction is greatly suppressed when oxygen molecules are replaced with oxygen adatoms. Therefore, it is very clear that oxygen atoms stabilized at three-fold hollow sites show little reactivity with NO.

The facile exchange reaction can be understood if $N^{16}O$ forms a complex with $^{18}O_2$ at 94 K. According to the coverage dependence of the overall-reaction yield, the simplest composition of the complex would be $NO_3$. In this case, $^{18}O$ atoms may be redistributed to fragment molecules in the process of thermal decomposition of the complex. Another possibility is the reaction between oxygen atoms with NO in the process of $O_2$ dissociation, since dissociation of molecular oxygen also takes place near the desorption temperature of NO. Although it is difficult to identify which mechanism dominates over the other solely by the TPD measurements, these results indicate that adsorbed oxygen molecules are responsible for the oxygen-exchange reaction.

## III—I Dynamical Processes in Electronically-and/or Vibrationally Excited Molecules

Fundamental molecular aspects of chemical reactions and energy transfer processes in the electronically or vibrationally excited states have been studied. Particular interest has been directed to the dynamics of vibrationally-excited weakly-

coupled complexes such as van der Waals and hydrogen-bonded complexes, and the "disproportionation" reaction caused by UV irradiation of the complexes. Dynamics of highly-excited vibrational states (local modes) and chemical reaction induced by their excitation have also been subjects of research.

### III-I-1 Stimulated-Emission-Pumping Laser-Induced-Fluorescence Spectroscopy of Phenol and Anisole

**Masao TAKAYANAGI and Ichiro HANAZAKI**

[*Laser Chem.*, in press]

The SEP-LIF (stimulated emission pumping-laser induced fluorescence) technique was applied to the investigation of dynamical behavior of vibrationally excited phenol and anisole produced in the supersonic expansion. In the SEP-LIF scheme, a molecule excited to a specific vibrational state by SEP is detected by measuring the LIF excitation spectrum with an appropriate delay to probe the vibrational relaxation. Four vibrational states, $6a_1$, $16a_2$, $12_1$ and $1_1$, of phenol, and six vibrational states, $18b_1$, $18b_2$, $6a_1$, $12_1$, $16a_2$ and $1_1$, of anisole were investigated. For both of phenol and anisole, it is found that the relaxation of the vibrational states below 1000 $cm^{-1}$ in the ground electronic state is so slow under the collisionless condition that only the transitions from the vibrational states initially prepared by SEP are observed as the SEP-induced bands in the SEP-LIF spectra. The low frequency torsional motion of methyl group in anisole does not accelerate IVR (intramolecular vibrational redistribution) much in this energy region.

### III-I-2 Geometry and Torsional Potential of 2,2′-Bithiophene in a Supersonic Jet

**Masao TAKAYANAGI, Tatsuo GEJO** *(Grad. Univ. Adv. Studies)*, **and Ichiro HANAZAKI**

Fluorescence-excitation, hole-burning and dispersed-fluorescence spectra of 2,2′-bithiophene in a supersonic jet were measured. Bands due to two species were observed in the fluorescence-excitation spectra. These species have the origin bands with the 91 $cm^{-1}$ shift to each other, and show almost the same vibronic structures. They are considered to be not due to the isomers of 2,2′-bithiophene around its single bond between the thiophene rings, but due to 2,2′-bithiophenes in the ground and low-lying excited vibrational states. Long and harmonic progressions due to the torsional vibration in the excited electronic state are observed in the LIF excitation spectra, suggesting a remarkable change of the torsional angle upon the electronic excitation. The equilibrium structure of 2,2′- bithiophene in the electronic excited state is considered to be *trans* planar. The torsional potential has a deep and harmonic single-minimum around the equilibrium structure. In the dispersed fluorescence spectra, short and unharmonic progressions due to the torsional vibration in the ground electronic state have been observed. By simulating the progressions observed in the dispersed fluorescence spectra, 2,2′-bithiophene in the ground electronic state is found to have a double minimum torsional potential, whose equilibrium structures are twisted by about 21° from the *trans* planar structure. The height of the barrier between the minima is estimated to be about 25 $cm^{-1}$.

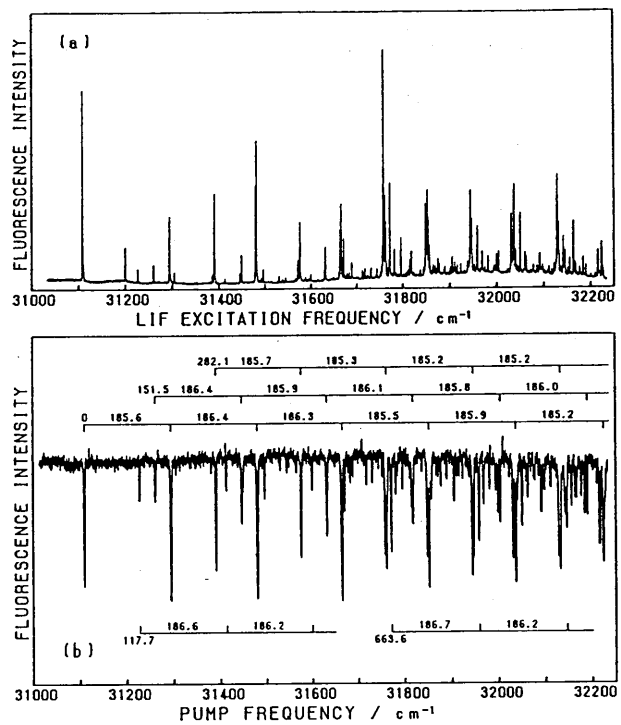


**Figure 1.** (a) LIF excitation and (b) hole-burning spectra of 2,2′-bithiophene in a supersonic jet. The latter is measured with the 31108 $cm^{-1}$ probe laser. The band at 31108 $cm^{-1}$ is the 0-0 band, while the band at 31199 $cm^{-1}$ observed in the LIF excitation spectrum is the origin band of 2,2′-bithiophene in the low-lying excited vibrational state. In both spectra, long and harmonic progressions due to the torsional vibration in the excited electronic state are observed.

### III-I-3 Reaction Dynamics of the 193 nm Photolysis of the $N_2O \cdot H_2O$ Complex

**Hong-Lae KIM** *(Kangweon National Univ.)*, **Masao TAKAYANAGI, and Ichiro HANAZAKI**

The reaction of $O(^1D)$ with $H_2O$ has been studied for the photolysis of the $N_2O \cdot H_2O$ van der Waals complex in a supersonic jet. The reaction has been initiated by irradiating the 193 nm laser light which dissociates the $N_2O$ moiety of the complex to produce $O(^1D)$. LIF excitation spectra of the product OH have been measured.

Figure 1 shows the part of the obtained spectrum. The product OH has been found to be vibrationally and rotationally much colder than that produced in the corresponding bimolecular reaction under the bulk condition.[1] The preference for the A′ state has been found for the $\lambda$-doublet fine state distribution. The $N_2O \cdot H_2O$ complex has been reported to have a planar structure in which $N_2O$ and oxygen atom in $H_2O$ form a T-shape.[2] The observed A′ preference suggests that the reaction proceeds via a planar insertion-type intermediate; The A′ preference cannot be accounted for by assuming the non-planar intermediate or the abstraction-type intermediate. The vibrationally and rotationally cold distribution would be attributed at least partly to the $N_2$ which takes away some of the available energy from the reaction intermediate as the internal or kinetic energy.

**References**
1) D. G. Sauder, J. C. Stephenson, D. S. King, and M. P. Casassa, *J. Chem. Phys.* **97**, 952 (1992).
2) D. Zolandz, D. Yaron, K. I. Peterson, and W. Klemperer, *J. Chem. Phys.* **97**, 2861 (1992).

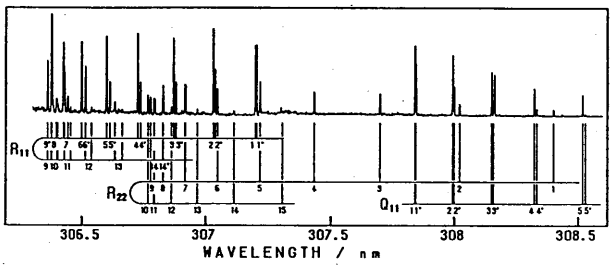


**Figure 1.** LIF excitation spectrum of OH($v$=0) produced by the photolysis of the $N_2O \cdot H_2O$ complex.

## III-I-4 Hole Burning Spectrum of the Vinoxy Radical in the $\tilde{B}$ ($^2A''$) State in a Supersonic Free Jet

**Tatsuo GEJO*, Takumi KONO*, Masao TAKAYANAGI, and Ichiro HANAZAKI** *(*Grad. Univ. Adv. Studies)*

[*Chem. Lett.*, 2065 (1993)]

Although the absorption spectrum in the $\tilde{B}$ ($^2A''$) state of the vinoxy radical consists of a series of vibronic progressions appearing between 350nm and 280nm, only four main bands near 0—0 band have been observed in the LIF excitation spectrum. The vibronic structure of the vinoxy radical in the $\tilde{B}$ ($^2A''$) state was investigated by the hole burning technique in a supersonic free jet. Several vibronic bands were observed as depletions in the hole burning spectrum, which cannot be observed in the LIF spectrum due to a rapid dissociation of the radical in the $\tilde{B}$ ($^2A''$) state. They are in agreement with the bands observed in the absorption spectrum but are obtained with higher resolution. Most of the observed vibronic bands are explained as combination bands of the $\nu_4$ ~ $\nu_9$ vibrational modes, in agreement with the previous caluculation.[1)]

**Reference**
1) M. Yamaguchi, T. Momose, and T. Shida, *J. Chem. Phys.* **93**, 4211 (1990).

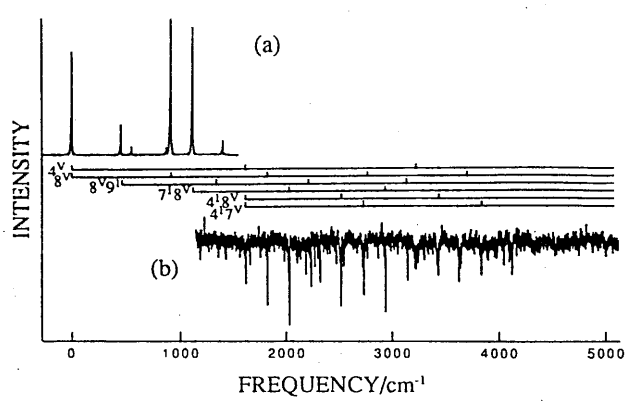


**Figure 1.** (a) LIF spectrum of the $\tilde{B}$ ($^2A''$)←$\tilde{X}$ ($^2A''$) transition of the vinoxy radical. The origin band locates at 28787cm$^{-1}$. (b) The hole burning spectrum of the vinoxy radical. The ordinate shows the fluorescence intensity.

## III-I-5 Photodissociation Dynamics of Acetaldehyde: Vibrational Energy Distribution in Photofragment HCO

**Tatsuo GEJO*, Takumi KONO*, Masao TAKAYANAGI, and Ichiro HANAZAKI** *(*Grad. Univ. Adv. Studies)*

Production of vibrationally excited HCO radicals (HCO*), in which either CO-stretch or bending vibration was excited, was observed in the photodissociation of acetaldehyde in a supersonic jet with the pump-probe technique. The relative populations of HCO* against the ground state HCO were measured with the excitation wavelength of 277.5—312.5 nm. The threshold wavelengths for the HCO* production were determined as 308.7 and 302.6 nm, respectively, for the CO-stretch and bending excitation. When the photolysis wavelength is longer than 295 nm (the available energy < 3000cm$^{-1}$), the observed vibrational distribution in HCO is found to agree with the distribution calculated with a model in which the excess energy above the reaction barrier is statistically distributed among the vibrations.

## III-I-6 Vibrational Structure in the $S_1$ ($\pi^*$←n) State of Acetaldehyde as Studied by the Photofragment Excitation Spectroscopy and the Fluorescence Excitation Spectroscopy in a Supersonic Free Jet

**Takumi KONO** *(Grad. Univ. Adv. Studies)*, **Masao TAKAYANAGI, and Ichiro HANAZAKI**

Vibrational structure was determined for the first time in the $\pi^*$←n transition ($S_1$←$S_0$) of acetaldehyde for the excitation wavelength down to 287 nm (corresponding to the excess energy of 5000 cm$^{-1}$ from the $S_1$ origin) by the photofragment excitation (PHOFEX) spectroscopy in a supersonic free jet. The excitation spectrum was measured by detecting one of the rotational lines in the LIF spectrum of the $\tilde{B}$ (0,0,2)←$\tilde{X}$ (0,0,0) transition of the photofragment HCO, while another laser was scanned to decompose acetaldehyde. Vibrational assignments in the $S_1$ state were attempted for the excess energy range of 0 ~ 5000 cm$^{-1}$. Bands below 1000 cm$^{-1}$ are coincident with the previous work[1)] which assigns most of them to the combinations of $\nu_{14}$ (CO out-of-plane-wagging), $\nu_{15}$ ($CH_3$ torsion) and $\nu_{10}$ (CCO deformation). In the higher energy region, most of the bands can be assigned to the combinations of $\nu_{14}$, $\nu_{15}$ and $\nu_{10}$ with $\nu_4$ (C=O stretching). The 1←0 and 2←1 frequencies of $\nu_4$ are 1259 cm$^{-1}$ and 1178 cm$^{-1}$, respectively.

**Reference**
1) M. Baba, I. Hanazaki, and U. Nagashima, *J. Chem. Phys.* **82**, 3938 (1985).

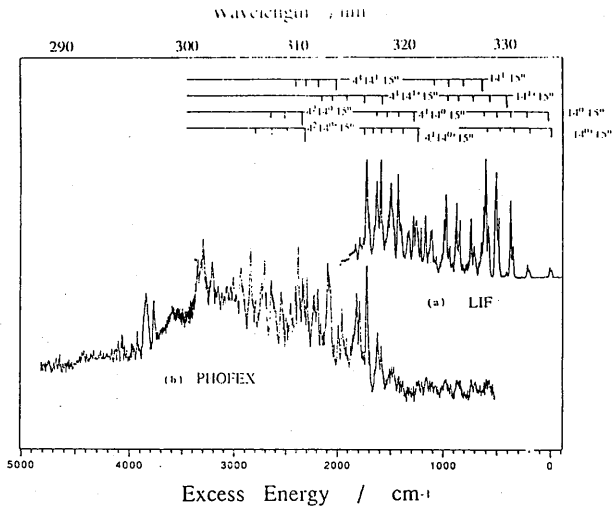


**Figure 1.** (a) Fluorescence excitation spectrum of acetaldehyde (b) PHOFEX spectrum of acetaldehyde obtained by monitoring $^{Q}P_0(5)$ of the $\tilde{B}$ (0,0,2)←$\tilde{X}$ (0,0,0) transition of HCO
Excess energy denotes from the $S_1$ origin.

### III-I-7 Rotational Excitation of HCO Produced by the Photodissociation of Acetaldehyde in a Supersonic Jet

**Takumi KONO** *(Grad. Univ. Adv. Studies)*, **Masao TAKAYANAGI, and Ichiro HANAZAKI**

[*J. Phys.Chem.*, in press]

The rotational excitation was studied for HCO produced by the photodissociation of acetaldehyde in the excitation wavelength range of 280–320 nm in a supersonic free jet. The laser induced fluorescence from $\tilde{B}$ state of HCO was used to determine the rotational energy in the $\tilde{X}$ (0,0,0) state. The rotational enrgy partitioned into HCO is estimated to be $6.2 \pm 0.5$ kJ mol$^{-1}$, which is independent of the excitation energy. The result is shown to be accounted for by the rotational excitation due to the torque imparted in the exit channel.

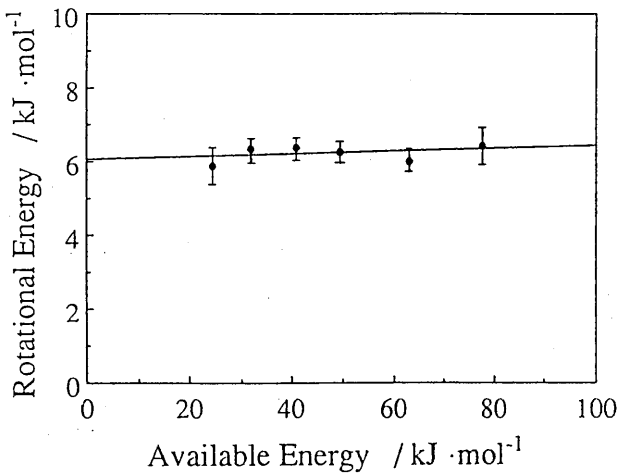


**Figure 1.** Rotational energy in HCO as a function of available energy.

## III-J Self-organization in Chemical Reactions

The self-organizing process in chemical systems is known to occur as a result of nonlinear chemical process. It exhibits the temporal chemical oscillation and the spatial pattern formation. We are particularly interested in the response of chemical oscillators to photo-irradiation. The mechanism of the photo- induction and photo-inhibition of chemically oscillating systems and the structure of related bifurcation phenomena are main subjects of research.

### III-J-1 Bifurcation Structure of the Chemical Oscillation in the $Fe(CN)_6^{4-}$–$H_2O_2$–$H_2SO_4$ System

**Yoshihito MORI and Ichiro HANAZAKI**

[*J. Phys. Chem.* **97**, 7375 (1993)]

pH oscillation was observed in the $Fe(CN)_6^{4-}$–$H_2O_2$-$H_2SO_4$ system under the flow condition. When the total flow rate of the starting materials into a reactor as an external parameter was increased, the system bifurcated from a high pH steady to an oscillatory states at a flow rate beyond a critical value. When the flow rate was increased further, the system bifurcated from the oscillatory to a low pH steady states at a flow rate beyond the higher critical value. The results were shown on the bifurcation diagram (Figure 1a). The diagram illustrates the bifurcation structure. The bifurcation structure of the present system depends on initial concentration of $H_2SO_4$ ($[H_2SO_4]_0$) which is the concentration of $H_2SO_4$ in a reactor if no reaction would take place. As shown in Figure 1b to f, when the parameter space for the oscillatory state shrinks and shifts for lower flow rates, as $[H_2SO_4]_0$ is increased. For $[H_2SO_4]_0 \geq 1.10$ mM, no oscillatory state was observed for any flow rate.

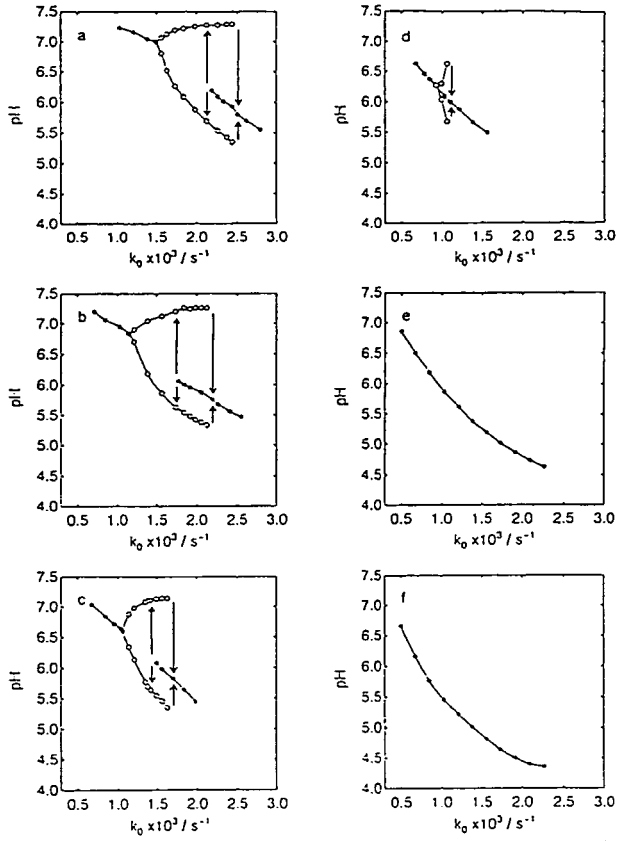


**Figure 1.** Bifurcation diagrams. $K_0$ is a generalized flow rate given by dividing total flow rate of starting materials into a reactor by volume of a reactor. A pair of open circles for a single $k_0$ indicates the maximum and minimum pH values of oscillation and the closed circle gives a steady-state pH value. The arrows indicate discontinuous transitions. Initial concentrations are $[Fe(CN)_6^{4-}]_0$=3.30 mM, $[H_2O_2]_0$=50.0 mM, and $[H_2SO_4]_0$=(a)0.800 mM, (b)0.900 mM, (c)1.00 mM, (d)1.10 mM, (e)1.20 mM and (f)1.30 mM.

## III-J-2 Photo-induction of Chemical Oscillation in the Belousov- Zhabotinsky Reaction under the Flow Condition

**Yoshihito MORI, Yoshihiro NAKAMICHI*, Tetsuo SEKIGUCHI**, Noriaki OKAZAKI**, Takeko MATSUMURA*, and Ichiro HANAZAKI** *(*Nara University of Education, **Grad. Univ. Adv. Studies)*

[*Chem. Phys. Lett.* **211**, 421 (1993)]

We have observed photo-induced oscillation in the $Ru(bpy)_3^{2+}$– $BrO_3^-$–$CH_2(COOH)_2$–$H_2SO_4$ system(Belousov-Zhabotinsky reaction) under the flow condition. As shown in the figure, when the system at a steady state is irradiated with visible light, oscillation starts. As the light power is increased further, the oscillation is inhibited completely and the system bifurcates again to the steady state. To explain the photoresponse, we have proposed the two fold function of the autocatalytic process of the present system, which plays a crucial role to determine the bifurcation. Irradiation of the present system with low and high light power results in acceleration and inhibition of the autocatalytic reaction, respectively. The primary light absorber was found to be the catalyst, $Ru(bpy)_3^{2+}$, in both cases.

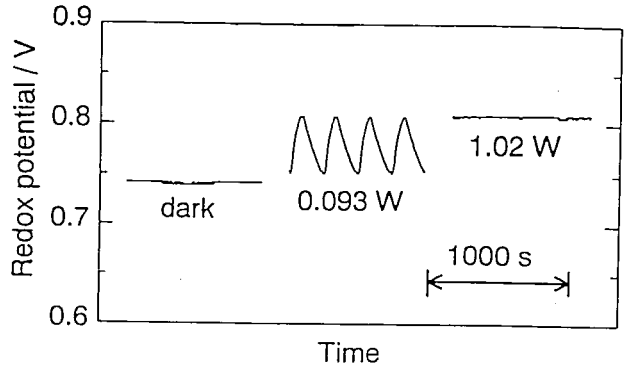


**Figure 1.** Time profiles of redox potential of the reaction mixture under irradiation. The initial concentrations of starting materials are $[Ru(bpy)_3^{2+}]_0$=0.2 mM, $[BrO_3^-]_0$=10 mM, $[CH_2(COOH)_2]_0$=72 mM, and $[H_2SO_4]_0$=0.8 M. The residence time is 355 s.

## III-J-3 Light Induced Bifurcation of Nonlinear Chemical Oscillator: The $Fe(CN)_6^{4-}$–$H_2O_2$–$H_2SO_4$ System

**Yoshihito MORI and Ichiro HANAZAKI**

The $Fe(CN)_6^{4-}$–$H_2O_2$–$H_2SO_4$ reaction system shows pH oscillation. The state of the system depends on a flow rate of starting materials into a reactor as an external parameter, and oscillatory and low pH steady states are observed at medium and higher flow rates, respectively. We have studied the photoresponse of the system at oscillatory and low pH steady states by irradiating the system with visible light (420 nm). As shown in the figure, when the system in the low pH steady state is irradiated, it bifurcates into the oscillatory state at the light power beyond a certain critical value. A further increase of the power results in the transition of the system into the high pH steady state at the light power beyond the higher critical value. A hysteresis is observed for the bifurcation between oscillatory and low pH steady states.

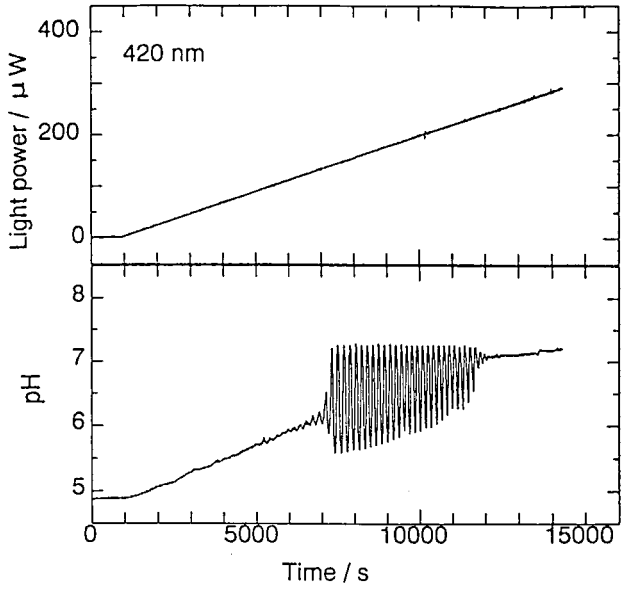


**Figure 1.** Time profiles of pH of the reaction mixture and light power for irradiating the system. The initial concentration of starting materials are $[Fe(CN)_6^{4-}]_0$ = 3.30 mM, $[H_2O_2]_0$ = 50.0 mM, and $[H_2SO_4]_0$ = 0.900 mM. The residence is 368 s.

## III-J-4 Effect of Adding Starch on the Photoinhibition of Oscillation in the Briggs-Rauscher Reaction

**Noriaki OKAZAKI** *(Grad. Univ. Adv. Studies)*, **Yoshihito MORI, and Ichiro HANAZAKI**

[*Chem. Lett.*, 1137 (1993)]

Wavelength dependence of the relative cross section (action spectrum) has been determined for the photoinhibition of oscillation in the starch-free and starch-added Briggs-Rauscher systems (Figure 1). In both cases, the action spectrum is characterized by the broad band at around 460 nm, indicating that the primary light absorber is the iodine molecule. The starch-iodine complex was found to be inert as to the primary photochemical process.

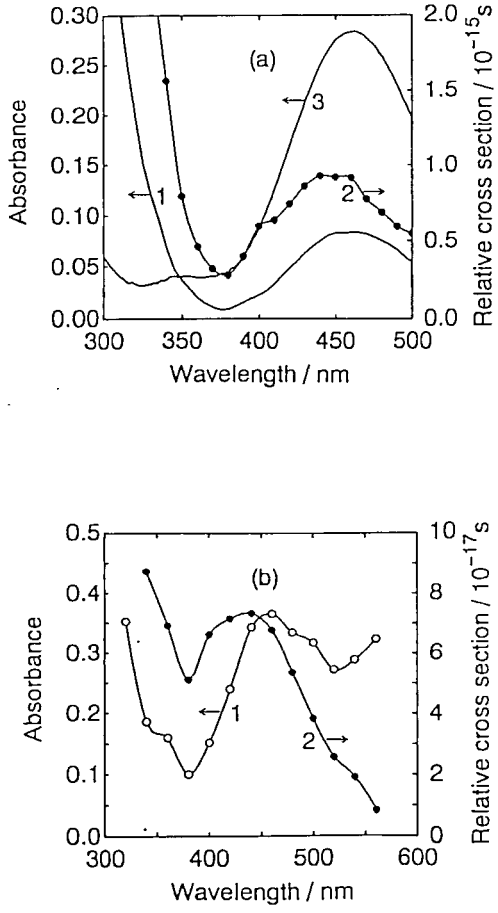


**Figure 1.** Wavelength dependence in the BR-systems: (a) starch-free, (b) starch-added. Curves labeled 1 and 2 correspond to the absorbance of reaction mixture at the bifurcation point and the relative cross section, respectively. For comparison, absorption spectrum of 0.4 mM aqueous solution of iodine (curve 3) is shown in panel (a).

## III-J-5 Direct Visualization of Bifurcation Structure by the Automatic Control Parameter Scanning Method

**Noriaki OKAZAKI** *(Grad. Univ. Adv. Studies)*, **Yoshihito MORI, and Ichiro HANAZAKI**

Continuous-flow Stirred Tank Reactor (CSTR) is one of powerful tools for the quantitative characterization of oscillating chemical reactions. In contrast to the batch-reactor configuration, it can provide a 'true' open-system condition by the continuous feeding of reactant solutions. Well-defined oscillatory/steady states can be realized by giving a set of fixed control parameters such as initial concentration of the reactant solutions, flow rate, temperature etc.

We have recently developed an experimental system which can visualize the transition between oscillatory/steady states (bifurcation structure) by the automatic control-parameter scanning method. Figure 1 (a) shows a typical system setup, in which light intensity is chosen as a control parameter. The scanning was made by applying PID control to the variable ND filter with reference to the sampled beam intensity. An experimental result for the starch-added Briggs-Rauscher system is shown in Figure 1 (b). A small amplitude oscillation region peculiar to the starch-added system has been successfully envisualized. The scanning method is expected to be especially advantageous for observing discontinuous bifurcation accompanying hysteresis phenomena.

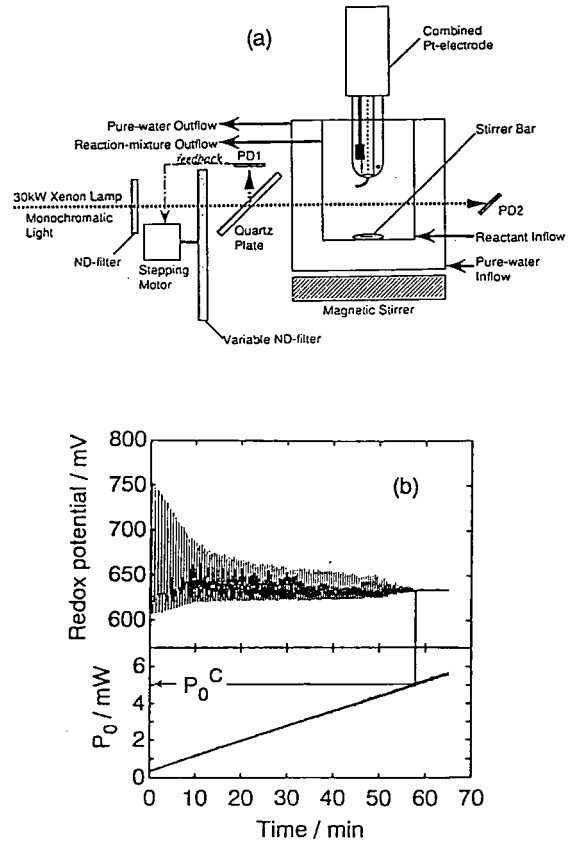


**Figure 1.** (a) Implementation of the automatic light intensity scanning method for the purpose of examining photo-induced bifurcation structure. (b) Bifurcation structure in the starch-added Briggs-Rauscher system. Incident light power ($P_0$) was continuously increased as indicated in the lower panel.

## III-J-6 Photo-responce of the $[Ru(bpy)_3]^{2+}/BrO_3^-/H^+$ System in a a Continuous-Flow Stirred Tank Reactor

**Tetsuo SEKIGUCHI** (*Grad. Univ. Adv. Studies*), **Yoshihito MORI, and Ichiro HANAZAKI**

[*Chem. Lett.*, 1309 (1993)]

Effect of photo-irradiation on the autocatalytic oxidation of $[Ru(bpy)_3]Cl_2$ by acidic bromate has been investigated in a continuous-flow stirred tank reactor. The photo-induced bifurcation structure and phase diagram have been determined by taking the irradiation light power ($P_0$) as an external control parameter. In Figure 1 plotted is a phase diagram in the $[BrO_3^-]_0$–$P_0$ plane. It is shown that, for a certain range of the bromate concentration, the photo-irradiation can either promote or inhibit the autocatalytic oxidation of $[Ru(bpy)_3]^{2+}$ depending on the irradiation light power.

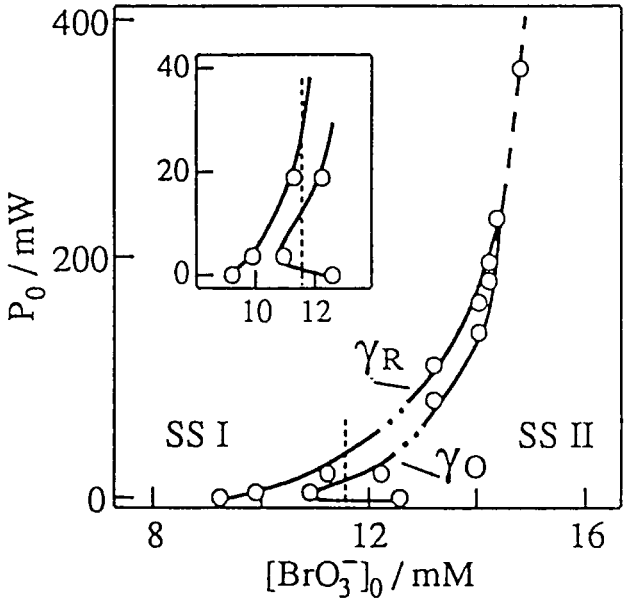


**Figure 1.** Phase diagram in the $[BrO_3^-]_0$-$P_0$ plane. External constraints are $[Ru(bpy)_3^{2+}]_0 = 0.256$ mM, $[H_2SO_4]_0 = 0.375$ M.

## III-J-7 Photo-responce of the $[Ru(bpy)_3]^{2+}$–catalyzed Minimal Bromate Oscillator

**Tetsuo SEKIGUCHI** (*Grad. Univ. Adv. Studies*), **Yoshihito MORI, and Ichiro HANAZAKI**

Photo-irradiation on the ruthenium-catalyzed BZ (Belousov-Zhabotinsky) system exhibits peculiar phenomena such as photo- induction and inhibition of chemical oscillation. We have found that the BZ system without substrate shows a bistability which can be controled by light irradiation [III-J-6]. It is interesting that the irradiation of the absorption band due to $[Ru(bpy)_3]^{2+}$ is efffective both in enhancing and inhibting the autocatalytic oxidation of the catalyst.

The cerous- or manganese-catalyzed BZ system without substrate is known to exhibit chemical oscillation where the system is properly coupled with the flow of materials.[1] They are known as the "minimal oscillator" characterized by a cross-shaped phase diagram.[2] We have found the minimal oscillator behavior also for the system with $[Ru(bpy)_3]^{2+}$ as a catalyst. The photo-irradiation of this system is found to result in both induction and inhibition of chemical oscillation. Figure 1 illustrates the photo-inhibition of chemical oscillation in the $[Ru(bpy)_3]^{2+}$–catalyzed minimal oscillator.

**References**

1) M.Orbáu et al., *J.Am.Chem.Soc.* **104**, 2657 (1982); W.Geisler, *Ber. Bunsenges. Phys. Chem.* **86**, 721 (1982).
2) J.Boissonade, P.De Kepper, *J.Phys.Chem.* **84**, 501(1980).

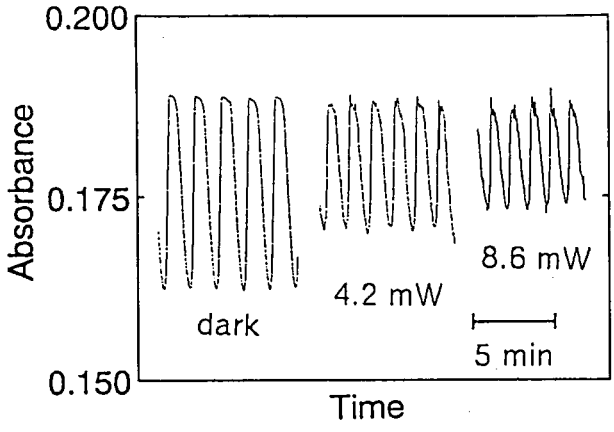


**Figure 1.** Irradiation effect on the $[Ru(bpy)_3]^{2+}$–catalyzed minimal bromate oscillator. The vertical axis shows time profiles of absorbance at 675.2 nm : optical-path length is 17.5 mm. External constraints are $[Ru(bpy)_3^{2+}]_0$=0.256 mM, $[BrO_3^-]_0$=167 mM, and $[Br^-]_0$=0.667 mM,$[H_2SO_4]_0$=0.375 M.

# III—K Laser Investigation of Photodissociation and Bimolecular Reactions

This research group, which started in June 1992, is planning to study fundamental chemical reactions in the gas phase by utilizing the monochromaticity and well-defined polarization of laser for preparing and examining scalar (e.g. energy) and vector (e.g. linear and angular momentum) quantities of molecules.

## III-K-1 Construction of REMPI Ion Imaging Apparatus

**Toshinori SUZUKI and Kenichi TONOKURA**

A newly developed technique, REMPI ion imaging, enables us to determine the velocity vector of reaction products with complete internal state selection.[1] Incorporation of such device with crossed molecular beams will allow the measurement of the fully state-resolved differential cross section in a bimolecular reaction. We have constructed the imaging device for such experiments and tested it through the observation of photodissociation processes. A molecular beam of 1 mm in diameter, produced by a pulsed nozzle and two skimmers, is introduced into a Wiley-McLaren

time-of-flight mass spectrometer. The two counter-propagating laser beams for pump and probe intersect the molecular beam 79 mm downstream from the nozzle. The reaction products are state-selectively ionized by REMPI (resonance enhanced multi-photon ionization), and the resulting ion cloud is accelerated and projected onto a microchannel plate of 40 mm in diameter. Secondary electrons emitted by the microchannel plate excite a phosphor screen and the transient image on the screen is captured by a CCD camera. An example is shown in Figure 1.

**Reference**

1) D.W.Chandler and P.L.Houston, *J.Chem.Phys.* **87**, 1445 (1987).

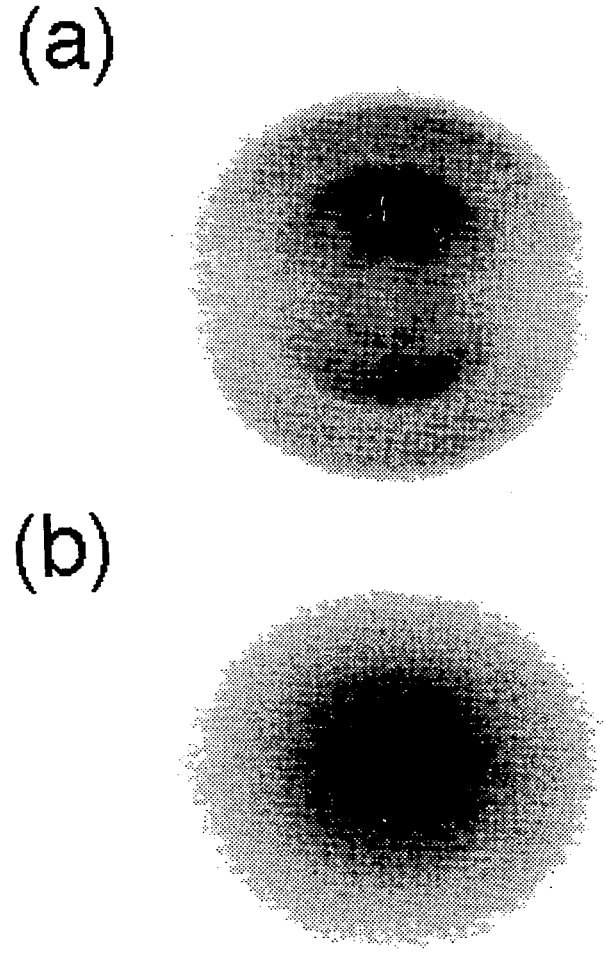


**Figure 1.** The ion images of oxygen atom ($^3P_2$) produced by 355 nm photodissociation of $NO_2$. The electric vector of the photolysis laser is (a) parallel and (b) perpendicular to the plane of the figure.

# III—L External Magnetic Field Effects on Chemical Reactions

## III-L-1 Mixing of the $B^2\Sigma^+$ and $A^2\Pi_i$ States of CN Radicals at High Rotational Levels

**Kaoru SUZUKI and Saburo NAGAKURA** (*Grad. Univ. for Adv. Studies*)

The external magnetic field effects on the perturbation between the electronically excited states of CN radicals at high rotational levels produced in the photodissociation of BrCN were studied. The local perturbation known in the high rotational levels of the $A^2\Sigma_i$ and $B^2\Sigma^+$ states of CN was observed and analyzed following the classic work by Radford and Broida. The high J levels were populated by the laser excitation of $CN(X^2\Sigma^+)$ with an excimer laser pumped dye laser (FL2002), produced in the photodissociation of BrCN with an ArF laser (LPX 110i). The analysis of the lifetimes of the main and extra lines in the zero magnetic field gave the lifetime of the unperturbed $A^2\Pi_i$ state as 140 ns, which is considerably smaller than those obtained from the direct observation of the decay of the $A^2\Pi_i$ state or theoretical values, but is consistent with the results by the anticrossing experiment and the analysis of the intensities of the perturbed lines. The magnetic field dependence of the mixing parameter, deduced from the lifetimes of the perturbed lines, is consistent with that calculated by the diagonalization of the Hamiltonian matrix including the perturbation and Zeeman terms.

# RESEARCH ACTIVITIES IV
# Department of Molecular Assemblies

## IV—A Solid State Properties of Phthalocyanine Salts and Related Compounds

Some phthalocyanine molecules contain unpaired d-electrons in the conjugated $\pi$-electron system. Owing to this special nature, the itinerant $\pi$-electrons and localized magnetic moment due to the d-electrons coexist in solid phthalocyanine salts. The exchange interaction of itinerant $\pi$-electrons with localized magnetic moments is a new aspect in the field of organic metals. For the basic understanding of these materials and to search for a new phenomenon, where a magnetic interaction takes an important role, we prepared and characterized solid phthalocyanine salts and related compounds.

### IV-A-1 Structure and Solid State Properties of Stable Ring-Oxidized Conductor $CoPc(AsF_6)_{0.5}$: Interaction between Ring $\pi$-Electrons and Cobalt d-Electrons

**Hideo YAMAKADO, Tadashi IDA, Akito UGAWA, Kyuya YAKUSHI, Kunio AWAGA, Yusei MARUYAMA, Kenichi IMAEDA, and Hiroo INOKUCHI**

[Synthetic Metals, submitted]

A conducting crystal of (phthalocyaninato)cobalt hexafluoroarsenate $CoPc(AsF_6)_{0.5}$ is prepared by an electrochemical method. The crystal belongs to a tetragonal system with the space group of $P4/mcc$, the lattice constant being $a$=14.234(2), $c$=6.296(2) Å , and Z=2. The infrared and visible spectra and thermopower indicate that the Pc (macrocyclic ligand) ring is mainly oxidized in contrast to the analogous compound, CoPcI. Thermopower and magnetic susceptibility strongly suggest that $CoPc(AsF_6)_{0.5}$ has a narrow bandgap at Fermi level due to strong electron correlations. The electrical conductivity having a broad peak (ca. 100 $Scm^{-1}$) around the room temperature can be understood by a narrow-gap-semiconductor model. Optical spectrum is also consistent with the large-U model. Optical conductivity $\sigma(\omega)$ indicates that the CoPc chain produces one-dimensional $\pi$- and d-bands along the conducting axis ($c$ axis). We discuss the large-U property based on the exchange interaction between these $\pi$- and d-electrons.

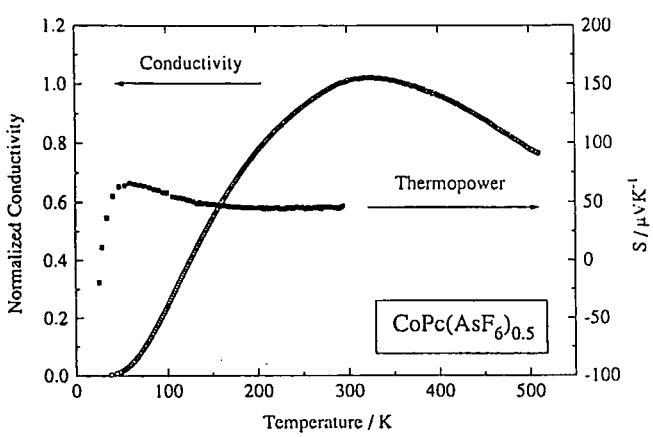


**Figure 1.** Electrical conductivity and thermopower of the $CoPc(AsF_6)_{0.5}$ single crystal. Almost temperature-independent positive value of thermopower implies that itinerant $\pi$-electrons produced by ring oxidation are rather localized by on-site Coulomb energy.

### IV-A-2 Attempt to Prepare 2D-polymer of CuPc under High Pressure and Characterization of Solid State Properties

**Kyuya YAKUSHI, Kentaro IWASAKI, Illias I. KHAIRULLIN, Yasuhiro NAKAZAWA, Kazushi KANODA, Ichimin SHIROTANI,* Sadamu TAKEDA,** and Nobuhiro KOSUGI** *(*Muroran Inst. of Tech., **Osaka Univ.)*

2D-polymer of CuPc has been attempted to prepare by heating the solid mixture of Cu and tetracyanobenzene (TCNB) in vacuum. The ideal structure of this polymer consists of 2D itinerant $\pi$-electrons and localized magnetic moments on $Cu^{2+}$ on a square lattice. The interaction between conduction electrons and local magnetic moments may produce a new solid state properties. However, well-defined 2D-polymer has not been prepared. We have tried to prepare the 2D-polymer under high pressure (3 GPa) by changing the temperature and reaction time, and obtained a conductive material ($\sigma_{max}$ ~ 100 $Scm^{-1}$ ). Characterization has been done by X-ray diffraction, EXAFS, $^{13}C$-NMR, FIR-IR-VIS-UV spectrum, electrical conductivity, magnetic susceptibility, and ESR. The structure is very disordered and the structural unit is different from what we expected but there exists conduction electrons in this polymer.

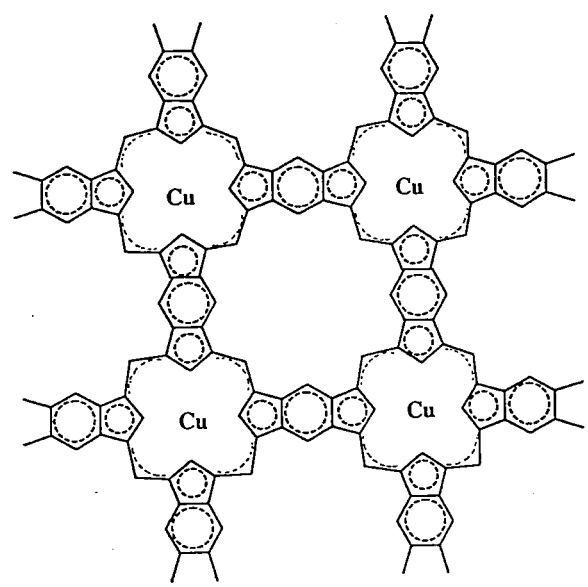


**Figure 2.** Chemical structure of 2D-polymer of CuPc. We have not arrived at this structure.

## IV-A-3 Intercalation of High-Tc Oxides with Organic Molecules

**Leonid GRIGORYAN, Yasuhiro NAKAZAWA, Kazushi KANODA, and Kyuya YAKUSHI**

[*Advances in Superconductivity* V, 287 (1993)]

Exposure of Bi- and Tl-oxides to vapor of benzene or phthalocyanines results in formation of intercalation compounds where c-axis is expanded with respect to that of the host oxide due to insertion of the organic molecules between the double Bi-O (or Tl-O) layers. electronic and vibrational modes of both the guest organic and host inorganic constituents are significantly modified as compared to the starting materials. the intercalated samples exhibit strongly enhanced non-linear magnetism with a complex filed dependence, which is tentatively scribed to the orbital magnetism of $\pi$-electrons of organic molecules.

## IV-A-4 Modification of Normal-State and Superconducting Properties of High-Tc Oxides via Treatment by Metal-Phthalocyanines

**Leonid GRIGORYAN, Kyuya YAKUSHI, A. V. NARLIKAR,* P. K. DUTTA,* and S. B. SAMANTA*** *(*National Phys. Lab. of India)*

[Mod. Phys. Letters B, submitted]

Exposure of Bi- or Tl-based high-Tc oxide powders to vapors of metal-phthalocyanines MPc (M is Zn or Ni) resulted in formation of a family of new compounds with modified crystal lattice parameters, electronic structure, phonon spectrum and magnetic properties as compared to the starting materials. Based on the combined X-ray diffraction, scanning tunneling microscopy, optical, FT-IR and microwave absorption data, a model of crystal structure is proposed where the key feature is intercalation of MPc molecules between the Bi-O (Tl-O) bilayers. Values of dc magnetization at 300 K varied over two orders of magnitude as a function of chemical composition and nature of the central metal ion in MPc. Measurements of temperature dependence of magnetization of the intercalated samples revealed a divergence at low temperatures between the zero-field and the field-cooled cycles, though of lower magnitude as compared to the starting high-Tc oxides. The results of this study suggest that treatment by MPc offers a possibility of controllable variation of key properties of high-Tc oxides.

## IV-A-5 Evolution of Optical Absorption and Superconductivity in Bi-2212 and 2223 Oxides Intercalated by Metal-Phthalocyanines: A Systematic Study as a Function of Intercalation Level

**Leonid GRIGORYAN, Kyuya YAKUSHI, Chia-Jyi LIU,* Satoru TAKANO,* Mitsunobu WAKATA,* and Hisao YAMAUCHI*** *(*ISTEC)*

[Physica C, submitted]

Exposure to vapors of the metal-phthalocyanines MPc (M=Zn, Ni, Fe, or Pb) brings about a systematic variation of optical and superconducting properties of Bi-2212 and

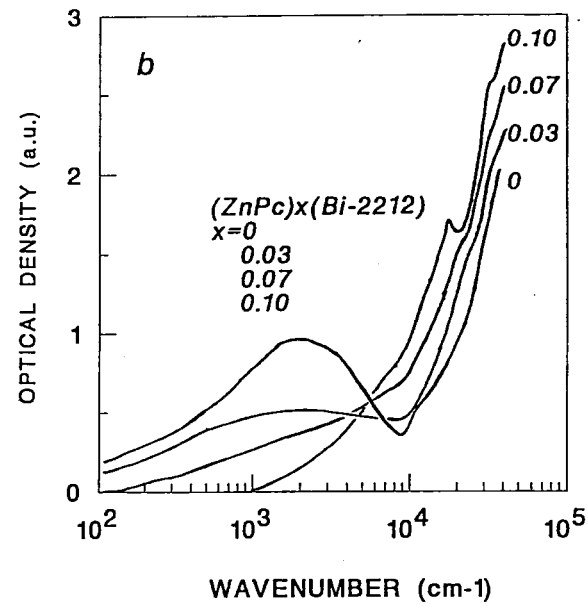


**Figure 3.** Evolution of the electronic absorption spectra as a function of x for $(ZnPc)_x(Bi2212)$. The spectral weight is gradually transferred from the low to high-frequency regions upon doping of ZnPc.

2223 high-Tc oxides. With increasing level of MPc uptake, the spectral weight is gradually transferred from the low to the high-frequency regions, accompanied by a decrease of Tc, diamagnetic response and magnetic hysteresis. Two different types of evolution patterns were observed: the first was characterized by a sharp change at the lowest level of MPc uptake (Tc hysteresis), while the second featured a gradual evolution (intensities of the electronic absorption bands, diamagnetism). The heavily intercalated Bi-oxides are brightly colored non-conducting materials with well-resolved vibrational features due to both the intercalated MPc molecules and the host oxides.

The above evolution patterns are ascribed to a combination of two mechanisms: the decrease of the charge carrier concentration as a result of electron doping into the host oxide, and the increase of anisotropy of the system due to incorporation of insulating MPc molecular layer between the Bi-O bilayers, thereby reducing the coupling along the c-axis. Hence, the intercalation by MPc is shown to be an effective technique for the electron doping leading to a reduction of the charge carrier concentration in the host oxides, in contrast to the intercalation by iodine which leads to a hole doping and to an increase of the number of charge carriers.

## IV-A-6 Contribution of Interblock Coupling to Tc in High-Tc Bi-Oxides

**Leonid GRIGORYAN, Kyuya YAKUSHI, A. V. NARLIKAR,* and S. B. SAMANTA*** *(*National Phys. Lab. of India)*

Magnetization, optical and scanning tunneling microscopy/spectroscopy studies of Bi-2212 and 2223 oxides intercalated by metal-phthalocyanine (MPc) are presented. At the low level of MPc uptake, the diamagnetic response of the Bi-2212 single crystals along the c-axis is severely suppressed accompanied by a sharp drop in Tc. Since at

that stage the number of charge carriers is not affected as evidenced by the optical spectra, the Tc drop is ascribed to the decoupling of the unit cell blocks due to insertion of the insulating MPc molecules between the Bi-O bilayers. Magnitude of the Tc drop is in a reasonable agreement with the estimates of the resonating valence bond model.

# IV—B Structure and Properties of Organic Metals

The study of organic metals rapidly developed when the dimensionality of an intermolecular charge-transfer interaction is expanded. This expansion of dimensionality has been brought about by the discovery of new molecules such as BEDT-TTF or $C_{60}$. In this project we treat one-, two-, and three-dimensional organic metals and superconductors to know what is most important for stabilizing a metallic state and for designing new superconducting materials.

## IV-B-1 ESR and Low-field Microwave Absorption Study of Sodium-doped $C_{60}$: Peculiarities of the Doping Using Sodium Azide

**Ilias I. KHAIRULLIN, Kenichi IMAEDA, Kyuya YAKUSHI, and Hiroo INOKUCHI**

[*Proceedings of IUMRS-ICAM-93*]

We have studied ESR and low-magnetic field microwave aborption in new superconducting sodium-nitrogen-$C_{60}$ ternary compound prepared utilizing the thermal decomposition of soidum azide ($NaN_3$). Depending upon the water content in the reactant, $NaN_3$, the final products of the doped $C_{60}$ show two SC phases with $T_{c1}$=10—12 K and $T_{c2}$=14.7—17.3 K, and with different volume fractions.

## IV-B-2 Infrared and Transport Properties of $K_xC_{60}$

**Akito UGAWA, Kyuya YAKUSHI, Koichi KIKUCHI,* Shinzo SUZUKI,* Yoji ACHIBA,* and Isao IKEMOTO***
*(*Tokyo Metropolitan Univ.)*

[*Synthetic Metals* **56**, 2997 (1993)]

Infrared reflectance spectra have been measured on high-quality bulk crystals of $K_xC_{60}$ during the K-doping process. The results support a rigid band picture of $K_xC_{60}$ for $0<x<3$ in contrast to the non-rigid band feature reported on the photoemission spectra of film samples. The spectrum of $K_3C_{60}$ demonstrates a metallic dispersion which is described by the Drude model with $\omega_p$=1.2 eV and $\gamma$=0.62eV, the plasma frequency being in good agreement with the theoretical calculation by Erwin and Pickett. An infrared-active $T_{1u}$ mode of 1429 $cm^{-1}$ in $C_{60}$ is found to decrease in proportion to the degree of charge-transfer $x$ with $\Delta\omega/\Delta x$=—20 $cm^{-1}$ up to $x$=6.

## IV-B-3 Fermi Surface and Magnetoresistance in β″-(BEDT-TTF)$_2$AuBr$_2$

**Shinya UJI,* Haruyoshi AOKI,* Madoka TOKUMOTO,** Akito UGAWA, and Kyuya YAKUSHI** *(*National Research Institute for Metals, **ETL)*

[*Proceeding of the 20th International Conference on Low Temperature Physics*, in press]

We have carried out the magnetoresistance measurements in β″-(BEDT-TTF)$_2$AuBr$_2$. SdH signals with at least two fundamental frequencies of 41.5 T and 139 T are observed for $H \| b^*$-axis. The angular dependence of both frequencies shows that the Fermi surfaces are cylindrical. An anormalous resistance maximum is found at 9.5 K when magnetic fields above 4 T are applied parallel to the $b^*$-axis, although no anomaly is observed for the fields in the $ac$-plane.

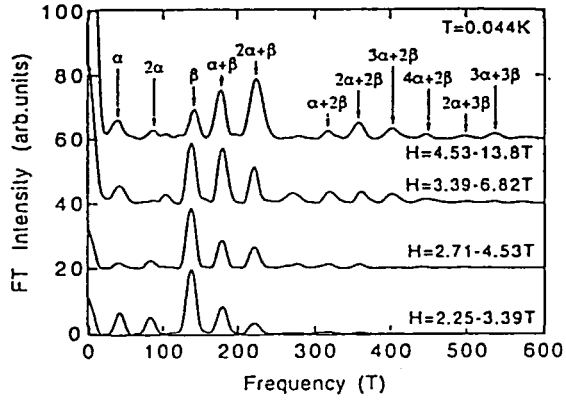


**Figure 4.** Fourier spectra of SdH signal of β″-(BEDT-TTF)$_2$AuBr$_2$ in various field regions.

## IV-B-4 Far-Infrared Reflectance and Microwave Properties of β″-(BEDT-TTF)$_2$AuBr$_2$

**Akito UGAWA,* David B. Tanner,* Hideo YAMAKADO, and Kyuya YAKUSHI** *(*Univ. of Florida)*

Temperature dependence of polarized far-infrared reflectance (35—4000 $cm^{-1}$) and microwave absorption (10 GHz) have been measured on β″-(BEDT-TTF)$_2$AuBr$_2$. The $\|c$ spectrum shows a Drude-like dispersion over the temperature range 15—300 K, although the (010) $\perp c$ spectrum is accompanied with strong phonon-structures as well as interband absorptions caused by the dimeric arrangement of BEDT-TTF molecules along $\|a$ direction. The dispersion analysis on both spectra at 20 K yields the plasma frequency $\omega_p\|_c$=1.2 eV and $\omega_p\perp_c$=0.1 eV, showing the highest optical anisotropy among the organic metals without metal-insulator transiton. The microwave conductivity completely agrees with the dc result at temperatures 4—300 K. We conclude that there is no positive evidence for SDW transition in β″-(BEDT-TTF)$_2$AuBr$_2$ argued by Pratt *et al.*

# IV—C NMR Study of Organic Conductors and Superconductors

## IV-C-1 Construction of Wide-Band Pulsed NMR System for Solid State Physics

**Kazushi KANODA, Atsushi KAWAMOTO** *(Ochanomizu Univ.)*, **and Kazuya MIYAGAWA**

The nuclear magnetic resonance (NMR) is a powerful method to examine electronic state of condensed matters. With this method, one can get further insight into nature of the metallic, superconducting and magnetic states than with other macroscopic measurements. For the purpose, we have constructed a NMR system, which is described here. Our system is composed of the spectrometer and the cryostat. The spectrometer was designed to have a frequency-band of 5—300 MHz, transmit rf peak power of 300 W and generate various rf pulse patterns with quadruture phase-modulation. The techniques such as the phase cycling and the solid echo are available. The recovery time of the receiver is 2.8 $\mu$sec at the frequency of 90 MHz. Transmission of rf pulse and numerical handling of the NMR signal are fully computer-controlled. The cryostat contains a superconducting magnet, which can generate magnetic field up to 11 Tesla, and an NMR probe. The probe has two variable capacitors near the sample coil for tuning and matching of the electrical system. Temperature of the sample can be varied in the range between 1.5 and 300 K. The whole system worked successfully, although electric discharge encountered at high power of rf pulse is a problem to be improved.

## IV-C-2 Substitution of $^{13}C$ Isotope for Central Carbon Sites of BEDT-TTF Molecules and NMR Study of BEDT-TTF Charge Transfer Salts

**Atsushi KAWAMOTO** *(Ochanomizu Univ.)*, **Yasuhiro NAKAZAWA, Kazuya MIYAGAWA, and Kazushi KANODA**

The $^1H$ is a nucleus of which the NMR signal is observed easiest. All the organic compounds have protons. Therefore, NMR measurements of organic conductors and superconductors have so far been performed extensively for the proton. However, the protons are located at edges of the molecule and, in many cases, have so small spin density of the molecular orbital responsible for conduction electrons that the proton is not the best probe nucleus. Unfortunately, many donor molecules have no other NMR-active nuclei. One way to overcome this difficulty is substitution of $^{13}C$ isotope which is NMR-active. For this purpose, we introduced $^{13}C$ isotope into the central carbon sites of the BEDT-TTF molecule which provides various types of conductors, superconductors and magnets. Selectively $^{13}C$-labeled BEDT-TTF molecule was synthesized according to the method by Larsen and Lenoir with slight modification. Examination of mass spectrum of the product showed successful substitution of $^{13}C$ into BEDT-TTF. Next, we proceeded to prepare charge transfer salts with electrochemical method. Several crystals of $\kappa$- and $\alpha$-phase compounds were obtained. Prior to NMR experiments, we measured magnetic susceptibility of the sample from room temperature down to 2 K to evaluate sample quality from a magnetic point of view. Almost all samples exhibited temperature-insensitive Pauli-like susceptibility with negligible Curie component. Samples of poor quality are excluded from NMR experiments. We observed $^{13}C$-NMR signal in the whole temperature range between 1.5 and 300 K. Preliminary results of $\kappa$-$(BEDT\text{-}TTF)_2Cu(NCS)_2$ shows that the relaxation rate is several tens msec at room temperature. Measurements of the temperature dependence is now in progress.

## IV-C-3 $^1H$-NMR Study of An Organic Conductor, $\kappa$-$(BMDT\text{-}TTF)_2Au(CN)_2$

**Kazuya MIYAGAWA, Atsushi KAWAMOTO** *(Ochanomizu Univ.)*, **Kazushi KANODA, and Takehiko MORI**

The title compound is known to show a steep increase in resistivity and decrease in spin susceptibility below 76 K, reminiscent of a metal-insulator transition. Above that, the temperature dependence of resistivity and susceptibility is metallic. Such an anomaly is unique in this compound among all the $\kappa$-phase compounds based on BMDT-TTF, BEDT-TTF, MDT-TTF and DMET. To clarify nature of the transition, we measured $^1H$ nuclear spin-lattice relaxation rate in the temperature range of 2 to 300 K. Since BMDT-TTF molecule is free from molecular motion such as vibration in the ethylene group or rotation in methyl group in the DMET molecule, dominant mechanism of the nuclear relaxation is considered to be electronic in origin. Relaxation of the nuclear magnetization was an exponential function of time above 75 K. Below that, however, the relaxation curve could not be fitted to a single exponential function, reflecting inhomogeneous relaxation. We fitted the data below 75 K to superposition of relaxation curves with three different $T_1$'s. The change of the relaxation profile at this temperature indicates some transition of the electronic state, in agreement with the resistive and magnetic behavior. However, it is noted that the longest $T_1$ behaves like a Korringa law even below 75 K. This fact suggests that the low temperature state is also metallic.

## IV-C-4 Pressure Dependence of the SDW Transition in $(MDT\text{-}TTF)_2Au(CN)_2$

**Toshihiro TAKAHASHI*, Yoshiaki KOBAYASHI*, Kazushi KANODA, Tetsuya INUKAI**, and Gunzi SAITO***** *(*Gakushuin Univ., **The Univ. of Tokyo, ***Kyoto Univ.)*

[*Synth. Met.* **55—57**, 2814 (1993)]

The pressure dependence of the SDW transition in the titled material has been investigated by the measurements of $^1H$-NMR relaxation rate, $T_1^{-1}$. In the metallic state, $^1H$-$T_1^{-1}$ follows a Korringa relation. The pressure dependence of $T_1^{-1}$ is large compared with other organic conductors. The large peak of $^1H$-$T_1^{-1}$ observed in the SDW state disappears at 5 kbar, in agreement with the resistivity measurement: The SDW order is completely suppressed at this pressure. There is still observed an appreciable

enhancement of $(T_1T)^{-1}$ below 8 K, which should be attributed to the short-range spin fluctuations near the SDW ordering. The temperature dependence of $T_1^{-1}$ and NMR linewidth was quite unusual for the standard SDW state, possible reasons of which were discussed.

### IV-C-5 $^1$H-NMR Studies of the Low Temperature Phase of $\alpha$-(BEDT-TTF)$_2$KHg(SCN)$_4$

**Toshihiro TAKAHASHI*, Ryota Tsuchiya*, Kazushi KANODA, Masashi WATABE*, Takahiko SASAKI**, and Naoki TOYOTA**** *(*Gakushuin Univ., **Tohoku Univ.)*

[*Synth. Met.*, **55–57**, 2513 (1993)]

We present the results of $^1$H-NMR relaxation and lineshape measurements in the organic conductor, $\alpha$-(BEDT-TTF)$_2$KHg(SCN)$_4$, aiming at clarifying the origin of electric and magnetic anomalies observed below 10 K. The relaxation rate in the metallic region follows a Korringa relation, $(T_1T)^{-1}$=1.0x10$^{-4}$s$^{-1}$K$^{-1}$. Above 200 K, the thermal motions of ethylene groups dominate the $^1$H-$T_1^{-1}$; the activation energy was estimated to be 4100 K, which is the highest in the BEDT-TTF salts ever studied. $(T_1T)^{-1}$ was found to show a prominent enhancement below 8 K, but there was not a peak anomaly such as observed at the standard SDW transition. The second moment of the resonance line was constant in temperature down to 1.9 K. No evidence for static SDW order was obtained. The upper bound for the possible SDW amplitude was estimated to be 1% $\mu_B$ per molecule.

### IV-C-6 Cu NMR Study on the Valence Fluctuating State in the Organic Conductor (DMe-DCNQI)$_2$Cu

**Kenji ISHIDA*, Yoshio KITAOKA*, H. Masuda*, Kunisuke ASAYAMA*, Toshihiro TAKAHASHI**, Kazushi KANODA, Akiko KOBAYASHI***, Reizo KATO***, and Hayao KOBAYASHI****** *(*Osaka Univ., **Gakushuin Univ., ***Univ. of Tokyo, ****Toho Univ.)*

[*Physica B*, **186–188**, 1059 (1993)]

An electronic property of a counterion site in the organic conductor (DMe-DCNQI)$_2$Cu has been investigated by Cu NMR experiments. The nuclear spin-lattice relaxation rate $1/T_1$ of $^{63}$Cu obeys a $T_1T$=constant law in the temperature range 0.33–90 K where the Knight shift $K$ remains constant. No anomalies have been observed in $^{63}T_1$ and $^{63}K$ around 6 K, at which temperature it has been suggested that magnetic ordering occurs.

### IV-C-7 Magnetism of DCNQI-Cu Salts

**Toshihiro TAKAHASHI*, Kazushi KANODA, Takao TAMURA*, Koichi HIRAKI*, Kumi IKEDA*, Reizo KATO**, Hayao KOBAYASHI***, and Akiko KOBAYASHI**** *(*Gakushuin Univ., **Univ. of Tokyo, ***Toho Univ.)*

[*Synth. Met.* **55–57**, 2281 (1993)]

Magnetic properties of (DMe-DCNQI)$_2$Cu, (DMeO-DCNQI)$_2$Cu and (DBr-DCNQI)$_2$Cu were investigated by $^1$H-NMR, ESR and magnetic susceptibility measurements. $^1$H-$T_1^{-1}$ was found to exhibit a step-like enhancement at the metal-insulator (M-I) transitions of DBr salt at ambient pressure and of DMe- and DMeO-salts under pressure. This reflects the appearance of localized $Cu^{2+}$ spins at the M-I transition. An antiferromagnetic (AF) ordering was observed in DBr- (at ambient pressure) and DMe-salts (under pressure). In both salts, $^1$H-NMR relaxation rates, $T_1^{-1}$, $T_2^{*-1}$ and $T_2^{-1}$, indicate the onset of inhomogeneous local field at the transition temperature, $T_N$: The lineshape below $T_N$ is well explained by the assumption that the magnetic $Cu^{2+}$-sites with $\mu_B$ form a regular three-fold lattice along the c-axis. In the DMe-salt, the pressure dependence of $T_N$ was determined. It was shown that the enhancement of static susceptibility in the metallic state of DMe-salt was due to the insulating domain induced by some stress within the sample.

## IV—D Electron Transport Study of Organic Conductors and Superconductors

### IV-D-1 Magnetic Penetration Depth and Vortex State of the Organic Superconductor, κ-(BEDT-TTF)$_2$Cu[N(CN)$_2$]Br

**Kazushi KANODA, Yasuhiro NAKAZAWA, and Atsushi KAWAMOTO**

The κ-phase layered organic superconductors with transition temperatures greater than 10 K are characterized by strong anisotropy of the electronic state. The superconductivity in these compounds has also two-dimensional character. It is a natural question whether the anisotropy has something to do with transition temperature, mechanism of superconductivity and so on. Systematic comparison of anisotropy and other superconducting parameters may give a clue to answer the question. It is, however, difficult to characterize anisotropy of the superconductivity quantitatively. We previously proposed that the magnetic penetration depth measurements can provide us with important information for this subject and reported the values of the parallel penetration depth at field parallel to the layers for a series of κ-phase compounds. Our method to obtain the depth was ac complex susceptibility $\chi=\chi'-i\chi''$ measurements. However, there was a criticism against our method; the earth field can affect the ac susceptibility and lead to spurious depth. To examine this effect, we measured the same quantity of the titled compound in an environment where residual field at the sample position is less than 1 mOe. The resultant value of 190 $\mu$m showed a good agreement with the previous value (200 $\mu$m). Moreover, application of a dc magnetic field of 0.5 Oe did not change the value of complex susceptibility. Therefore, we conclude that the earth field has no influence on the present measure-

ments.

In addition to this, the measurements were extended under higher dc magnetic field up to 10 kOe parallel to the layers. In the field range of several hundreds of Oe, we observed two-step transition in $\chi'$ and broad double peaks in $\chi''$ against temperature. Such a unique profile is unexpected in usual type-II superconductors. Appreciable frequency dependence (0.01—1000 Hz) of $\chi$ reflects flux creep in the vortex state.

### IV-D-2 Complex Susceptibility and Magnetic Penetration Depth of $\alpha$-(BEDT-TTF)$_2$NH$_4$Hg(SCN)$_4$

**Yasuhiro NAKAZAWA, Atsushi KAWAMOTO** *(Ochanomizu Univ.)*, **Hirohiko SATO, Kiyonori KATO, and Kazushi KANODA**

The titled compound has a layered structure in which conducting BEDT-TTF layers are separated by thick insulating blocks. Anisotropy of electrical resistivity is extremely high among quasi-two-dimensional organic conductors. Therefore, superconductivity is also expected to be highly two-dimensional. We have investigated the superconductivity of this material in terms of complex susceptibility measurements down to 30 mK, using a dilution refrigerator. First, ac field was applied perpendicular to the layers. Relatively sharp transition in $\chi'$ and peak formation in $\chi''$ was observed below 1 K. At lower temperatures, $\chi'$ reaches a constant value which corresponds to the complete diamagnetism after correcting the demagnetizing factor. Second, the ac field was applied parallel to the layers. In contrast to the perpendicular case, $\chi'$ grows gradually below 1 K and the value of $\chi'$ at the lowest temperature is only 5% of the complete diamagnetism. This fact suggests that the parallel penetration depth under the field parallel to the layers are comparable with the sample size. The resultant preliminary value of 1.4 mm, which is considerably greater than those of κ-phase superconductors, shows extremely week coupling between the superconducting layers, that is, highly two-dimensional nature.

Small dc field perpendicular to the layers suppresses the superconductivity. For example, the onset of the transition is depressed to 500 mK.

### IV-D-3 Resistive Transition of the Organic Superconductor, $\alpha$-(BEDT-TTF)$_2$NH$_4$Hg(SCN)$_4$

**Hirohiko SATO, Yasuhiro NAKAZAWA, Atsushi KAWAMOTO** *(Ochanomizu Univ.)*, **Kiyonori KATO, and Kazushi KANODA**

The superconductivity of the title compound has been investigated by resistive measurements. Eight electrical contacts were made on a single crystal so that both resistivities parallel and perpendicular to the layers can be measured for identical crystals; this method avoids ambiguity of sample dependence when comparing the in-plane and out-of-plane resistive transitions. The measurements were made down to 0.5 K for several crystals. The transition at a zero field is characterized by an onset of decrease of resistivity around 2 K and gradual decrease at lower temperatures. This characteristics was reproduced for all the samples measured. We encountered sample dependence below 1 K. For one sample, both in-plane and out-of-plane resistivities vanished below 1 K, but with different temperature dependence above that. The transition to a zero resistance was very sensitive to the field perpendicular to the layer although the 2-K transition was insensitive to the field. For other samples, finite resistivity remains even at 0.5 K.

Field-insensitive broad transition, gradual decrease of resistivity and subtle nature of the transition to a zero resistance leads us to speculate on the possibility of some sophisticated state, such as vortex-antivortex excitation below the mean-field transition, inherent in two-dimensional superconductivity.

Further characterization of the superconductivity and clarification of origin of the sample dependence are needed.

## IV—E Ultra-Thin Organic Film Systems Prepared by Molecular Beam Epitaxy (MBE) Technique

As a strategy for a development of new molecular systems of organic materials, we have undertaken the fabrication of ultra-thin organic multi-layer systems with the use of an MBE technique. We are expecting the preparation of such novel 2-dimensional materials as molecular superlattice systems or intercalation compounds in which special electronic states in the bulk and/or new charge-transfer states in the interfaces could be realized.

We have prepared ultra-thin epitaxially grown phthalocyanine films on alkali halide single crystal substrates. On the basis of this single crystalline film, we are now fabricating double-layer systems of phthalocyanines.

Nonlinear optical effects are found to be significantly correlated with the film structure. The spectral responses of the nonlinear susceptibilities are now going to be studied for the phthalocyanine thin film systems.

### IV-E-1 Epitaxial Growth of Lead Phtholocyanine Film on KI crystal

**Hajime HOSHI, Shaoli FANG, and Yusei MARUYAMA**

[*J. Appl. Phys.*, **73**, 3111 (1993)]

The molecular-beam epitaxy technique is applied to grow an epitaxial film of lead phthalocyanine (PbPc). The epitaxy found, KI (100) (5×10/7) R45° -PbPc, is a new type with the incommensurate factor 10/7.

### IV-E-2 $\chi^{(3)}$ Components of Single-Crystalline Vanadyl Phthalocyanine Film

**Hajime HOSHI, Keiichi KOHAMA** *(Toyota Motor Corp. and IMS)*, **Shaoli FANG, and Yusei MARUYAMA**

[*Appl. Phys. Lett.*, **62**, 3080 (1993)]

Single-crystalline vanadyl phthalocyanine film has been grown by the molecular-beam epitaxy technique. The $\chi^{(3)}$ components, $\chi_{1111}$ and $\chi_{1221}$, have been determined by third-harmonic generation using a fundamental Nd:YAG laser source. The relation, $\chi_{1221} \sim 0.8\ \chi_{1111}$, reveals that the nondiagonal component significantly contributes to the nonlinear optical response, which originates in two-dimensional $\pi$-electron systems of this molecule.

### IV-E-3 Dependence of Off-Diagonal Components of $\chi^{(3)}$ on Substrate Temperature of Epitaxially Grown Vanadyl Phthalocyanine Films

**Shaoli FANG, Keiichi KOHAMA** *(Toyota Motor Corp. and IMS)*, **Hajime HOSHI** *(Tokyo Institute of Technology)*, **and Yusei MARUYAMA**

[*Jpn. J. Appl. Phys.*, in press]

Single-crystalline vanadyl phthalocyanine films have been grown by the molecular beam epitaxy technique. The normalized off-diagonal ratio $3\ \chi_{1221}/\chi_{1111}$ has been determined by circular-polarization third harmonic generation measurement. It is revealed that the single-crystalline phase with 4mm symmetry can be distinguished from the $C\infty_v$ polycrystalline phase by circular-polarization third harmonic generation measurement, and the quality of the epitaxial film can be quantitatively analyzed by the normalized off-diagonal ratio of $3\ \chi_{1221}/\chi_{1111}$.

### IV-E-4 Epitaxial Growth of Chloroaluminum Phthalocyanine and Vanadyl Phthalocyanine Double-Layer Structure by the Molecular Beam Epitaxy

**Shaoli FANG, Keiichi KOHAMA** *(Toyota Motor Corp. and IMS)*, **Hajime HOSHI** *(Tokyo Institute of Technology)*, **and Yusei MARUYAMA**

[Submitted to *Appl. Phys. Lett.*]

The epitaxial growth of chloroaluminium phthalocyanine on vanadyl phthalocyanine single-crystalline film on KBr substrate is realized using the highly controlled technique of molecular beam epitaxy. Scanning electron microscopy studies indicate that the chloroaluminum phthalocyanine layer exhibits unidirectional epitaxy and the epitaxial growth is further confirmed by the low temperature spectral studies of the chloroaluminium phthalocyanine and vanadyl phthalocyanine double-layer structure.

## IV—F Novel Molecular System $C_{60}$: Fullerites and Fullerides

In the early stage of the research of $C_{60}$ solids we used single crystals which were grown from $CS_2$ solution. Now we succeeded in the vapor-phase growth of $C_{60}$ and $C_{70}$ single crystals which are free from solvent inclusion. We have studied transport properties of $C_{60}$ single crystals without or with doping of alkali metals.

### IV-F-1 Electronic Structure of Alkali Metal Doped $C_{60}$ Derived from Thermoelectric Power Measurements

**Tamotsu INABE** *(Hokkaido Univ.)*, **Hironori OGATA, Yusei MARUYAMA, Yohji ACHIBA*, Shinzo SUZUKI*, Koichi KIKUCHI*, and Isao IKEMOTO*** *(*Tokyo Metropolitan Univ.)*

[*Phys. Rev. Lett.*, **69**, 3797 (1992)]

The thermoelectric power of K- and Rb-doped $C_{60}$ superconductors prepared from single crystals grown from a $CS_2$ solution is reported. Nearly linear temperature dependences of the thermoelectric power with negative sign are observed above the superconducting transition temperatures for both materials. From the slope of the linear correlation, the ratio of the density of states at the Fermi energy, $N^{Rb}(E_F)/N^{K}(E_F)$, is estimated to be 1.5—1.8.

### IV-F-2 Vapor Phase Growth of $C_{60}$ or $C_{70}$ Single Crystals

**Hironori OGATA, Tamotsu INABE** *(Hokkaido Univ.)*, **and Yusei MARUYAMA**

Intensively purified $C_{60}$ or $C_{70}$ powder was sublimed in a vacuum and the collected sublimate was sealed in a quartz tube with helium gas ($\sim$ 10 Torr). The tube was set in a horizontal electric furnace in which the temperature distribution was adjusted to keep a little lower temperature at the middle point of the horizontal tube. In this way we can grow millimeter-size $C_{60}$ or $C_{70}$ single crystals at the portion of lower temperature zone.

### IV-F-3 Mobilities of Charge Carriers in $C_{60}$ Orthorhombic Single Crystal

**Eugene L. FRANKEVICH** *(Institute for Energy Problems of Chemical Physics, Russian Aca. Sci. and IMS)*, **Yusei MARUYAMA, Hironori OGATA, Yohji ACHIBA*, and Koichi KIKUCHI*** *(*Tokyo Metropolitan Univ.)*

[*Solid State Commun.*, in press]

Time-of-flight technique has been used to measure mobilities of electrons and holes in $C_{60}$ orthorhombic single crystals at room temperature. Single crystals of $C_{60}$ grown from the $CS_2$ solution have been characterized as having about $10^{14}$ $cm^{-3}$ deep trapping sites for electrons and holes, The mobility for holes ($\mu_h$) at room temperature is $1.1 \pm 0.1$ $cm^2/V.s$ and that for electrons is found within the same limits. Temperature dependence of $\mu_h$ is revealed to be almost constant from 325 to 250K. $\mu_h$ starts increasing and below 250K may be approximated by the law $\mu_h \sim \exp$

($\Delta E/kT$) with $\Delta E$=0.053eV. Coincidence of the point of the increase of hole mobility with the phase transition temperature is worthy to be noted.

### IV-F-4 Mobility of Charge Carriers in Vapor-Phase Grown $C_{60}$ Single Crystals

**Eugene L. FRANKEVICH** *(Institute for Energy Problems of Chemical Physics, Russian Acad. Sci., and IMS)*, **Yusei MARUYAMA, and Hironori OGATA**

[*Chem. Phys. Lett.*, in press]

Transport properties of charge carriers in the fullerene $C_{60}$ single crystal grown from the vapor phase were studied by using the time-of-flight technique, and absolute values of mobility for electrons $\mu_e$=0.5±0.2 $cm^2/V$ s, and holes $\mu_h$=1.7±0.2 $cm^2/V$ s at room temperature were measured. Crystals were characterized as having about $3\times10^{13}$ $cm^{-3}$ deep trapping sites for holes. Temperature dependence of $\mu_h$ was measured within the broad range of temperature. Two features are revealed: (i) A step-wise increase of the mobility below the phase transition temperature and (ii) almost-temperature independence of mobility in regions from 50 to 200 K and from 250 to 310 K.

### IV-F-5 Electronic Properties of Some $C_{60}$ Derivatives

**Yusei MARUYAMA, Toshiyasu SUZUKI, Roger WHITEHEAD** *(Durham Univ. and IMS)*, **and Atsushi SUZUKI**

Some derivatives based on $C_{60}$ have been synthesized aiming at the change in electronegativity of $C_{60}$ molecule. We started to measure such solid state properties as magnetic susceptibity or electrical conductivity for the alkali metal doped $C_{61}H_2$ powder samples.

## IV—G Electrochemical Properties of the Organofullerene and Metallofullerene

Buckminsterfullerene, $C_{60}$ is an electronegative molecule which can accept up to six electrons in the solution and solid state. Because of this property, superconducting and ferromagnetic materials have been produced by doping with alkali metals and organic donors. We have been interested in the electronic structures of its derivatives such as organofullerenes and metallofullerenes and performed electrochemical measurements by cyclic voltammetry and differential pulse voltammetry.

### IV-G-1 Redox Properties of Organofullerenes

**Toshiyasu SUZUKI, Yusei MARUYAMA, Takeshi AKASAKA** *(Tsukuba Univ.)*, **Wataru ANDO** *(Tsukuba Univ.)*, **Kaoru KOBAYASHI** *(Yokohama National Univ.)*, **and Shigeru NAGASE** *(Yokohama National Univ.)*

[Submitted to *J. Am. Chem. Soc.*]

A comparative voltammetric study was done on oxygen-, carbon-, and silicon-substituted organofullerenes by cyclic voltammetry, differential pulse voltammetry, and Osteryoung square wave voltammetry. Electron affinities of organofullerenes increase with increasing electronegativities of attached atoms. $C_{60}O$ is a stronger electron acceptor than $C_{60}$. In the carbon-substituted derivatives, hybridization of the attached carbons and electron-withdrawing groups also affect their reduction potentials. Electron-donating groups such as alkyl and silyl lower the oxidation potentials of organofullerenes.

### IV-G-2 Electrochemical Properties of La@$C_{82}$

**Toshiyasu SUZUKI, Yusei MARUYAMA, Tatsuhisa KATO, Koichi KIKUCHI** *(Tokyo Metropol. Univ.)*, **and Yohji ACHIBA** *(Tokyo Metropol. Univ.)*

[Submitted to *J. Am. Chem. Soc.*]

We show that La@$C_{82}$ has unusual redox properties which significantly differ from empty fullerenes. Two oxidation and five reduction processes were observed by cyclic voltammetry and differential pulse voltammetry. Our results indicate that La@$C_{82}$ is a moderate electron donor as well as a stronger electron acceptor than any empty fullerenes.

## IV—H Preparation and Characterization of Copper Oxide High $T_c$ Superconductor Films

After the discovery of novel high $T_c$ superconductors, a lot of works including the film preparation have been carried out. We have carried out to fabricate thin films of such superconductors by a sputtering method and an electron-beam evaporation technique with the purpose of searching for new composition, structures, and elements in high $T_c$ superconductors.

### IV-H-1 Atomic Layer-by-Layer Deposition of Well-Oriented Crystalline La-Sr-Cu-O Films

**Toshifumi TERUI, Robert J. FLEMING** *(Monash Univ., and IMS)*, **and Yusei MARUYAMA**

[*Chem. Lett.*, 137 (1993)]

La-Sr-Cu-O films have been prepared as-deposited condition by an atomic layer-by-layer deposition technique in a high vacuum evaporation system with multi-electron beam-bun sources. The film quality is crucially dependent on the substrate temperature, oxidation gas, and source material. It is found that the layer-by-layer successive deposition of the

three elements is superior to the simultaneous deposition.

# IV—I Scanning Probe Microscopic Study on Some Functionality Materials

Scanning Probe Microscopy is a powerful technique to study microscopic surface structure or morphology at atomic or molecular level. Scanning Tunneling Microscopy (STM) and Atomic Force Microscopy (AFM) are becoming popular recently and we have applied these microscopies for some functionality materials to reveal the correlation between functionality and microscopic structure.

## IV-I-1 Scanning Tunneling Microscopy Observations of Zinc Naphthalocyamine on $MoS_2$

**Ayyakkannu MANIVANNAN** *(Univ. of Tokyo and IMS)*, **Larry A. NAGAHARA** *(Univ. of Tokyo)*, **Hisao YANAGI*, Takeshi KOUZEKI*, Michio ASHIDA***, *(*Kobe Univ.)*, **Yusei MARUYAMA, Kazuhito HASHIMOTO** *(Univ. of Tokyo)*, **and Akira FUJISHIMA** *(Univ. of Tokyo)*

[*Thin Solid Films*, **226**, 6 (1992)]

We have used STM to probe the molecular structure of ZnNc deposited on $MoS_2$ at 250°C. Columnar arrays were routinely observed with a periodicity of approximately 0.9 nm. Based on STM and X-ray data, the ZnNc molecules are believed to be stacked with the molecular planes standing canted to the $MoS_2$ surface.

## IV-I-2 Scanning Probe Microscopic Investigation of Epitaxially Grown $C_{60}$ Film on $MoS_2$

**Ayyakkannu MANIVANNAN** *(Univ. of Tokyo and IMS)*, **Hajime HOSHI, Larry A. NAGAHARA** *(Univ. of Tokyo)*, **Yoshihisa MORI, Yusei MARUYAMA, Koichi KIKUCHI*, Yohji ACHIBA*** *(*Tokyo Metropol. Univ.)*, **and Akira FUJISHIMA** *(Univ. of Tokyo)*

[*Jpn. J. Appl. Phys.*, **31**, 3680 (1992)]

$C_{60}$ thin films have been fabricated on $MoS_2$ surface by the molecular-beam epitaxy (MBE) and their monolayer coverage on this substrate have been investigated by scanning tunneling microscopy (STM) and atomic force microscopy (AFM). STM study indicates that the $C_{60}$ molecules pack either in a square lattice with lattice parameter of 11 $\pm$1 Å or a hexagonal close packed structure with lattice parameter of 10$\pm$1 Å. The AFM images show column like structures similar to the square lattice pattern of STM images. The substrate lattice has been imaged together with $C_{60}$ molecular contours by STM in order to determine the epitaxial nature of the film.

## IV-I-3 Scanning Prove and Transmission Electron Microscopy Observations of Cobalt Naphthalocyanine Molecules Deposited onto a NaCl Substrate

**Larry A. NAGAHARA** *(Univ. of Tokyo)*, **Ayyakkannu MANIVANNAN** *(Univ. of Tokyo and IMS)*, **Hisao YANAGI*, M. TORIDA*, Michio ASHIDA***, *(*Kobe Univ.)*, **Yusei MARUYAMA, Kazuhito HASHIMOTO** *(Univ. of Tokyo)*, **and Akira FUJISHIMA** *(Univ. of Tokyo)*

[*J. Vac. Sci. Technol.*, **A11**, 781 (1993)]

We have used scanning probe microscopy and transmission electron microscopy (TEM) to investigate the molecular orientation of cobalt naphthalocyanine (CoNc) vacuum deposited onto a NaCl substrate. Atomic force microscopy observations taken on CoNc deposited at room temperature reveal mostly amorphous grains with only few regions showing columnar structure. For CoNc films deposited at 250°C, scanning tunneling microscopy and TEM showed domains of columnar structure arranged in various orientation. The X-ray and electron diffraction analysis indicates that the molecules are standing with their planes perpendicular to the underlying NaCl substrate surface.

# IV—J Phase Transitions and Molecular Dynamics in Polar Liquid Crystals

Experimental studies on the microscopic nature of the liquid crystalline state was started. Special emphasis was placed on the unusual phase transitions and molecular dynamics in the polar smectic liquid crystals: A number of nematic (N) liquid crystalline compounds bearing strongly polar end group condense in the partially bilayered smectic A ($S_{Ad}$) state where the one-dimensional lattice period is incommensurate with the molecular length in its most extended form, due to antiferroelectric coupling among the molecules. Instability inherent to this ordering, *i.e.*, reentrant phase transition (the phase sequence, N-$S_{Ad}$- and the reentrant nematic, RN, on lowering the temperature) and a highly disordered nature of the $S_{Ad}$ state were investigated by applying various NMR techniques.

## IV-J-1 Proton NMR Study of CBOOA, NBOOA, and Their Chain Deuterated Homologues in Smectic Ad and Nematic Mesophases

**Seiichi MIYAJIMA* and Takehiko CHIBA**** *(*IMS and Nihon Univ., **Nihon Univ.)*

[*Liquid Cryst.*, **11**, 283 (1992)]

The nature of the smectic Ad to nematic phase transition and the modes of molecular motion were investigated for

the homologous mesogens, 4-octyloxy-*N*-(4-cyanobenzylidene)aniline (CBOOA), 4-octyloxy-*N*-(4-nitrobenzylidene)aniline (NBOOA), and their chain-deuterated compounds. In NBOOA, the $S_{Ad}$-N phase transition was found to be of first order with pronounced pretransitional decrease of the orientational order parameter $<P_2>$ both above and below the transition point, while in CBOOA such anomaly in $<P_2>$ was very small. Despite the different behaviors in terms of the orientational order, the dynamical aspects of molecular motion probed by the NMR relaxation are quite similar. The motional mode characteristic of the N phase was order director fluctuation, but translational self-diffusion became the dominant relaxation mechanism in the $S_{Ad}$ phase. It was also recognized that relative importance of these mechanisms changed in a continuous manner as a function of temperature.

### IV-J-2 Pulsed-Field-Gradient Stimulated-Spin-Echo NMR Study of Anisotropic Self-Diffusion in Smectic Ad Liquid Crystal CBOOA

**Seiichi MIYAJIMA*, A. F. MCDOWELL**, and R. M. COTTS**** *(*IMS and Cornell Univ., **Cornell Univ.)*

[*Chem. Phys. Lett.* **212**, 277 (1993)]

Anisotropic self-diffusion tensor was determined in the smectic Ad ($S_{Ad}$) phase of a polar mesogen CBOOA. The pulsed-field-gradient stimulated-spin-echo NMR technique was applied in combination with angular displacement of a quadrupole coil, to obtain the diffusion coefficient components both parallel ($D_{/\!/}$) and perpendicular ($D_{\perp}$) to the director for the sample oriented at the magic angle from the large static magnetic field. It was found that $D_{/\!/} > D_{\perp}$ ($D_{/\!/}/D_{\perp}$=2.3—3.0) and the activation energies were similar for the two components. These features are different from the known facts for classical $S_A$ state consisting of essentially nonpolar mesogens, and are similar to the diffusion in the N state. The unusual diffusion anisotropy is related to the highly disordered nature of the $S_{Ad}$ liquid crystal.

### IV-J-3 NMR Detection of the Director Realignment in Reentrant Liquid Crystals

**Seiichi MIYAJIMA**

In many of the liquid crystals formed by cooling from the isotropic melt in the magnetic field, the director is aligned along the external field due to diamagnetic anisotropy. When the direction of the external field is suddenly switched, the director follows the equation of motion consisting of magnetic and viscous torques. Since the magnitude of the internuclear dipole-dipole coupling is a function of the angle between the director and the external field, the realignment process is probed by the NMR line shape. In the present study the kinetics was detected through the unusual phase transition sequence, N-$S_{Ad}$-N-$S_{AI}$, on lowering the temperature. This method was also proved to be applicable for the detection of the phase transition with very subtle thermal anomaly.

### IV-J-4 Alkyl-Deuteration of CBOBP by the Carbon-Carbon Cross Coupling and the Effect of Isotopic Exchange on the Reentrant Phase Transition

**Takamasa HOSOKAWA, Toshiyasu SUZUKI, and Seiichi MIYAJIMA**

Perdeuteration of the alkyl chains of reentrant mesogens is an interesting work due to the necessity for deuterium NMR. It is also interesting to know the effect of isotopic exchange on the phase transitions and the molecular motion. In this study the chain-deuterated 4-cyanobenzoyloxy-(4-octylbenzoyloxy)-*p*-phenylene (CBOBP-$d_{17}$) was prepared by applying the nickel-phosphine complex-catalyzed cross coupling of perdeuterated alkyl Grignard reagent with bromobenzene. In the phase transition sequence, N-$S_{Ad}$-N-$S_{AI}$, only the reentrant phase transition, $S_{Ad}$ to N on lowering the temperature, was significantly affected by the chain-deuteration, suggesting that this transition is strongly correlated with the chain motion.

### IV-J-5 Liquid Crystals of Terminally Trifluoromethyl- and Trifluoromethoxy-Derivatives of 4-Octyloxy-*N*-Benzylideneaniline

**Seiichi MIYAJIMA, Ayumi NAKAZATO*, Noriko SAKODA*, and Takehiko CHIBA*** *(*Nihon Univ.)*

Seven compounds of 4-octyloxy-*N*-(substituted benzylidene)aniline (XBOOA) family were synthesized, and the fundamental liquid crystalline properties were studied to explore possibly novel characteristics of the polar mesogens. 4-trifluoromethyl and 4-trifluoromethoxy derivatives exhibited stable smectic B and A phases, respectively, while both of the methyl and methoxy derivatives have monotropic nematic phases. None of the 3,5-bis(trifluoromethyl)-, 3,5-dimethyl-, and 3,5-dimethoxy-derivatives were mesogenic. The effect of terminal trifluoromethylation on the liquid crystalline properties was discussed.

## IV—K Solid State High Resolution NMR Studies of Organic Conductors

Structural and electronic properties of the single-component organic conductors were studied.

### IV-K-1 $^{13}C$ Solid State High Resolution NMR Study of the Organic Conductors, TTF and Its Derivatives (BEDT-TTF and TTCn-TTF)

**Seiichi MIYAJIMA*, Takehiko CHIBA**, Gunzi SAITO***, and Hiroo INOKUCHI** *(*IMS and Nihon Univ., **Nihon Univ., ***Kyoto Univ.)*

Cross polarization-magic angle sample spinning-$^{13}C$ NMR experiment was carried out for the single component

organic conductors, TTF and its derivatives. In TTF and BEDT-TTF, the central ethylene carbons were found to be most shielded among the ring carbons, and tend to be even more shielded in the long-chain homologues of TTCn-TTF, reflecting the $\pi$-band formation. As the chain length increases, the shielding of the ethylene and methylene carbons directly attached to the outer sulfer atoms exhibited discontinuous change between n=6 and 7 consistent with the change in molecular stacking evidenced by the X-ray structural analysis.

# IV—L Organic Metals

In an attempt to develop new organic superconductors and to explore the related phenomena, new organic conductors have been prepared and the physical properties have been investigated. Particularly, this year detailed physical properties of organic superconductors (BEDT-TTF)$_4M$(CN)$_4$H$_2$O [$M$ = Pt and Pd] were investigated. In addition, extensive study was carried out for crystal structures and conducting properties of "double-TTF" series salts.

## IV-L-1 Physical Properties of New Organic Superconductors, (BEDT-TTF)$_4M$(CN)$_4$H$_2$O [$M$ = Pt and Pd]

**Takehiko MORI, Kiyonori KATO, Yusei MARUYAMA, Hiroo INOKUCHI, Hatsumi MORI*, Izumi HIRABAYASHI*, and Shoji TANAKA*** *(ISTEC)*

[*Synth Metals*, **56**, 2911 (1993)]

New organic conductors (BEDT-TTF)$_4M$(CN)$_4$H$_2$O [$M$ = Pt, Pd, and Ni] exhibit metallic conductivity down to *ca.* 80 K, below which the resistivity increases slightly. The measurements of thermoelectric power (Fig. 1) and ESR indicate that there is no energy gap even at low temperatures. The Pt and Pd salts undergo superconducting transitions at $T_c$ = 2 K under 6.5 kbar, and $T_c$ = 1.2 K under 7 kbar, respectively, whereas the Ni salt shows no superconducting transition under similar conditions.

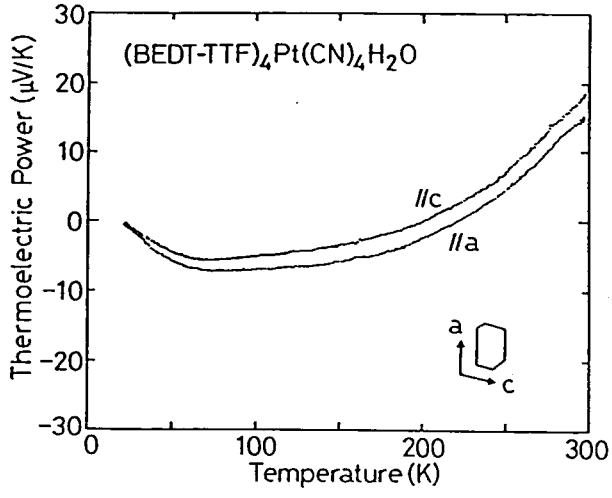


**Figure 1.** Thermoelectric Power of (BEDT-TTF)$_4$Pt(CN)$_4$H$_2$O.

## IV-L-2 Bis(methylthio) Substituted Unsymmetrical 2,5-Bis(1′,3′-dithiol-2′-ylidene)-1,3,4,6-tetrathiapentalenes

**Yohji MISAKI,* Hiroyuki NISHIKAWA,* Tokio YAMABE,* Takehiko MORI, Hiroo INOKUCHI, Hatsumi MORI,** and Shoji TANAKA**** *(*Kyoto Univ., **ISTEC)*

[*Chem. Lett.*, **1993**, 729]

2,5-Bis(1′,3′-dithiol-2′-ylidene)-1,3,4,6-tetrathiapentalenes were synthesized as the donor components for organic conductors, and preparation and electrical properties of their cation radical salts were investigated. Among various cation radical salts obtained so far, $AsF_6$ salt of ethylenedithio derivative and $SbF_6$ salt of ethylenedioxy derivative showed metallic temperature dependence of conductivities down to 0.6 K.

## IV-L-3 Structure and Conducting Properties of TMET-TTP Radical-Cation Salts

**Takehiko MORI, Hiroo INOKUCHI, Yohji MISAKI,* Hiroyuki NISHIKAWA,* Tokio YAMABE,* Hatsumi MORI,** and Shoji TANAKA**** *(*Kyoto Univ., **ISTEC)*

[*Chem. Lett.*, **1993**, 733]

Radical cation salts of TMET-TTP (2-(4′,5′-bis(thiomethyl)-1′,3′-dithiol-2′-ylidene)-5-(4″,5″-ethylenedithio-1″, 3″-dithiol-2″-ylidene)-1,3,4,6-tetrathiapentalene) with various anions show high electrical conductivity. Many of them have a similar $\theta$-type structure (Fig. 1) with two-dimensional donor arrangement.

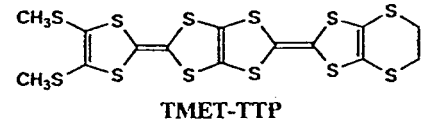


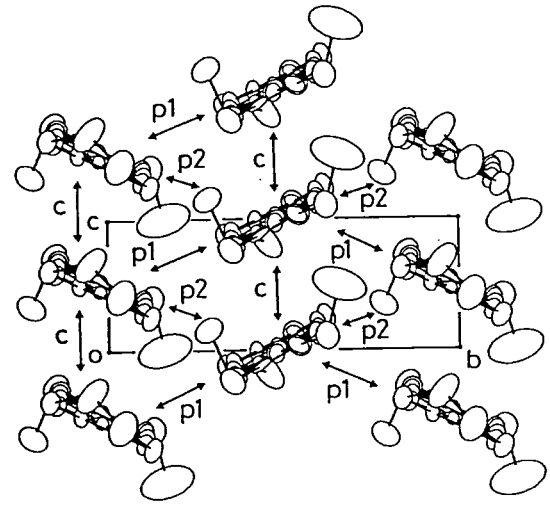


**Figure 1.** $\theta$-type donor arrangement of (TMET-TTP)$_3$ReO$_4$.

### IV-L-4 Structure and Electrical Properties of MeDTET Salts

**Yohji MISAKI,* Hiroyuki NISHIKAWA,* Tokio YAMABE,* Takehiko MORI, Hiroo INOKUCHI, Hatsumi MORI,** and Shoji TANAKA**** *(*Kyoto Univ., **ISTEC)*

[*Chem. Lett.*, **1993**, 1341]

Several cation radical salts of MeDTET-TTF (2-isopropylidene-1,3-dithiolo[4,5-d]ethylenedithiotetrathiafulvalene) showed metallic temperature dependence of conductivity down to 0.6 K. X-ray crystal structure of (MeDTET-TTF)$_3$PF$_6$TCE$_x$ revealed that the donors have κ-type arrangement in the conducting sheet (Fig. 1). This is the first example of a κ-type salt that has a composition other than 2:1.

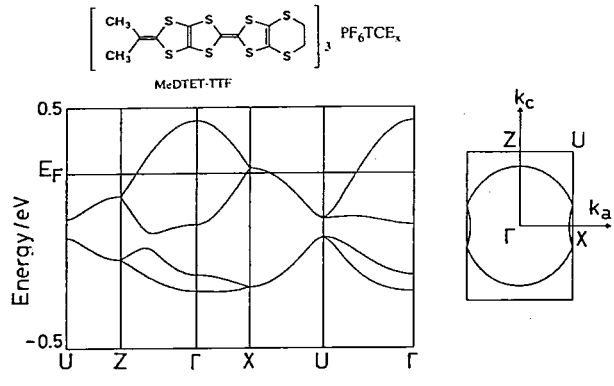


**Figure 1.** Energy band structure of (MeDTET-TTF)$_3$PF$_6$TCE$_x$.

### IV-L-5 Structure and Physical Properties of (TMEO-TTP)$_2$Au(CN)$_2$

**Takehiko MORI, Hiroo INOKUCHI, Yohji MISAKI,* Hiroyuki NISHIKAWA,* Tokio YAMABE,* Hatsumi MORI,** and Shoji TANAKA**** *(*Kyoto Univ., **ISTEC)*

[Chem. Lett. **1993**, 2085]

Radical cation salts of TMEO-TTP with linear and octahedral anions exhibit metallic conductivity down to 0.6 K (Fig. 1). The title salt has "$ClO_4$-type" donor arrangement, and the measurements of electrical conductivity, thermoelectric power, and ESR show a characteristic metal-to-metal transition.

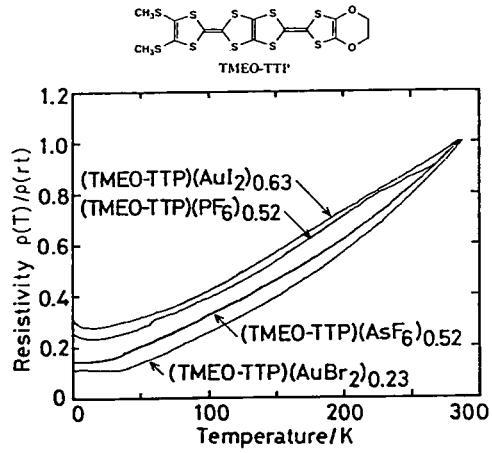


**Figure 1.** Electrical resistivity of TMEO-TTP salts.

## IV—M Photoelectron Spectroscopy of Organic Solids in Vacuum Ultraviolet Region

The works of ultraviolet photoelectron spectroscopy (UPS) and also of UPS with synchrotron radiation lightsource (UVSOR-UPS) of organic materials have been proceeded to find their quantitative electronic structures.

### IV-M-1 Valence Electronic Structure of a Long-Chain Alkane in Random Coil Forms: Gas Phase UPS of *n*-$C_{36}H_{74}$ and MO Calculations

**Kazuhiko SEKI*, Naoki SATO**, and Hiroo INOKUCHI** *(*Nagoya University, **Kyoto University)*

[*Chem. Phys.*, in press]

Electronic structure of a long chain alkane in random coil forms was studied by the combination of ultraviolet photoelectron spectroscopy (UPS) of *n*-$C_{36}H_{74}$ in the gas phase and *ab initio* MO calculations of alkanes in various conformations. The observed spectra were generally similar with those of the crystalline state characterized by extended chain form, except for the disappearance of a feature in the C2p+H1s band. Spectral simulation by MO calculations with taking account of the statistical weights of conformers gave results consistent with the above observations. The similarity of the occupied states between the extended-chain and random-coil forms is in sharp contrast with the drastic change of unoccupied state structure between crystalline and molten (liquid) states.

### IV-M-2 Angle-Resolved Photoemission Spectroscopy of Ultrathin Films of $H_2$-Phthalocyanine on $MoS_2$ Surfaces

**Nobuo UENO*, Katsumi SUZUKI*, Shinji HASEGAWA, Koji KAMIYA**, Kazuhiko SEKI**, and Hiroo INOKUCHI** *(*Chiba University, **Nagoya University)*

[*J. Chem. Phys.*, in press]

The take-off-angle dependence of photoelectrons from the top most valence band of $\pi$ state was measured using synchrotron radiation at normal incidence condition and $h\nu$=40 eV for thin films of $H_2$-phthalocyanine deposited on cleaved $MoS_2$ surfaces. A sharp angular distribution of the photoelectrons was observed with a maximum intensity at the take-off-angle of about 34°. The results were analyzed with Independent-Atomic-Center approximation combined with MNDO molecular orbital calculations. As in the case of bis(1,2,5-thiadiazolo)-*p*-quinobis(1,3-dithiole) on graphite, the experimental angular distribution agreed well the calculated one for flat-lie orientation of $H_2$-phthalocyanine molecule. So far such a reasonable analysis has never been

performed for the angle-resolved ultraviolet photoelectron spectra of thin films of large and complex organic molecules. Although the analysis model should involve the photoelectron scattering for a much better agreement between experimental and calculated results, our analysis method is useful in the quantitative analysis of photoelectron angular distribution from thin films of functional organic molecules and in determining molecular orientation of them.

### IV-M-3 Mono- and Multilayers of Novel Molecular Complex of Thiophene Derivative with Long-Chain TCNQ

**Hiroo NAKAHARA*, Akira NAGASAWA*, Akihiko ISHII*, Juzo NAKAYAMA*, Masamatsu HOSHINO*, Kiyoshige FUKUDA*, Kouji KAMIYA**, Chikako NAKANO, Unpei NAGASHIMA, Kazuhiko SEKI**, and Hiroo INOKUCHI** *(*Saitama University , **Nagoya University)*

[*Mol. Cryst. Liq. Cryst.*, **227**, 13 (1993)]

Electronic structures of the 2,5-dihydrothiophene derivatives were characterized by UPS spectra together with crystallographic analysis. A novel complex between the thiophene derivative and $C_{18}$TCNQ was obtained and the multilayer of the complex was prepared. Electrical conductivities with respect to the parallel and perpendicular direction to the film plane have been studied to the film structures.

## IV—N Electrical Conduction and its Related Properties of Organic Solids

The electronic properties of single component organic semiconductors and $C_{60}$ complexes have been observed.

### IV-N-1 ESR and Low-Field Microwave Absorption Studies of Potassium Doped $C_{70}$: Observation of Possible Metallic State in $K_xC_{70}$

**Kenichi IMAEDA, Kyuya YAKUSHI, Hiroo INOKUCHI, Koichi KIKUCHI*, Isao IKEMOTO*, Shinzo SUZUKI*, and Yohji ACHIBA*** *(*Tokyo Metropolitan University)*

[*Solid State Commun.*, **84**, 1019 (1992)]

The magnetic property of $K_xC_{70}$ upon K doping process was investigated by electron spin resonance (ESR) and low-magnetic field microwave absorption (low-field signal: LFS). In the early stage of K doping (doping time $t_d < 40$ h), ESR signal with a Curie-like behavior was observed, which means an insulating state of a doped phase in this stage. In $t_d > 40$ h, ESR spectra broadened suddenly and the almost temperature-independent behavior of ESR intensity appeared in the high temperature region. This suggests a change from an insulating $K_xC_{70}$ phase to a metallic $K_xC_{70}$ phase. The chemical analysis has presented that the insulating phase corresponds to $K_3C_{70}$ and the metallic phase corresponds to $K_4C_{70}$. A very weak LFS below *ca.* 9 K was observed in the doping stage of $t_d \geq 10$ h, indicating the coexistence of a small volume of some superconducting phase. A possible origin of the superconducting phase is described.

### IV-N-2 New Superconducting Sodium-Nitrogen-$C_{60}$ Ternary Compound

**Kenichi IMAEDA, Ilias I. KHAIRULLIN** *(Uzbek Acad. of Sci.)*, **Kyuya YAKUSHI, Masaaki NAGATA, Nobuo MIZUTANI, Hiroshi KITAGAWA, and Hiroo INOKUCHI**

[*Solid State Commun.*, **87**, 375 (1993)]

We have prepared sodium-doped $C_{60}$ utilizing the thermal decomposition of sodium azide ($NaN_3$). The strong low-magnetic field microwave absorption with a clear hysteresis was observed in the samples of $Na_nC_{60}$ ($n=3 \sim 4$), indicating the superconducting nature. By means of a SQUID measurement, the superconducting transition temperature is found to be around 12 K. Significantly, elemental analysis detected a nitrogen which was surely produced in the process of the thermal decomposition of $NaN_3$. We suppose that this new superconducting phase will be $Na_xN_yC_{60}$ where x is between 3 and 4, and y is unknown. This is the first superconducting material in Na-doped $C_{60}$ without other alkali metals.

## IV—O Electron Transport in Cytochromes

Using x-ray photoelectron spectroscopy (XPS) and Langmuir-Blodgett film preparation technique, the detailed electronic structures of cytochrome *c* series has been analyzed.

### IV-O-1 Electronic States of Oxidized and Reduced Cytochrome *c* Observed by X-ray Photoelectron Spectroscopy

**Kenji ICHIMURA** *(Kumamoto Univ.)*, **Yusuke NAKAHARA** *(Tech. Coll. Miyakonojo)*, **Keisaku KIMURA** *(Himeji Inst. Tech.)*, **and Hiroo INOKUCHI**

[*J. Mater. Chem.*, **2**, 1185 (1992)]

To understand the measurement of electrical conducti-

vities of cytochromes in terms of the electronic and valence states, x-ray photoelectron spectra of oxidized and reduced cytochrome *c* were measured in the Fe 2p, S 2p, O 1s, N 1s and C 1s regions. The difference between the spectra of both forms shows that changes occur in the electronic states at the sites of porphyrin ring and sulfur-containing amino acids (methionine and cysteine residues). Two peaks appear at 165.3 and 170.7 eV in the spectrum for the oxidized form. After reduction, four peaks are observed at 162.2, 165.4, 170.4 and 172.4 eV. The Fe 2p spectra show changes in the chemical shift and the satellite structure. The higher conductivity of ferrocytochrome *c* (reduced form) than ferricytochrome *c* (oxidized form) is attributed to the change multiplicity of sulfur atoms in addition to $\pi$-electron system.

## IV-O-2 Direct Observation of the Secondary Structure of Unfolded Pseudomonas-cytochrome $c_{551}$ by Scanning Tunneling Microscopy

**Zhong Fan LIU, Ayyakkannu MANIVANNAN, Hisao YANAGI*, Michio ASHIDA*, Akira FUJISHIMA**, and Hiroo INOKUCHI** (**Kobe University, **Tokyo University)*

[*Surface Sci. Lett.*, **284**, L411 (1993)]

The denaturation of pseudomonas-cytochrome $c_{551}$ at the air-water interface was studied using scanning tunneling microscopy (STM). The STM images indicate that the native secondary and tertiary structures of this protein has been virtually lost at such interface. The polypeptide chains of the unfolded protein are nearly fully extended, and higher aggregated in a localized region, forming a crystalline or a twisted rope-like structure. Our observation demonstrates the capability of STM in studying the unfolding of protein, and also suggests the possibility of using STM to directly sequence the amino acid residues of a protein.

# RESEARCH ACTIVITIES V
# Department of Applied Molecular Science

## V—A New Multi-Stage Redox Systems

Interdisciplinary cooperation between synthetic chemistry, physical chemistry, and solid state physics has opened a new field of science which forcuses on the development and study of molecular materials having interesting electrical, magnetic, and optical properties in the solid state. In general, molecular level correlation of molecular solid state micro structure and bulk material properties is essential to construct new molecular materials. Such consideration regarding highly electrically conducting behavior reveals the importance of conjugated electronic systems having multi-stage redox nature, which can transfer electrons smoothly by multi-stage manners. We have designed and synthesized two classes of new multi-stage redox systems, such as peri-condensed Weitz type donors, and amphoteric multi-stage redox systems. The peri-condensed Weitz type redox systems are designed by replacing two of the $sp^2$ carbon atoms in a polycyclic arene by two sulfur atoms. Such heterocycles have produced new organic molecular metals which contain non-TTF and non-TCNQ type components. The amphoteric multi-stage redox systems are designed so as to decrease the difference between the oxidation and the reduction potentials of a molecule. We have already reported the synthesis and properties of conjugated hydrocarbons with the highest amphotericity. Design and synthesis of new types of multi-stage redox systems, and investigations of their physical and solid state properties are actively continued.

## V—B New Conjugated Electronic Systems

Design and synthesis of novel conjugated electronic systems are continuing in the exploration of new molecular materials which might have interesting chemical reactivities and physical properties. In this research project, new electronic systems having closed shell and open shell electronics are actively searched for. Chemical modifications of known electronic systems are also important. An example is as follows. Stable, conjugated, neutral radicals have attracted much attention as new materials having potentially interesting solid state properties, as single component conductors, and magnetically interesting materials. We have utilized odd alternant hydrocarbon, phenalenyl, as the basic skeleton for neutral radicals, and modified the phenalenyl skeleton by introducing donor and acceptor substituents to suppress the thermodynamic and kinetic instability. Such modification is one of the typical procedure in physical organic chemistry to stabilized unstable electronic systems.

### V-B-1 Oxidation Reaction of 3-Hydroxyphenalenone

**Kunio HATANAKA, Yasushi MORITA, and Kazuhiro NAKASUJI**

In order to explore stable neutral radicals based on phenalenyl systems, we designed 3- and 6-oxophenalenoxyl radicals, **1** and **2**. As a basic study to clarify the chemical reactivities of **1**, we performed oxidation of 2-phenyl-3-hydroxyphenalenone derivatives with three different reagents, $K_3[Fe(CN)_6]$, $PbO_2$, and $Ag_2CO_3$. The product obtained from these reactions was determined as the C-C dimer at 2-position of the phenalenyl moiety of the desired radical species from the elemental analysis and the spectroscopic measurements. The result is consistent with the characteristics of the spin delocalization and indicates that more bulky substituent than phenyl group needs at 2-position to isolate the desired neutral radical.

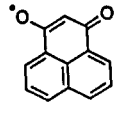

1

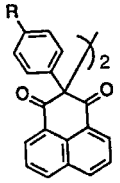


2

### V-B-2 Crystal Structure of the Dimeric Product Obtained by Oxidation of 2-*p*-Methoxyphenyl-3-hydroxyphenalenone

**Kunio HATANAKA, Yasushi MORITA, Jiro TOYODA, and Kazuhiro NAKASUJI**

The chemical structure of the oxidation product of 2-aryl-3-hydroxy-phenalenones was determined as the dimer of the desired neutral radical from the elemental analysis and spectroscopic measurements. However, there are some ambiguities since $^1$H-NMR spectrum of the oxidation product of 3-hydroxyphenalenones showed more complicated signal than the expected symmetrical structure and the broad signal in some part, which suggest the existence of some dynamic behavior in the molecule. In order to determine the chemical structure unequivocally, we performed X-ray crystal structure analysis of 2-*p*-methoxyphenyl-3-hydroxyphenalenone. As shown in the figure, the product is actually the dimer which has the longer C-C single bond length, 1.59 Å. The steric congestion between aromatic hydrogens of the methoxyphenyl and oxygens of the phenalenyl is expected to produce the restricted rotations and make the $^1$H-NMR signal complicated.

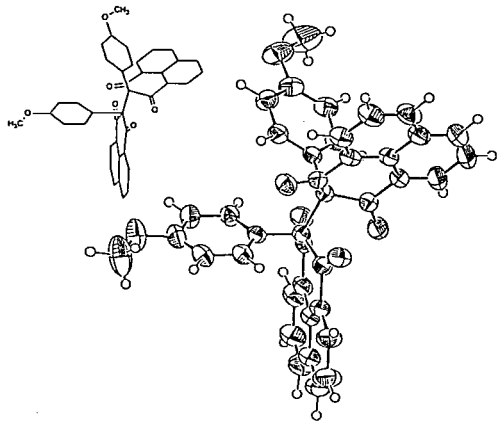

### V-B-3 Oxidation Reaction of 2-Naphthyl-3-hydroxyphenalenone

**Kunio HATANAKA, Yasushi MORITA, and Kazuhiro NAKASUJI**

In order to understand the reactivities of the 3-oxophenalenoxyl radical system, we performed oxidation of 2-naphthyl-3-hydroxyphenalenone (**1**) with $K_3[Fe(CN)_6]$, $PbO_2$, or $Ag_2CO_3$. We obtained the extended conjugated phenalenone derivatives, **2** and **3**, whose chemical structures were determined by the elemental analysis and spectroscopic measurements. Interestingly, the compound **3** can be characterized as an oxa-ketone derivative of unique condensed polycyclic aromatic, Zethrene.

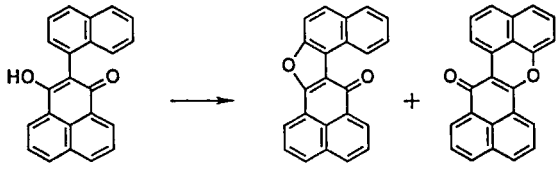


1 2 3

### V-B-4 Synthesis of 1,6-Diazaphenalene Derivatives

**Yasushi MORITA, Koichi TAMAKI, and Kazuhiro NAKASUJI**

Phenalenyl, an odd alternant hydrocarbon with one NBMO, plays an important role to design new conjugated electronic systems. Heterocyclic analog of phenalenyl can also be utilized for such purposes. We pay attention to the 1,6-diazaphenalenyl skeleton to explore new molecular systems. In addition to the redox properties, the hydrogen bonding ability and the coordination ability of the nitrogen atoms make the electronic system unique. J. M. Cook and his coworker reported the synthesis of several derivatives of 1,6-diazaphenalenyl derivatives. We synthesized new derivatives **2** of 1,6-diazaphenalene from 2,4-dichloroaniline by four steps. This synthetic procedure can be applied to introduce substituents regio-selectively to the diazaphenalene skeleton.


1 2

## V—C New Cooperative Proton-Electron Transfer (PET) Systems

From the viewpoint of synthetic chemistry, we have begun exploration of molecular materials having interesting chemical reactivities and physical properties, while constructing an interdisciplinary strategy for interesting materials. Our particular attention in this research project is paid to the hydrogen-bonded charge-transfer (HBCT) systems which exhibit cooperative proton-electron interactions in the solid state. If a cooperative proton-electron transfer (PET) occurs inter-molecularly in such systems, a state which can be characterized as a molecular assembly of *H-bonded neutral radicals* might be produced. The type and strength of the proton-electron cooperativity can control the solid state properties in an interesting way. A stepwise consideration on the PET phenomenon leads to two reasonable molecular design strategies to realize such a PET state under milder conditions: (1) the exploration of new electronic systems having a smaller intermolecular CT gap and (2) an electronic modification to stabilize H-bonded neutral radicals. Our current fundamental efforts are concentrated on the design and synthesis of a wide range of HBCT systems having the cooperative interaction between H-bonding and electron transfer process, in both organic materials and transition metal complexes.

### V-C-1 Molecular Design of H-Bonded Charge-Transfer Complexes Composed of the Transition Metal Complex

**Makoto TADOKORO, Jiro TOYODA, Tetsuji ITOH, Kiyoshi ISOBE, and Kazuhiro NAKASUJI**

It is important to explore new PET systems having a smaller intermolecular charge-transfer gap. As one of the approaches, we are now designing H-bonded transition metal complexes. In such metal complexes, the redox property of metal atoms and the intermolecular interactions through metal atoms can be utilized as the intermolecular CT interactions. The interaction between metal atom and ligand are also possible for the intermolecular electronic interaction. The biimidazole skeleton which possesses the potential ability to form inter-ligand H-bonding is widely

used as a chelating ligand to transition metals. Furthermore, depending on the structural characteristics in the metal complex the ligand show the donor and acceptor properties of proton and electron in systematic fashion. Paying attention to the characteristics, we began to construct biimidazole transition metal complexes having networks of H-bondings between the ligands. As a first step, we synthesized **1**. The crystal structure analysis showed the H-bonding interaction between the biimidazole ligand and the counter anion perchlorate, but no H-bonding interaction between the biimidazole ligands.

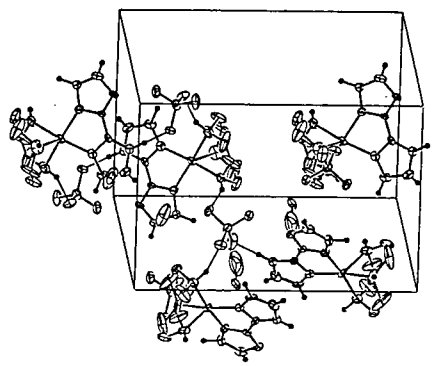

## V-C-2 Crystal Structure of the H-Bonded Dimer of the Biimidazole Transition Metal Complex

**Makoto TADOKORO, Jiro TOYODA, Tetsuji ITOH, Kiyoshi ISOBE, and Kazuhiro NAKASUJI**

The biimidazole ligand in the metal complexes basically exists in the three forms, such as di-protonated, mono-protonated, and non-protonated forms. In order to construct a H-bonded dimer of the biimidazole transition metal complexes, the neutral complex of copper(II) with the mono-protonated form of biimidazole ligand was synthesized. The crystal structure analysis showed the existence of dimeric H-bonds of the type NH···N type between the mono-protonated biimidazole ligands as a first example among the biimidazole transition metal complexes.

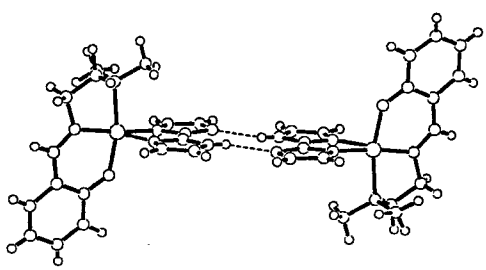

## V-C-3 Synthesis and Crystal Structure of Bis(ethylenedithioglyoxime)nickel

**Tetsuji ITOH, Jiro TOYODA, Makoto TADOKORO, and Kazuhiro NAKASUJI**

Generally, the fundamental structural characteristics of PET systems can be expanded to the H-bonded transition metal complexes. In such complexes, we can utilize the additional characteristics of redox properties of the metal atoms and the intermolecular interactions between the metal atoms or between the metal atom and the ligand. Recently, Endres and his coworkers have intensively studied the crystal structures and physical properties of the metal complexes containing the diaminoglyoxime ligand. In order to understand the role of the H-bonding in such metal complexes, we modified the ligand so as to decrease the site for the intermolecular H-bondings. We prepared bis(ethylenediaminoglyoxime)metal complexes and bis(ethylenedithioglyoxime)metal complexes. Bis(ethylenedithioglyoxime)-nickel gave single crystals for crystal structure analysis.

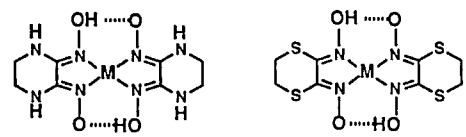

## V-C-4 Crystal Structure of Charge-Transfer Complex of Bis(ethylenediaminoglyoxime)Pd with Tetracyanoquinodimethane

**Jiro TOYODA, Tetsuji ITOH, Makoto TADOKORO, and Kazuhiro NAKASUJI**

In order to expand the examples of the H-bonded CT complexes, we have recently prepared the transition metal complexes of ethylenediaminoglyoxime ligand ($H_2$edag). Using this transition metal complex as an electron donor component, we prepared CT complexes with organic acceptors. One of the CT complexes, [Pd($H_2$edag)(Hedag)] TCNQ, formed black single crystals. Crystal structure analysis showed that this complex contains the segregated stacks of the donor and acceptor columns. There were found the intermolecular H-bonds between NH group of the metal complex and CN group of TCNQ. Therefore, the donor and acceptor columns are connected by the H-bonding. Furthermore, in the columns of the transition metal complexes, there exist OH···O type intermolecular H-bonds between the oxime moieties.

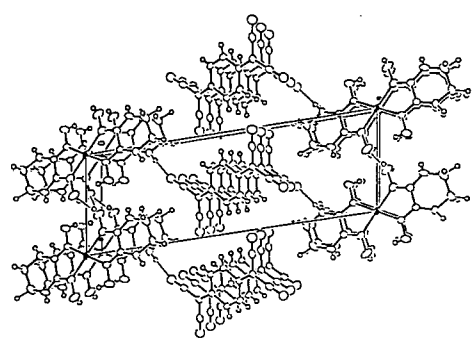

## V-C-5 *Ab-initio* Molecular Orbital Studies for the Dimer Model of Quinhydrone

**Jiro TOYODA, Satoshi MINAMINO, Kazuo KITAURA, and Kazuhiro NAKASUJI**

In order to analyze the cooperative PET type phase transition at the molecular level in more detail, we have undertaken *ab-initio* molecular orbital calculations of the

benzoquinone-benzohydroquinone complex (quinhydrone). Semi qualitative basic properties, such as optimized molecular geometries, electronic structures, and molecular energies were calculated using the UHF/3-21G* basis set for relevant quinone related model species; benzoquinone, hydroquinone, benzoquinone anion radical, hydroquinone cation radical, semiquinone anion, semiquinone cation, semiquinone radical. The energies of both hydrogen bonded hydroquinone-quinone complex (Figure 1) and semiquinone dimer (Figure 2) are more stable than the sum of energies of the corresponding components by about 12 kcal $mol^{-1}$. The stability can be attributed to the intermolecular H-bonding.

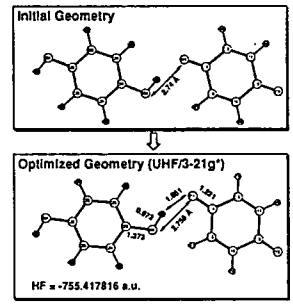


Figure 1.

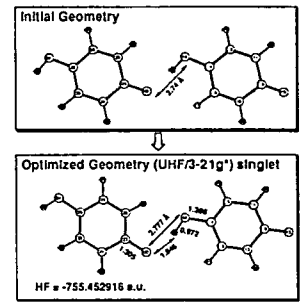


Figure 2.

# V—D Transition Metal Oxide Clusters

Recently, we have directed our efforts primarily toward the synthesis of integrated cubane-type clusters as potential models for inorganic solid surfaces to understand the chemistry on them. We have synthesized the triple cubane-type oxide cluster, $[(RhCp^*)_4Mo_4O_{16}]$ (**1**) which shows novel fragmentaion and extention of cube size. Cluster **1** have three kinds of the M-O bonds with oxygen atoms of different charge density and basicity. These functionalities will be important facter for determination of its reactivity. We are also studing reactivities of cluster **1** toward organic molecules containing sulfur atom. In addition, we will see how transformation of the cluster framework takes place during the reaction.

## V-D-1 Synthesis and Molecular Structure of Tetranuclear Complex with Two $Rh(\mu\text{-}SMe)_3Mo$ Groups, $[\{Cp^*Rh(\mu\text{-}SMe)_3MoO\}_2(\mu\text{-}O)(\mu\text{-}S)]$ ($Cp^*=\eta^5\text{-}C_5Me_5$)

**Xi RIMO** *(Grad. Univ. for Adv. Studies and IMS)*, **Bateer WANG** *(IMS and Inner Mongolia Norm. Univ.)*, **Yoshiki OZAWA** *(IMS and Himeji Institute of Technology)*, **and Kiyoshi ISOBE**

In the course of studying the reactivity of the triple-cubane type cluster, $[(RhCp^*)_4Mo_4O_{16}]$, toward MeSH, we have synthesized a new $Rh_2Mo_2$ tetranuclear complexe, $[\{Cp^*\text{-}Rh\ (\mu\text{-}SMe)_3MoO\}_2\ (\mu\text{-}O)(\mu\text{-}S)]$ (**1**) according to eq. 1.

$$[(RhCp^*)_4Mo_4O_{16}]\cdot 2H_2O + 18MeSH \rightarrow 2[\{Cp^*Rh(\mu\text{-}SMe)_3MoO\}_2(\mu\text{-}O)(\mu\text{-}S)] + 2MeSSMe + 2Me\cdot + 12H_2O$$

In **1** the $\mu$-S ligand may arise from the bond cleavage of the C-S bond of MeSH, but the resulting alkyl moiety was not detected. The products were recrystallized from $CH_2Cl_2$ at room temperature and characterized by single crystal X-ray analysis. The molecular structure is shown in Figure 1. The three SMe ligands in **1** link different two metal atoms, Rh (III) and Mo (V), to make $Cp^*Rh(\mu\text{-}SMe)_3Mo$ moieties which are bridged by O1 and S7 atoms in a syn arrangement with their groups on the same side of the bridge. The $OMo(\mu\text{-}O)(\mu\text{-}S)MoO$ framework was also found to have a syn arrangement. All six sulfur atoms of the SMe ligands prefer the Rh atoms in unequal bridging of the Rh···Mo spacing. In particular, the Mo-S (SMe) bond trans to the Mo-O (terminal) bonds are substantially longer (2.734(2) and 2.717(2) Å) than the others (2.547(2)-2.615(3) Å). The complexe has metal-metal bonds (2.666(1) Å) between the molybdenum atoms with a $d^1$ configuration, and hence are diamagnetic. Two sets of the three bridging SMe groups are disposed as in an anticlockwise symmetric arrangement for **1**, viewed along the Rh1···Mo1 and Rh2···Mo1 axes.

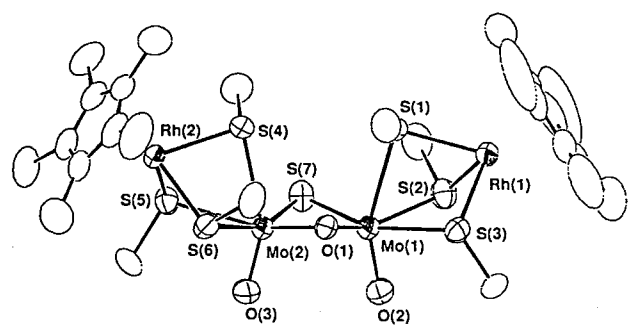


**Figure 1.** Perspective view of $[\{Cp^*Rh(\mu\text{-}SMe)_3MoO\}_2(\mu\text{-}O)(\mu\text{-}S)]$

## V-D-2 A Novel System for Studying Stereodynamics of Tetranuclear Thiolate Complexes $[\{Cp^*Rh(\mu\text{-}SMe)_3MoO\}_2(\mu\text{-}O)_2]$ and $[\{Cp^*Rh(\mu\text{-}SMe)_3MoO\}_2(\mu\text{-}O)(\mu\text{-}S)]$ ($Cp^*=\eta^5\text{-}C_5Me_5$)

**Xi RIMO** *(Grad. Univ. for Adv. Studies and IMS)*, **Masaaki ABE, Yoshiki OZAWA** *(IMS and Himeji Institute of Technology)*, **and Kiyoshi ISOBE**

To date, several binuclear metal complexes with three bridging SR ligands, $L_nM(\mu\text{-}SR)_3M\text{-}L_n$, have been prepared, and some of them show interesting fluxional behaviors in solution due to the inversion at the pyramidal sulfur center.

In the course of studying the reactivity of the triple-cubane type cluster, $[(RhCp^*)_4Mo_4O_{16}]$, toward MeSH, we have synthesized new $Rh_2Mo_2$ tetranuclear complexes, $[\{Cp^*Rh(\mu\text{-}SMe)_3MoO\}_2(\mu\text{-}O)_2]$ (**1**) and $[\{Cp^*Rh\ (\mu\text{-}SMe)_3\text{-}MoO\}_2\ (\mu\text{-}O)(\mu\text{-}S)]$ (**2**), which have two $Rh(\mu\text{-}SMe)_3Mo$ groups in the molecule (see V-D-1 and Annual

Rev., 1992, p. 79). These tetranuclear complexes provide a novel system to investigate the stereodynamics of thiolate complexes.

Complexes **1** and **2** show temperature-dependent $^1H$ NMR spectra in $C_6D_5NO_2$. On warming in $C_6D_5NO_2$, broadening then coalescence of the signals of the $\mu$-SMe ligands (three signals for **1** and six signals for **2**) occurs. At respective coalescence temperatures of 120°C and 100°C, singlets at $\delta$ 2.267 and $\delta$ 2.374 result for compounds **1** and **2**, respectively. These changes, which are reversed on cooling, may not simply be interpreted as the onset of rapid pyramidal inversion of the bridging sulfur atoms effecting a symmetry⇋asymmetry arrangement interconversion such as that found in $L_nMo(\mu\text{-}SR)_3MoL_n$ systems. The asymmetric isomers of **1** or **2**, even if produced at a higher temperature, may also give three or six signals for the $\mu$-SMe ligands, but such an interconversion would not attain the observed averaging of the $\mu$-SMe ligands. A rapid isomerization between the syn and the anti configuration of the $OMo(\mu\text{-}O)(\mu\text{-}X)MoO$ (X=O or S) framework in **1** and **2** is also not consistent with the results of the $^{17}O$ NMR measurements. A plausible explanation of the complete averaging of the protons of $\mu$-SMe ligands is breaking of the Mo-S ($\mu$-SMe) bond. The $\mu$-SMe ligands in **1** and **2** form weak bonds with Mo atoms: molybdenum-sulfur distances generally fall within the range 2.411–2.549 Å, but the corresponding distances in both **1** and **2** are much longer except for Mo2-S6 (2.547(2) Å) in **1**. This is particularly true for the Mo-S bond which is trans to the Mo-O (terminal) bond. This bond is very long and is likely to be broken at high temperature. We believe that this bond cleavage induces the complete averaging of all protons of $\mu$-SMe ligands. M-$\mu$-SR bond cleavage has also been proposed for the cis ⇌ trans isomerization of $[\{M(CO)(\mu\text{-}SR)(\eta^5\text{-}C_5H_5)\}_2]$ (M=Fe and Ru). The details of this averaging process are currently under investigation.

## V-D-3 Doubly Bridged-1,2-Benzenedithiolato and 1,2-Benzenethiolatosulfenato Rhodium Dimer Derived from Reaction of Triple Cubane-Type Oxide Cluster $[RhCp^*MoO_4]_4$ with 1,2-Benzenedithiol

**Xi RIMO** *(Grad. Univ. for Adv. Studies and IMS)*, **Takanori NISHIOKA, Takayoshi SUZUKI, and Kiyoshi ISOBE**

We have extended the reactions of the triple cubane-type cluster $[RhCp^*MoO_4]_4$ with organic monothiols to those with dithiols to compare the fragmentation patterns of the cluster framework. Here we report the reaction with 1,2-benzenedithiol which breaks the cubane framework completely. From the reaction mixture, $[(RhCp^*)_2(\mu\text{-}S_2C_6H_4)_2]$ (**1**) and $[(RhCp^*)_2(\mu\text{-}o\text{-}S(O)C_6H_4S)_2]$ (**2**) were isolated.

Molecular strucures of **1** and **2** are shown in Figure 1. Both complexes have dinuclear structures with inversion center. The $RhS_2C_2$ metallacycles in **1** and **2** are not planar and the dihedral angles between planes $RhS_2$ and $S_2C_2$ are 30.0 (2)° for **1** and 31.7 (3)° for **2**. These angles are larger than that in $[(\eta^5\text{-}C_5H_5)Co(S_2C_6H_4)]_2$ (20.9°) which has a structure similar to **1** and **2**. In complex **2**, the lone-pair electrons of sulfurs can be oriented to certain directions and sulfurs are asymmetric centers, but in the solid state **2** is racemic. In $CD_2Cl_2$, **2** gives two series of $^1H$ signals of Me groups in Cp* in the NMR spectrum which were assigned to two diastereoisomers. Complex **1** can be converted into **2** through the oxidation by *t*-BuOOH in $CH_2Cl_2$. The difference of S-C bond distances in **1** and **2** are not significant, but the bond length of Rh-S2 is shorter in **2** than in **1**. This may be attribute to stronger backbonding of S to Rh in **2** than that in **1**.

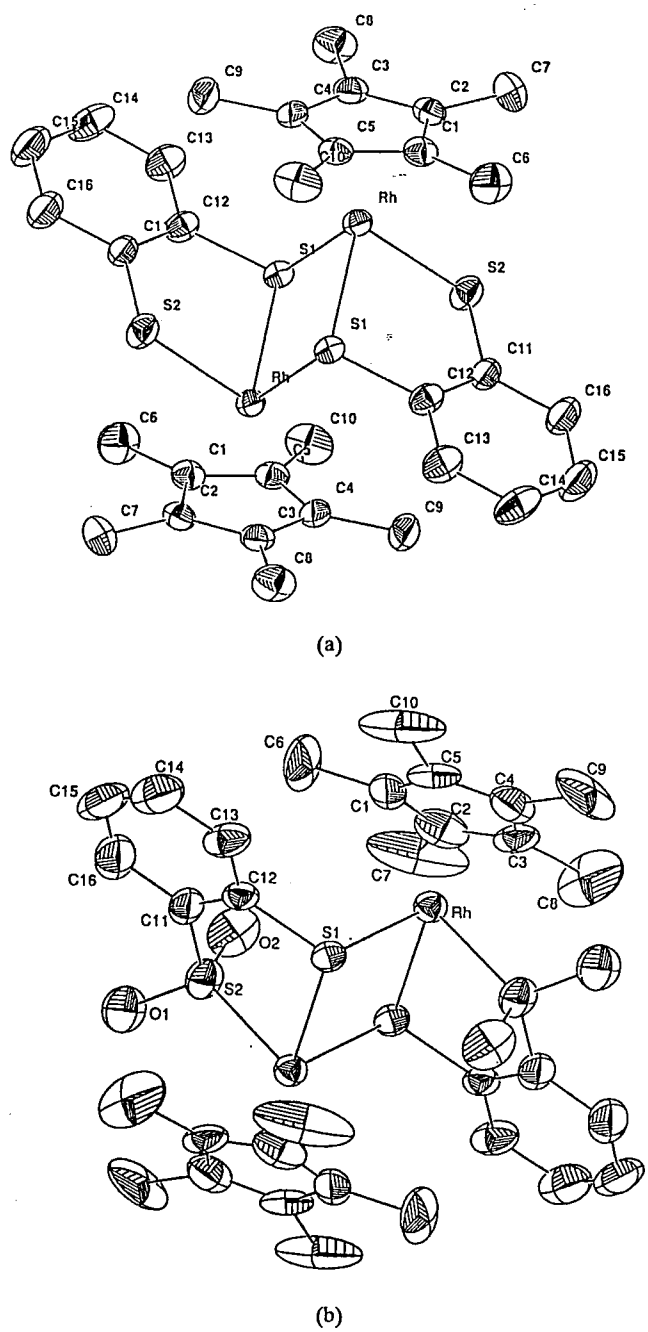


**Figure 1.** Perspective view of $[(RhCp^*)_2(\mu\text{-}S_2C_6H_4)_2]$ (a) and $[(RhCp^*)_2(\mu\text{-}o\text{-}S(O)C_6H_4S)_2]$ (b)

# V—E Transition Metal Sulfide Compounds

Transition-metal thiol (M-SH) complexes are currently under intensive investigation because of their intrinsic chemical interest in oxidation, deprotonation, nucleophilic reactions, as well as their significance in biological, mineralogical, and industrial processes. The corresponding chemistry of M-($\mu$-SH)-M complexes, however, has little developed. Recently our group has synthesized the bridged hydrosulfide rhodium (Rh-Rh) complex, $[Cp^*_2Rh_2(\mu\text{-}CH_2)_2(\mu\text{-}SH)]^+$ (**1**). From comlex **1**, several sulfur clusters have been derived by oxidation, deprotonation, and partial abstraction of the $\mu$-SH ligand.

## V-E-1 Tetranuclear Rhodium Complex with $\mu_4$-S Ligand, $[\{Cp^*_2Rh_2(\mu_2\text{-}CH_2)_2\}_2(\mu_4\text{-}S)]^{2+}$ ($Cp^*=\eta^5\text{-}C_5Me_5$), Obtained from Stepwise Abstraction of $SH^-$ Ligand from Dinuclear Rhodium Dihydrosulfide Precursor by $Ag^+$

**Takanori NISHIOKA, Vadim Yu. KUKUSHKIN** *(St. Petersburg State University and IMS)*, **Kiyoshi ISOBE, and Amelio VAZQUEZ DE MIGUEL** *(University of Alcala of Henares)*

Recently our group reported synthesis and X-ray structures of the terminal and bridged hydrosulfide rhodium dinuclear (Rh-Rh) complexes, *trans*-$[Cp^*_2Rh_2(SH)_2(\mu_2\text{-}CH_2)_2]$ (**1**) and $[Cp^*_2Rh_2(\mu_2\text{-}SH)(\mu_2\text{-}CH_2)_2]^+$ (**2**). In the presence of $O_2$ and excess $H_2S$, the latter complex undergoes an unusual oxidative coupling to yield the novel compound with a rectangular $S_4$ framework, $[\{Cp^*_2Rh_2(\mu_2\text{-}CH_2)_2\}_2(\mu_4\text{-}S_4)]^{2+}$ (**3**). In the course of our investigation of the oxidation of **1**, we have found that a strong oxidant — $Ag^+$ in $CH_2Cl_2$, instead of oxidation, induces an intriguing partial abstraction of the terminal $SH^-$ ligand in **1** to give **2** followed by likewise abstraction of the bridging $SH^-$ ligand in **2** to form the tetranuclear $\mu_4$-S cationic complex $[\{Cp^*_2Rh_2(\mu_2\text{-}CH_2)_2\}_2(\mu_4\text{-}S)]^{2+}$ (**4** in Figure 1).

Reaction of *trans*-$[Cp^*_2Rh_2(SH)_2(\mu_2\text{-}CH_2)_2]$ with an equimolar amount of silver trifluoromethanesulfonate, $AgSO_3CF_3$, took place immediately in $CH_2Cl_2$ and was accompanied by a color change from red to orange-brown, the evolution of $H_2S$ gas, and precipitation of $Ag_2S$. From the reaction mixture, $[Cp^*_2Rh_2(\mu_2\text{-}SH)(\mu_2\text{-}CH_2)_2](SO_3CF_3)$ (**2**-$SO_3CF_3$) was obtained in an 87% yield. The silver salt induces an elimination of one terminal SH ligand from **1** to give **2**-$SO_3CF_3$. The stoichiometry of the reaction is as follows ($H_2S$ gas was identified by a $H_2S$ detector-tube but was not quantified):

$$\textit{trans}\text{-}[Cp^*_2Rh_2(SH)_2(\mu_2\text{-}CH_2)_2] + AgSO_3CF_3 \rightarrow [Cp^*_2Rh_2(\mu_2\text{-}SH)(\mu_2\text{-}CH_2)_2](SO_3CF_3) + 1/2\ Ag_2S + 1/2\ H_2S \quad \text{(eq. 1)}$$

On similar treatment of **2**-$SO_3CF_3$ with one equivalent of $AgSO_3CF_3$ in dichloromethane dark grayish solids containing $Ag_2S$ and Ag precipitated, and further ligand abstraction was observed, this time, of the $\mu_2$-SH ligand. After subsequent workup $[\{Cp^*_2Rh_2(\mu\text{-}CH_2)_2\}_2(\mu_4\text{-}S)](SO_3CF_3)_2$ (**4**-$SO_3CF_3$) was isolated in a 68% yield as an orange solid. The main reaction may proceeds according to eq. 2:

$$[Cp^*_2Rh_2(\mu_2\text{-}SH)(\mu_2\text{-}CH_2)_2](SO_3CF_3) + AgSO_3CF_3 \rightarrow 1/2[\{Cp^*_2Rh_2(\mu\text{-}CH_2)_2\}_2(\mu_4\text{-}S)](SO_3CF_3)_2 + 1/2\ Ag_2S + H^+ + CF_3SO_3^- \quad \text{(eq. 2)}$$

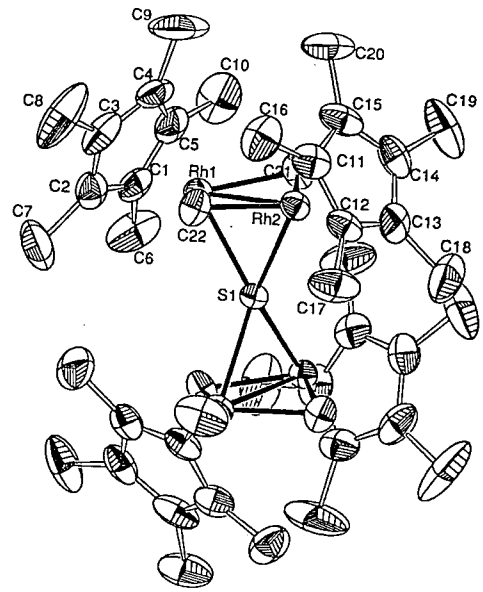


**Figure 1.** Perspective view of $[\{Cp^*_2Rh_2(\mu_2\text{-}CH_2)_2\}_2(\mu_4\text{-}S)]^{2+}$

## V-E-2 Synthesis and Structures of Triangular Rhodium Complexes Monocapped and Bicapped with $\mu_3$-S Ligand.

**Takanori NISHIOKA, Yoshiki OZAWA** *(IMS and Himeji Institute of Technology)*, **and Kiyoshi ISOBE**

To date, we have revealed that the Rh-($\mu$-SH)-Rh functionality in complex $[Cp^*_2Rh_2(\mu_2\text{-}SH)(\mu_2\text{-}CH_2)_2]^+$ (**1**) shows a variety of intriguing reactivities and is transformed into terminal-SH, $\mu_4$-S, and $\mu$-$S_4$ functionalities with the formation of the clusters having two, four nuclearity of Rh atom. Here we report that the Rh-($\mu$-SH)-Rh functionality in **1** is also converted to the $\mu_3$-S functionality.

Compound **1** reacts with $[Cp^*_2Rh_2(\mu_2\text{-}OH)_3]^+$ containing the basic OH ligands to take the proton of the $\mu$-SH ligand and offers a monocapped and a bicapped trinuclear $\mu_3$-S complexes of $[Cp^*_3Rh_3(\mu_2\text{-}CH_2)(\mu_3\text{-}S)]^{2+}$ (**2**) and $[Cp^*_3Rh_3(\mu_3\text{-}S)_2]^{2+}$, respectively (**3**). **2** and **3** make mixed-crystals in any ratio, and the separation of these compounds is very difficult.

Figure 1 shows X-ray structures of the cationic moiety of **3**-$BF_4$. The complex has three rhodium atoms in the plane of a regular triangle and is capped with two sulfur atoms. If the crystal consists of only **3**-$BF_4$, there would be no disordered atom. In fact it, however, contains **2**-$BF_4$ having the disordered sulfur atom and $\mu$-$CH_2$ into two positions with 0.9 population and into six with 0.03, respectively. Although, actually, the values of structure data are averaged values of those of **2**-$BF_4$ and **3**-$BF_4$ corresponding to the composition ratio of $[\mathbf{2}\text{-}BF_4]_{0.19}[\mathbf{3}\text{-}BF_4]_{0.81}$, they are probably close to the values of the pure **3**-$BF_4$ sample.

There was no significant difference in the bond distances between **2-$BF_4$** and **3-$BF_4$** except for the Rh—S bond distance. The corresponding bond in **3-$BF_4$** (2.239(3) Å) was shorter than that in **2-$BF_4$** (2.2761(8) Å).

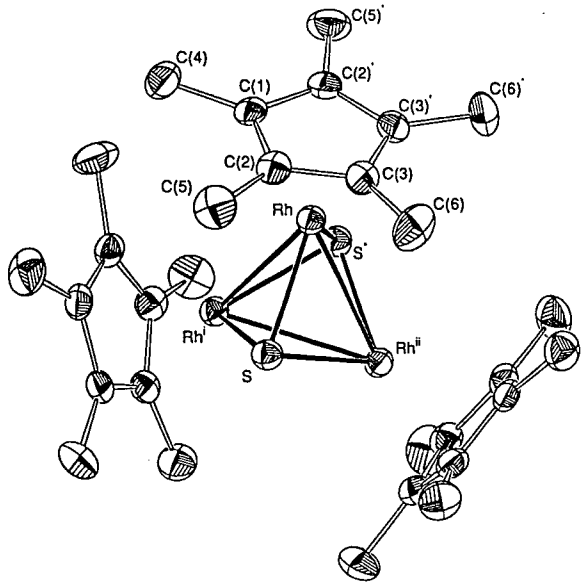


**Figure 1.** Perspective view of $[Cp^*_3Rh_3(\mu_3\text{-}S)_2]^{2+}$

## V-E-3 Synthesis and Molecular Structure of Novel Octanuclear Mixed Metal Complex, [Cp*Rh{P(OEt)$_3$}W($\mu_2$-S)$_2$($\mu_3$-S)$_2$CuClCu($\mu$-Cl)]$_2$

**Seiji OGO** *(Grad. Univ. for Adv. Studies and IMS)*, **Takayoshi SUZUKI, and Kiyoshi ISOBE**

In many cases the formation of sulfide clusters are under thermodynamic control and the resulting cluster frameworks are not predicted from reaction conditions. We are trying to overcome this lack of control and develop methodology for the rational synthesis of the clusters by using the metal compounds as building blocks. We have successfully built up a novel octanuclear mixed metal complex, [Cp*Rh{P(OEt)$_3$}W($\mu_2$-S)$_2$($\mu_3$-S)$_2$CuClCu($\mu$-Cl)]$_2$ from [Cp*Rh{P(OEt)$_3$}Cl$_2$], $WS_4^{2-}$, and CuCl.

The title compound was prepared from [Cp*Rh{P(OEt)$_3$}$WS_4$] and CuCl (1:3) as follows: [Cp*Rh{P(OEt)$_3$}$WS_4$] (4.80 g, 6.70 mmol) was added to a solution of CuCl (1.99 g, 20.1 mmol) in acetonitrile (480 cm$^3$). After stirring for 10 h at room temperature the mixture was filtered and dried. Red crystals were obtained (5.52 g, yield 90%).

Crystal data for [Cp*Rh{P(OEt)$_3$}W($\mu_2$-S)$_2$($\mu_3$-S)$_2$CuClCu($\mu$-Cl)]$_2$: monoclinic, $P2_1/n$, $a$ = 10.156(5), $b$ = 14.483(7), $c$ = 19.403(5) Å, $\beta$ = 104.33(3)°, $V$ = 2765(2) Å$^3$, and $Z$ = 2.

Inversion center generates the [Cp*Rh{P(OEt)$_3$}W($\mu_2$-S)$_2$($\mu_3$-S)$_2$CuClCu($\mu$-Cl)]$_2$ dimer. The geometry at the Cu(1) atom is distored tetrahedral. On the other hand, atom Cu(2) displays a trigonal-planar geometry. As expected the Cu-Cl distance of 2.28(2) Å at the $\mu$-Cl bridge is longer than that of 2.14(1) Å at the terminal Cl ligand. The Rh····Mo distance shows no direct metal-metal interaction.

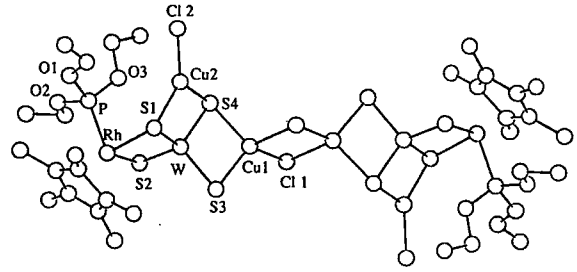


**Figure 1.** Perspective view of [Cp*Rh{P(OEt)$_3$}W($\mu_2$-S)$_2$($\mu_3$-S)$_2$CuClCu($\mu$-Cl)]$_2$.

# V—F Enantioselective Synthesis and Structures of Helical Metal Complexes

Helical metal complexes termed by "helicates" are the compounds of current interest in coordination chemistry. Since the helicate has an optical activity, the left-handed and its right-handed helicate are helical enantiomers. Recent studies of this field are directed toward the enantioselective synthesis of the helicate using an optically active bridging ligand and diastereoisomerism. For this purpose, we have developed a powerful method to prepare optically active bridging ligands, 1,3-dioxolane derivatives. With these ligands enantioselective synthesis of helicates has been performed in this study. Further, in order to understand the helical enantioselectivity and the chiral molecular recognition process, preparation of the complex with the racemic ligand has also been carried out.

## V-F-1 Synthesis and Characterization of a Left-handed and a Right-handed Helical Infinite Chain Complex of Silver(I)

**Takayoshi SUZUKI, Kiyoshi ISOBE, Hiyoshizo KOTSUKI** *(Kochi Univ. and IMS)*, **Narimasa MORIYA,* Yuichi NAKAGAWA,* and Masamitsu OCHI*** *(*Kochi Univ.)*

The chiral ligands used for construction of helical framework are derived from optical active tartaric acids as (4*R*,5*R*)-*trans*-4,5-bis[2-(2-pyridyl)ethyl]-1,3-dioxolane (**R,R-L**) and its enantiomer (**S,S-L**). Treatment of **R,R-L** or **S,S-L** with silver trifluoromethanesulfonate (**AgOTf**) in methanol provided colorless prismatic crystals, respectively. Both of the crystals (**Ag(R,R-L)OTf** and **Ag(S,S-L)OTf**) have been analyzed by X-ray diffraction method, and it has been found that they are enantiomorphic. Crystal data and Final $R$ values are: for **Ag(R,R-L)OTf**, $FW$ = 541.30, orthorhombic, $P2_12_12_1$, $a$ = 13.065(5), $b$ = 18.684(7), $c$ = 8.810(5) Å, $V$ = 2151(2) Å$^3$, $Dx$ = 1.67 Mg m$^{-3}$, and $Z$ = 4, $R$ = 0.056 for 2315 reflections. For **Ag(S,S-L)OTf**, $FW$ = 541.30, orthorhombic, $P2_12_12_1$, $a$ = 13.063(3), $b$ =

18.689(5), $c$ = 8.817(3) Å, $V$ = 2153(1) Å$^3$, $Dx$ = 1.67 Mg m$^{-3}$, and $Z$ = 4, $R$ = 0.068 for 2263 reflections. The absolute structures were determined with references to the known absolute configurations of ligand moieties.

The structure of the compounds can be assigned as an infinite chain with $Ag^+$ that has a slightly distorted linear coordination geometry and the bridging ligand, **L** (Fig. 1). The chain runs along the crystallographic $b$ axis, which is a twofold screw axis. Since the $Ag^+$ ion is not sited on the axis, the chain has a "helical" structure. In Fig. 2, perspective views along the screw axis are shown for both compounds. It shows clearly that these compounds are helical enantiomers. At the both sides of the Ag centers, the conformation of the bridging ligand makes itself helical, that is, **R,R-L** makes a right-handed helical bridge and **S,S-L** a left-handed. These helicities due to the bridging ligand might cause the infinite chain of the compound to be helical, left-handed for **Ag(R,R-L)OTf**, and right-handed for **Ag(S,S-L)OTf**.

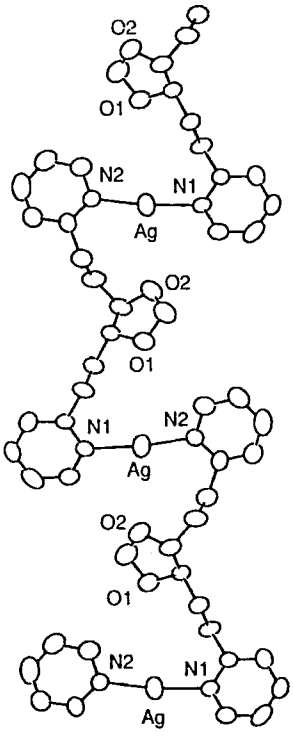


**Figure 1.** The ORTEP drawing of cationic part of **Ag(R,R-L)OTf**.

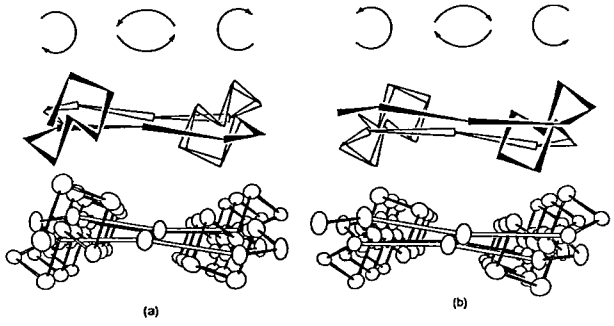


**Figure 2.** Perspective views of chains of (a) **Ag(R,R-L)OTf** and (b) **Ag(S,S-L)OTf**, each along its individual screw axis.

## V-F-2 Stereoselective Formation of Meso-dimeric Complex from Racemic Bridging Ligand and Silver(I).

**Takayoshi SUZUKI, Kiyoshi ISOBE, Hiyoshizo KOTSUKI** *(Kochi Univ. and IMS)*, **Narimasa MORIYA,* Yuichi NAKAGAWA,* and Masamitsu OCHI*** *(*Kochi Univ.)*

The reaction of a racemic mixture of *trans*-4,5-bis{2-(2-pyridyl)ethyl}-1,3-dioxolane (**rac-L**) with silver trifluoromethanesulfonate (**AgOTf**) in methanol has yielded a dimeric $Ag^+$ complex, **$Ag_2$(rac-L)$_2$(OTf)$_2$** quantitatively, in contrast to the reaction of an optically active ligand and **AgOTf**. The same dimeric complex has been also obtained by mixing of optically active infinite chain complexes, **Ag(R,R-L)OTf** and **Ag(S,S-L)OTf** (see V-F-1), in methanol. The complex crystallizes in monoclinic space group $P2_1/c$, $a$ = 9.281(5), $b$ = 23.518(6), $c$ = 9.802(6) Å, $V$ = 2058(2) Å$^3$, $Dx$ = 1.75 Mg m$^{-3}$, and $Z$ = 2. The final $R$ value is 0.057 for 2417 reflections.

The molecular structure is depicted in Fig. 1. Since the dimeric complex has symmetry center, the bridging ligands must be an enantiomeric pair, and then the dimeric complex is a meso-form. The stereoselective formation of the meso-dimeric complex from the racemic ligand is a remarkable feature, because it contains a somewhat enantioselective molecular recognition. The origin of the selectivity might be a hydrogen bond-like interaction between two dioxolane rings of the bridging ligands. The C10···O2′ distance of 3.42(1) Å is just the same as the sum of van der Waal's radii of C, H, and O, and the infrared spectrum of **$Ag_2$(rac-L)$_2$(OTf)$_2$** shows that $\nu$(C-O) stretching bands are slightly shifted compared to those of **Ag(R,R-L)OTf** and **Ag(S,S-L)OTf**, but the other regions are quite similar to one another.

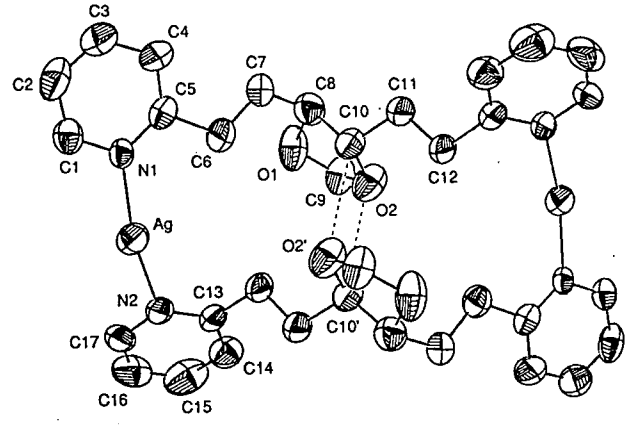


**Figure 1.** The ORTEP drawing of cationic part of **$Ag_2$(rac-L)$_2$(OTf)$_2$**.

# V—G Organic Synthesis with Lanthanoids

The fifteen elements from lanthanum to lutetium constitute a unique family of closely related elements. Recent progress on the utilization of such lanthanoids in organic synthesis has aroused a growing interest among organic chemists. For several years, we have been working in this field by using samarium(II) iodide and developed a number of new synthetic reactions, in which a unique property of the lanthanide ion was found to play an important role. In this project, we have prepared new samarium(II) and ytterbium(II) species and examined their reactivities.

## V-G-1 Preparation and Reactivity of New Samarium(II) and Ytterbium(II) Species

**Takeshi HANAMOTO, Yuichi SUGIMOTO, and Junji INANAGA**

Despite a large number of investigations of samarium(II) iodide, less attention has been paid to other samarium(II) species. We found that new samarium(II) and ytterbium(II) species, presumed to be samarium(II) trifluoromethanesulfonate [$Sm(OTf)_2$] and ytterbium (II) trifluoromethanesulfonate [$Yb(OTf)_2$], are cleanly prepared as tetrahydrofuran solutions from $Sm(OTf)_3$ and $Yb(OTf)_3$, respectively, by treating them with organomagnesium or organolithium reagents at room temperature. The Sm(II) species is fairly unstable; it gradually decomposes at −3°C even in the presence of Sm metal as a stabilizer. These low-valent lanthanide(II) species are fairly Lewis acidic and effectively promote the pinacol coupling reaction of a variety of aldehydes and ketones. The precise mechanism of the formation and the scope of reactivity of these lanthanoid(II) triflates are currently under investigation.

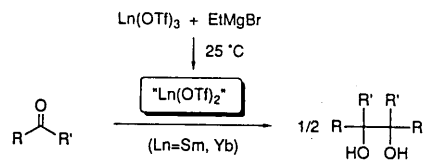


by T. Hanamoto et al.

# V—H Synthesis and Conformational Study of Multibridged [3n]Cyclophanes

[3₆](1,2,3,4,5,6)Cyclophane **1**, in which two benzene rings are bridged with six -$CH_2CH_2CH_2$- chains, is one of the final target molecules in the field of [3.3]cyclophane chemistry. A stereochemical feature of **1** is associated with the chair-boat inversion of a trimethylene bridge. Six trimethylene chains of **1** are expected to undergo correlated inversion in solution (Scheme 1). This compound is a promising precursor to propella-[3₆]prismane **2** since photochemical isomerization of **1** to **2** has been predicted based on semi-empirical MO calculations[1] (Scheme 2). Hexaprismane **3** is a theoretically and structurally intriguing compound, but its synthesis has not been accomplished yet. Synthesis of hexaprismane derivative **2** and parent compound **3** will be the final goal of this study.

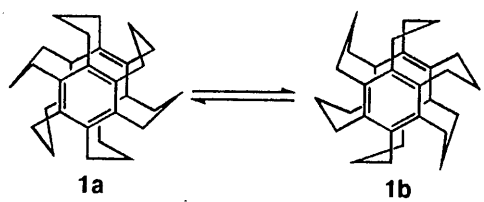


**Scheme 1.** Correlated inversion process of the six trimethylene bridges of **1**

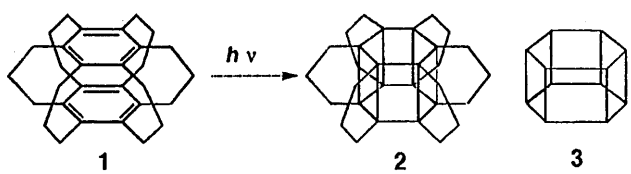


**Scheme 2.** Predicted photochemical isomerization of **1** to hexaprismane derivative **2**

## V-H-1 Synthesis of [3₄](1,2,3,5)- and (1,2,4,5)Cyclophanes

**Teruo SHINMYOZU, Shirou KUSUMOTO, Sachiyo NOMURA, Haruo KAWASE,* and Takahiko INAZU***
*(*Kyusyu Univ.)*

[*Chem. Ber.*, **126**, 1815 (1993)]

Efforts have been made to synthesize **1** by two different approaches: (a) a stepwise approach *via* stepwise introduction of additional trimethylene bridges starting from [3₃](1,3,5)cyclophane **7** and (b) a direct approach *via* cyclotrimerization of cyclodeca-1,6-diyne **17** in the presence of a metal catalyst. In the stepwise approach, we developed an acid-catalyzed cyclization reaction of a pseudogeminally substituted acetyl group and a chloromethyl group, and synthesized [3₄](1,2,3,5)cyclophane **4**. An isomer of **4**, [3₄](1,2,4,5)cyclophane **5** was also prepared by the one-step TosMIC coupling reaction of tetrabromide **10** and subsequent reduction of the carbonyl groups (Scheme 3).

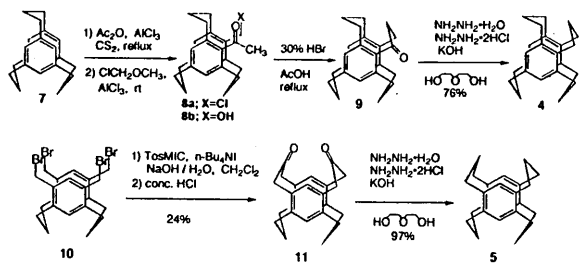


**Scheme 3.** Synthetic route to [3₄](1,2,3,5)cyclophane **4** and [3₄](1,2,4,5)cyclophane **5**

## V-H-2 Synthesis of [3$_5$](1,2,3,4,5)Cyclophane

**Teruo SHINMYOZU, Shirou KUSUMOTO, Mihoko HIRAKIDA,* and Takahiko INAZU*** *(*Kyusyu Univ.)*

In the acid-catalyzed cyclization reaction described above, the raise of the reaction temperature to 130–140°C resulted in the formation of bromo-olefin **13** (75–85%). This was assumed by the conversion of the ketone **9** to bromohydrin **12** and subsequent dehydration. Two-step hydrogenation of **13** afforded [3$_4$](1,2,3,5)cyclophane **4** in high yield (92%). By the same series of reactions, [3$_5$](1,2,3,4,5)cyclophane **6** was prepared from **4** (Scheme 4). Introduction of the final bridge is currently under way.

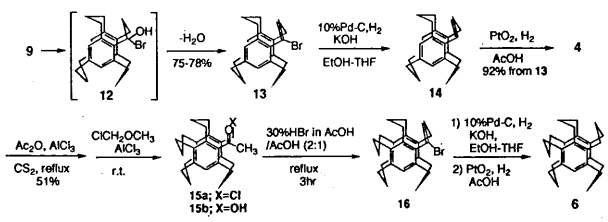


**Scheme 4.** Synthetic route to [3$_5$](1,2,3,4,5)cyclophane **6**

## V-H-3 A Synthetic Study of [3$_6$](1,2,3,4,5,6)Cyclophane by Metal Catalyzed Cyclotrimerization of Cyclodeca-1,6-diyne

**Teruo SHINMYOZU, Yoichi SAKAMOTO,* and Takahiko INAZU*** *(*Kyusyu Univ.)*

In an alternative approach, cyclotrimerization of cyclodeca-1,6-diyne **17** in the presence of a metal catalyst has been studied. First we developed an improved synthetic method of **17**; the intramolecular cyclization of lithium acetylide and iodine of **18** in THF-PMDETA (pentamethyldiethylenetriamine) afforded **17** in 8% yield, whereas a mixture of **17** (2%), dimer (3%), and trimer (1%) was obtained when HMPA was used instead of PMDETA. Palladium catalyzed cyclization of **17** afforded a dimerization product **19** (Scheme 5). This agreed with Gleiter's results,[2] and indicated that the cyclodimerization was more favorable process than trimerization. Our search for suitable catalysts is now in progress.

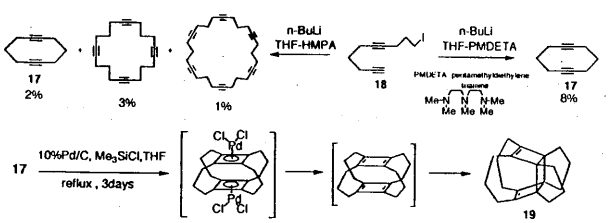


**Scheme 5.** Synthesis of cyclodeca-1,6-diyne **17** and its Pd-catalyzed cyclization

## V-H-4 A Conformational Study of [3.3]Metacyclophanes through Variable Temperature $^1$H NMR and Optical Rotation

**Katsuya SAKO,[a] Teruo SHINMYOZU, Hiroyuki TAKEMURA,[b] Masahiko SUENAGA,[b] and Takahiko INAZU[b]** *([a]Nagoya Inst. Tech., [b]Kyushu Univ.)*

[*J. Org. Chem.*, **57**, 6536 (1992)]

Conformational study of 2,2,11,11-tetradeuterio[3.3]-metacyclophanes (**1-d$_4$**, **2-d$_4$**) based on a variable temperature (VT) $^1$H NMR method as well as racemization experiments of (−)- and (+)-**3** revealed that the energy barrier for benzene ring inversion is much lower than that of trimethylene bridge inversion ($\Delta G^{\ddagger}$=11–12 kcal/mol). The most stable conformer of **1-d$_4$** and **2-d$_4$** is a syn(chair-chair), and the less stable conformer is estimated to be a syn(chair-boat) based on the $^1$H NMR data (Scheme 6).

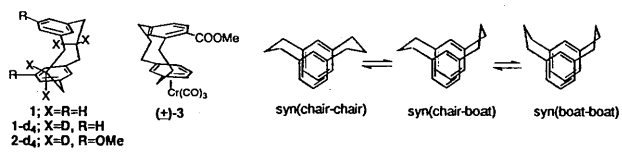


**Scheme 6.** Structures **1-3** and conformational isomerism of [3.3]metacyclophane *via* chair-boat type inversion of the trimethylene bridges.

## V-H-5 Conformational Analysis of [3.3]Azacyclophanes

**Teruo SHINMYOZU, Jerzy M. RUDZIŃSKI,[a] Hiroyuki TAKEMURA,[b] Katsuya SAKO,[c] and Takahiko INAZU[b]** *([a]Fujitsu Kyushu System Engineering, [b]Kyushu Univ., [c]Nagoya Inst. Tech.)*

Conformational behavior of 2,11-diaza[3.3]para- and metacyclophanes **4-7** based on VT $^1$HNMR method and theoretical calculations (semi-empirical MO calculations and molecular mechanics calculations) have been studied. The relative stability order of three conformers of azametacyclophane **6** and **7** (chair-boat > boat-boat > chair-chair) are different from those of the parent compound **1** (chair-chair > chair-boat > boat-boat), whereas the relative stabilities of chair and boat conformers and the energy barrier for the bridge inversion are very similar to those of the parent [3.3]paracyclophane **2** (boat > chair) in the azaparacyclophanes **4** and **5** (Scheme 7). Only MM3 calculations can be well reproduced the experimental results in [3.3]azacyclophanes **4-7**.

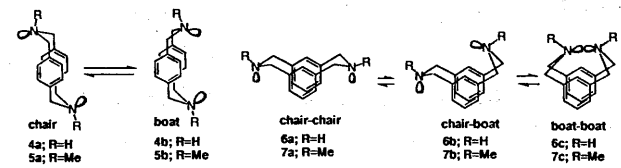


**Scheme 7.** Chair-boat type inversion process of the -$CH_2NCH_2$- bridges in 2,11-diaza[3.3]para- and metacyclophanes **4-7**.

## V-H-6 A Simple Synthetic Method of Tetraaza[3.3.3.3]meta- and Paracyclophanes by Alkylation of N-Substituted Trifluoroacetamide[1]

**Teruo SHINMYOZU, Nobuhiko SHIBAKAWA,[a] Ken'ichi SUGIMOTO,[a] Hiroko SAKANE,[a] Hiroyuki TAKEMURA,[b] Katsuya SAKO,[b] and Takahiko INAZU[a]** *([a]Kyushu Univ., [b]Nagoya Inst. Tech.)*

[*Synthesis*, in press]

A simple and practical synthetic method of tetraaza[3.3.3.3]meta- and paracyclophanes **1b** and **2b** as artificial host molecules is described. Alkylation of N-substituted trifluoroacetamides (**3**) with appropriate dibromides (**4**) in the presence of NaH in DMF at 100°C or powdered KOH in refluxing acetone, followed by removal of the trifluoroacetyl group and N-methylation of the resultant amines provides desired **1b** and **2b** in 21 and 19% overall yields, respectively, along with their lower and higher homologs (Scheme 8).

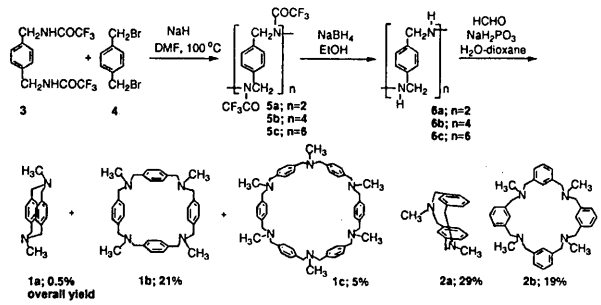


**Scheme 8.** Synthetic method of tetraaza[3.3.3.3]cyclophanes (**1b** and **2b**) by alkylation of N-substituted trifluoroaetamide.


**References**

1) O.K. Cha, E. Ōsawa, and S. Park, J. Mol. Struc. in press.
2) R. Gleiter, M. Karcher, M. Ziegler, and B. Nuber, Tetrahedron Lett. 28, 195 (1987).


# V—I Transannular $\pi-\pi$ Interaction of (4n)$\pi$ Systems

In cyclic conjugated planar systems, molecules with (4n+2)$\pi$-electrons are stabilized by delocalization of the $\pi$-system and called aromatic compounds. On the other hand, the $\pi$-delocalization causes an increase in the energy of the system in planar (4n)$\pi$ monocyclic systems. These types of systems have been defined as antiaromatic. It is our interest to study how two $\pi$-systems mutually interact when they are overlapped each other in a close proximity. According to the frontier molecular orbital calculations, Greenberg *et al.* predicted a destabilizing $\pi-\pi$ interaction in a (4n+2)$\pi$-(4n+2)$\pi$ system, a stabilizing interaction in a (4n+2)$\pi$-(4n)$\pi$ system, and greater stabilization in a (4n)$\pi$-(4n)$\pi$ system than in the (4n+2)$\pi$-(4n)$\pi$ system.[1] To verify these interesting predictions experimentally, we considered that [3.3]cyclophanes containing annulene rings must be the most suitable models since two $\pi$-systems in [3.3]cyclophane are located in the most optimal transannular distance and they are almost planar. [3.3]Cyclophane, therefore, permits exact evaluation of $\pi-\pi$ interaction without interference of the strain effect.

## V-I-1 Synthesis and Transannular $\pi-\pi$ Interaction of [3.3]Cyclophanes Containing 1,6-Methano[10]annulenes


**Teruo SHINMYOZU, Tomonori MATSUNAGA,[a] Takahiko INAZU,[a] and Jerzy M. RUDZIŃSKI[b]** *([a]Kyushu Univ., [b]Fujitsu Kyushu System Engineering)*


We undertook the synthesis of [3.3]cyclophanes containing Vogel's 1,6-methano[10]annulene **1**[2] as a model compound for the study of (4n+2)$\pi$-(4n+2)$\pi$ interaction (n≧2). The precursor of cyclization reactions, 2,7-bis(bromomethyl)-1,6-methano[10]annulene **2**, was prepared from **1** in four steps. After several cyclization reactions were attempted, the synthesis of annulenophanes **3** could be achieved by the cyanamide method. **3** was obtained as a mixture of **3a** and **3b** in a ratio of 1.0:2.4, which were separated by HPLC and characterized (Scheme 1). These compounds are the first example of [m.n]cyclophanes containing two annulene rings. Their transannular $\pi-\pi$ interactions were studied based on the electronic spectra and theoretical calculations (MNDO-PM3).

The syntheses of layered annulene **5** in which Boekelheide's trans-15,16-dimethyldihydropyrene [**4**; (4n+2)$\pi$, n=3][3] are linked by a -$CH_2CH_2$- bridge, as well as [3.3]cyclophanes **7** containing Paudler's 8b, 8c-diazacyclopenta-[fg]acenaphtylene [**6**; (4n)$\pi$, n=3][4] are now under way (Scheme 2).


**References**

1) A. Greenberg, J.F. Liebman, "*Strained Organic Molecules*", Academic Press, New York, 1978, p.170.
2) E. Vogel, H.D. Roth, *Angew. Chem. Int. Ed. Engl.*, 3, 228 (1964).
3) W.S. Lindsay, P. Stokes, L.G. Humber, V. Boekelheide, J. Am. Chem. Soc., 89, 4468 (1967).
4) W.W. Paudler, E.W. Stephan, *J. Am. Chem. Soc.*, 92, 4468 (1970).


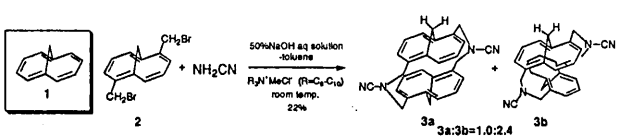


**Scheme 1.** Synthesis of the annulenophanes **3a** and **3b** by cyanamide coupling method.

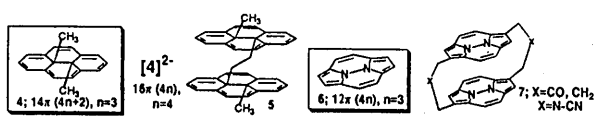


**Scheme 2.** The target layered annulene **5** and anulenophane **7** for the (4n+2)(4n+2) and (4n)(4n) interactions, respectively.

# V—J Modeling Reaction of Metalloenzyme Active Center

Metalloenzymes play key roles in various chemical conversion in biological systems. Most of them have not well-characterized structurally and/or mechanistically due to their instability. To build new reaction systems and to obtain further insight into the natural systems, artificial models of several important metalloenzyme active centers were prepared and was used to simulate the natural enzymatic reactions. In this research project, three major enzymes, plant water oxidation enzyme, manganese catalase, and cytochrome P-450, have been studied with use of suitably desighned artificial reaction center models.

## V-J-1 Functional Modeling Reaction of Water Oxidation Enzyme in Plant Photosynthetic Reaction Center

**Yoshinori NARUTA, Masa-aki SASAYAMA,[a] and Nobuyuki SAWADA[a]** *([a]Kyoto Univ.)*

Manganese porphyrin dimers **1-3** linked by *o*-phenylene molecule showed oxygen evolution under anodic oxidation conditions in an aqueous acetonitrile solution (Figure 1). Evolved oxygen in an electrochemical cell was assinged by a mass spectrometer and its isotopic composition in the reaction containing $H_2{}^{16}O$ and $H_2{}^{18}O$ (1:1) was determined to be $^{16}O_2$:$^{16}O$-$^{18}O$:$^{18}O_2$ = 1:2:1, which is same as that expected from the statistical distribution. Evolved $O_2$ was quantitatively determined by a Clark-type oxygen electrode and its faradaic efficiency was 5—16%. Without these Mn complexes, any $O_2$ was not detected even in the presence of the corresponding Mn porphyrin monomers. By means of rotating-electrode method, the number of electrons concerning water oxidation was also determined to be four. This is the first example of the catalytic water oxidation with dimanganese complexes.

$$2H_2O \xrightarrow[-4e^-]{\text{Mn catalyst}} O_2 + 4H^+$$

## V-J-2 Modeling Reaction of Manganese Catalase with Dimanganese Porphyrin Dimers. Part 1. Dependency of Oxygen Evolution Rate on Mn-Mn Separation

**Yoshinori NARUTA and Masa-aki SASAYAMA[a]** *([a]Kyoto Univ.)*

Manganese catalase (Mn CAT) contains dimanganese complexes in their active center and they disproportionate hydrogen peroxide to oxygen and water.

$$2H_2O_2 \xrightarrow{\text{Mn catalyst}} O_2 + 2H_2O$$

We prepared dimanganese porphyrin dimers (Figure 2) with various metal-metal separations and measured their catalase activity in an aprotic solvent by means of an oxygen electrode. This reaction requires a nitrogen base and two Mn ions with an appropriate separation. Oxygen evolution rate was intensively affected by the metal-metal separation and it was greatly decreased when the separation is exceed 10 Å and the direction of their coordination sites becomes divergent. The highest turnover rate ($> 10^3$ min$^{-1}$) of $H_2O_2$ dismutation was observed in the catalytic reaction of *o*-phenylene-linked Mn porphyrin dimers. Electron-withdrawing groups on the porphyrins make the catalyst robust and showed high catalytic turnovers ($> 10^4$).

**References**

Y. Naruta and K. Maruyama, *J. Am. Chem. Soc.*, **113**, 3595 (1991); Y. Naruta, M. Sasayama, and K. Maruyama, *Chem. Lett.*, 1267 (1992)

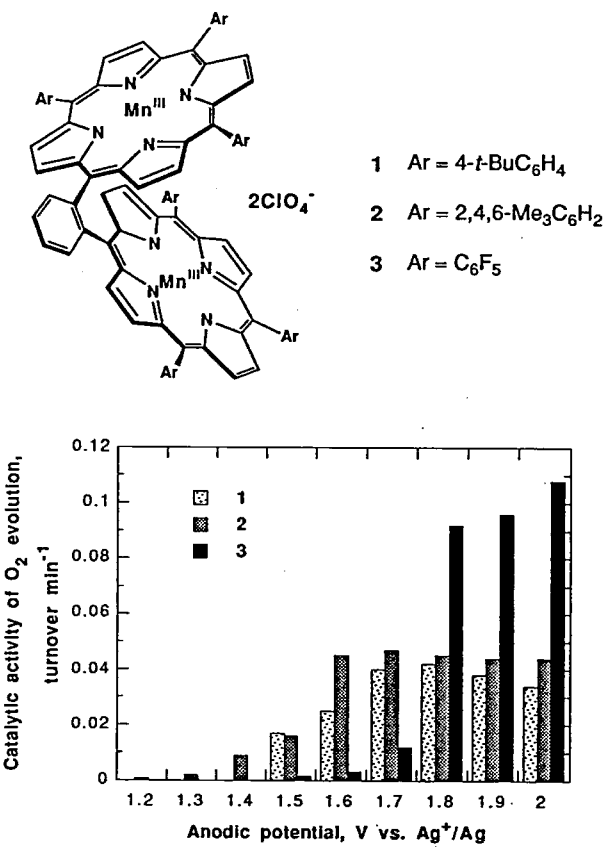


**Figure 1.** Oxygen evolution rate with dimanganese porphyrin dimer catalysts **1-3** under anodic oxidation conditions in an aqueous acetonitrile solution.

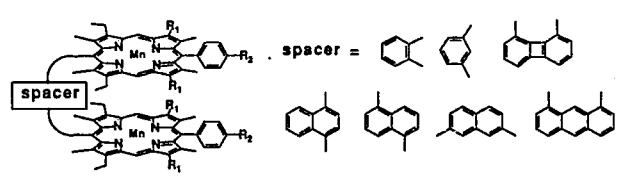


**Figure 2.** Dimanganese porphyrin dimers linked by various aryl groups.

## V-J-3 Modeling Reaction of Manganese Catalase with Dimanganese Porphyrin Dimers. Part 2. Mechanistic Study of $H_2O_2$ Dismutaion with Manganese Porphyrins

**Yoshinori Naruta and Masa-aki SASAYAMA**[a] *([a]Kyoto Univ.)*

Modeling reaction of Mn CAT with dimanganes porphyrin dimers was analyzed from the mechanistic stand point with use of 1,8-anthracene-linked dimer. The reaction rate is first-order to the catalyst and pseudo-first order to $H_2O_2$. When $H_2{}^{16}O_2$ and $H_2{}^{18}O_2$ (1:1) was used, the evolved $O_2$ is $^{16}O_2{:}^{18}O_2 = 1{:}1$ and no isotope scrambling to $^{16}O$-$^{18}O$ was observed. Characteristic absorbance corresponding to $Mn^{IV}$ or $Mn^{V}$ was not detected during the reaction even at low temperature. Based on these results, the catalytic cycle was proposed to include $Mn^{III}{}_2/Mn^{IV}{}_2$ cycle and the rate determining step of this reaction is the formation of the $Mn^{IV}{}_2$ complex by the oxidation of the initial $H_2O_2$.

The role of the base is quantitatively evaluated both as the general base and as the axial ligand according to the following equation;

$$V = k_1[H_2O_2][\mathbf{Mn_2P}] + k_2[H_2O_2][\mathbf{Mn_2P{:}B}]$$

where $V$, $\mathbf{Mn_2P}$, and $\mathbf{Mn_2P{:}B}$ are velocity of $O_2$ evolution, concentration of the N base-unligated Mn porphyrin dimer, and the ligated dimer, respectively. Linear relationship between log $k_1$ and basicity of the applied N base was found and $k_2/k_1$ was in the range of 4-6. These experiments lead the fair evaluation of the two roles of the N base to the hydrogen peroxide decomposition.

### V-J-4 Synthesis of an Accurate Model of Cytochrome P-450 Monooxygenase

**Yoshinori NARUTA, Mari ICHIHARA**[a]**, and Fumito Tani**[a] *([a]Kyoto Univ.)*

The active center of cytochrome P-450 has substrate/$O_2$ binding and thiolate ligating sites. For demonstration of $O_2$ binding to the $Fe^{II}$ with a thiolate axial ligand, chiral binaphthalene-linked "twin-coronet (**TC**)" porphyrins have been prepared (Figure 3). These porphyrins have two chiral cavities on their both faces and they are protected by the bulky binaphthalene groups. Both for the stabilization of coordinated $O_2$ inside the cavity and for the catalytic function of the protonation to the $O_2$ terminus, new **TC** porphyrins have four phenolic OHs inside the cavities. Their preparation was performed by the coupling reaction of *meso*-tetra(2,6-dihydroxyphenyl)porphyrine and 2,2′-dimethoxymethyl-3,3-dichloromethylbinaphthalene and deprotection of MOM groups. The OH groups inside the cavity can function to stabilize the coordinated $O_2$ by making hydrogen bonding and are used as the functional group for modification of a thiolate appendage inside the other cavity.

**References**

Y. Naruta, F. Tani, N. Ishihara, and K. Maruyama, *J. Am. Chem. Soc.*, **113**, 6865 (1991); *Bull. Chem. Soc. Jpn.*, **66**, 158 (1993).

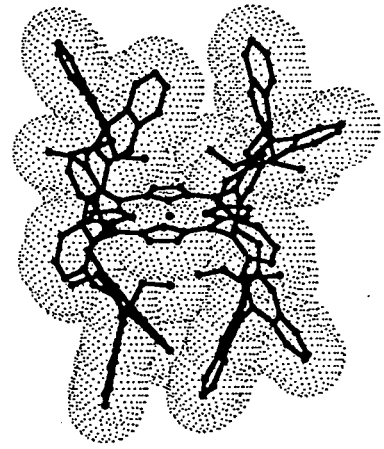

**Figure 3.** Computer generated model of "twin-coronet" porphyrin (eclipsed form). The interactive modeling was performed on a Silicon Graphics IRIS 4D/35 using MAXIMIN2 package inside SYBYL 5.5.

## V—K Design, Properties and Reactivity of New Organometallic Compounds

A variety of carbon-metal bonds can produce unconventional reactivities and properties of the organometallic compounds. At present, development of new organometallic reagents for organic chemical transformations especially asymmetric reactions is one of our important projects. The other is synthesis of new organometallic compounds, especially organoboron compounds having strong affinity to cancer cells for Neutron Capture Therapy (**NCT**).

### V-K-1 Synthesis and Properties of Organoboron Compounds Bearing a Water-solubilizing Cascade Type of Polyol for Boron Neutron Capture Therapy

**Hisao NEMOTO, Jianping CAI**[a]**, Satoshi IWAMOTO**[a]**, Naoki SADAYORI**[a]**, Hiroyuki NAKAMURA**[a]**, and Yoshinori YAMAMOTO**[a] *([a]Tohoku Univ.)*

If sufficient amount of boron atoms can be located in cancer cells, irradiation of thermal neutron beam produces 2.4 MeV/mol of energy to kill the cancer cell. We have synthesized new boron atom containing nucleoside and amino acid derivatives. The *in vitro* examinations of some of our new organoboron compounds gave promising results for BNCT. Two typical examples, BPA-$(OH)_2$ (**1**) and $5B_{10}U$ (**2**), are shown in Figure 1.

*p*-Boronophenylalanine (**BPA**) is now clinically used for the therapy of Melanoma cancer (Figure 2). The compound **1** was designed based on the chemical structure of **BPA**, and synthesized from **BPA** with 2-amino-1,3-benzyloxypropane. The incorporation of **1** into B16 Melanoma of human cells (the model of cancer cell) were 1.5 times more than **BPA**. In contrast, into TIG-1-20 (A cell of human's baby, the model of normal cell), the incorporation of **1** was one-fifth to that of **BPA**. Dodecaboranethiol (**BSH**) is clinically used for the therapy of brain tumor. Incorporation of our $5B_{10}U$ (**2**) is 100 times more than **BSH** into Glioma cells of human brain.

To investigate the molecular design, we are now prepar-

ing BPA-$(OH)_2$ analogue to examine the relationship between water-solubility and incorporation to the cells. Thus, BPA-$(OH)_1$ and BPA-$(OH)_4$ were synthesized and are now being examined *in vitro* (Figure 3).

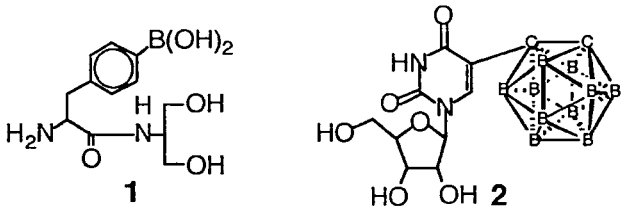


**Figure 1.** Newly Synthesized Organoboron Compounds Having Affinity to Cancer Cells

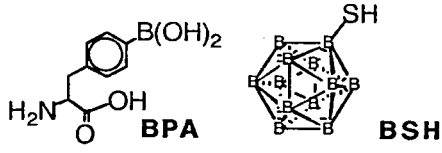


**Figure 2.** The Compounds Clinically Used

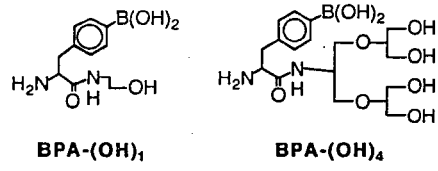


**Figure 3.** Newly Designed BPA-$(OH)_2$ Analogue.

## V-K-2 Carbon-carbon Bond Formation Reactions of $ROCH(CN)_2$ and the Related Compounds Using Transition Metal Complexes

**Hisao NEMOTO, Yoshihiro HONDA,[a] Md. Al MASUM,[a] and Yoshinori YAMAMOTO[a]** *([a]Tohoku Univ.)*

We have developed a new acyl anion equivalent, $ROCH(CN)_2$ (**4**) as a masked acyl cyanide (**4** + $E^+$ → E-$(RO)C(CN)_2$ → E-$(HO)C(CN)_2$ → E-COCN + HCN). Alkyl halides were reacted with **4** in the presence of weak bases. Allylic carbonates, aldehydes, and activated imines (RCH=N-EWG, EWG = $-SO_2R$, $-CO_2R$, $-C_6H_4$-*p*-$CO_2Me$, and $-P(O)Ph_2$) were reacted with **4** *under neutral conditions* in the presence of transition metal catalysts or at high pressured conditions.

Now, we are investigating the reactions of **4** and the related compounds mainly the active methyne or methylene compounds bearing cyano group.

## V-K-3 Intramolecular Michael Addition of γ-Alkylsulfonyloxy-α,β-Unsaturated Esters by Using Higher Order Cyano Copper or Silver Amides as a Base. Synthesis of Sultones

**Naoki ASAO, Meguro MASAKI,[a] Hisao NEMOTO, and Yoshinori YAMAMOTO[a]** *([a]Tohoku Univ.)*

Synthesis of heterocyclic compounds *via* intramolecular conjugate addition of heteronucleophiles is a well known process. However, intramolecular Michael addition of carbanions often causes undesired side reactions especially when an anion stabilizing heteroatom is substituted at the γ-position, since the use of a significantly strong base is needed to generate the carbanions from the corresponding heteroalkyls and the base abstracts the γ-hydrogen atom competitively. However, we found that the use of the higher order cyano copper (or silver) amide $2LiN^iPr_2$-CuCN (or AgCN) enables to transform γ-alkylsulfonyloxy-α,β-unsaturated esters **1** into γ-sultones **2** in good to high yields. For example, the treatment of **1a** with $LiN^iPr_2$ gave the cyclization product **2a** in 69% yield. However, the use of higher order silver amide $2LiN^iPr_2$-AgCN afforded **2a** in 93% yield in nearly 100% de. On the other hand, the ring cleavage of sultones was succeeded with $3LiAlH_4$-$AlCl_3$ to afford thiodiol. From these two steps, i.e. intramolecular Michael addition followed by ring opening reaction, 1,2-asymmetric induction was accomplished with excellent stereoselectivity.

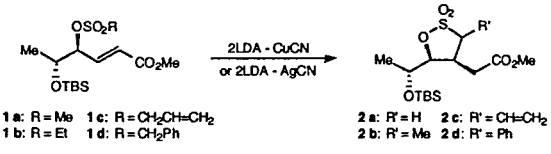


# V—L Kinetic Studies on Photosolvolytic Reactions

Reactivities of photochemical reactions are considerably different from what are observed for the ordinal thermally initiated reactions. The contrast of the two reactions are mainly due to the differences in electronic states of the substrates between the excited and the ground states. Thus, photochemical reactions often proceed through highly reactive intermediates of which structures and reactivities are of great interest in physical chemistry as well as in synthetic chemistry. Furthermore, the reactivities of intermediate in photochemical reactions can be directly elucidated by the aid of transient techniques, and the results will greatly help the understanding of the photochemical reaction mechanisms as well as thermal ones. On this point of view, we are interested in the mechanisms of photosolvolytic reactions. Especially, our investigations are focused on the carbocationic intermediate and/or transition state in the photoinduced phenyl migration of α-chloropropiophenones where a phenyl-bridged, charge-delocalized carbocation is postulated as a reaction intermediate. Though the structure of the intermediate resembles "phenonium ion" well known as a carbocation intermediate in aryl-assisted solvolysis, an electron withdrawing carbonyl group is directly attached to the carbocation structure. Such a charge-delocalized and destabilized carbocation has not appeared in the ordinal solvolyses, and the reactivity of the carbication is of great interest. In this project, the transition state and/or intermediates in the photoinduced phenyl migration of α-chloropropiophnenone is kinetically investigated.

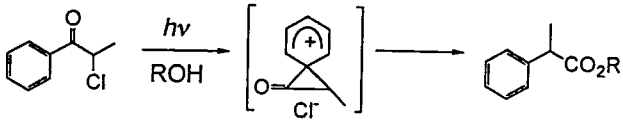

**Figure 1.** The proposed rectoion intermediate for the photoinduced phenyl-rearrangement reaction of α-chloropropiophenone

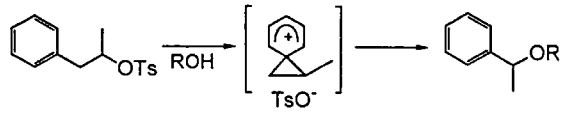

**Figure 2.** Reaction mechanism of the aryl-assisted solvolysis of 2-phenyl-1-methyl ethyl tosylate.

## V-L-1 Nucleophilic Substitution Reaction in the Photosolvolysis of α-Chloropropiophenone

**Satoshi USUI, Hitoshi ISHIDA,[a] and Katsutoshi OHKUBO[a]** *([a]Kumamoto University)*

Nucleophilic substitution reaction in the photosolvolysis of α-chloropropiophenone (1) was investigated. The irradiation of 1 in 2,2,2-trifluoroethanol (TFE) with UV light ($\lambda > 280$ nm, pyrex filter) predominantly gave a product 2 with minor products 3 and 4 as indicated in Scheme 1. The main product 2 is formed by a phenyl migration reaction involving carbocationic intermediates while 4 is formed by the hydrogen abstraction of α-methylphenacyl radicals. The result is interpreted as a mix of ionic and radical reaction paths for the photosolvolysis mechanism of 1. When the photosolvolysis was carried out in the presence of *n*-propanethiol (PrSH), the yield of 2 was remarkably reduced and propyl sulfide 5a was additionally obtained; however, the yields of 3 and 4 did not change. The addition of sodium azide ($NaN_3$) similarly decreased the yield of 2 and gave an azide adduct 5b with little change in the yield of 3 or 4. The results indicate that the decrease of 2 is due to the nucleophilic substitution of $Cl^-$ by PrSH or $N_3^-$ ($k_s$) which competes with the phenyl migration process ($k_\Delta$) as described in Scheme 2. Then the $k_s$ values for a series of nucleophilies can be evaluated as rate ratios to $k_\Delta$ from the product analysis. Because the adducts 5 disappesared by the further photochemical decomposition, the $k_s/k_\Delta$ ratios were calculated from the nucleophile concentration dependency of the yield of 2. The $k_s/k_\Delta$ values obtained for the reaction with PrSH and $N_3^-$ are 950 and 1200 $M^{-1}$, respectively, and the $k_s/k_\Delta$ values for the reactions with other nucleophilies are now under investigation.

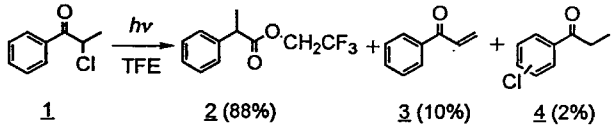

1 2 (88%) 3 (10%) 4 (2%)

**Scheme 1.**

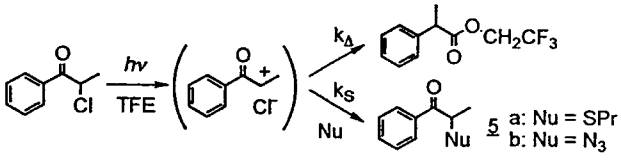

5 a: Nu = SPr b: Nu = $N_3$

**Scheme 2.**

## V-L-2 Substituent Effect on the Photoinduced Phenyl Rearrangement of α-Chloropropiophenone

**Satoshi USUI, Junji NISHIMOTO,[a] Hitoshi ISHIDA,[a] and Katsutoshi OHKUBO[a]** *([a]Kumamoto University)*

Substituent effect on the photoinduced phenyl rearrangement of α-chloropropiophenone was investigated in 2,2,2-trifluoroethanol (TFE). Because photosolvolysis of α-chloropropiophenone shows concurrent phenyl migration ($k_\Delta$) and nucleophilic substitution ($k_s$) processes, the rates of photoinduced phenyl migration for a seriese of phenyl substituted derivatives were evaluated as $k_\Delta/k_s$ rate ratios. The rate ratios were calculated from the decrease of phenyl rearranged product by the addition of *n*-propanethiol (PrSH) as a nucleophile. The $k_\Delta/k_s$ ratios decreased with the increase of electron withdrawing ability of the aryl substituent but were not linearly correlated with either $\sigma^\circ$ nor $\sigma^+$. As shown in Fig. 1, the $k_\Delta/k_s$ ratios for more deactivated derivatives than p-Me were almost linearly correlated with $\sigma^\circ$ values while that of p-MeO derivative is plotted far above the correlation line. The result indicates the enhancement of $k_\Delta$ in the presence of strong p-π-donnating substituent and suggests stbilization of the positive charge in the transition state by the conjugation through π-orbital of phenyl ring. The application of the Yukawa-Tsuno LArSR equation $\log k/k_H = \rho(\sigma^\circ + r^+\Delta\bar{\sigma}_R^+)$ to the $k_\Delta/k_s$ ratios gave $\rho = -1.70 \pm 0.32$ and $r^+ = 0.65 \pm 0.24$. The $\rho$ and $r^+$ values for $k_\Delta$ path are estimated as $\rho = -2.18$ and $r^+ = 0.51$ assuming that $\rho$ and $r^+$ values for the $k_s$ process in the photosolvolysis are equal to those of the nucleophilic substitution reaction for the 2-aryl-1-methylethyl solvolysis ($\rho = -0.48$ and $r^+ = 0.00$ in 50% aqueous TFE).[1] The intermediate $r^+$ value of 0.51 is a typical one for β-arylalkyl solvolyses and suggests a phenyl-bridged, delocalized carbocation for a transition state of the photoinduced phenyl migration reaction of α-chloropropiophenone.

**Reference**

1) M. Goto, K. Funatsu, N. Arita, M. Mishima, M. Fujio, and Y. Tsuno, *Mem. Fac. Sci. Kyushu Univ., Ser. C*, 17 (1), 123 (1989).

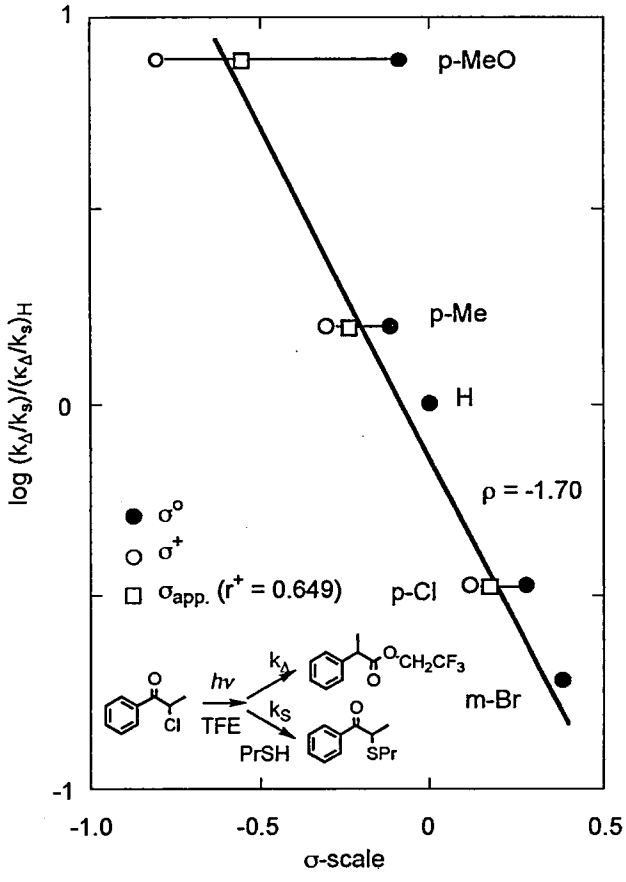


**Figure 1.** LArSR plot for the $k_\Delta/k_s$ ratios of the photosolvolysis of $\alpha$-chloropropiophenone.

# RESEARCH ACTIVITIES VI
# Department of Vacuum UV Photoscience

## VI—A Electronic Structure and Decay Mechanism of Inner-shell Excited Molecules

This project is being carried out in collaboration with Photon Factory, Institute for High-Energy Physics (KEK-PF). We successfully measured ion-yield spectra for the Σ ($\Delta\Lambda$=0) and Π ($\Delta\Lambda=\pm1$) distributions of fragment ions ("symmetry-resolved" spectra) emitted following the inner-shell photoabsorption of open-shell diatomic molecules, $O_2$ and NO, and clarified electronic structures with complicated spin coupling and exchange interaction between the valence and core electrons [See, N. Kosugi et al., *Chem. Phys. Lett.* **190**, 481 (1992); *J. Chem. Phys.* **97**, 8842 (1992)]. In the next stage we have started in revealing Rydberg-valence mixing and dissociation dynamics for triatomic linear molecules in addition to diatomic molecules.

### VI-A-1 Angular Distribution of the Fragment Ions after the O 1s-$\pi^*$ Excitation of $O_2$ and $N_2O$

**Nobuhiro KOSUGI, Jun-ichi ADACHI*, Eiji SHIGEMASA*, and Akira YAGISHITA*** *(*KEK-PF)*

Figure 1 shows the angular distribution of fragment ions, with kinetic energies larger than 2 eV, emitted after the 1s-$\pi^*$ excitation of $O_2$ and $N_2O$. $\theta$ is the angle between the electric vector of the incident photons and the emitted photoion direction. Dots with error bars correspond to experimental data points. The experimental distribution for $O_2$ behaves according to $\sin^2\theta$ as predicted in the Π ($\Delta\Lambda$=+1) excitation, indicating that the molecular orientation on the photoabsorption is preserved on the fragmentation. This is related to the axial-recoil approximation. The experimental distribution for $N_2O$ behaves according to $A+(1-A)\sin^2\theta$ (=$A\cos^2\theta+\sin^2\theta$), where A is 0.48. The O 1s-$\pi^*$ excited state of $N_2O$ has a stably bent structure due to the Renner-Teller effect; therefore, some bending modes are easily excited and the fragmentation through the Auger decay takes place after bending. In this case, the angular distribution does not strictly obey either Σ ($\Delta\Lambda$=0) or Π ($\Delta\Lambda$=+1) distribution. On the other hand, the O 1s ionized state and $\sigma$-type Rydberg states in $N_2O$ have stably linear structures and accept the axial-recoil approximation. The situation is almost the same in the $\pi$-type Rydberg states, because the Renner-Teller effect is very weak.

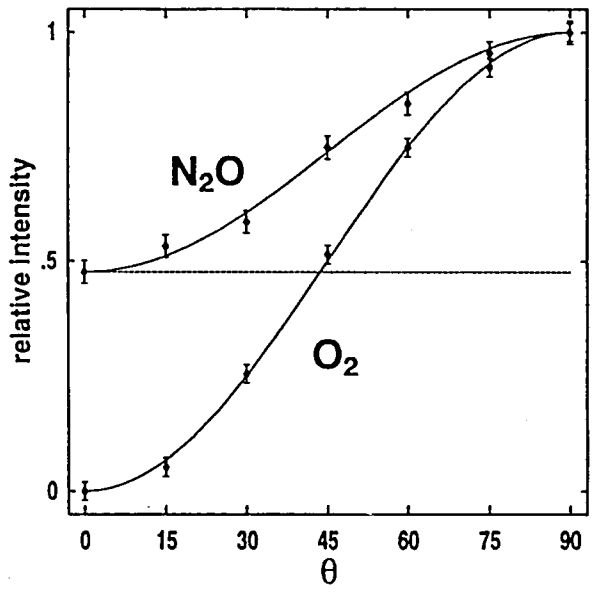


**Figure 1.** Angular distribution of photoions emitted after the O 1s→$\pi^*$ excitation of $O_2$ and $N_2O$.

### VI-A-2 Rydberg-valence Mixing near the O 1s Absorption Edge of $O_2$

**Akira YAGISHITA*, Eiji SHIGEMASA*, and Nobuhiro KOSUGI** *(*KEK-PF)*

The Rydberg series near the O 1s absorption edge in the open-shell $O_2$ molecule are superimposed on the two broad resonance features assigned to the 1s-2p$\sigma^*$ valence transitions; therefore, it is difficult to definitely understand the Rydberg states. In the present work we have measured the "symmetry-resolved" spectra with a much improved energy resolution, but the near-edge features are still complicated as shown in Figure 1 (Σ ($\Delta\Lambda$=0) spectrum).

The exchange splitting in the Rydberg series is not so different from the splitting in the core-ionized states of $^4\Sigma^-$ and $^2\Sigma^-$, whereas due to large exchange integrals between the 1s and $\sigma^*$ electrons the exchange splitting in the $\sigma^*$ resonances is so different that the lower $\sigma^*$ state is correlated to the $^2\Sigma^-$ ion core and the higher one to the $^4\Sigma^-$. The 3s$\sigma$ ($^4\Sigma^-$) Rydberg state lies simply on the lower $\sigma^*(^2\Sigma^-)$ resonance with no Rydberg-valence mixing. On the other hand, it is possible that the higher $\sigma^*(^4\Sigma^-)$ resonance interacts with some np$\sigma$ ($^4\Sigma^-$) Rydberg states. As shown in Figure 1

the npσ ($^4\Sigma^-$) Rydberg series (n≥4) and npσ ($^2\Sigma^-$) series (n≥3) show single structures, but the 3pσ ($^4\Sigma^-$) Rydberg transition cannot be assigned to a single peak. We believe that the 1s-3pσ ($^4\Sigma^-$) Rydberg excited state is strongly perturbed by the 1s-2pσ*($^4\Sigma^-$) excited state with a repulsive potential energy curve and shows unusual vibrational structures.

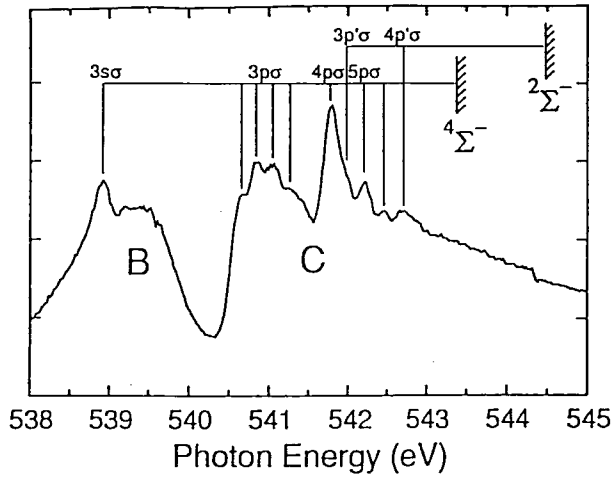


**Figure 1.** The Rydberg series and 1s-2pσ* resonances near the O 1s absorption edge in $O_2$. The symmetry-resolved Σ (ΔΛ=0) spectrum.

# VI—B Two-Color cm$^{-1}$-Resolution Threshold Photoelectron Spectroscopy for Studying Molecular Cations

In this Institute we have developed a compact cm$^{-1}$-resolution photoelectron analyzer, which collects threshold photoelectrons at several hundreds nanoseconds after each laser shot in our two-color experiment. Such a threshold photoelectron technique is equivalent to so-called ZEKE [Zero Kinetic Energy] photoelectron spectroscopy.

In the present project, we have carried out vibrational spectroscopy of cation molecules, including interesting phenomena induced due to charged molecules, by using this threshold photoelectron analyzer.

## VI-B-1 The Role of Electronic and Geometric Factors in "Proton Tunneling": A Comparative Study of Tropolone and 9-hydroxyphenalenone by Threshold Photoelectron Spectroscopy

**Hiroyuki OZEKI, Masahiko TAKAHASHI** *(Tohoku Univ.)*, **Katsuhiko OKUYAMA and Katsumi KIMURA** *(JAIST)*

[*J.Chem.Phys.*, **99**, 56 (1993)]

High resolution two-color threshold photoelectron spectra of tropolone and 9-hydroxyphenalenone (9-HPO) isolated in a free jet expansion have been measured to study the proton tunneling phenomena in the cation ground state ($D_0$). The tunneling splitting width of the $D_0$ zeroth vibrational level for the both molecules like within our experimental accuracy (2 cm$^{-1}$), indicating that the proton tunneling is inhibited when compared to that obtained in their respective neutral states. By means of a comparative study of these two molecules, the tunneling inhibition has been explained in terms of a large contribution from the electronic factor which represents the changes in charge distribution of the $\pi$ electrons upon ionization. The geometric factor, which is associated with the ring planarity is less important in determining the rate of tunneling in the $D_0$ state. In the case of tropolone, we have found that the measurement of an out-of-plane skeletal vibration in various electronic states make it possible to describe the tunneling path at a higher level that a simple one-dimensional description. Moreover, the adiabatic ionization energies of 9-HPO and the deuterated 9-HPO have been determined accurately to be 65338±5 cm$^{-1}$ (8.1009±0.0006 eV) and 65350±5 cm$^{-1}$ (8.1024±0.0006eV), respectively.

## VI-B-2 Structural Isomers and Tautomerism of 2-Hydroxypyridine in the Cation Ground State Studied by a Laser Threshold Photoelectron [Zero Kinetic Energy (ZEKE)-Photoelectron] Spectroscopy

**Hiroyuki OZEKI, Martin C. R. COCKETT, Katsuhiko OKUYAMA, Masahiko TAKAHASHI** *(Tohoku Univ.)* **and Katsumi KIMURA** *(JAIST)*

The investigation of structural isomers and proton transfer phenomenon of 2-pyridinone/2-hydroxypyridine system in the cation ground state ($D_0$) has been performed by two-color (1+1′) resonantly enhanced multiphoton ionization threshold photoelectron spectroscopy. The ionization energies of each keto/enol tautomer have been determined to be 68137±5 cm$^{-1}$ and 72093±5 cm$^{-1}$ for 2-pyridinone and 2-hydroxypyridine, respectively. The keto tautomers having different geometries in the $S_1$ state show the same ionization energies, indicating that no structural isomers of the keto tautomer exist in the $D_0$ state. The keto tautomer adopts a planar geometry in the $D_0$ state similar to that in the neutral ground state. In addition, no spectroscopic evidence for fast proton transfer from the enol form to the keto form in the $D_0$ state has been obtained from the analysis of the spectral line width.

### VI-B-3 Vibronic Coupling in the Ground Cationic State of Naphthalene: A Laser Threshold Photoelectron [Zero Kinetic Energy (ZEKE)-Photoelectron] Spectroscopic Study

**Martin C. R. COCKETT, Hiroyuki OZEKI, Katsuhiko OKUYAMA, and Katsumi KIMURA** *(JAIST)*

[*J. Chem. Phys.*, **98**, 7763 (1993)]

The two-color (1+1′) threshold photoelectron spectra of naphthalene in a supersonic free jet have been reported via nine vibronic levels of the $S_1$ electronic state up to about 1420 $cm^{-1}$ above the $S_1$ band origin. The threshold photoelectron spectra recorded via the $S_1$ band origin and via totally symmetric $a_g$ vibronic levels show significant intensity in $\Delta v$=+1 transitions in nontotally symmetric vibrations having $b_{1g}$ symmetry indicating that the ionization transition gains significant intensity through a vibronic coupling mechanism between the two lowest doublet cationic states. The strongest departure from the expected $\Delta v$=0 propensity in the threshold photoelectron spectra occurs through excitation of the totally symmetric 8 mode having $a_g$ symmetry indicating that a considerable displacement occurs along the normal coordinate of this 8 mode upon ionization from the $S_1$ state. The superior resolution of the threshold photoelectron technique over conventional photoelectron methods has allowed accurate values for the fundamental vibrational frequencies of naphthalene in its ground cationic state to be determined and it has also allowed a more rigorous investigation of the vibronic coupling mechanism that occurs between the two lowest doublet cationic states. Moreover, an improved value for the adiavatic ionization energy of naphthalene of 65 687±7 $cm^{-1}$ (8.1442±0.0009 eV) has been determined.

### VI-B-4 Photoelectron Spectra of Acetone and Acetone Dimer

**Kenji FURUYA, Shunji KATSUMATA** *(Iwaki Meisei Univ.)*, **and Katsumi KIMURA** *(JAIST)*

[*J. Electron Spectrosc.*, **62**, 237 (1993)]

In order to study the ionic states of acetone produced in a supersonic jet, we have carried out threshold photoelectron spectroscopy (TPES) with synchrotron radiation in the region 122.0–130.0 nm. Acetone has also been re-investigated by 58.4 nm He(I) photoelectron spectroscopy (PES). It has been found from a comparison of the PES and TPES spectra that there is an autoionizing state at 9.893±0.015 eV. Forethermore, a threshold-photoelectron photoion coincidence (TPEPICO) spectrum due to the acetone dimer has been obtained for the first time in the region 124.0–135.0 nm with an interval of 0.2 nm. The dimer intensity in each spectrum was plotted against the excitation wavelength, giving rise to intensity distribution corresponding to a TPES spectrum of the non-dissociative aceton dimer. In contrast to the PES and TPES spectra of the acetone monomer, no vibrational structure appears in the dimer spectrum. From this spectrum the appearance ionization potential of the acetone dimer has been evaluated as being 9.210±0.015 eV. Two bands appear in the dimer spectra, one of which may be assigned to a Rydberg state of the neutral dimer, and the other to the electronic ground state of the dimer cation.

## VI—C Molecular Beam Studies of Gas Phase and Surface Reaction Dynamics

In the present project we investigate dynamics of bimolecular reactions using a crossed molecular beams technique and also surface reaction dynamics using molecular beam-surface scattering techniques. Experimental data obtained in this project are angular and velocity distributions of the scattered species detected by a rotatory quadrupole mass spectrometer using a time-of-flight (TOF) technique as a function of reactant collision energy and, in the case of surface reactions, surface conditions such as substrate temperature, incident angle, and surface structure and coverage. We are interested in obtaining interaction energies between a molecule and the characterized surface in relation to the reactivities. Molecular Beam Chemistry apparatus-I (MBC-1) and -II (MBC-II) which are modified for ultrahigh vacuum specifications are employed for the present project.

### VI-C-1 A Scattering Experiment of Molecular Beams for Estimation of the Adsorption Probability

**Tetsuo FUJIMOTO*, T. NI-IMI*, Kosuke SHOBATAKE, and K. KONDO*** *(*Nagoya Univ.)*

[*Vacuum*, **44**, 429 (1993)]

Scattering experiment using molecular beams on a target enables us to estimate the adsorption probability. Time-of-flight (TOF) spectra of He and Ar scattered from a Ag ion-plated stainless steel (SUS 304) surface and a naked one have been obtained for various angles of incidence and reflection. For the naked surface, a TOF spectrum of Ar scattered from the naked surface can be analyzed in terms of a Maxwell-Boltzmann distribution function without invoking drift velocity. This shows that the scattering proceeds following adsorption and desorption process. For the ion-plated surface on the other hand, the spectrum analysis requires superposition of two distribution functions with and without drift velocity. The former corresponds to the direct scattering or inelastic scattering. For He, the two velocity distribution functions with and without drift velocity are required for both surfaces. From the relative magnitude of the two velocity distribution functions, the adsorption and desorption process is dominant for the naked surface, leading to higher adsorption probability.

# VI—D Vacuum UV Photochemistry of Gaseous Molecules and Molecular Clusters

In the present project we seek to obtain detailed information about, 1) photodissociative excitation processes from highly excited molecules, 2) photochemistry of excited van der Waals (vdw) molecules and clusters formed in a supersonic expansion, and 3) collision induced relaxation and reactions of the photoexcited molecules. The techniques applied are absorption and fluorescence spectroscopies of gaseous molecules and vdw molecules on an apparatus constructed on the beam line BL2A of UVSOR facility. In particular we use fluorescence excitation, fluorescence polarization, time-resolved fluorescence, and dispersed fluorescence spectroscopies to identify product species and obtain information on the dynamics of photochemical reactions.

## VI-D-1 Photo-induced Processes of $Cl_2$ ($1^1\Sigma^+_u$) State Studied by VUV/UV Fluorescence Lifetime Measurements

**Kiyohiko TABAYASHI, Mitsuhiko KONO, Atsunari HIRAYA** *(UVSOR)*, **and Kosuke SHOBATAKE**

The time-resolved fluorescence decay measurements were done to study relaxation processes of the SR excited ion-pair state $Cl_2$ ($1^1\Sigma^+_u$) and the laser emitting state $Cl_2$ ($2^3\Pi_g$) formed by the collision-induced process of the ion-pair state. Figure 1 shows the Stern-Volmer plot for the bound-free transition $Cl_2$ ($1^1\Sigma^+_u$-$X^1\Sigma^+_g$) observed in the region $185 < \lambda_{obs} < 215$ nm via a VUV monochromator and with a multichannel detector. The decay rate $k_d$ ($=1/\tau_d$ where $\tau_d$ is the fluorescence lifetime) is plotted against the rare gas pressure $P_{Rg}$ from which the quenching rate of $Cl_2$ ($1^1\Sigma^+_u$) state by Xe gas has been estimated as $1.3\times10^{-9}$ $cm^3/s$ which corresponds to average quenching cross section of $\sigma_Q$=350 $Å^2$, while the quenching rate for Ne is $1.4\times10^{-10}$ $cm^3/s$. From the risetime measurement for the XeCl* excimer emission its formation rate has been also estimated as $7.7\times10^{-11}$ $cm^3/s$ which corresponds to the average quenching cross section of 21 $Å^2$. It is thus found that the quantum yield for excimer formation is about 6.0% of the quenching rate of $Cl_2$ ($1^1\Sigma^+_u$) state. This value is comparable with the quantum yield for excimer formation from the Xe-$Cl_2$ van der Waals molecule excited at $\lambda_{exc}$=142.5 nm which was estimated as about 3%.

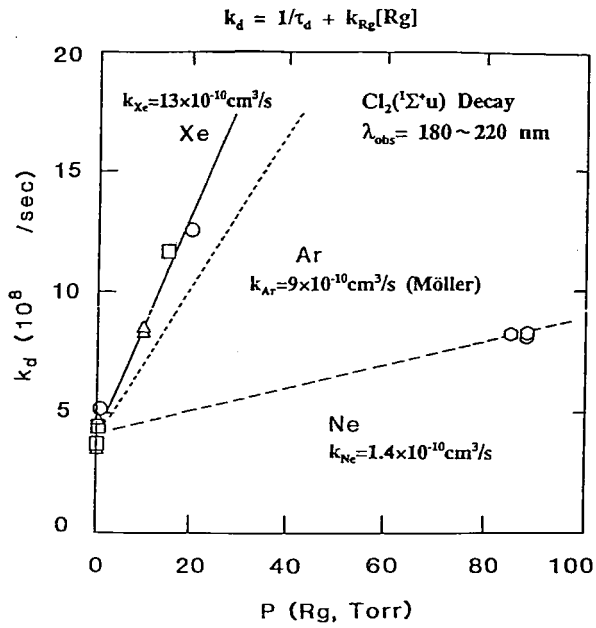


**Figure 1.** Stern-Volmer plot for the decay rate of the $Cl_2$ ($1^1\Sigma^+_u$-$X^1\Sigma^+_g$) emission observed in the region $185 < \lambda_{obs} < 215$ nm as a function of pressure of rare gas Rg (Rg=Xe, Ar, and Ne). The decay rate for Xe and Ne partner are $1.3\times10^{-9}$ and $1.4\times10^{-10}$ $cm^3/s$, respectively. The literature value for Ar is $9.0\times10^{-10}$ $cm^3/s$.

## VI-D-2 Absorption Spectra of Alkali Cyanide Molecules in the Vacuum Ultraviolet Region: Transitions to Direct-dissociative and Predissociative States

**Hisato YASUMATSU*, Tamotsu KONDOW*** *(Univ. of Tokyo)*, **Kaoru SUZUKI** *(Dept. of Electronic Structure)*, **Kiyohiko TABAYASHI, and Kosuke SHOBATAKE**

The absorption spectra of alkali cyanide molecules, MCN (M=Na, K, and Rb), in the gas phase were measured in the energy region from 4.0 to 11 eV (300—110 nm) using SR. A windowless absorption cell which enables us to measure absorption spectra at high temperatures up to 750°C was specially made. Figure 1 illustrates the absorption spectra of MCN molecules. The major features of the spectra obtained for all of the cyanides were explained in terms of the electronic transitions to two types of excited states of MCN, the repulsive and excited ion-pair states with the aid of the preliminary *ab initio* SCF-CI calculations of alkali cyanides. The absorption bands having a FWHM of about 1 eV are assigned to the bound-free transitions to the repulsive Rydberg states correlating to M($^2$S, $^2$P)+CN($X^2\Sigma^+$, $A^2\Pi$, $B^2\Sigma^+$). The broad band at about

8.0 eV observed for all the alkali cyanides studied are assigned to the transition to the direct dissociative state. The bands observed at 8.0, 7.4, 7.1 eV for NaCN, KCN, and RbCN, respectively, are associated with the transitions to the lowest excited ion-pair states of MCN correlating to $M^+ + CN^-(^3\Sigma^+)$. The bands associated with the transitions to the lowest excited ion-pair states seem to pile up with the high Rydberg transitions and exhibit an almost continuous absorption feature.

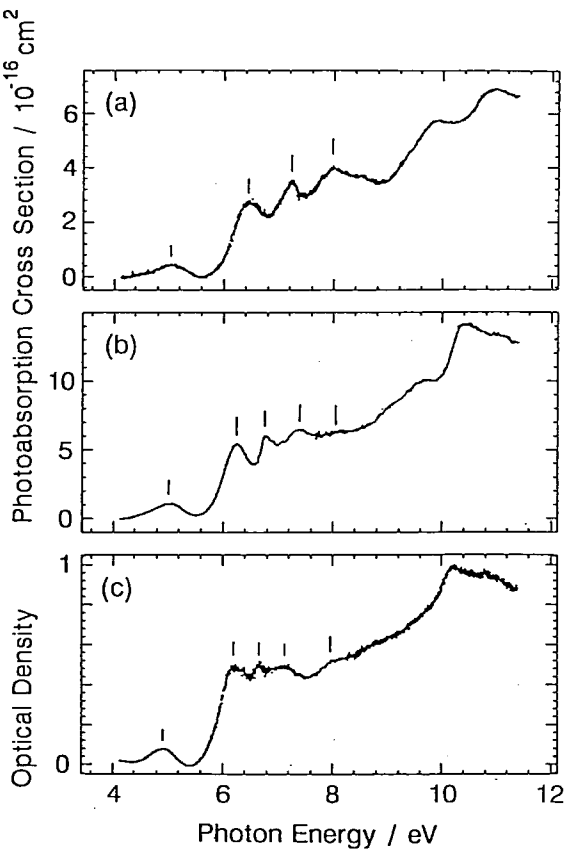


**Figure 1.** Photoabsorption spectra of (a) NaCN, (b) KCN, and (c) RbCN. The ordinates for the NaCN and KCN are scaled as the absolute absorption cross section with the estimated uncertainty of 60%, while that for the RbCN spectrum is scaled as the optical density, $-\log(I/I_0)$, where $I_0$ and I denote the transparent intensities without and with alkali cyanide vapor.

## VI-D-3 Fluorescence Polarization Measurements of CN(B→X) Formed in the Photodissociative Excitation Process of $CD_3CN$ and $CH_3CN$

**Mitsuhiko KONO, Kiyohiko TABAYASHI, and Kosuke SHOBATAKE**

Photodissociative excitation process of $CD_3CN$ and $CH_3CN$ forming $CN(B^2\Sigma^+)$ fragments in the wavelength region from 107 to 150 nm was studied using synchrotron radiation as a polarized light source. The fluorescence emitted to the direction perpendicular to both the exciting light beam and its electric vector was detected. Figure 1 shows $CN(B^2\Sigma^+ \rightarrow X^2\Sigma^+)$ fluorescence anisotropy, R, along with its fluorescence excitation spectrum for gaseous $CD_3CN$ as a function of the excitation wavelength $\lambda_{exc}$ in the region $105 < \lambda_{exc} < 140$ nm. The fluorescence anisotropy R was estimated as $R = (I_\parallel - I_\perp)/(I_\parallel + 2I_\perp)$ where $I_\parallel$ and $I_\perp$ are the observed polarized fluorescence intensities parallel and perpendicular to the polarization vector of the incident light. Although not shown the fluorescence quantum yield smoothly increases with photoexcitation energy up to 107 nm where maximum value of about 4% is obtained. The anisotropy factor decreases to zero as the excitation wavelength longer than 130 nm, which is in sharp contrast with the trend of the ClCN photodissociation where the anisotropy factor stays as high as the theoretically allowed maximum value of 0.10. The maximum anisotropy factor R observed is about 0.05 for the bands at 115 nm, which is indicative of the longer lifetimes of the excited states for $CD_3CN$ than the those of ClCN. It is also found that the anisotropy factor does not depend on the gas pressure in the pressure region below 20 mTorr.

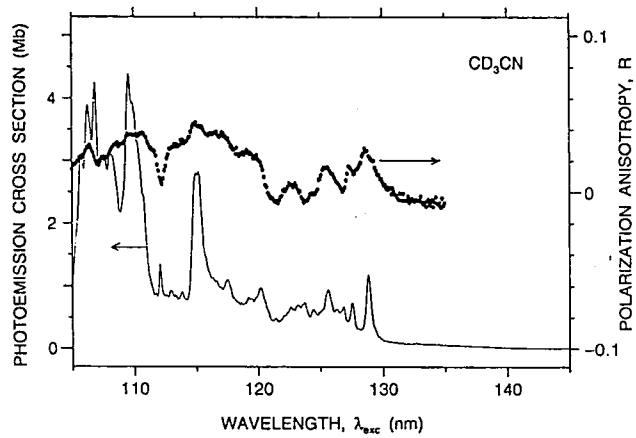


**Figure 1.** $CN(B^2\Sigma^+ \rightarrow X^2\Sigma^+)$ fluorescence anisotropy factor, R, along with its fluorescence excitation spectrum for gaseous $CD_3CN$ as a function of the excitation wavelength $\lambda_{exc}$ in the region $105 < \lambda_{exc} < 140$ nm. The resolution of the incident light for the fluorescence polarization measurement was 0.5 nm and the pressure was 20 mTorr.

## VI-D-4 Photodissociation of BrCN in the Vacuum Ultraviolet Region

**Kazuhiro KANDA[a], Shunji KATSUMATA[a]** *([a]Iwaki Meisei Univ.)*, **Takashi NAGATA[b], Yasushi OZAKI[b], Tamotsu KONDOW[b], Kozo KUCHITSU[b]** *([b]Univ. of Tokyo)*, **Atsunari HIRAYA** *(UVSOR)*, **and Kosuke SHOBATAKE**

[*Chem. Phys.* **175**, 399 (1993)]

The absolute cross sections for the production of $CN(A^2\Pi_i)$ and $CN(B^2\Sigma^+)$ from BrCN were measured over the excitation wavelength range 105–150 nm (67000–95000 $cm^{-1}$), using synchrotron radiation. The quantum yields for the CN(A) and CN(B) productions were also determined. The yields were observed to increase with the excitation energy from ~0.02 at 145 nm to 0.1 at 105 nm. The production of $CN(X^2\Sigma^+)$ is possibly the dominant photochemical channel of BrCN in the vacuum ultraviolet (UVU) region. The fragment $CN(B^2\Sigma^+ - X^2\Sigma^+)$ emission was found to be partially polarized with respect to the direction of the electric vector of the incident radiation. The polarization anisotropy of the emission depends on the type of transitions relevant to photodissociation; an examination of the polarization vs. excitation energy curve has

provided on the symmetry of the upper electronic states. Based on these experimental results, the assignments of the Rydberg and/or intravalence transitions of BrCN in the VUV region are discussed in connection with the photochemical properties of the high-energy electronic states. The absorption spectrum of BrCN below 105 nm was also reported.

# VI—E Synchrotron Radiation-excited Etching Reactions of Semiconductor Material Surfaces Studied by Velocity Distribution Measurements of Desorbed Species

In this project the mechanism of synchrotron radiation excited etching reactions of semiconductor material surfaces is being investigated by characterizing the product states as a function of the experimental conditions such as the pressure of the etchant, the sample temperature, the integrated dose of synchrotron radiation (SR), and the time-correlation between the irradiation time and the instant of product desorption. The experimental technique applied is the mass spectroscopic detection of the neutral species combined with the velocity distribution measurement using the time-of-flight (TOF) technique. For the present experiment an apparatus which consists of a reaction chamber, a TOF chopper chamber, and a detector chamber has been assembled. The electron bombardment ionization quadrupole mass spectrometer detector used for the crossed molecular beam apparatus (see VI-C) is employed.

## VI-E-1 Synchrotron Radiation-excited Etching of Silicon Surface Studied by Velocity Distribution Measurements of Desorbed Species: I. Excitation by Undulator Radiation at 35.8 eV

**Haruhiko OHASHI, Kiyohiko TABAYASHI, and Kosuke SHOBATAKE**

Synchrotron radiation excited etching of Si(100) surface with $XeF_2$ as an etchant is studied by measuring the velocity distributions of the desorbed neutral species using a TOF technique and an electron bombardment ionization mass spectrometer on a new apparatus constructed on the beamline BL3A1. The undulator radiation of the photon energy of 35.8 eV was shown on the Si(100) surface at an incident angle of 75 degrees and the desorbed species leaving the surface at an angle of 15 degrees from the surface normal were measured. The flight length from the correlation chopper to the ionizer was 31 cm.

Figure 1 shows the TOF spectra observed at mass m/e=85 ($SiF_3^+$) with the SR on and off. The pressure of the $XeF_2$ pressure was kept at $1.1\times10^{-5}$ Torr and the substrate was kept at room temperature. It is noted that the velocity distribution of the desorbed species are identical within the experimental error except for the higher intensities observed for the SR on. The solid curves are the Maxwell-Boltzmann distributions calculated assuming the translational temperature of the species is 300 K and the mass of the neutral species is 104, that is $SiF_4$. The results indicate that the excitation with 35.8 eV light enhances the etching reaction but it does not accelerate the departure speed of the etching product of $SiF_4$.

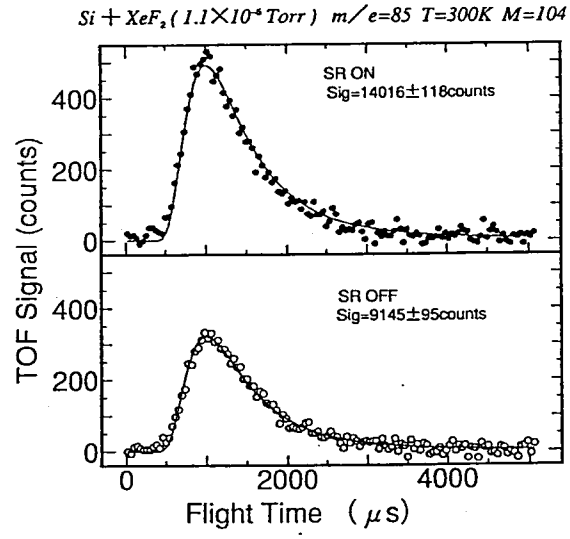


**Figure 1.** TOF spectra of desorbed species from the etching reaction of Si(100) with $XeF_2$ detected at mass m/e=85 ($SiF_3^+$) with undulator beam on and off. The solid curves correspond to the calculated Maxwell-Boltzmann distributions for mass M=104 ($SiF_4$) and translational temperature of 300 K.

## VI-E-2 Synchrotron Radiation-excited Etching of Silicon Surface Studied by Velocity Distribution Measurements of Desorbed Species: II. Excitation by Bending Magnet Light

**Haruhiko OHASHI and Kosuke SHOBATAKE**

Synchrotron radiation excited etching of Si(100) surface with $XeF_2$ is studied by measuring the velocity distributions of the desorbed neutral species using a TOF technique and an electron bombardment ionization mass spectrometer detector. A new reaction chamber was constructed to lower the residual gas background due to the desorbed species. Focused synchrotron radiation from a bending magnet was shown on the Si(100) sample in $XeF_2$ environment. The angle between the incident light beam and the velocity vector of desorbing product detected is 135 degrees. The flight length from the correlation chopper to the ionizer was 31 cm.

Figure 1 shows the TOF spectra observed at mass m/e=85 ($SiF_3^+$) with the SR on and off. The conspicuous difference between the two distributions is that with the SR on a fast moving species appears as a shoulder in addition to the slow species which can be fitted by the Maxwell-Boltzmann (MB) distribution. From a series of measurements under different experimental conditions it has been found that the substrate temperature goes up as much as about 200°C depending upon the irradiation time and the stored current level. The peak for the fast moving species in the TOF spectrum for SR on is not always observed, but after some twenty minutes of irradiation. The mechanism for formation of the fast moving species is not well understood at the moment.

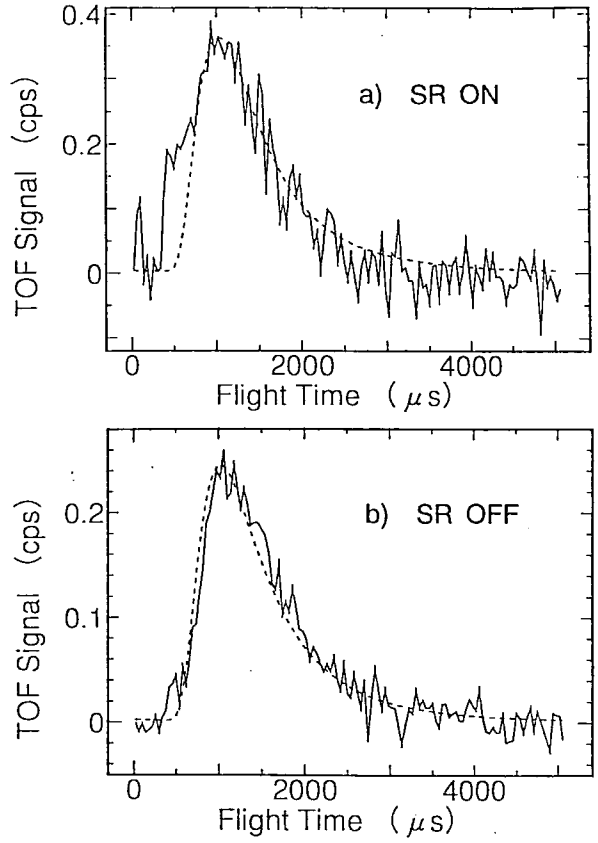


**Figure 1.** TOF spectra of desorbed species detected at mass m/e=85 ($SiF_3^+$) with SR beam on and off. The dashed curve corresponds to the calculated MB distribution for mass M=104 ($SiF_4$) and a translational temperature of 300 K fitted to the experiment.

# VI—F Synchrotron Radiation Stimulated Surface Reactions

Study of synchrotron radiation (SR) stimulated surface reaction is a promising topic in fundamental science, because dynamical processes induced by the photostimulated core-electron excitations on surfaces are scarcely explored so far. This field is important also in applied science, since the fundamental study is expected to develop the new techniques for semiconductor processing such as SR stimulated etching and SR stimulated epitaxial growth.

## VI-F-1 Reaction Chamber for the Study of the Synchrotron Radiation Stimulated Etching, Chemical Vapor Deposition and Epitaxial Growth

**Tsuneo URISU, Akitaka YOSHIGOE, Mitsuru NAGASONO, Kazuhiko MASE, Haruhiko OHASHI, and Kosuke SHOBATAKE**

A new reaction apparatus consisting of five chambers for the study of synchrotron radiation (SR) etching, and chemical vapor deposition (CVD) or epitaxial growth has been almost constructed. The base pressure of the chamber is designed to be less than $1\times10^{-9}$ Torr. Sample surfaces can be heated up to more than 1000°C in the epitaxial chamber, by use of the graphite carbon thin film heater covered by boron nitride. In-situ measurements by the reflection high energy electron diffraction (RHEED) and FTIR are the important subjects of these experiments. For this purpose, the filament room of the RHEED is differentially pumped by the turbo molecular pump for the operation under the reaction gases. For the measurements of the FTIR, a pair of $BaF_2$ windows are used as the IR beam input and output ports.

## VI-F-2 Highly Sensitive Single-reflection FTIR Spectroscopy for In Situ Monitoring Photoreaction upon Synchrotron Radiation Processing of Semiconductor Materials

**Yanping ZHANG, Shinri SATO*** *(*Hokkaido Univ.)*, **Hisayoshi OHSHIMA****, **Tadashi HATTORI**** *(**Nippondenso Co. Ltd)*, **Kazuhiko MASE, and Tsuneo URISU**

[*Appl. Surf. Sci.*, submitted]

In order to monitor photoreaction upon VUV synchrotron radiation processing of semiconductor materials, combined with the specially prepared substrate that has a buried metal layer, FTIR reflection-absorption spectroscopy was developed to carry out highly sensitive in situ detection of chemical changes on Si surfaces. For organometallic $Fe(CO)_5$ adsorbates, the sensitivity using the Si substrate with a buried metal layer was found to be an order of magnitude higher than that using standard Si substrates and thus $Fe(CO)_5$ submonolayer could be detected. Upon

application of this technique for in situ real time monitoring photoreaction of the $Pd(\mu\text{-}O_2CCH_3)_3$ spin-on film under VUV synchrotron irradiation, not only was the photolysis observed, but also the photo-thermal effect.

### VI-F-3 Study of Synchrotron Radiation Stimulated Surface Dynamics by Using Electron-Ion Coincidence Spectroscopy

**Kazuhiko MASE and Tsuneo URISU**

The aim of the present project is to clarify the detailed mechanism of surface dynamics induced by synchrotron radiation (SR). The apparatus is an ultra-high vacuum chamber equipped with an SR inlet port, sample manipulation system, sample cleaning system, gas inlet line, low-energy electron diffraction (LEED) optics, and electron-ion coincidence spectroscopy analyzer. The last instrument detects an electron and ions emitted in the same photochemical process by using electron energy analyzer and time-of-flight ion mass analyzer, respectively. The excited state responsible for the photochemical process is identified by the energy of emitted electron. The probability of the ion desorption from the excited state is estimated by the ion counting rate.

## VI—G Study of Ion-pair Formation in the Vacuum Ultraviolet Region Using Synchrotron Radiation

Photoexcitation of molecules to highly-excited states is often accompanied by dissociation into a pair of positive and negative ions in the photon energy range of 10—50 eV. The detection of negative ions produced by such ion-pair processes provides a sensitive probe to investigate the properties of superexcited states lying in the vacuum ultraviolet. This year we investigate the ion-pair formation from photoexcitation of $SO_2$ and saturated hydrocarbons.

### VI-G-1 Ion-pair Formation from $SO_2$ in the Vacuum Ultraviolet

**Koichiro MITSUKE, Shinzo SUZUKI** *(Tokyo Met. Univ.)*, **Takashi IMAMURA** *(Natl. Inst. Environ. Studies)*, **and Inosuke KOYANO** *(Himeji Inst. of Tech.)*

[*Org. Mass Spectrom.*, **28**, 335 (1993)]

Experiments are made by using synchrotron radiation emitted from the beam line BL3B installed in the UVSOR storage ring. Negative ions $O^-$ from $SO_2$ are observed by mass spectrometry. Figure 1 shows the $O^-$ photodissociation efficiency curve. The appearance energy for $O^-$ is in good agreement with the thermochemical threshold of 14.49 eV for the formation of $O^-(^2P_u)+SO^+(\tilde{X}\,^2\Pi)$. The cross section for the ion-pair formation at ~765 Å is estimated to be $(2.6\pm1)\times10^{-20}$ cm$^2$.

The $O^-$ efficiency rises markedly at the wavelengths of 622 and 570 Å. These onsets are attributed to the formation of triplets of fragments: $O^-(^2P_u)+S^+(^4S_u)+O(^3P_g)$ and $O^-(^2P_u)+S^+(^2D_u)+O(^3P_g)$. In the wavelength range of 680–860 Å, there are a number of vibrational progressions which may be identified to Rydberg states with a variety of symmetry and principal quantum numbers. We can extract and assign three vibrational progressions in the symmetric stretching mode $\nu_1$ for the s-type Rydberg states converging to $SO_2^+$ ($\tilde{D}\,^2A_1$). Some of the vibrational progressions reported in the photoionization efficiency curve of $SO_2^+$ from $SO_2$ are not discernible in the present $O^-$ efficiency curve. We can explain this discrepancy in terms of the specificity of the Rydberg states in autoionization branching.

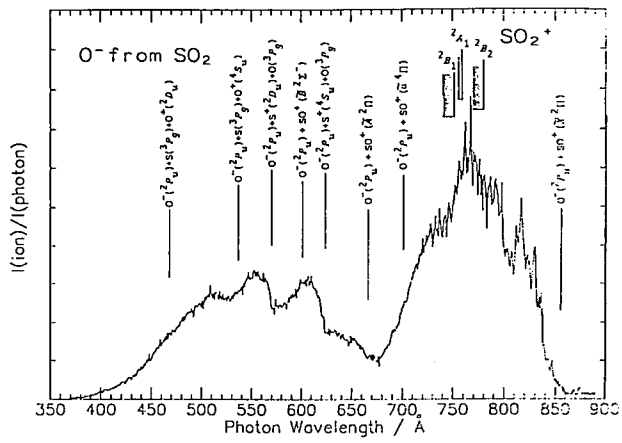


**Figure 1.** Photodissociation efficiency curve of $O^-$ produced from $SO_2$ taken at a wavelength resolution (FWHM) of 0.8 Å and wavelength intervals of 1 Å. The vertical lines indicate the ionization limits for $SO_2^+(\tilde{C}\,^2B_2$, $\tilde{D}\,^2A_1$, and $\tilde{E}\,^2B_1)$ and the thermochemical thresholds for possible ion-pair channels.

### VI-G-2 Ion-pair Formation from Saturated Hydrocarbons

**Hideo HATTORI, Hiroaki YOSHIDA, and Koichiro MITSUKE**

[*J.Chem.Phys.*, **99**, 6642 (1993)]

We study the ion-pair formation from several saturated hydrocarbons (methane, ethane, propane, butane, isobutane, neopentane) by negative-ion mass spectrometry of $H^-$ produced by photoexcitation in the vacuum ultraviolet. Figure 1 shows the efficiency curve of $H^-$ produced from propane. The intense peaks around 18.55 eV and 20.4 eV are attributed to predissociation of the Rydberg states formed by promotion of an electron in carbon *2s*-type molecular orbitals ($C_{2s}$ orbitals) designated as $3a_1$, $2b_2$, and $4a_1$. On the contrary, the curve shows no peak resulting from predissociation of the Rydberg states formed by excitation of an electron in carbon *2p*-type molecular orbitals

($C_{2p}$ orbitals) such as $1b_1$, $5a_1$, $3b_2$, and $1a_2$, although the excitation energies for these states are higher than the thermochemical threshold for the ion-pair formation. In the case of the other molecules, almost all Rydberg states produced by removal of an electron from $C_{2s}$ orbitals are found to undergo predissociation into ion pairs, but those produced by removal of a $C_{2p}$ electron scarcely lead to ion pairs.

This remarkably different behavior between the two types of Rydberg state can be explained in terms of competition between predissociation into ion pairs and other decay pathway, particularly autoionization process. The Rydberg states with the $C_{2p}$-hole character have higher transition probabilities of autoionization due to considerable overlap between two $C_{2p}$ orbitals involved in electron exchange. Since only a little overlap occurs between $C_{2s}$ and $C_{2p}$ orbitals, the Rydberg states with the $C_{2s}$-hole character have much longer lifetime with respect to autoionization and, as a result, large branching ratio for production of ion pairs.

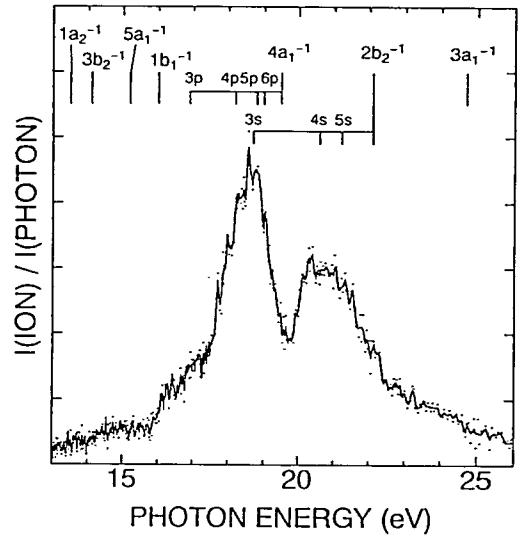


**Figure 1.** Photodissociation efficiency curve of $H^-$ produced from propane plotted as a function of the photon energy. The vertical ionization potentials for valence molecular orbitals and assignments of the Rydberg states are indicated.

# VI—H Positive Ion-Negative Ion Coincidence Spectroscopy (PINICO) Using Synchrotron Radiation

For full understanding of the ion-pair formation, we have developed a new coincidence technique, PINICO, utilizing the flight-time correlation of a pair of positive and negative ions produced by single photon excitation. The basic design of the apparatus and the principles of operation are described elsewhere [*Z. Phys. D*, **27**, 267 (1993)]. By using PINICO spectroscopy we could discuss about the symmetry of the Rydberg states $O_2^{**}$ and $H_2^{**}$ which are predissociated into $O^+ + O^-$ and $H^+ + H^-$, respectively. This year PINICO method is applied to the study of the ion-pair formation from $O_2^{**}$ converging to $O_2^+(\tilde{c}^4\Sigma_u^-)$ and from $N_2O^{**}$ in doubly-excited states.

## VI-H-1 Angular Dependence of the Ion-pair Formation from $O_2$ in 20–25 eV

**Hiroaki YOSHIDA, Hideo HATTORI, and Koichiro MITSUKE**

The relative photodissociation efficiency curve for the ion-pair formation from $O_2$ is measured in the energy region of 20–25 eV by using synchrotron radiation. In Figure 1, the solid line denotes the efficiency curve obtained by extracting $O^+$ and $O^-$ perpendicularly to the electric vector of the linearly polarized light (perpendicular extraction), while the broken line by extracting $O^-$ almost parallel to the vector (parallel extraction). The results indicate that ion pairs are produced through not only direct transitions to $^3\Sigma_u^-$ and $^3\Pi_u$ ion-pair states but also conversion of the $ns\sigma_g{}^3\Sigma_u^-$ and $nd\sigma_g{}^3\Sigma_u^-$ Rydberg states converging to $O_2^+(\tilde{c}^4\Sigma_u^-)$ to $^3\Sigma_u^-$ ion-pair states. If a $\Sigma \rightarrow \Sigma$ parallel transition to a Rydberg state is followed by predissociation into ion pairs, the ion detection efficiency is expected to be much lower for perpendicular extraction than for parallel extraction. This consideration suggests that the broad peak around 21.5 eV in Figure 1 results from a $\sigma \rightarrow \sigma^*$ shape resonance, since the intensity of this peak is quite low in the efficiency curve for perpendicular extraction.

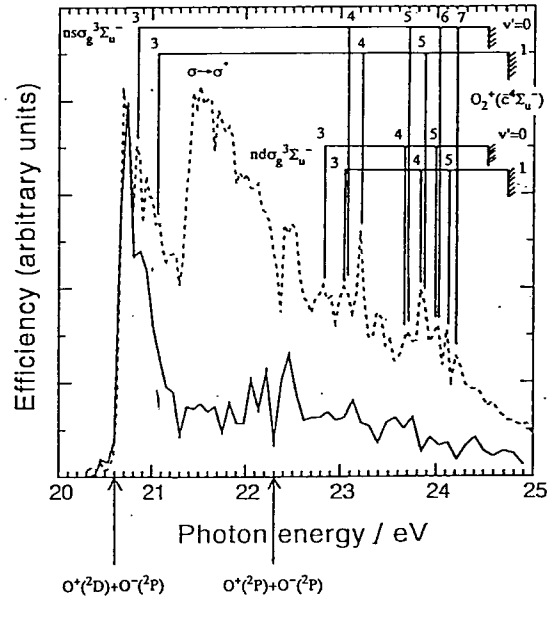


**Figure 1.** Photodissociation efficiency curves for the ion-pair formation from $O_2$ in the energy region of 20–25 eV. Produced negative ions are extracted perpendicularly (—) or parallel (– –) to the electric vector of the linearly polarized light. Vertical lines indicate the thermochemical threshold for the formation of $O^+(^2D)+O^-(^2P)$ and $O^+(^2P)+O^-(^2P)$ and the Rydberg series $O_2^{**}(ns\sigma_g{}^3\Sigma_u^-$ and $nd\sigma_g{}^3\Sigma_u^-)$ converging to $O_2^+(\tilde{c}^4\Sigma_u^-)$.

### VI-H-2 Positive Ion-Negative Ion Coincidence Spectroscopy of $N_2O$

**Hiroaki YOSHIDA and Koichiro MITSUKE**

Ion-pair formation from photoexcitation of $N_2O$ has been studied in detail by PINICO spectroscopy using synchrotron radiation in the 360–512 Å photon wavelength region. We can distinguish the following two processes: dissociation into three bodies of $O^-+N^++N$ and that into two bodies of $O^-+N_2^+$. The photodissociation efficiency curve for each process is shown in Figure 1. The onset of efficiency curve for dissociation into three bodies is in good agreement with the thermochemical threshold of 506.5 Å for the formation of $O^-(^2P_u)+N^+(^3P_g)+N(^4S_u)$. The efficiency for this process surpasses that for dissociation into two bodies above 25.30 eV(=490.0 Å). Both of the curves show several resonance peaks which can be assigned to the Rydberg states converging to two-electron-excited ionic states lying in the energy range of 25–35 eV.

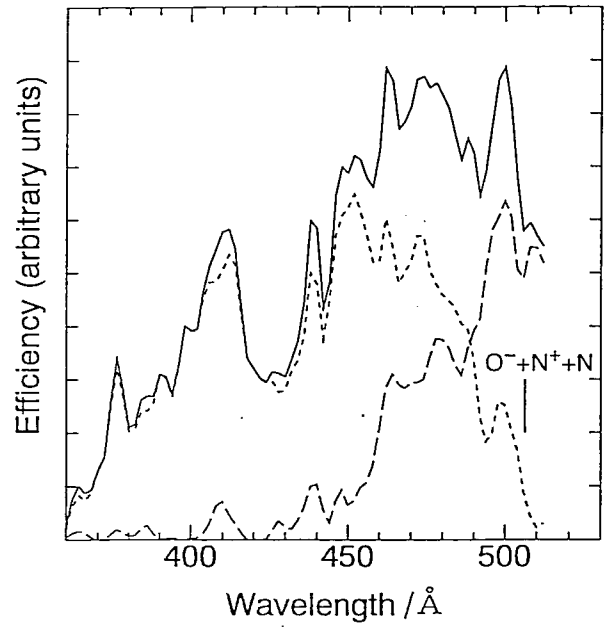


**Figure 1.** Photodissociation efficiency curves for the ion-pair formation from $N_2O$ as a function of the photon wavelength: $O^-+N_2^+$ (——), $O^-+N^++N$(----), and total $O^-$ yield (—). The thermochemical threshold of 506.5 Å for the formation of $O^-(^2P_u)+N^+(^3P_g)+N(^4S_u)$ is indicated.

## VI-I Construction of New Apparatus on the Beam Lines in UVSOR

In UVSOR, six beam lines are now devoted to studies of elementary atomic and molecular processes in the gas phase. First, the monochromator equipped in BL3B supplies well-collimated photon beam with relatively high flux, high resolution and excellently negligible contamination of the higher-order radiation. These advantages encourage us to develop a new apparatus for the study of photoionization with valence excitations and reactions of state-selected photoions. The experimental apparatus, containing an electron energy analyzer and a time-of-flight mass spectrometer, is designed and set up for photoelectron spectroscopy, photoionization mass spectrometry, and electron-ion coincidence measurements. On the other hand, the apparatus installed on the beam line BL2B2 has great capability in spectroscopic measurements on supercooled molecular species or ions, since this machine is composed of mobile vacuum chambers of great volume which are differentially pumped with high efficiency. Making full use of its features, we are planning to construct an intense source of metal cluster anions for studies of the electronic properties of neutral metal clusters by using photodetachment spectroscopy.

### VI-I-1 Construction of a Versatile Photoionization Spectrometer on UVSOR BL3B

**Hideo HATTORI and Koichiro MITSUKE**

A new photoionization spectrometer has been constructed on the beamline BL3B at UVSOR. The main components of the apparatus are a double-field type time-of-flight mass spectrometer and a spherical sector electrostatic energy analyzer as shown in Figure 1.

The sample gas expanded from a 50 $\mu$m nozzle is introduced into the photoionization region. The molecular beam is irradiated by a monochromatized VUV photon beam. Ejected electrons are focused onto the entrance slit of the energy analyzer. The mean radius of the electron orbit and the spacing between two concentric spherical sector surfaces are 54.7 and 11.9 mm, respectively. Upon detection of an electron, photoions are pushed out by a pulsed electric field (duration ~1 $\mu$s; amplitude 1–2 kV) and mass analyzed by a TOF spectrometer of 50 cm length. This apparatus is designed to provide a wide range of information on the products of a single photoionization event. In constant-ionic-state photoelectron spectroscopy, which is one possible mode of experiment, the difference between the photon energy and the kinetic energy of electrons is kept constant. Thus we can measure the partial cross section for a particular ionic state as a function of the photon energy. Photoelectron-photoion coincidence spectroscopy is another mode of experiment. With this method, we investigate unimolecular dissociation of state-selected ions and the electronic structure of van der Waals clusters.

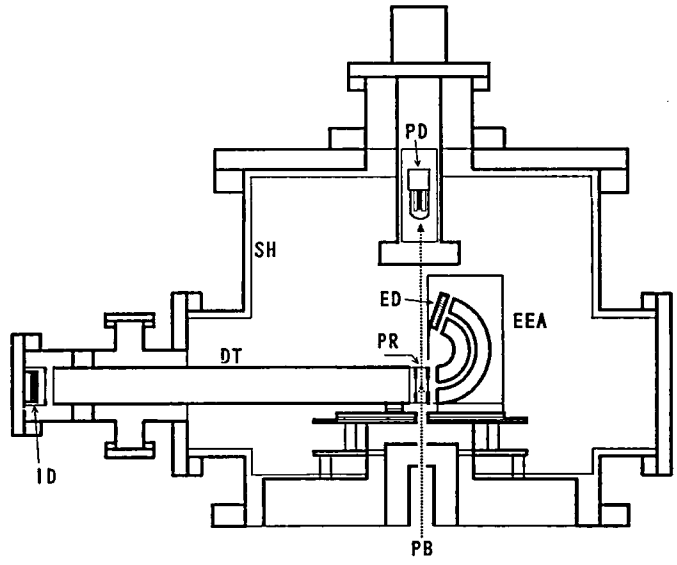


**Figure 1.** Schematic diagram of the photoionization spectrometer. PB: monochromatized photon beam, PR: photoionization region, DT: drift tube for ions, EEA: electron energy analyzer, ID: ion detector, ED: electron detector, PD: photon detector, SH: $\mu$-metal shield. The molecular beam is introduced into the photoionization region perpendicularly to both the photon beam and the symmetric axis of drift tube.

### VI-I-2 Development of Intense Source of Metal Cluster Anions

**Minoru KANNO and Koichiro MITSUKE**

Study of photodetachment spectroscopy of metal cluster anions is very useful to obtain valuable information on the ground and electronically excited states of neutral clusters. We are constructing a source of metal cluster anions using plasma sputtering. This source is a cluster-ion version of the "BLAKE V" ion source which has been developed by Mori *et al.* to generate intense beam of heavy-mass negative metal ions such as $Au^-$ and $Cu^-$ at National Laboratory for High Energy Physics (KEK) in cooperation with Tsukuba University.

Schematic diagram of the apparatus is shown in Figure 1. Negative ions are produced at the surface of the sample metal which is placed in a Xe plasma confined by a multi-cusp magnetic field. The sputtered atomic ions are decelerated by collisions in a He gas flow, and then cluster ions condense out of the quenched vapor. Atomic and cluster ions extracted from the source are mass-separated by a magnetic mass spectrometer and are allowed to intersect at 90° with the dispersed light from a 1 m Seya-Namioka monochromator. The extraction voltage is set to 10–20 kV. In the first stage, we are planning to measure threshold photoelectron spectra of size-selected metal cluster anions.

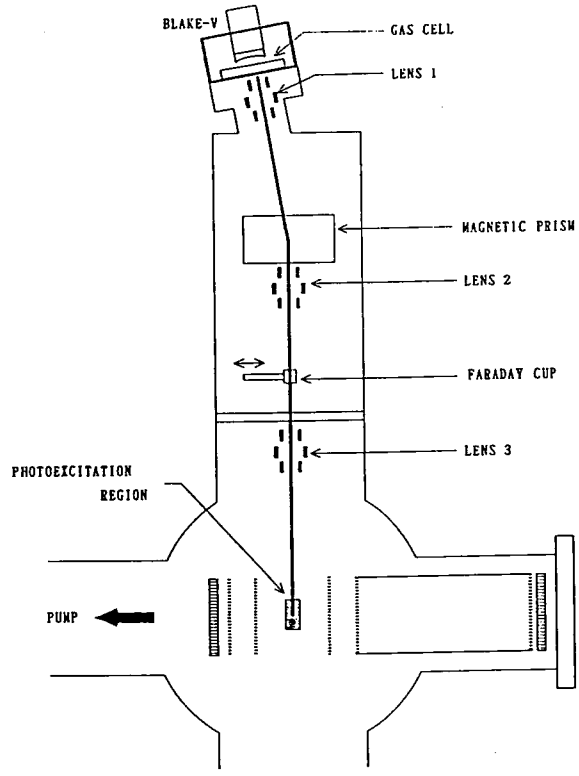


**Figure 1.** Schematic diagram of the apparatus for the metal cluster anion source and the threshold photoelectron spectrometer.

## VI—J Desorption Induced by Electronic Transitions on the Solid Surface of Condensed Gases

Photon-stimulated desorption (PSD) of molecules or ions from condensed gases is a direct probe of surface reactions induced by electronic excitation of adsorbed molecules and diverse relaxation processes which subsequently occur. It is proposed by several authors that surface and bulk excitons play important roles in PSD of rare gas solids. In this study, we perform time-of-flight measurements of desorbed metastable atoms from a Ne and Ar mixture to estimate their kinetic energies. Using monochromatized synchrotron radiation allows us to discuss the detailed mechanism of excitation and decay of excitons.

### VI-J-1 Desorption of Metastable Atoms from the Surface of a Ne and Ar Solid Alloy

**Daniel E. WEIBEL*, Toshiki NAGAI*, Ichiro ARAKAWA*, Minoru KANNO, Koichiro MITSUKE, and Makoto SAKURAI**** *(*Gakushuin Univ., **Kobe Univ.)*

Photon-stimulated desorption of metastable atoms, Ne* and Ar*, from the surface of a Ne and Ar solid alloy is studied using monochromatized synchrotron radiation at the beam line BL5B of UVSOR. The sample is prepared by deposition of the gas mixture on a Cu(100) substrate at T ~ 6 K and the thickness of the alloy is about 100 atomic layers. The experiments are performed in an ultrahigh vacuum chamber with a base pressure of $\sim 4\times10^{-8}$ Pa. Desorbed metastable atoms are detected by a secondary electron multiplier situated at a distance of 120 mm from the sample. Their kinetic energy distribution is measured by a TOF technique.

The inset of Figure 1 shows a TOF spectrum of desorbed particles from the sample. The two peaks at 0.095 and 0.25 ms are assigned respectively to Ne* and Ar* desorbed by the cavity-ejection mechanism in which an excited atom is ejected by repulsion between a self-trapped exciton and surrounding atoms. Figure 1 shows the dependences of the Ar* yield on the photon energy in the wavelength range of 50—110 nm for pure Ar and the alloy (12% of Ne). It is clearly observed that the presence of Ne leads to significant increase in the Ar* yield in the range of 50—75 nm. This enhancement at higher photon energy strongly suggests that the excitonic excitations of Ne contribute to the formation of Ar* through energy transfer between heteroatoms.

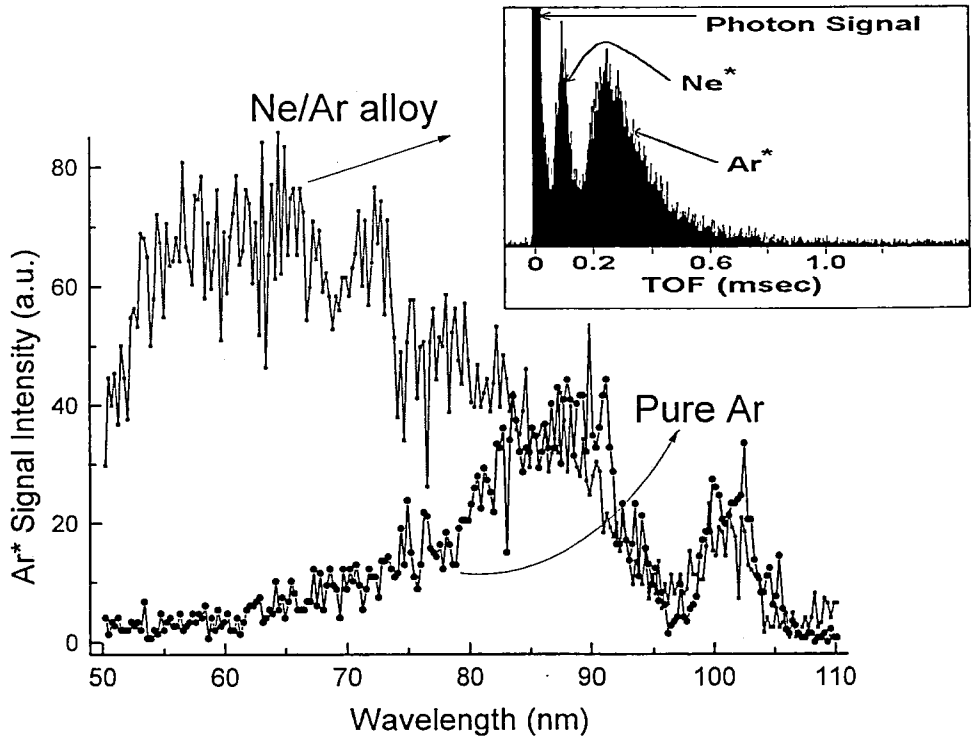


**Figure 1.** Dependences of the yield of desorbed Ar* on the photon energy measured for the samples of pure Ar and an alloy (Ne:Ar = 12:88). The inset shows a time-of-flight spectrum of desorbed particles from the alloy sample.

## VI—K Preparation and Characterization of Semiconductor Thin Films by New Excitation Processes

Crystalline and amorphous semiconductor thin films of high quality, especially prepared at low temperatures, are essential for the development of VLSI (Very Large-Scale Integration) and new functional devices in the near future. Synchrotron radiation-assisted, plasma-enhanced, and photo-excited CVD (Chemical Vapor Deposition) are believed to be powerful and fine fabrication processes are required. We have been developing new semiconducting thin films and new devices by these excitation methods.

### VI-K-1 Structural Properties of $CuIn_xGa_{1-x}Se_2$ Thin Films Prepared by RF Sputtering

**Toshiyuki YAMAGUCHI** *(Wakayama College of Tech.)*, **Jiro MATSUFUSA** *(Toyohashi Univ. of Tech.)*, **and Akira YOSHIDA** *(Toyohashi Univ. of Tech. and IMS)*

[*J. Appl. Phys.*, **72**, 5657 (1992)]

Cu-In-Ga-Se alloy thin films were prepared by rf sputtering from powder targets previously synthesized in various ratios. From x-ray diffraction analyses, these thin films have chalcopyrite structure of $CuIn_xGa_{1-x}Se_2$, and the lattice

parameters (a and c) are varied linearly with indium content x. The preferred orientation factor f(112) in these thin films was estimated. Its value was always more than 0.79, specifically 0.96 in a $CuInSe_2$ thin films. From scanning electron microscope images, the grain sizes in these thin films decrease with the decrease of indium content. From x-ray photoelectron spectroscopy analyses, the binding energies of Se, In, Cu and Ga in these thin films shift to higher energies with decreasing indium content, where a slight bowing behavior is observed.

### IV-K-2 Optical Properties in RF Sputtered $CuIn_xGa_{1-x}Se_2$ Thin Films

**Toshiyuki YAMAGUCHI** *(Wakayama College of Tech.)*, **Jiro MATSUFUSA** *(Toyohashi Univ. of Tech.)*, **and Akira YOSHIDA** *(Toyohashi Univ. of Tech. and IMS)*

[*Appl. Surf. Sci.*, **70/71**, 669 (1993)]

The optical absorption coefficients of $CuIn_xGa_{1-x}Se_2$ thin films produced over the entire range of $0 \leq x \leq 1$ by RF sputtering were evaluated in the temperature range between 4 and 300 K. In the optical absorption spectra at 300 K, three kinds of energy gaps, which are attributed to the fundamental edge and band splitting by crystal-field and spin-orbit splitting, are observed. The expression of the primary transition energies are obtained and definite bowing behavior is observed. The spin-orbit and crystal-field parameters are estimated. The temperature dependence of the primary transition energies can be reproduced by Varshni's expression.

### VI-K-3 Optical Constants of Indium Nitride

**QiXin GUO, Osamu KATO** *(Toyohashi Univ. of Tech.)*, **Masami FUJISAWA** *(Tokyo Univ.)*, **and Akira YOSHIDA** *(Toyohashi Univ. of Tech. and IMS)*

[*Solid State Commun.*, **83**, 721 (1992)]

Indium nitride epitaxial layers were grown by microwave-excited metalorganic vapor phase epitaxy. The reflectance spectra of single crystalline InN were obtained in the range from 2 to 20 eV using synchrotron radiation for the first time. The optical constants have been determined from the Kramers-Kronig analysis of the reflectance spectra with extrapolation beyond the experimental range.

### VI-K-4 Thermal Stability of Indium Nitride Single Crystal Films

**QiXin GUO, Osamu KATO** *(Toyohashi Univ. of Tech.)*, **and Akira YOSHIDA** *(Toyohashi Univ. of Tech. and IMS)*

[*J. Appl. Phys.*, **73**, 7969 (1993)]

We examine the thermal stability of InN single crystal films. The films are not entirely stable and degrade at relatively low temperatures. No change on the surface of the film is found after heating the samples up to 500°C in nitrogen atmosphere. However, if the films are heated above 550°C, the surface undergoes a considerable change, owing to the decomposition and desorption of nitrogen.

## VI—L Photochemistry of Organometallic Complexes Adsorbed on Solid Surfaces

Photochemistry of organometallic complexes adsorbed on solid surfaces has received increasing attention in recent years. The driving force behind this stems from its potential use in catalysis and microelectronics. Interest in the surface photochemistry also arises from the fact that its products are often quite different from those observed in gas phase or in liquid solution. We have studied the surface-chemistry and the surface-photochemistry of metal carbonyls over solid surfaces to investigate catalytic effects of the surface on a photochemical secondary process using infrared, X-ray photoelectron, and Auger electron spectroscopy. Geometry of adsorbed species is discussed in terms of a surface selection rule of infrared reflection absorption spectroscopy. As a result the geometry of reaction intermediate is found to depend on the nature of surface.

### VI-L-1 IRAS, XPS, and TPD Study on the Adsorption and Decomposition of $Fe(CO)_5$ on Silver Surface

**Shinri SATO, Yuji UKISU, Hisashi OGAWA*, and Yoshio TAKASU*** *(*Shinshu Univ.)*

[*J. Chem. Soc. Faraday Trans.*, in press]

The adsorption and decomposition of $Fe(CO)_5$ on silver surfaces has been studied by infrared reflection absorption spectroscopy (IRAS), X-ray photoelectron spectroscopy (XPS), and temperature-programmed desorption (TPD) technique. TPD spectra showed that $Fe(CO)_5$ physisorbs at temperatures below 120 K on uncleaned silver surface while chemisorbed species is formed on the surface cleaned by Ar ion sputtering. The active sites for chemisorption may be defect sites produced by the sputtering. At lower coverage of adsorbed $Fe(CO)_5$ than monolayer, IRAS and XPS revealed that the chemisorbed species undergoes decarbonylation upon rising temperature to 182 K and converts into $Fe(CO)_4$ which has a planar structure parallel to the surface. The $Fe(CO)_4$ species undergoes conformation change with further rise in temperature and releases all the carbonyls at temperatures above 350 K. When physisorbed $Fe(CO)_5$ presents on the chemisorbed species, the $Fe(CO)_4$ species reacts weakly with the physisorbed species to form an adduct which decomposes at around 350 K. The intermediate species $Fe(CO)_4$ exhibits a very similar behavior to $Fe(CO)_4$ species produced by the photolysis of $Fe(CO)_5$.

### VI-L-2 Geometry of Surface Intermediates formed during Thermal and Photolytic Decomposition of Iron Pentacarbonyl over Silver Surfaces

**Shinri SATO, Yuji UKISU, Hisashi OGAWA*, and Yoshio TAKASU*** (**Shinshu Univ.*)

[*Langmuir*, submitted]

Geometry of surface intermediates formed during the thermal and photolytic decarbonylation of iron pentacarbonyl ($Fe(CO)_5$) adsorbed on Ag surfaces was studied using infrared reflection absorption spectroscopy (IRAS). While physisorption of $Fe(CO)_5$ occurs on uncleaned Ag surfaces, chemisorption takes place partly on a Ag surface cleaned by Ar ion sputtering. Chemisorbed $Fe(CO)_5$ exhibits an intense C-O stretching band at 2062 $cm^{-1}$ with a weak band at 2116 $cm^{-1}$, and physisorbed $Fe(CO)_5$ an intense 2058 $cm^{-1}$ band alone. Chemisorbed $Fe(CO)_5$ undergoes thermal decarbonylation at ca. 180 K to form intermediate, $Fe(CO)_4$, which is decomposed completely at $>300$ K depositing Fe metal on the surface. Upon heating Ag substrate, the intermediate first exhibits a broad band centered at 2040 $cm^{-1}$, which disappears at 250 K. A new band at 2050 $cm^{-1}$ develops at 210 K, grows up with decrease of the 2040 $cm^{-1}$ band, and disappears at 330 K. Adsorbed $Fe(CO)_5$ undergoes photolytic decarbonylation to produce subcarbonyl intermediate with CO/Fe=ca.4. The intermediate produced from physisorbed $Fe(CO)_5$ shows no C-O stretching band, while the one from isolated chemisorbed $Fe(CO)_5$ displays two bands at 2062 and 2038 $cm^{-1}$, which merge together at 2060 $cm^{-1}$ with increasing coverage. These IRAS results were discussed in terms of a surface selection rule of IRAS, and possible geometries of surface intermediates are proposed.

### VI-L-3 Photochemistry of $Fe(CO)_5$ Adsorbed on Silver Surfaces

**Shinri SATO, Yuji UKISU, Hisashi OGAWA*, and Yoshio TAKASU*** (**Shinshu Univ.*)

Photolysis of $Fe(CO)_5$ adsorbed on silver surfaces has been studied by infrared reflection absorption spectroscopy (IRAS), X-ray photoelectron spectroscopy (XPS), and temperature-programmed desorption (TPD) technique. $Fe(CO)_5$ adsorbed on a silver surface undergoes photodecarbonylation to release CO under irradiation of the light of wavelengths shorter than 390 nm. The yield of CO photo-evolution increases with increasing adsorption amount up to more than 20 monolayers, indicating fast energy relaxation of photoexcited molecules near the surface. The maximum quantum yield of photo-decarbonylation is estimated less than 1%. The CO/Fe ratio in the subcarbonyl species produced by photolysis is ca.4 at the monolayer coverage and decreases with increase in adsorption amount. The ratio drops to less than 3 at the three monolayer coverages. IRAS spectra after photolysis are broad and shift to higher frequencies with increase in the coverage of $Fe(CO)_5$. When the coverage is less than monolayer, a band assignable to $Fe(CO)_4$ develops and disappears with increase in the coverage, suggesting $Fe(CO)_4$ reacts with each other to form oligomers in overlayers.

## VI—M Studies on Catalysis for Automobile Exhaust and Energy Resources

The measures against global air pollution and the development of new energy resources instead of fossil fuel are current problems. Catalysts play important roles in the cleaning of exhaust gases from industrial factories and gasoline engines. We are now aiming the catalytic reduction of $NO_x$ from diesel engines, and have recently found a new catalytic system hopeful for this purpose. A mechanistic study on the $NO_x$ reduction is under progress in our laboratory. We have also studied a photocatalyst which converts light energy to chemical energy from the viewpoint of solar-to-chemical energy conversion.

### VI-M-1 Possible Role of Isocyanate Species in $NO_x$ Reduction by Hydrocarbons over Copper-Containing Catalysts

**Yuji UKISU, Shinri SATO, Akira ABE*, and Kiyohide YOSHIDA*** (**Riken Co. Ltd.*)

[*Appl. Catal.*, **2**, 147 (1993)]

The behavior of an isocyanate intermediate (-NCO) formed during $NO_x$ reduction has been studied on alumina-supported Cu-Cs oxide catalyst in the presence of oxygen and hydrocarbons (propene, acetylene, propane, and n-heptane) using infrared spectroscopy. While a reaction involving NO, $O_2$, and acetylene needs some heat treatment to produce the isocyanate species on the catalyst, no heat treatment is required in a NO/$O_2$/propylene or n-heptane system. No isocyanate intermediate is formed in a NO/$O_2$/propane system by an ordinary procedure. Adsorbed water on the catalyst surface is found to suppress the formation of the isocyanate species. This inhibition effect is smaller in the acetylene or n-heptane containing system than in the propylene containing system. The role of isocyanate species is discussed with reference to the results of the practical reduction of $NO_x$.

### VI-M-2 IR Study on the Catalytic Reduction of $NO_x$ in the Presence of Oxygen and Ethanol

**Akira ABE*, Kiyohide YOSHIDA*, and Shinri SATO** (**Riken Co. Ltd.*)

Alumina-supported Ag catalysts are found to show high activity for the reduction of $NO_x$ in the presence of oxygen and alcohol. The behavior of adsorbed species formed during the reaction is studied by IR spectroscopy. When the catalyst is exposed to ethanol, ethoxide bands are observed, which grow up upon addition of oxygen. The surface ethoxide reacts with NO to form $NO_3$ and a complex similar to that observed in the NO reduction process with propene. When the sample is heated to temperatures above 100°C, a

new band appears at around 2080 $cm^{-1}$, which is assignable to a reaction intermediate involving CN. This intermediate is different from the intermediate produced during the $NO_x$ reduction with hydrocarbons.

### VI-M-3 Photochemical Diodes of a $TiO_2$ Film Prepared by a Sol-Gel Method

**Shinri SATO, Hisato KOSHIBA*, Hitoshi MINAKAMI*, Noriyoshi KAKUTA*, and Akifumi UENO**,** *(*Toyohashi Univ. of Tech., **Shizuoka Univ.)*

Photochemical diodes were prepared using a thin film of $TiO_2$ made from titanium isopropoxide by a sol-gel method. A half part of a conductive $SnO_2$ film plated on a quartz plate was coated with the $TiO_2$ film by a spin-coating method, and another part of the $SnO_2$ substrate was coated with a thin Pt film by vacuum evaporation. The photochemical diode thus prepared shows photocatalytic activity for hydrogen evolution from aqueous ethanol solutions containing NaOH or $HClO_4$. No other products are detected in the gas phase. Hydrogen evolution from the Pt part is definitely observed, indicating electron transfer from the $TiO_2$ film to the Pt film. Hydrogen is also evolved from the $TiO_2$ film, suggestive of the photo-dehydrogenation of intermediate species. Another type of photochemical diode, the $TiO_2$ film coated on a Pt plate, is found to show higher activity than the $TiO_2/SnO_2/Pt$ device for the hydrogen photo-evolution without any support electrolyte. Hydrogen evolution on this device, however, occurs on the $TiO_2$ side but not on the Pt side. These results are discussed in terms of a photoelectrochemical mechanism at semiconductor surfaces.

## VI—N Electronic Structure Design of Wide Gap Conductors and Control of Their Conduction Behavior

Wide gap conductors are interesting materials from scientific viewpoint: the conductivity of the material reaches $1\times10^4$ $S\cdot cm^{-1}$ irrespective of their wide band gap ($\gtrsim$3.1 eV). These are also technologically important as transparent electrodes, gas sensors and semiconductor-catalysts. In the present study it is aimed to give a firm basis of the materials design of wide gap conductors. The ongoing study includes proposition of a working hypothesis for searching new materials, preparation of materials, estimation of physical properties, characterization of electronic structures by spectroscopic methods using synchrotron radiation and energy band calculations.

### VI-N-1 New UV-Transparent Electroconductive Oxide, $ZnGa_2O_4$ Spinel

**Takahisa OMATA*, Naoyuki UEDA*, Kazushige UEDA*** *(*Tokyo Inst. Tech.),* **and Hiroshi KAWAZOE**

$ZnGa_2O_4$ with spinel structure was prepared, and optical and electrical properties of the material were measured. By the measurements of diffuse reflectance spectra, $ZnGa_2O_4$ was found to have wider band gap (−5eV) than ITO (Indium Tin Oxide). Electrical conductivity of the $H_2$ annealed ceramic of $ZnGa_2O_4$ was $3\times10^1$ $S\cdot cm^{-1}$. Thus $ZnGa_2O_4$ spinel was found to be a new UV-transparent electronic conductor.

### VI-N-2 Preparation of $MgIn_2O_{4-X}$ Thin Films on Glass Substrate by RF-Sputtering

**Hiroshi UN'NO*, Naoko HIKUMA*, Takahisa OMATA*, Naoyuki UEDA*** *(*Tokyo Inst. Tech.),* **Takuya HASHIMOTO, and Hiroshi KAWAZOE**

$MgIn_2O_{4-X}$ thin films were deposited on to a silica glass plate by RF-sputtering method. The highest conductivity observed for the film post-annealed under $H_2$ flow was $2.3\times10^2$ S/cm, with a carrier concentration of $6.3\times10^{20}$ $cm^{-3}$ and a mobility of 2.2 $cm^2.V^{-1}\cdot s^{-1}$. No distinct optical absorption band was observed in the visible region.

### VI-N-3 New Oxide Phase $Cd_{1-X}Y_XSb_2O_6$ with a Wide Band Gap and High Electrical Conductivity

**Kazuhiko YANAGAWA*, Yoshimichi OHKI*** *(*Waseda Univ.),* **Naoyuki UEDA**, Takahisa OMATA**,** *(**Tokyo Inst. Tech.),* **Takuya HASHIMOTO, and Hiroshi KAWAZOE**

It was found that $Cd_{1-X}Y_XSb_2O_6$ (X=0−0.05) is a promising material as a transparent conductor. By measurements of diffuse reflectance spectra, the optical band gap of $CdSb_2O_6$ was found to be wide enough as a transparent conductor. Electrial conductivity of the Y-doped $CdSb_2O_6$ ceramic was found to be at least larger than $1S\cdot cm^{-1}$, while that of the non-doped $CdSb_2O_6$ was under $10^{-5}$ $S\cdot cm^{-1}$ at room temperature.

## VI—O Effects of Oxygen Nonstoichiometry on Crystal Structure and Conduction Behavior of BPBO

It was well establishied that substitution of Bi in $BaBiO_3$ with Pb in the range $0.6\lesssim x\lesssim 0.9$, where x is the substitution ratio in $BaBi_{1-x}Pb_xO_3$, results in superconductivity below 13 K. However, concentration of oxygen has been assumed to be 3 in the current studies. We have found that crystal structure, electronic structure and conductive properties are highly dependent on the oxygen nonstoichiometry.

### VI-O-1 Effect of Substitution of Bi with Pb in $BaBi_{1-x}Pb_xO_3$ on Crystal Structure, Chemical State of Bi and Conduction Behavior

**Takuya HASHIMOTO, Hiroshi KAWAZOE, and Harunari SHIMAMURA*** *(*Tokyo Inst. Tech.)*

Crystal structure and electrical conduction mechanism of $BaBi_{1-x}Pb_xO_3$ and $Ba_{1-x}K_xBiO_3$ were discussed from the viewpoint of chemical description of these materials. Crystal structure of $BaBi_{1-x}Pb_xO_3$ was investigated by X-ray diffraction, which showed monoclinic symmetry containing two Bi sites in the range of $0.0<X<0.5$, and orthorhombic indluding one Bi site in $0.5<X<1.0$. This suggests Bi exhibits the disproportion to two different chemical state, +3 and +5, supplying no electron carrier in $0.0<x<0.5$ and that Bi takes one state, +4, supplying electron carrier in $0.5<x<1.0$ Optical reflection and X-ray absorption showed good agreement with above mentioned Bi chemical state. Electron carrier in $Ba_{0.6}K_{0.4}BiO_3$ could also be explained from the consideration of relation between crystal structure and chemical state of Bi. Crystal structute varies from monoclinic symmtry to cubic one as concentration of K increases. Simultaneously, chemical state of Bi changes from coexistence of $Bi^{3+}$ and $Bi^{5+}$ to $Bi^{4+}$ which serves electron carriers.

Keywords: $BaBi_{1-x}Pb_xO_3$, $Ba_{1-x}K_xBiO_3$, crystal structure, XAFS, chemical state of Bi

### VI-O-2 Effect of Oxygen-deficiency on the Structure and Conduction Behavior of $BaPb_{0.75}Bi_{0.25}O_{3-\delta}$

**Takuya HASHIMOTO and Hiroshi KAWAZOE**

Oxygen-deficiency ($\delta$) and its effect on the structure and electrical preperties of $BaPb_{0.75}Bi_{0.25}O_{3-\delta}$ were studied. $\delta$ could be controlled from 0.00 to 0.15. It was observed that the crystal symmetry varied with increasing $\delta$ from orthorhombic ($\delta = 0.00 \pm 0.005$) through tetragonal ($\delta = 0.09 \pm 0.005$, $0.11 \pm 0.005$) and to cubic ($\delta = 15 \pm 0.005$). Electrical resistivity increased by increasing $\delta$. The superconducting transition was observed at 13 K and 10 K in the specimens of $\delta = 0.00 \pm 0.005$ and $0.15 \pm 0.005$, superconductivity was not observed.

### VI-O-3 Oxygen Nonstoichiometry of $BaBi_{0.25}Pb_{0.75}O_{3-\delta}$ and Its Effect on the Conduction Behavior and Crystal Structure

**Takuya HASHIMOTO, Hiroshi KAWAZOE, Toshikazu YOSHIDA*, Junichiro MIZUSAKI*, and Hiroaki TAGAWA*** *(*Yokohama National Univ.)*

Dependence of oxygen deficiency, $\delta$, of $BaBi_{0.25}Pb_{0.75}O_{3-\delta}$ on temperature, T, and oxygen partial pressure, $Po_2$, was measured by thermogravimetry. Based on the determined $\delta$-T-$Po_2$ relationships, the samples with various oxygen deficiency were prepared. Variations of electric conduction behavior and crystal structure with $\delta$ were investigated by resistivity measurements and X-ray diffraction. As $\delta$ increases, resistivity increased and critical temperature of superconductivity, Tc, became low. For $\delta \geq 0.08$, Tc disappeared from the temperature range above 4K. Powder X-ray diffraction analysis revealed that crystal symmetry changed from orthorhombic with different lattice constants through tetragonal to pseudo-cubic with increase of $\delta$. Some possible discussions on the elimination of superconductivity by increase of $\delta$ are presented.

## VI—P Growth and Characterization of II-VI Compound Semiconductor Thin Film Using Metalorganic Sources

Epitaxial growth at low temperature is essential to control the electrical and optical properties of the layer in the fields of II-VI materials. We believe that metalorganic vapor phase epitaxy (MOVPE) and photo-assisted MOVPE using visible light or synchrotron radiation (SR) light are useful in this field. We have investigated the low temperature growth of the II-VI semiconductors by these methods.

### VI-P-1 ZnTe Growth by Photo-assisted Metalorganic Vapor Phase Epitaxy at Atmospheric Pressure

**Makoto IKEJIRI*, Hitoshi NAKAYAMA*, Mitsuhiro NISHIO, Hiroshi OGAWA*, and Akira YOSHIDA****
*(*Saga University, **IMS)*

[*Appl. Surf. Sci.*, **70/71**, 755 (1993)]

ZnTe is promising for application as a purely green LED. To obtain the information for the understanding of the growth process of ZnTe under illumination, the effect of illumination wavelength, carrier gas and alkylzinc source upon the growth rate of ZnTe layer have been investigated by $Ar^+$ ion laser or xenon lamp-assisted MOVPE. The growth rate is greatly enhanced when light is used with photon energies higher than the band gap of ZnTe. The increase in growth rate is smaller for He than for $H_2$. The combination of dimethylzinc and diethyltelluride is more effective for the growth rate enhancement than that of diethylzinc and diethyltelluride. We have concluded that the growth rate enhancement is due to the photocatalysic effect.

### VI-P-2 Growth of Low Resistivity n-type ZnTe by Metalorganic Vapor Phase Epitaxy

**Mitsuhiro NISHIO, Hiroshi OGAWA*, Hitoshi NAKAYAMA*, Gheyas Syed IRFAN*, and Akira YOSHIDA**** *(*Saga University, **IMS)*

ZnTe usually shows only p-type conductivity. Many studies on the fabrication of n-type ZnTe by doping ZnTe with donor type dopant have been published. However, n-type ZnTe with low resistivity, which is important for fabricating highly efficiently LED, could not be achieved. Al-doped ZnTe layers have been grown using triethylalumi-

nium as a dopant source. N-type ZnTe layer with carrier concentration of $(1-4)\times10^{17}$ $cm^{-3}$ and resistivity as low as 0.1—0.3 Ωcm has been obtained when triethylaluminium flow rate is kept between 15—20 nmol/min and substrate temperature at 380°C. The Al-doped ZnTe layer is characterized by the donor-acceptor pair emission together with the small emission from the exicitons bound to neutral donors, implying that Al is incorporated and acts as a shallow donor quite effectively in the epitaxial layer. It has also been shown by the electrical properties of a p-n diode that triethylaluminium dopant is useful for n-type doping of ZnTe.

### VI-P-3 Epitaxial Growth of ZnTe by Synchrotron Radiation

**Mitsuhiro NISHIO, Hiroshi OGAWA*, Makoto IKEJIRI*, Toshihiro OGATA*, and Akira YOSHIDA****
*(*Saga University, **IMS)*

Since SR has a high photon flux density in the vacuum ultraviolet region, any metalorganic sources can be decomposed efficiently by SR light source. Very recently, several investigations on the prepartion of thin film by the irradiation of SR have been published using metalorganic sources. We have investigated the SR-assisted growth of ZnTe at room temperature. Irradiation of SR to the adsorbed surface of diethylzinc and diethyltelluride molecules has been employed for growth. The formation of ZnTe epitaxial layer on (100) GaAs substrate has been experimentally demonstrated. It has been shown by XPS measurement that no carbon is included in the film.

### VI-P-4 Construction of Vacuum Metalorganic Chemical Vapor Deposition System for Growth of II-VI Compound Semiconductors

**Mitsuhiro NISHIO, Toshihiro OGATA*, Makoto IKEJIRI*, and Gheyas Syed IRFAN*** *(*Saga University)*

Low temperature growth is one of the key factors for growing II-VI compound semiconductors of high quality. We have demonstrated that SR provides a powerful light source for a novel low-temperature growth technique of ZnTe. In order to investigate the growth of II-VI compounds in the beam line BL-4A, we are now constructing the growth system. The apparatus has been designed to introduce SR into the growth chamber via a prepared differential pumping system.

# RESEARCH ACTIVITIES VII
# Coordination Chemistry Laboratories

Prof.H. Ohtaki retired from the position of the Director in March, 1993 and moved to Ritsumeikan University as Prof. of Graduate school. We sincerely thank his effort and the progress made during his period here. His contribution to the Coordination Chemistry Laboratories (CCL) is immense and highly acknowledged. Prof. Akira Nakamura (Osaka University) took the position of the Director and the laboratory of Complex Catalysis from April, 1993. Prof. Yutaka Fukuda, and Prof. Kiyoshi Sawada and Dr. Hikaru Ichida, and Dr. Keiichi Sato continued their positions at the laboratory of Synthetic Coordination Chemistry. Dr. Thomas Daniel took the position of assistant in the laboratory of Complex Catalysis from June, 1993. Prof. Hisanobu Ogoshi and Assoc. Prof. Kawaizumi continued as Adjunct Prof, of the laboratory of Complex Catalysis. Prof. Kazuko Matsumoto (Waseda University) and Assoc. Prof. M. Nagasawa (Saitama University) newly appointed as the Adjunct Prof. of the laboratory of Coordination Bond. Prof. Tasuku Ito and Assoc. Prof. Masatatsu Suzuki finished their term as Adjunct Prof. and returned to Tohoku and Kanazawa Universities, respectively. Their effort during their term is gratefully acknowledged.

## VII—A Syntheses, Structures and Functions of Chromotropic Complexes

### VII-A-1 Synthesis of Spin-crossover Complexes of Fe(II) and Fe(III), and Their Chromotropic Phenomena in Solution

**Junko YUZURIHARA*, Kayoko KASAI*, Yuichi MASUDA*, Masaaki HAGA**, Hikaru ICHIDA, Keiichi SATO, and Yutaka FUKUDA** *(*Ochanomizu Univ., **Mie Univ.)*

We have synthesized some Fe(II) complexes with 1,1,1-tris (2-aminomethylpyridylmethyl) propane (AMPMP) and its oxidized form (tris(diimine)-type(AMPMP-6H) chelating reagent). The complex with the former ligand shows typical spin-crossover transition in solution and the latter one is not a spin-crossover but a low- spin complex at room temperature. We have studied thermodynamic properties of these complexes in solution and their solvent dependent spin-transition phenomena by means of NMR and electronic spectral measurements and compared these results with the data of simple bidentate aminomethylpyridine (AMP)-Fe(II) complex reported before. Now we try to get good crystals for X-ray structural analyses. We also continue to study these types of spin-crossover phenomena with Fe(III) complexes with different kinds of polydentate Schiff-base ligands obtained from polyamine and salicylaldehyde (and its derivatives). In some cases, we could get dinuclear complexes containing the polydentate Schiff-base and a bridging ligand such as a bis(diimine)-type ligand, which also show spin-crossover phenomena.

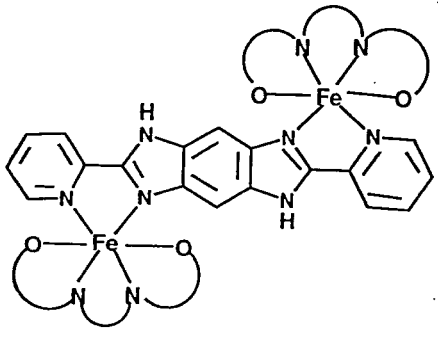


### VII-A-2 Studies on Mixed Ligand Complexes. Mono- and Binuclear Nickel(II) and Copper(II) Complexes with N,N,N′, N″, N‴, —N‴-Hexamethyltriethylenetetramine(hmtt) and β-Diketonates (dike)

**Noriko SHINTANI*, Junko KOTAKI*, Kozo SONE*, and Yutaka FUKUDA** *(*Ochanomizu Univ.)*

[*Bull. Chem. Soc. Jpn.*, **66**, 784 (1993).]

Nine mixed chelates of Ni(II) and Cu(II) with hmtt and dike ligands were prepared and characterized. Except for [Ni(dipm)(hmtt)] $ClO_4$ (where dipm=dipivaloylmethanate), all of them to be dinuclear chelates: (i) $[M_2(dike)_4(hmtt)]$ (where M-Ni, dike-dipm, acac (=acetylacetonate), tfac, hfac (tri- or hexafluoroacetylacetonates); M=Cu, dike= hfac), (ii) $[Ni_2(NO_3)_2dike)_2$-hmtt)](where dike=dipm or acac), and (iii) $[Cu_2(acac)_2(hmtt)]$-$(ClO_4)_2$. Although they are similar to their mononuclear analogues containing N,N,N′,N′-tetramethylethylenediamine (tmen), a number of characteristic differences exist. Though the Ni(II) chelates are only slightly solvatochromic, the Cu(II) chelates are strongly so.

### VII-A-3 Studies on Mixed Ligand Complexes. Synthesis and Crystal Structure of the Binuclear Ni(II) Complex, μ-(Oxalato)bis-[(acetylacetonato)(N,N,N′, N′-tetramethylethylenediamine)-nickel(II)]

**Kasumi YAMADA*, Tetsuya KAWAMOTO**, Yoshihiko KUSHI**, Wasuke MORI**, Kei UNOURA***, and Yutaka FUKUDA** *(*Ochanomizu Univ., **Osaka Univ., ***Yamagata Univ.)*

[*Bull. Chem. Soc. Jpn.*, **66**, 2758 (1993)]

A new binuclear nickel(II) complex having the formula $[Ni_2(acac)_2(tmen)_2(ox)]$ (acac=acetylacetonate, tmen=N,N, N′,N′-tetramethylethylenediamine, ox=oxalate) has been characterized, and its crystal structure has been determined at room temperature. This crystal was obtained in its solvated form, $[Ni_2(acac)_2(tmen)_2(ox)] \cdot 2TCE$ (TCE=1,1,2,2-tetrachloroethane); orthorhombic system, space group

Pcab(No.61), with a=20.172(4), b=17.180(5), c=13.132-(3) Å, z=4, R=0.044. The oxalate ligand acts as a bridging tetradentate ligand between two Ni (II) moieties.

### VII-A-4 Glass Transition Phenomenon due to Freezing-in of Conformational Disorder of Ethylenediamine Framework in Crystalline [Ni(acac)(tmen)-$(H_2O)_2$]$ClO_4$

**Tomoko YOSHIDA*, Masaharu OGUNI*, Yukie MORI**, and Yutaka FUKUDA** *(*Tokyo Institute of Technology, **Ochanomizu Univ.)*

[Solid State commun., in press]

Heat capacities of crystalline [Ni(acac)(tmen)$(H_2O)_2$]-$ClO_4$ were measured with an adiabatic calorimeter in the range of 10 to 300 K, where acac and tmen are acetylacetonate and N,N,N′,N′-tetramethylethylenediamine, respectively. A glass transition in this crystal was found at 107.2 K with the accompanied heat capacity jump of 2.6 $JK^{-1}$ $mol^{-1}$, and interpreted as due to the freezing-in of disorder between the two, $\delta$ and $\lambda$, conformations of the ethylenediamine framework of tmen. The energy difference between the two conformations and the activation energy for the conformational change were determined by analyses of the calorimetric data to be 1.26 $kJmol^{-1}$ and 31.0 $kJmol^{-1}$, respectively.

### VII-A-5 $^{95}$Mo-NMR Studies of Dioxomolybdenum(VI) Complexes with Dithiocarbamates. The Correlation between the Chemical Shifts and the Coordination Abilities of Various Kinds of Dithiocarbamate Derivatives.

**Kei UNOURA*, Akira NAGASAWA**, Riko KIKUCHI*, and Yutaka FUKUDA** *(*Yamagata Univ., **Saitama Univ.)*

$^{95}$Mo-NMR study on cis-dioxomolybdenum(VI) complexes with various dithiocarbamates, $[MoO_2(R_2dtc)_2]$ (where $R_2dtc^-$: dithio-carbamate, R=$CH_3$(=Me), $C_2H_5$-(=Et), iso-$C_3H_4$(i-Pr), iso- $C_4H_9$(=i-Bu), $C_6H_5$(=Ph), $C_6H_5CH_2$(=Bzyl)), has been done. The chemical shift of the $^{95}$Mo nucleus showed rather wide range between $\delta$=151 (R=Me) and 216 (R=i-Pr) depending on the substituent groups in the dithiocarbamates. The significant correlation was found between the chemical shifts and the rate constants ($k_1$) of oxygen transfer reaction as follows:

$$[MoO_2(R_2dtc)_2] + P(Ph)_3 \xrightarrow{k_1} MoO(R_2dtc)_2] + OP(Ph)_3$$

### VII-A-6 4-, 5- and 6-Coordinate Complexes of Ni(II) and Cu(II) Containing Tetraacetylethanate and Various Kinds of Poly-amines

**Akiko SEINO*, Hide KAMBAYASHI*, Yuichi MASEDA*, Hiroko NAKAGAWA**, Hiroshi MIYAMAE**, Keiichi SATO, and Yutaka FUKUDA** *(*Ochanomizu Univ., **Josai Univ.)*

We have synthesized dinuclear complexes of Ni(II) and Cu(II) containing tetraacetylethanate(taet)(and its derivatives) and various kinds of polyamines(plam) such as N,N,N′,N′-tetramethylethylenediamine(tmen), N,N,N′, N″,N″-pentamethyldiethylenetriamine(pmdt), general formula $M_2(taet)(plam)_2X_2$ where X=$B(Ph)_4^-$, $ClO_4^-$, $NO_3^-$, halide, pseudohalide. The obtained dinuclear complexes show various structural forms in the dinuclear unit such as 4-coordinate(square planar=Sp)-4coordinate(Sp), 5-coordinate(square pyradidal=$C_{4v}$)-5-coordinate($C_{4v}$), 6-coordinate-(octahedral=Oh)-6-coordinate(Oh), 4-coordinate-(Sp)-6-coordinate-(Oh), 4-coordinate(Sp)-5coordinate-($C_{4v}$), and 5-coordinate($C_{4v}$)-6-coordinate(Oh). These complexes show characteristic solvatochromism and thermochromism in organic solutions according to not only the donor abilities of the anions used and solvents but also the acceptor properties of the solvents.

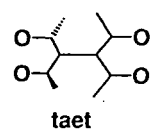


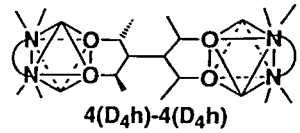


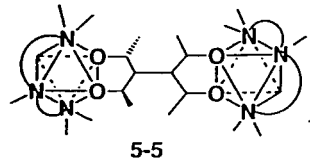


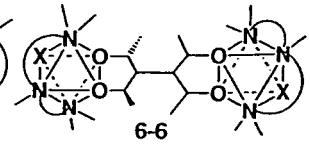


## VII—B Structures and Thermodynamics of Ionic and Molecular Ensembles in Solution

The interactions of ion-ion and ion-molecule in solution have been studied for various kinds of systems of complex formation and solvents. The weak interactions such as ion-pair, intermolecular, and solvation, play an important role to determine the general feature of thermodynamics and structures of complexes in solution. The studies of transfer phenomena between two phases are also important to understand the reactions in homogeneous solution.

### VII-B-1 Formation and Protonation of Aminopolyphosphonate Complexes of Alkaline Earth and Divalent Transition Metal Ions in Aqueous Solution

**Kiyoshi SAWADA, Takashi KANDA*, Yasuo NAGANUMA*, and Toshio SUZUKI*** *(*Niigata Univ.)*

[*J. Chem. Soc., Dalton Tans.* in press]

The complex formation and protonation of *N*-methyliminodi(methylenephosphonic acid) (MIDMP, $H_4L$) and *N,N*-dimethylamino(methylenephosphonic acid)(DMAMP, $H_2L$) complexes with alkaline earth (M=$Mg^{2+}$, $Ca^{2+}$, $Sr^{2+}$, $Ba^{2+}$) and divalent transition metals (M=$Mn^{2+}$, $Fe^{2+}$, $Co^{2+}$, $Ni^{2+}$, $Cu^{2+}$, $Zn^{2+}$, $Cd^{2+}$) have been investigated at 25.0°C and at an ionic strength of 0.1 M ($KNO_3$) by means of

potentiometry and $^{31}P$ NMR spectroscopy. The complex formation constants, $K_{ML}$, for the alkaline earth metals decrease with increase in the ion size. The order of $K_{ML}$ for the transition metal complexes agree with Irving-Williams series for each ligand. The first protonation constants, $K_{MHL}$, of the alkaline earth-MIDMP and transition metal-DMAMP complexes are quite large compared with the first protonation constants of the phosphonate group of free ligand (the second protonation constants of ligand $K_{H2L}$), and decrease with the increase in the complex formation constant. The value of $K_{MHL}$ of the transition metal-MIDMP complexes are the same order of magnitude of the value of $K_{H2L}$ of ligand. The second protonation constants $K_{MH2L}$ of all complexes are smaller than $K_{H2L}$ and there is no significant difference among the complexes. The $^{31}P$ NMR spectra of the metal-ligand solutions have been measured at 25°C as a function of pH and the chemical shift of each species was evaluated. The results of the potentiometric and NMR studies suggest that the M-N of the ML complex is weakened by the decrease of the number of methylenephosphonate group of ligand, i.e., the protonation of MIDMP complexes of alkaline earth and some of transition metal-MIDMP and all the DMAMP complexes occurs on the nitrogen atom of the ligand rupturing the M-N bond.

### VII-B-2 Structure and Thermodynamic Properties of Aminopolyphosphonate Complexes of the Alkaline Earth Metal Ions

**Kiyoshi SAWADA, Toshihiko MIYAGAWA*, Tomoko SAKAGUCHI**, and Kunio DOI*** *(*Nagoya Inst. Tech., **Niigata Univ.)*

[*J. Chem. Soc. Dolton Trans.* in press]

The formation equilibria and thermodynamic properties of the alkaline earth metal (M: $Mg^{2+}$, $Ca^{2+}$, $Sr^{2+}$, $Ba^{2+}$) complexes of nitrilotris(methylenephosphonic) acid ($H_6$ntmp) and ethylenediaminetetrakis(methylenephosphonic acid) ($H_8$edtmp) have been studied by means of potentiometry, NMR spectroscopy and calorimetry at 25.0°C and at an ionic strength of 0.1 M $KNO_3$. The complex formation constants and the protonation constants of the complexes were determined from the potentiometric titration data. Thermodynamic parameters of the protonation of ligand, and the formation and protonation of the metal complexes of ntmp and edtmp were evaluated from the calorimetric titration data. The first protonation on nitrogen atom of ntmp is significantly exothermic and it is followed by the endothermic protonation on phosphonate $O^-$. The protonations of edtmp are exothermic up to the third step. The formation of magnesium complexes of ntmp and edtmp is endothermic and entropy driven, whereas that of the $Ca^{2+}$, $Sr^{2+}$, and $Ba^{2+}$ complexes is weakly exothermic. This behavior is analogous to that of aminopolycarboxylate complexes. The results of calorimetric measurements of ntmp complexes support the structure of protonated complexes of alkaline earth metal-ntmp predicted from the stability and NMR data, i.e., the first protonation of the metal complexes occurs on the nitrogen atom of the ligand, rapturing the M-N bond. The thermodynamic behavior of edtmp complexes is considerably complicated. In the analysis of the pH dependence of the $^{31}P$ NMR signals, the chemical shift of each species of ligand and metal complexes was evaluated by using the formation constants potentiometrically obtained. The change in the chemical shift of complexes by the protonation supports the structures of the alkaline earth metal complexes predicted by the thermodynamic parameters.

### VII-B-3 Crystal and Molecular Structures of Pyridine Base Complexes of Cadmium (II) Chloride

**Keiichi SATOH, Toshio SUZUKI* and Kiyoshi SAWADA** *(*Niigata Univ.)*

Crystal and molecular structures of dichlorobis(pyridine)cadmium(II)(**1**), dichlorobis(3-methylpyridine)cadmium(II)(**2**), dichlorobis(4-methylpyridine)cadmium(II)(**3**), and dichloromono(4-methylpyridine)cadmium(II)(**4**) were determined by means of single-crystal X-ray diffraction method. All crystal were monoclinic. Cadmium atoms of **1, 2, and 3** are octahedrally coordinated with four chloride ions in di-$\mu$-chloro polymeric linear chain and two nitrogen atoms of pyridine base in trans configuration. In **4** cadmium atom is coordinated with five chloride ions in which four chloride ions form di-$\mu$-chloro polymeric chain and one belongs another polymeric chain and with one nitrogen atom of 4-methylpyridine. The crystal structures indicate the absence of peculiar interaction between polymeric chains such as hydrogen bond.

### VII-B-4 Determination of Bismuth (III) by Graphite Furnace Atomic Absorption Spectrophotometry Combined with Solvent Extraction by Trioctylmethylammonium Nitrate

**Asako MINAGAWA*, Kiyoshi SAWADA*, and Toshio SUZUKI**** *(*Niigata Pharm. Coll., **Niigata Univ.)*

[*Anal.Chim.Acta*, **278**, 287 (1993)]

A method for determining a trace amount of bismuth(III) in environmental samples by graphite furnace atomic absorption spectrophotometry (GFAAS) after extractive separation with trioctylmethylammonium nitrates (TOMA · $NO_3$) is described. Bismuth(III) was quantitatively extracted and concentrated with 6 %(W/V) TOMA · $NO_3$ in xylene from the mixture of 0.1 M hydrobromic acid - 0.5 M nitric acid solution. The organic phase was then washed by 1.0 M nitric acid to remove other coextracted metal ions, where bismuth (III) remained quantitatively in xylene solution. Bismuth(III) in the organic phase was directly determined by GFAAS. The present method was applied to the standard reference materials. The results obtained agreed well with certified values.

### VII-B-5 Preconcentration of Cadmium by Column Extraction with Trioctylmethylammonium Chloride and Determination by Graphite Furnace Atomic Absorption Spectroscopy

**Kiyoshi SAWADA, Satoshi OHGAKE*, Michiko KOBAYASHI*, and Toshio SUZUKI*** *(*Niigata Univ.)*

[*Bunseki Kagaku*, in press]

The solvent-extraction system of cadmium with trioctylmethylammonium chloride (TOMA · Cl) from a chloride solution was applied to the column-extraction preconcentration of cadmium. After elution from the column, the cadmium ion was determined by atomic absorption spectroscopy. The optimum conditions for column extraction were investigated.

One percent of a TOMA · Cl xylene solution was supported on an inorganic resin, the surface of which was coated by lipophilic silicone. The cadmium ion was collected on the resin supporting the organic phase from sea water, or a 0.5 M NaCl solution acidified by 0.1 M HCl. The cadmium ion was quantitatively collected on one gram of resin from 200 ml of sample solution at a flow rate of 6 ml $min^{-1}$. Most of the diverse ions were separated by this procedure. The loaded cadmium ion was eluted by 1 ml of 0.1 M $HClO_4$. The concentration of cadmium was determined by graphite furnace atomic absorption spectroscopy. A two-hundred-fold concentration of cadmium and separation from diverse ions were achieved much more conveniently compared with batch extraction or by using a chelating resin column. The detection limit of cadmium was obtained as 5 ppt. The method was applied to sea-water samples.

### VII-B-6 Hydration of Poly(oxyethylene) Derivative Complexes of Alkali Metal Ions and Barium Ion in 1,2-Dichloroethane

**Yoichi KIKUCHI*, Mitsuru KUBOTA**, Toshio SUZUKI**, and Kiyoshi SAWADA** (**Iwate Univ., **Niigata Univ.*)

The water molecules were coextracted into 1,2-dichloroethane (1,2-DCE) with the ion pairs of various poly(oxyethylene) derivative (POE compound) complexes of alkali metal ions and barium ion with picrate ion. The mean number of water attached to POE compounds, $X_{H20,S}$, and its complex, $X_{H20,\ comp}$, in water saturated 1,2-DCE was determined by means of aquametry. The value of $X_{H20,S}$ increases with the increase in the number of the oxyethylene unit (EO unit) of the POE compound. The value of $X_{H20,\ comp}$, decreases in the order $Li^+ > Na^+ > K^+ = Rb^+ = Cs^+$ in any POE compound systems, and increases with the increase in the number of EO units of the POE compounds for a given metal ion. The water molecules attached to the complex are interpreted by the hydration of the central metal ion, and the hydrated metal ion is surrounded by the EO chain in the complex. The large number of water molecules are coordinating to the lithium ion complexes and bring about a serious distortion in the structure.

## VII—C Structures of Solvated Metal Ions and Complexes in Solution

### VII-C-1 Structure and Dynamics of Hydrated Ions

**Hitoshi OHTAKI and Tamas RADNAI*** (*IMS and Hungarian Academy of Sciences, Budapest, Hungary*)

[*Chem.Rev.*, **93**, 1157 (1993)]

Structure and dynamic properties of hydrated ions in water, as well as water molecules, have been reviewed. Contents: I Introduction, II Methods for Determination of the Structure of Hydrated Ions, II A Scattering Method, II B Spectroscopic Methods, II C Computer Simulations, III Structural Aspects of Ionic Hydration, III A First Hydration Shell of Ions, III B Second Hydration Shell of Ions, III C Influence of Ion-Pair and Complex Formation on Hydration of Ions, III D Influences of Temperature and Pressure on the Hydtation Structure of Ions, IV Dynamic Aspects of Ionic Hydration, IV A Self-Diffusion Coefficients of Water Molecules and Ions, IV B Rotational Correlation Time of Hydrated Water Molecules, IV C Reorientational Time of Hydrated Water Molecules, IV D Residence Time of Water Molecules in the First Hydration Shell of Ions, IV E Rates of Water Substitution Reactions of Ions, V Concluding Remarks, VI References. 417 References are cited. Total pages are 48.

## VII—D Molecular Dynamics Simulations of Electrolyte Solutions

### VII-D-1 Molecular Dynamics Simulations for Dissolution and Nucleation Processes of Alkali Halide Crystals in Water

**Hitoshi OHTAKI, Masuhiro MIKAMI*, and Yoshio TAGO*** (**Fujitsu Ltd.*)

[*Computer Aided Innovation of New Materials II*, 265 (1993)]

Dissolution and nucleation processes of various alkali halide crystals in water have been investigated by means of molecular dynamics (MD) simulations at 25°C. Anions in the LiCl, NaCl and CsF crystals have dissolved but no dissolution of cations has been observed within 12 to 20 ps. Crystals having cations and anions with similar size, e.g., KCl, NaF and KF, no ions have dissolved within 20 ps. In supersaturated aqueous solutions of NaCl and CsF ionic clusters are formed. Solution X-ray diffraction measurements show that 1:1 ion pairs are formed in almost saturated aqueous solutions of NaCl and KCl. On the other hand, ion clusters larger than 1:1 ion pairs are formed in supersaturated KF and CsF solutions. The results are in good agreement with those obtained by the MD simulations.

# VII—E Structural Studies on Superionic Glasses

## VII-E-1 A Structural Study on AgI-$Ag_2O$-$CrO_3$ Glass

**S. PATNAIK*, M. SESHASAYEE*** *(*Indian Inst. Technol., Madras, India)*, **Toshio YAMAGICHI**** *(**Fukuoka Univ.)*, **Masaharu NOMURA***** *(***Natl. Lab. High Energy Phys.)*, **and Hitoshi OHTAKI**

[*J. Phys. Soc. Jpn.*, **62**, 536 (1993)]

A structural investigation for a 50AgI-20$Ag_2O$- 30$CrO_3$ (in mole %) glass has been carried out by using X-ray diffraction (XRD) and the extended X-ray absorption fine structure (EXAFS) techniques. The analysis of the EXAFS spectrum of the glass at the Ag K-edge reveals that the distance between a silver (I) and an iodide ions, $r_{Ag\text{-}I}$, and the average number of iodide ions around an $Ag^+$, $n_{Ag\text{-}I}$, are 2.874(4) Å and 1.6(1), respectively. Two Ag-O distances separated by only 0.38 Å ($\Delta r_{Ag\text{-}I}$) are deconvoluted from the total Ag-O peak in the spectrum. The results by the X-ray diffraction measurement coincide with those by the EXAFS study within experimental uncertainties: $r_{Ag\text{-}I}$=2.860(1) Å, $n_{Ag\text{-}I}$=1.34(1), and $\Delta r_{Ag\text{-}I}$=0.35 Å. The intramolecular structural parameters of $CrO_3$ are determined to be $r_{Cr\text{-}O}$=1.718 Å, and $n_{Cr\text{-}O}$=5.58. Short range ordering of atoms is discussed on the basis of the radial distribution function (RDF).

## VII-E-2 An X-ray RDF Study of the Glass 30AgI-45$Ag_2O$-25$V_2O_5$

**S. PATNAIK*, A. RAJALAKSHMI*, M. SESHASAYEE*** *(*Indian Inst. Technol., Madras, India)*, **Hitoshi OHTAKI**

[*Solid State Ionics*, in press]

X-Ray radial distribution function of the glass with the composition 30AgI-45$Ag_2O$-25$V_2O_5$ (mole % units) has been investigated and compared with that of 50AgI-30$Ag_2O$-20$V_2O_5$ previously investigated in order to analyze the effect of compositional change of the basic glass network. Results indicate that the coordination number of the V-O interactions remains at 5 and that the glass network is more closely packed in the present case, the V-O distance being 172 pm. The results also show the shift of the strong Ag-O interaction around 190 pm to 217 pm. AgI is dispersed in the glassy matrix.

# VII—F Complexes of Biochemical Significance

## VII-F-1 Cis-dioxo(benzenedithiolato)tungsten and the Related Monooxotungsten(V) and -(IV) Complexes. Models of Tungsten Oxidoreductases

**Norikazu UEYAMA*, Hiroyuki OKU*, and Akira NAKAMURA** *(*Osaka University)*

[*J.Am.Chem.Soc.*, **114**, 7310 (1992)]

Chemically important catalytic species responsible for the enzymatic redox reactions of tungsten enzymes found in deep sea are indicated to contain a dithiolene ligand coordinated to tungsten (VI). The title compounds are thus prepared and their structure determined for the first time as models of the tungsten spieces which carry out O-atom transfer reactions.

## VII-F-2 Intramolecular NH—S Hydrogen Bond in Acylaminobenzenethiolato Complexes of Cobalt(II) and Iron(II)

**Norikazu UEYAMA*, Taka-aki OKAMURA*, and Akira NAKAMURA** *(*Osaka University)*

[*JCS.Chem.Comm.*, 1019 (1992)]

Importance of NH—S hydrogen bonds in many metalloenzymes which contain cysteinato-metal sites has been recognized. This paper reports preparation of models of such metal sites by utilizing a unique thiolato ligand, ortho-acylaminobenzenethiolato. The structure of cobalt(II) and iron(II) complexes of this ligand is determined to support the characteristic NH—S hydrogen bonds at the thiolato functions. A remarkable effect of the hydrogen bonds is found in their redox properties.

## VII-F-3 Structure and Properties of Molybdenum-(IV,V) Arenethiolates with a Neighboring Amide Group. Significant Contribution of NH—S Hydrogen Bonds to the Positive Shift of Redox Potential of Mo(V)/Mo(IV)

**Norikazu UEYAMA*, Taka-aki OKAMURA*, and Akira NAKAMURA** *(*Osaka University)*

[*J.Am.Chem.Soc.*, **114**, 8129 (1992)]

Monooxomolybdenum(V) and monooxomolybdenum (IV) complexes with o-(acylamino)benzenethiolate were synthesized and characterized by visible, ESR, NMR, and Raman spectroscopies, and electrochemical analysis. Two of these complexes were subjected to X-ray analysis for their molecular structure. Thus, both complexes was found to have a distorted square-pyramidal structure with an axial Mo=O and two distinct kinds of Mo-S bonds. All four acylamino groups of both complexes are located at the Mo=O side. Al four NH groups are involved in intraligand hydrogen bonds with which contribute to the positive shift of the redox potential in acetonitrile.

## VII-F-4 Synthesis of 16 Electron Half-sandwich Ru(II)—Thiolate Complexes Ru(SAr)$_2$($\eta^6$-*p*-cymene) (Ar=2,6-dimethyl-phenyl, 2,4,6-trimethylphenyl)

**Kazushi MASHIMA*, Aki MIKAMI*, and Akira NAKAMURA** *(*Osaka University)*

[*Chem.Lett.* 1473 (1992)]

Treatment of [$RuCl_2$(*p*-cymene)]$_2$ (**1**) with 4 equiv. of sodium salt of 2,6-dimethylphenylthiolate in methanol af

forded intense blue colored solution, from which air-sensitive metallothiolate **2a** was isolated in 47% yield upon recrystallization from a chloroform–hexane solution. Similarly, complex **2b** was prepared by the reaction of **1** with 4 equiv of sodium salt of 2, 4, 6-trimethylphenylthiolate in THF. Complexes **2b** are more soluble in organic solvents and may be crystallized from a saturated hexane solution.

Structure of mononuclear Ru(II) complexes **2** was established by an *X*-ray crystallographic study of **2a**. Figure 1 shows the structure of **2a** with atom labeling scheme. The molecule **2a** is best represented as the two-legged piano stool geometry (Y-shape) and the mononuclear five-coordinated structure. Thus, complex **2** is the first example of the isolated 16-electron ruthenium molecule with Y-shaped geometry. The "half-sandwich" complexes of the type $(C_nH_n)ML_2$ having 16 electrons have been considered as the key intermediates in organometallic chemistry. The reaction of **2** with different kinds of donor molecules is now in progress.

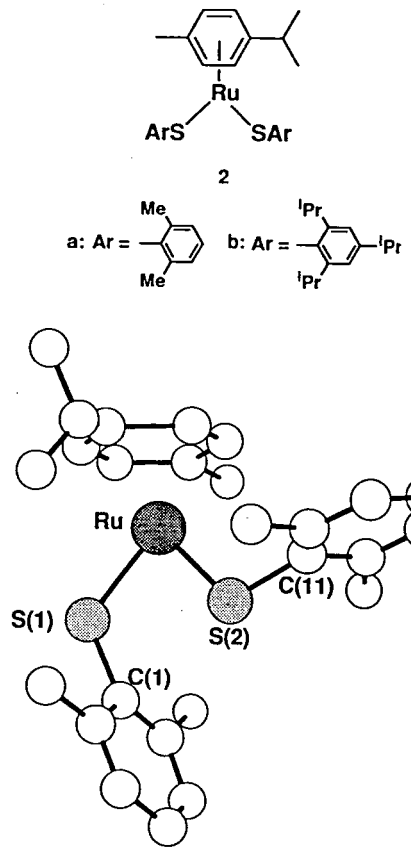


**Figure 1.** An ORTEP drawing of **2a**.

## VII-F-5 Bulky Aryloxo Complexes of Tungsten and Niobium as Catalyst Precursors for High Polymerization of Alk-1-ynes

**Yuushou NAKAYAMA*, Kazushi MASHIMA*, and Akira NAKAMURA** *(*Osaka University)*

[*J.Chem.Soc., Chem.Commun.*, 1496 (1992)]

Metathesis polymerization of some alkynes has been studied in terms of the kind of metals at the catalytic center, but the variation of ligands attached to the metal has been little studied. We found that the tungsten and niobium complexes bearing bulky aryloxo ligands with a reducing reagent such as a Grignard reagent or alkyl aluminum become effective catalysts for the polymerixation of 1-alkynes.

2,6-Dimethylphenoxo complexes of tungsten and niobium complexes were used as catalyst precursors for the polymerization of 3,3-dimethyl-1-butyne. When a bis-aryloxo complex of tungsten/$AlEt_3$ was used as initiator, an extra high molecular mass polymer ($M_n > 2\times10^6$) with narrow molecular mass distribution ($M_W/M_n=1.2$) was obtained.

The polymerization of monosubstituted acetylenes with smaller substituents than 3,3-dimethyl-1-butyne, such as 3-methyl-1- butyne, and 1-butyne in the catalyst system of $WCl_2(OAr)_4$/EtMgBr afforded high molecular mass polymers ($M_n=3.7\times10^5$ and $M_n=9.4\times10^4$, respectively).

Thus, we have found that the bulkiness around the active metal center dramatically enhances the molecular mass of the resulting polymer with narrow molecular mass distribution and prevents side reactions such as cyclotrimerization.

## VII-F-6 Convenient Synthesis of Pentamethylcyclopentadienyl-Tantalum–Diene Complexes via the Reaction of $Cp^*TaCl_4$ with Methylated–allyl Anions

**Kazushi MASHIMA*, Yoshimichi YAMANAKA*, Shinjiro FUJIKAWA*, Hajime YASUDA**, and Akira NAKAMURA** *(*Osaka University, **Hiroshima University)*

[*J.Organometal.Chem.* **428**, C5 (1992)]

Treatment of $Cp^*TaCl_4$ (**1**) with two equiv of 2-butenyl Grignard reagent in THF afforded tantalum–1,3-butadiene complex, $Cp^*TaCl_2(C_4H_6)$ (**2a**). Similarly, reaction of **1** with methylated-allyl anions gave the corresponding diene complexes, $Cp^*TaCl_2$(diene) (**2;b:** diene=isoprene, **c:** 2,3-dimethyl-1,3-butadiene, **d:** 1,3-pentadiene).

The formation of these complexes may be rationalized by bis(allyl) intermediate, which undergoes hydrogen transfer to give allyl–hydride–diene species and the following reductive elimination of allyl and hydride afforded the diene complexes **2**.

The fragment of $Cp^*Ta(diene)Cl_2$ (**2**) is isoelectronic to that of metallocene of group 4. The catalytic aspect of complexes **2** is now in progress.

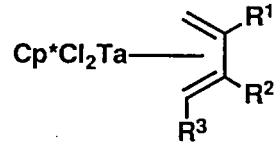


**2**

**a:** $R^1 = R^2 = R^3 = H$

**b:** $R1 = CH_3$, $R^2 = R^3 = H$

**c:** $R^1 = R^2 = CH_3$, $R^3 = H$

**d:** $R^1 = R^2 = H$, $R^3 = CH_3$

# VII—G Thermodynamic Approach to Ion-Solvent Interaction in Solutions

The ion-solvent interactions in solutions have been studied mainly from macroscopic points of view. Emphasis has been placed on the following three points: First, determination of the partial molar volume $V_2^0$ of the complex ion $[18\text{-crown-6-M}]^+$ in water and in methanol based on the measurement of sedimentation potentials. Second, that of the partial molar adiabatic compressibilities of ions of halogeno complexes. And finally evaluation of volume changes accompanying the stepwise complex formation between divalent metal ion and the ligands phenanthroline and 2,2′-bipyridine.

## VII-G-1 Sedimentation Potential Measurement of Alkali Chloride in Water and Methanol Containing 18-Crown-6

**Hiromitu HIRAKAWA** *(Kagoshima Univ.)*, **Fumio KAWAIZUMI** *(Nagoya Univ. and IMS)*, **and Hiroyasu NOMURA** *(Nagoya Univ.)*

[*Denki Kagaku*, **61**, 936 (1993)]

Aqueous and methanolic solutions of 18-crown-6 have been used for solvent for NaCl, KCl, and CsCl and the sedimentation potentials(SP) have been measured. Difference of SP in pure water and in water containing 18-crown-6 became progressively apparent with the increase of the complex formation constants, while the significant differences between SP in methanol and that in methanol containing 18-crown-6 have been observed. The $V_2^0$ ([18-crown-6-M]Cl) was determined from the density data of solutions of KCl dissolved in methanol containing 18-crown-6. Division of $V_2^0$([18-crown-6-M]Cl) into $V_2^0$([18-crown-6-M]$^+$) and $V_2^0(Cl^-)$ based on the SP values leads to the $V_2^0(Cl^-)$ which is equal to the one determined from $V_2^0$(KCl) in pure methanol.

## VII-G-2 Partial Molar Adiabatic Compressibilities of Halogeno Complexes of Platinum and Palladium in Aqueous Solutions

**Fumio KAWAIZUMI** *(Nagoya Univ. and IMS)*, **Yasuharu AMAKASU** *(Nagoya Univ.)*, **and Hiroyasu NOMURA** *(Nagoya Univ.)*

[*J. Solution Chem.*, to be submitted]

Ultrasonic propagation velocities measured at 25°C in aqueous solutions of $K_2[PtX_4]$ $K_2[PtX_6]$ $K_2[PdX_4]$, and $K_2[PdX_6]$ (X=Cl, Br or SCN) have been used together with our previously reported density data to determine the apparent molar adiabatic compressibilities. The partial molar adiabatic compressibilities $K_s^0$ showed that the values $K_s^0(K_2[PtCl_4])$ and $K_s^0(K_2[PtCl_6])$ are appromimately the same, while $K_s^0(K_2[PdCl_4]) > K_s^0(K_2[PdCl_6])$. For the tetracoordinated complexes, the order is $K_2[PtCl_4]) < K_2[PdCl_4] < K_2[PdBr_4] < K_2[Pd(SCN)_4]$. The far weaker interaction of the complex ions $[Pt(SCN)_4]^{2-}$ and $[Pt(SCN)_6]^{2-}$ with water molecules than the case of the other complex ions reflects the soft nature of the linear form ion $SCN^-$.

## VII-G-3 Volume Changes Accompanying the Stepwise Complex Formation in Aqueous Solutions. II Cu(II)-phen and Zn(II)-bpy Complexes

**Fumio KAWAIZUMI** *(Nagoya Univ. and IMS)*

[*J. Solution Chem.*, to be submitted]

Following the procedure described in our previous study (Chem. Lett., 1755 (1991)), the amount of volume change has been evaluated for the complex formation between the metal ions Cu(II) and Zn(II) and the ligands phenanthroline and 2,2′-bipyridine in aqueous solutions. The net volume change, namely the volume change after subtructing the volume contribution of the newly coordinated ligand molecule, was highest for the first coordination step $M^{2+}+L \rightarrow [ML]^{2+}$, while for the second coordination step $[ML]^{2+}+L \rightarrow [ML_2]^{2+}$, it is still positive but is not so high. For the third coordination step $[ML_2]^{2+}+L \rightarrow [ML_3]^{2+}$ it was very low or practically neglegible.

# VII—H Molecular Motion of Polymer Chain Ends

## VII-H-1 Molecular Motion of Polyethylene Chain-ends Tethered on the Surface of Polytetrafluoroethylene in vacuo at Extremely Low Temperatures

**Masato SAKAGUCHI** *(Ichimura Gakuen College)*, **Shigetaka SHIMADA** *(Nagoya Inst. Technol.)*, **Yasuro HORI** *(Nagoya Inst. Technol.)*, **Fumio KAWAIZUMI** *(Nagoya Univ. and IMS)*, **Shunji BANDOW, and Masahiro SAKAI**

The ESR technique has been applied for the study of motions of polyethlene (PE) chain-ends tethered on the surface of polytetrafluoroethylene (PTFE). Samples were prepared by block copolymerization of ethylene with PTFE molecules on the surface of PTFE and measurements were carried out in the temperature ranges from 2.6 K to 77 K. Following conclusion has been deduced: The isolated PE chain-ends ($3 \pm 1$ % of all PE chain-ends) can rotate around the $C_\alpha - C_\beta$ bond axis even at 2.6 K. The mobile fraction of the PE chain-ends increases with temperataure and at 77 K, $30 \pm 10$ % of PE chain ends seem to be in the rotating state.

# VII-I Density Functional Calculations on Structures and Energies of Solvated Metal Ions and Complexes

The density functional methods recently developed made it possible to carry out the accurate calculations of structures and energies to relatively large chemical systems. We have applied the methods to investigations of structures and energies of various solvated metal ions and complexes.

## VII-I-1 A Molecular Approach to the Formation of KCl and $MgCl^+$ Ion-pairs in Aqueous Solution by Density Functional Calculations

**Kenji WAIZUMI, Hideki MASUDA*** *(*Nagoya Inst. of Technol.),* **and Nobuhiro FUKUSHIMA**** *(**Cray Research Japan)*

[*Chem.Phys.Lett.*, **205**, 317, (1993)]

Full geometry optimizations have been carried out on molecular models of $[M(H_2O)_6]^{n+}$,$[M(H_2O)_6\cdots H_2O]^{n+}$ and $[M(H_2O)_6\cdots Cl]^{(n-1)+}$(M=K and Mg, n=1 for K and 2 for Mg) using the density functional methods. The optimized geometries of $[K(H_2O)_6]^+$ and $[Mg(H_2O)_6]^{2+}$ were a regular octahedron. In the optimizations of $[M(H_2O)_6\cdots H_2O]^{n+}$ and $[M(H_2O)_6\cdots Cl]^{(n-1)+}$, the octahedral structures of $[M(H_2O)_6]^{n+}$ units were completely broken for $K^+$ complexes and almost kept for $Mg^{2+}$ complexes. The results have been discussed in connection with the formation of KCl and $MgCl^+$ ion-pairs in aqueous solutions.

## VII-I-2 Geometry Optimization of $[M(H_2O)_6]^{2+}$ by Self Consisten Nonlocal Density Functional Method. M=Cr,Mn,Fe,Co,Ni,Cu and Zn.

**Nobuhiro FUKUSHIMA*** *(*Cray Research Japan)* **and Kenji WAIZUMI**

[*Chem.Express*,**8**,265 (1993)]

Geometries of the titled complexes were fully optimized by a self consistent nonlocal density functional method. The calculated M-O distances, on the average, increase by about 7 pm in comparison with those optimized by a local density functional method, which are in very good agreement with experimental values.

## VII-I-3 Intrinsic Structures and Dissociation Energies of $[Zn(NCS)_4]^{2-}$ and $[Zn(SCN)_4]^{2-}$ Ions Examined by Density Functional Calculations

**Nobuhiro FUKUSHIMA*** *(*Cray Research Japan)* **and Kenji WAIZUMI**

[*Chem.Express*,**8**,269(1993)]

The most stable structures of $[Zn(NCS)_4]^{2-}$ and $[Zn(SCN)_4]^{2-}$ were examined by density functional methods. The former was optimized to a regular tetrahedral arrangement with the Zn-N distance of 199 pm and Zn-N-C angle of 180°, while the latter to a twisted tetrahedral geometry with the Zn-S distance of 242 pm and Zn-S-C angles of 105°. The former was more stable than the latter by about 150 kJ/mol.

## VII-I-4 Intrinsic Structures of $[CuCl_4]^{2-}$ and $[CuBr_4]^{2-}$ Anions by *Ab Initio* Density Functional Calculations

**Kenji WAIZUMI, Hideki MASUDA*** *(*Nagoya Inst. of Technol.),* **and Nobuhiro FUKUSHIMA**** *(**Cray Research Japan)*

[*Chem.Lett.*, 1145 (1993)]

The intrinsic structures of $[CuCl_4]^{2-}$ and $[CuBr_4]^{2-}$ have been investigated by ab initio density functional method and determined to be $D_{2d}$ symmetry with the flattening X-Cu-X angles of 138° and 130° for the case of X=Cl and Br, respectively, and the Cu-X distances of 228 pm and 241 pm, respectively, which are good agreement with the experimental data.

## VII-I-5 Structural Rigidity of First Hydration Spheres of $Na^+$ and $Ca^{2+}$ in Cluster Models. Full Geometry Optimizations of $[M(H_2O)_6]^{n+}$, $[M(H_2O)_6\cdots H_2O]^{n+}$ and $[M(H_2O)_6{-}Cl]^{(n-1)+}$(M=Na and Ca, n=1 for Na and 2 for Ca) by Density Functional Calculations.

**Kenji WAIZUMI, Hideki MASUDA*** *(*Nagoya Inst. of Technol.),* **and Nobuhiro FUKUSHIMA**** *(**Cray Research Japan)*

[*Inorg.Chim.Acta*,**209**,207(1993)]

The intrinsic structural rigidity of hexaaqua complexes of $Na^+$ and $Ca^{2+}$ has been examined on the basis of full geometry optimizations on cluster models of $[M(H_2O)_6]^{n+}$, $[M(H_2O)_6\cdots H_2O]^{n+}$ and $[M(H_2O)_6\cdots Cl]^{(n-1)+}$ (M=Na and Ca, n=1 for Na and 2 for Ca) by use of the ab initio density functional method with Gaussian-type basis sets. The optimized geometries of $[Na(H_2O)_6]^+$ and $[Ca(H_2O)_6]^{2+}$ were both a regular octahedron. In the optimization for adding a water molecule or a chloride anion to $[Na(H_2O)_6]^+$ model, $[Na(H_2O)_6\cdots H_2O]^+$ and $[Na(H_2O)_6\cdots Cl]$, each octahedral $[Na(H_2O)_6]^+$ unit was kept within six-coordination, although both structures were strongly distorted. On the other hand, in the $[Ca(H_2O)_6\cdots H_2O]^{2+}$ and $[Ca(H_2O)_6\cdots Cl]^+$ system, the additional ligand, $H_2O$ and $Cl^-$, was participated in the coordination to the $Ca^{2+}$ ion and the coordination number of $Ca^{2+}$ was changed from six to seven. The results were compared with those of the $K^+$ and $Mg^{2+}$ complexes previously reported, and the differences in the intrinsic structural rigidity of the hexaaqua complexes of $Na^+$, $K^+$, $Mg^{2+}$ and $Ca^{2+}$ were explained in terms of the charges and ionic radii of the cations. The formation of $M^{n+}$-$Cl^-$ ion-pair in an aqueous solution was also discussed.

# VII-J Chemical Simulation of Biological Nitrogen Cycle and Carbon Dioxide Fixation

Assimilatory and dissimilatory reductions of $NO_3^-$ and $NO_2^-$ are the key reactions in the nitrogen cycle, which regulates the amounts of inorganic nitrogen compounds on earth. There are longstanding arguments for the precursors to NO and $N_2O$ in dissimilatory reduction of $NO_2^-$ by nitrite reductases containing iron heme and copper proteins; NO evolution during the turnover despite of very strong affinity of NO for iron heme proteins and the $N_2O$ formation from N1 compounds in the pathway from $NO_2^-$ to $N_2$. The catalytic reduction of $NO_2^-$ to $N_2O$ via NO by copper and iron complexes, therefore, is of much interest in connection with the longstanding questions. Multi-electron carbon dioxide fixation with carbon-carbon bond formation by homogeneous catalysts is expected to contribute for not only utilization of $CO_2$ as C1 resources for various chemicals but also elucidation of biological $CO_2$ fixation. The purpose of this project is to investigate the precursors to NO and $N_2O$ in the dissimilatory reduction of $NO_2^-$, and to develop a new catalytic system that allows to proceed the multi-electron reduction of $CO_2$.

## VII-J-1 Comparative Study of Crystal Structures of $[Ru(bpy)_2(CO)_2](PF_6)_2$, $[Ru(bpy)_2(CO)(C(O)OCH_3)]$ $-B(C_6H_5)_4 \cdot CH_3CN$, and $[Ru(bpy)_2(CO)(\eta^1\text{-}CO_2)] \cdot 3H_2O$ (bpy=2,2′-Bipyridyl)

**Hiroaki TANAKA, Biing-Chiau TZENG*, Hirotaka NAGAO, Shie-Ming PENG*, and Koji TANAKA**
*(*Natl. Taiwan Univ.)*

[*Inorg. Chem.*, **32**, 1508 (1993)]

The molecular structures of $[Ru(bpy)_2(CO)_2](PF_6)_2$, $[Ru(bpy)_2(CO)(C(O)OCH_3)]B(C_6H_5)_4.CH_3CN$ as a model of $[Ru(bpy)_2(CO)(C(O)OH)]^+$, $[Ru(bpy)_2(CO)(\eta^1\text{-}CO_2)].3H_2O$ have been determined by X-ray analysis. The observation that the Ru-$C(O)OCH_3$ bond distance of $[Ru(bpy)_2(CO)(C(O)OCH_3)]^+$ is shorter than the Ru-$CO_2$ one of $[Ru(bpy)_2(CO)(CO_2)]$ suggests that the multibond character of the Ru-$CO_2$ bond is not larger than that for Ru-$C(O)OCH_3$. One extra electron pair involved in $[Ru(bpy)_2(CO)(CO_2)]$ resulting from dissociation of a terminal proton of $[Ru(bpy)_2(CO)(C(O)OH)]^+$ may be localized in the $CO_2$ ligand rather than delocalized over the Ru-$CO_2$ moiety, and the extended three-dimentional network of hydrogen bonding between the $CO_2$ ligand and three hydrated water molecules compensates the increase in the electron density of the $CO_2$ moiety of $[Ru(bpy)_2(CO)(CO_2)].3H_2O$.

## VII-J-2 Carbon-carbon Bond Formation in Electrochemical Reduction of Carbon Dioxide by Ruthenium Complex

**Hirotaka NAGAO, Tetsunori MIZUKAWA, and Koji TANAKA**

We have demonstrated that $[Ru(bpy)_2(CO)_2]^{2+}$ (**1**) exists as an equilibrium mixture with $[Ru(bpy)_2(CO)(C(O)OH)]^+$ and $[Ru(bpy)_2(CO)(\eta^1\text{-}CO_2)]$ (bpy=2,2′-bipyridine) in aqueous solutions, and those three complexes serve as the precursors of CO and HCOOH, and the $CO_2$ carrier in electro- and photochemical reduction of $CO_2$ in protic media. In accordance with this, the carbonyl ligand of $[Ru(bpy)(trpy)(CO)](PF_6)_2$ (**2**) (trpy=2,2′:6′,2″- terpyridine) is reversibly converted to hydroxycarbonyl and $\eta^1$-$CO_2$ ones by treatment with $OH^-$ in $CH_3CN$. **1** and **2** react with $NaBH_4$ to afford $CH_3OH$ *via* formyl and hydroxymethyl complexes, and the molecular structure of $[Ru(bpy)_2(CO)(CH_2OH)]PF_6$ was determined by X-ray structure analysis. The controlled potential electrolysis of **2** at −1.75 V *vs.* $Ag|Ag^+$ in $CO_2$-saturated $C_2H_5OH/H_2O$ (8:2 v/v) at −20°C produced HC(O)H, $CH_3OH$, H(O)CCOOH, and $HOCH_2COOH$ together with CO and HCOOH, while the similar electrochemical $CO_2$ reduction in the presence of **1** gave only CO and HCOOH. The multi-electron reduction of $CO_2$ by **2** as the first example in homogeneous reactions is ascribed to the formation of $[Ru(bpy)(trpy)(CHO)]^+$ by two-electron reduction of **2** in protic media as similar to the reduction of **1** with $BH_4^-$.

## VII-J-3 Carbon-carbon Bond Formation in Multielectron Reduction of Carbon Dioxide Catalyzed by $[Ru(bpy)(trpy)(CO)]^{2+}$ (bpy=2,2′-bipyridine; trpy= 2,2′:6′2″-terpyridine)

**Hirotaka NAGAO, Tetsunori MIZUKAWA, and Koji TANAKA**

[*Chem. Lett.*, 955 (1993)]

Two electron reduction of $[Ru(bpy)(trpy)(CO)]^{2+}$ lead dissociation of CO at room temperature, while $[Ru(bpy)(trpy)(CO)]^0$ is stable at −20°C. The reaction of $[Ru(bpy)(trpy)(CO)]^0$ with proton produces $[Ru(bpy)(trpy)(CHO)]^+$, which undergoes protonation and carboxylation in $CO_2$-saturated $H_2O/C_2H_5OH$ to afford HC(O)H, $CH_3OH$, H(O)CCOOH, and $HOCH_2COOH$. In accordance with this, the controlled potential electrolysis of $[Ru(bpy)(trpy)(CO)]^{2+}$ at −1.70 V vs. $Ag/Ag^+$ in $CO_2$-saturated $C_2H_5OH/H_2O$ (8:2 v/v) at −20°C produced not only HCOOH and CO but also HC(O)H, $CH_3OH$, H(O)CCOOH, and $HOCH_2COOH$.

## VII-J-4 Evaluation of Acidity of $CO_2$ in Protic Media. Carboxylation of Reduced Quinone

**Hiroaki TANAKA, Hirotaka NAGAO, and Koji TANAKA**

[*Chem. Lett.*, 541 (1993)]

There is a controversy about the mechanism for electo- and photochemical $CO_2$ reduction; which of proton or $CO_2$ attacks low valent coordinatively unsaturated metal centers at the initial stage of the reduction? In the former, metal formato complexes (M-OC(O)H) are produced by insertion of $CO_2$ to M-H bonds, while metal carboxylates (M-C(O)OH) would be generated by protonation of metal-$CO_2$

complexes. This arguments partly results from lack of the information about the acidity of $CO_2$ in protic media. Interactions of $CO_2$ with reduced 2,3,5,6-tetramethylquinone (TMQ), therefore, were investigated by means of cyclic voltammetry in $CH_3CN$, $CH_3OH$, and $CH_3CN/H_2O$. Predominant carboxylation of reduced TMQ in $CH_3OH$ and $CH_3CN/H_2O$ (9:1 v/v) indicates that the acidity of $CO_2$ is substantially equivalent or stronger than that of proton in both media.

### VII-J-5 Stabilization of Superoxidized Form of Synthetic $Fe_4S_4$ Cluster as the First Model of High Potential Iron Sulfur Proteins in Aqueous Media

**Hide KAMBAYASHI, Hirotaka NAGAO, Koji TANAKA, Masami NAKAMOTO*, and Shie-Ming PENG**** *(*Osaka Municipal Tech. Res. Inst., **Natl. Taiwan Univ.)*

[*Inorg. Chim. Acta.*, **209**, 143 (1992)]

The adamantane ligated $Fe_4S_4$ cluster, $[Fe_4S_4(SAd)_4]^{2-}$, exhibits two stable $[Fe_4S_4]^{2+/+}$ and $[Fe_4S_4]^{3+/2+}$ redox couples in dry DMF, while $[Fe_4S_4(SAd)_4]^-$ readily undergoes a hydrolysis reaction by the addition of a small amount of $H_2O$ in DMF (3 vol.%). The hydrolysis of $[Fe_4S_4(SAd)_4]^-$ can be effectively depressed by the presence of free AdSH in $H_2O$/DMF, and also by solubilization in aqueous PDAH solutions (PDAH=poly[2-(dimethylamino)-hexanamide]). The observation that the crystal structure of $(Ph_4As)_2[Fe_4S_4(SAd)_4]$ has enough space for coordination of $H_2O$ to the $Fe_4S_4$ core indicates that stabilization of $[Fe_4S_4(SAd)_4]^-$ in aqueous media is described to depression of dissociation of $AdS^-$ rather than hydrophobic spheres around the $[Fe_4S_4]^{3+}$ core.

### VII-J-6 Crystal Structure of $(Ph_4As)_2[Fe_4S_4(SAd)_4]$ and Stabilization of $[Fe_4S_4(SAd)_4]^-$ State in Aqueous Media

**Hide KAMBAYASHI, Masami NAKAMOTO*, Shie-Ming PENG**, Hirotaka NAGAO, and Koji TANAKA** *(*Osaka Municipal Tech. Res. Inst., **Natl. Taiwan Univ.)*

[*Chem. Lett.*, 919 (1992)]

In contrast to high potential iron-sulfur proteins (Hipip), one electron oxidation of synthetic $[Fe_4S_4(SR)_4]^{2-}$ clusters readily causes decomposition of the cluster in aqueous media. The stable $[Fe_4S_4]^{3+/2+}$ redox couple of Hipip are believed to result from protection of nucleophilic attack of water molecules to the $Fe_4S_4$ cores by hydrophobic spheres formed by peptide chains. We have shown that $[Fe_4S_4(SAd)_4]^{2-}$ ($AdS^-$: 1- adamantanethiolate) undergoes a reversible one-electron oxidation reaction as the first example in aqueous media. Molecular structure of $(Ph_4As)_2[Fe_4S_4(SAd)_4]$, however, revealed that $[Fe_4S_4(SAd)_4]^{2-}$ has enough space for coordination of solvent molecules to the $[Fe_4S_4]^{2+}$ core. Stability of $[Fe_4S_4(SAd)_4]^-$ in aqueous micellar solutions, therefore, is ascribed to depression of a substitution reaction between $AdS^-$ ligated and $H_2O$ due to low solubility of $AdS^-$ in $H_2O$.

### VII-J-7 Molecular Structure of Copper Nitrito Complexes as the Reaction Intermediate of Dissimilatory Reduction of $NO_2^-$

**Nobutoshi KOMEDA*, Hirotaka NAGAO, Gin-ya ADACHI*, Masatatsu SUZUKI**, Akira UEHARA**, and Koji TANAKA** *(*Osaka Univ. **Kanazawa Univ.)*

[*Chem. Lett.*, in press]

A controlled potential electrolysis of an aqueous solution (pH 7.0) containing $[Cu(tpa)(H_2O)](ClO_4)_2$ (tpa=tris[(2-pyridyl)methyl]amine) and $NaNO_2$ at −0.40 V (*vs.* Ag/AgCl) catalytically produced NO and $N_2O$. Based on the fact that both $[Cu(tpa)(ONO)]^+$ and $[Cu(tpa)(NO_2)]^+$ exist as equilibrium mixtures in solutions, electrochemical reduction of $NO_2^-$ is concluded to result from irreversible protonation of oxygen of the $NO_2^-$ ligands of $[Cu(tpa)(ONO)]^+$ and $[Cu(tpa)(NO_2)]^+$. Removal of the bound- or terminal-oxygen from the Cu-ONO moiety presumably result in NO dissociation due to the Cu-O bond cleavage or lability of the Cu-ON bond. Free NO thus formed will form a nitrogen-bound nitrosyl adduct, $[Cu(tpa)(NO)]^{2+}$, which also may be formed in the reduction of $[Cu(tpa)(NO_2)]^+$ in $H_2O$ without the Cu-NO bond cleavage because of the removal of the terminal-oxygen of the nitro ligand. Thus, dissimilatory reduction of $NO_2^-$ via $[Cu(tpa)(ONO)]^+$ reasonably explains NO evolution.

### VII-J-8 Nitro- and Nitrito-Copper Complexes as Reaction Intermediate in the Pathways from Nitrite to Nitrouos Oxide

**Nobutoshi KOMEDA*, Hirotaka NAGAO, Gin-ya ADACHI*, Masatatsu SUZUKI**, Akira UEHARA**, and Koji TANAKA** *(*Osaka Univ., **Kanazawa Univ.)*

Dissimilatory reduction (denitrification) of $NO_2^-$ by nitrite reductase containing heme and copper proteins is the key reaction of the nitrogen cycle. There are, however, controversies about the precursors of NO and $N_2O$ evolution in the pathway from $NO_2^-$ to $N_2O$. Although $NO_2^-$ coordinates to a metal in a variety of forms such as nitro, nitrito, chelating nitro, and bridging nitro, it is exclusively assumed that $NO_2^-$ is linked by the nitrogen atom to the active center of nitrite reductases. The reaction of $[Cu(tpa)Cl]^+$ with $NO_2^-$ in $H_2O$ afford an equilibrium mixture of $[Cu(tpa)(NO_2)]^+$ and $[Cu(tpa)(ONO)]^+$ in $H_2O$, and the molecular structures of both complexes are determined by X-ray analysis (Figure 1). The fact that electrochemical reduction of both complexes afford $N_2O$ strongly suggests that not only nitro but also nitrito complexes have an ability to catalyze dissimilatory reduction of $N_2O$, and the nitrito adduct functions as the precursor for NO evolution.

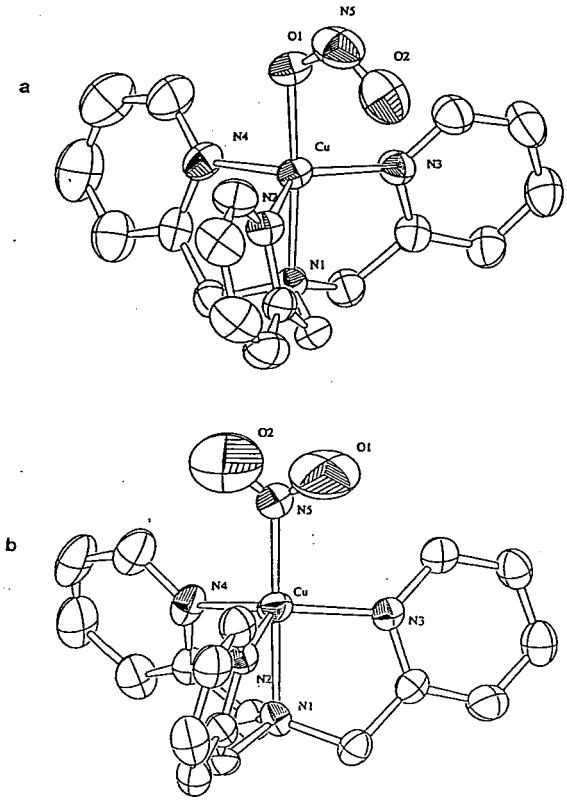


**Figure 1.** Molecular structures of $[Cu(tpa)(ONO)]^+$ (a) and $[Cu(tpa)(NO_2)]^+$ (b).

# VII-K Development of Highly Selective Reactions Using Early Transition Metal Complexes

Highly selective bond formation have been investigated using early transition metal complexes, especially zirconium complexes. Zirconocene alkene or alkyne complexes could be used for selective C-C bond formation or selective functionalization of molecules.

## VII-K-1 Zirconium Catalyzed Novel Catalytic C-C Bond Formation Reactions

**Noriyuki SUZUKI, Denis KONDAKOV, and Tamotsu TAKAHASHI**

[*J. Am. Chem. Soc.*, **115**, 8485 (1993)]

Zirconium catalyzed novel type of allylation reaction was investigated using allylic ethers and EtMgBr. Allylic ethers such as 2-hexenyl ethers and 2-cyclopentenyl ethers gave highly regioselective allylation products, 3-ethyl-1-hexene and 3-ethylcyclopentene, respectively, in 50—77% yields. When 2,5-dihydrofuran was treated with 1.2 equiv of EtMgBr in the presence of $Cp_2ZrCl_2$, similar type of catalytic allylation proceeded to give 2-ethyl-3-buten-1-ol after hydrolysis. Further catalytic ethylation of the first allylation product proceeded when treated with 5 equiv of EtMgBr.

Stoichiometric reaction of $Cp_2ZrEt_2$, which is zirconocene ethylene complex precursor, with 2-hexenyl phenyl ether revealed that 3-propyl-4-pentenylzirconocene compound was formed as an intermediate species. Reaction of this intermediate species with EtMgBr afforded 3-ethyl-1-hexene, and regenerated the zirconocene-ethylene complex. A reaction of zirconacyclopentene, which was prepared from $Cp_2ZrEt_2$ and alkyne, with allyl phenyl ether afforded the allylation product of alkyne after hydrolysis. The plausible mechanism of the catalytic reaction was proposed.

The following is the proposed mechanism for this zirconium catalyzed allylation reactions.

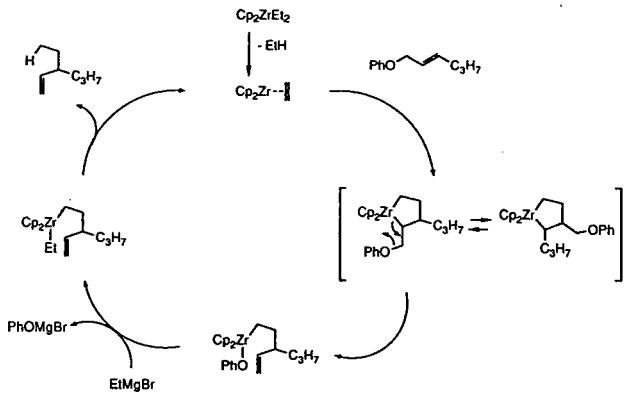

## VII-K-2 Facile Cleavage of the Cβ-Cβ′ Bond of Zirconacyclopentenes. Convenient Method for Selective Coupling of Alkynes with Alkynes, Nitriles, and Aldehydes

**Tamotsu TAKAHASHI, Motohiro KAGEYAMA, Victor DENISOV, Ryuichiro HARA, and Ei-ichi NEGISHI***
*(*Pudue Univ.)*

[*Tetrahedron Lett.*, **34**, 687 (1993)]

The reaction of zirconacyclopentenes (**1**) with alkynes, nitriles, and aldehydes proceeds via cleavage of the Cβ-Cβ′ bond of **1** and displacement of ethylene by the donors to give the corresponding five-membered zirconacycles, providing a convenient means of selective coupling of alkynes with π-donor compounds.

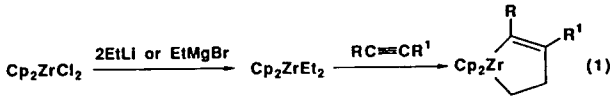


1a (80-90%, R = R¹ = *n*-Pr) 1b (87%, R = R¹ = Et) 1

1c (87%, R = R¹ = Ph) 1d (84%, R = Ph, R¹ = Me)

1e (74-87%, R = H, R¹ = *n*-Hex) 1f (40%, R = $Me_3Si$, R¹ = H)

The reaction of alkynes with diethylzirconocene, generated *in situ* by treatment of $Cp_2ZrCl_2$ with 2 equivalents of ethylmagnesium halides or ethyllithium, can selectively produce the corresponding zirconacyclopentenes (**1**) in good yields (eq 1). Interestingly, zirconacyclopentenes (**1**) react at room temperature with various π-donors to give selectively the corresponding five-membered zirconacycles(**2-4**), while their reaction with a phosphine gives zirconocene-alkyne-phosphine complexes (**5**) (Scheme 1). The facile cleavage of the Cβ-Cβ′ bond of zirconacyclopentenes is analogous to that of zirconacyclopentanes. It is, however, in striking contrast with the inertness of zirconacyclopentadienes which do not react with any of the reagents mentioned above under comparable conditions. The known procedures for the synthesis of **2-4** mostly require preformed $Cp_2Zr$-alkyne-phosphine complexes containing costly phosphines, e.g., $PMe_3$ and $PPh_2Me$, and/or cumbersome preparation of $Cp_2Zr(H)Cl$ for hydrozirconation of alkynes. Consequently, the Cβ-Cβ′ bond cleavage route herein reported offers a convenient alternative for selective coupling of alkynes with alkynes, nitriles, and aldehydes.

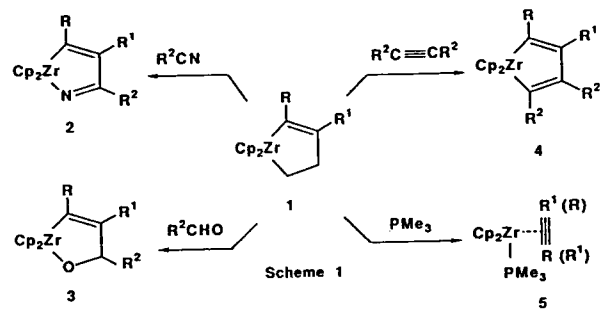


## VII-K-3 Highly Chemoselective Reactions of Zirconacyclopentenes for Selective Functionalization

**Tamotsu TAKAHASHI, Koichiro AOYAGI, Ryuichiro HARA, and Noriyuki SUZUKI**

[*J. Chem. Soc., Chem. Commun.*, 1042 (1993)]

Cross coupling of alkynes with alkenes on zirconium complexes results in the formation of zirconacyclopentenes which contain two different zirconium-carbon bonds. In order to transform the zirconacyclopentenes to useful organic compounds, for example, stereodefined trisubstituted alkenyl iodide, chemoselective reactions of these two different zirconium-carbon bonds are important.

bonds are important.

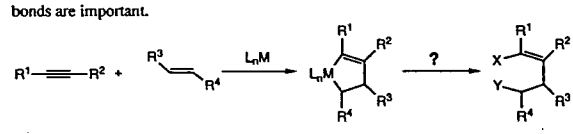


Alcoholysis of zirconacyclopentenes proceeded at alkyl carbon on Zr with high chemoselectivity in sharp contrast to monoiodination of zirconacyclopentenes with iodine, and alcoholysis followed by iodination of zirconacyclopentenes produced stereodefined trisubstituted alkenyl iodides in high yields with high isomerical purities.

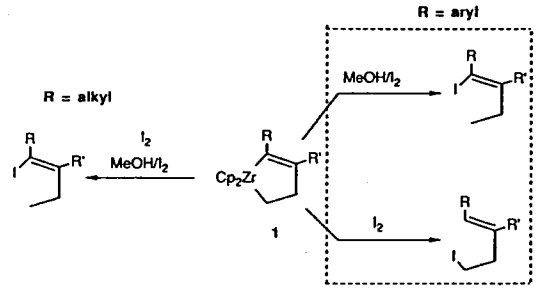


## VII-K-4 Allylzirconation of Alkynes by the Reactions of Zirconocene-Alkyne Complexes with Allylic Ethers

**Tamotsu TAKAHASHI, Noriyuki SUZUKI, Motohiro KAGEYAMA, Denis, Y. KONDAKOV, and Ryuichiro HARA**

[*Tetrahedron Lett.*, **34**, 4811 (1993).]

Although allylmetalation of alkynes is very attractive reaction for organic synthesis, only allylmetals containing Li, Mg, B, Zn or Al have been used. No precedents have been reported for allylzirconation of alkynes. Mechanistic studies of these allylations suggested six-centered or four-centered intermediate stage was plausible. We describe here a novel type of allylzirconation of alkynes by the reactions of zirconocene-alkyne complexes with allylic ethers.

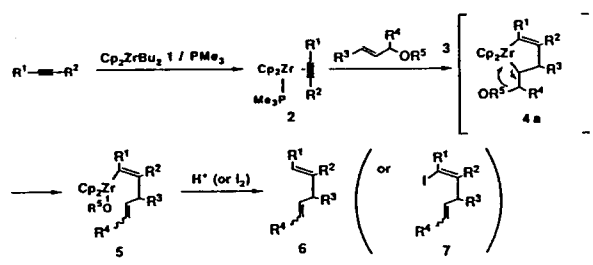

### VII-K-5 Pair Selective Coupling Reactions of Alkynes with Alkenes on Zirconocene

**Tamotsu TAKAHASHI, Zhenfeng XI, Christophe J. ROUSSET, and Noriyuki SUZUKI**

[*Chem.Lett.*, 1001 (1993).]

When ethylene and alkynes such as 4-octyne and diphenylacetylene were treated with $Cp_2ZrBu_2$, highly pair selective coupling products were formed in high yields. Similarly, styrene or trimethylvinylsilane also afforded cross coupling products with alkynes on zirconocene complex.

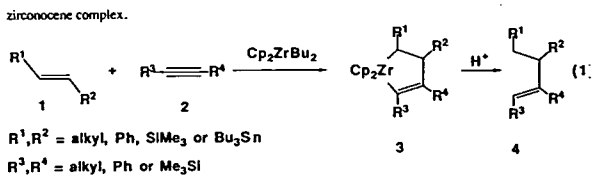


### VII-K-6 Reactions of Alkynes with Homoallylic Halides Mediated by Zirconocene-Ethylene Complex

**Tamotsu TAKAHASHI, Denis Y. KONDAKOV, and Noriyuki SUZUKI**

[*Tetrahedron Lett.*, **34**, 6571 (1993)]

Recently we have developed allylzirconation reactions of alkenes and alkynes using allylic ethers and zirconocene-alkene and -alkyne complexes, respectively, as described above. These reactions proceeded via five membered ring intermediates. The reaction mechanism was quite different from that involving four centered or six centered intermediates proposed for allylmetalation reactions of alkynes using allylmetals. In order to extend this type of reactions we investigated reactions of alkynes with homoallylic compounds.

Homoallylic ethers, however, were not reactive towards zirconocene-alkyne complexes. Although homoallylic bromides were reactive, they reacted with trimethylphosphine of zirconocene-alkyne complex first. Finally we found that zirconocene-ethylene complex $Cp_2Zr(CH_2{=}CH_2)$, prepared in situ from $Cp_2ZrCl_2$ and 2 equiv of EtMgBr, was a suitable reagent for reactions of alkynes with homoallylic bromides. Treatment of alkynes with zirconocene-ethylene complex and homoallylic halides gave allylcyclopropane derivatives as shown in the following Scheme.

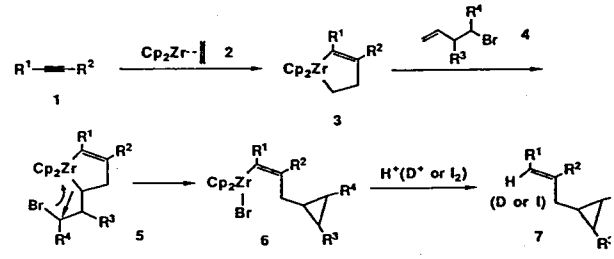


## VII—L Chemistry of Polynuclear Metal Complexes

Cooperative phenomena based on direct or indirect metal-metal interaction in polynuclear metal complexes give rise to interesting and sometimes useful chemistry. And a polynuclear complex often exhibits unique reactivity with the use of polymetallic reaction site. We are trying to synthesize new polynuclear metal complexes with the cooperative metal-metal interaction to develop chemistries along such a line.

### VII-L-1 Dinucleating Bis-dimethylcyclam Ligand and Its Dinickel(II) and Dizinc(II) Complexes with the Face-to-face Ring Arrangement

**Takashi KAJIWARA** *(Tohoku Univ.)*, **Tadashi YAMAGUCHI** *(Tohoku Univ.)*, **Hiroaki KIDO** *(Tohoku Univ.)*, **Satoshi KAWABATA** *(Tohoku Univ.)*, **Reiko KURODA** *(The Univ. of Tokyo)*, **Tasuku ITO** *(Tohoku Univ. and IMS)*

Chemistry of metal complexes with cyclam or related tetraaza macrocyclic ligands has been extensively developed. Preparation of dinucleating ligands with two such macrocyclic rings was also attempted, aiming at the cooperative interaction of two metallic sites in the metal complexes. To our knowledge, however, no one has succeeded in synthesizing metal complex with the cofacial ring arrangement, except for the face-to-face diporphyrin complexes. In this study, we prepared a new dinucleating ligand (L) comprized of two dimethylcyclams bridged at the carbon center with *ortho*-xylylene group, and its bridged dinicker(II) and dizinc(II) complexes with a cofacial ring arrangement, $[Ni_2(\mu\text{-}Br)Br_2(L)]Br \cdot H_2O$ (Figure 1) and $[Zn_2(\mu\text{-}CO_3)(L)](ClO_4)_2 \cdot 2H_2O$ (Figure 2). Introduction of two methyl groups to each cyclam ring skeleton makes it possible to arrange two rings in a face-to-face manner. Ni-Ni and Zn-Zn separations are 5.802(2) and 5.806(2) Å, respectively. $[Zn_2(\mu\text{-}CO_3)(L)](ClO_4)_2 \cdot 2H_2O$ has been obtained via the spontaneous $CO_2$ uptake from the air by $[Zn_2(L)](ClO_4)_4$ in 0.1 M NaOH aqueous solution. The $CO_2$ uptake originates from the designed dinuclear structure.

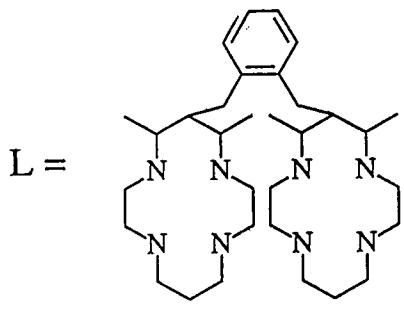

The free ligand can easily be prepared in a large scale and it is possible to make its complexes of various metal ions. Therefore, a variety of the use of the bimetallic site such as substrate binding in a catalytic process and creation of novel type of M-M interaction would be possible, by combining metal ions and bridging ligands.

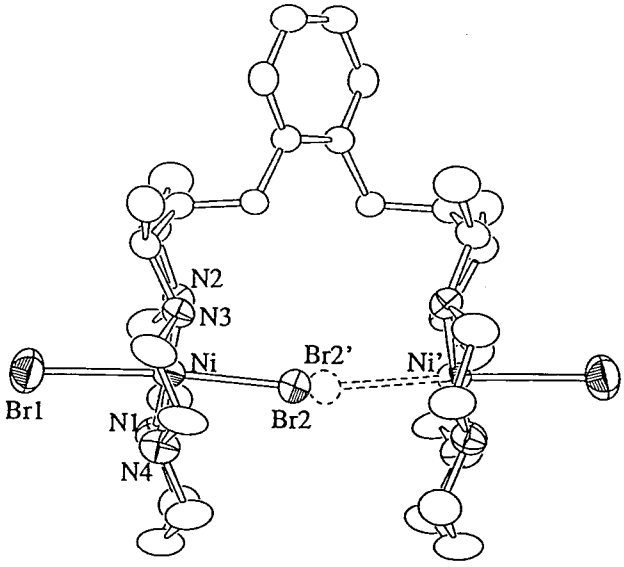


**Figure 1.** ORTEP drawing of $[Ni_2(\mu\text{-}Br)Br_2(L)]^+$. Dotted atom and bond show disorder of the Br(2) atom.

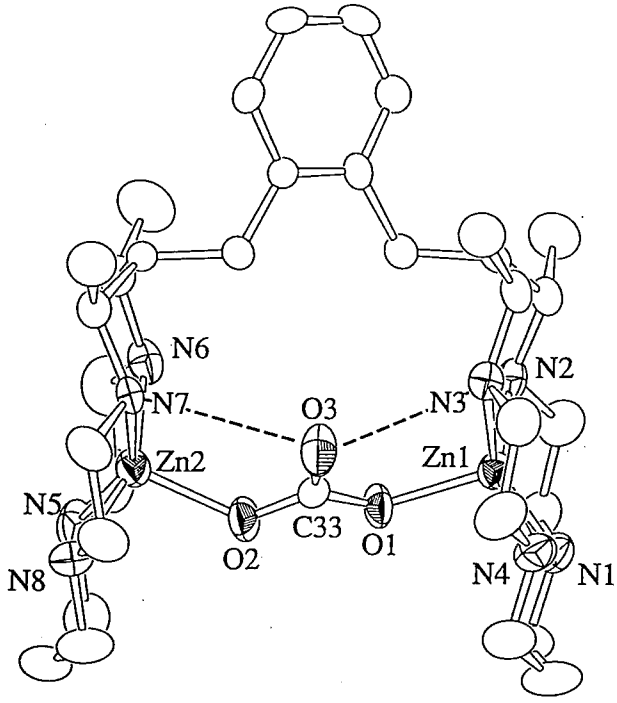


**Figure 2.** ORTEP drawing of $[Zn_2CO_3(L)]^{2+}$.

## VII-L-2 Tetranuclear Platinum(II) Cluster Complexes Having Non-bridging Chelate Ligands in the Plane of Square Planer Cluster Core,$[Pt_4(CH_3COO)_4(en)_4]Cl_4 \cdot 4H_2O$ and $[Pt_4(CH_3COO)_4(pic)_4] \cdot CH_3OH \cdot 4H_2O$ (en=ethylenediamine and picH= picolinic acid)

**Tadashi YAMAGUCHI** *(Tohoku Univ.)*, **Tetsuuji UENO** *(Tohoku Univ.)*, **and Tasuku ITO** *(Tohoku Univ. and IMS)*

$[Pt_4(CH_3COO)_8]$**(1)** is a well-known cluster complex of divalent platinum with Pt-Pt bonds and has unique structure and reactivity. It has square-planar cluster core comprized of four Pt(II) ions. The coordination geometry around each Pt(II) ion is a distorted octahedron if the Pt-Pt bond is included, while Pt(II) adopts normally the square-planar four coordinate geometry.

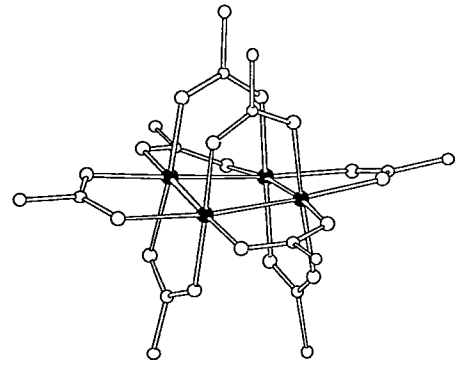

$[Pt_4(CH_3COO)_8]$**(1)**

Previously, we reported derivatives of **1**, $[Pt^{II}{}_4(\mu\text{-}CH_3COO)_4(\mu\text{-}RCOO)_4]$ and $[Pt^{II}{}_4(\mu\text{-}CH_3COO)_4(\mu\text{-acac-}O,C^3)_4]$. In all the so far known compounds derived from **1**, eight bidentate ligands bridge doubly four edges of the square-planar cluster core. Although there exist the direct Pt-Pt single bonds, it has been believed that the double bridging stabilizes the cluster core and thereby gives rise to the rather unusual octahedral geometry around Pt(II) ion. In this study, we prepared for the first time tetranuclear Pt(II) cluster complexes having non-bridging chelate ligands in the plane of the square planar cluster core (Chart, in which only the cluster core and the coordination mode of the in-plane ligands are shown).

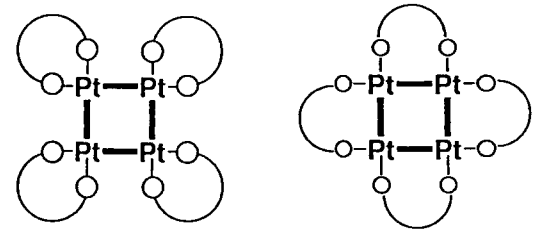


The titled two new complexes were synthesized through the acetate ligand substitution of **1** by ethylenediamine and picolinic acid, respectively. X-ray analyses of both the compound show that ethylenediamine and picolinate ion are in the plane of the square planar Pt(II) cluster core and adopt the chelate coordination mode. Figure 1 shows the structure of $[Pt_4(CH_3COO)_4(pic)_4]$ as an example. The loss of the bridge coordination in the plane of the cluster core resulted in the slight lengthening of Pt-Pt bond (2.545(1)—2.557(1) Å) and distortion of the cluster core.

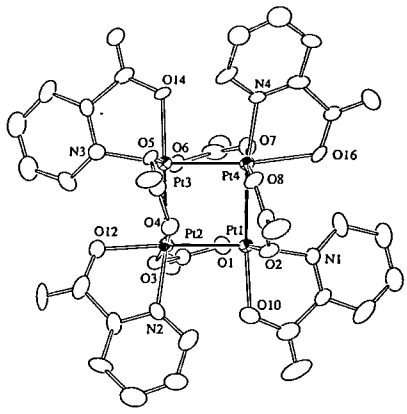


**Figure 1.** ORTEP drawing of $[Pt_4(CH_3COO)_4(pic)_4]$

## VII-L-3 $^{195}Pt$ NMR of Tetranuclear Platinum(II) Cluster Complexes, $[Pt_4(CH_3COO)_7(CH_3CONH)]$ and $[Pt_4(CH_3COO)_5(CH_3CONH)_3]$, Which Have Chemically Non-equivalent Nuclei

**Tadashi YAMAGUCHI** *(Tohoku Univ.)*, **Koji Abe** *(Tohoku Univ.)*, **and Tasuku ITO** *(Tohoku Univ. and IMS)*

Both of the titled compounds with direct Pt-Pt bonds have four chemically nonequivalent platinum nuclei and show very complicated $^{195}Pt$ NMR spectra because of four different Pt-Pt coupling and the existence of isotopomers owing to the natural abundance of $^{195}Pt$ nucleus. Each spectrum was successfully analysed on the basis of spectral patterns of eight possible isotopomers, the line broadning caused by the nitrogen donation, and the cyclic structure of the cluster core. Chemical shifts and Pt-Pt coupling constants in the mono-acetoamidate complex in $CD_3CN$ were 912, 959, 1109, and 1176 ppm vs $K_2PtCl_4$ and $^1J_{Pt\text{-}Pt}$= 5980, 6050, 6410, and 7370 Hz. Those in the tris-acetoamidate complex were 825, 931, 1087, and 1189 ppm and $^1J_{Pt\text{-}Pt}$=5680, 6720, 7380, and 7560 Hz. As an example, $^{195}Pt$ NMR spectrum of $[Pt_4(CH_3COO)_7(CH_3CONH)]$ in $CD_3CN$ and the assignments are shown in Figure 1.

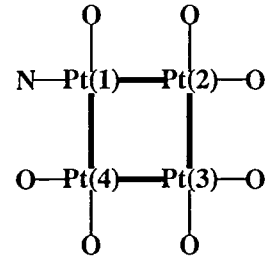


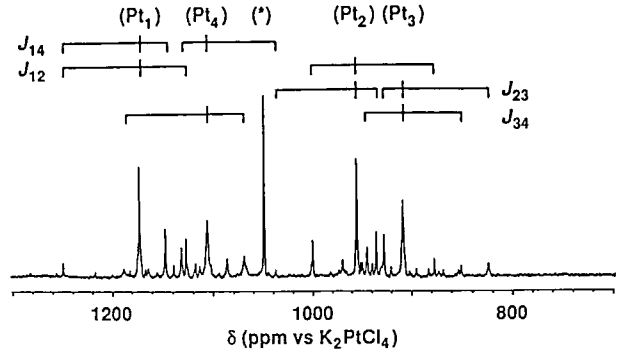


**Figure 1.** $^{195}Pt$ NMR of $[Pt_4(CH_3COO)_7(CH_3CONH)]$ in $CD_3CN$

# RESEARCH ACTIVITIES VIII
# Computer Center

## VIII—A Theoretical Studies of Highly Excited Vibrational States in Polyatomic Molecules

Research activities of this year spread over the wide field of molecular problems. These include: (a) molecular dynamics simulations of liquids, (b) electronic structure and dynamics of small polyatomic molecules, and (c) development of parallel computational environment for large scale electronic structure calculations. Dr. Kitaura left IMS in March 1993 and became Professor at University of Osaka Prefecture. Dr. Aoyagi joined as Associate Professor in May 1993.

### VIII-A-1 Rotation Induced Vibrational Mixing in Highly Excited Vibrational States of Formaldehyde

**Mutsumi AOYAGI**

The effects of both anharmonic and Coriolis interactions on the intramolecular dynamics in Formaldehyde are investigated quantum mechanically. Variational calculations including all of the vibrational modes, and the rotational modes are performed using the ab initio SDCI potential energy surface. Both time-dependent and time-independent analyses are made on the calculated eigenstates (up to 12000 $cm^{-1}$) to elucidate the role of Coriolis interaction in highly excited vibrational states. We found that the anharmonic couplings assisted by b- and c-type Coriolis interactions and extensive K-mixings[1] play a crucial role in the intramolecular dynamics at high energy region ($E > 7500$ $cm^{-1}$). Viewing from the parametric motion of ro-vibrational eigenvalues (Figure 1), we also found that the mechanism of rotation induced vibrational mixing can be interpreted as the multiple avoided crossing in parameter space among many ro-vibrational states spreading over the wide energy range.

**Reference**

1) M. Aoyagi and S. Gray, *J. Chem. Phys.*, **94**, 195 (1991).

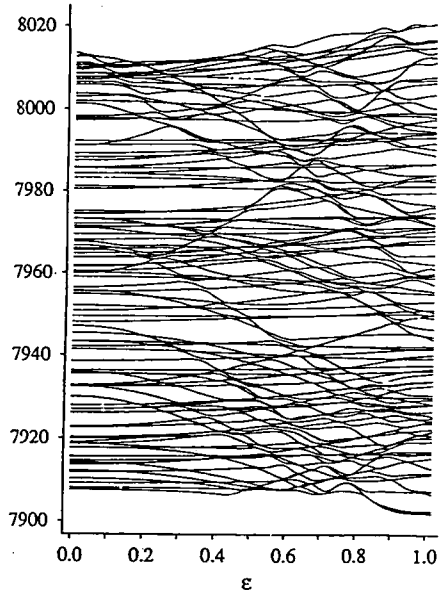


**Figure 1.** Parametric motion of ro-vibrational eigenvalues. Energy levels ($cm^{-1}$) are variationally determined with changing ro-vib interaction parameter ($\varepsilon$) in $H=H_{rot}+H_{vib}+\varepsilon H_{ro\text{-}vib}$.

### VIII-A-2 Theoretical Study of the Photoabsorption Spectrum and Photodissociation Dynamics of Fluoroformyl Radical FCO

**Shinkoh NANBU, Masahiro GOMYO*, and Suehiro IWATA*** *(*Keio University)*

[submitted to *Chem. Phys.*]

Potential energy surfaces for electronic ground and four excited states of the fluoroformyl radical, FCO, were calculated with the *ab initio* molecular orbital (MO) configuration interaction (CI) method. The electronic transition related with progressions I and II in the photoabsorption spectra observed by Jacox[1] was found to be the $1^2A''(1^2\Pi) \leftarrow 1^2A'$ transition. To assign the vibrational progressions, 60 vibrational levels in the $1^2A''$ state were numerically evaluated by using the TRIATOM program developed by Tennyson and Miller[2]. The theoretically obtained progressions of the CO stretching mode in the $1^2A''$ state corresponded successfully with the experimentally assigned progressions of the CO stretching mode between 340 and 280 nm. The calculated level spacings for the CO stretching and bending modes were 873 and 459 $cm^{-1}$, respectively, while the experimental spacings for those modes were 700 and 350 $cm^{-1}$, respectively. The saddle point on the pathway to the dissociation $CO(^1\Sigma^+)+F(^2P)$ was also found at a non-linear structure in the $1^2A''$ state, and the excitation energy from the bottom of the ground state surface was 4.57 eV. We support the Jacox's report, according to which the photodissociation of FCO into F+CO was observed with a threshold near 4.43 eV ($\sim$280 nm).[1]

**References**

1) M. E. Jacox, *J. Mol. Spectrosc.*, **80**, 257 (1980).
2) J. Tennyson and S Miller, Comput. *Phys. Commun.* **55**, 149 (1989).

### VIII-A-3 Development of Parallel Direct SCF Program and Applications to Large Scale Molecular Orbital Calculations on Loosely Coupled Networks of Workstations

**Mutsumi AOYAGI, Satoshi MINAMINO, and Shinkoh NANBU**

We are developing a parallel code of a direct SCF program on loosely coupled networks of workstations (WS), and are applying it to large scale molecular orbital calculations. This program system can be used on several distributed computing tools, including PVM, TCGMSG, and

EXPRESS. Benchmark calculations of retinal molecule with DZP basis set are carried out to test the scalability of this problem. Figure 1 presents the elapsed time required to solve one SCF iteration, as the number of processors increased. Calculations were performed on cluster of nine IBM RS/6000, including four WS of Model 560 (node No. 1–4) and five WS of Model 350 (node No. 5–9). From Figure 1, we see that almost linear scalability was obtained for this problem, and that the load unbalance appears at 5 processor nodes where node increases from four to five. To enhance the total throughput, we are now improving the code so as to take account of the dynamic load-balance for the future use of heterogeneous WS cluster.

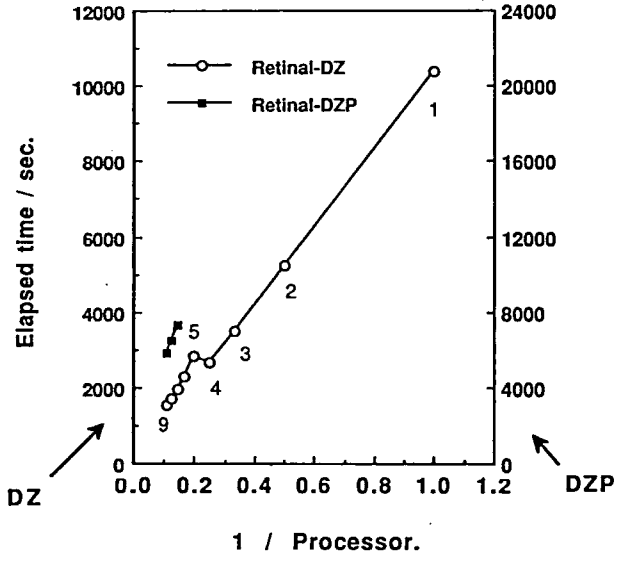


**Figure 1.** Direct SCF timings for an SCF iteration on Retinal/DZ and DZP calculations.

## VIII-A-4 Theoretical Study of Quinhydrone Complex: Cooperative Proton-Electron Transfer (PET) Mechanism

**Satoshi MINAMINO, Kazuo KITAURA, Jiro TOYODA, and Kazuhiro NAKASUJI**

The benzoquinone-hydroquinone (1:1) complex (quinhydrone) is a DA-type CT-complex which exists as one-dimensional hydrogen bonded networks. The vibrational spectra under high pressure condition suggested a proton-electron transfer (PET) takes place coorperatively to give semiquinone radical. To clarify this type of PET mechanism (Figure 1) at the molecular level, we have carried out ab initio UHF calculations on cluster models with 3-21G* basis set. We have calculated the equilibrium structures and energies along the reaction path of hydroquinone-benzoquinone complex and semiquinone dimer. Our results support cooperative PET rather than simple mechanism caused by hydride shifts.

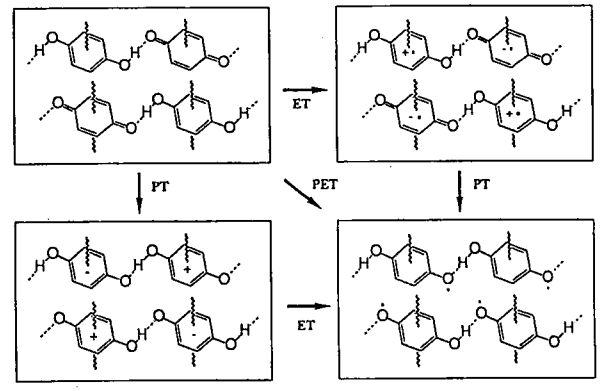


**Figure 1.** Sequential and direct proton-electron transfer (PET) models for Quinhydrone crystal.

## VIII-A-5 Theoretical Study on Binding Enthalpies and Populations of Isomers of $Cl^-(H_2O)_n$ Clusters at Room Temperature

**Toshio ASADA*, Kichisuke NISHIMOTO*, and Kazuo KITAURA** *(*Osaka City Univ.)*

[*J. Phys. Chem.*, **97**, 7724 (1993)]

Monte Carlo simulations were performed for $Cl^-(H_2O)_n$(n=1–8) at room temperature. New potential functions for the systems were generated, which well reproduced ab initio intermolecular interaction energies. The calculated enthalpy changes were in reasonable agreement with the experiments. We found that the population of ion-centered structure (IC) was larger than that of pyramidal structure (PY) at 300 K, though the former was energetically less stable than the latter. PY gains hydrogen bonding energy between the coordinated water molecules by about 2 kcal/mol per bond. While IC is entropy-favored, since it has large vibrational density of states due to low frequency modes. The enthalpy change was calculated for $Cl^-(H_2O)_2+H_2O \rightarrow Cl^-(H_2O)_3$ by a Partition function. The result suggests that the enthalpy change has large temperature dependence below 150K (Figure 1).

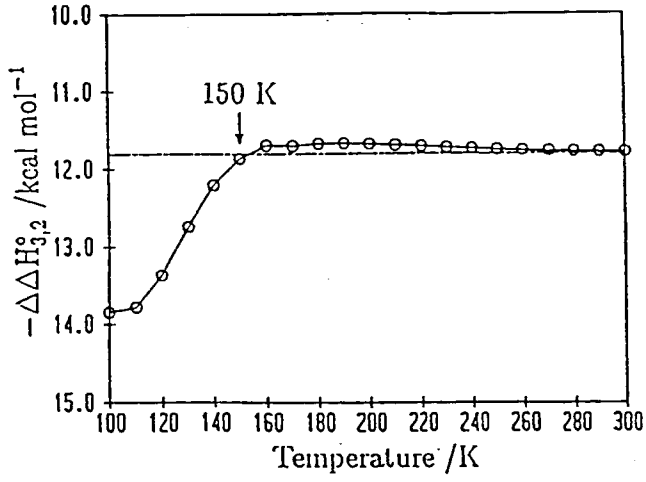


**Figure 1.** Temperature dependence of the enthalpy change for the reaction $Cl^-(H_2O)_2+H_2O \rightarrow Cl^-(H_2O)_3$. Experimental data at standard conditions (dash-dotted line) and calculated data (solid line) are shown.

# Chemical Materials Center

## VIII—B Preparation and Properties of Novel Heterocyclic Compounds

Heterocycles containing sulfur or nitrogen atoms are useful as components of organic conductors because heteroatoms in their rings are helpful to stabilize ions or ion-radical species, and extended $\pi$-conjugation decreases Coulombic repulsion. In addition intermolecular interactions caused by heteroatom contacts can be expected to form unique molecular assemblies. In this project novel electron acceptors and donors based on heterocycles such as 1,2,5-thiadiazole and 1,3-dithiole were synthesized and their properties including those of the charge-transfer complexes or ion-radical salts were investigated. Thiophene derivatives were also prepared and led to new types of polythiophenes by electrochemical oxidation.

### VIII-B-1 Preparation and Properties of Bis[1,2,5]thiadiazolo-*p*-quinobis(1,3-dithiole) and Its Derivatives. Novel Organic Semiconductors

**Yoshiro YAMASHITA, Shoji TANAKA, Kenichi IMAEDA, Hiroo INOKUCHI, and Mizuka SANO*** *(*International Christian Univ.)*

[*J. Org. Chem.*, **57**, 5517 (1992)]

Bis[1,2,5]thiadiazolo-*p*-quinobis(1,3-dithiole) (BTQBT) (**1a**) and its derivatives **1b-f** were prepared by using a Wittig-Horner reaction. The conductivity of BTQBT was good as a single component, while those of the derivatives **1b-f** were poorer. This fact indicates that the unique crystal structure of BTQBT involving a sheet-like network by short S---S contacts is needed for the good conductivity. The selenadiazolo analogues TSQBT **2a** and BSQBT **2b** were also prepared. They have isomorphous structures with BTQBT, and the conductivities were a little higher than that of BTQBT due to the stronger intermolecular interactions caused by the selenium atom.

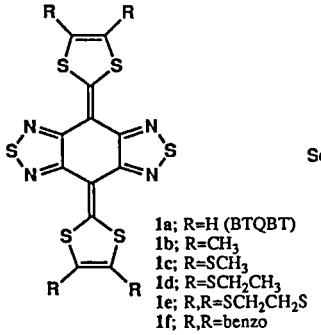

1a; R=H (BTQBT)
1b; R=$CH_3$
1c; R=$SCH_3$
1d; R=$SCH_2CH_3$
1e; R,R=$SCH_2CH_2S$
1f; R,R=benzo

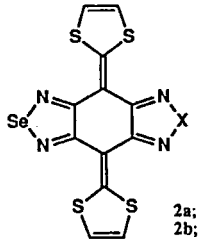

2a; X=S (TSQBT)
2b; X=Se (BSQBT)

### VIII-B-2 Single Component Organic Conductors Based on Neutral Radicals Containing the Pyrazino-TCNQ Skeleton

**Yoshiaki TSUBATA*, Takanori SUZUKI*, Tsutomu MIYASHI*, and Yoshiro YAMASHITA** *(*Tohoku Univ.)*

[*J. Org. Chem.*, **57**, 6749 (1992)]

Pyrazino-TCNQ **1a** prepared from 5,8-diiodoquinoxaline was a strong electron acceptor giving highly conductive complexes. Substituted derivatives **1b-g** were also prepared from 3,6-diiodo-1,2-phenylenediamine as a common intermediate. Neutral radicals **2d-g** derived from the corresponding pyridyl-substituted derivatives **1d-g** are open-shell donor-$\pi$-acceptor systems with high electrical amphotericity designed as a new motif for single-component organic conductors. The oxidation and reduction potentials of **2f** were observed at +0.33 V and −0.22 V vs. SCE, respectively, and the powder conductivity was as high as $3.2\times10^{-5}$ S $cm^{-1}$.

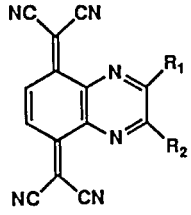

1

a: $R_1 = R_2 = H$
b: $R_1 = R_2 = Me$
c: $R_1 = R_2 = Ph$
d: $R_1$ = 2-pyridyl, $R_2 = H$
e: $R_1$ = 3-pyridyl, $R_2 = H$
f: $R_1$ = 4-pyridyl, $R_2 = H$
g: $R_1 = R_2$ = 2-pyridyl

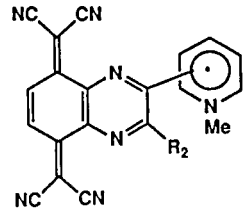

2

### VIII-B-3 Molecular Recognition through C-H · · O Hydrogen Bonding in Charge-Transfer Crystals: Highly Selective Complexation of 2,4,7-Trinitrofluorenone with 2,6-Dimethylnaphthalene

**Takanori SUZUKI*, Hiroshi FUJII,* Tsutomu MIYASHI*, and Yoshiro YAMASHITA** *(*Tohoku Univ.)*

[*J. Org. Chem.*, **57**, 6744 (1992)]

Treatment of a dimethylnaphthalene (DMN) isomer mixture with 2,4,7-trinitrofluorenone (TNF) resulted in the predominant formation of 2,6-DMN · TNF (1:1) complex accompanied by a small amount of 2,7-DMN · TNF (1:1). X-Ray structural analyses of these charge-transfer crystals showed that coplanar "ribbon"-like networks are formed by C-H ··· O hydrogen bonding of TNF. The 2,6-DMN complex is thermodynamically more stable than the 2,7-DMN complex due to the larger interactions through C-H ··· O contacts. This complexation was applied to separate pure 2,6-DMN from a DMN isomer mixture.

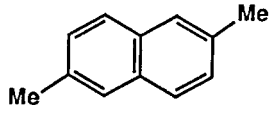

2.6-DMN

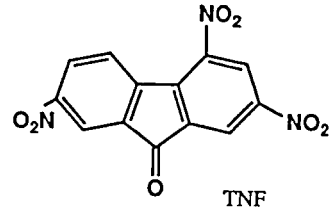

TNF

## VIII-B-4 Crystal Structure of Cation-Radical Salts of a Bis(1,3-dithiole) Donor Containing a 1,2,5-Thiadiazole Unit

**Yoshiro YAMASHITA and Shoji TANAKA**

[*Chem. Lett.*, 73 (1993)]

A bis(1,3-dithiole) compound **1** containing a fused 1,2,5-thiadiazole ring gave highly conductive cation-radical salts as single crystals ($\sigma$/S cm$^{-1}$ at room temperature, $ClO_4$ salt; 16, $BF_4$ salt; 23, $PF_6$ salt; 110, $AsF_6$ salt; 68) whose molar ratios are all 2:1. The $PF_6$ and $AsF_6$ salts showed metallic temperature dependence of conductivities down to 100 K, while the $ClO_4$ and $BF_4$ salts showed semiconductive behaviors. X-Ray analyses of $PF_6$ and $BF_4$ salts reveal that the $PF_6$ salt has a uniform stacking of donor molecules, while the $BF_4$ salt has a dimeric structure. This result indicates that a uniform stacking is essential for occurrence of a metallic property in one-dimensional conductors.

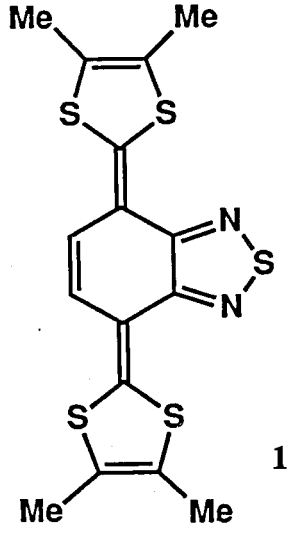


1

## VIII-B-5 Benzidine Type Electron Donors Fused with 1,2,5-Chalcogenadiazole Units

**Takanori SUZUKI*, Tsuneyuki OKUBO*, Akihisa OKADA*, Yoshiro YAMASHITA, and Tsutomu MIYASHI*** *(*Tohoku Univ.)*

[*Heterocycles*, **35**, 395 (1993)]

The title electron donors **1** and **2** were prepared from 4-bromo-7-dialkylaminobenzo[c][1,2,5]thiadiazole. They are electrochemically amphoteric (for instance, the oxidation and reduction potentials of **1a** were observed at +0.56 and −1.50 V vs. SCE in DMF, respectively). The absorption maxima in the 500−550 nm region were assigned to the intramolecular charge-transfer (CT) bands. The X-ray analyses of **1b** and $\mathbf{1b}^+ \cdot PF_6^-$ revealed that the twisted geometry of **1b** became planar upon one-electron oxidation, and a coplanar ribbon-like network was formed by S---N interactions in the crystal of the cation-radical salt.

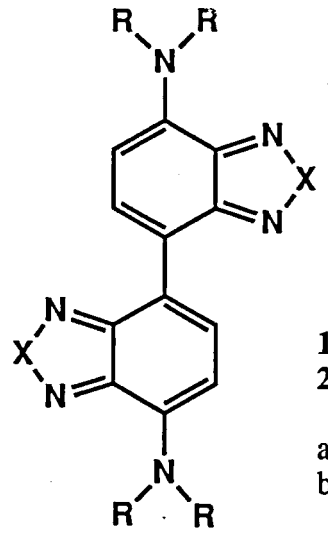


1; X=S
2; X=Se

a; R=Me
b; R,R= -$(CH_2)_4$-

## VIII-B-6 2,2′-(Cyclopenten-3,5-diylidene)bis(1,3-dithiole)s: Novel Electron Donors Undergoing Deprotonation by Oxidation

**Yoshiro YAMASHITA, Shoji TANAKA, and Masaaki TOMURA**

[*J. Chem. Soc., Chem. Commun.*, 652 (1993)]

The title bis(1,3-dithiole) donors **1** containing a dimethylenecyclopentene skeleton were prepared by a Wittig-Horner reaction of the corresponding carbanions derived from the phosphonate esters of 1,3-dithioles with cyclopen-4-ene-1,3-dione. The cyclic voltammograms (CV) of the donors showed irreversible waves and the cathodic peaks were observed at very low potentials, indicating that during the CV measurements some reaction occurred to give products which have reduction potentials at the observed positions. The products **2** could be isolated by oxidation with $NOBF_4$ in high yields. The formation of the cations **2** can be explained by deprotonation from the dication states of **1** whose acidity becomes high. The cations are interesting ones which have a resonance contribution of **2′** and show intense absorptions in the long wavelength region due to intramolecular charge transfer.

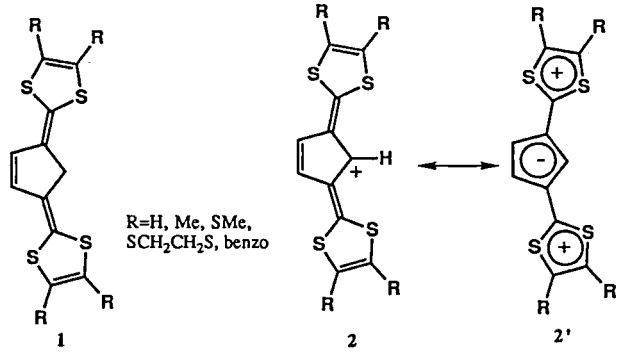


## VIII-B-7 Preparation and Properties of 7-(1,3-dithiol-2-ylidene)-7H-cyclopenta[1,2-b;4,3-b′]dithiophenes and Their Polymers

**Masatoshi KOZAKI, Shoji TANAKA, and Yoshiro YAMASHITA**

[*Chem. Lett.*, 533 (1993)]

The title 1,3-dithiole compounds **1** were synthesized using a Wittig-Horner reaction from the corresponding ketone. The X-ray analysis of the parent compound **1a** revealed that **1a** has a planar structure with both inter- and intramolecular short S---S contacts. The molecules of **1a** are uniformly stacked along the *b* axis with good overlapping. The electrochemical oxidation of **1** gave polythiophene derivatives **2** which have lower oxidation potentials than polythiophene. The conductivity of **1a** was $3.5\times10^{-3}$ in the doping state. The superficial morphology observed by a scanning electron microscope was very smooth.

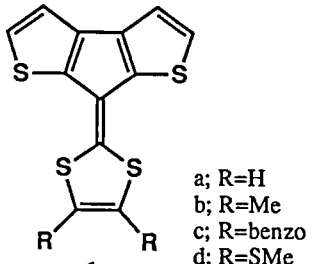

1

a; R=H
b; R=Me
c; R=benzo
d; R=SMe
e; R=$CO_2Me$

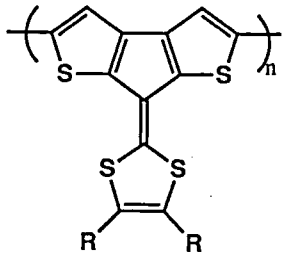

2

## VIII-B-8 Synthesis and Characterization of Poly(4,7-dithienylthieno[3,4-b]pyrazine). A New Small Band Gap Heterocyclic Copolymer

**Shoji TANAKA, Masaaki TOMURA, and Yoshiro YAMASHITA**

Heterocyclic conjugated copolymers with alternate aromatic-qunonoid and/or donor-acceptor moieties in the main chain have been predicted to be promising candidates for narrow bandgap organic materials. In order to establish the structure-bandgap relationship for polymers of this category, we have synthesized the title copolymer **2a** and compared the properties with those of the isoelectronic system **2b**.[1] The X-ray structural analysis revealed that molecule **1a** is planar. In contrast MNDO-PM3 calculations predict a nonplanar structure for **1b**. The momoner **1a** has an $E_{p,a}$ of +0.99 V and an $E_{p,c}$ of −1.20 V *vs.* SCE, and afforded the electroactive polymer **2a** by anodic oxidation. The $\pi$-$\pi^*$ absorption of the neutral state of **2a** ($\lambda_{max}$=734 nm, $E_{gap}\approx1.0$ eV) appears at significantly lower energy region compared with that of the isoelectronic system **2b** ($\lambda_{max}$=534 nm, $E_{gap}\approx1.7$ eV). The smaller bandgap of **2a** can be attributed to the higher coplanarity of the polymer backbone with respect to **2b**. Polymer **2a** remains stable to n-doping as well as p-doping after repeated anodic and cathodic scans, whereas polymers based on benzo[c]thiophene reported previously are unstable in the n-doping state. The bandgap value estimated from the difference in the threshold potentials for p- and n-doping of **2a** is in agreement with that obtained from the spectral data.

**Reference**

1) S. Musmanni and J. P. Ferraris, *J. Chem. Soc., Chem. Commun.*, 172 (1993).

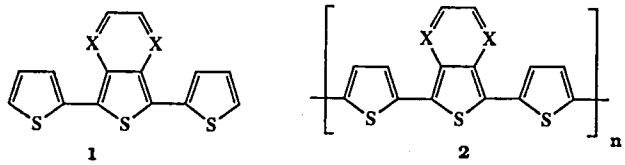

1 2

a: X=N b: X=CH

## VIII-B-9 Synthesis, Structure, and Properties of the Novel Conducting Dithiolato-metal Complexes Having Dicyanopyrazine Moieties

**Masaaki TOMURA, Shoji TANAKA, and Yoshiro YAMASHITA**

Recently dithiolato-metal complexes have received much attention as molecular conductors and molecular superconductors. We have synthesized the novel metal complexes from 2,3-dicyano-5,6-dimercaptopyrazine ($H_2$dcdmp) ligand which may enhance intermolecular interactions in the solid state by S···N heteroatom contacts. The Ni complex, $(n\text{-}Bu_4N)_2$ [Ni(dcdmp)$_2$] and Pd complex, $(n\text{-}Bu_4N)_2$ [Pd(dcdmp)$_2$] were prepared by a one-pot reaction of 2,3-dichloro-5,6-dicyanopyrazine with $Na_2S$, $NiCl_2$ or $PdCl_2$, and $n\text{-}Bu_4NBr$ in acetone. The first oxidation potential of the Ni complex ($E^{ox}_{1/2}$=+0.52 V vs. SCE, in $CH_3CN$) is considerably higher than that of $(n\text{-}Bu_4N)_2$[Ni(dmit)$_2$] ($E^{ox}_{1/2}$=−0.15 V).[1] Metathesis of $(n\text{-}Bu_4N)_2$[M(dcdmp)$_2$] (M=Ni, Pd) with $(TTF)_3(BF_4)_2$ in an acetonitrile solution by the diffusion method gave $(TTF)_5$[M(dcdmp)$_2$]$_2$ as black brown needles. Electrical conductivities of these complexes at room temperature were $8.3\times10^{-2}$ (M=Ni) and $9.1\times10^{-3}$ (M=Pd) S cm$^{-1}$, respectively. Temperature dependance of the conductivity shows that these complexes were semiconductors with small activation energies (M=Ni; $E_a$=0.067 eV, M=Pd; $E_a$=0.084 eV). The X-ray structural analysis of $(TTF)_5$[Pd(dcdmp)$_2$]$_2$ indicates that the intermolecular S···N and S···S contacts within the sum of van der Waals radii exist in the crystal, as shown in Figure 1. Two Pd(dcdmp)$_2$ molecules and one TTF molecule form mixed stacks along the c axis, and other TTF molecules stack along the b axis.

**Reference**

1) G. Steimecke, H-J. Sieler, R. Kirmse, and E. Hoyer, *Phosphorus and Sulfur*, **7**, 49 (1979).

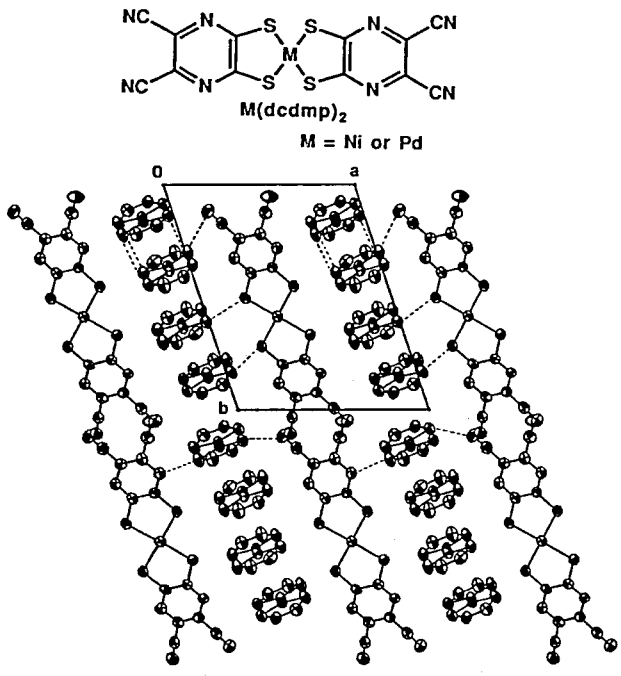


**Figure 1.** Crystal structure of $(TTF)_5[Pd(dcdmp)_2]_2$ viewed along the c axis. The dotted lines show intermolecular heteroatom contacts within the sum of van der Waals radii.

# Instrument Center

## VIII—C Studies of Solvated Metal Clusters

Solvated metal ions and metal cluster ions afford a particularly interesting collection of systems for study because they bridge the gap between bare, isolated ions and ionic solids and electrolyte solutions. From the point of view of cluster chemistry, the question of charge delocalization, the formation of solvation shells, and the interaction of solvent with metal surfaces appear especially attractive.

In this project we investigate the photoionization, photodissociation, and chemical reaction processes of various kinds of solvated metal atom (ion) clusters to unveil the microscopic aspect of solvation.

### VIII-C-1 Photodissociation Spectra of $Ca^+(H_2O)_n$ for $n$=1–4

**Masaomi SANEKATA, Fuminori MISAIZU, and Kiyokazu FUKE**

Photodissociation spectra of size-selected $Ca^+(H_2O)_n$ ($n$=1–4) have been examined in the wavelength region from 335 nm to 720 nm using a reflectron mass spectrometer. As in the case of $Mg^+(H_2O)_n$,[1] the dissociation process of $Ca^+(H_2O)_n$ was found to be not only the simple evaporation of water molecules but also the photoinduced intracluster reaction including the hydrogen atom elimination. The dissociation spectra were obtained by plotting the total yield of fragment ions ($Ca^+(H_2O)_m$ and $CaOH^+(H_2O)_m$) as a function of wavelength.

Figure 1 shows the dissociation spectra of $Ca^+(H_2O)_n$ for $n$=1–4. As for $n$=1 and 2, the theoretical transition energies[2] are also indicated by bars. The ground state of the $Ca^+(H_2O)$ ion has a planar structure with $C_{2v}$ symmetry. Upon the complex formation, the $^2P$ atomic ion level of calcium (25303 $cm^{-1}$) splits into the three states: the transition energies for these states were calculated to be 21300 $cm^{-1}$ ($^2B_2$), 23100 $cm^{-1}$ ($^2B_1$) and $<$29600 $cm^{-1}$ ($^2A_1$),[2] and agree well with the observed band positions. The cross sections for $n \geqq 2$ exhibit large redshifts with the increase of $n$: The amounts of redshifts are 0.4 eV for $n$=1, 0.66 eV for $n$=2, 1.0 eV for $n$=3, and $>$1.8 eV for $n$=4 with respect to the $Ca^+$ resonance line, respectively. In the case of $Mg^+(H_2O)_n$, the spectra show a clear evolution of solvation shell closing at $n$=3,[1] and for larger clusters, the spectra do not change appreciably. In contrast, the band positions of $Ca^+(H_2O)_n$ decrease monotonically with increasing $n$ and show no indication of the shell closing. These results seem to consistent with the prediction of the Monte Carlo calculations, which presents that the first shell around the $Ca^+$ ion closes with five and/or six water molecules.[3] The other reason of the observed large redshifts may be a change in the bonding character of the excited state to an ion-pair character $[Ca^{2+}(H_2O)_n^-]$ as was proposed for $Sr^+(NH_3)_n$. This issue and the dynamics of the photoinduced reaction are currently under investigation in our laboratory.

**References**

1) F. Misaizu, M. Sanekata, K. Tsukamoto, K. Fuke, and S. Iwata, *J. Phys. Chem.* **96**, 8259 (1992).

2) C.W. Bauschlicher, Jr., M. Sodupe, and H. Partridge, *J. Chem. Phys.* **96**, 4453 (1992).
3) E. Kochanski and E. Constantin, *J. Chem. Phys.* **87**, 1661 (1987).

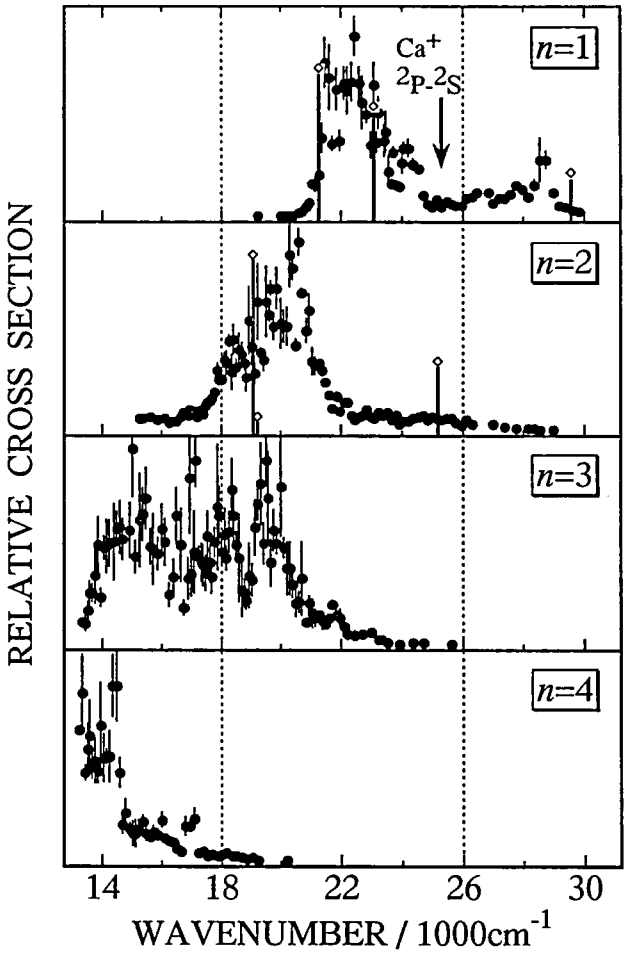


**Figure 1.** Photodissociation spectra of $Ca^+(H_2O)_n$ ($n$=1–4). The intensities of the spectra are normalized at their peak positions.

## VIII-C-2 Photodissociation Study on $Mg^+(H_2O)_n$, $n$=1–5: Electronic Structure and Photoinduced Intracluster Reaction

**Fuminori MISAIZU, Masaomi SANEKATA, Kiyokazu FUKE, and Suehiro IWATA** *(Keio Univ.)*

[*J. Chem. Phys.*, in press]

Photodissociation spectra of $Mg^+(H_2O)_n$ ($n$=1–5) cluster ions were examined in the wavelength region from 720 to 250 nm by monitoring the total yield of the fragment ions. The absorption bands exhibit redshifts as large as 17000 $cm^{-1}$ and were explained by the shift of the $^2P$-$^2S$ transition of the free $Mg^+$ ion. The spectra also exhibit clear evolution of solvation shell and the first shell closing with $n$=3, being consistent with the theoretical prediction. The mass spectra of the fragment ions show the existence of two dissociation processes: the evaporation of water molecules and the photoinduced intracluster reaction to produce $MgOH^+(H_2O)_m$. The branching fraction between the two processes depends strongly on the solvent number $n$ and also on the photolysis wavelength as shown in Figure 1. As for $Mg^+(H_2O)$, the branching fraction of this reaction is independent of the photolysis energy and the reaction seems to take place on the ground-state surface. In contrast, the reaction cross sections for $Mg^+(H_2O)_2$ depend on the photolysis energy and show a strong enhancement at the energy above 28600 $cm^{-1}$, which corresponds to the onset energy of the transition to the $2^2B$ state. This result as well as the results of the laser-fluence-dependence experiment suggests that the reaction proceeds directly through the $2^2B$ state and probably also through $2^2A$. The $Mg^+(H_2O)_3$ ion exhibits the similar tendency for the fraction of the reaction products and its reaction mechanism is discussed in line with those for $n$=2. For larger clusters, the fractions of reaction products are independent of the photolysis energy. One of the possible reasons may be that the rapid increase of internal conversion rate enhanced by the second shell water molecule suppresses the excited state channel.

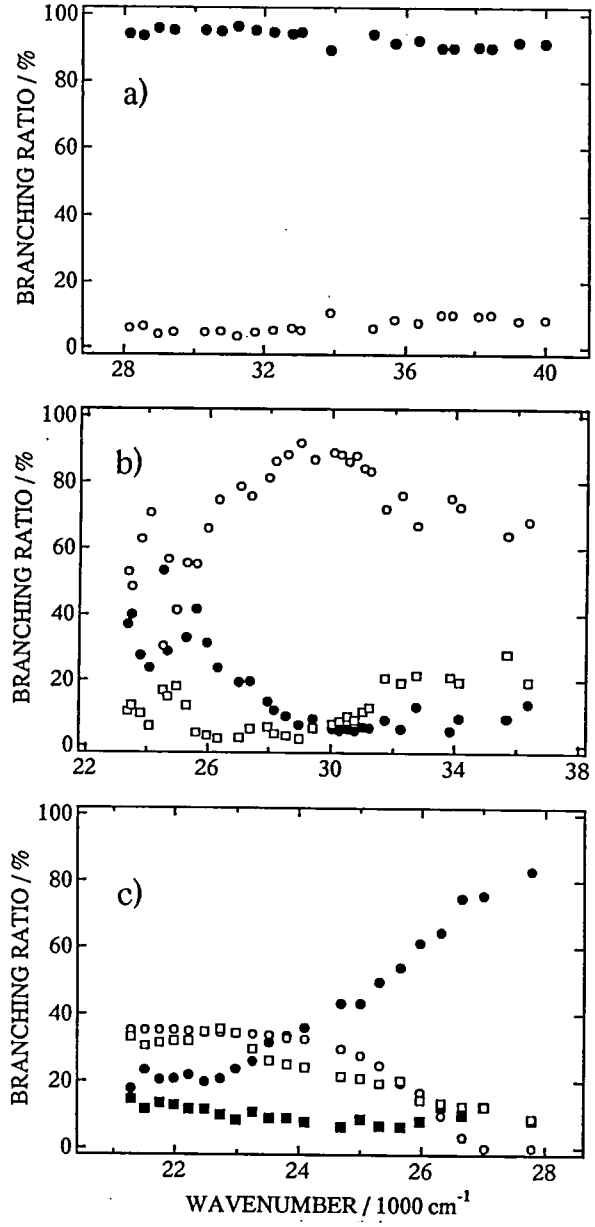


**Figure 1.** Branching ratios of the fragment ions produced by the photodissociation of $Mg^+(H_2O)_n$ ions. a) $n$=1. ●: $MgOH^+$ and ○: $Mg^+$. b) $n$=2. ○: $MgOH^+(H_2O)$, □: $MgOH^+$, and ●: $(Mg^+(H_2O)+Mg^+)$. c) $n$=3. ■: $Mg^+(H_2O)$, □: $Mg^+(H_2O)_2$, ●: $MgOH^+(H_2O)$, and ○: $MgOH^+(H_2O)_2$.

## VIII-C-3 Kinetic Energy Dependence on the Reaction between $Mg^+$ Ion and $(H_2O)_n$ Clusters

**Masaomi SANEKATA, Fuminori MISAIZU, and Kiyokazu FUKE**

Recently we found that both $Mg^+(H_2O)_n$ and $MgOH^+(H_2O)_{n-1}$ ions are formed with characteristic size distribution in a pick-up type cluster source: For $1 \leqq n \leqq 5$ and $n \geqq 15$, $Mg^+(H_2O)_n$ are dominant, while $MgOH^+(H_2O)_{n-1}$ is exclusively observed for $6 \leqq n \leqq 14$.[1] To gain further insight into this issue, we investigated the kinetic energy (KE) dependence on the product ions for the reaction between $Mg^+$ and $(H_2O)_n$ using a crossed beam assembly. The $Mg^+$ ions produced by a laser vaporization source were guided by ion optics and was crossed perpendicularly with the water cluster beam. The product ions were collimated by a skimmer and analyzed by a reflectron-type time-of-flight mass spectrometer.

Figure 1 shows the KE-dependence on the mass spectrum of the product ions. At lower KE, the mass distribution is the same as that produced by the cluster source mentioned previously. This result clearly shows that $MgOH^+(H_2O)_n$ reported previously[1] is formed not by direct evaporation of $MgOH^+$ from the metal rod but by an H-atom elimination reaction in the nascent $Mg^+(H_2O)_n$ ions. Large clusters disappear with increasing KE of $Mg^+$, indicating the enhancement of evaporation by an excess energy deposited in the nascent cluster ions. The critical size for the transition to metal-hydroxide clusters does not change within the present KE range: the result is consistent with the previous prediction that the transition occurs due to the difference in the hydration energies between $Mg^+(H_2O)_n$ and $MgOH^+(H_2O)_n$.[2] A possible explanation for the occurrence of second transition (at $n$=15) may be the stabilization of solvated ion-pair state such as $Mg^{2+}(H_2O)_n^-$. For the clusters as large as $n$=15, the ion-pair state may become thermodynamically more stable than $MgOH^+(H_2O)_n$ and, as a result, the reaction is expected to be suppressed. We plan further experiments at the energy lower than 20 eV to elucidate the contribution of the ion-pair state.

**References**

1) F. Misaizu, M. Sanekata, K. Tsukamoto, K. Fuke, and S. Iwata, *J. Phys. Chem.* **96**, 8259 (1992).
2) F. Misaizu, M. Sanekata, K. Fuke, and S. Iwata, *J. Chem. Phys.*, in press.

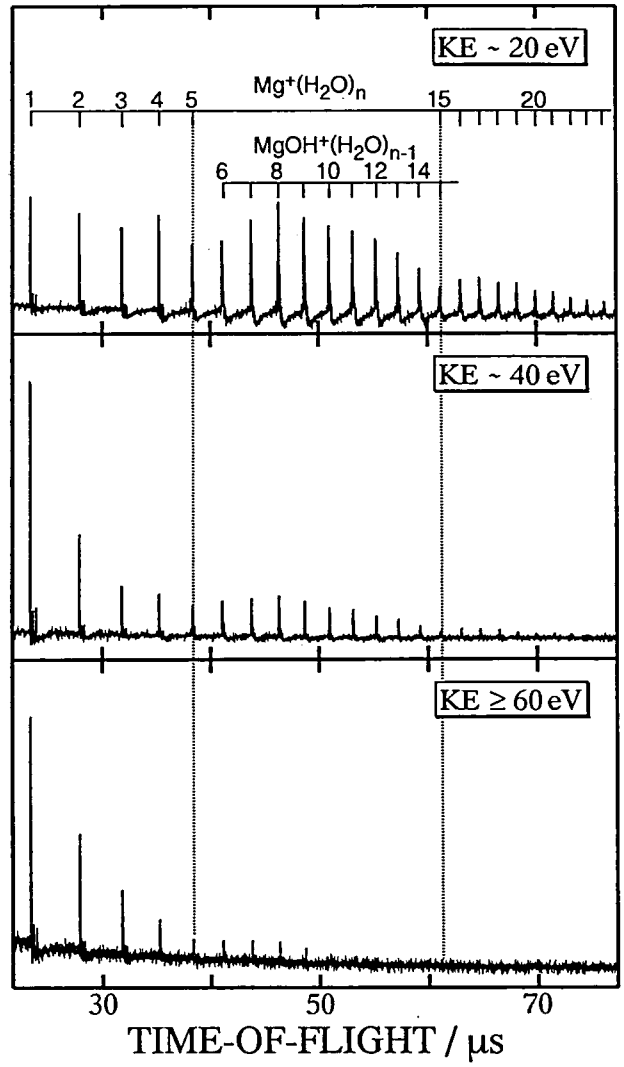


**Figure 1.** Kinetic energy dependence on the mass spectrum of the product ions for the reaction between $Mg^+$ and water clusters.

## VIII-C-4 Photoionization and Photodissociation Studies on Aluminum-Water Clusters and Their Ions

**Fuminori MISAIZU, Keizo TSUKAMOTO, Masaomi SANEKATA, and Kiyokazu FUKE**

[*Z. Phys. D* **26**, S177 (1993)]

Clusters of aluminum atoms solvated with water molecules, $Al(H_2O)_n$, have been studied by one-photon ionization and time-of-flight mass spectroscopy. Characteristic feature was observed in the photoionization mass spectrum: The intensities of the product $Al^+(H_2O)_n$ ions are about one order of magnitude larger for $n \leqq 4$ than for $n \geqq 5$. The ionization potentials were determined for $n$ up to 4. The obtained results are discussed in connection with the recent theoretical works.[1] The photodissociation spectroscopy has also been applied to the $Al^+(H_2O)_n$ ions with $n$=1–10. The observed spectra were ascribed to the transition localized on the $Al^+$ ion in comparison with the recent theoretical work on the structure and stability of these ions.

**Reference**

1) H. Watanabe, M. Aoki, and S. Iwata, *Bull. Chem. Soc. Jpn.*, **66**, 3245 (1993).

## VIII-C-5 Construction of a Magnetic-Bottle Photoelectron Spectrometer for the Study of Mass-Selected Negative Cluster Ions

**Fuminori MISAIZU, Keizo TSUKAMOTO, Masaomi SANEKATA, and Kiyokazu FUKE**

Negative ion photoelectron spectroscopy serves information not only about the stability of the ions but also on the excited electronic states of a neutral molecule. This technique is also useful to study the electronic structures of the neutral clusters size-specifically. Especially for solvated metal atom clusters, such studies provide microscopic informations about the interaction between the solute atomic ion and the solvent molecules. For this purpose, we have constructed a new apparatus as depicted in Figure 1.

Negative cluster ions were produced by laser vaporization method. Occasionally, the density of the negative ions can be increased by additional electron beam source equipped in front of the nozzle source. The negative ions were accelerated to ca. 750 eV at right angles by pulsed electric fields and were mass-selected in a time-of-flight mass spectrometer. After flying 50 cm, ions with a given mass-to-charge ratio were selected with a pulsed mass gate, and were decelerated to less than 100 eV with a pulsed potential switching method. Decelerated ions were focused with Gustafsson-Lindholm-type electrostatic lenses to the detachment region where the ions were irradiated with a detachment laser at right angles. The magnetic bottle photoelectron spectrometer has an advantage to collect almost all of the electrons emitted over $4\pi$ steradian with magnetic fields produced by a combination of a strong field magnet near the detachment region and a weak field solenoid at the electron flight tube. Under the condition that the magnetic fields of the detachment region and in the flight tube are set about 400 G and 2 G, respectively, detached photoelectrons are found to be detected efficiently and the resolution of the photoelectron spectra is less than 200 meV for the $Cu^-$ ion detachment as shown in VIII-C-6.

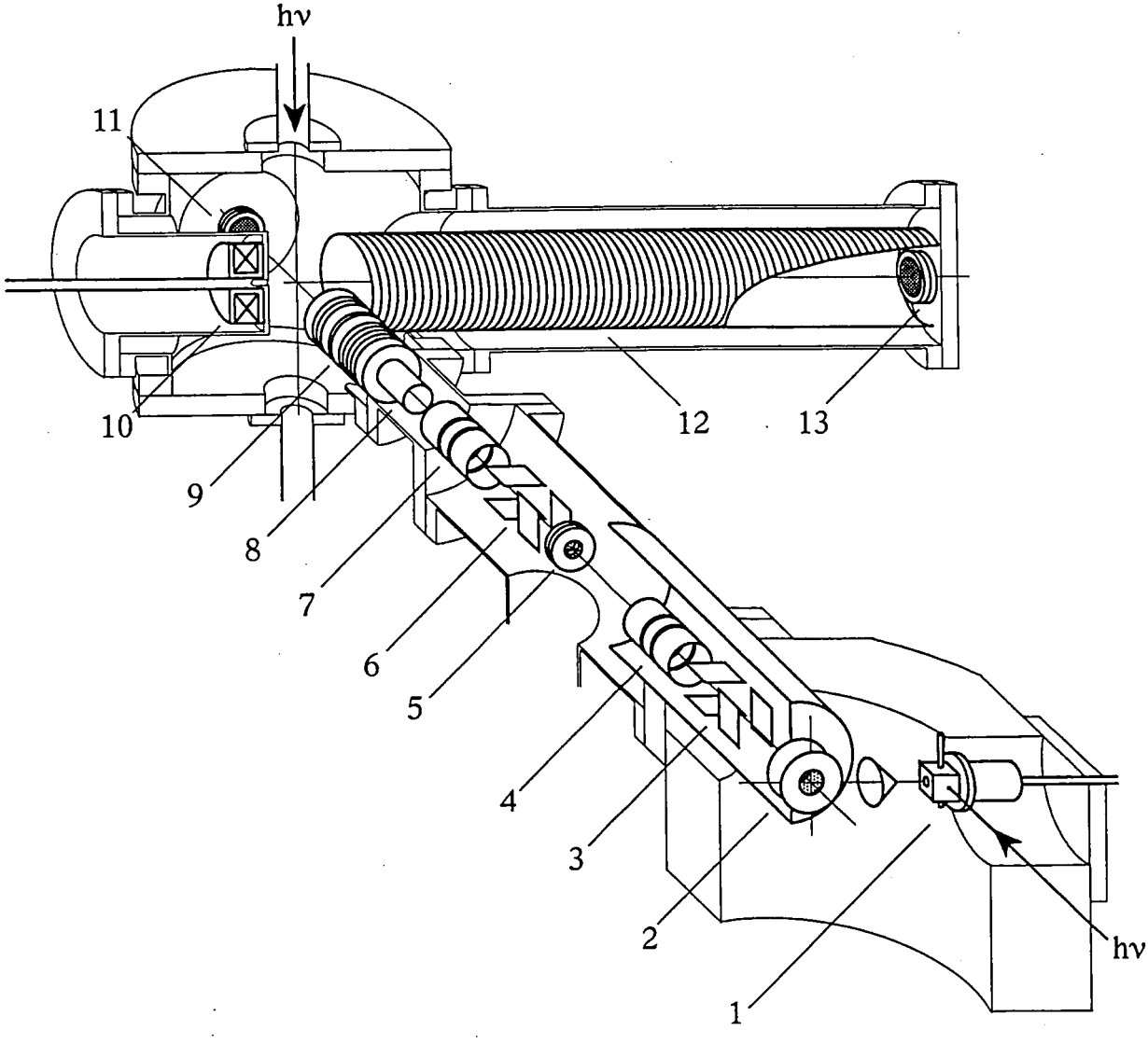


**Figure 1.** Schematic drawing of the apparatus. 1: cluster beam source, 2: acceleration plates, 3,6: deflectors, 4,7: einzel lenses, 5: pulsed mass gate, 8: potential switch, 9: deceleration lenses, 10: pulsed solenoid, 11: ion detector, 12: guiding solenoid, 13: electron detector.

### VIII-C-6 Photoelectron Spectroscopy of $Cu(H_2O)_n^-$ Cluster Anions

**Fuminori MISAIZU, Keizo TSUKAMOTO, Masaomi SANEKATA, and Kiyokazu FUKE**

Negative-ion photoelectron spectroscopy has been applied in order to obtain size dependent information about the electronic structures of clusters of metal atoms solvated with polar molecules. In the present work, we have investigated photoelectron spectra of $Cu(H_2O)_n^-$ cluster ions with $n$=0–3. Cluster negative ions were directly produced by laser vaporization and were mass selected in a time-of-flight (TOF) mass spectrometer. After decelerating the ions by a potential switching method, the negative ions were irradiated with a detachment laser pulses: the third harmonic of a Nd:YAG laser, 355 nm, was used for the detachment. Detached electrons were collected by a magnetic bottle photoelectron spectrometer and the photoelectron spectra were obtained by the TOF measurement of the electrons. Figure 1 shows the photoelectron spectra of $Cu(H_2O)_n^-$ with $n$=0–3. The ground state of the $Cu^-$ ion is in the $^1S(3d^{10}4s^2)$ state and thus the $s$ and $d$ electron detachment to produce $^2S(3d^{10}4s^1)$ and $^2D(3d^94s^2)$ states of the Cu atom should be observed at 1.23 and 2.7 eV in the photoelectron spectrum, respectively. However, the latter transitions are hardly observed in the figure, though the former is strongly observed. For $Cu(H_2O)^-$, the lowest energy peak is found to be blue-shifted as large as 0.5 eV from that of $Cu^-$. In contrast, several peaks which probably correspond to the transitions to different electronic states of the neutral clusters are observed in the photoelectron spectra of $n$=2 and 3. For $Cu(H_2O)_2^-$, the lowest energy peak lies at 1.4 eV and intense peaks are observed around 2.1 eV. For $n$=3, the first band has a peak at 2.3 eV and the second band shows narrow peaks at 2.5 eV. Electron affinities of the Cu atom and the $H_2O$ molecule are reported to be 1.23 and 0 eV, respectively. Therefore, the observed spectral shifts are considered to be due to the stabilization of $Cu^-$ by the solvation of water molecules.

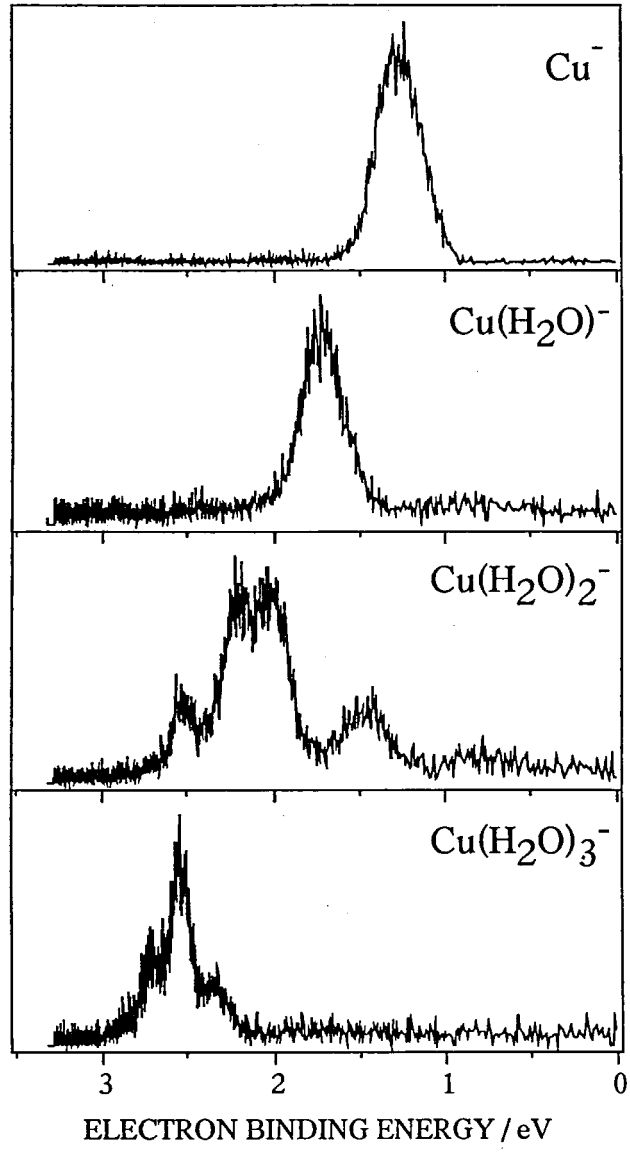


**Figure 1.** Photoelectron spectra of $Cu(H_2O)_n^-$ ($n$=0–3). Third harmonic of a Nd:YAG laser (355 nm, 3.49 eV) was used for electron detachment.

## VIII—D Physical Properties of Semiconductor Clusters

The study of structures and properties of small elemental clusters has been an extremely active area of current research. Particularly, the covalently bonded semiconductor clusters such as silicon and germanium clusters have attracted considerable attention. In the past several years a considerable amount of experimental and theoretical efforts has been expended in the study of these clusters, but the complexity and variety of bonding modes that exist in these clusters have not been recognized. To gain further insight on the physical properties of semiconductor clusters, we have studied the photoionization process of these clusters.

### VIII-D-1 Near Threshold Photoionization of Silicon Clusters in the 248-146 nm Region: Ionization Potentials for $Si_n$

**Kiyokazu FUKE, Keizo TSUKAMOTO, Fuminori MISAIZU, and Masaomi SANEKATA**

[*J. Chem. Phys.*, **99**, 7807 (1993)]

Photoionization thresholds for $Si_n$ ($n$=2–200) have been examined with an unprecedentedly wide photoionization energy (5.0–8.5 eV) using a laser photoionization-time-of-flight mass spectrometry. A high-output vacuum ultraviolet (VUV) laser was used as the ionization light source in the energy above 6.42 eV (ArF laser), in addition to the second harmonic of an excimer-pumped dye laser in the region below this energy. In Figure 1, the results of ionization potentials (IPs) are plotted against $n^{-1/3}$, which is based on a classical conducting spherical droplet (CSD) model. A characteristic size dependence of IPs was found for $n$<22, featuring major maxima at $n$=10 and 20. The rather high IP of $Si_{10}$ in comparison with its neighbors is consistent with

the results of the collision-induced-dissociation study of $Si_n^+$. We also found a large gap in IPs between $n$=20 and 22 (see Figure 1). This gap was ascribed to the structural transition of neutral clusters in analogy with that found recently for small silicon cluster ions: two structural isomers such as prolate and oblate forms coexist for $Si_n^+$ throughout the size range of $n$=24–34. The result in Figure 1 may suggest the growth of new isomer starting with 21 atoms for neutral clusters. The IPs for $n$=100–200 were found to be 5.0–5.17 eV, which are lower than the ionization energy but still higher than the work function of bulk Si(111) surface. This discrepancy may be due to the difference in the nature of surface states for both phases.

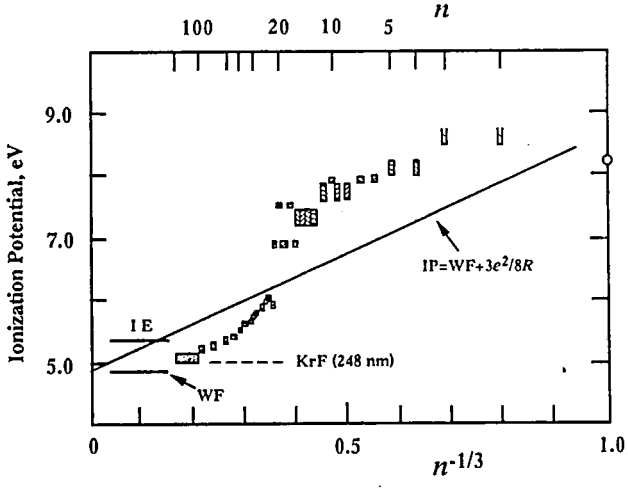


**Figure 1.** Ionization potentials of $Si_n$, $n$=2–200, plotted versus $n^{-1/3}$ and the bulk ionization energy and work function for Si(111). The solid line is the prediction of the CSD model.

### VIII-D-2 Photoionization Process of Small Germanium Clusters

**Kiyokazu FUKE, Fuminori MISAIZU, and Masaomi SANEKATA**

Photoionization process of small germanium clusters produced by a laser vaporization technique has been investigated by using an ArF excimer laser and the second harmonic of an excimer laser pumped dye laser. Figure 1 shows the typical photoionization mass spectra of $Ge_n$ recorded with 6.42-eV ionizing laser photon energy at three different fluences. At lower fluence, the signals of $Ge_n$ ($n \geqq 20$) are prominent, however, these signals are completely disappear at the laser fluence higher than 1 mJ/cm$^2$; an extensive photofragmentation of cluster ions occurs through the multiphoton absorption process. At the intermediate fluence, a characteristic size distribution was observed as shown in Figure 1b: the $Ge_n^+$ clusters with $n$=11 (10), 16(15), 23 (22), 32 (31), and 45 (44) are much abundant than its neighbors. These magic numbers suggest the special stabilities of the cluster ions. Interestingly, these numbers agree with those of $Si_n^+$ clusters, which are particularly unreactive toward $NH_3$, $O_2$, etc. These results seem to suggest the structural similarity of $Si_n^+$ and $Ge_n^+$ clusters. The laser fluence dependence of mass spectrum shows that the first germanium cluster with an ionization potential (IP) lower than 6.42 eV ArF excimer laser photon may be $Ge_{19}$. The IPs of $Ge_n$ ($n$=19–21) are 6.0–6.42 eV, while those of $n$=22–31 are 5.65–5.7 eV. The IP of $Ge_n$ as large as $n$=50 was determined to be 5.5 eV.

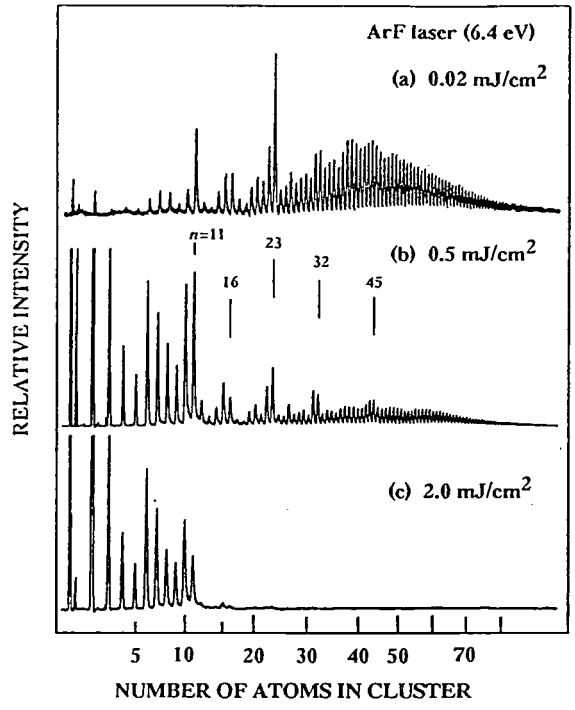


**Figure 1.** Time-of-flight mass spectra of $Ge_n$ clusters ionized by an ArF excimer laser at three different fluences.

## VIII—E Collisional Relaxation and Chemical Reaction Dynamics of the Excited Group IIB Metal Atoms

The collisional quenching and chemical reaction of electronically excited metal atoms have been the subject of extensive studies because of its importance in photophysics and photochemistry. In the present project we seek to obtain more detailed information about the reaction dynamics of the excited group IIB metal atoms.

### VIII-E-1 Nascent Rotational and Vibrational Distributions in Both Products of the Reaction: $Zn(4^1P_1)+H_2O \rightarrow ZnH(X^2\Sigma^+)+OH(X^2\Pi)$

**Kazuya KUWAHARA, Hiroyuki IKEDA, Hironobu UMEMOTO, Tohru SATO, Kazuto TAKANO, Sigeru TSUNASHIMA** *(Tokyo Inst. of Tech.)*, **Fuminori MISAIZU, and Kiyokazu FUKE**

[*J. Chem. Phys.*, **99**, 2715 (1993)]

The reaction $Zn(4^1P_1)+H_2O \rightarrow ZnH(X^2\Sigma^+)+OH(X^2\Pi)$ was studied under thermal equilibrium conditions at 700K. The nascent internal state distributions of both products, ZnH and OH, were determined by using a pump-and-probe technique. The experimental results show the preferential energy partitioning into the internal degrees of freedom. ZnH was severely excited in rotation as shown in Figure 1. The vibrational distribution of ZnH was slightly inverted and peaked at $v'=1$. In contrast, no excitation was observed in the internal motion of OH. Such a non-statistical energy partitioning into ZnH and OH was explained in terms of the abstraction mechanism through a Zn-H-OH intermediate. However, an idealized direct stripping process is ruled out. This is because a large fraction of the available energy is released in translation, which indicates the translational excitation of OH.

The upper limit of the branching ratio to produce ZnH+OH in this reaction was also determined. The relatively small ZnH yield predicts the existence of other exit channels. Considering the highly excited rotational distribution of ZnH, there must be the three-body dissociative Zn+H+OH pathway as an exit channel.

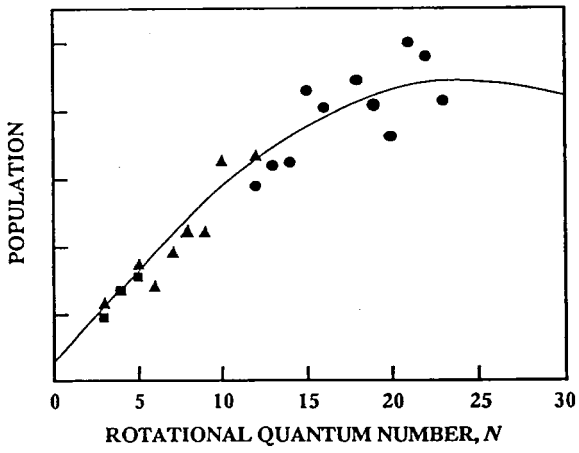


**Figure 1.** The rotational state distributions of $ZnH(X^2\Sigma^+, v'=0)$. The solid line represents the Boltzmann distribution at 12000K for the $F_1$ component. (●): $P_1$; (▲): $Q_1$; (■): $R_1$.

### VIII-E-2 Nascent Rotational State Distributions of $ZnH(X^2\Sigma^+)$ Produced in the Reactions of $Zn(4^1P_1)$ with Simple Alkane Hydrocarbons

**Hironobu UMEMOTO, Tohru SATO, Kazuto TAKANO, Sigeru TSUNASHIMA, Kazuya KUWAHARA, Kei SATO, Hiroyuki IKEDA,** *(Tokyo Inst. of Tech.),* **Fuminori MISAIZU, and Kiyokazu FUKE**

[*Chem. Phys. Lett.*, **214**, 271 (1993)]

The reactions of $Zn(4^1P_1)$ with $CH_4$, $C_2H_6$, $C_3H_8$, and $C(CH_3)_4$ were studied by employing a laser pump and probe technique. The nascent rotational state distributions of $ZnH(X^2\Sigma^+, v'=0)$ were determined. In all cases, the experimentally obtained rotational distributions could be approximated by Boltzmann distributions. These results were compared with the theoretical distributions predicted by a statistical model. The results of Boltzmann temperatures are summarized in Table 1.

As for $C(CH_3)_4$, the experimental distribution agrees well with the statistical distribution, suggesting that the reaction proceeds with a long-lived intermediate complex. The excess energy is randomized during the long lifetime. The geometry of the long-lived complex for $C(CH_3)_4$ must be an insertive one, $H\text{-}Zn\text{-}CH_2C(CH_3)_3$. The geometries of the intermediates for other hydrocarbons are also considered to be insertive, because the experimental rotational state distributions change smoothly with the size of hydrocarbons. The deviation of the experimentally obtained Boltzmann temperatures for light hydrocarbons from the theoretical results may be ascribed to that the intermediate complex for light hydrocarbons decomposes before the intramolecular vibrational redistribution.

**Table 1.** The Best-Fit Boltzmann Temperatures for the Rotational State Distributions of $ZnH(X^2\Sigma^+, v'=0)$ in K and the Available Energies in kJ/mol[a)]

| Alkane | $E_{AVL}$ | Boltzmann temperature | |
|---|---|---|---|
| | | Experimental | Prior |
| $CH_4$ | 224 | 9000 | 4100 |
| $C_2H_6$ | 243 | 5000 | 2700 |
| $C_3H_8$ | 249[b)] | 2900 | 2000 |
| $C(CH_3)_4$ | 244 | 1600 | 1600 |

a): Exothermicity + 3RT.
b): Weighted average of primary and secondary C-H bonds.

## VIII—F Studies of Ultrafine Particles

Study of the size effect of spin ordering in ultrafine particles is very interesting to know the nature of magnetic properties in finite system. Ultrafine Fe particles are produced by vacuum deposition method. The magnetic properties are studied by the static magnetic susceptibility measurement.

### VIII-F-1 Magnetic Properties of Small Fe Particles Dispersed in $SiO_2$ Film

**Masahiro SAKAI and Shunji BANDOW**

Very small particles what are called *nanoscale materials* have been prepared and investigated in this study. Samples are produced by the simultaneous vacuum deposition technique[1)] to form a $Fe/SiO_2$ composite film. Average size of Fe particles was controlled by changing the deposition ratio of Fe and $SiO_2$. Transmission electron microscope was used to check the crystal structure and the size distribution. Temperature and size dependences of the magnetic properties were measured by Faraday-type magnetic balance in the temperature range from 2 to 240 K and the average size from 2.4 to 4.9 nm.

Temperature dependence of the inverse of the magnetic

susceptibility near zero magnetic filed shows a superparamagnetic behavior at temperature higher than 140 K for all samples. Magnetization curves for the various sizes of particles are shown in Figure 1. To explain the experimental results, it is necessary to use at least two kinds of magnetic moments existing in a particle. The fitting results using a superposition of Langevin functions are shown by the solid lines in the figure. Above results suggest a core-shell type structure where the core consists of metallic Fe and the shell is Fe oxides.[2] The shell oxides have not been specified, but these consist of the same materials independent of the particle size.

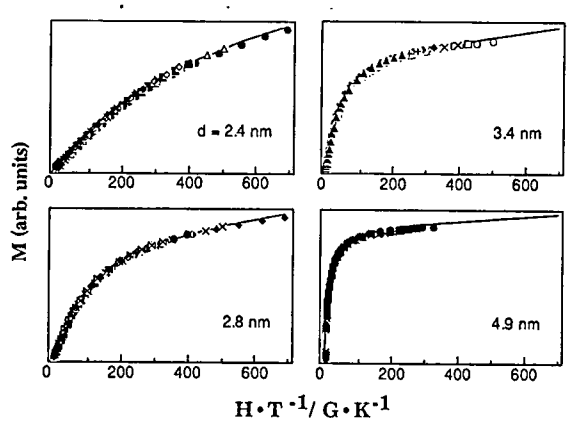


**Figure 1.** Magnetization curves of small Fe particles in the superparamagnetic region. Data points for various temperatures are on the same curve. Average sizes are indicated in the figure. The solid lines are the fitting curves obtained by the superposition of Langevin functions.


**References**

1) M. Sakai and S. Bandow, *IMS Ann. Rev.*, 124 (1991).
2) S. Gangopadhyay, G.C. Hadjipanayis, B. Dale, C.M. Sorensen, K.J. Klabunde, V. Papaefthymiou and A. Kostikas, *Phys. Rev.*, **B45**, 9778 (1992).


# VIII—G Formation of Metallofullerenes and Graphite Nanoballs

Synthesis technique for lanthanofullerenes and graphite nanoballs is investigated for the purpose to study the formation mechanism of new carbon allotropes. It is found that lanthanum carbide is playing an important role in generating lanthanum endhedral metallofullerenes.

## VIII-G-1 High Yield Synthesis of Lanthano-Fullerenes via Lanthanum Carbide


**Shunji BANDOW, Hisanori SHINOHARA** *(Mi'e University, Nagoya University)*, **Yahachi SAITO** *(Mi'e University)*, **Masato OHKOHCHI*, and Yoshinori ANDO*** *(*Meijo University)*



[*J. Phys. Chem.*, **97**, 6101 (1993)]


A high yield synthesis for lanthano-fullerenes has been studied by a newly developed fullerene arc-generator equipped with an *anaerobic* sampling apparatus. The yield of the lanthano-fullerene, La@$C_{82}$, has increased by a factor of 10 or more, when $LaC_2$-enriched composite carbon rods are used for the generation of soot, instead of hydro-oxidized or oxidized lanthanum composite rods. The fact is characterized by electron spin resonance (ESR) and by powder X-ray diffraction method. Furthermore, the yields of other types of lanthano-fullerenes, $LaC_{2n}$, has also increased, when the $LaC_2$-enriched composite rod is used as an arc-burning material.

## VIII-G-2 A New Characterization of Lanthanum- and Scandium-Endohedral Metallofullerenes


**Hisanori SHINOHARA** *(Mi'e Univ., Nagoya Univ.)*, **Hiroki YAMAGUCHI*, Hiroyasu SATO*, Motoki INAGAKI*, Yahachi SAITO*** *(*Mi'e Univ.)*, **Shunji BANDOW, Hiroshi KITAGAWA, and Tadaoki MITANI**



[*Mater. Sci. Engin.*, **B19**, 25 (1993)]


Several endohedral metallofullerenes involving La and Sc atom(s) were characterized by electron spin resonance (ESR) and mass spectrometry. In particular, new types of lanthanofullerenes including $LaC_{76}$ and $LaC_{82}$ were produced and extracted by a newly developed fullerene arc-generator equipped with an anaerobic (air-free) sampling and extraction mechanism of metallofullerenes. The newly extracted metallofullerenes exhibit equally spaced octet ESR lines of equal signal intensities with different hyperfine coupling constants (0.44 G, 3.15 G, 2.12 G) and $g$ values (2.0043, 2.0042, 2.0010). These lanthanofullerenes are found to be air sensitive, in contrast to reported metallofullerenes such as La-$C_{82}$, Y-$C_{82}$ and Sc-$C_{82}$. The probable candidates for these fullerenes are presented, including $LaC_{76}$ and $LaC_{84}$. Furthermore, Sc-$C_{82}$ and La-$C_{82}$ fullerenes can be well separated from $Sc_3$-$C_{82}$ and La-$C_{84}$, respectively, by liquid chromatography with an ethanol-deactivated silica-gel column.

## VIII-G-3 Interlayer Spacings in Carbon Nanotubes


**Yahachi SAITO*, Tadanobu YOSHIKAWA*** *(*Mi'e Univ.)*, **Shunji BANDOW, Masato TOMITA**, and Takayoshi HAYASHI**** *(**NTT)*



[*Phys. Rev.*, **B48**, 1907 (1993)]


Electron and X-ray diffraction studies of nanotubes have revealed that the distance between the graphitic sheets are larger by a few percent than those in bulk graphite. The mean value of the interlayer spacings is 0.344±0.001 nm.

## VIII-G-4 Encapsulation of ZrC and $V_4C_3$ in Graphite Nanoballs via Arc Burning of Metal Carbides/ Graphite Composites


**Shunji BANDOW and Yahachi SAITO** *(Mi'e Univ.)*



[submitted to *Jpn. J. Appl. Phys.*]


Ultrafine particles surrounded by graphitic carbon layers have been produced by the arc burning of a composite carbon rod containing ZrC or VC. The size of the ultrafine

particles are typically in the range of 20–40 nm in diameter and the number of graphitic carbon layers surrounding a core particle is ranging from about 10 to 30. The core ultrafine particles are found to be ZrC (via ZrC-graphite composite rod) and $V_4C_3$ (via VC-graphite composite rod) by selected area electron diffraction from each composite nanoball (graphite nanoball with a core particle). One of the graphite nanoballs encapsulating ZrC and $V_4C_3$ are shown in Figure 1 (a) and (b), respectively.

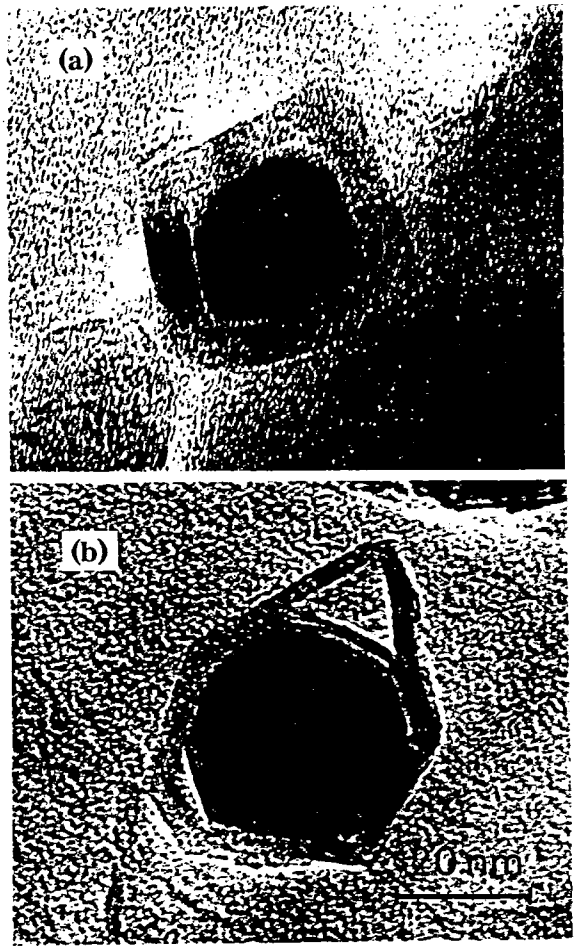


**Figure 1.** Encapsulated (a) ZrC and (b) $V_4C_3$ in graphite nanoballs.

### VIII-G-5 Formation of Carbon Nanotubes by Evaporation of a Carbon Rod Containing Scandium Oxide

**Masato OHKOHCHI*, Yoshinori ANDO*** *(*Meijo Univ.)*, **Shunji BANDOW, and Yahachi SAITO**** *(**Mi'e Univ.)*

[submitted to *Jpn. J. Appl. Phys.*]

Carbon nanotubes and nanoparticles formed by dc arc-discharge evaporation of a carbon composite rod containing scandium oxide were studied by high resolution scanning electron microscopy (SEM). Nanotubes obtained from the composite rod were more abundant than those obtained from pure carbon rod. A lot of fibrous nanotubes were gathered together and bunched to form long bundles. Moreover, a number of nanoparticles whose size was nearly the same with the diameter of nanotubes were attached to the surface of each tube forming bundles. It became clear that scandium had an effect promoting the growth of nanotubes.

# Low-Temperature Center

## VIII—H Electronic Properties of Novel Molecular Materials

### VIII-H-1 XAFS Studies of Oxidation Process in $Rb_xCs_yC_{60}$(x=3, y=0 and x=2, y=1)

**Yoshiro KUBOZONO*, Tamotsu FUJIMOTO*, Hironobu MAEDA*, Akiko HIRANO*, Setsuo KASHINO*, Kokichi OSHIMA*** *(IMS)*, **Hitoshi YAMAZAKI*, Hiroyuki ISHIDA*, Tadao ISHII*, Shuichi EMURA**, and Kiyonori KATO** *(*Okayama Uni. and **Osaka Univ.)*

[*Physica C.* to be published]

The first EXAFS measurement of the alkali-doped fullerene superconductors, $Rb_xCs_yC_{60}$(x=3, y=0 and x=2, y=1 with $T_c$=30 and 31 K, respectively), has been made at the Rb K-edge as a function of exposure time to $O_2$ gas. The distance $r_{Rb\text{-}C}$=3.35±0.02 and 3.31±0.02 Å were obtained for the pristine $Rb_xCs_yC_{60}$ of x=3, y=0 and x=2, y=1, respectively, in good agreement with the reported value of 3.33 A at the tetrahedral site determined by X-ray diffraction study. The analysis of the Rb-O EXAFS in the $O_2$ exposed $Rb_3C_{60}$ for 40 h gives $^r$Rb-O=2.89±0.05 A and N=4±1, consistent with the crystallographic values of rubidium oxide ($Rb_2O$: $^r$Rb-O=2.89 and N=4 at room temperature). The result indicates that the Rb in $Rb_xCs_yC_{60}$ is converted into $Rb_2O$ through the oxidation.

### VIII-H-2 A New FISDW (Field Induced Spin Density Wave) Family, (DMET-TSeF)$_2$X

**Kokichi OSHIMA*, Kiyonori KATO, Yusei MARUYAMA, Reizo KATO**, Akiko KOBAYASHI**, and Hayao KOBAYASHI***** *(*Okayama Univ. and IMS, **Tokyo Univ. and ***Toho Univ.)*

[*Synthetic Metals*, **55—57**, 2780 (1993)]

A new family of metallic 1-D system which includes one superconductor has been studied at IMS Low Temperature Center using the 12 T magnet and the dilution refrigerator. The family is made from the new donor molecule DMET-TSeF (dimethyl ethylene dithio tetraselena fulvalene). The Fermi surface of the family is similar to that of the famous TMTSF system. And three compounds in this family have been actually confirmed to show FISDW states, two at ambient pressure and one under pressure.

# Equipment Development Center

## VIII—I Activities of Division of "IMS Machines"

Equipment Development Center has the division for construction of so-called "IMS Machines", which are designed on the basis of ideas and/or proposals from the members of the Institute for Molecular Science. New technologies required for their construction are developed by the staff of this division with an introduction of recently developed engineering and in collaboration with researchers of other institutes, universities and facilities of industries. The main aim of these activities is to expand technical capability of this center, intending a development of future technology of the molecular science.

In this fiscal year, 1992, the project themes listed below were adopted as IMS Machines. Their construction was successfully executed as described separately, and one part is under way.

**1. Fast Stabilizer for Fabry-Perot Interferometer**
(Kazuo HAYAKAWA, Tatsuhisa KATO, and Shuji ASAKA)
**2. Liquid Helium Automatic Supply System**
(Hisashi YOSHIDA, Mitsukazu SUZUI, Keiichi HAYASAKA, Kiyonori KATO, Takashi TAKAYAMA, and Shuji ASAKA)
**3. Infra-red Cryostat Windows**
(Norio OKADA)
**4. Multi-channel Spectroscopic System in MID-IR**
(Jeung Sun AHN and Shuji ASAKA).

For fiscal year of 1993, two themes listed below were newly selected as IMS Machines.
**1. Broad-band Infra-red Window for Ultra-high-vacuum Apparatus**
(proposed by Tsuneo URISU and Norio OKADA)
**2. Time-of-flight-type Mass Spectrometer for High-Mass Materials**
(proposed by IMS Machine Division).

Application of patents is promoted in this division. For fiscal year of 1992, two titles listed below were applied.
**1. Sealing Mechanism of Optical Window**
**2. Method of Spectrum Determination from Two-Dimensional Interferogram**

### VIII-I-1 Fast Stabilizer for Fabry-Perot Interferometer

Fabry-Perot interferometers are usually sensitive to environmental conditions such as temperature change or mechanical vibrations, and easily degrade their optical adjustments causing a loss of spectral resolution during a long time measurement.

We have newly developed a stabilizer for a Fabry-Perot interferometer based on direct optical inspection of non-parallelism of mirrors. After deciding the degree of deviation from optimum adjustment by using a computer, the apparatus applies proper bias voltages on the piezoelectric elements between the mirrors. Our method of stabilization is characteristic in a sense that it is more "direct" compared with commercial one, enabling rather simple and quick feedback. Refinement of control software is now under way.

### VIII-I-2 Automatic Liquid Helium Supply System

Supply of liquid helium to researchers in this institute has been performed by an automated liquid helium transfer system that was developed under the cooperation of the low-temperature center and the equipment development center. The present project is aimed at improvement in transfer speed, reduced loss and easy maintenance of the system.

The features of the present system include:

(1) cold liquid transfer with a newly developed miniature centrifugal pump, which enables a high flow rate and a low loss,

(2) use of a transfer tube with a new motorized needle valve, enabling precise flow adjustment and easy maintenance of the valve, and

(3) digital-data transmission through optical fiber for sensing (pressures etc.) and controlling, enabling enough noise tolerance.

### VIII-I-3 High-sensitivity and High-resolution Multichannel FT Spectrometer

**Satoshi TAKAHASHI, Jeung Sun AHN, Shuji ASAKA, and Teizo KITAGAWA**

[Appl. Spectrosc. **47**, 863 (1993)]

(This is one of the projects of IMS Machines of 1991)

A compact multichannel Fourier-transform (MCFT) spectrometer without mechanical moving parts has been constructed. The spectrometer consists of a birefringent interferometer based on the Savart plate and a CCD detector, as illustrated schematically in Figure 1, which is basically the same as the system explained by Hashimoto and Kawata.[1] In the present system, we have succeeded in expanding the observable frequency region of the MCFT spectrum without reducing its resolution by using the two-dimensional property of a CCD chip. The resolution has reached the theoretical value, 40 $cm^{-1}$, by correcting the geometrical distortion of the interferogram. Main features of the present system are the following.

(1) Utilization of a birefringent common-path interferometer without moving components. This approach makes it easy to construct a compact interferometer and to circumvent the noises due to mechanical vibrations, and also provides the ability to measure transient spectrum of a single event by using a pulse source.

(2) Use of a large solid angle as a consequence of the linearly arranged optics of the birefringent interferometer.

(3) No requirement of the entrance and exit slits.

Features 2 and 3 serve to make the throughput of the interferometer quite large, and this is the main advantage of this spectrometer over conventional Fourier transform and dispersive spectrometer.

**Reference**

1) M. Hashimoto and S. Kawata, Appl. Opt. **31**, 6096 (1992).

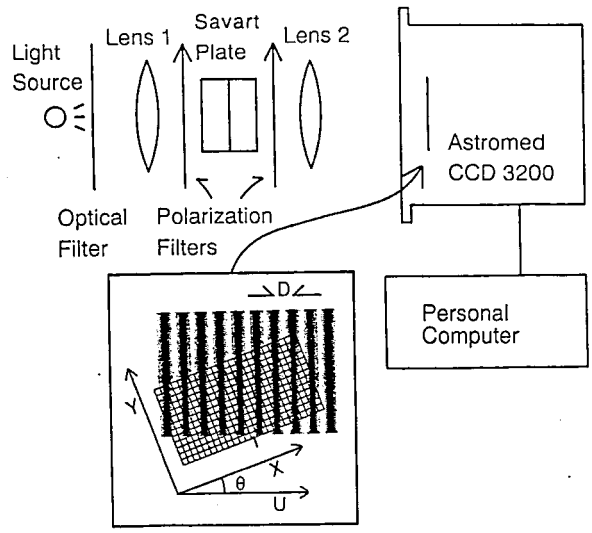


**Figure 1.** Schematic diagram of the MCFT system constructed. The inset illustrates the way of CCD arrangement.

## VIII—J Site-selective Fluorescence Spectroscopy on Dye Molecules in Amorphous Matrices

Recently, we have developed a technique to measure the laser-induced fluorescence spectrum, including the narrow resonance fluorescence line appearing at the same wavelength as the exciting light, for localized centers with short fluorescent decay times in condensed matter. A method to obtain the fluorescence spectrum of dye molecules in a single site in disordered host matrices by the use of saturation effect of the laser-induced fluorescence has also been devised [see, J.S. AHN et al., J. Lumin. **48/49**, 405 (1991); Phys. Rev. B, in press]. These methods give us valuable information on guest-host interactions and host dynamics.

### VIII-J-1 Site-selective Fluorescence Spectroscopy in Zn-substituted Myoglobin

**Jeung Sun AHN, Shuji ASAKA, Teizo KITAGAWA, Yoshito NISHIKAWA*, Yasuo KANEMATSU*, and Takashi KUSHIDA*** *(*Osaka Univ.)*

Site-selective fluorescence spectroscopy has been performed for Zn-substituted myoglobin (ZnMb) in the lowest optical band at sufficiently low temperatures. The distribution of the zero-phonon transition energy has been obtained from the excitation profile of the resonance fluorescence line. The spectral width (FWHM) of the distribution function is rather narrow ($\sim 110$ $cm^{-1}$) in comparison with that of MgOEP in PMMA ($\sim 210$ $cm^{-1}$) and polystyrene ($\sim 160$ $cm^{-1}$). This difference may come from the fact that ZnMb has an almost fixed structure, while the structure of the surroundings of the dye molecule is random in polymers. The single-site fluorescence spectrum has also been determined by making use of the saturation effect of the laser-induced fluorescence. The large Debye-Waller factor ($\sim 0.8$) obtained for ZnMb reveals that the coupling between the electrons of the chromophore and the vibrations of the polypetide chain is very weak. The origin of weak coupling is attributed to the close packing of the chromophore into a hydrophobic environment in myoglobin.

## VIII—K Studies of Halogen-bridged Mixed-valence Systems

The search for high-temperature superconductivity and novel superconducting mechanisms is one of the most challenging tasks of condensed-matter physicists and materials research scientists. Bednorz and Müller considered mixed-valent and

Jahn-Teller effects of Cu ions in the $La_{2-x}Ba_xCuO_4$ system as a mechanism for strong electron-phonon interactions allowing a high $T_c$. It is well known that their breakthrough in discovering superconductivity in $La_{2-x}Ba_xCuO_4$ was inspired partly by their knowledge of the superconducting properties of $BaPb_{1-x}Bi_xO_3$. The valence state of Bi has been considered as a very important factor for a comprehension of the physical properties of $BaPb_{1-x}Bi_xO_3$ system. The insulating state of the end-member compound $BaBiO_3$ was explained by the charge disproportionation of the Bi cations (+IV into +III and +V) which couples to lattice deformation or the stabilization of a commensurate charge-density wave (CDW). To our interest, a possibility of an unusual superconducting state, which results from condensation of bipolarons, is postulated under a strongly coupled electron-phonon system such as $BaPb_{1-x}Bi_xO_3$. According to this model, Cooper-pair formation due to the condensation of bipolarons occurs under some electron-phonon coupling constant *l*, while in the large *l* limit bipolarons' formation occurs. The insulating $BaBiO_3$ is regarded as on-site bipolaronic state where bipolarons form a three-dimensional lattice and localize at $Bi^{III}$ site. On the other hand, a large number of perovskite-type metal halides $ABX_3$ or $A_2BX_4$ (A=alkali metal; B=metal; X=F,Cl,Br,I) have been known. However, there has been few materials researches on these compounds, except for the studies on magnetism or structural phase transition. We consider perovskite-type metal halide with mixed valency of metal, a crystal of cesium gold iodide $CsAuI_3$, as "model materials" for searching for high-temperature superconductivity due to its structure analogous to $BaBiO_3$ or high-$T_C$ Cu oxides.

### VIII-K-1 Pressure-induced Metallization and Band-type Jahn-Teller Transition in Perovskite-type Mixed-valence Metal Halide $CsAuI_3$

**Hiroshi KITAGAWA, Norimichi KOJIMA,* Hiroki TAKAHASHI,** and Nobuo MORI**** *(*Kyoto Univ., **ISSP)*

[*Physical Review Letters*, Submitted]

The effect of hydrostatic pressure on the electrical resistivity of perovskite-type mixed-valence metal halide $CsAuI_3$ has been investigated at low temperatures using a newly developed very-high-static-pressure apparatus. We have found two pressure-induced transitions at room temperature: one is the gradual insulator-metal transition resulting in a valence fluctuation of the Au atoms between $Au^{I}$ and $Au^{III}$ and the other is the metal-semimetal transition with a giant resistance jump by four orders of magnitude driven by a valence proportionation of $Au^{I}$ and $Au^{III}$ into $2Au^{II}$. The latter transition is considered to be associated with the band-type Jahn-Teller transition. At low temperatures, unusual conducting behaviors were observed under the pressures below the metal-semimetal transition, which is considered to be attributed to valence fluctuations of Au atoms. The observed anomalous properties indicate that the perovskite-type metal halide $CsAuI_3$ is a strongly coupled electron-lattice system.

## VIII—L Studies of H-bonded CT Complexes

The dynamics of hydrogen bond (H-bond) in solids has been a subject of prolonged interest, and a great deal of spectroscopic data of the H-bond has been accumulated. Nevertheless, there remain many fundamental problems when the proton is dynamically correlated with electrons, particularly with regard to the quantum-mechanical dynamics of proton in H-bonded condense phases. Unquestionably, this is a reflection of the cooperation of H-bond with electron and lattice systems through a unique interaction in solids. The subject of this study is to elucidate the cooperation of proton-electron and proton-lattice in CT complexes.

### VIII-L-1 Two-band System of *d* and $\pi$ with Interband H Bridges

**Hiroshi KITAGAWA, Tadaoki MITANI, J. TOYODA, K. NAKASUJI, Hiroshi OKAMOTO,* and Masahiro YAMASHITA**** *(*RISM, Tohoku Univ., **Nagoya Univ.)*

[Synthetic Metals, **56**, 1783 (1993)]

Since the discoveries of organic conductor in TTF-TCNQ and highly conductive 1-D transition-metal complexes in $K_2Pt(CN)_4 \cdot Br_{0.3} \cdot 3H_2O$, a large number of new molecular metals have been synthesized and some of them exhibit superconductivity. As an extension of these materials, it is expected to construct a hybrid system composed of 1-D transition-metal-complex chains and 1-D organic acceptor (or donor) chains.

A two-band system of *d* and $\pi$ with interband H bridges provides a unique opportunity for construction of novel molecular assemblies, in which many electronic systems are combined *via* H-bond system. When the partial CT occurs between the chains, *d* holes (or electrons) in the metal-complex chains and $\pi$ electrons (or holes) in the organic acceptor (donor) chains are expected to show a unique cooperation through the interchain H bonds. As the first demonstration of this system, we have investigated single crystals of [M($H_2$DAG)(HDAG)]TCNQ (M=Ni, Pd, Pt). These complexes consist of segregated stacks of bis(oxamidoximato)M(II) complex donors and TCNQ acceptors, whose chains are connected to each other by interchain H bonds.

The optical, electrical resistivity, and X-ray photoelectron spectroscopy (XPS) measurements on [M($H_2$DAG)(HDAG)]TCNQ (M=Ni, Pd, Pt, $H_2$DAG= diaminoglyoxime) have been made under low temperature. The results show unusual behavior around 250 K. In the case of Pt or Pd complex, it exhibits $M^{II-IV}$ mixed valency below 250 K.

# Ultraviolet Synchrotron Orbital Radiation Facility

## VIII—M Development of the UVSOR Light Source

### VIII-M-1 Double RF System for Suppression of Longitudinal Coupled Bunch Instability on the UVSOR Storage Ring

**Kazuhiro TAMURA*, Toshio KASUGA*, Makoto TOBIYAMA*, Hiroyuki HAMA, Toshio KINOSHITA, and Goro ISOYAMA** *(*Hiroshima University)*

A higher harmonic RF system whose frequency is the third harmonic of the main RF frequency has been installed on the UVSOR storage ring in order to suppress longitudinal coupled bunch instability with a double RF system. The RF acceleration field with the double RF system is shown in Figure 1, where the voltage of the third harmonic field is maintained at one third of that of the main RF field. The electron bunch is located at a phase position close to zero. Since the synchrotron oscillation frequency is proportional to the square root of the slope of the RF field and the bunch length is inversely proportional to the synchrotron oscillation frequency, we can control the bunch length by varying the phase of the third harmonic field relative to the main field. Two extreme cases are shown in Figure 1. In the zero-mode (b), the slope of the combined field is twice as much as that of the main RF field alone so that the bunch length is expected to decrease to 70% of the normal value. In the $\pi$-mode (a), slopes of the respective field components cancel out, so that not only the bunch length becomes longer but also the frequency spread of the synchrotron oscillation increases due to the non-linearity of the RF field at the electron bunch. The frequency spread leads to Landau damping against the coherent oscillation of electron bunches due to the longitudinal instability.

First, we measured the synchrotron oscillation frequency, the frequency spread and the bunch length in single bunch operation at an electron energy of 600 MeV, in order to see whether the double RF system worked as expected. The main RF system was operated in the same conditions as usual; the frequency is 90.115 MHz, the peak RF voltage is 47 kV and the tuning angle is around −60 degrees. The tuning angle of the harmonic cavity was set at −60 degrees in order to avoid Robinson instability. The bunch length and the synchrotron oscillation frequency were measured in the zero and $\pi$-modes as a function of the RF voltage of the harmonic cavity. The measured values agreed well with theoretical predictions for the double RF system. Next, we carried out experiments in multi-bunch operation to suppress longitudinal coupled bunch instability. The peak RF voltage in the harmonic cavity was set at 15.6 kV, which is one third of the voltage in the main cavity, and the phase was adjusted to operate the system in the $\pi$-mode. When the beam current was low, the instability was completely suppressed with the double RF system. As the beam current increased, however, it became difficult to keep the phase of the harmonic field in the $\pi$-mode due to the beam-induced RF field in the harmonic cavity, and the instability appeared again. Meanwhile, it turned out that the instability could be suppressed even at the higher beam current if the tuning angle of the harmonic cavity was set at a positive value. This result indicates that the strong instability excited by the fundamental resonance of the harmonic cavity can be suppressed by Landau damping with the double RF system. Since the beam induced field in the harmonic cavity at the negative tuning angle is in the same phase as the RF field in the $\pi$-mode, this operation mode works even at a very high beam current.

The double RF system is routinely used for user experiments in multi-bunch operation to suppress longitudinal coupled bunch instability. Another advantage of this system is that the beam lifetime becomes longer because the bunch is 2 ~ 3 times longer. The lifetime at the beam current of 200 mA increases from 240 min to 350 min. The maximum beam current in multi-bunch operation had been limited by the instability to 500 ~ 700 mA. With the double RF system, it could be increased to more than 1 A.

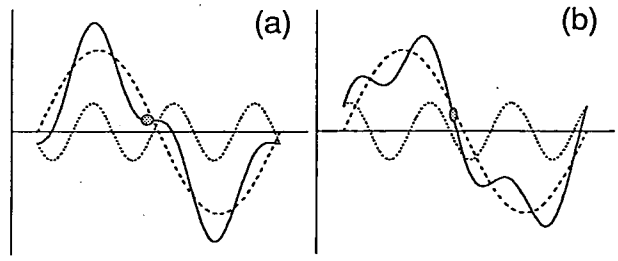


**Figure 1.** RF field in the double RF system. The peak voltage of the third harmonic field (dotted line) is one third of the main RF field (broken line). The solid line is the combined field. In the $\pi$-mode (a), the phase of the higher harmonic field is adjusted such that the slope of the combined field becomes zero at the bunch position. In the zero-mode (b), the slope becomes higher and the bunch length is reduced.

### VIII-M-2 FEL Experiment on the UVSOR Storage Ring

**Hiroyuki HAMA, Jun-ichiro YAMAZAKI, and Goro ISOYAMA**

We have been conducting free electron laser experiments on the UVSOR storage ring. The first lasing was obtained at wavelengths around 460 nm in Spring, 1992. Since then, we have been preparing for experiments in the ultraviolet region. Because the FEL gain and the reflectivity of mirrors used for the optical cavity are anticipated to decrease as the wavelength becomes shorter, we have developed a gain-enhancement technique using a higher harmonic cavity, which makes the peak current of the electron beam higher by reducing the bunch length. The FEL gain was increased to be 1.7 times higher over the whole range of the wavelength and the beam current.

At first, we chose the wavelength around 340 nm for experiments in the UV region. However, lasing continued only for a few seconds because the reflectivity of mirrors used for the experiments went down very quickly. We have not identified exactly the origin of the mirror degradation.

It seems that an absorption band appeared in the region from 340 to 440 nm. Based on this experience, we decided to choose the wavelength of 300 nm for the experiment, where the mirror degradation is less serious.

The experimental procedure for lasing in the UV region was almost same as that used in the visible region except that fluorescent plates to see the UV light were used for the alignment of the optical cavity. We obtained the first lasing in the UV region at 303 nm on July 5, 1993. As shown in Figure 1, we could vary the laser wavelength from 310 to 290 nm by changing the undulator gap.

We are continuing experiments in the visible region around 500 nm to study dynamics of the FEL on the storage ring. In order to derive the effective gain, which is the gain minus the cavity loss, time spectra of the laser power were detected with a biplanar photodiode and processed with a digital oscilloscope. Lasing was controlled by gain-switching with a repetition rate of 1 Hz in order to secure enough time for beam cooling by radiation damping, in which the RF frequency was shifted by 200 Hz to stop lasing. Figure 2 shows the gain as a function of the beam current. The solid line is the calculated gain which is enhanced by use of the harmonic cavity, and the broken line is the gain with the main RF system alone. The measured gain is in good agreement with the gain enhanced by the harmonic RF system.

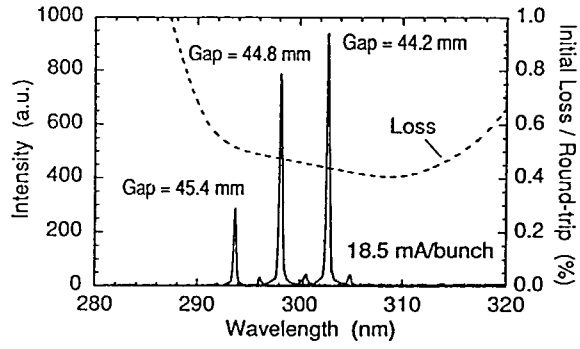


**Figure 1.** Laser spectra in the UV region measured with a monochromator for various undulator gaps. The initial round-trip loss of the optical resonator is shown by the dashed line.

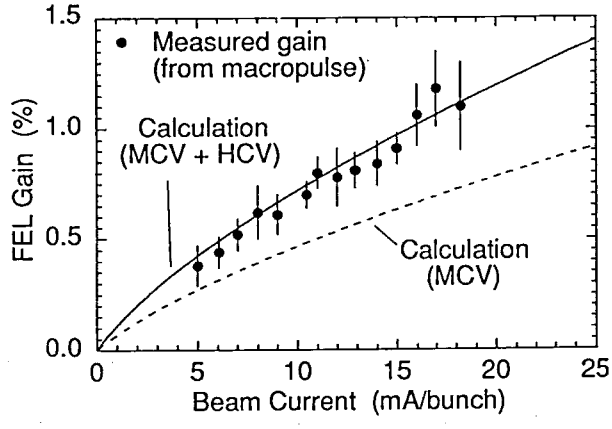


**Figure 2.** Beam current dependence of the measured gain derived from the macro pulse (the solid circles) and the calculated one (the solid line). The calculated gain for the normal operation with the main RF system alone is also shown by the dashed line.

# VIII—N Development of Beamlines and Equipment for UVSOR

## VIII-N-1 Reflectance of Multilayer Gratings in the Soft X-ray Region

**Eiji ISHIGURO** *(Osaka City Univ. and IMS)*, **Tsutomu KAWASHIMA** *(Osaka City Univ.)*, **Kojun YAMASHITA***, **Hideyo KUNIEDA***, **Yuzuru TAWARA***, **Takashi YAMAZAKI***, **Hidenori YOSHIOKA,*** **Akihiro FURUSAWA*** *(*Nagoya Univ.)*, **Kuninori SATO** *(NIFS)*, ****Masaru KOEDA, Tetsuya NAGANO****, **and Kazuo SANO**** *(**Shimadzu Corp.)*

The reflectance for a laminar Pt/C multilayer grating has been measured in the region from 1.2 keV to 2.8 keV by using monochromatized light from a crystal monochromator in the BL7A beamline of UVSOR. The grating comprises 10 pairs of Pt and C layers with 2d=100 Å on a $SiO_2$ laminar grating which was produced by means of a holographic exposure and reactive ion-beam etching. The groove density was 100 l/mm and the groove depth 100 Å. Figure 1 shows the reflectances for m=−1, 0, and +1 which are plotted as a function of the glancing angle, together with the total reflectance measured with a detector having a large acceptance angle and that of a multilayer mirror which was fabricated at the same time when the multilayer was deposited on the grating. A high total reflectance at the glancing angle less than 2 deg. are due to the total reflection of Pt, and a peak around the glancing angle of 5.8 deg. to Bragg reflection of the multilayer. The dependence of the reflectance of the spectral orders in the Bragg peak on the glancing angle can be qualitatively interpreted by a kinematical theory of multilayer gratings.[1] The maximum reflectance of m=0, +1, and −1 order in the Bragg region were 6.4% (5.8°), 1.8% (5.7°), and 1.6% (6.2°), respectively, at E=1.2 keV, 9.0% (4.1°), 2.1% (4.3°), and 1.6% (4.3°) at E=1.7 keV, 6.4% (3.5°), 1.2% (3.3°), and 1.3% (3.2°) at E=2.0 keV, and 8.8% (2.5°), 1.5% (2.2°), and 1.4% (2.0°) at E=2.8 keV.

**Reference**

1) W.K. Warburton, *Nucl. Instrum. and Methods*, **A291**, 278 (1990).

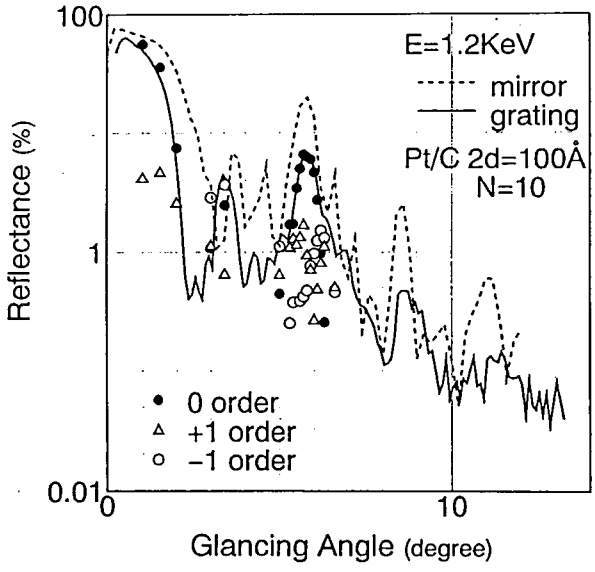


**Figure 1.** Reflectance of the m=0, +1, and −1 spectral orders as a function of the incident glancing angle, together with the total reflectance of the grating (solid line), and that of the multilayer mirror (broken line).

### VIII-N-2 Performance Test of β-Alumina as a Soft X-ray Monochromator Crystal

**Atsunari HIRAYA, Kazunori MATSUDA** *(Naruto Univ. of Education)*, **Yang HAI** *(Inst. of High Energy Physics, China)*, **and Makoto WATANABE**

In order to extend the lower photon energy limit of double crystal monochromator, a synthesized inorganic crystal β-alumina was tested as a monochromator crystal. Performance (intensity, resolution, and resistivity to radiation damage) of β-alumina was compared with that of beryl crystal which is only one practical crystal in the photon energy below 1.5 keV (820–2450 eV) with synchrotron radiation source. The photon energy range of 580–1740 eV can be covered with β-alumina crystal, which is extended to lower energy side by 240 eV than that with beryl crystal. Monochromatized x-ray intensity with β-alumina crystal was more than ten times higher than that with beryl crystal. Resolution with β-alumina crystal was estimated to be 0.75 eV at 900 eV which is narrow enough for EXAFS measurements, though broader than that of beryl crystal (0.46 eV). No degradation in intensity and in resolution were observed even after 1 month exposure to synchrotron radiation under normal operating conditions.

## VIII—O Researches by the Use of UVSOR

### VIII-O-1 Solid-State Effects on Nonradiative Decay of $4d^94f^1$ States in Barium Halides

**Masao KAMADA, Kouichi ICHIKAWA*, and Osamu AITA*** *(*Univ. Osaka Pref.)*

[*Physical Review*, **B47**, 3511 (1993)]

The nonradiative decay of $4d^94f^1$ states in barium halides was investigated by using resonant photoemission spectroscopy. Constant-final-state spectra with the final states at $N_{4,5}$-$O_{2,3}O_{2,3}$ Auger electron peak and constant-initial state spectra with the initial state at Ba 5p levels were enhanced in the Ba 4d excitation-energy region, indicating Auger and direct recombination decay processes, respectively. It was noticed that the decay probability through the direct recombination process and the degree of the anomalous branching ratio increases in the order of $BaF_2$, $BaCl_2$, and $BaBr_2$. This result indicates that the nonradiative decay of the $4d^94f^1$ states in the barium halides is affected by crystalline environments.

### VIII-O-2 Sputtering of Excited-State Alkali Atoms from Alkali Halides Irradiated with Synchrotron Radiation

**Masao KAMADA and Sayumi HIROSE**

[Submitted to *Nuclear Instrum. and Methods B*]

Photon-induced sputtering of excited-state alkali atoms from alkali-halide crystals was investigated with synchrotron radiation. It was found that time response of the sputtering of excited-state sodium atoms from NaCl consists of two components, and that the fast component is several orders as fast as the existing results of time response for ground-state alkali atoms. It is suggested that the fast sputtering of excited-state alkali atoms may be interpreted in terms of lattice instability due to electronic excitation in the surface layer.

### VIII-O-3 Co-adsorption of K and Cl on the Si(100) surface

**Shin-ichiro TANAKA and Masao KAMADA**

Co-adsorption of K and Cl on the Si(100) surface was investigated with photoelectron and XANES (X-ray Absorption Near Edge Structure) spectroscopy. Experiments were performed by using the grasshopper monochromator and a double-pass CMA at BL2B1 of UVSOR. The Si(100) surface were firstly covered with a monolayer of K and subsequently exposed to Cl [Si(100)/K/Cl]. The Si(100)/Cl/K system was also prepared in a similar way. The valence-band photoelectron spectra of these systems were very similar to that of the KCl film evaporated on gold, indicating that K and Cl atoms are ionic on both surfaces. This is consistent with the results obtained from XANES spectra around the K-$L_{2,3}$ edge. Both surfaces showed the diffused (2×1) LEED pattern. It is considered that quasi-two dimensional KCl surfaces are produced in these systems. However, the Si-2p photoelectron spectra showed that the bonding configuration in the Si(100)/K/Cl system is different from that in the Si(100)/Cl/K system.

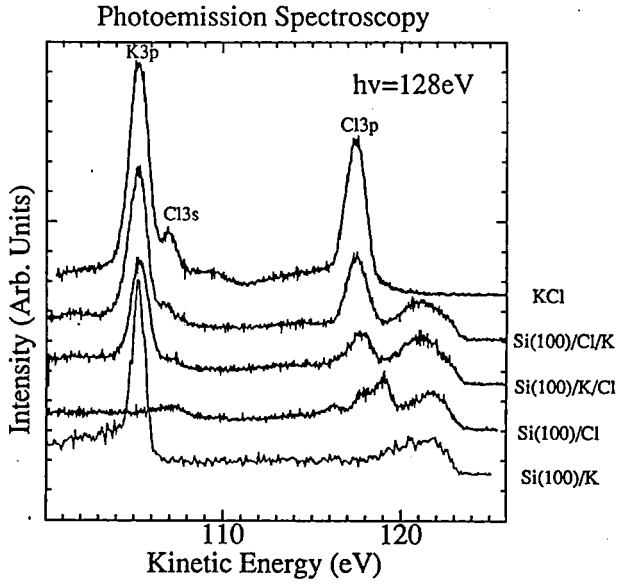


**Figure 1.** Photoelectron spectra of the Si(100) surfaces covered with a monolayer of K atoms [Si(100)/K], the Si(100) surface with a monolayer of Cl [Si(100)/Cl], the Si(100)/K surface after an exposure to Cl [Si(100)/K/Cl], the Si(100)/Cl surface after a deposition of K [Si(100)/Cl/K], and the KCl film evaporated on the gold substrate. The energy scale of the spectrum of KCl film were shifted by +0.6 eV. The sample preparation and the measurements were made at room temperature. Photon energy was about 128 eV, and the kinetic energy corresponding to the valence band maximum was 123.5 eV.

# RESEARCH FACILITIES

For the sake of brevity the present issue includes only the newly installed facilities and the activities since September 1992. Concerning the activities and facilities before September 1992, please refer to older IMS Annual Review issues (1978 ~ 1992).

## Computer Center

The main computers at the Center are a supercomputer HITAC S-820/80 and a main-frame computer HITAC M-680H. The computers are linked to international networks through Tokyo University International Science Network (TISN). About 40% of the computer time is used by the research staff at IMS, and the remaining 60% is given out as research grants to scientists outside the Institutes in molecular science and related field. As of March 1993, the number of project group was 271, consisting of 804 users.

In January, 1994, the S-820/80 is to be replaced by NEC SX-3/34R, which has a peak speed of 19.2 GFLOPS. This new generation of supercomputer, equipped with a main memory of 2GB and an extended memory of 8GB, will provide a very powerful computational environment for molecular science.

A system for making video movies has been adopted to S-820/80. Using this system, one can make video movies of one minute long in one job on S-820/80. The system is especially useful for the visualization of molecular dynamics simulations.

The library programs of the Center amount to 803. Among them, about 200 programs can be executed immediately. Recent additions include GAUSSAN 90 and FLEX32 (a program for generating conformers). The Quantum Chemistry Literature Database (QCLDB) has been developed by the Center in collaboration with the QCDB group. The database, CMQCA, IR2, STERIC, and QCBDB are also available at the Center.

## Chemical Materials Center

The Chemical Materials Center plays an important role in the synthesis and purification of chemical substances in IMS. The scientists and technical associates of this facility support other people in IMS to carry out the above works. Upon request, technicians carry out elemental and mass spectrometric analyses of new compounds prepared at IMS. They also carry out their own researches on synthesis of new interesting compounds, developments of new selective chemical transformations, elucidation of reaction mechanism, and application of new methodologies developed in IMS to the analysis of chemical substances and reactions.

## Instrument Center

For the efficient use of instruments, the Center is equipped with various types of instruments for general use.[1] One instrument has been newly installed in 1992.

**Tunable Ultrashort Pulse Laser and Photodetection System** (Spectra-Physics Tsunami, TAS-1, and Hamamatsu Photonics Picosecond Fluorometer)

The system consists of a pico- and femtosecond laser and a picosecond time-resolved fluorometer. The laser light source comprises a Ti-sapphire laser (Tsunami) pumped by an $Ar^+$ ion laser (2080-12S) and a Ti-sapphire regenerative amplifier. The laser generates a pulse with pulse energy of 5 mJ/pulse at 800 nm (at 10 Hz), pulse width of $<2$ ps and/or $<200$ fs, and tuning range of 720–900 nm. The fluorometer comprises a streak scope (C-4334), a monochromator (C5094), a CCD detection unit, and a microcomputer (Macintosh Quadra 700). The time resolution of the fluorometer is 5 ps with a deconvolution mode.

**Reference**

1) *List of Instruments*, No.8, IMS Instrument Center (1992).

## Low-Temperature Center

The main must of Low-Temperature Center is constant supply of liquid helium and liquid nitrogen to the Institute. The total amounts of liquid helium and liquid nitrogen supplied in 1992 were 23,029 *l* and 60,377 *l*, respectively.

Newly equiped machines for low-temperature physics study are a dilution refrigerator (KELVINOX 36115, Oxford Instruments) and a SQUID magnetometer (MPMS 2, Quantum Design).

## Equipment Development Center

A number of research instruments have been designed and constructed by making use of the mechanical, electric and glass-blowing technologies at this Facility. Representative instruments developed during this fiscal year of 1992 are listed below.

$\phi$8 cm Mirror for a Submillimeter-Wave Radiometer
$^3$He Cryostat for Superconducting Magnet
UHV Chamber System for Synchrotron Radiation Stimulated Surface Reaction
UHV Compact Sample Transfer System with Radiative Heater
Calorimeter
Cryostat for Clamp-Type High-Pressure Cell
Electron Bombardment Ionization Mass Spectrometer Detector
Dual Multi-Channel Scaler Using Digital Signal Processor
High-speed High-Voltage Pulse Generator for MCP
Vacuum Apparatus Protection System against Momentary Power Failure
Thermo-Controller for Semiconductor Samples
Pulse Nozzle Driver for Molecular Beam Source

### Division of IMS Machines

Equipment Development Center has the division of IMS Machines. Activities of this division is described in detail in the research activities section.

## Ultraviolet Synchrotron Orbital Radiation Facility

The UVSOR light source is ususally operated at an electron energy of 750 MeV with an initial current of 200 mA. A higher harmonic RF system has been installed in order to suppress longitudinal coupled bunch instability with a double RF system. The instability was successfully suppressed in machine study and the system is routinely used for user experiments in multi-bunch operation. Another advantage of the double RF system is that the beam lifetime increases from 220 to 350 min. in multi-bunch operation at 200 mA because the bunch length becomes 2—3 times longer. The facility for the calibration of light detectors on BL5B was transferred from Institute for Nuclear Fusion Science to IMS. This beam-line is open to the users outside and inside of IMS from the April of 1993. Four beam lines are now under construction. They are BL4B for the basic research on the photo-assisted etching reactions, BL5A for spin polarized photoelectron spectroscopy, BL6B for far-infrared microspectroscopy, and BL8B1 equipped with a grazing incidence monochromator for soft X-ray spectroscopy.

# SPECIAL RESEARCH PROJECTS

IMS has special research projects supported by national funds. Two projects presently in progress are:

(1) Development and evaluation of molecular synergistic systems and their application to chemical energy conversion (1990–).

(2) Materials science on molecular devices (1990–).

These projects are being carried out with close collaboration between research divisions and facilities. Collaborators from outside also make important contributions. Research fellows join these projects. The results in 1992 are reviewed in this report.

# (1) Development and Evaluation of Molecular Synergistic Systems and their Application to Chemical Energy Conversion

## 1. Studies on Dynamical Processes of Highly Excited Atoms and Molecules

## 2. Studies of Laser Cooling and Trapping of Neutral Atoms

**Norio MORITA, Asuka FUJII, and Mitsutaka KUMAKURA**

The competing process between rotational autoionization and predissociation in superexcited *np* Rydberg states ($n \geq 23$, $v=0$, $N^+=12$) of NO has been studied with rotational-state-resolved multistep laser excitation of NO and multiphoton ionization detection of dissociation fragments. In this study, it has been concluded that the decay dynamics of these states are governed by predissociation, not by rotational autoionization. This is the first experimental study that has clarified the mutual relation between the efficiencies of rotational autoionization and other decay processes (see II-C-1).

Next, we have performed a high resolution spectroscopy of *ng* superexcited Rydberg states of NO and also investigated their decay dynamics. There have been very few studies on the dynamics of such high orbital-angular-momentum states. The three-color triple resonance technique has been used to perform rotational-state-resolved excitation of *ng* superexcited Rydberg states. Highly excited *ng* Rydberg states up to $n=70$ have been observed, and their term energies and quantum defects have been determined. One of the important results other than spectroscopic data is that the decay dynamics of the *ng* Rydberg states are governed by autoionization, not by predissociation (see II-C-2).

Regarding the laser cooling and trapping experiment, we have completed the construction of a new vacuum chamber that can be evacuated to ultrahigh vacuum. With this chamber, the trapping time has been increased by about thirty times that in the previous low-vacuum chamber. This improvement has allowed us to measure the temperature of the trapped metastable helium atoms, and it has been found to be 230 $\mu$K at the optimal condition, at which the number of trapped atoms has been estimated to be about $10^5$ and they have been confined in a nearly spherical region with a diameter of 0.8 mm. Using these trapped atoms, we have then demonstrated the atomic wave diffraction by a transmission grating (2000 lines/mm). Although this has not been achieved at the lowest atomic temperature mentioned above, a diffraction pattern of atomic waves has successfully been observed at a trap temperature of 1.2 mK. This is a first-stage experiment to construct an atomic interferometer consisting of three gratings, and we expect that some improvements would allow us to make it (see II-D-1).

## Mechanism of Oxygen Activation by Cytochrome Oxidase in a Respiratory Chain

**Teizo KITAGAWA, Takashi OGURA, Shun HIROTA, Denis A. PROSHYLAKOV, Shinya YOSHIKAWA** *(Himeji Inst. Tech.)*, **and Evan H. APPELMAN** *(Argonne Natl. Lab.)*

Cytochrome oxidase is the terminal enzyme of the respiratory electron transfer chain of aerobic organisms. The $aa_3$-type enzyme contains two heme A groups ($Fe_A$ and $Fe_B$) and two copper ions ($Cu_A$ and $Cu_B$) as the redox active metal centers and couples the dioxygen reduction reaction with proton translocation across the membrane. A functional unit containing the $Fe_A$ and $Cu_A$ ions serves as an electron transfer protein from cytochrome *c* to another functional unit containing the $Fe_B$-$Cu_B$ binuclear dioxygen-reducing site. A mechanism of dioxygen reduction by the $Fe_B$-$Cu_B$ is a current topic of spectroscopic studies. We investigated reaction intermediates present in the time interval between 0.1 and 5.4 ms following initiation of the reaction by using time-resolved resonance Raman spectroscopy combined with our original Artificial Cardiovascular System. We succeeded in resolving an oxygen isotope-sensitive band of intermediates at 788 $cm^{-1}$ into two components at 804 and 785 $cm^{-1}$ by using a monochromator with higher resolution. The latter was shifted to 796 $cm^{-1}$ in $D_2O$, while the former was insensitive to deuteration of the protein. Temperature dependence experiments clarified that the two bands arose from different intermediates. Experiments with $^{16}O^{18}O$ indicated that the two bands cannot be O-O stretching mode and accordingly, the 785 and 804 $cm^{-1}$ bands were assigned to the Fe-O stretching of the $Fe^{III}$-O-O-H intermediate and the $Fe^{IV}$=O stretching of the $Fe^{IV}$=O intermediate of $Fe_{a3}$, respectively.

In order to develop a new technique for obtaining time-resolved resonance Raman spectra, a multichannel Fourier transform Raman spectrometer was constructed by using a CCD detector and an interferometer consisting of Savart plate held between two polarizers. A novel idea of this system lies in avoiding the aliasing distortion by inclined disposition of the principal axis of CCD from the axis of the fringe pattern of interferogram. By using this system and a ps Nd:YAG laser, Raman spectrum of benzene was observed successfully.

## The Application of 2 Dimensional Raman and Resonance Raman Spectroscopy to the Condensed Phase

**Tatsuhisa KATO and Michio MATSUSHITA**

The success of the 2 dimensional (2D) expansion of IR absorption spectra by I. Noda suggested to us a new direction for IR spectroscopy in the condensed phase. The technique of 2D correlation analysis is applicable to spectroscopies other than IR, as he mentioned, and we are constructing the apparatus for 2D Raman and 2D resonance Raman spectroscopy. The purpose of the application of the technique to Raman spectroscopy is not only to obtain complementary data to IR spectroscopy but also to get more precise information about condensed phase molecular dynamics.

To investigate the Raman line shape, a tandem type spectrometer, which is the combination of a Fabry-Perot (F-P) interferometer with a conventional grating monochrometer, is used. There are two noteworthy features of the apparatus. One is a new stabilizing system for the F-P interferometer. This system is capable of a quick response and high stability due to graphic data processing. This makes possible the detection of weak signals through very long accumulation of data. The other feature is a multichannel type detection, making simultaneous line shape analysis for several Raman lines possible. This feature will play an important part for our anlaysis of Raman line shape as mentioned below.

The enhanced resolution of the 2D Raman spectrometer will reveal whether the broad feature is composed of many components, or is broadened by homogeneous broadening effects. In this way the 2D patterns of each Raman lines would look different depending on whether the line broadening mechanism is homogeneous or inhomogeneous. Consequently the analysis of Raman line-shapes using a 2D expansion technique provides useful information about the nature of intermolecular interaction in the condensed phase.

## Studies of Laser-induced Photochemistry on Solid Surfaces

**Yoshiyasu MATSUMOTO, Kyoichi SAWABE, Kazuo WATANABE, and Hiroyuki KATO** *(Graduate Univ. for Advanced Studies)*

Light sources such as lasers and synchrotron radiation can be very useful for the various processes in the fabrication of microelectronics, including etching, chemical vapor deposition, atomic layer epitaxy. On the other hand, it has also been well recognized that there is an important class of catalytic reactions with the aid of photon irradiation. Although those applications of light are practically useful and important, fundamental understandings of these processes are still lacking. Therefore, this project is mainly aimed for investigating how the interaction of light and adsorbates and/or substrates promote chemical reactions from the fundamental point of view.

Besides the conventional techniques in surface science such as low energy electron diffraction, Auger electron spectroscopy, and temperature programmed desorption, we have developed time-of-flight (TOF) spectroscopy of neutral species desorbed from the surface with sub-monolayer coverage. This approach is particularly useful because this provides the information on what species are desorbed from the surface, but also how energetic the desorbed species are. We have investigated photodissociation dynamics of nitrous oxide adsorbed on metal and semiconductor surfaces. Under the irradiation of uv photons $N_2O$ is partially desorbed and partially dissociated into O and $N_2$. TOF distributions of $N_2$ and $N_2O$ from Pt(111) clearly indicate that desorption and dissociation processes of $N_2O$ are nonthermal in origin. Furthermore, we have found that an energetic oxygen atom produced via photodissociation of $N_2O$ adsorbed on Pt(111) reacts with a chemisorbed oxygen adatom before accommodating with the surface. Thus, the reaction dynamics is completely different from that of the thermal recombination reaction governed by the Langmuir-Hinshelwood mechanism.

## Self-organization in Chemical Reactions

**Ichiro HANAZAKI, Yoshihito MORI, Noriaki OKAZAKI*, and Motoo SEKIGUCHI*** *(Graduate Univ. for Advanced Studies)*

The self-organizing process in chemical systems is known to occur as a result of nonlinear chemical process. It exhibits the temporal chemical oscillation and the spatial pattern formation. We are particularly interested in the response of chemical oscillators to photo-irradiation. The mechanism of the photo-induction and photo-inhibition of chemically oscillating systems and the structure of related bifurcation phenomena are main subjects of research. We have investigated several systems such as $Fe(CN)_6^{4-}$-$H_2O_2$-$H_2SO_4$, the Belousov-Zhabotinsky system, and Briggs-Rauscher system. We are especially interested in the photoresponce of these self-organizing chemical systems and are trying to establish the bifurcation and phase diagrams taking the irradiation light power as one of the external parameters.

## Studies on Gas Phase Reaction Dynamics by Crossed Beam Ion-imaging

**Toshinori SUZUKI, Kenichi TONOKURA, and Nobuhisa HASHIMOTO** *(Graduate Univ. for Advanced Studies)*

The differential cross section obtained in a crossed beam experiment would be one of the most detailed information

on chemical reaction dynamics. The electron impact-quadrupole mass analysis that has been commonly used in such experiments does not provide sufficient state resolution to discriminate rovibrational excitation within the products. A state-resolved experiment would allow the observation of dynamical resonance in a chemical reaction and the unraveling of the mechanism of energy randomization in chemically activated reaction intermediates. We have constructed an ion imaging apparatus for the measurement of state-resolved differential cross sections, and tested its performance through the observation of photodissociation events. The reaction products are state-selectively ionized by resonance enhanced multiphoton ionization and the ion cloud of the products is projected onto a two-dimensional position sensitive detector. With this technique, the state-resolved differential cross section is measured in the center-of-mass frame with all the scattering angles detected simultaneously. The atomic and radical beam sources for the crossed beam experiment is under construction.

### Development of Electron-Ion Coincidence Spectroscopy for Study of Desorption Induced by Electronic Transitions

**Kazuhiko MASE and Tsuneo URISU**

Desorption induced by electronic transitions (DIET) has developed into an attractive topic in the field of surface science, as well as molecular physics, photochemistry, and surface technology, because it is one of the most fundamental dynamical processes on surfaces. To clarify the detailed mechanism of DIET, we started a project to develop electron-ion coincidence spectroscopy. This novel method is most powerful for the study of surface dynamics which emit an electron and desorb an ion simultaneously. The equipment is consisted of an electron gun, a cylindrical mirror analyzer (CMA), and a time-of-flight (TOF) ion detection assembly. A surface is excited by electron beam or synchrotron radiation, and the energy of emitted electrons is analyzed by CMA. When an electron is detected, pulsed high voltage is applied on the first grid of the TOF assembly, so that ions simultaneously desorbed are mass-selected and detected. The excited state responsible for the ion desorption is identified by the energy measurement of the emitted electron.

### Highly Sensitive FTIR Systems for *In-Situ* Observation of the Synchrotron Radiation Stimulated Surface Photochemical Reactions

**Tsuneo URISU, Mitsuru NAGASONO, Akitaka YOSHIGOE, Yanping ZHANG, and Kazuhiko MASE**

Fourier Transformed Infrared Spectroscopy (FTIR) is one of the most promising technique for in-situ monitoring important for the study of the surface photochemical reactions. In this project, a highly sensitive FTIR system having S/N ratio of $10^{-4}$ order which enable the observation of the surface reactions with submonolayer adsorbate species is under construction. The fourier transformed infrared beam is focused into the SR reaction chamber, and the reflected beam from the sample surface is detected by the MCT detector. The optical pass is purged with dry $N_2$ gas. The $BaF_2$ and ZnSe are going to be used as the input and output window materials. To obtain a sufficient sensitivity for semiconductor or insulator materials, we are now developing a new observation technique using BML (buried metal layer) substrate, the semiconductor or insulator substrate having thin buried metal layer at the depth of 10 to 20 nm, which has characteristics of semiconductors or insulators for surface chemical reactions, but shows enhancement effects of IR absorption like on the surface of metal.

### Laser Photodetachment Spectroscopy of Solvated Cluster Anions

**Koichiro MITSUKE**

The detail properties of the transition states in chemical reactions are not fully understood on account of short lifetime and low concentration of transient species. We are planning to perform laser photodetachment spectroscopy of solvated cluster anions, *e.g.* $XHX^-(H_2O)_{20}$, for the purpose of investigating the transition-state region of the corresponding neutrals in an exchange reaction. Negative cluster ions are produced by electron impact on the free jet expanded from a pulsed nozzle and sampled through a conical skimmer. Cluster ions are mass-selected with a beam-modulated time-of-flight mass spectrometer. The cluster ion bunch of the desired mass is photoirradiated with the third or fourth harmonic of a Nd:YAG laser. Electrons produced by photodetachment are energy-analyzed by using time-of-flight technique. We observe $O^-$ and negative cluster ions $O^-(N_2O)_n$ produced by electron impact on an $N_2O$ jet. The photodetachment spectrum of $O^-$ at the 355 nm excitation shows a single peak at the electron binding energy $E_b$ of 1.46 eV, which is in good agreement with the electron affinity of the oxygen atom. The photodetachment spectrum of $O^-(N_2O)_{1,3}$ taken at the same photon energy exhibits a broad peak centering at $E_b \sim 1.46$ eV.

# (2) Materials Science on Molecular Devices

### d-$\pi$ Interaction in Molecular Metals

**Kyuya YAKUSHI, Akito UGAWA, and Kentaro IWASAKI**

We have undertaken a systematic study on the solid molecular systems in which transition metals are embedded in a $\pi$-conjugated system from the viewpoint of the future design of the superconducting material. Through the systematic study of phthalocyanine radical salts, we continue the study on $CoPc(AsF_6)_{0.5}$, in which itinerant $\pi$-electrons are coupled with the local magnetic moments on Co atoms. This year we have measured the electrical conductivity in high-temperature region up to 500 K. This compound has a broad conductivity peak around room temperature. (see

IV-A-1). This behavior can be understood by the 1D narrow-gap semiconductor model. Contrary to the expectation, CoPc has a stronger d-$\pi$ interaction than CuPc. The electrical conductivity under high pressure is now planned to make this compound metallic.

We started to prepare 2D-polymer of CuPc to extend the d-$\pi$ interacting materials, where local magnetic moments on the square lattice are embedded in a 2D Fermi sea. (see IV-A-2) Heat treatment of the mixture of Cu and tetracyanobenzene under high pressure produced conducting polymers. Characterizations by X-ray diffraction, EXAFS, $^{13}$C-NMR, FIR-IR-VIS-UV spectrum, electrical conductivity, magnetic susceptibility, and ESR are now in progress.

## Intercalation of Phthalocyanine into the Superconducting Layer Compounds, Bi2212 and Bi2223

**Leonid S. GRIGORYAN and Kyuya YAKUSHI**

Modification of the physical properties of superconducting materials Bi2212 and Bi2223 has been conducted by exposing Bi2212 and Bi2223 in the vapors of several metal-phthalocyanine. Exposure to vapors of the metal-phthalocyanines MPc (M=Zn, Ni, Fe, or Pb) brings about a systematic variation of optical and superconducting properties of Bi-2212 and 2223 high-Tc oxides. With increasing level of MPc uptake, the color changes from black, dark green, and to pink, and accordingly the spectral weight is gradually transferred from the low to the high-frequency regions, accompanied by a decrease of Tc, diamagnetic response and magnetic hysteresis. We found that phthalocyanine treatment of Bi-Oxides was a unique method to change the carrier concentration by electron donation. (see IV-A-3, 4, 5) This is a joint research with a Yamauchi group of ISTEC, who provides us a well-characterized Bi2212 and Bi2223.

## Discovery of a New Superconducting Na-N-$C_{60}$ Ternary Compound

**Illias I. KHAIRULLIN and Kyuya YAKUSHI**

Many superconducting compounds has been found in alkali-metal-doped $C_{60}$. Because of the small size of Na cation, $Na_xC_{60}$ was prepared up to x=11, and especially $Na_3C_{60}$ undergoes a phase separation into $Na_2C_{60}$ and $Na_6C_{60}$ at 250 K. We prepared the Na-doped $C_{60}$ by means of the thermal decomposition of $NaN_3$. By this method we found a new superconducting Na-doped $C_{60}$, in which nitrogen atoms are incorporated in the face-centered-cubic lattice of $C_{60}$. We suppose that these nitrogen species play a role in preventing from the phase separation. The nitrogen species incorporated in the crystal lattice is likely to be $N_3^-$, since strong peaks (stretching and bending modes) attributable to $N_3^-$ was found in the infrared spectrum. The critical temperature of superconducting phase transition is *ca.* 12 K. After the careful examination of the preparation method, we found the importance of the residual water in $NaN_3$. A small amount of water in $NaN_3$ plays a role in stabilizing the superconducting Na-N-$C_{60}$ and even raises the critical temperature up to *ca.* 16 K. Since Na-$C_{60}$ system has a possibility to accommodate various molecules in the interstitial site, it will expand a new family of $C_{60}$ superconductors. (see IV-B-1) This is a joint research with the new materials section of Equipment Development Center and Inokuchi group.

## Mechanism of Superconductivity in Organic Materials and Possibility of Molecular Systems with the Josephson Effect

**Kazushi KANODA, Yasuhiro NAKAZAWA, Atsushi KAWAMOTO** *(Ochanomizu Univ.)*, **Hirohiko SATO, and Kazuya MIYAGAWA**

One important branch of study on the superconducting materials is search for novel functionality associated with superconductivity. We have our eyes on organic superconductors as promising materials. A class of organic superconductors have quasi-two-dimensional layered structure, which is considered as an serial array of the Josephson junctions. This particular nature is fascinating for forthcoming molecular device. In spite of such a great interest, fundamental problems of organic superconductors remains unsolved. We aim at clarifying the following two problems of organic superconductors, important for possible molecular device.

(a) Mechanism of the superconductivity

There have been observed a lot of anomalous superconducting properties in organic materials. Mechanism of the superconductivity is still an open question. We planned to perform two experiments deeply involved in this problem. First, magnetic penetration depth is determined by high resolution measurements of complex susceptibility on single crystals. The temperature dependence of penetration depth probes type of symmetry of electron pairing; exponential temperature-dependence corresponds to the usual S-wave pairing while power law to the unusual non-S wave pairing. The measurements for some $\kappa$-phase compounds with transition temperature greater than 10 K supports the latter case. Second, we make $^{13}$C-NMR measurement, which also probes type of electron pairing from the microscopic point of view. This experiment is now in progress. (see IV-C-2)

(b) Anisotropy of the superconductivity

Prior to search for the Josephson effect in organic systems, we have to characterize anisotropy of the superconductivity. The ac susceptibility and resistive measurements under magnetic field tells us important information on this aspect. Among various superconducting systems, $\alpha$-$(BEDT\text{-}TTF)_2NH_4Hg(SCN)_4$ was found to have extremely two-dimensional character and curious behavior. (see IV-D-2 and IV-D-3). This material may be a good candidate of functional molecular system. Search for Josephson effect in this material is now going on.

## Fabrication of Novel Organic Molecular Assemblies with the Use of the Molecular Beam Epitaxy Technique

**Yusei MARUYAMA, Hajime HOSHI, Keiichi KOHAMA** *(Toyota Motor Corp. and IMS)*, **and Shaoli FANG**

In order to prepare new materials which could be useful for molecular devices elements, we have started to design and fabricate ultra-thin organic multi-layered systems. In the first place, we have prepared ultra-thin single component phthalocyanine thin films to investigate epitaxial growth conditions on alkali halide single crystals. Fairly well oriented, uni-or bi-directionally, crystalline films are obtainable on the alkali halide substrates. Based on this kind of mono-film, we are going to fabricate a multi-layered system.

The SHG and/or THG of the films are investigated from the view point of the molecular structure and the epitaxy or orientation of the films.

## Fabrication of High $T_c$ Metal Oxide-superconducting Films by Layer-by-Layer Deposition from Multi-electron-beam Gun Sources

**Toshifumi TERUI and Yusei MARUYAMA**

Successive deposition of each component of metal oxides has been undertaken to achieve the layer-by-layer construction for high $T_c$ oxide superconductors. The high vacuum evaporation machine is equiped with three electron-beam guns and it can be operated under a differential pumping when oxygen inclusion is required. As an initial trial, an La-Sr-Cu-O system is now investigated.

## Study on the Solid State Properties of Fullerenes

**Yusei MARUYAMA, Hironori OGATA, Roger WHITEHEAD** *(Durham Univ. and IMS)*, **Toshiyasu SUZUKI, and Atsushi SUZUKI**

In order to clarify the nature of novel molecular systems, fullerenes, we have started to measure the electronic properties of fullerene solids, mainly concerning on the transport properties of pure and/or alkali metal-doped fullerene crystals.

Charge-carrier drift mobilities of pure $C_{60}$ single crystals were measured with the use of time-of-flight technique and the temperature dependence of the mobilities was also investigated. As for the alkali metal (K or Rb) doped $C_{60}$ crystals, the temperature dependences of the electrical conductivities and the thermoelectric power were observed, and the "metallic" nature of these substances was revealed. Through these measurements we are going to understand the electronic nature of this novel molecular system.

## NMR Studies of Novel Condensed Matter Systems

**Seiichi MIYAJIMA, Hironori OGATA, and Noriko YAMAMURO**

To investigate new functional materials based on molecular assemblies, experimental solid state NMR studies were started. In the last period our study centered on the phase transitions and molecular dynamics of polar smectic liquid crystals and a high resolution solid state NMR study of organic conductors (IV-J and K). At the same time preliminary results are being obtained for new projects. (1) $^{13}C$ NMR study is in progress for vapor phase grown single crystals of $C_{60}$, $C_{70}$, and their doped conductors. (2) In an organic binary complex, tetramethylbenzidine/11,11,12,12-tetracyano-2,6-naphtoquinodimethan, a dimerizing phase transition was found without accompanying charge transfer. The proton, carbon, nitrogen, and electron spin resonance studies were conducted to study the spin dynamics. (3) The nature of the bond-orientationally-ordered (BOO) phase and the phase transitions which are analogous to the two-dimensional liquid-hexatic(BOO)-crystal phase changes, are being studied by using a model liquid crystalline compound, 4-propionyl-(4-heptanoyloxy)azobenzene.

## Exploration of New Cooperative Proton-Electron Transfer (PET) Systems

**Kazuhiro NAKASUJI, Jiro TOYODA, Yasushi MORITA, Makoto TADOKORO, Tetsuji ITOH, Minoru MITSUMI, Kunio HATANAKA, and Koichi TAMAKI**

Search for new molecular materials based on the cooperative interactions between proton and electron has been actively continued. We are now developing a general strategy to explore new molecular materials. Cooperative proton-electron transfer (PET) in the hydrogen-bonded charge transfer (HBCT) systems might produce a molecular assembly of H-bonded neutral radicals. The solid state properties of such PET systems depend on the type and strength of the proton-electron cooperativity. Realization of a PET system under milder physical conditions can open an opportunity toward new molecular materials which possess interesting solid state properties. A molecular level stepwise consideration leads to two reasonable molecular design strategies: the exploration of new electronic systems having smaller intermolecular CT gap and an electronic modification to stabilize H-bonded neutral radical state. Our current approaches to synthesize new PET systems are as follows: (1) the donor and acceptor substituted quinhydrones, (2) the extended conjugated quinhydrones, and (3) the transition metal complexes having H-bonding networks. For example, as for the approach (1), we continue to modify the prototype benzoquinhydrone by introducing the electron donor and the acceptor substituents. As for (2), we have already reported the synthesis and solid state properties of naphtho-, bipheno-, and stilben-quinhydrone as extended conjugated quinhydrones. In these quinhydrones, we found cooperative phenomena between H-bonding and CT interaction. In order to expand the PET systems, new approach (3) are now actively performed. In the H-bonded transition metal complexes, we can utilize the additional characteristics of redox properties of the metal atoms and the intermolecular interactions between the metal atoms or between the metal atom and the ligand. As a first step, we succeeded to construct a H-bonded dimer model of the biimidazole transition metal complex.

## Synthetic Study of Sulfide Clusters with RhCp* Group

**Kiyoshi ISOBE**

The chemistry of M-SH functionality has been intensively studied in several metal complexes in connection with its significance in biological, mineralogical, and industrial

processes. It has been revealed that the reaction pathway and the number of electrons participating in the reaction are dependent on the metal ions. There has been, however, few reports of the corresponding chemistry of the M($\mu$-SH)M functionality in metal complexes. As the M($\mu$-SH)M functionality occurs commonly in those processes we felt that this chemistry warranted further investigation.

From $[Cp^*_2Rh_2(\mu_2\text{-}SH)(\mu_2\text{-}CH_2)_2]^+$ (1) synthesized by our group, several small sulfur clusters are derived by oxidation, deprotonation, and partial abstruction of the SH ligand. These clusters are summarized in Scheme 1.

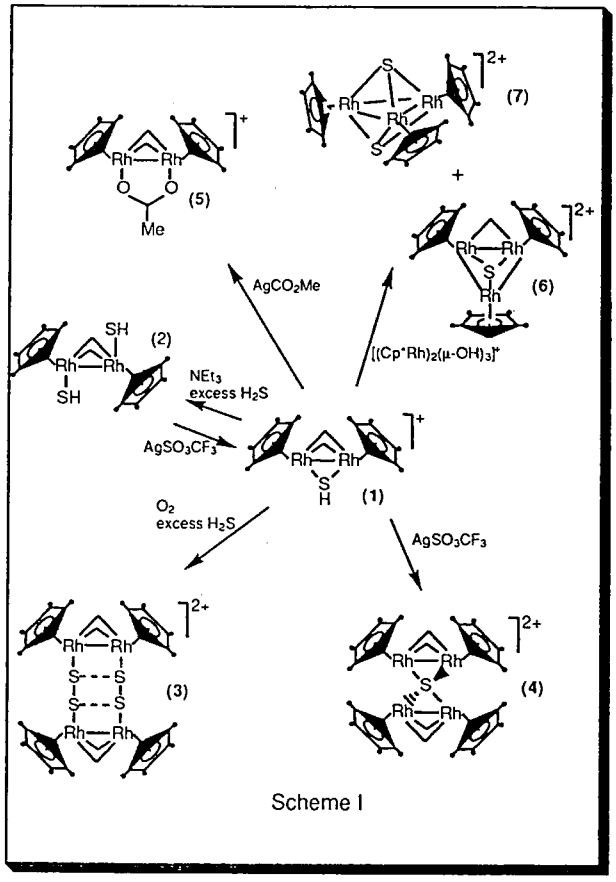

Scheme I

## Transannular $\pi$-$\pi$ Interaction of (4n)$\pi$ Systems

**Teruo SHINMYOZU, Tomonori MATSUNAGA*, Ikutarou SUGIMOTO*, Makoto OHE*, Kenji NODA*, Takahiko INAZU*** *(*Kyushu Univ.)*, **and Jerzy M. RUDZIŃSKI** *(Fujitsu Kyushu System Engi.)*

Transannular $\pi$-$\pi$ interactions between two $\pi$ systems were estimated by semi-empirical MO calculations (PM3 method) and the result was in good agreement with that of Greenberg's prediction. The predicted attractive $\pi$-$\pi$ interaction in stacked (4n)$\pi$ systems, which are unstable by nature, suggested the successful synthesis of (4n)$\pi$-(4n)$\pi$ compounds. As model compounds for this study, we designed [3.3]cyclophanes containing annulene rings since two $\pi$-systems are located in the most optimal transannular distance and they are almost planar.

We first undertook the synthesis of [3.3]cyclophanes containing 1,6-methano[10]annulene for the study of (4n+2)$\pi$-(4n+2)$\pi$ interaction (n$\geqq$2), and accomplished the synthesis of 2,16-dicyano-2,16-diaza[3.3](2.7)(1,6-methano[10]annuleno)phanes using cyanamide cyclization method, which was newly developed and might be applicable to the cyclization of unstable antiaromatic compounds. Their $^1$H NMR spectra showed significant ring current effect of the annulene ring. The electronic spectra also showed the strong $\pi$-$\pi$ interaction.

The syntheses of layered annulene in which trans-15,16-dimethyldihydropyrene [(4n+2)$\pi$, n=3] are linked by a $-CH_2CH_2-$ bridge, as well as [3.3]cyclophanes containing 8b, 8c-diazacyclopenta[fg]acenaphtylene [(4n)$\pi$, n=3] are now under way. More detailed description are given in V-section.

## Development of New Asymmetric Auxiliaries, Ligands, and Catalysts for Remote Asymmetric Inductions

**Junji INANAGA and Takeshi HANAMOTO**

In connection with our continuous interest in the development of new chiral auxiliaries, ligands, and catalysts which are effective for remote asymmetric inductions, *dl*-trans-2,5-bis(*m*-terphenylethynyl)pyrrolidine and *dl*-trans-2,5-bis($\beta$-naphthylethynyl)pyrrolidine were designed and synthesized as promising candidates. Succinaldehyde derived from 2,5-dimethoxytetrahydrofuran just before use was reacted with an excess amount of lithium acetylide. The resulting bis-propargylic alcohol was mesylated and then cyclized with *p*-methoxybenzylamine to give a mixture of N-protected cis- and trans-2,5-bis(ethynyl)pyrrolidine. The trans-isomer, purified by column chromatography on silica gel, was cross-coupled with 1-bromo-3,5-diphenylbenzene or 2-bromonaphthalene with the aid of palladium catalyst. Deprotection of the N-protective group of the corresponding N-(*p*-methoxybenzyl)-2,5-bis(*m*-terphenylethynyl)pyrrolidine and N-(*p*-methoxybenzyl)-2,5-bis($\beta$-naphthylethynyl)pyrrolidine afforded the desired free amines. Optical resolution of the amines and their use in asymmetric reactions are under investigation.

## Studies on Photosensible Dinuclear Complexes Containing Stilbene Moiety

**Haruko HOSOI*, Farideh JALILEHVAND*, Yukie MORI*, Yuichi MASUDA*, and Yutaka FUKUDA,** *(*Ochanomizu Univ.)*

We have synthesized a photosensible bridging ligand which contains stilbene moiety as the photosensible part. It is well known that the stilbene moiety changes the conformation from the trans-form to the cis one by ultraviolet light irradiation. We have synthesized tetradentate ligands (L) having the stilbene moiety and two sites of chelating parts, by which we could obtain trans-dinuclear Cu(II) complexes as shown below: (acac)Cu(L)Cu(acac)$X_2$, and $Cu_2(L)Cl_4$. The aim of this research is to obtain the cis-dinuclear complexes by UV light irradiation and to trap the cis-dinuclear complexes with second bridging ligand (Y) which is called the cis-trapping ligand like an ambidentate ligand. A part of the work was reported at the 10th

ISPPCC(International Symposium on Photochemistry and Photophysics of Coordination Chemistry, July, 1993).

L: $R_2NCH_2CH_2NHCH_2(C_6H_4)CH$
$=CH(C_6H_4)CH_2NHCH_2CH_2NR_2$

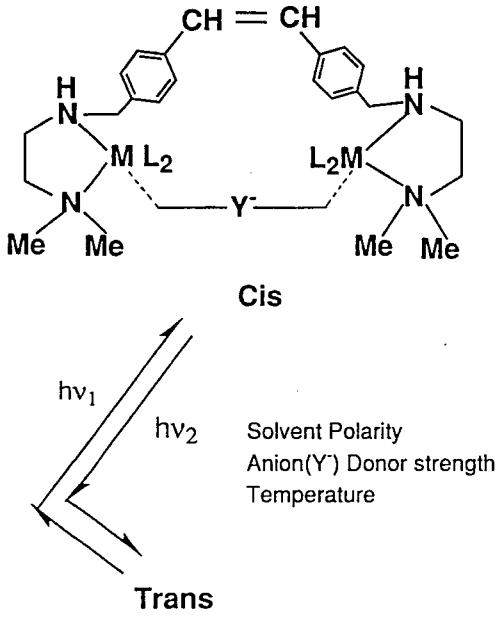


## The Mechanism of Reaction of Aminopolyphosphonates with $Pt^{II}(NH_3)_2$

**Kiyoshi SAWADA, Keiichi SATOH, and Hiroyuki YOKOYAMA**

The reactions of $Pt^{II}(NH_3)_2(H_2O)_2$ with aminopolyphosphonates, APP, were investigated at 0°C by means of $^{31}P$ NMR spectroscopy. APP used were nitrilotris(methylenephosphonate) (NTMP), methyliminodi(methylenephosphonate), (MIDMP) and dimethylaminophosphonate (DMAMP). In the acidic solution, O-monodentate complex is formed and followed by the formation of N,O-bidentate complex. These complexes form protonated complexes. The protonation constants and the structures of the protonated complexes were estimated. No complex formation occurs at alkaline solution. The O-monodentate complex changes to N,O-bidentate complex via N-monodentate complex in alkaline solution. The rate constants of these reactions revealed that the mechanisms of the ring-closure are given by schemes 1 and 2.

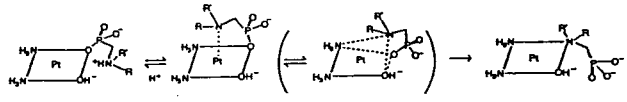

**Scheme I.** O-monodentate to N-monodentate

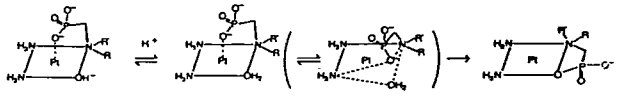

**Scheme II.** N-monodentate to N,O-bidentate

## Multi-electron Reduction of Carbon Dioxide by Homogeneous Catalysts

**Koji TANAKA, Tetsunori MIZUKAWA, and Hirotaka NAGAO**

Much attention has been paid to electro- and photochemical $CO_2$ reduction by homogeneous catalysts, since various reaction products are expected in artificial homogeneous $CO_2$ reduction in contrast to biochemical $CO_2$ reduction in $H_2O$. However, the reduction products in photo- and electrochemical reduction of $CO_2$ by homogeneous catalysts have been limited to CO and HCOOH so far. Multi-electron reduction of $CO_2$ accompanied by carbon-carbon bond formation, therefore, is highly desired in the viewpoint of the utilization of $CO_2$ as C1 resources. The purpose of this project is to develop new catalytic systems that allow multi-electron reduction of $CO_2$ to proceed in homogeneous reactions. We have already established a smooth conversion from $\eta^1$-$CO_2$ metal complexes to metal-carbonyl complexes through metal-carboxylic acid compounds by acid-base equilibria in aqueous media. Predominant evolution of CO from metal-carbonyl intermediates is caused by a decrease in the coordination number of metal complexes upon electro- and photochemical reduction of the complexes. On the other hand, a metal-carbonyl bond cleavage from reduced forms of metal complexes is effectively lowered when extra electrons are accommodated by $\pi^*$ orbitals of ligands rather than metal centers. In fact, we have found that $[Ru(bpy)(trpy)(CO)]^{2+}$ (bpy=bipyridine; trpy=terpyridine) can accept two electrons in the $\pi^*$ orbitals of the polypyridyl ligands without Ru-CO bond cleavage, and $[Ru(bpy)(trpy)(CHO)]^+$ that is formed by the reaction of $[Ru(bpy)(trpy)(CO)]^0$ with proton, affords HC(O)H, $CH_3OH$, HOOCCH(O), and $HOOCCH_2OH$ for the first time under electrochemical reduction in $CO_2$-saturated aqueous media.

## Selective Carbon-carbon Bond Formation Reactions on Zirconocene Complexes

**Tamotsu TAKAHASHI, Noriyuki SUZUKI, Koichiro AOYAGI*, Ryuichiro HARA*, Kayoko KASAI*** *(*Graduated Univ. for Advanced Studies),* **Denis KONDAKOV, Marina KONDAKOVA, Zhenfeng XI, Martin KOTORA, Victor DENISOV, and Motohiro KAGEYAMA**** *(**Tokyo Univ.)*

Zirconocene (II) chemistry is a new area. We have investigated the reactions using this zirconocene (II) species, especially zirconocene alkene complexes or zirconocene alkyne complexes. When zirconocene dichloride is reduced by metal such as magnesium amalgam, a very useful alkyne dimerization reagent is formed. Zirconocene dibutyl $Cp_2ZrBu_2$, which is called 'Negishi Reagent', also can be used as a zirconocene equivalent "$Cp_2Zr$". This reagent is very convenient for alkyne dimerization, diyne cyclization and enyne cyclization reactions. However, we found that zirconocene diethyl $Cp_2ZrEt_2$ reacted with alkynes to give not a dimer of alkynes but a cross coupling product of alkynes with ethylene. This result is very interesting because previous reduced zirconium species have been a very useful

reagent for dimerization of alkynes. Zirconocene diethyl $Cp_2ZrEt_2$ was converted into a zirconocene ethylene complex $Cp_2Zr(CH_2{=}CH_2)$ which is very reactive species. When it reacted with unsaturated bonds, an ethylene molecule was always incorporated in the products.

## Electronic Structure and Reaction Dynamics of Solvated Metal Cluster Ions

**Kiyokazu FUKE and Fuminori MISAIZU**

Metal ions are intimately involved in chemistry and biochemistry and play a crucial role in many reactions. Although there has been extensive progress in the thermodynamic and kinetic studies of solvated metal ions, the study of microscopic aspect of solvation dynamics has been rather limited. Spectroscopic studies of the solvated metal ion clusters as a function of cluster size can provide detailed information on energetic and dynamics of solvation. The advent of mass spectrometer and metal cluster beam techniques in conjunction with laser probes now allow an attack on the problem for the solvation of metal ions and metal cluster ions through studies probing energy levels and dynamical processes occurring in solvated metal clusters.

In the present research project, we have investigated the photodissociation spectra and photoinduced hydrogen-atom elimination reaction of mass-selected $Mg^+(H_2O)_n$, $Ca^+(H_2O)_n$, and $Al^+(H_2O)_n$ (see VIII-C-1, 2, 3, and 4) using a reflectron-type TOF mass spectrometer. We have constructed a magnetic-bottle type photoelectron spectrometer and have investigated the photoelectron spectra of $Cu^-(H_2O)_n$ (see VIII-C-5, 6).

## Organic Conductors Based on Novel Heterocyclic Compounds

**Yoshiro YAMASHITA, Shoji TANAKA, and Masaaki TOMURA**

Bis(1,3-dithiole) donors with Extended $\pi$-conjugation are of interest as components of organic conductors due to their highly electron-conducting properties as well as the decreased Coulombic repulsion. We have now prepared new types of bis(1,3-dithiole) donors. For example, bis(1,3-dithiole) donors containing a 3,5-dimethylenecyclopentene skeleton were prepared using a Wittig-Horner reaction from 4-cyclopentene-1,3-dione. They afforded a novel type of deeply colored cations by deprotonation from the dication states. A derivative containing a fused-[1,2,5]thiadiazole gave cation-radical salts as single crystals whose X-ray analyses revealed that the $PF_6$ salt showing a metallic behavior has a uniform stacking of donor molecules, while the $BF_4$ salt showing a semiconductive behavior has a dimeric structure. 7-(1,3-Dithiol-2-ylidene)-7H-cyclopenta-[1,2-b;4,3-b']dithiophene was found to have a planar structure with both inter- and intramolecular short S---S contacts. The electrochemical oxidation led to the formation of conductive polythiophene derivatives with low oxidation potentials and smooth superficial morphology. The selenadiazolo analogues of bis[1,2,5]thiadiazolo-*p*-quinobis(1,3-dithiole) (BTQBT) were prepared. They have isomorphous structures with BTQBT and the conductivities as single components were a little higher than that of BTQBT. Details of these works are described in VIII-B section.

## New Development of Electron-Proton Cooperation Systems

**Tadaoki MITANI and Hiroshi KITAGAWA**

The electron-proton cooperation systems provide a unique opportunity for construction of novel functional assemblies. [T. Mitani and T. Inabe, "Spectroscopy of New Materials"; Advances in spectroscopy Vol.22, ed. by R.J.H. Clark and R.E. Hester, John Wiley & Sons, Chichester, 1993, p.291]. As a typical model of this system, [M($H_2$DAG)(HDAG)]TCNQ (M=Ni, Pd, Pt, and $H_2$DAG: diaminogllyoxime) single crystals have been investigated by optical, vibrational and XPS measurements in details. The results indicate that the $d_z^2$ electronic state of the metal (M) chain and the $\pi$-electronic state of acceptor (TCNQ) stack closely correlate through the intra-H-bonds in ligands (HDAG and $H_2$DAG) and the interchain H-bonds. This gives the strongly temperature-dependent mixed-valence state of metals, which unquestionably indicate a promising of our proposal of creation of novel H-bonded molecular systems.

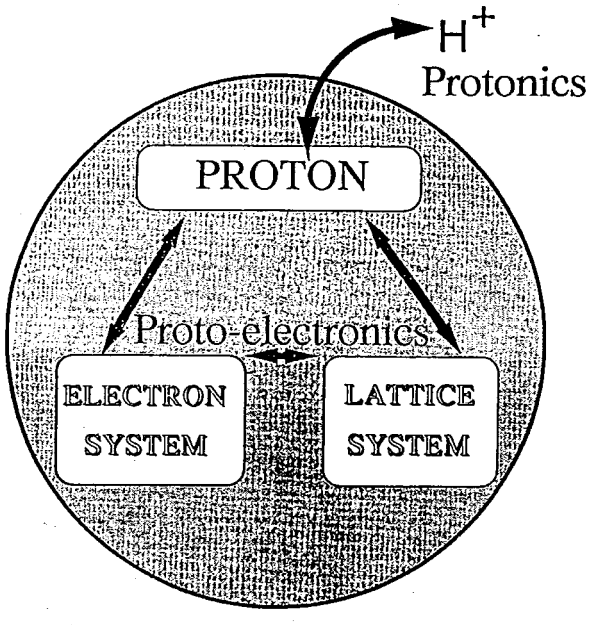

# OKAZAKI CONFERENCES

"Okazaki Conferences" are principal symposia at IMS, which are held on the subjects related to the "Special Research Projects". They are held two or three times a year, with a moderate number of participants around 50, including several invited foreign speakers. The formal language for the conference is Engligh. Outlines of the forty-forth, forty-fifth, and forty-sixth conferences are as follows.

### The Forty-forth Okazaki Conference

### New Development in Theory of Chemical Reactions *(November 4−6, 1992)*

**Organizers: K. MOROKUMA** *(IMS)*, **H. NAKAMURA** *(IMS)*, **H. NAKATSUJI** *(Kyoto Univ.)*, **and S. IWATA** *(Keio Univ.)*
**Invited Speakers: H.J. WERNER** *(Univ. Bielefeld, Germany)*, **T. ZIEGLER** *(Univ. Calgary, Canada)*, **J. BOWMAN** *(Emory Univ., U.S.A.)*, **D. CLARY** *(Cambridge Univ., U.K.)*, **K. WILSON** *(Univ. Calif. San Diego, U.S.A.)*, **and K. SCHULTEN** *(Univ. Illinois, U.S.A.)*

Fifty-seven leading theoreticians (six from abroad and fifty-one domestic) together with fourteen scientists from IMS gathered to discuss and exchange opinions and ideas on the theory of chemical reactions. This conference was composed of three basic fields in the theory of chemical reactions: (1) Theory of electronic structure, (2) Theory of chemical reaction dynamics, and (3) Theory of reaction in condensed medium. In addition to six outstanding invited talks by the foreign invited speakers (two in each field), ten Japanese scientists gave nice talks. These talks represented the recent methodological and computational developments in each field and stimulated vivid discussions. Actually, thanks to these developments interplay and knowledge exchange among the three fields are becoming possible and useful. In this sense, this conference played an important role of step stone for the future. The vivid discussions were made on the subjects such as accurate *ab initio* calculations, density functional theory, accurate treatment of gas-phase reaction dynamics, nonadiabatic transitions, and reactions in liquid, protein and cluster.

## The Forty-fifth Okazaki Conference

**Chemistry of Intra- and Intermolecular Charge Transfer of Metal Complexes *(December 8–10, 1992)***

**Organizers: H. OHTAKI** *(IMS)* **and A. NAKAMURA** *(Osaka Univ.)*
**Invited Overseas Speakers: A.G. SYKES** *(Univ. of Newcastle upon Tyne, UK)*, **and N.D. YORDANOV** *(Bulgarian Acad. of Sci., Bulgaria)*

The conference was organized so that the discussions were focused on the following subjects (1) Electron transfer in metal proteins (2) Redox properties of metal clusters (3) Activation of small molecules by redox reactions of metal centers (4) Intramolecular electron transfer in molecular assembly. The conference consisted of three plenary talks, nineteen invited talks and fourteen poster presentations. The total number of participants were sixty-nine. Organizers and participants believe that the conference was successful in exchanging information on the new aspect of charge transfer of metal complexes.

## The Forty-sixth Okazaki Conference

### Application of Synchrotron Radiation to Molecular Science; Present Status and Future Prospects *(December 16–18 1992)*

**Organizers: K. SHOBATAKE, M. WATANABE, M. KAMADA, and G. ISOYAMA** *(IMS)*
**Invited Overseas Speakers: W. BRAUN** *(BESSY, Germany)*, **S. KRINSKY** *(NSLS, BNL, U.S.A.)*, **P. LABLANQUIE** *(LURE, Univ. Paris Sud, France)*, **Y.T. LEE** *(Univ. of Calif., Berkeley, U.S.A.)*, **I. LINDAU** *(MAX-Lab., Univ. of Lund, Sweden)*, **P. WEIGHTMAN** *(IRCSS, Univ. of Liverpool, U.K.)*, **and G. ZIMMERER** *(Univ. of Hamburg and DESY-HASYLAB, Germany)*

Because about 10 years had passed since the commissioning of the UVSOR (a 750 MeV electron storage ring), we held this conference to review the present status and discuss future prospects of synchrotron radiation (SR) research in molecular science in the vacuum ultraviolet (VUV). The conference was divided into five oral sessions: light sources, instrumentation, gases, solids and surfaces/interfaces. The number of talks was 27. In addition, the status of SR facilities in Asia was reported in the poster session. The facilities are: Indus-I, India reported by **P.M. RAJA RAO** *(BARC)*; SRRC, Taiwan reported by **P.-K. TSENG** *(Natl. Taiwan Univ.)*; BSRL, China reported by **Y. HAI** *(IHEP)*; HESYRL, China reported by **C.Y. XU** *(HESYRL)*; and PLS, Korea reported by **S.Y. RAH** and **Y. CHUNG** *(POSTECH)*. The names and parameters of the Japanese light sources (6 government institutes and 11 private companies) were listed. At IMS, a users' meeting is held once a year around December, so it was integrated into this Okazaki Conference. Research carried out in 1992 using UVSOR was also reported in the poster session. A few topics were reported from each beamline and 30 posters were contributed. About 100 scientists, including 17 overseas researchers, participated in active and fruitful discussions. Through the discussions, we are convinced that in the near future, various spectroscopic research using SR will expand in molecular science and SR will be applied more to the detailed study of photochemical reaction processes in the VUV region.

# JOINT STUDIES PROGRAMS

As one of the important functions of an inter-university research institution, IMS undertakes joint studies programs for which funds are available to cover research expenses as well as travel and living expenses of individuals. The proposals from domestic scientists are reviewed and controlled by the inter-university commitee. The programs are carried out under one of five categories:

1) Joint Studies on special projects (a special project of significant relevance to the advancement of molecular science can be carried out by a team of several groups of scientists).
2) Research Symposia (on timely topics in collaboration with both outside and IMS scientists).
3) Cooperative Research (carried out in collaboration with both outside and IMS scientists).
4) Use of Facility (the Computer Center, Instrument Center and other research facilities at IMS are open to all researchers throughout the country).
5) Joint studies programs using UVSOR facilities.
   a) Special Project, b) Cooperative Research, c) Use of UVSOR Facility.
   In the fiscal year 1992, numbers of joint studies programs accepted amounted to 4, 8, 129, and 300 for categories 1)–4), respectively 2, 46 and 109 for 5a)–5c), respectively.

## 1) Special Projects

### A. Static and Dynamic Solvent Effects in Elementary Reactions

*Contributors:* **Okitsugu KAJIMOTO** *(Kyoto Univ.)*, **Tadamasa SHIDA** *(Kyoto Univ.)*, **Hisanori SHINOHARA** *(Mie Univ.)*, **Masaru NAKAHARA** *(Kyoto Univ.)*, **Nobuyuki NISHI** *(Kyusyu Univ.)*, **and Kritaro YOSHIHARA**

This research project aims at the molecular-level understanding of both static and dynamic solvent effects by means of recently developed techniques such as molecular beam, supercritical solution and pico-second spectroscopy.

#### (1) Solvent-induced Spectral Shift in the Raman Spectra Observed in Supercritical Fluids

Supercritical fluid offers an important molecular-level information on both the static and dynamic solvent effects because of its unique cluster structure. In order to get a local picture of solvation, we have measured the Raman spectra of acetone and acetonitrile in several supercritical fluids. Figures 1 and 2 display the spectral shifts of the C=O stretching of acetone and the C≡N stretching of acetonitrile, respectively, as a function of fluid reduced density. In this density region, the frequencies were shifted monotonously to lower values with the increase of the solvent density. The CO stretching vibration shows considerable red-shift in supercritical $CF_3H$ whereas the shift becomes less significant in $CO_2$, $CF_3Cl$ and Ar.

The observed trends of the shift of the C=O stretching are in fair accordance with the continuum model using Onsager's reaction field. However, a closer look at the plots reveals that, at low density, the observed shifts are larger than those expected from the polarity parameter of homogeneous supercritical fluids. This discrepancy indicates the enhancement of local concentration by the formation of clusters just around the solute molecule. The large discrepancy in $CO_2$ may reflect the anisotropy in the polarizability, $\alpha$, of the linear $CO_2$ molecule. The orientation of $CO_2$ should be taken into account for a correct prediction. On the other hand, in the case of the C≡N stretching of acetonitrile, a large discrepancy appears in $CF_3H$. This may indicate the small contribution of the dipole interaction to the shift in the acetonitrile-solvent interaction.

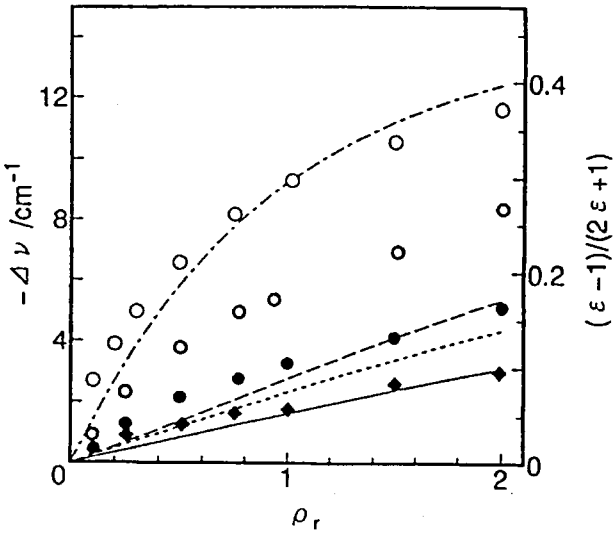


**Figure 1.** The density dependence of the shifts in the C=O stretching vibration of acetone in Ar (◆), $CO_2$ (◎), $CF_3Cl$ (●) and $CF_3H$ (○). The density dependence of the polarity parameters for the same fluids are also plotted by the lines from the top to the bottom.

#### (2) Formation of the Charge-transfer State in the Microsolvated Bianthryl

The bianthryl(BA)-acetone complex formed in a supersonic jet was found to give a charge-transfer(CT) state on photoexcitation. Even the 1:1 complex can produce the CT state. The rate of formation of the CT state was measured using a single photon counting system. A 1.5ps-pulse from a Ti:$Al_2O_2$ laser was doubled and used to excite the BA-acetone complex. Since the component of the $S_1$ emission is small compared with the CT emission, all photons above 400 nm were collected for the photon counting. From the rise time of the CT emission, the 1:1 BA-acetone complex was estimated to form the CT state within 34 psec. The rate for the 1:2 complex was found to be much faster, less than 10 psec. This fact indicates that the increasing solvation by

acetone molecules diminishes the barrier to the electron transfer.

### (3) Rotational Coherence Measurements for Solvated Van Der Waals Complexes

For the detailed discussion of environmental effects in van der Waals complexes, the unambiguous information of their structure is essential. In our previous report of the polar excited state formation in bianthryl-acetone complex, we suggested that the location of the solvent molecules are quite important for the reaction to occur. The measurement of rotational coherence i.e., the determination of the rotational period, provides us with an important structural information for heavy molecules. As a preliminary test, we measured the rotational coherence signal of free BA in its $S_1$ state at several internal rotation levels. Since the excited state BA in its lowest twisting level is about 30° twisted from the orthogonal position and the average twisting angle varies with the internal rotational levels, the rotational constants depend on the photo-excited levels. Such a change is most clearly reflected in the rotational coherence signal of each internal rotation level. The excited level corresponding to the largest absorption peak has the average twisting angle of 90°. With the increase or the decrease in excitation wavelength, the average angle gradually deviates from 90° and as a result the molecule deviates from a symmetric top. Such a change significantly weaken the coherence signal though the recurrence time changes only slightly.

We also measured preliminarily the rotational coherence signal of BA-Ar complex. The signal was found to be rather faint, which means the large deviation from a symmetric top.

## B. The Solid State Properties of the Transition Metal Complexes and the Control of Interaction between d- and $\pi$-electrons

*Coordinators:* **Hayao KOBAYASHI** *(Toho Univ.)*, **Kyuya YAKUSHI, Ichimin SHIROTANI** *(Muroran Inst. of Tech.)*, **Toshiaki ENOKI** *(Tokyo Inst. of Tech.)*, **Norimichi KOJIMA** *(Kyoto Univ.)*, **Masahiro YAMASHITA** *(Nagoya Univ.)*, **and Koshiro TORIUMI** *(Himeji Inst. of Tech.)*

This research project aims at a basic investigation which covers wide variety of compounds from the organics through to metal complexes.

### (1) DCNQI-Cu System

2,5-substituted-N,N'-dicyanoquinonediimine(abrreviated to $R_1,R_2$-DCNQI or more simply DCNQI) is one of the $\pi$-acceptor molecules as well as well-known TCNQ and forms complexes with such cations as Cu, Ag and alkali ions with 2:1 stoichiometry. Soon after Hunig et al. reported that $(DMe\text{-}DCNQI)_2Cu(R_1,R_2=CH_3)$ retained the stable metallic properties, the authors pointed out that such metallic state is particularly characteristic because Cu would be in mixed-valence state and thus the d(Cu) level could be located around the Fermi level of $\pi$-metallic band. Furthermore the authors demonstrated the crucial role of the hybridization of $\pi$ and d levels from the reflectance spectra. In fact, the anomalies of DCNQI-Cu system have since proven attributable to the fact that almost localized 3d(Cu) electrons actually play an important role together with $\pi$-electrons in the metallic band. In the present research project, the synthesis of new DCNQI's of novel substitutions $R_1,R_2$ and the synthesis and characterizations of thin films of DCNQI-Cu system were examined. In regard to the latter, the absorption spectra, X-ray diffraction and electrical resistivity were measured on the thin films which were prepared by the vacuum evaporation of CuI and DMe-DCNQI on the quartz or pyrex glass. They remained highly conductive down to 4 K and exhibited the metallic conductivity in high temperature region.

### (2) Metallo-phthalocyanines

To investigate an effect of the interaction between itinerating $\pi$-electrons and almost localized d-electrons, we examined the single crystal of one dimensional radical salt; (phthalocyaninato) cobalt and that of two dimensional polymer; (phthalocyaninato) copper.

(1) One-dimensional radical salt: $CoPc(AsF_6)_{0.5}$

The electrical resistivity, thermo power, magnetic susceptibility, vibration spectrum and polarized reflectance spectrum of $CoPc(AsF_6)_{0.5}$ were measured. Their results showed the following three facts: (1) though the transfer integral between the molecules is as large as ca.0.3 eV, the electronic structure is one-dimensional and has strong electron-electron corelation; (2) there exists antiferromagnetic interaction (J=240 K) between the neighboring unpaired electrons on the chain of Co which penetrates in the middle of the conduction path of $\pi$-electrons; (3) the interaction between conduction electrons and phonon is too weak to cause the lattice distortion. From these results it is concluded that CoPc's have far stronger interaction between $\pi$- and d-electrons than CuPc's and that the interaction causes the localization of $\pi$-electrons.

(2) Two-dimensional polymer: $(CuPc)_x$

We tried the synthesis of two-dimensional polymer, $(CuPc)_x$ by the thermopolymerization under 50000 atm. Although the condition of the synthesis remained to be further examined, a compound with rather low resistivity ($\rho RT=10^{-2}\Omega$ cm) was prepared. The elemental analysis, X-ray diffraction, NMR, electrical resistivity, magnetic susceptibility, ESR and far- and infrared spectrum are being measured.

### (3) The Organic Compounds with Magnetic Ions

$(BEDT\text{-}TTF)_6Cu_2Br_8$ was examined. Above 6 Kbar, the metallic state appears. From ESR, heat capacity and conductivity measurements, the transition at 59 K can be attributed to the distortion of the tetrahedral $CuBr_4^{2-}$. The spin on $Cu^{2+}$ can be explained by two-dimensional Heisenberg model with the spin-spin interaction J=−17 K, which suggests that $\pi$-d interaction through BEDT-TTF molecules should be important. By examination of the magnetization curve we found a spin flop transition at several kilooersted. The magnetic anisotropy fields were also measured.

### (4) M(dmit)$_2$(M=Ni, Pd) Superconductors

A new superconductor $[(CH_3)_2(C_2H_5)_2N][Pd(dmit)_2]_2$ was found this year. It exhibits superconductivity under 2.4 Kbar or more but under higher pressure than 7 Kbar it turns into an insulator. The insulating phase again starts to disappear with increasing pressure. Further study under higher pressures are in progress. Also this year (EDT-TTF)$[Ni(dmit)_2]_2$ was found to be the first example of the metal complex superconductor under ambient pressure.

### (5) Mixed-valence Compounds with Bridged Halogens

#### 5-a) One-dimensional Compounds

$Cs_2[Pt(NO_2)Cl_2(NH_3)][Pt(NO_2)Cl_4(NH_3)](Pt\text{-}NO_2)$ and $K_2[Pt(Py)Cl_3][Pt(Py)Cl_5](Pt\text{-}Py)$ were synthesized and their reflectance spectra were measured. On both spectra of the complexes strong $Pt^{II}$-$Pt^{IV}$ charge-transfer bands polarized along the one-dimensional direction were observed. The transition energies decreases as follows;
$Cs_2[Pt(NO_2)Cl_2(NH_3)][Pt(NO_2)Cl_4(NH_3)](Pt\text{-}NO_2) >$
$[Pt(en)_2][PtCl_2(en)_2](ClO_4)_4(Pt\text{-}en) >$
$K_2[Pt(Py)Cl_3][Pt(Py)Cl_5](Pt\text{-}Py)$.

#### 5-b) Three-dimensional Compounds

On $Cs_2Au_2X_6$(X=Cl, Br, I) the relation between the conductivity and the structure under high pressures was investigated. $Cs_2Au_2I_6$ was observed to make a first order transition around 5.5 GPa. The c-axis suddenly elongates and the resistivity jumps by the magnitudes of 3 or 4 orders. Under higher pressures the band Jahn-Teller transition are thought to occur, which is peculiar to $d^9$ configuration, while under lower pressures the valence fluctuation of Au is thought to occur, which might have something to do with the anomaly in the resistivity. The cubic phase at high pressures and high temperatures is meta-stable metallic phase, where the oxidation state of Au is conceived to be +II. As for the Cl and Br salts similar transitions were observed under high pressures.

## C. Electronic Relaxation and Reaction of Electronically Excited Metal Atoms

*Coordinators:* **Shigeru TSUNASHIMA** *(Tokyo Inst. of Tech.)*, **Suehiro IWATA** *(Keio Univ.)*, **Shunzo YAMAMOTO** *(Okayama Univ.)*, **Kazuo KASATANI** *(Fukuoka Women's College)*, **Kaoru YAMANOUCHI** *(Tokyo Univ.)*, **Hironobu UMEMOTO** *(Tokyo Inst. of Tech.)*, **Fuminori MISAIZU, and Kiyokazu FUKE**

In order to understand reaction dynamics, the information on the reaction rates as well as the initial product state distributions are inevitable. In the present projects, both full- and half-collision processes of excited metal atoms are studied by employing pulsed laser techniques. In the half-collision studies, pico second spectroscopic studies are also planned.

### (1) Nascent Rotational and Vibrational Distributions in Both Products of the Reaction: $Zn(4_1P_1)+H_2O \rightarrow ZnH(X^2\Sigma^+)+OH(X^2\Pi)$

The reaction $Zn(4^1P_1)+H_2O \rightarrow ZnH(X^2\Sigma^+)+OH(X^2\Pi)$ was studied under thermal equilibrium conditions at 700K. The nascent internal state distributions of both products, ZnH and OH, were determined by using a pump-and-probe technique. The rotational distributions of ZnH and OH were both Boltzmann-like for their $v'=0$ vibrational levels. However, the rotational temperatures were significantly different; 12000K for ZnH and 900K for OH. ZnH was also vibrationally excited. The nascent vibrational distribution of ZnH was determined to be $10(v'=0):13(v'=1):7(v'=2):2(v'=3)$. In contrast, no excitation in the OH vibration was observed. Such a non-statistical energy partitioning is explained by considering a short-lived Zn-H-OH intermediate in a non-linear geometry.

### (2) Nascent Rotational State Distributions of $ZnH(X^2\Sigma^+)$ Produced in the Reaction of $Zn(4^1P_1)$ with Simple Alkane Hydrocarbons

The reactions of $Zn(4^1P_1)$ with $CH_4$, $C_2H_6$, $C_3H_8$ and $C(CH_3)_4$ were studied by employing a laser pump-and-probe technique. The nascent rotational state distributions of $ZnH(X^2\Sigma^+, v'=0)$ were determined. The rotational distributions could be approximated by Boltzmann distributions in all cases. The corresponding Boltzmann temperature decreased with the size of the hydrocarbons; 9000K for $CH_4$, 5000K for $C_2H_6$, 2900K for $C_3H_8$ and 1600K for $C(CH_3)_4$. These distributions were compared with those predicted by a statistical model.

### (3) Half Collision Processes of Excited Cd Atoms

The half collision processes of excited Cd atoms and $H_2$ are going to be studied under beam conditions. The real time measurement of the dynamical behavior of short-lived species such as electronically excited $CdH_2$ complexes are going to be carried out. The ground state $CdH_2$ complexes can be formed in a supersonic expansion. These species are excited to the lowest singlet or triplet excited states by a tunable dye laser. The photofragments such as H atoms as well as the excited $CdH_2$ complexes are probed by using nano- or pico-second lasers.

## D. Properties of Complexes with Electron-lacking Transition Metals

*Contributors:* **Koichi NARASAKA** *(Tokyo Univ.)*, **Kazuyuki TATSUMI** *(Osaka Univ.)*, **Akira MIYASHITA** *(Saitama Univ.)*, **Toshikazu HIRAO** *(Osaka Univ.)*, **Koichi MIKAMI** *(Tokyo Institute of Tech.)*, **Kazuhiko TAKAI** *(Kyoto Univ.)*, **Kazushi MASHIMA** *(Osaka Univ.)*, **Atsunori MORI** *(Tokyo Univ.)*, **and Tamotsu TAKAHASHI** *(IMS)*

The purpose of this joint studies program is to understand the properties of electron-lacking transition metal complexes in order to develop this area. This area consists

of early transition metal chemistry and lanthanide chemistry.

### (1) Asymmetric Bond Formation Reactions Using Early Transition Metal Complexes or Lanthanide Complexes

Chiral Lewis-acidic complexes could be used for asymmetric carbon-carbon bond formation reactions. Peptide-titanium or zirconium complexes were prepared.

### (2) Relation between a Reaction Activity and a Structure of Complexes

Bridged titanocene or zirconium complexes were designed and prepared. These complexes were very active for $\alpha$-olefin polymerization reactions with high stereoselectivities.

### (3) Development of an Effective Redox System

Vanadium has various oxidation states. One electron transfer reactions is an usual way for vanadium. Development of a novel useful organic synthesis method using vanadium complexes have been tried.

### (4) Preparation of Complexes with Novel Properties

Soluble transition metal chalcogenides represent one of the most fruitful specialties in coordination chemistry, in view of their structural and electrochemical diversity. The preparation of chalcogenide complexes of early transition metals is often beset with problems arising from the propensity of (poly)charcogenide anions to form insoluble polymeric residues. One way to avoid this problem was to introduce organic auxiliary ligands, e.g., Cp* , which could promotes solubility of metal chalcogenides and thereby make their chemistry tractable.

### (5) Selective Carbon-carbon Bond Formation Reactions

A low valent tantalum compound, which was prepared from pentachlorotantalum and zinc metal, reacted with alkynes to produce tantalum-alkyne complexes. The reactivities and properties of this tantalum-alkyne complexes were investigated.

## 2) Research Symposia

1. Symposium on Molecular Dynamics and Chemical Reactivity
   (October 12th–15th, 1992)
   Organizer: I. Ohmine
2. Dynamical Processes in Molecules and Molecular Assembles
   (January 11th–13th, 1993)
   Organizer: I. Hanazaki
3. Current Status and Future Prospects of Intersteller Chemistry and Physics with Submillimeter-wave Telescopes
   (February 22th–23th, 1993)
   Organizer: S. Yamamoto
4. Symposium on Physical Chemistry for Young Researchers in Molecular Science
   (May 9th, 1993)
   Organizer: O. Takahashi
5. Chemistry of Metal Complexities in Mesoscopic Phase
   (July 9th–11th, 1993)
   Organizer: S. Kaifu
6. Photochemistry of Coordination Compounds
   (August 3rd, 1993)
   Organizer: Y. Fukuda

## 3) Cooperative Research

This is one of the most important programs IMS undertakes for conducting its own research of the common interest to both outside and IMS scientists by using the facilities at IMS. During the first half of fiscal year of 1992 ending on September 30, 56 outside scientists including 1 invited collaborated with IMS scientists; and during the second half of the fiscal year, 71 outside scientists and 1 invited scientists worked in collaboration with IMS scientists, the names and the affiliations of these collaborators are found in the Research Activities.

## 4) Use of Facilities

The number of projects accepted for the Use of Facility Program of the Computer Center during the fiscal year of 1992 amounted to 215 (661 users) and the computer time spent for these projects is 9286 hours (converted to the HITAC M-680H time), and amounted to 62% of the total annual CPV time used.

Projects (250 users) were accepted for the Use of Facility Program of the Instrument Center during the fiscal year of 1992.

## 5) UVSOR

In the UVSOR Facility with the 750 MeV electron storage ring, there are nineteen beam lines available for synchrotron radiation research (see "UVSOR ACTIVITY REPORT 1993"). The Experimental Facility of each beam line is described in the introductory pamphlet "OUTLINE OF UVSOR". The Japanese and English versions are available through UVSOR Facility. Under the following programs, a number of SR studies have been carried out by many users outside and inside IMS: a) the UVSOR Special Project, b) the UVSOR Cooperative Research Projects, c) the UVSOR Invited Research Projects, and d) the User-of-UVSOR Projects. Furthermore, the 12th UVSOR User's Symposium was held on December 18, 1992 as a satellite meeting combined with 46th Okazaki Conference "Present Status and Future Prospect of Synchrotron Radiation Science".

## 5-a) UVSOR Special Project

### Development of the Infrared and Far-infrared Spectroscopy Using Synchrotron Radiation

**Kyuya YAKUSHI, Akito UGAWA, Tadaoki MITANI, Hiroshi OKAMOTO,** Takao NANBA,*** Makoto WATANABE, and Kusuo SAKAI** *(*Univ. of Tokyo, **Tohoku Univ., ***Kobe Univ.)*

Application of Synchrotron Radiation (SR) has been performed at the beamline BL-6B of the UVSOR facility in IMS. We are conducting three projects for the use of infrared region of SR using the characteristic natures of SR such as a high collimation, high brilliance, wide-range tunability, and pico-second pulse width. (1) The former three natures are the ideal properties as the light source of a microspectrophotometric apparatus. We are constructing a microspectrophotometer to measure optical reflectivity of a small ($\sim$20 $\mu$m) single crystal in the wide range (50 $cm^{-1}$–13000 $cm^{-1}$). This apparatus will be mainly used for the study of organic conductors and superconductors. (2) The last property of SR is appropriate to the time-resolved spectroscopy. Delay-time modulation spectrometer has been designed and constructed using the pico-second light pulse of SR synchronized with a cw mode-locked Nd-YAG laser. This method is applied to the transient photo-induced absorption spectroscopy in the infrared region by combining with FT-IR to increase the sensitivity. (3) Another experiment is prepared for the grazing-angle infrared spectroscopy for the surface absorbed molecules. This optical system uses also the high collimation and high brilliance of SR.

### Studies of Dissociation Processes in Inner-shell and Multiple Ionized Molecular Ions

*Coordinator:* **Inosuke KOYANO** *(Himeji Institute of Technology)*

This project started in 1990 with the objective to understand the dissociation mechanisms of molecules following the inner-shell and multiple (double and triple) photoionization in the vacuum ultraviolet. The multiple photoionization includes both the direct type and via-Auger type processes. The apparatus on beamline 3A2,[1] which has been designed to allow measurements of angle-resolved TOF mass and PIPICO spectra of ionic products of the dissociation, is utilized in the wavelength range of 30–140 eV. The project has successfully been performed owing to the tremendous efforts of the members of the project, notably Drs. T. Masuoka, S. Nagaoka, T. Imamura, and T. Ibuki. Two scientists from abroad, C.E. Brion (Canada) and B.H. Boo (Korea), have also joined and contributed greatly to the project.

The main results obtained in this year (the last year of the project) are summarized as follows.

(i) Relation between the ionized molecular orbitals and dissociation pathways of doubly charged ions of $CH_2$=$CD_2$ and $CH_2$=$CF_2$ (key person: T. Ibuki).[2]

The PIPICO studies of the title molecules have been performed extensively in the valence double photoionization region. Comparison of the results with the recent theoretical studies of the electric states of the electronic states of doubly changed ethenes made it clear that the double ionization involving release of at least one $\pi_{C=C}$ electron results in the C=C bond cleavage, while that involving release of two electrons from either the $\sigma_{CH_2}$,$\sigma_{CC}$, or C 2s orbitals of ethene forms two smaller fragment ions of the form $H^+$+$CX_m^+$.

(ii) Photoelectron-photoion-photoion triple coincidence (PEPIPICO) study of OCS (key person: T. Masuoka).[3]

The PEPIPICO measurements, which provide further detailed dynamical information on the dissociation of multiple-charged molecular ions, have been made possible and applied to the OCS molecule. The spectra obtained clearly distinguished several dissociation mechanisms of $OCS^{2+}$, i.e., simultaneous three body dissociation into $C^+$+$O^+$+S, sequential dissociation into $C^+$+$S^+$+O via $OC^+$+$S^+$, simultaneous three-body dissociation into $O^+$+$S^+$+C with the central C atom being a spectator, and two-body dissociations into $O^+$+$CS^+$ and $OC^+$+$S^+$.

(iii) Inner-shell photoionization and search for site-specific dissociation processes (key person: S. Nagaoka).[4]

Several interesting molecules from the viewpoint of inner-shell vs valence ionization and the site-specific dissociation have been synthesized and studied. Although definite site-specificity has not been recognized in the wavelength regions studied, characteristic fragmentation patterns for the inner-shell ionization have been observed in some molecules, for example, in $(CH_3)_3SiCH_2SiF_3$ and $Si_2(CH_3)_3Cl_3$.

**References**

1) T. Masuoka, T. Horigome, and I. Koyano, *Rev. Sci. Instrum.* **60**, 2179 (1989).
2) T. Ibuki, T. Imamura, I. Koyano, T. Masuoka, and C.E. Brion, *J. Chem. Phys.* **98**, 2908 (1993).
3) T. Masuoka, *J. Chem. Phys.* **98**, 6989 (1993).
4) S. Nagaoka, J. Ohshita, M. Ishikawa, T. Masuoka, and I. Koyano, *J. Phys. Chem.* **97**, 1488 (1993).

## 5-b) UVSOR Cooperative Research Projects

Under this joint-study program, many synchrotron radiation experiments have been carried out with the beam lines of in-house staff in cooperation with scientists who were invited from other institutions. The total number of the projects in this category was 39 in the fiscal year of 1992.

## 5-c) The UVSOR Invited Research Projects

Under this joint-study program, several scientists were invited from other institutions to help for construction of new beam lines and improvement of the UVSOR storage ring and others. The total number of the projects in this category was 7 in the fiscal year of 1992.

## 5-d) The Use-of-UVSOR Projects

Ten out of the total of nineteen UVSOR beam lines are available for general users outside and inside IMS for their synchrotron radiation studies in the field of molecular science. The total number of the projects in this category was 107 in the fiscal year of 1992.

# FOREIGN SCHOLARS

Visitors from abroad play an important role in research activities and are always welcome at IMS. The following is the list of foreign scientists who visited IMS in the past year (Aug. 1992 – July 1993). The sign *[1] indicates an attendant to an Okazaki Conference, *[2] an IMS or Japan Society for the Promotion of Science Invited Foreign Scholar, *[3] an IMS councillor, *[4] an IMS visiting scientist, and *[5] an IMS adjunct professor or associate professor from abroad (period ofstay is from 9 to 12 months). Scientists who wish to visit IMS under program *[2] and *[5] are invited to make contact with an IMS faculty in a related field.

| | | | |
|---|---|---|---|
| Dr. F. Maseras*[4] | Univ. Autonama Barcelona | (Spain) | Oct. 1991 - Dec. 1993 |
| Dr. Bongsoo Kim*[2] | Univ. of California, Berkeley | (USA) | Nov. 1991 - |
| Dr. P. J. Jewsbury*[2] | Univ. of Edinburgh | (UK) | Feb. 1992 - |
| Dr. J.-F. Riehl*[2] | Centre Paris-Sud | (France) | Feb. 1992 - |
| Dr. R. J. Whitehead*[2] | Univ. of Durham | (UK) | Mar. 1992 - |
| Dr. D. Y. Kondakov*[2,4] | St. Petersburg State Univ. | (Russia) | Jun. 1992 - Jun. 1993 |
| | | | Jun. 1993 - |
| Dr. A. Mebel*[4] | Inst. of New Chem. Problems | (Russia) | Jun. 1992 - Mar. 1993 |
| Dr. T. Radnai*[2] | Hungarian Acad. Sci. | (Hungary) | - Aug. 1992 |
| Prof. A. D. Bandrauk*[5] | Univ. of Sherbrooke | (Canada) | - Aug. 1992 |
| Mr. Huh Chul*[4] | Inha Univ. | (Korea) | - Aug. 1992 |
| Dr. Hong Lae Kim*[2] | Kangweon Natl. Univ. | (Korea) | - Aug. 1992, Jan. - Mar. 1993 |
| Prof. Joon Taik Park*[2] | KAIST | (Korea) | - Aug. 1992 |
| | | | Dec. 1992 - Feb. 1993 |
| Prof. R. L. Christensen*[4] | Bowdoin College | (USA) | - Aug. 1992, May 1993 |
| Mr. Jeong - Min Kweon | Kyungpook Natl. Univ. | (Korea) | - Aug. 1992 |
| Ms. D. Choueiri*[4] | Purdue Univ. | (Lebanon) | - Aug. 1992 |
| Prof. Tsun-Kong Sham*[2] | Univ. Western-Ontario | (Canada) | - Aug. 1992 |
| Dr. Dongho Kim | Korea Inst. of Stand. and Sci. | (Korea) | Aug. 1992 |
| Prof. T. J. Schaafsma | Wageningen Agricultural Univ. | (Holland) | Aug. 1992 |
| Prof. Sehun Kim*[2] | KAIST | (Korea) | Aug. 1992 |
| Prof. Bong-Hyun Boo | Chungnam Natl. Univ. | (Korea) | Aug. 1992, Jan. 1993 |
| Prof. M. Okumura | Univ. of California | (USA) | Aug. 1992 |
| Prof. I. H. Munro | Daresbury Lab. | (UK) | Aug. 1992 |
| Prof. V. A. Ivanov | Russian Acad. of Science | (Russia) | Aug. 1992 |
| Dr. M. E. Couprie | Univ. Paris-Sud | (France) | Aug. 1992 |
| Dr. A. D. Hammerich*[4] | Hebrew Univ. | (Israel) | Aug. - Sep. 1992 |
| Dr. R. Serra*[4] | Univ. Autonoma Barcelona | (Spain) | Aug. - Nov. 1992 |
| Dr. D. J. Wales*[2] | Univ. of Cambridge | (UK) | - Sep. 1992, Jul. 1993 |
| Dr. Sung-Hong Kim*[4] | Kyungpook Natl. Univ. | (Korea) | - Sep. 1992 |
| Prof. Young S. Choi*[4] | Inha Univ. | (Korea) | - Sep. 1992 |
| | | | Dec.1992 - Feb. 1993 |
| | | | Jun. - Aug. 1993 |
| Prof. K. A. Nelson*[2] | Massachusetts Inst. of Tech. | (USA) | - Sep. 1992 |
| Dr. C. J. Rousset*[2] | Purdue Univ. | (France) | - Sep. 1992 |
| Mr. M. Cho | Univ. of Chicago | (USA) | Sep. 1992 |
| Dr. L. Powers | Natl. Center for the Design of Mol. Function | (USA) | Sep. 1992 |
| Prof. E. I. Solomon | Stanford Univ. | (USA) | Sep. 1992 |
| Prof. H. Metiu | Univ. of California, Santa Barbara | (USA) | Sep. 1992 |
| Prof. W. G. Klemperer | Univ. of Illinois | (USA) | Sep. 1992 |
| Prof. L. Sanche*[2] | Univ. of Sherbrooke | (Canada) | Sep. 1992 |
| Prof. B. Venkataraman | Tata Inst. of Fundam. Res. | (India) | Sep. 1992 |
| Dr. J. Durrant | Imperial College | (UK) | Sep. 1992 |
| Dr. Young Mok Park | Korea Basic Sci. Center | (Korea) | Sep. 1992 |
| Dr. Jong Soon Choi | Korea Basic Sci. Center | (Korea) | Sep. 1992 |
| Prof. P. F. Barbara | Univ. of Minnesota | (USA) | Sep. 1992 |
| Dr. G. P. Morley | Univ. of Bristol | (UK) | Sep. 1992 |
| Prof. M. J. Cook | Univ. of East Anglia | (UK) | Sep. 1992 |
| Prof. S. Leon | Univ. of Scherbrooke | (Canada) | Sep. 1992 |

| | | | |
|---|---|---|---|
| Prof. Tang Ao Qing | Natl. Nature Sci. Foundation | (China) | Sep. 1992 |
| Prof. Xu Guang Xian | Beijing Univ. | (China) | Sep. 1992 |
| Dr. Zhang Cun Hao | Natl. Nature Sci. Foundation | (China) | Sep. 1992 |
| Prof. Cao Yang | Suzhou Univ. | (China) | Sep. 1992 |
| Mr. Liu Feng | Jilin Univ. Foreign Affairs Dept. | (China) | Sep. 1992 |
| Prof. Y. Haas | Hebrew Univ. | (Israel) | Sep. - Oct. 1992 |
| Prof. Jiabo Li*4 | Xiamen Univ. | (China) | Sep. - Mar. 1993 |
| Mr. A. E. Johnson | Univ. of Minnesota | (USA) | Sep. - Dec. 1992 |
| Prof. M. Suzuki*4 | State Univ. New York | (USA) | Sep. - Dec. 1992 |
| Dr. I. S. Suzuki*4 | State Univ. New York | (USA) | Sep. - Dec. 1992 |
| Prof. E. L. Frankevich*5 | Russ. Acad. Sci. | (Russia) | Sep. 1992 - Jul. 1993 |
| Prof. Jihwa Lee*2 | Seoul Natl. Univ. | (Korea) | Sep. 1992 - Aug. 1993 |
| Prof. L. S. Grigoryan*5 | Armenian Acad. of Sci. | (Armenia) | Sep. 1992 - |
| Dr. J. Gorecki*5 | Polish Acad. Sci. | (Poland) | - Oct. 1992 |
| Dr. Shuqin Zhou*4 | Academia Sinica | (China) | - Oct. 1992 |
| Dr. A. Dedieu | Univ. Louis Pasteur | (France) | Oct. 1992 |
| Prof. N. N. Greenwood | Univ. of Leeds | (UK) | Oct. 1992 |
| Prof. R. Kosloff | Hebrew Univ. of Jerusalem | (Israel) | Oct. 1992 |
| Prof. M. Shapiro | Weizmann Inst. of Sci. | (Israel) | Oct. 1992 |
| Prof. J. Jortner | Tel-Aviv Univ. | (Israel) | Oct. 1992 |
| Prof. R. D. Levine | Hebrew Univ. of Jerusalem | (Israel) | Oct. 1992 |
| Prof. A. Nitzan | Tel-Aviv Univ. | (Israel) | Oct. 1992 |
| Prof. T. P. Fehlner | Notre Dame Univ. | (USA) | Oct. 1992 |
| Prof. J. C. Polanyi*3 | Univ. of Toronto | (Canada) | Oct. 1992 |
| Prof. Zhenghe Zhu | Inst. of Atomic & Mol. Phys. Chengdu | (China) | Oct. 1992 |
| Prof. R. H. Herber | Univ. of New Jersey | (USA) | Oct. 1992 |
| Dr. C. Bellitto | Int. of Theory and Electronic Structure, CNR | (Italy) | Oct. 1992 |
| Dr. M. Larsson | Royal Inst. of Tech. | (Sweden) | Oct. 1992 |
| Prof. Renyuan Qian | Academia Sinica | (China) | Oct. 1992 |
| Prof. Fosong Wang | Academia Sinica | (China) | Oct. 1992 |
| Prof. Wenzao Qian | Academia Sinica | (China) | Oct. 1992 |
| Prof. Daoben Zhu | Academia Sinica | (China) | Oct. 1992 |
| Prof. Xian-Tong Bi | Academia Sinica | (China) | Oct. 1992 |
| Prof. Peiji Wu | Academia Sinica | (China) | Oct. 1992 |
| Dr. Fenglian Bai | Academia Sinica | (China) | Oct. 1992 |
| Prof. Cheng Ye | Academia Sinica | (China) | Oct. 1992 |
| Dr. Yunqi Liu | Academia Sinica | (China) | Oct. 1992 |
| Prof. Deqing Zhang | Academia Sinica | (China) | Oct. 1992 |
| Dr. Suzhen Li | Academia Sinica | (China) | Oct. 1992 |
| Prof. You-Ming Chang | Academia Sinica | (China) | Oct. 1992 |
| Dr. Yongfang Li | Academia Sinica | (China) | Oct. 1992 |
| Prof. Ji-Min Yan | Academia Sinica | (China) | Oct. 1992 |
| Prof. Wenxin Zhang | Academia Sinica | (China) | Oct. 1992 |
| Prof. Shaolin Mu | Yangzhou Teacher's College | (China) | Oct. 1992 |
| Prof. Rong Tang Fu | Fudan Univ. | (China) | Oct. 1992 |
| Prof. Dian-Lin Zhang | Academia Sinica | (China) | Oct. 1992 |
| Prof. Songyu Huang | East China Univ. of Chem. Tech. | (China) | Oct. 1992 |
| Prof. Wenbin Zhang | Academia Sinica | (China) | Oct. 1992 |
| Prof. Renkuan Yuan | Nanjing Univ. | (China) | Oct. 1992 |
| Prof. Jinqui Qin | Wuhan Univ. | (China) | Oct. 1992 |
| Prof. Xiaabin Jing | Academia Sinica | (China) | Oct. 1992 |
| Prof. Tiejin Li | Jilin Univ. | (China) | Oct. 1992 |
| Prof. Mujie Yang | Zhejiang Univ. | (China) | Oct. 1992 |
| Prof. Ki-Jung Paeng | Yonsei Univ. | (Korea) | Oct. 1992 |
| Prof. V. Aquilanti*2 | Univ. of Perugia | (Italy) | Oct. - Nov. 1992 |
| Dr. D. C. Clary*1 | Univ. of Cambridge | (UK) | Oct. - Nov. 1992 |
| Dr. Ping Wang*4 | Univ. of Alabama | (USA) | Oct. - Nov. 1992 |
| Prof. J. Kincaid | Marquette Univ. | (USA) | Oct. - Nov. 1992 |
| Dr. Yong-Fang Li*4 | Academia Sinica | (China) | Oct. - Dec. 1992 |

| | | | |
|---|---|---|---|
| Dr. Yang Hai | Inst. of High Energy Phys. | (China) | Oct. 1992 - Jul. 1993 |
| Dr. I. I. Khairullin*2 | Uzbekistan Akademy of Sciences | (Uzbek) | Oct. 1992 - |
| Prof. K. Schulten*1 | Univ. of Illinois | (USA) | Nov. 1992 |
| Prof. J. M. Bowman*1 | Emory Univ. | (USA) | Nov. 1992 |
| Prof. H. J. Werner*1 | Univ. Bielfeld | (Germany) | Nov. 1992 |
| Prof. K. R. Wilson*1 | Univ. of California, San Diego | (USA) | Nov. 1992 |
| Prof. T. Ziegler*1 | Univ. of Calgary | (Canada) | Nov. 1992 |
| Prof. Zhang Cuo Dong | HESYRL, Univ. of Sci. & Tech. | (China) | Nov. 1992 |
| Dr. Qiuping Wang | HESYRL, Univ. of Sci. & Tech. | (China) | Nov. 1992 |
| Prof. Shu-Qin Yu | Univ. of Sci. & Tech. of China | (China) | Nov. 1992 |
| Dr. Chuan Jan Ding | Chinese Academy of Sci. | (China) | Nov. 1992 |
| Prof. P. Day*3 | Royal Institution | (UK) | Nov. 1992 |
| Dr. D. Robin | Lawrence Berkeley Lab. | (USA) | Nov. 1992 |
| Dr. J. McMurdo*4 | Univ. of East Anglia | (UK) | Nov. - Dec. 1992 |
| Prof. Poh-Kun Tseng | Natl. Taiwan Univ. | (Taiwan) | Nov. - Dec. 1992 |
| Prof. Way-Faung Pong | Natl. Taiwan Univ. | (Taiwan) | Nov. - Dec. 1992<br>Apr. - May 1993 |
| Prof. K. Stefanski*5 | Nicolas Copernicus Univ. | (Poland) | Nov. 1992 - Aug. 1993 |
| Prof. T. C. Steimle | Arizona State Univ. | (USA) | Nov. 1992 - Feb. 1993 |
| Dr. Yan-Ping Zhang | Max-Planck Inst. | (Germany) | Nov. 1992 - |
| Prof. R. Osman | Mount Sinai School of Medical | (USA) | Dec. 1992 |
| Prof. I. I. Morozov | Inst. of Chem. Phys., Acad. Sci. of Russia | (Russia) | Dec. 1992 |
| Mr. Taek-Soo Kim*4 | Inha Univ. | (Korea) | Dec. 1992 - Feb. 1993 |
| Dr. S. R. Meech*4 | Heriot-Watt Univ. | (UK) | Dec. 1992 - Jan. 1993<br>Jun. - Aug. 1993 |
| Dr. D. J. Fox | Gaussian INC. | (USA) | Dec. 1992 |
| Dr. M. J. Frisch | Gaussian INC. | (USA) | Dec. 1992 |
| Prof. B. Schlegel | Wayne State Univ. | (USA) | Dec. 1992 |
| Prof. J. A. Pople | Carnegie-Mellon Univ. | (USA) | Dec. 1992 |
| Prof. W. Buarn*1 | BESSY | (Germany) | Dec. 1992 |
| Dr. S. Krinsky*1 | NSLS, BNL | (USA) | Dec. 1992 |
| Prof. Y. T. Lee*1 | Univ. of Calif., Berkeley | (USA) | Dec. 1992 |
| Dr. P. Lablanquie*1 | Univ. Paris Sud | (France) | Dec. 1992 |
| Prof. I. Lindau*1 | MAX-Lab., Univ. of Lund | (Sweden) | Dec. 1992 |
| Prof. P. Weightman*1 | Univ. of Liverpool | (UK) | Dec. 1992 |
| Prof. Georg Zimmerer | Univ. of Hamburg | (Germany) | Dec. 1992 |
| Prof. A. C. Sykes | Univ. of Newcastle Upon Tyne | (UK) | Dec. 1992 |
| Prof. N. D. Yordanov | Bulgarian Academy of Science | (Bulgaria) | Dec. 1992 |
| Prof. C. W. Neilson | Univ. of Bristol | (UK) | Dec. 1992 |
| Dr. P. M. Rajo Rao | BARC | (India) | Dec. 1992 |
| Prof. C. Y. Xu | Univ. Sci. & Tech. | (China) | Dec. 1992 |
| Dr. J. D. Bozek | Univ. Western-Ontario | (Canada) | Dec. 1992 |
| Dr. S. Y. Rah | Postech, Pohang | (Korea) | Dec. 1992 |
| Dr. Y. Chung | Postech, Pohang | (Korea) | Dec. 1992 |
| Prof. Joon Taik Park | KAIST | (Korea) | Dec. 1992 - Feb. 1993 |
| Prof. V. Y. Kukushkin*2 | St. Petersburg State Univ. | (Russia) | Dec. 1992 - Apr. 1993 |
| Dr. M. C. R. Cokett*2 | Univ. of Southampton | (UK) | - Jan. 1993 |
| Dr. D. G. Musaev*2 | Inst. New Chem. Problems | (Russia) | - Jan. 1993 |
| Dr. J. Moc*2 | Univ. Wraclaw | (Poland) | - Jan. 1993 |
| Prof. Mu Shik Jhon | KAIST | (Korea) | Jan. 1993 |
| Prof. Jong-Jean Kim | KAIST | (Korea) | Jan. 1993 |
| Prof. Kyoung Tai No | Soongsil Univ. | (Korea) | Jan. 1993 |
| Prof. Nark Nyul Choi | Kumoh Natl. Inst. of Tech. | (Korea) | Jan. 1993 |
| Prof. Heon Kang | Pohang Inst. of Sci. &Tech. | (Korea) | Jan. 1993 |
| Prof. Ryong Ryoo | KAIST | (Korea) | Jan. 1993 |
| Prof. Hosung Sun | Pusan Natl. Univ. | (Korea) | Jan. 1993 |
| Dr. Dae Won Moon | KAIST | (Korea) | Jan. 1993 |
| Dr. Dongho Kim | KAIST | (Korea) | Jan. 1993 |
| Prof. Seong Keun Kim | Seoul Natl. Univ. | (Korea) | Jan. 1993 |
| Prof. Du-Jeon Jang | Seoul Natl. Univ. | (Korea) | Jan. 1993 |

| | | | |
|---|---|---|---|
| Prof. Sung-Ho Sack Salk | Pohang Inst. of Sci. & Tech. | (Korea) | Jan. 1993 |
| Prof. Youngkyu Do | Korea Adv. Inst. of Sci. & Tech. | (Korea) | Jan. 1993 |
| Prof. Jakang Ku | Pohang Inst. of Sci. & Tech. | (Korea) | Jan. 1993 |
| Prof. Jisoon Ihm | Seoul Natl. Univ. | (Korea) | Jan. 1993 |
| Prof. Byoung Jip Yoon | Kangreung Natl. Univ. | (Korea) | Jan. 1993 |
| Prof. Young Kee Kang | Chungbuk Natl. Univ. | (Korea) | Jan. 1993 |
| Mr. Hang-Woo Lee | Pohang Inst. of Sci. & Tec. | (Korea) | Jan. 1993 |
| Prof. A. Underhill | Univ. of Wales (Bangor) | (UK) | Jan. 1993 |
| Dr. R. Bushby | Leeds Univ. | (UK) | Jan. 1993 |
| Dr. M. Grossel | Univ. of Southampton | (UK) | Jan. 1993 |
| Dr. G. Ashwell | Cranfield Inst. of Tech. | (UK) | Jan. 1993 |
| Dr. K. Seddon | Univ. of Sussex | (UK) | Jan. 1993 |
| Prof. H. Heller | Univ. of Wales (Cardif) | (UK) | Jan. 1993 |
| Dr. J. King | SERC | (UK) | Jan. 1993 |
| Mr. Chul Huh | Inha Univ. | (Korea) | Jan. - Feb. 1993 |
| Prof. Dong-Eon Kim | Pohang Inst. of Sci. & Tec. | (Korea) | Jan. - Feb. 1993 |
| Mr. Seong-Ho Kim | Pohang Inst. of Sci. & Tec. | (Korea) | Jan. - Feb. 1993 |
| Mr. Jang-Chul Seo*4 | Korea Res. Inst. of Standard & Sci. | (Korea) | Jan. - Feb. 1993 |
| Prof. Jung Chul Seo | Cheonbuk Natl. Univ. | (Korea) | Jan. - Mar. 1993 |
| Dr. Hong Lae Kim*2 | Kangweon Natl. Univ. | (Korea) | Jan. - Mar. 1993 |
| Dr. Jeongwon Kim | Cheonbuk Natl. Univ. | (Korea) | Jan. - Mar. 1993 |
| Mr. Hanwoong Yeom | Cheonbuk Natl. Univ. | (Korea) | Jan. - Mar. 1993 |
| Dr. Zhenfeng Xi*4 | Henan Inst. of Chem. | (China) | Jan. 1993 - |
| Prof. A. J. McCaffery | Univ. of Sussex | (UK) | Feb. 1993 |
| Prof. J. R. Reynolds | Univ. of Florida | (USA) | Feb. 1993 |
| Prof. Seung Min Park | Kyunghee Univ. | (Korea) | Feb. 1993 |
| Dr. Hackjin Kim | Chungnam Natl. Univ. | (Korea) | Feb. 1993 |
| Mr. Qi-Ming Wang | Chinese Academy of Science | (China) | Feb. 1993 |
| Mr. Gui-Hai Wang | Chinese Academy of Science | (China) | Feb. 1993 |
| Mr. Xue-Zhen Gu | Chinese Academy of Science | (China) | Feb. 1993 |
| Ms. Shu-Hui Deng | Chinese Academy of Science | (China) | Feb. 1993 |
| Mr. Yang-Fan Ou | Chinese Academy of Science | (China) | Feb. 1993 |
| Dr. F. H. Mies*2 | Natl. Inst. of Standards and Tech. | (USA) | Feb. - Mar. 1993 |
| Mr. Young-Sei Park*4 | Seoul Natl. Univ. | (Korea) | Mar. - May 1993 |
| Prof. S. F. A. Kettle*2 | Univ. of East Anglia | (UK) | Mar. 1993 |
| Dr. A. Marcellic | INFN, Lab. Naz. Frascati | (Italy) | Mar. 1993 |
| Prof. J. Prochorow | Polish Acad. of Sci. | (Poland) | Mar. 1993 |
| Prof. D. G. Whitten | Univ. of Rochester | (USA) | Mar. 1993 |
| Dr. M. Terekhin | Kurchatov Inst. of Atomic Energy | (Russia) | Mar. 1993 |
| Dr. K. M. Evenson | Natl. Inst. Stand. Tech. | (USA) | Mar. 1993 |
| Ms. Mei Du | Univ. of Chicago | (USA) | Mar. 1993 |
| Dr. F. Schälers | BESSY | (Germany) | Mar. - Apr. 1993 |
| Dr. A. P. Yartsev*2 | Inst. of Spectroscopy | (Russia) | - Apr. 1993 |
| Dr. I. Novak*2 | Natl. Univ. of Singapore | (Singapore) | Apr. 1993 |
| Prof. F. Siebert | Univ. Freiburg | (Germany) | Apr. 1993 |
| Prof. E. Källne | Royal Inst. of Tech. Stockholm | (Sweden) | Apr. 1993 |
| Prof. P. Erman | Royal Inst. of Tech. Stockholm | (Sweden) | Apr. 1993 |
| Dr. V. Kamalov | Inst. of Russian Acad. | (Russia) | Apr. 1993 |
| Prof. Poh-Kun Tseng | Natl. Taiwan Univ. | (Taiwan) | Apr. - May 1993 |
| Mr. Kung-Te Wu | Natl. Taiwan Univ. | (Taiwan) | Apr. - May 1993 |
| Dr. M. E. Kondakov*4 | Leningrad Paper Industry Inst. | (Russia) | Apr. 1993 - |
| Dr. Zhongfang Liu*4 | Beijing Univ. | (China) | - May 1993 |
| Dr. V. Denisov*4 | St. Petersburg State Univ. | (Russia) | - May 1993 |
| Prof. P. Stein | Duquesne Univ. | (USA) | May - Jul. 1993 |
| Dr. M. Kotora*2 | Inst. Chem. Process Fundamentals | (Czechoslovakia) | May 1993 - |
| Prof. J. Herbich | Polish Acad. of Sci. | (Poland) | Jun. 1993 |
| Prof. Young Kee Kang*2 | Chungbuk Natl. Univ. | (Korea) | Jun. 1993 |
| Dr. S. F. C. O'Rourke | Queen's Univ. of Belfast | (UK) | Jun. 1993 |
| Prof. Shaojian Xia | BSRL, Inst. of High Energy Phys. | (China) | Jun. 1993 |
| Dr. S. Umapathy | Indian Inst. of Sci. | (India) | Jun. 1993 |

| | | | |
|---|---|---|---|
| Dr. Youngmin Chung | Pohang Inst. of Sci. & Tec. | (Korea) | Jun. 1993 |
| Prof. Tai Jong Kang*[4] | Taegu Univ. | (Korea) | Jun. - Aug. 1993 |
| Prof. Young S. Choi | Inha Univ. | (Korea) | Jun. - Aug. 1993 |
| Mr. Taek-Soo Kim | Inha Univ. | (Korea) | Jun. - Aug. 1993 |
| Mr. Jae Young Kim*[4] | Seoul Natl. Univ. | (Korea) | Jul. 1993 |
| Prof. J. Connor | Manchester Univ. | (UK) | Jul. 1993 |
| Prof. Yoon Sup Lee | KAIST | (Korea) | Jul. 1993 |
| Prof. M. A. Robb | Univ. of London | (UK) | Jul. 1993 |
| Prof. H. S. Rzepa | Univ. of London | (UK) | Jul. 1993 |
| Prof. B. T. Sutcliffe | Univ. of York | (UK) | Jul. 1993 |
| Dr. A. Dedieu | Lab. de Chimie Quantique | (France) | Jul. 1993 |
| Prof. Kee Hag Lee | Wonkwang Univ. | (Korea) | Jul. 1993 |
| Prof. T. R. Rizzo | Univ. of Rochester | (USA) | Jul. 1993 |
| Dr. K. Kalyanasundaram | Ecole Polytechnique Federal de Lausaune | (Switzerland) | Jul. 1993 |
| Dr. A. Barnes | Univ. of Salford | (UK) | Jul. 1993 |
| Prof. J. Michl | Univ. of Colorado | (USA) | Jul. 1993 |
| Prof. P. Carsky | Heyrovsky Inst. of Phys. Chem. | (Czechoslovakia) | Jul. 1993 |
| Dr. Xu Chao Yin | Academia Sinica | (China) | Jul. 1993 |
| Dr. Liu Shun Cheng | Beijing Univ. | (China) | Jul. 1993 |
| Ms. J. M. Rehm | Univ. of Rochester | (USA) | Jul. - Aug. 1993 |
| Ms. L. Schilling | Univ. of Rochester | (USA) | Jul. - Aug. 1993 |
| Mr. J. W. Leon | Univ. of Rochester | (USA) | Jul. - Aug. 1993 |
| Prof. Sang K. Lee | Pusan Natl. Univ. | (Korea) | Jul. 1993 - Sept. 1993 |

# AWARD

## Emeritus Professor Hirota's Scientific Achievements

Emeritus Professor Eizi Hirota received the Award of Japan Academy of Science in 1992 for his contribution to "Precise Structure and Dynamical Behavior of Free Radical Molecules".

Transient molecules such as free radicals and unstable molecules are produced as intermediates in chemical reactions, and are very active. High resolution spectroscopy of free radicals have been a difficult subject for a long time. Professor Hirota established the microwave and infrared spectroscopic methods studying free radicals. He detected many fundamental free radicals and determined their detailed molecular structures precisely. Furthermore, he applied his spectroscopic methods to clarification of the dynamical processes of chemical reactions generating free radicals, and founded an interface between molecular structure and chemical reacion, both of which are of fundamental importance in physical chemistry.

## Associate Professor Takahashi's Scientific Achievements

Associate Professor Tamotsu Takahashi of Coordination Chemistry Laboratories received 'Progress Award in Synthetic Organic Chemistry, Japan' in 1992 for his contributions to "Development of Selective Reactions using Zirconocene Alkene Complexes" as follows.

1. Preparation of zirconocene-alkene complex
   He prepared the first zirconocene-alkene complex [$Cp_2Zr(PhHC{=}CHPh)(PMe_3)$] and determined the structure by X-ray study.
2. Development of selective carbon-carbon bond formation reactions
   He found that zirconocene-alkene complexes reacted with alkenes to give zirconacyclopentane compounds with high regioselectivities and stereoselectivities. Especially, when the ethylene complex [$Cp_2Zr(CH_2{=}CH_2)$], which was in situ prepared from $Cp_2ZrEt_2$, was used, pair selective cross coupling reactions with alkenes such as 1-decene and styrene proceeded.
3. Development of selective catalytic reactions
   He made a catalytic cycle for the highly selective cross coupling reactions described above. He made clear that the final product of a stoichimetric reaction, zirconacyclopentane, reacted with EtMgBr and the coupling product on zirconocene was transfered from zirconium to magnesium. This transmetalation reaction was also a very high selective reaction.
4. Development of a selective skeletal rearrangement by C-C bond activation
   He found that 2,5-dimethylmetallacyclopentane compounds were converted into 3,4-dimethylmetallacyclopentane compounds by carbon-carbon bond activation.
5. Catalytic hydrosilation reactions of alkenes using zirconocene-alkene complexes.
   He found that hydrosilation reactions of alkene proceeded with high regioselectivities using zirconocene-alkene complexes.

## Dr. Ogura's Scientific Achievements

Dr. Takashi Ogura of Department of Molecular Structure received the Award of the Chemical Society of Japan for Young Chemists in 1993 for his studies of "The Reaction Mechanism of Oxygen Activation by Cytochrome c Oxidase". Cytochrome c oxidase is the respiratory enzyme, which catalyzes reduction of dioxygen to water in all aerobic organisms, has been studied with various techniques for a long time, but Dr. Ogura has made a breakthrough in elucidating its reaction mechanism by combining Raman spectroscopy with his original devices. Dr. Ogura's contributions are summarized as follows;

1) Classification of observed Raman bands into those of cytochrome a and cytochrome $a_3$, and the assignment of the Fe-histidine stretching band of cytochrome $a_3$.
2) Construction of the daily usable time-resolved Raman measurement unit using two-color excitation and a flow cell.
3) Construction and successful application of simultaneous measurement device for Raman and absorption spectra.
4) Construction of a novel flowing and continuous regenerating system of the enzyme for Raman measurements, named "artificial cardiovascular system for analyzing enzymic reactions".
5) Structure determination of four reaction intermediates involved in reduction of $O_2$ to water.

# LIST OF PUBLICATIONS

**H. KAWAMURA-KURIBAYASHI, N. KOGA, and K. MOROKUMA,** "An Ab Initio MO and MM Study on Homogeneous Olefin Polymerization with Silylene-Bridged Zirconocene Catalyst and Its Regio- and Stereoselectivity", *J. Am. Chem. Soc.* **114,** 8687 (1992).

**K. SAWABE, N. KOGA, and K. MOROKUMA,** "An Ab Initio MO Study on Adsorption at the MgO Surface I. $H_2$ Chemisorption on the $(MgO)_4$ Cluster", *J. Chem. Phys.* **97,** 6871 (1992).

**N. KOGA and K. MOROKUMA,** "Ab Initio MO Calculation of $(\eta^2\text{-}C_{60})Pt(PH_3)_2$: Electronic Structure and Interaction between $C_{60}$ and Pt", *Chem. Phys. Lett.* **202,** 330 (1992).

**H. FUKUNAGA and K. MOROKUMA,** "Cluster and Solution Simulation of Formaldehyde-Water Complexes and Solvent Effect on Formaldehyde $^1(n,\pi^*)$ Transition", *J. Phys. Chem.* **97,** 59 (1993).

**M. OHSAKU, N. KOGA, and K. MOROKUMA,** "Triplet-Singlet Intersystem Crossing as the Second Step of Cycloaddition of Triplet Penta-1,4-Diene. An Ab Initio MO Study", *J. Chem. Soc. Perkin 2,* **71,** (1993).

**E. NAKAMURA, M. NAKAMURA, Y. MIYACHI, N. KOGA, and K. MOROKUMA,** "Theoretical Studies on Carbometallation of Cyclopropene. Transition Structures of Addition of $Me^-$, MeLi, MeCu, and $MeCu^-$ and Origin of High Reactivity of Strained Double Bond", *J. Am. Chem. Soc.* **115,** 99 (1993).

**J. MOC, A. DORIGO, and K. MOROKUMA,** "Transition Structures for $H_2$ Elimination from $XH_4$ Hypervalent Species (X=S, Se and Te): Ab Initio MO Study", *Chem. Phys. Lett.* **204,** 65 (1993).

**K. HASHIMOTO, S. HE, and K. MOROKUMA,** "Structure, Stability and Ionization Potential of $Na(H_2O)_n$ and $Na(NH_3)_n$(n=1–6) Clusters. An Ab Initio MO Study", *Chem. Phys. Lett.,* **206,** 297 (1993).

**D. MUSAEV, N. KOGA, and K. MOROKUMA,** "Ab Initio MO Study of the Electronic and Geometrical Structure of $RhCH_2^+$ and the Reaction Mechanism: $RhCH_2^+ + H_2 \rightarrow Rh^+ + CH_4$", *J. Phys. Chem.* **97,** 4064 (1993).

**H. ITAGAKI, N. KOGA, K. MOROKUMA, and Y. SAITO,** "An Ab Initio MO Study on Two Possible Stereochemical Reaction Paths for Methanol Dehydrogenation with $Ru(OAc)Cl(PEtPh_2)_3$", *Organometallics* **12,** 1648 (1993).

**H. ITAGAKI, Y. NAKAOKI, T. OGATA, N. KOGA, K. MOROKUMA, and Y. SAITO,** "Quantum-Chemical and Experimental Analyses on $H_2$ Elimination from $IrCl(H)_2(CO)(PR_3)_2$", in *Computer Aided Innovation of New Materials II,* M. Doyama, J. Kihara, M. Tanaka, and R. Yamamoto, Eds, Elsevier, p.785 (1993).

**D. BROWN, N. FITZPATRICK, P. GROARKE, N. KOGA, and K. MOROKUMA,** "A Theoretical Study of Hydride Attack on the $\eta^5$-Cyclopentadienyltricarbonyliron Cation", *Organometallics,* **12,** 2521 (1993).

**J. ENDO, N. KOGA and K. MOROKUMA,** "A Theoretical Study on Hydrozirconation", *Organometallics,* **12,** 2777 (1993).

**A. MEBEL, D. MUSAEV, and K. MOROKUMA,** "Ab Initio MO Study of Mechanisms of the Reaction of $B_2H_6$ with $SH_2$", *J. Phys. Chem.* **97,** 7543 (1993).

**N. KOGA, and K. MOROKUMA,** "SiH, SiSi, and CH Bond Activation by Coordinatively Unsaturated $RhCl(PH_3)_2$. Ab Initio MO Study", *J. Am. Chem. Soc.* **115,** 6883 (1993).

**D. WALES and I. OHMINE,** "Structure, Dynamics and Thermodynamics of Model of $(H_2O)_8$ and $(H_2O)_{20}$ Clusters", *J. Chem. Phys.* **98,** 7245 (1993).

**D. WALES and I. OHMINE,** "Rearrangements of Model $(H_2O)_8$ and $(H_2O)_{20}$ Clusters", *J. Chem. Phys.* **98,** 7257 (1993).

**C. ZHU and H. NAKAMURA,** "The Two-State Linear Curve Crossing Problems Revisited, II. Analytical Approximations for the Stokes Constant and Scattering Matrix: The Landau-Zener Case", *J. Chem. Phys.* **97,** 8497 (1992).

**C. ZHU and H. NAKAMURA,** "Numerical Method for the Two-State Linear Curve Crossing: Nonadiabatic Tunneling Case", *Comp. Phys. Commun.* **74,** 9 (1993).

**K. SOMEDA, R. RAMASWAMY, and H. NAKAMURA,** "Decoupling Surface Analysis of Classical Irregular Scattering and Clarification of its Icicle Structure", *J. Chem. Phys.* **98,** 1156 (1993).

**C. ZHU and H. NAKAMURA,** "The Two-State Linear Curve Crossing Problems Revisited III. Analytical Approximations for Stokes Constant and Scattering Matrix: Nonadiabatic Tunneling Case", *J. Chem. Phys.* **98,** 6208 (1993).

**M. IWAI, S. LEE and H. NAKAMURA,** "Electron Correlation in Doubly Excited States of the Hydrogen Molecule", *Phys. Rev.* **A47,** 2686 (1993).

**I. BANNO,** "Electron Density in a Half-Filled Shell Atom", *Prog. Theor. Phys.* **89,** 935 (1993).

**L. LI, X. SUN, and K. NASU,** "Spectrum of Third Harmonic Generation of MX Complex", *Chinese Phys. Lett.* **9,** 431 (1992).

**X. SUN, K. NASU, C. WU, L. LI, D. LIN, and T. GEORGE,** "Frequency Dependence of Two-photon Resonance and Damping in Polymers", *Synthetic Metals* **49/45,** 141 (1992).

**B.S. LEE and K. NASU,** "Stationary Localized Modes in an Anharmonic Molecular Crystal Model", *Phys. Lett.* **A167,** 205 (1992).

**Y. INADA and K. NASU,** "Enhancement, Reduction and Inversion of Isotope Effect Due to Anharmonic Phonons, — Migdal-Eliashiberg Theory for Superconductivity —", *J. Phys. Soc. Jpn.* **61,** 4511 (1992).

**Y. INADA and K. NASU,** "Superconductivity of a Many-electron System Coupling Strongly with Nonlinear Phonons", *Solid State Physics (in Japanese)* **27,** 578 (1992).

**K. IWANO and K. NASU,** "Nonlinear Optical Spectra in Halogen Bridged Mixed-valent Platinum Complexes", *J. Phys. Soc. Jpn.* **62,** 1778 (1993).

**S. SAITO and M. GOTO,** "Laboratory Submillimeter-Wave Observation of the N=1−0 Transition of the ND($^3\Sigma^-$) Radical", *Astrophys. J.* **410,** L53 (1993).

**T.C. STEIMLE, S. SAITO, and S. TAKANO,** "Laboratory Measurement of the Millimeter-Wave Spectra of Calcium Isocyanide", *Astrophys. J.* **410,** L49 (1993).

**A.FUJII and N. MORITA,** "Laser Investigation of the Competition between Rotational Autoionization and Predissociation in Superexcited *np* Rydberg States of NO", *J. Chem. Phys.* **98,** 4581 (1993).

**N. MORITA, K. OHTSUKI, and T. YAMAZAKI,** "Laser Spectroscopy of Metastable Antiprotonic Helium Atomcules", *Nucl. Instrum. Methods,* **A330,** 439 (1993).

**E. WIDMANN, H. DANIEL, J. EADES, T. von EGIDY, F.J. HARTMANN, R.S. HAYANO, W. HIGEMOTO, J. HOFFMANN, T.M. ITO, Y. ITO, M. IWASAKI, A. KAWACHI, N. MORITA, S.N. NAKAMURA, N. NISHIDA, W. SCHMID, I. SUGAI, H. TAMURA, and T. YAMAZAKI,** "Antiproton Trapping in Various Helium Media: Report of the HELIUMTRAP Experiment at LEAR", *Nucl. Phys.* **A558,** 679 (1993).

**S. SATO, K. KAMOGAWA, K. AOYAGI, and T. KITAGAWA,** "Time-Resolved Resonance Raman Investigation of Photoreduction of Iron-octaethylporphyrin Complexes by Using Quasi-simultaneous Pump/probe Measurement Technique", *J. Phys. Chem.* **26,** 10676 (1992).

**S. KAMINAKA and T. KITAGAWA,** "A Novel Idea for Practical UV Resonance Raman Measurement with a Double-monochromator and Its Application to Protein Structural Studies", *Appl. Spectrosc.* **46,** 1804 (1992).

**S. ADACHI, S. NAGANO, K. ISHIMORI, Y. WATANABE, I. MORISHIMA, T. EGAWA, T. KITAGAWA, and R. MAKINO,** "Role of Proximal Ligand in Heme Proteins: Replacement of Proximal Histidine of Human Myoglobin with Cysteine and Tyrosine by Site-directed Mutagenesis as Models for P-450, Chloroperoxidase, and Catalase", *Biochemistry* **32,** 241 (1993).

**S. TAKAHASHI, T. OGURA, K. SHINZAWA-ITOH, S. YOSHIKAWA, and T. KITAGAWA,** "Resonance Raman Studies on the $Cu_A$ Site of Cytochrome *c* Oxidase Using a Multichannel Scanning Raman Spectrometer with a CCD Detector", *Biochemistry* **32,** 3664 (1993).

**T. LIAN, B. LOCKE, T. KITAGAWA, M. NAGAI, and R.M. HOCHSTRASSER,** "Determination of Fe-CO Geometry in the Subunits of Carbonmonoxy Hemoglobin M Boston using Femtosecond Infrared Spectroscopy", *Biochemistry* **32,** 5809 (1993).

**Y. SAKAN, T. OGURA, T. KITAGAWA, F.A. FRAUNFELTER, R. MATTERA, and M. IKEDA-SAITO,** "Time-resolved Resonance Raman Study on the Binding of Carbonmonoxide to Recombinant Human Myoglobin and its Distal Histidine Mutants", *Biochemistry* **32,** 5815 (1993).

**T. KITAGAWA, Y. SAKAN, T. OGURA, F.A. FRAUNFELTER, R. MATTERA, and M. IKEDA-SAITO,** "Time-resolved Resonance Raman Study of Recombination Intermediates of Photodissociated CO of Myoglobin and its E7 Mutants", in "Laser Spectroscopy of Biological Molecules", J.E.I. Korppi-Tommola, Ed., *SPIE* **1921,** 187 (1993).

**Y. MIZUTANI, S. TOKUTOMI, S. KAMINAKA, and T. KITAGAWA,** "Ultraviolet Resonance Raman Spectra of Pea Intact, Large, and Small Phytochromes: Differences in Molecular Topography of the Red and Far-red Absorbing Forms", *Biochemistry* **32,** 6916 (1993).

**I. YUMOTO, S. TAKAHASHI, T. KITAGAWA, Y. FUKUMORI, and T. YAMANAKA,** "The Molecular Features and Catalytic Activity of $Cu_A$-containing $aco_3$-type Cytochrome *c* Oxidase from a Facultative Alkalophilic *Bacillus*", *J. Biochem (Tokyo)* **114,** 88 (1993).

**S. TAKAHASHI, J.S. AHN, S. ASAKA, and T. KITAGAWA,** "Multichannel Fourier Transform Spectroscopy Using Two-dimensional Detection of Interferogram and its Application to Raman Spectroscopy", *Appl. Spectrosc.* **47,** 863 (1993).

**T. OGURA, S. TAKAHASHI, S. HIROTA, K. SHINZAWA-ITOH, S. YOSHIKAWA, E.H. APPELMAN, and T. KITAGAWA,** "Time-resolved Resonance Raman Elucidation of the Pathway for Dioxygen Reduction by Cytochrome *c* Oxidase", *J. Am. Chem. Soc.* **115,** 8527 (1993).

**S. SUZUKI, S. KAWATA, H. SHIROMARU, K. YAMAUCHI, K. KIKUCHI, T. KATO, and Y. ACHIBA,** "Isomers and $^{13}C$ Hyperfine Structure of Metal Encapsulated Fullerenes, $M@C_{82}$(M=Sc, Y, and La)", *J. Chem. Phys.* **96,** 7159 (1992).

**S. NAGASE, K. KOBAYASHI, T. KATO, and Y. ACHIBA,** "A Theoretical Approach to $C_{82}$ and $La@C_{82}$", *Chem. Phys. Lett.* **201,** 475 (1993).

**T. KATO, T. KODAMA, and T. SHIDA,** "Spectroscopic Studies of the Radical Anion of $C_{60}$: Detection of the Fluorescence and Reinvestigation of the ESR Spectrum", *Chem. Phys. Lett.* **205,** 405 (1993).

**K. KAWAGUCHI, E. KAGI, T. HIRANO, S. TAKANO, and S. SAITO,** "Laboratory Spectroscopy of MgNC: The First Radioastronomical Identification of Mg-bearing Molecule", *Astrophys. J. Lett.* **406,** L39 (1993).

**R. INABA, H. OKAMOTO, K. YOSHIHARA, and M. TASUMI,** "Observation of the Dephasing of the C≡N Stretching Vibration in Liquid Nitriles by Femtosecond Time-Resolved Coherent Anti-Stokes Raman Scattering", *J. Phys. Chem.* **96,** 8385 (1992).

**J. HERBICH, J. KARPIUK, Z.R. GRABOWSKI, N. TAMAI, and K. YOSHIHARA,** "Modification of the Intramolecular Electron Transfer by Hydrogen Bonding: 4-(Dialkylamino) Pyrimidines", *J. Lumines.* **54,** 165 (1992).

**H. KANDORI, K. YOSHIHARA, and S. TOKUTOMI,** "Primary Process of Phytochrome: Initial Step of Photomorphogenesis in Green Plants", *J. Am. Chem. Soc.* **114,** 10958 (1992).

**K. YOSHIHARA, H. PETEK, Y. FUJIWARA, J.H. PENN, and J.H. FREDERICK,** "Vibrational Mode Dynamics of Photocyclization in cis-Stilbene and Its Related Compounds", Time Resolved Vibrational Spectroscopy V, H. Takahashi Ed., Springer, Berlin, 194 (1992).

**M.J.E. MORGENTHALER, S.R. MEECH, and K. YOSHIHARA,** "The Inhomogeneous Broadening of the Electronic Spectra of Dyes in Glycerol Solution. A Time-resolved Fluorescence Study", *Chem. Phys. Lett.* **197,** 537 (1992).

**H. OKAMOTO and K. YOSHIHARA,** "Femtosecond Time-Resolved CARS: Time Domain Observation of Molecular Vibrational Dynamics", Time Resolved Vibrational Spectroscopy V, H. Takahashi Ed., Springer, Berlin, 231 (1992).

**H. OKAMOTO, R. INABA, K. YOSHIHARA, and M. TASUMI,** "Femtosecond Time-Resolved Polarized Coherent Anti-Stokes Raman Studies on Reorientational Relaxation in Benzonitrile", *Chem. Phys. Lett.* **202,** 161 (1993).

**B. KIM and K. YOSHIHARA,** "Determination of Adiabatic Ionization Potentials of $Cs_2$ and $Cs_3$ in a Very Cold Molecular Beam Using Time-of-Fight Mass Spectrometry", *Chem. Phys. Lett.* **202,** 437 (1993).

**B. KIM and K. YOSHIHARA,** "Triplet-triplet Transition of $Cs_2$ Studied by Multiphoton Ionization Spectroscopy in a Very Cold Pulsed Molecular Beam", *Chem. Phys. Lett.* **204,** 407 (1993).

**R.B. PANSU, K. YOSHIHARA, T. ARAI, and K. TOKUMARU,** "Convolution Analysis of the Pyrene Excimer Formation in Membranes", *J. Phys. Chem.* **97,** 1125 (1993).

**H. PETEK, A.J. BELL, Y.S. CHOI, K. YOSHIHARA, B.T. TOUNGE, and R.L. CHRISTENSEN,** "The $2^1$Ag State of trans, trans-1,3,5,7-octatetraene in Free Jet Expansions", *J. Chem. Phys.* **98(5),** 3777 (1993).

**A. YARTSEV, Y. NAGASAWA, A. DOUHAL, and K. YOSHIHARA,** "Solvent and Nuclear Dynamics in Ultrafast Intermolecular Electron Transfer in a Diffusionless, Weakly Polar System", *Chem. Phys. Lett.* **207,** 546 (1993).

**H. OKAMOTO, R. INABA, M. TASUMI, and K. YOSHIHARA,** "Femtosecond Vibrational Dephasing of the C≡N Stretching in Alkanenitriles with Long Alkyl Chains. Dependence on the Chain Length and Hydrogen Bonding", *Chem. Phys. Lett.* **206,** 388 (1993).

**R.F. BORKMAN, A. DOUHAL, and K. YOSHIHARA,** "Picosecond Fluorescence Decay in Photolyzed Lens Protein $\alpha$-Crystalline", *Biochem.* **32,** 4787 (1993).

**B. KIM and K. YOSHIHARA,** "The 480 nm System of $Cs_2$ Studied in a Very Cold Molecular Beam: Direct Observation of a New E′ and the Ion-pair State", *J. Chem. Phys.* **98,** 5990 (1993).

**K. YOSHIHARA, A. YARTSEV, Y. NAGASAWA, H. KANDORI, A. DOUHAL, and K. KEMNITZ,** "Femtosecond Intermolecular Electron Transfer: Dye in Weakly Polar Electron-Donating Solvent", Ultrafast Phenomena VIII Eds. J.L. Martin, A. Migus, G. Mourou, A. Zewail, Springer, Berlin, 571 (1993).

**V.F. KAMALOV, R. INABA, and K. YOSHIHARA,** "Dephasing and Beats of Excitonic-Enhanced Transitions of J-Aggregates Measured by Femtosecond Time-Resolved Resonance CARS", Ultrafast Phenomena VIII Eds. J.L. Martin, A. Migus, G. Mourou, A. Zewail, Springer, Berlin, 87 (1993).

**H. KANDORI, K. YOSHIHARA, H. TOMIOKA, H. SASABE, and Y. SHICHIDA,** "Subpicosecond Time-Resolved Spectroscopy of Halorhodopsin and Comparison with Bacteriorhodopsin", Ultrafast Phenomena VIII Eds. J.L. Martin, A. Migus, G. Mourou, A. Zewail, Springer, Berlin 566 (1993).

**R.F. BORKMAN, A. DOUHAL, and K. YOSHIHARA,** "Picosecond Fluorescence Decay of Lens Protein $\gamma$-II Crystalline", *Biophys. Chem.* **47,** 203 (1993).

**K. YOSHIHARA, A. YARTSEV, Y. NAGASAWA, H. KANDORI, and K. KEMNITZ,** "Femtosecond Intermolecular Electron Transfer between Dyes and Electron-Donating Solvents", *Pure & Appl. Chem.* **65,** 1671 (1993).

**R. INABA, H. OKAMOTO, K. YOSHIHARA, and M. TASUMI,** "Femtosecond Time-Resolved Coherent Anti-Stokes Raman Scattering of the C≡C Stretching in Liquid Alkanes", *J. Phys. Chem.* **97,** 7815 (1993).

**R. INABA, K. TOMINAGA, M. TASUMI, K.A. NELSON, and K. YOSHIHARA,** "Observation of Homogeneous Vibrational Dephasing in Benzonitrile by Ultrafast Raman Echoes", *Chem. Phys. Lett.* **211,** 183 (1993).

**B. KIM and K. YOSHIHARA,** "Multichannel Quantum Interference in the Predissociation of $Cs_2$: Observation of q-reversal in a Complex Resonance", *J. Chem. Phys.* **99,** 1433 (1993).

**A.E. JOHNSON, S. KUMAZAKI, and K. YOSHIHARA,** "Pump-Probe Spectroscopy of Exciton Dynamics of J-aggregate at High Pump Intensity", *Chem. Phys. Lett.* **211,** 511 (1993).

**H. KANDORI, K. YOSHIHARA, H. TOMIOKA, H. SASABE, and Y. SHICHIDA,** "Comparative Study of Primary Photochemical Events of Two Retinal Proteins, Bacteriorhodopsin and Halorhodopsin, by Use of Subpicosecond Time-Resolved Spectroscopy", *Chem. Phys. Lett.* **211,** 385 (1993).

**Y. NAGASAWA, A.P. YARTSEV, K. TOMINAGA, A.E. JOHNSON, and K. YOSHIHARA,** "Substituent Effects on Intermolecular Electron Transfer: Coumarins in Electron-Donating Solvents", *J. Am. Chem. Soc.* **115,** 7922 (1993).

**B. KIM and K. YOSHIHARA,** "$^3\Delta$-$^1\Sigma^+$ Transition of RbCs Observed in a Very Cold Molecular Beam", *Chem. Phys. Lett.* **212,** 271 (1993).

**K. SAWABE and Y. MATSUMOTO,** "Laser-induced Photochemistry of Nitrous Oxide on a Pt(111) Surface", *Surf. Sci.* **283,** 126 (1993).

**K. SAWABE, J. LEE, and Y. MATSUMOTO,** "Dynamics of the Oxygen Combination Reaction on Pt(111) Initiated by Photodissociation of $N_2O$ at 193 nm: O*+O(ad) → $O_2$(g)", *J. Chem. Phys.* **99,** 3143 (1993).

**Y. MORI and I. HANAZAKI,** "Primary Photochemical Processes of Light-Induced pH Oscillation in the $Fe(CN)_6^{4-}/H_2O_2$ System", *J. Phys. Chem.* **96,** 9083 (1992).

**M. TAKAYANAGI and I. HANAZAKI,** "SEP-LIF Spectra of Some Molecules and van der Waals Molecules in a Molecular Beam", *Springer Proceedings in Physics* **68,** 245 (1992).

**I. HANAZAKI,** "Formation of Lambda-doublet Components of OH in the Bimolecular Reactions: H+OX → OH+X', *Chem. Phys. Lett.* **201,** 301 (1993).

**T. KONO, M. TAKAYANAGI, T. NISHIYA, and I. HANAZAKI,** "Photodissociation of Acetaldehyde Studied by the Photofragment Excitation Spectroscopy in a Supersonic Free Jet", *Chem. Phys. Lett.* **201,** 166 (1993).

**M. YOSHIMOTO, K. YOSHIKAWA, Y. MORI, and I. HANAZAKI,** "Experiment in Coupled Chemical Oscillators. Asymmetric Coupling Stabilizes Anti-Phase Mode", *Forma* **7,** 39 (1992).

**M. TAKAYANAGI and I. HANAZAKI,** "Dynamics of Vibrationally Excited van der Waals Complexes: Stimulated-emission-pumping Laser-induced-fluorescence Spectroscopy of the Anisole · Ar Complex" *J. Chem. Phys.* **98,** 6985 (1993).

**M. TAKAYANAGI and I. HANAZAKI,** "Observation of Intermolecular Vibrational Modes in the 2,3-Dihydrobenzofuran Dimer", *Chem. Phys. Lett.* **208,** 5 (1993).

**Y. MORI and I. HANAZAKI,** "Bifurcation Structure of the Chemical Oscillation in the $Fe(CH)_6^{4-}$-$H_2O_2$-$H_2SO_4$ System", *J. Phys. Chem.* **97,** 7375 (1993).

**N. OKAZAKI, Y. MORI, and I. HANAZAKI,** "Effect of Adding Starch on the Photoinhibition of Oscillation in the Briggs- Rauscher Reaction", *Chem. Lett.*, 1135 (1993).

**I. HANAZAKI, Y. MORI, T. SEKIGUCHI, and N. OKAZAKI,** "Photoresponse of Oscillatory Chemical Reactions", *Tech. Report IEICE* **93,** no.58, 25 (1993) (in Japanese).

**T. SEKIGUCHI, Y. MORI, and I. HANAZAKI,** "Photo-response of the $[Ru(bpy)_3]^{2+}/BrO_3^-/H^+$ System in a Continuous-Flow Stirred Tank Reactor", *Chem. Lett.*, 1309 (1993).

**T. SUZUKI and E. HIROTA,** "Vibrational Distribution of $CH_3$ Produced by the Reaction of $O(^1D_2)$ Atom with $CH_4$", *J. Chem. Phys.* **98,** 2387 (1993).

**H. YASUMATSU, K. SUZUKI, and T. KONDOW,** "Vibrational Distributions of the $CN(B^2\Sigma^+)$ in the Dissociative Excitation of KCN and NaCN with Ar Metastable Atoms: Bimodal Vibrational Distribution from KCN", *J. Phys., Chem.* **97,** 6788 (1993).

**H. ITO, K. SUZUKI, T. KONDOW, and K. KUCHITSU,** "An Analysis of the $B^2\Sigma^+$-$X^2\Sigma^+$ Emission of SiN. Dependence of the Electronic Transition Moment on the Si-N Internuclear Distance", *Chem. Phys. Lett.* **208,** 328 (1993).

**A.A. ZAKHIDOV, K. YAKUSHI, K. IMAEDA, H. INOKUCHI, K. KIKUCHI, S. SUZUKI, I. IKEMOTO, and Y. ACHIBA,** "Microwave Spectroscopy of Fullerene-based Molecular Superconductors in Low Magnetic Field: $M_xC_{60}$(M=K, Rb, $I_2$, Ga, In), $M_xC_n$ (n=70, 76, 78, 84, 90) and $M_x(C_{60})_{1-y}(C_{70})_y$(M=K, Rb)", *Mol. Cryst. Liq. Cryst.* **218,** 299 (1992).

**V.N. DENISOV, A.A. ZAKHIDOV, R. DANIELI, G. RUANI, R. ZAMBONI, C. TALIANI, K. IMAEDA, K. YAKUSHI, H. INOKUCHI, and Y. ACHIBA,** "Evidence for Jahn-Teller Coupling and Fano Resonance of Lower $H_g$ Modes in $K_xC_{60}$ and $Rb_3C_{60}$ Films from Raman Scattering", *Int. J. Mod. Phys. B* **6,** 4019 (1992).

**K. TANAKA, A.A. ZAKHIDOV, K. YOSHIZAWA, K. OKAHARA, T. YAMABE, K. YAKUSHI, K. KIKUCHI, S. SUZUKI, I. IKEMOTO, and Y. ACHIBA,** "Ferromagnetic TDAE-$C_{60}$ versus Paramagnetic TDAE-C70: Faradey Balance and ESR Study", *Int. J. Mod. Phys. B* **6,** 3953 (1992).

**K. IMAEDA, K. YAKUSHI, H. INOKUCHI, K. KIKUCHI, I. IKEMOTO, S. SUZUKI, and Y. ACHIBA,** "ESR and Low-Field Microwave Absorption Studies of Potassium Doped $C_{70}$: Observation of Possible Metallic State in $K_xC_{70}$", *Solid State Commun.* **84,** 1019 (1992).

**A. UGAWA, K. YAKUSHI, K. KIKUCHI, S. SUZUKI, K. SAITO, Y. ACHIBA, and I. IKEMOTO,** "Infrared and Transport Properties of $K_xC_{60}$", *Synth. Met.* **56,** 2997 (1993).

**A.A. ZAKHIDOV, I.I. KHAIRULLIN, P.K. KHABIBULLAEV, V. Yu. SOKOLOV, K. IMAEDA, K. YAKUSHI, H. INOKUCHI, and Y. ACHIBA,** "Air Stability of $K_3C_{60}$ Superconductors: Low Field Microwave Absorption and ESR Study", *Synthetic Metals* **55–57,** 2967 (1993).

**S. HINO, K. MATSUMOTO, S. HASEGAWA, K. IWASAKI, K. YAKUSHI, T. MORIKAWA, T. TAKAHASHI, K. SEKI, K. KIKUCHI, S. SUZUKI, I. IKEMOTO, and Y. ACHIBA,** "Photoelectron Spectra of Higher Fullerence Compound $C_{82}$ and its Potassium Complex", *Synthetic Metals* **55–57,** 3191 (1993).

**K. TANAKA, A.A. ZAKHIDOV, K. YOSHIZAWA, K. OKAHARA, T. YAMABE, K. YAKUSHI, K. KIKUCHI, S. SUZUKI, I. IKEMOTO, and Y. ACHIBA,** "Magnetic Properties of TDAE-$C_{60}$ and TDAE-$C_{70}$", *Phys. Rev. B* **47,** 7554.

**K. IMAEDA, I.I. KHAIRULLIN, K. YAKUSHI, M. NAGATA, N. MIZUTANI, H. KITAGAWA, and H. INOKUCHI,** "New Superconducting Sodium-Nitrogen-$C_{60}$ Ternary Compound", *Solid State Commun.* **87,** 375 (1993).

**K. IWASAKI, T. IDA, A. KAWAMOTO, A. UGAWA, Y. YAMASHITA, K. YAKUSHI, and T. SUZUKI,** "Structure of the Charge-Transfer Complex of (DBTTF)(BTDA-TCNQ)", *Acta Cryst. C* **48,** 1982 (1992).

**K. IWASAKI, A. UGAWA, A. KAWAMOTO, Y. YAMASHITA, K. YAKUSHI, T. SUZUKI, and T. MIYASHI,** "Crystal Structures of Metallic and Insulating Molecular Complexes between Tetraseleno-naphthacene and bis(1,2,5-thiadiazolo)tetracyanoquinodimethane: (TSeN)(BTDA-TCNQ) and (TSeN)(BTDA-TCNQ)($C_6H_5Cl$)", *Bull. Chem. Soc. Jpn.* **65,** 3350 (1992).

**H. YAMAKADO, K. YAKUSHI, K. AWAGA, Y. MARUYAMA, T. NAKANO, and K. KASUGA,** "Ferromagnetic Interaction in Solid Octabutoxyphthalocyaninato Cobalt", *Mol. Cryst. Liq. Cryst.* **218,** 219 (1992).

**K. YAKUSHI, H. YAMAKADO, T. IDA, A. UGAWA, K. AWAGA, Y. MARUYAMA, K. IMAEDA, and H. INOKUCHI,** "Structure and Solid State Properties of Conductive (Phthalocyaninato)cobalt Salt, $CoPc(AsF_6)_{0.5}$", *Synthetic Metals* **55–57,** 1699 (1993).

**L.S. GRIGORYAN, Y. NAKAZAWA, and K. YAKUSHI,** "Intercalation of High-Tc Oxides with Organic Molecules," *Advances in Superconductivity* **V,** 287 (1993).

**K. KANODA, Y. TSUBOKURA, K. IKEDA, T. TAKAHASHI, N. MATSUKAWA, G. SAITO, H. MORI, T. MORI, B. HILTI, and J.S. ZAMBOUNIS,** "Magnetic Penetration Depth of the $\kappa$-Phase Family of Organic Superconductors", *Synth. Met.* **55–57,** 2865 (1993).

**S. KAGOSHIMA, A. MIYAZAKI, T. OSADA, Y. SAITO, N. WADA, H. YANO, T. TAKAHASHI, K. KANODA, H. KOBAYASHI, A. KOBAYASHI, and R. KATO,** "Charge and Spin State of DCNQI-Cu Salts" *Synth. Met.* **55–57,** 1832 (1993).

**T. TAKAHASHI, Y. KOBAYASHI, K. KANODA, T. INUKAI, and G. SAITO,** "Pressure Dependence of the SDW Transition in $(MDT\text{-}TTF)_2Au(CN)_2$", *Synth. Met.* **55–57,** 2814 (1993).

**K. KANODA, K. KATO, Y. KOBAYASHI, M. KATO, T. TAKAHASHI, K. OSHIMA, B. HILTI, and J.S. ZAMBOUNIS,** "Upper Critical Field and NMR Relaxation Studies of an Organic Superconductor, $\kappa$-$(MDT\text{-}TTF)_2AuI_2$", *Synth. Met.* **55–57,** 2871 (1993).

**K. ISHIDA, Y. KITAOKA, H. MASUDA, K. ASAYAMA, T. TAKAHASHI, K. KANODA, A. KOBAYASHI, R. KATO, and H. KOBAYASHI,** "Cu NMR Study of the Organic Conductor $(DMe\text{-}DCNQI)_2Cu$", *Physica B* **186–188,** 1059 (1993).

**T. TAKAHASHI, R. TSUCHIYA, K. KANODA, M. WATABE, T. SASAKI, and N. TOYOTA,** "$^1$H-NMR Studies of the Low Temperature Phase of $\alpha$-$(BEDT\text{-}TTF)_2KHg(SCH)_4$", *Synth. Met.* **55–57,** 2513 (1993).

**K. KANODA, K. KATO, A. KAWAMOTO, K. OSHIMA, T. TAKAHASHI, K. KIKUCHI, K. SAITO, and I. IKEMOTO,** "de Haas-van Alphen Effect in $\kappa$-$(DMET)_2AuBr_2$", *Synth. Met.* **55–57,** 2309 (1993).

**T. TAKAHASHI, K. KANODA, T. TAMURA, K. HIRAKI, K. IKEDA, R. KATO, H. KOBAYASHI, and A. KOBAYASHI,** "Magnetism of DCNQI-Cu Salts", *Synth. Met.* **55–57,** 2281 (1993).

**A. WILSON, G.P. RIGBY, J.D. WRIGHT, S.C. THORPE, T. TERUI, and Y. MARUYAMA,** "Effect of Heat Treatment on Chemical, Morphological and $NO_2$-Sensing Properties of Lead Phthalocyanine Films", *J. Mater. Chem.* **2,** 303 (1992).

**A. MANIVANNAN, H. HOSHI, L.A. NAGAHARA, Y. MORI, Y. MARUYAMA, K. KIKUCHI, Y. ACHIBA, and A. FUJISHIMA,** "Scanning Probe Microscopic Investigation of Epitaxially Grown $C_{60}$ Film on $MoS_2$", *Jpn. J. Appl. Phys.* **31,** 3680 (1992).

**T. INABE, H. OGATA, Y. MARUYAMA, Y. ACHIBA, S. SUZUKI, K. KIKUCHI, and I. IKEMOTO,** "Electronic Structure of Alkali Metal Doped $C_{60}$ Derived from Thermoelectric Power Measurements", *Phys. Rev. Lett.* **69,** 3797 (1992).

**A. MANIVANNAN, L.A. NAGAHARA, H. YANAGI, T. KOUZEKI, M. ASHIDA, Y. MARUYAMA, K. HASHIMOTO, and A. FUJISHIMA,** "Scanning Tunneling Microscopy Observations of Zinc Naphthalocyanine on $MoS_2$", *Thin Solid Films* **226,** 6 (1992).

**T. TERUI, R.J. FLEMING, and Y. MARUYAMA,** "Atomic Layer-by-Layer Deposition of La-Sr-Cu-O Films", *Chem. Lett.* **1993,** 137.

**H. HOSHI, S.L. FANG, and Y. MARUYAMA,** "Epitaxial Growth of Lead Phthalocyanine Film on KI Crystal", *J. Appl. Phys.* **73,** 3111 (1993).

**Y. MARUYAMA, T. INABE, H. OGATA, Y. ACHIBA, K. KIKUCHI, S. SUZUKI, and I. IKEMOTO,** "Electron Transport Probes of Alkali Metal-Doped $C_{60}$ Single Crystals", *Mater. Sci. Eng.* **B19,** 162 (1993).

**H. HOSHI, K. KOHAMA, S.L. FANG, and Y. MARUYAMA,** "$\chi^{(3)}$ Components of Single-Crystalline Vanadyl Phthalocyanine Film", *Appl. Phys. Lett.* **62,** 3080 (1993).

**T. NAKAMURA, T. KOMATSU, G. SAITO, K. KATO, Y. MARUYAMA, and T. MORI,** "Transport Properties and Electronic Structure of the Novel Organic Superconductor $\kappa$-$(BEDT\text{-}TTF)_2$ $Cu(CN)$ $[N(CN)_2](T_c$=11.2K)", *Synth. Met.* **55–57,** 2905 (1993).

**K. AWAGA, T. INABE, Y. MARUYAMA, T. NAKAMURA, and M. MATSUMOTO,** "Ferromagnetic Properties and Crystal Structures of Pyridyl and Pyredinium $\alpha$-Nitronyl Nitroxides", *Synth. Met.* **55–57,** 3311 (1993).

**A. YAMAGUCHI, K. AWAGA, T. INABE, T. NAKAMURA, M. MATSUMOTO, and Y. MARUYAMA,** "Crystal Structures and Magnetic Properties of the *p*-*N*-Methylpyridinium Nitronyl Nitroxide Cation Radical Salts, *p*-MPYNN · $ClO_4$", *Chem. Lett.* **1993,** 1443.

**K. OICHI, E. ITO, K. SEKI, T. ARAKI, S. NARIOKA, H. ISHII, T. OKAJIMA, T. YOKOYAMA, T. OHTA, T. INABE, and Y. MARUYAMA,** "XANES Spectroscopic Study of Chemical Bonding in Amides and *N*-Salicylideneanilines", *Jpn. J. Appl. Phys.* **32,** 818 (1993)

**L.A. NAGAHARA, A. MANIVANNAN, H. YANAGI, M. TORIIDA, M. ASHIDA, Y. MARUYAMA, H. HASHIMOTO, and A. FUJISHIMA,** "Scanning Probe and Transmission Electron Microscopy Observations of Cobalt Naphthalocyanine Molecules Deposited onto a NaCl Substrate", *J. Vac. Sci. Technol.* **A11,** 781 (1993).

**K. OSHIMA, H. YAMAZAKI, K. KATO, Y. MARUYAMA, R. KATO, A. KOBAYASHI, and H. KOBAYASHI,** "De Haas-van Alphen Effect and the Fermi Surface in $\kappa$-(BEDT-TTF)$_2I_3$", *Synth. Met.* **55—57,** 2334 (1993).

**K. OSHIMA, T. DOI, Y. TOKUDA, H. YAMAZAKI, K. KATO, Y. MARUYAMA, H. MORI, and S. TANAKA,** "Quantum Oscillation and Transport Property in $\kappa$-(BEDT-TTD)$_2$Ag(CN)$_2H_2O$", *Synth. Met.* **55—57,** 2339 (1993).

**K. OSHIMA, K. KATO, Y. MARUYAMA, R. KATO, A. KOBAYASHI, and H. KOBAYASHI,** "The Field-Induced Transitions in a Novel Organic System, (DMETSeF)$_2AuI_2$", *Synth. Met.* **55—57,** 2780 (1993).

**S. MIYAJIMA and T. CHIBA,** "Proton NMR Study of CBOOA, NBOOA, and Their Chain-Deuteriated Homologues in Smectic Ad and Nematic Mesophases", *Liquid Cryst.* **11,** 283 (1992).

**T. MORI, K. KATO, Y. MARUYAMA, H. INOKUCHI, H. MORI, I. HIRABAYASHI, and S. TANAKA,** "Physical Properties of New Organic Superconductors, (BEDT-TTF)$_4M$(CN)$_4H_2O$ [*M*=Pt and Pd]", *Synth Metals* **56,** 2911 (1993).

**H. MORI, I. HIRABAYASHI, S. TANAKA, T. MORI, Y. MARUYAMA, and H. INOKUCHI,** "Preparation and Crystal Structures of New Organic Superconductors, (BEDT-TTF)$_4$Pt(CN)$_4H_2O$ ($T_c$=2 K, 6.5 kbar), (BEDT-TTF)$_4$Pd(CN)$_4H_2O$ ($T_c$=1.2 K, 7 kbar), and Related Materials", *Synth. Metals* **56,** 2044 (1993).

**H. MORI, I. HIRABAYASHI, S. TANAKA, T. MORI, Y. MARUYAMA, and H. INOKUCHI,** "Critical Temperature ($T_c$) and Crystal Structures of $\kappa$-(BEDT-TTF)$_2$Ag(CN)$_2H_2O$ ($T_c$=5 K) and $\kappa$-(BEDT-TTF-d8)$_2$Ag(CN)$_2H_2O$ ($T_c$=6 K)", *Synth. Metals* **56,** 2437 (1993).

**H. MORI, I. HIRABAYASHI, S. TANAKA, T. MORI, H. INOKUCHI, K. OSHIMA, and G. SAITO,** "Magnetic Susceptibility and Electrical Resistivity of (BEDT-TTF)$_2M$Hg(SCN)$_4$ (*M*=K, $NH_4$, and Rb)", *Synth. Metals* **56,** 2443 (1993).

**G. SAITO, H. YAMOCHI, T. NAKAMURA, T. KOMATSU, N. MATSUKAWA, T. INOUE, H. ITO, T. ISHIGURO, M. KUSUMOTO, K. SAKAGUCHI, and T. MORI,** "Structural and Physical Properties of Two New Ambient Pressure $\kappa$-type BEDT-TTF Superconductors and their Related Salts", *Synth. Metals* **56,** 2883 (1993).

**T. NAKAMURA, T. KOMATSU, G. SAITO, K. KATO, Y. MARUYAMA, T. MORI, K. OSHIMA, T. OSADA, K. KAGOSHIMA, N. MIURA, and T. TAKAHASHI,** "Transport Properties and Electronic Structure of the Novel Organic Superconductor $\kappa$-(BEDT-TTF)$_2$Cu(CN)[N(CN)$_2$] ($T_c$=11.2 K)", *Synth. Metals* **56,** 2905 (1993).

**R. MASUDA, H. TAJIMA, H. KURODA, H. MORI, S. TANAKA, T. MORI, and H. INOKUCHI,** "Reflectance Spectra of $\kappa$-(BEDT-TTF)$_2X$", *Synth. Metals* **56,** 2489 (1993).

**H. NISHIKAWA, K. KAWAKAMI, H. FUJIWARA, T. UEHARA, Y. MISAKI, T. YAMABE, T. MORI, and M. SHIRO,** "Synthesis and Properties of New Tetrathiafulvalenes Condensed with 1,3-Dithiol-2-ylidenes", *Synth. Metals* **56,** 1983 (1993).

**Y. MISAKI, H. NISHIKAWA, T. YAMABE, T. MORI, H. INOKUCHI, H. MORI, and S. TANAKA,** "Bis(methylthio) Sustituted Unsymmetrical 2,5-Bis(1′,3′-dithiol-2′-ylidene)-1,3,4,6-tetrathiapentalenes", *Chem. Lett.* **1993,** 729.

**T. MORI, H. INOKUCHI, Y. MISAKI, H. NISHIKAWA, T. YAMABE, H. MORI, and S. TANAKA,** "Structure and Conducting Properties of TMET-TTP Radical-Cation Salts", *Chem. Lett.* **1993,** 733.

**H. MORI, I. HIRABAYASHI, S. TANAKA, T. MORI, Y. MARUYAMA, and H. INOKUCHI,** "New Organic Superconductor, (BEDT-TTF)$_4M$(CN)$_4H_2O$ (*M*=Pt and Pd)", in "*Advances in Superconductivity V*", ed by Y. Bando and H. Yamauchi, Springer, Berlin (1993) p.259.

**Y. MISAKI, H. NISHIKAWA, T. YAMABE, T. MORI, H. INOKUCHI, H. MORI, and S. TANAKA,** "Structure and Electrical Properties of MeDTET Salts", *Chem. Lett.* **1993,** 1341.

**H. FUJIMOTO, K. KAMIYA, S. TANAKA, T. MORI, Y. YAMASHITA, H. INOKUCHI, and K. SEKI,** "Electronic Strucure of Bis[1,2,5]thiadiazolo-*p*-quinobis(1.3-dithiole) (BTQBT) Studied by Ultraviolet Photoemission Spectroscopy", *Chem. Phys.* **165,** 135 (1992).

**S. HINO, K. MATSUMOTO, S. HASEGAWA, H. INOKUCHI, T. MORIKAWA, T. TAKAHASHI, K. SEKI, K. KIKUCHI, S. SUZUKI, I. IKEMOTO, and Y. ACHIBA,** "Photoelectron Spectra of $C_{76}$ and $K_xC_{76}$", *Chem. Phys. Lett.* **197,** 38 (1992).

**T. TAKAHASHI, T. MORIKAWA, H. KATAYAMA-YOSHIDA, S. HASEGAWA, H. INOKUCHI, K. SEKI, S. HINO, K. KIKUCHI, S. SUZUKI, K. IKEMOTO, and Y. ACHIBA,** "Electronic Structure of Doped $C_{60}$: Strong Correlation or Lattice Distortion?", *Physica* **B186,** 1068 (1993).

**S. HASEGAWA, S. TANAKA, Y. YAMASHITA, H. INOKUCHI, H. FUJIMOTO, K. KAMIYA, K. SEKI, and N. UENO,** "Molecular Orientation in Thin Films of Bis(1,2,5-thiadiazolo)-*p*-quinobis(1,3-dithiole) on Graphite Studied by Angle-Resolved Photoelectron Spectroscopy", *Phys. Rev.* **B48,** 2596 (1993).

**H. NAKAHARA, A. NAGASAWA, A. ISHII, J. NAKAYAMA, M. HOSHINO, K. FUKUDA, K. KAMIYA, C. NAKANO, U. NAGASHIMA, K. SEKI, and H. INOKUCHI,** "Mono- and Multilayers of Novel Molecular Complex of Thiophene Derivative with Long-Chain TCNQ", *Mol. Cryst. Liq. Cryst.* **227,** 13 (1993).

**K. IMAEDA, K. YAKUSHI, H. INOKUCHI, K. KIKUCHI, I. IKEMOTO, S. SUZUKI, and Y. ACHIBA,** "ESR and Low-Field Microwave Absorption Studies of Potassium Doped $C_{70}$: Observation of Possible Metallic State in $K_xC_{70}$", *Solid State Commun.* **84,** 1019 (1992).

**K. IMAEDA, I.I. KHAIRULLIN, K. YAKUSHI, M. NAGATA, N. MIZUTANI, H. KITAGAWA, and H. INOKUCHI,** "New Superconducting Sodium-Nitrogen-$C_{60}$ Ternary Compound", *Solid State Commun.* **87,** 375 (1993).

**K. ICHIMURA, Y. NAKAHARA, K. KIMURA, and H. INOKUCHI,** "Electronic States of Oxidized and Reduced Cytochrome *c* Observed by X-ray Photoelectron Spectroscopy", *J. Mater. Chem.* **2,** 1185 (1992).

**Z.F. LIU, A. MANIVANNAN, H. YANAGI, M. ASHIDA, A. FUJISHIMA, and H. INOKUCHI,** "Direct Observation of the Secondary Structure of Unfolded Pseudomonas-cytochrome $c_{551}$ by Scanning Tunneling Microscopy", *Surface Sci. Lett.* **284,** L411 (1993).

**Y. MORITA, T. OHMAE, J. TOYODA, S. MATSUDA, F. TODA, and K. NAKASUJI,** "Synthesis and Properties of 1,6-Diselenapyrene (DSPY) and Its Methyl Chalcogeno Derivatives", *Chem. Lett.* **1993,** 443.

**J. TOYODA, A. ODA, I. MURATA, A. KAWAMOTO, J. TANAKA, and K. NAKASUJI,** "Crystal Structure of an Alternated Stacking Charge-Transfer Complex of 2,7-Bis(methylthio)-1,6-dithiapyrene (MTDTPY) with Tetracyano-2,6-naphthoquinodimethane (TNAP)", *Bull. Chem. Soc. Jpn.* **66,** 2115 (1993).

**J. INANAGA, Y. SUGIMOTO, Y. YOKOYAMA, and T. HANAMOTO,** "One-Carbon Extrusion from Carbohydrates via Cl-Alkoxy Radical Fragmentation. An Easy Access to Erythrose and Threose", *Tetrahedron Lett.* **33,** 8109 (1992).

**J. INANAGA, Y. YOKOYAMA, and T. HANAMOTO,** "Study on the Catalytic Activities of Lanthanoid(III) Triflates in the Glycosylation of 1-*O*-Methoxyacetyl Sugar", *Nippon Kagaku Kaishi, Special Articles on Lanthanide Chemistry* (in Japanese), 52 (1993).

**J. INANAGA, Y. YOKOYAMA, and T. HANAMOTO,** "Utility of 3,4-Dimethoxybenzyl (DMPM) Glycosides. A New Glycosylation Triggered by 2,3-Dichloro-5,6-dicyano-*p*-benzoquinone (DDQ) Oxidation", *Chem. Lett.* 85 (1993).

**J. INANAGA, O. UJIKAWA, Y. HANDA, K. OTSUBO, and M. YAMAGUCHI,** "Samarium-Mediated Acyclic Stereoselection in a Radical Reaction", Proceedings of the International Conference, Rare Earths '92 in Kyoto: *J. Alloy and Compounds,* **192,** 197 (1993).

**J. INANAGA, Y. BABA, and T. HANAMOTO,** "Organic Synthesis with Trialkylphosphine Catalysts. Conjugate Addition of Alcohols to $\alpha,\beta$-Unsaturated Alkynic Acid Esters", *Chem. Lett.* 241 (1993).

**J. INANAGA, Y. YOKOYAMA, and T. HANAMOTO,** "1-*O*-Methoxyacetyl Sugars as a New Glycosyl Donor. Zinc(II)-Promoted Synthesis of *O*- and *S*-Glycosides", *Chem. Express* **8,** 165 (1993).

**T. HANAMOTO, Y. BABA, and J. INANAGA,** "Utility of Phosphomium-Substituted Ester Enolates as Synthetic Intermediates. A Novel Trialkylphosphine-Catalyzed [3,3] Rearrangement of Allylic Acrylates", *J. Org. Chem.* **58,** 299 (1993).

**J. INANAGA, Y. YOKOYAMA, and T. HANAMOTO,** "Lanthanoid(III) Triflates as New Glycosylation Catalysts. Selective and Efficient Activation of 1-*O*-Methoxyacetyl Sugars", *Tetrahedron Lett.* **34,** 2791 (1993).

**J. INANAGA, Y. YOKOYAMA, and T. HANAMOTO,** "Catalytic *O*- and *S*-Glycosylation of 1-Hydroxy Sugars", *J. Chem. Soc., Chem. Commum.* 1090 (1993).

**H. TAKEMURA, K. YOSHIMURA, I.U. KHAN, T. SHINMYOZU, and T. INAZU,** "The First Synthesis and Properties of Hexahomotriazacalix[3]arene", *Tetrahedron Lett.* **33,** 5775 (1992).

**K. SAKO, T. SHINMYOZU, H. TAKEMURA, M. SUENAGA, and T. INAZU,** "A Conformational Study of [3.3]Metacyclophane Through Variable Temperature $^1$H NMR and Optical Rotations", *J. Org. Chem.* **57,** 6536 (1993).

**T. SHINMYOZU, S. KUSUMOTO, S. NOMURA, and T. INAZU,** "Synthesis of [3.3.3.3](1,2,3,5)- and (1,2,4,5)Cyclophanes", *Chem. Ber.* **126,** 1815 (1993).

**I.U. KHAN, H. TAKEMURA, M. SUENAGA, T. SHINMYOZU, and T. INAZU,** "Azacalixarenes: New Macrocyclic Molecules with Dimethyleneaza Bridging of Calix[4]arene System", *J. Org. Chem.* **58,** 3158 (1993).

**Y. KUBOZONO, T. MIYAMOTO, T. SHINMYOZU, M. AOYAGI, Y. GONDO, H. TAKEMURA, and M. SHIOTANI,** "An ESR and MO Study of the Butatriene and Tetramethylbutatriene Radical Cations", *Spectrochimica Acta.* **49A,** 1187 (1993).

**S. NAKAGAWA and N. KOSUGI,** "Polarized One-electron Potentials Fitted by Multicenter Polarizabilities and Hyperpolarizabilities", *Chem. Phys. Lett.* **210,** 180 (1993).

**M. TAKAHASHI and K. KIMURA,** "Cation Vibrational Spectroscopy of *Trans* and *Gauche n*-Propylbenzene Rotational Isomers, Two-Color Threshold Photoelectron Study and *Ab Initio* Calculations", *J. Chem. Phys.* **97,** 2920 (1992).

**J.M. DYKE, H. OZEKI, M. TAKAHASHI, M.C.R. COCKETT, and K. KIMURA,** "A Study of Phenylacetylen (PA) and Styrene (ST), and Their Argon Complexes, PA-Ar and ST-Ar, with Laser Threshold Photoelectron Spectroscopy", *J. Chem. Phys.* **97,** 8926 (1992).

**M. TAKAHASHI and K. KIMURA,** "Reply to the Comment on: Cation Vibrational Spectroscopy of *Trans* and *Gauche n*-Propylbenzene Rotational Isomers, Two-Color Threshold Photoelectron Study and *Ab Initio* Calculations", *J. Chem. Phys.* **98,** 5109 (1993).

**M.C.R. COCKETT, H. OZEKI, K. OKUYAMA, and K. KIMURA,** "Vibronic Coupling in the Ground Cationic State of Naphthalene: A Laser Threshold Photoelectron [Zero Kinetic Energy (ZEKE)-Photoelectron] Spectroscopic Study", *J. Chem. Phys.* **98,** 7763 (1993).

**H. OZEKI, M. TAKAHASHI, K. OKUYAMA, and K. KIMURA,** "The Role of Electronic and Geometric Factors in 'Proton Tunneling', as Revealed by A Comparative Photoelectron Spectroscopic Study of Tropolone and 9-Hydroxyphenalenone in Their Cation Ground States", *J. Chem. Phys.* **99,** 56 (1993).

**K. FURUYA, S. KATSUMATA, and K. KIMURA,** "Photoelectron Spectra of Acetone and Acetone Dimer", *J. Electron Spectroscopy* **62,** 237 (1993).

**S. HIRAYAMA, M. KONO, Y. KUBO, F. TANAKA, and K. SHOBATAKE,** "Single Vibronic Level Relaxation in Photoreactive 9-tert-Butylanthracence", *J. Phys. Chem.* **96,** 10666 (1992).

**T. MATSUSHIMA, K. SHOBATAKE, and Y. OHNO,** "Spatial and Velocity Distributions of Product Desorption in Carbon Monoxide Oxidation over Palladium (110) and Reconstructed Platinum (110)(1×2) Surfaces", *Surf. Sci.* **283,** 101 (1993).

**H. OHASHI, A. YOSHIDA, K. TABAYASHI, and K. SHOBATAKE,** "Mechanisms of Synchrotron Radiation-Excited Etching Reactions of Semiconductor Materials", *Appl. Surf. Sci.* **69,** 20 (1993).

**K. KONDO, T. FUJIMOTO, T. NI-IMI, and K. SHOBATAKE,** "Molecular Beam Study of Materials for Vacuum Technology: I. Interaction of Gas Molecules with Stainless Steel Surface", *Trans. Jpn. Soc. Mech. Eng.* (in Japanese) **59B,** 1057 (1993).

**K. KONDO, T. FUJIMOTO, T. NI-IMI, and K. SHOBATAKE,** "Molecular Beam Study of Materials for Vacuum Technology: II. Improvement of Surface Characteristics by Ag Ion-Plating", *Trans. Jpn. Soc. Mech. Eng.* (in Japanese) **59B,** 1946 (1993).

**T. FUJIMOTO, T. NI-IMI, K. SHOBATAKE, and K. KONDO,** "A Scattering Experiment of Molecular Beams for Estimation of the Adsorption Probability", *Vacuum* **44,** 429 (1993).

**K. MITSUKE, S. SUZUKI, T. IMAMURA, and I. KOYANO,** "Negative-Ion Mass Spectrometric Study of Ion-Pair Formation in the Vacuum Ultraviolet. VII. $SO_2 \rightarrow O^- + SO^+$, $O^- + S^+ + O$", *Org. Mass Spectrom.* **28,** 335 (1993).

**K. MITSUKE, H. YOSHIDA, and H. HATTORI,** "Positive Ion-Negative Ion Coincidence Spectroscopy of $O_2$ and $H_2$ Using Synchrotron Radiation", *Z. Phys. D* **27,** 267 (1993).

**T. YAMAGUCHI, J. MATSUFUSA, and A. YOSHIDA,** "Structural Properties of $CuIn_xGa_{1-x}Se_2$ Thin Films Prepared by RF Sputtering", *J. Appl. Phys.* **72,** 5657 (1992).

**Q.X. GUO, O. KATO, M. FUJISAWA, and A. YOSHIDA,** "Optical Constants of Indium Nitride", *Solid State Commun.* **83,** 721 (1992).

**T. YAMAGUCHI, J. MATSUFUSA, and A. YOSHIDA,** "Thermal Crystallization of Copper Indium Diselenide Film with Oxygen-Doped Layer", *Jpn. J. Appl. Phys.* **31,** 2877 (1992).

**Y. SAITO and A. YOSHIDA,** "A Simple Process for Removing Residual Fluorine and Chlorine on Silicon Surface by Low Temperature Annealing in Hydrogen Ambient", *J. Electrochem. Soc.* **139,** L115 (1992).

**Y. HIRAO, M. HARAGUCHI, M. FUKUI, Q.X. GUO, and A. YOSHIDA,** "Degradation Mechanism of $Au/AlO_x/Al$ Tunnel Junction", *J. Phys. Soc. Japan* **62,** 1286 (1993).

**T. YAMAGUCHI, J. MATSUFUSA, and A. YOSHIDA,** "Optical Properties in RF Sputtered $CuIn_xGa_{1-x}Se_2$ Thin Films", *Appl. Surf. Sci.* **70/71,** 669 (1993).

**Q.X. GUO, O. KATO, and A. YOSHIDA,** "Thermal Stability of Indium Nitride Single Crystal Films", *J. Appl. Phys.* **73,** 7969 (1993).

**K. KOMORITA, H. NISHIMURA, and A. YOSHIDA,** "Structural Change Due To Thermal Treatment and Dielectric Properties of Anodic Oxide Films of Bismuth", *Thin Solid Films* **229,** 156 (1993).

**Y. UKISU, S. SATO, and T. OHMORI,** "Spectroscopic Studies on Adsorption States of Iron Pentacarbonyl Adsorbed on Titanium Dioxide", *J. Molecular Catal.* **78,** 287 (1993).

**S. SATO and Y. UKISU,** "Mechanism of the Photolysis of Iron Pentacarbonyl Adsorbed on a Pt Surface", *Surf. Sci.* **283,** 137 (1993).

**Y. UKISU, S. SATO, G. MURAMATSU, and K. YOSHIDA,** "Activity Enhancement of Copper-containing Oxide Catalysts by Addition of Cesium in the Reduction of Nitric Oxide", *Catal. Lett.* **16,** 11 (1992).

**Y. UKISU, S. SATO, A. ABE, and K. YOSHIDA,** "Possible Role of Isocyanate Species in $NO_x$ Reduction by Hydrocarbons over Copper-Containing Catalysts", *Appl. Catal.* **2,** 147 (1993).

**M. IKEJIRI, H. NAKAYAMA, M. NISHIO, H. OGAWA, and A. YOSHIDA,** "ZnTe Growth by Photo-Assisted Metal-organic Vapor Phase Epitaxy", *Appl. Surf. Sci.* **70/71,** 755 (1993).

**K. YAMADA, K. HORI, and Y. FUKUDA,** "Structure of $\mu$-Carbonato-1$\kappa^2O^1,O^2$: 2$\kappa^2O^1,O^3$-bis[(acetylacetonato)(*N,N,N',N'*-tetramethylethylenediamine)nickel(II)] [(Acetylacetonato)agua(methanol)(*N,N,N',N'*-tetramethylethylenediamine)nickel(II)] Tetraphenylborate", *Acta Cryst.* **C49,** 445 (1993).

**N. SHINTANI, J. KOTAKI, K. SONE, and Y. FUKUDA,** "Studies on Mixed Chelates. XX. Mono- and Binuclear Nickel(II) and Copper(II) Complexes with *N,N,N'N'',N''',N'''*-Hexamethyltriethylenetetramine and $\beta$-Diketonates", *Bull. Chem. Soc. Jpn.* **66,** 784 (1993).

**K. YAMADA, Y. FUKUDA, T. KAWAMOTO, Y. KUSHI, W. MORI, and K. UNOURA,** "Studies on Mixed Chelates. XXI. Synthesis and Crystal Structure of the Binuclear Nickel(II) Complex, $\mu$-(Oxalato)bis[(acetylacetonato)(*N,N,N',N'*-tetramethylethylenediamine)nickel(II)]", *Bull. Chem. Soc. Jpn.* **66,** 2758 (1993).

**N. SATO and Y. FUKUDA,** "Anion-sensing electrodes based on nickel(II) and copper(II) mixed ligand complexes", *Sensors & Actuators* **B, 13–14,** 743 (1993).

**K. SAWADA, S. YOSHIDA, and T. SUZUKI,** "Adsorption of Phosphate on Vaterite", *J. Chem. Soc. Faraday Trans.* **88,** 2227 (1992).

**M. HANDA, H. MIYAMOTO, T. SUZUKI, K. SAWADA, and Y. YUKAWA,** "Formation of Acetylacetonato Iron Complexes in Acetonitril and their Resonance Raman Spectra", *Inorg. Chim. Acta* **203,** 61 (1992).

**K. SAWADA, K. SATOH, C. HONDA, T. ISHIYAMA, and T. SUZUKI,** "Thermodynamic Study of Steric Effect on the Formation of Tetrahedral Pyridine Base Complexes of Cadmium Halides", *J. Chem. Soc. Dalton Trans.* 377 (1993).

**A. MINAGAWA, K. SAWADA, and T. SUZUKI,** "Determination of Bismuth(III) by Graphite Furnance Atomic Absorption Spectroscopy Combined with Liquid-liquid Extraction with Trioctylmethylammonium Nitrate", *Anal. Chim. Acta* **278,** 287 (1993).

**K. WAIZUMI, H. MASUDA, H. OHTAKI, K.A. BURKOV, and L. CHERNYKH,** "Structure of $2RbCl \cdot CuCl_2 \cdot 2H_2O$", *Acta Crystallogr.* **C48,** 1374 (1992).

**H. OHTAKI,** "Dissolution and Nucleation Phenomena of Salts in Water. Molecular Dynamics Approaches and Supporting Solution X-Ray Diffraction Measurements", *Pure Appl. Chem.* **65,** 203 (1993).

**T. RADNAI and H. OHTAKI,** "Intramolecular and Liquid Structures of Tetramethylurea Studied by Means of X-Ray Diffraction", *Z. Naturforsch.* **47a,** 1003 (1992).

**S. PATNAIK, M. SESHASAYEE, T. YAMAGUCHI, M. NOMURA, and H. OHTAKI,** "A Structural Study on AgI-$Ag_2O$-$CrO_3$ Glass", *J. Phys. Soc. Jpn.* **62,** 536 (1993).

**W.-Y. SUN, A. KAJIWARA, N. UEYAMA, and A. NAKAMURA,** "An Iron(II) Complex with a Tetradentate Peptide Ligand, cis-1,2-$C_6H_{10}$(CO-Cys-Pro-Leu-Cys-OMe)$_2$-1,2, as a Model of Reduced Rubredoxin", *J. Chem. Soc. Dalton Trans.* 3255 (1992).

**N. UEYAMA, W.-Y. SUN, and A. NAKAMURA,** "Evidence for Intramolecular NH···S Hydrogen Bonds from $^2$H-NMR Spectroscopy of Reduced Rubredoxin Model Fe(II) Complexes with Bidentate Peptide Ligands", *Inorg. Chem.* **31,** 4053 (1992).

**N. UEYAMA, H. OKU, and A. NAKAMURA,** "cis-Dioxobis(benzenedithiolato)tungsten(VI) and the Related Monooxotungsten(V) and -(IV) Complexes. Model of Tungsten Oxidoreductases", *J. Am. Chem. Soc.* **114,** 7310 (1992).

**W.-Y. SUN, N. UEYAMA, and A. NAKAMURA,** "Spectral and electrochemical properties of an iron(II) complex of Z-Cys-Ala-Pro-Cys-OMe and new synthesis of the corresponding Z-Cys-Ala-Ala-Cys-OMe analogue", *Inorg. Chim. Acta* **197,** 47 (1992).

**N. UEYAMA, H. OKU, and A. NAKAMURA,** "Two-Electron-Transfer Oxidation by Polymer-supported $[Fe_4S_4(SR)_4]^{2-}$ Complex", *J. Mol. Catal.* **74,** 451 (1992).

**H. ADACHI, N. UEYAMA, and A. NAKAMURA,** "$^{199}$Hg NMR Investigation on the Solution Structure of Hg(II) Complexes of Oligopeptides Containing Cysteine and Histidine Residues", *Inorg. Chim. Acta* **198–200,** 805 (1992).

**N. UEYAMA, T. OKAMURA, and A. NAKAMURA,** "Intramolecular NH···S Hydrogen Bond in o-Acylamino Substituted Benzenethiolate Iron(II) and Cobalt(II) Complexes", *J. Chem. Soc. Chem. Commun.* 1019 (1992).

**N. UEYAMA, T. OKAMURA, and A. NAKAMURA,** "Structure and Properties of Molybdenum(IV,V) Arenethiolates with a Neiboring Amide Group. Significant Contribution of NH···S Hydrogen Bond to Positive Shift of Redox Potential of Mo(V)/Mo(IV)", *J. Am. Chem. Soc.* **114,** 8129 (1992).

**U. UEYAMA, S. UENO, A. NAKAMURA, K. WADA, H. MATSUBARA, S. KUMAGAI, S. SAKAKIBARA, and T. TSUKIHARA,** "A Synthetic Analogue for the Active Site of Plant-Type Ferredoxin: Two Different Coordination Isomers by a Four-Cys-Containing [20]-Peptide", *Biopolymers* **32,** 1535 (1992).

**N. UEYAMA, H. OKU, W.-Y. SUN, A. NAKAMURA, and K. FUKUYAMA,** "Nature of Fe-Se Bond in $(NR_4)_2$ $[Fe(SePh)_4]$", *Phosphorus, Sulfur, and Silicon* **67,** 151 (1992).

**W.-Y. SUN, N. UEYAMA, and A. NAKAMURA,** "Catalytic Oxidation of Benzoin and p-Substituted Benzhydrol by p-Benzoquinone or Air in the Presence of $[Fe^{II}(SPh)_4]^{2-}$ and $[Fe^{II}(SePh)_4]^{2-}$", *J. Mol. Catal.* **71,** 391 (1992).

**W.-Y. SUN, N. UEYAMA, and A. NAKAMURA,** "Air Oxidation of p-Substituted Benzoin to the Corresponding Benzil Catalyzed by Fe(II)-Cysteine Petide Complexes", *Tetrahedron* **48,** 1557 (1992).

**K. MASHIMA, Y. YAMANAKA, S. FUJIKAWA, H. YASUDA, and A. NAKAMURA,** "Convenient Synthesis of Pentamethylcyclopentadienyltantalum-Diene Complexes via the Reaction of Cp*$TaCl_4$ with Methylated-allyl Anions", *J. Organometal. Chem.* **428,** C5 (1992).

**K. MASHIMA, A. MIKAMI, and A. NAKAMURA,** "16 Electron Half-sandwich Ru(II)-Thiolate Complexes, $Ru(SAr)_2(\eta^6$-p-cymene) (Ar=2,6-dimethyl-phenyl; 2,4,6-triisopropylphenyl)", *Chem. Lett.* 1473 (1992).

**K. MASHIMA, A. MIKAMI, and A. NAKAMURA,** "Preparation and Crystal Characterization of Cationic Dinuclear Ru(II)-Thiolate Complex, $[Ru_2(SPh)_3(\eta^6$-p-cymene$)_2]Y$(Y=Cl and $PF_6$)", *Chem. Lett.* 1795 (1992).

**Y. NAKAYAMA, K. MASHIMA, and A. NAKAMURA,** "Bulky Aryloxo Complexes of Tungsten and Niobium as Catalyst Precursors for High Polymerization of 1-Alkynes", *J. Chem. Soc., Chem. Commun.* 1496 (1992).

**N. KITAJIMA, K. FUJISAWA, C. FUJIMOTO, Y. MORO-OKA, S. HASHIMOTO, T. KITAGAWA, K. TORIUMI, K. TATSUMI, and A. NAKAMURA,** "A New Model for Dioxygen Binding in Hemocyanin. Synthesis, Characterization, and Molecular Structure of the $\mu$-$\eta^2$:$\eta^2$ peroxo Dinuclear Copper(II) Complexes, $[Cu(HB(3,5\text{-}R_2pz)_3)]_2(O_2)$(R=i-Pr and Ph)", *J. Am. Chem. Soc.* **114,** 1277 (1992).

**H. YASUDA, M. FURO, H. YAMAMOTO, A. NAKAMURA, S. MIYAKE, and N. KIBINO,** "New Approach to Block Copolymerizations of Ethylene with Alkyl Methacrylates and Lactones by Unique Catalysis with Organolanthanide Complexes", *Macromolecules* **25,** 5115 (1992).

**N. KANEHISA, Y. KAI, N. KASAI, H. YASUDA, Y. NAKAYAMA, and A. NAKAMURA,** "Unique Molecular Structures of Tungsten Phenoxides", *Bull. Chem. Soc. Jpn.* **65,** 1197 (1992).

**H. YASUDA, H. YAMAMOTO, K. YOKOTA, S. MIYAKE, and A. NAKAMURA,** "Synthesis of Monodispersed High Molecular Weight Polymers and Isolation of an Organo-lanthanide(III) Intermediate Coordinated by a Penultimate Poly(MMA) Unit", *J. Am. Chem. Soc.* **114,** 4908 (1992).

**K. MASHIMA and A. NAKAMURA,** "Agostic Interaction in Early Transition Metal Alkyls and Their Role in Catalytic Activity for Olefin Polymerizations", *J. Organometal. Chem.* **428,** 49 (1992).

**H. HIRAKAWA, F. KAWAIZUMI, and H. NOMURA,** "Sedimentation Potential Measurement of Alkali Chloride in Water and Methanol Containing 18-Crown-6", *Denki Kagaku* **61,** 936 (1993).

**K. WAIZUMI, H. MASUDA, and N. FUKUSHIMA,** "A Molecular Approach to the Formation of KCl and $MgCl^+$ Ion-Pairs in Aqueous Solution by Density Functional Calculations", *Chem. Phys. Lett.* **205,** 317 (1993).

**N. FUKUSHIMA and K. WAIZUMI,** "Geometry Optimization of $[M(H_2O)_6]^{2+}$ by Self Consistent Nonlocal Density Functional Method. M=Cr, Mn, Fe, Co, Ni, Cu and Zn", *Chem. Express* **8,** 265 (1993).

**N. FUKUSHIMA and K. WAIZUMI,** "Intrinsic Structures and Dissociation Energies of $[Zn(NCS)_4]^{2-}$ and $[Zn(SCN)_4]^{2-}$ Ions Examined by Density Functional Calculations", *Chem. Express* **8,** 269 (1993).

**K. WAIZUMI, H. MASUDA, and N. FUKUSHIMA,** "Intrinsic Structures of $[CuCl_4]^{2-}$ and $[CuBr_4]^{2-}$ Anions by Ab Initio Density Functional Calculations", *Chem. Lett.* 1145 (1993).

**K. WAIZUMI, H. MASUDA, and N. FUKUSHIMA,** "Structural Rigidity of First Hydration Spheres of $Na^+$ and $Ca^{2+}$ in Cluster Models. Full Geometry Optimizations of $[M(H_2O)_6]^{n+}$, $[M(H_2O)_6 \cdots H_2O]^{n+}$ and $[M(H_2O)_6 \cdots Cl]^{(n-1)+}$ (M=Na and Ca, n=1 for Na and 2 for Ca) by Density Functional Calculations", *Inorg. Chim. Acta* **209,** 207 (1993).

**H. TANAKA, H, NAGAO, and K. TANAKA,** "Evaluation of Acidity of $CO_2$ in Protic Media. Carboxylation of Reduced Quinone", *Chem. Lett.* 541 (1993).

**H. NAGAO, T. MIZUKAWA, and K. TANAKA,** "Carbon-Carbon Bond Formation in Multi-electron Reduction of Carbon Dioxide Catalyzed by $[Ru(bpy)(trpy)(CO)]^{2+}$ (bpy=2,2′-bipyridine; trpy=2,2′:6′,2″-terpyridine)", *Chem. Lett.* 955 (1993).

**H. TANAKA, B-C. TZENG, H. NAGAO, S-M. PENG, and K. TANAKA,** "Comparative Study on Crystal Structure of $[Ru(bpy)_2(CO)_2](PF_6)_2$, $[Ru(bpy)_2(CO)(C(O)OCH_3)]B(C_6H_5)_4CH_3CN$, and $[Ru(bpy)_2(CO)(\eta^1\text{-}CO_2)] \cdot 3H_2O$ (bpy=2,2′bipyridine)", *Inorg. Chem.* **32,** 1508 (1993).

**H. KAMBAYASHI, H. NAGAO, K. TANAKA, M. NAKAMOTO, and S-M. PENG,** "Stabilization of Superoxidized form of Synthetic $Fe_4S_4$ Cluster as the First Model of High Potential Iron Sulfur Proteins in Aqueous Media", *Inorg. Chim. Acta.* **209,** 143 (1993).

**N. KOMEDA, H. NAGAO, G. ADACHI, M. SUZUKI, A. UEHARA, and K. TANAKA,** "Molecular Structure of Copper Nitrito Complexes as the Reaction Intermediate of Dissimilatory Reduction of $NO_2^-$", *Chem. Lett.*, 1521 (1993).

**T. TAKAHASHI, M. KAGEYAMA, V. DENISOV, R. HARA, and E. NEGISHI,** "Facile Cleavage of the $C_\beta$-$C_\beta$ Bond of Zirconacyclopentenes. Convenient Method for Selective Coupling of Alkynes with Alkynes, Nitriles, and Aldehydes", *Tetrahedron Lett.* **34,** 687 (1993).

**N. SUZUKI, D. KONDAKOV, and T. TAKAHASHI,** "Zirconium Caalyzed Novel Catalytic C-C Bond Formation Reactions", *J. Am. Chem. Soc.* **115,** 8485 (1993).

**T. TAKAHASHI, K. AOYAGI, R. HARA, and N. SUZUKI,** "Highly Chemoselective Reactions of Zirconacyclopentenes for Selective Functionalization", *J. Chem. Sos., Chem. Commun.* 1042 (1993).

**T. TAKAHASHI, N. SUZUKI, M. KAGEYAMA, D.Y. KONDAKOV, and R. HARA,** "Allylzirconation of Alkynes by the Reactions of Zirconocene-Alkyne Complexes with Allylic Ethers", *Tetrahedron Lett.* **34,** 4811 (1993).

**T. TAKAHASHI, Z. XI, C.J. ROUSEET, and N. SUZUKI,** "Pair Selective Cross Coupling Reactions of Alkynes with Alkenes on Zirconocene", *Chem. Lett.* 1001 (1993).

**T. TAKAHASHI, D.Y. KONDAKOV, and N. SUZUKI,** "Reactions of Alkynes with Homoallylic Halides Mediated by Zirconocene-Ethylene Complex", *Tetrahedron Lett.* **34,** 6571 (1993).

**Y. SASAKI, Y. YOSHIDA, A. OHTO, A. TOKIWA, T. ITO, H. KOBAYASHI, N. URYU, and I. MOGI,** "Mixed Chromiuum(III)-Ruthenium(III) Trinuclear Complex, $[CrRu_2(\mu_3\text{-}O)(\mu\text{-}CH_3COO)_6(pyridine)_3]^+$", *Chem. Lett.*, 69 (1993).

**T. YAMAGUCHI, N. NISHIMURA, and T. ITO,** "Triangular Platinum(II) Cluster Complexes $[Pt_3(CH_3COO)_4(cdoH)_2(cdoH_2)]$ and $[Pt_3(CH_3COO)_4(dmgH)_2(dmgH_2)]$($cdoH_2$=cyclohexanedionedioxime and $dmgH_2$=dimethylglyoxime)", *J. Am. Chem. Soc.* **115,** 1612 (1993).

**K. TORIUMI, M. YAMASHITA, S. KURITA, I. MURASE, and T. ITO,** "Phase Transitions of the Halogen-Bridged $M^{II}$-X-$M^{IV}$ Mixed-Valence Complexes of $[M(en)_2][MX_2(en)_2](ClO_4)_4$(M=Pt, Pd; X=Cl, Br). Structural Studies of the High- and Low-Temperature Phases of $[Pt(en)_2][PtBr_2(en)_2](ClO_4)_4$", *Acta Crystallogra.* Sect. **B49,** 497 (1993).

**Y. SATAKE, Y. IHARA, H. SENDA, M. SUZUKI, and A. UEHARA,** "Study on Cis-Folded Macrocylic Nickel(II) Complex. Molecular Structure and Thermal Reaction of Cis-Diaqua(1,4,7,11-tetraazacyclotetra-decane)nickel(II) Chloride", *Inorg. Chem.* **31,** 3248 (1992).

**K. UOZUMI, Y. HAYASHI, M. SUZUKI, and A. UEHARA,** "Reactivity of Copper(I) Complexes Containing Various Tetradentate Tripodal Ligands with Molecular Oxygen", *Chem. Lett.*, 963 (1993).

**T. ASADA, K. NISHIMOTO, and K. KITAURA,** "Theoretical Study on Binding Enthalpies and Population of Isomers of $Cl^-(H_2O)_n$(n=1–8) Clusters at Room Temperature", *J. Phys. Chem.* **97,** 7724 (1993).

**M. KOZAKI, S. TANAKA, and Y. YAMASHITA,** "Preparation and Properties of Poly-4-(1,3-dithiol-2-ylidene)-4H-cyclopenta[2,1-b; 3,4-b']dithiophene and its Derivatives", *J. Chem. Soc., Chem. Commun.* 1137 (1992).

**E. HASEGAWA, K. ISHIYAMA, T. KATO, T. HORAGUCHI, T. SHIMIZU, S. TANAKA, and Y. YAMASHITA,** "Photochemically and Thermally Induced Free-Radical Reactions of $\alpha,\beta$-Epoxy Ketones with Tributyltin Hydride: Selective $C_\alpha$-O Bond Cleavage of Oxiranylmethyl Radicals Derived from $\alpha,\beta$-Epoxy Ketones", *J. Org. Chem.* **57,** 5352 (1992).

**Y. YAMASHITA, S. TANAKA, K. IMAEDA, H. INOKUCHI, and M. SANO,** "Preparation and Properties of Bis[1,2,5]thiadiazolo-*p*-quinobis(1,3-dithiole) (BTQBT) and Its Derivatives. Novel Organic Semiconductors", *J. Org. Chem.* **57,** 5517 (1992).

**T. SUZUKI, H. FUJII, T. MIYASHI, and Y. YAMASHITA,** "Molecular Recognition through C-H···O Hydrogen Bonding in Charge-Transfer Crystals: Highly Selective Complexation of 2,4,7-Trinitrofluorenone with 2,6-Dimethylnaphthalene", *J. Org. Chem.* **57,** 6744 (1992).

**Y. TSUBATA, T. SUZUKI, T. MIYASHI, and Y. YAMASHITA,** "Single-Component Organic Conductors Based on Neutral Radicals Containing the Pyrazine-TCNQ Skeleton", *J. Org. Chem.* **57,** 6749 (1992).

**Y. YAMASHITA and S. TANAKA,** "Crystal Structures of Cation Radical Salts of a Bis(1,3-dithiole) Donor Containing a 1,2,5-Thiadiazole Unit", *Chem. Lett.* 73 (1993).

**M. KOZAKI, S. TANAKA, and Y. YAMASHITA,** "Preparation and Properties of 7-(1,3-Dithiol-2-ylidene)-7H-cyclopenta[1,2-b;4,3-b']dithiophenes and Their Polymers", *Chem. Lett.*, 533 (1993).

**M. TOMURA, S. TANAKA, and Y. YAMASHITA,** "Preparation and Properties of Bis[1,2,5]thiadiazolotetrathiafulvalene", *Heterocycles* **35,** 69 (1993).

**T. SUZUKI, T. OKUBO, A. OKADA, Y. YAMASHITA, and T. MIYASHI,** "Benzidine Type Electron Donors Fused with 1,2,5-Chalcogenadiazole Units", *Heterocycles* **35,** 395 (1993).

**Y. YAMASHITA, S. TANAKA, and M. TOMURA,** "2,2'-(Cyclopenten-3,5-diylidene)bis(1,3-dithiole)s: Novel Electron Donors Undergoing Deprotonation by Oxidation", *J. Chem. Soc., Chem. Commun.* 652 (1993).

**S. TANAKA and Y. YAMASHITA,** "Synthesis of a Narrow Band Gap Heterocyclic Polymer: Poly-4,6-di(2-thienyl)thieno[3,4-c][1,2,5]thiadiazole", *Synthetic Metal* **55–57,** 1251 (1993).

**K. FUKE, K. TSUKAMOTO, M. SANEKATA, and F. MISAIZU,** "Near Threshold Photoionization of Silicon Clusters in the 248–146 nm Region: Ionization Potentials for $Si_n$", *J. Chem. Phys.* **99,** 7807 (1993).

**K. FUKE, F. MISAIZU, M. SANEKATA, K. TSUKAMOTO, and S. IWATA,** "Electronic Structure and Reactivity of $Mg^+(H_2O)_n$ Cluster Ions", *Z. Phys.* **D26,** S180 (1993).

**F. MISAIZU, K. TSUKAMOTO, M. SANEKATA, and K. FUKE,** "Photoionization and Photodissociation Studies on Aluminum-Water Clusters and Their Ions", *Z. Phys.* **D26,** S177 (1993).

**K. FUKE, K. TSUKAMOTO, and F. MISAIZU,** "Photoionization of Small Silicon Clusters: Ionization Potentials for $Si_2$ to $Si_{40}$", *Z. Phys.* **D26,** S204 (1993).

**K. KUWAHARA, H. IKEDA, H. UMEMOTO, T. SATO, K. TAKANO, S. TSUNASHIMA, F. MISAIZU, and K. FUKE,** "Nascent Rotational and Vibrational Distributions in Both Products of the Reaction: $Zn(4^1P_1)+H_2O \rightarrow ZnH(X^2\Sigma^+)+OH(X^2\Pi)$", *J. Chem. Phys.* **99,** 2715 (1993).

**H. UMEMOTO, T. SATO, K. TAKANO, S. TSUNASHIMA, K. KUWAHARA, K. SATO, H. IKEDA, F. MISAIZU, and K. FUKE,** "Nascent Rotational State Distributions of $ZnH(X^2\Sigma^+)$ Produced in the Reactions of $Zn(4^1P_1)$ with Simple Alkane Hydrocarbons", *Chem. Phys. Lett.* **214,** 271 (1993).

**F. MISAIZU, P.L. HOUSTON, N. NISHI, H. SHINOHARA, T. KONODOW, and M. KINOSHITA,** "Formation of Protonated Ammonia Cluster Ions: Two-Color Two-Photon Ionization Study", *J. Chem. Phys.* **98,** 234 (1993).

**P. WANG, R.M. METZGER, S. BANDOW, and Y. MARUYAMA,** "Superconductivity in Langmuir-Blodgett Multilayers of $C_{60}$ Doped with Potassium", *J. Phys. Chem.* **97,** 2926 (1993).

**S. BANDOW, H. SHINOHARA, Y. SAITO, M. OHKOHCHI, and Y. ANDO,** "High Yield Synthesis of Lanthanumfullerenes via Lanthanum Carbide", *J. Phys. Chem.* **97,** 6101 (1993).

**H. SHINOHARA, H. YAMAGUCHI, N. HAYASHI, H. SAITO, M. INAGAKI, Y. SAITO, S. BANDOW, H. KITAGAWA, T. MITANI, and H. INOKUCHI,** "A New Characterization of Lanthanum- and Scandium-endohedral Metallofullerenes", *Mater. Sci. Engin.* **B19,** 25 (1993).

**Y. SAITO, T. YOSHIKAWA, S. BANDOW, M. TOMITA, and T. HAYASHI,** "Interlayer Spacings in Carbon Nanotubes", *Phys. Rev.* **B48,** 1907 (1993).

**M. MIKURIYA, T. KOTERA, F. ADACHI, and S. BANDOW,** "A Tetranuclear Vanadium-(III,III,IV,IV) Complex Formed by a Reaction of Bis(acetylacetonato)-oxovanadium(IV) with a Thiolate Ligand", *Chem. Lett.* 945 (1993).

**H. KITAGAWA, N. KOJIMA, H. TAKAHASHI, and N. MORI,** "Electrical Conductivity of the Perovskite-Type Mixed-Valence Compound $Cs_2Au_2I_6$ under High Pressures and Low Temperature", *Synthetic Metals* **56,** 1726 (1993).

**H. KITAGAWA, T. MITANI, J. TOYODA, K. NAKASUJI, H. OKAMOTO, and M. YAMASHITA,** "A New Two-Band Sytstem of *d* and $\pi$ with interband H Bridges", *Synthetic Metals* **56,** 1783 (1993).

**H. KITAGAWA, H. OKAMOTO, T. MITANI, and M. YAMASHITA,** "New Type of H-Bonded CT Complexes; [M($H_2$DAG)(HDAG)]TCNQ(M=Ni,Pd,Pt)", *Mol. Cryst. Liq. Cryst.* **228,** 155 (1993).

**H. OKAMOTO, T. MITANI, K. TORIUMI, and M. YAMASHITA,** "Photogeneration of Solitons and Polarons in 1-D Halogen-Bridged Metal Complexes", *Phys. Rev. Lett.* **69,** 2248 (1992).

**H. OKAMOTO, T. MITANI, K. TORIUMI, and M. YAMASHITA,** "FTIR Study of Photo-Induced Gap States in the MX Compounds", *Synthetic Metals* **55,** 524 (1993).

**M. YAMASHITA, E. TSURUTA, K. INOUE, T. FURUTA, H. OKAMOTO, T. MITANI, K. TORIUMI, H. OHKI, and R. IKEDA,** "Halogen-Bridged One-Dimensional $Ni^{II}$-$Ni^{IV}$ Mixed-Valence State and $Ni^{III}$ Mott-Hubbard State", *Synthetic Metals* **57,** 524 (1993).

**S. BANDOW, H. KITAGAWA, T. MITANI, H. INOKUCHI, Y. SAITO, H. YAMAGUCHI, N. HAYASHI, H. SATO, and H. SHINOHARA,** "Anaerobic Sampling and Characterization of Lanthano-Fullerenes: Extraction of $LaC_{76}$ and other $LaC_{2n}$", *J. Phys. Chem.* **26,** 9609 (1992).

**T. TERASHIMA, N. KOJIMA, H. KITAGAWA, H. OKAMOTO, and T. MITANI,** "Optical Reflectivity Spectra of Incommensurate Layer Compounds $(CeS)_{1.2}NbS_2$ and $(CeS)_{0.6}NbS_2$", *J. Phys. Soc. Jpn.* **62,** 2166 (1993).

**N. KOJIMA, F. AMITA, H. KITAGAWA, H. SAKAI, and Y. MAEDA,** "$^{197}$Au Mössbauer Spectroscopy of the Cubic Phase in the Halogene Bridged Mixed-Valence Complex $Cs_2Au_2I_6$", *Nuclear Instruments and Methods in Physics Research,* **B76,** 321 (1993).

**H. SHINOHARA, H. YAMAGUCHI, N. HAYASHI, H. SATO, M. INAGAKI, Y. SAITO, S. BANDOW, H. KITAGAWA, T. MITANI, and H. INOKUCHI,** "A New Characterization of Lanthanum- and Scandium-Endohedral Metallofullerenes", *Materials Sci. & Engineering* **B19,** 25 (1993).

**K. IMAEDA, I. KHAIRULLIN, K. YAKUSHI, M. NAGATA, N. MIZUTANI, H. KITAGAWA, and H. INOKUCHI,** "New superconducting sodium-nitrogen-$C_{60}$ ternary compound", *Solid State Communications* **87,** 375 (1993).

**S. TAKANO, H. HAMA, G. ISOYAMA, A. LIN, and N.A. VINOKUROV,** "Gain Measurement of a Free Electron Laser on the UVSOR Storage Ring", *Jpn. J. Appl. Phys.* **31,** 2621 (1992).

**S. TAKANO, H. HAMA, and G. ISOYAMA,** "Gain Measurement of a Free Electron Laser with an Optical Klystron on the UVSOR Storage Ring", *Jpn. J. Appl. Phys.* **32,** 1285 (1993).

**H. HAMA, S. TAKANO, and G. ISOYAMA,** "Control of the Bunch Length on an Electron Storage Ring", *Nucl. Instr. Meth. Phys. Res.* **A329,** 29 (1993).

**S. TAKANO, H. HAMA, and G. ISOYAMA,** "Lasing of a Free Electron Laser in the Visible on the UVSOR Storage Ring", *Nucl. Instr. Meth. Phys. Res.* **A331,** 20 (1993).

**E. ISHIGURO, H. MAEZAWA, M. SAKURAI, M. YANAGIHARA, M. WATANABE, M. KOEDA, T. NAGANO, K. SANO, Y. AKUNE, and K. TANINO,** "Test of Holographic SiC Gratings for High-Power Synchrotron Radiation", *SPIE* **1739,** 592 (1992).

**T. MURATA, K. HARADA, S. EMURA, M. NOMURA, K.R. BAUCHSPIESS, H. MAEDA, A. HIRAYA, and M. WATANABE,** "X-Ray Excited Luminescence Yield Spectra of NaBr and NaBr:Cu Single Crystals", *Jpn. J. Appl. Phys.* **32, Supple. 32-2,** 217 (1993).

**W.F. PONG, R.A. MAYANOBIC, K.T. WU, P.K. TSENG, B.A. BUNKER, A. HIRAYA, and M. WATANABE,** "X-Ray Absorption Near Edge Structure (XANES) Studies of Diluted Magnetic Semiconductors (DMS) $Zn_{1-x}Y_xS$ (Y=Mn, Fe, Co) Systems", *Jpn. J. Appl. Phys.* **32, Suppl. 32-2,** 722 (1993).

**V.G. STANKEVITCH, N. YU. SVECHNIKOV, K.V. KAZNACHEEV, M. KAMADA, S. TANAKA, S. HIROSE, R. KINK, G.A. EMEL'CHENKO, S.G. KARABACHEV, T. WOLF, H. BERGER, and F. LEVY,** "Luminescence of High-temperature Single-crystal Superconductors Cleaved in Ultrahigh Vacuum", *Phys. Rev.* **B47,** 1024 (1993).

**M. KAMADA, K. ICHIKAWA, and O. AITA,** "Solid-state Effects on Nonradiative Decay of $4d^94f^1$ States in Barium Halides", *Phys. Rev.* **B47,** 3511 (1993).

**Y. OHNO, T. MATSUSHIMA, S. TANAKA, and M. KAMADA,** "Desorption, Dissociation and Orientation of Oxygen Admolecules on a Reconstructed Platinum(110)(1×2) Surface Studied by Thermal Desorption and Near-edge X-ray-Absorption Fine-Structure", *Jpn. J. Appl. Phys.* **32 Suppl. 32-2,** 383 (1993).

**J. YOSHINOBU, S. TANAKA, and M. NISHIJIMA,** "Elementary Chemical-Reaction Processes of Silicon Surfaces", *Jpn, J. Appl. Phys.* **32,** 1171 (1993).

**K. KUWAHARA, H. IKEDA, H. UMEMOTO, T. SATO, K. TAKANO, S. TSUNASHIMA, F. MISAIZU, and K. FUKE,** "Nascent Rotational and Vibrational Distributions in Both Products of the Reaction: $Zn(4^1P_1)+H_2O \rightarrow ZnH(X^2\Sigma^+)+OH(X_2\Pi)$", *J. Chem. Phys.* **99,** 2715 (1993).

# Review Articles and Textbooks

**S. SAITO**, "Free Radicals in Cosmic Space", *Kagaku to Kogyo* (in Japanese), **45**, 2024 (1992).

**S. SAITO**, "Chemistry of Interstellar Matters", *Kagaku to Kyoiku* (in Japanese), **41**, 451 (1993).

**A. FUJII and N. MORITA**, "Laser Investigation of Decay Dynamics in Superexcited Rydberg States of NO", in "*Laser Techniques for State-Selected and State-to-State Chemistry*" ed. by C.Y.Ng, The International Society for Optical Engineering, pp.184–195 (1993).

**T. KITAGAWA and T. OGURA**, "Time-resolved Resonance Raman Spectroscopy of Heme Proteins: Visible to UV and ns to ms.", *Advance in Spectroscopy* **21**, Part B, 139–188 (1993).

**T. KITAGAWA**, "Characteristics at the Heme Locus of Cytochrome P-450 in Comparison with Other Oxygen-binding Heme Proteins", in "Cytochrome P-450.", T. Omura, Y. Ishimura and Y. Fujii-Kuriyama Eds., Kodansha (Tokyo), pp.31–44 (1993).

**K. YOSHIHARA**, "Picosecond and Femtosecond Time-Resolved Spectroscopy", Introduction to Laser Technology-Application to Organic and Polymer Materials" (in Japanese), Ed. M. Kato, Kyoritsu, Tokyo, pp.61–78 (1993).

**S.R. MEECH and K. YOSHIHARA**, "Applications of Second Order Nonlinear Optical Effects to the Study of Surfaces and Interfaces", *Butsuri* (in Japanese) **48**, pp.29–36 (1993).

**T. SUZUMOTO, K. KEMNITZ, K. YOSHIHARA, and T. TANI**, "Measurement of Picosecond Fluorescence Lifetimes of J-Aggregates of Cyanine Dye Adsorbed on AgBr", in Chemistry of Functional Dyes Vol.2, Eds. Z. Yoshida and Y. Shirota, Mita Publ., Tokyo, pp.140–144 (1993).

**H. KANDORI, K. YOSHIHARA, H. TOMIOKA, H. SASABE, and Y. SHICHIDA**, "Primary Events in Retinal Proteins", in "Recent Advances in Photosciences", Eds. M. Yong and P.S. Song, Chungnam National University, Taejon (Korea) pp.90–102 (1993).

**Y. MATSUMOTO**, "State-to-state Chemistry in Surface Science", in *Hyomen Kagaku (J. Surf. Sci. Soc. Japan)* (in Japanese) **13**, 572 (1992).

**Y. MATSUMOTO, K. SAWABE, and J. LEE**, "Photochemistry and Photodissociation Dynamics of $N_2O$ on Metal Surfaces", in "Laser Techniques for State-selected and State-to-state Chemistry", C.-Y. Ng Ed., SPIE- The International Society for Optical Engineering, Vol.1858, p.378 (1993).

**Y. MATSUMOTO**, "Diode Laser Spectroscopy and Double Resonance", in Textbook of Experimental Chemistry, Spectroscopy III", H. Inokuchi Ed., Maruzen (in Japanese), p.148 (1993).

**I. HANAZAKI**, "Nonlinear Phenomena and Self-organization", *Kagaku*, June (1993) (in Japanese).

**K. SUZUKI**, "Vacuum Techniques", in "Experimental Chemistry 4th Edition, Spectroscopy III", H. Inokuchi Ed. (in Japanese), Maruzen, pp.85–90 (1993).

**A. UGAWA**, "Superconductivity of Alkali-Fulleride", *TANSO* (in Japanese) **157**, 99–106 (1993).

**T. INABE, K. OKANIWA, H. OGATA, H. OKAMOTO, T. MITANI, and Y. MARUYAMA**, "Crystal Structure and Transport Properties of a Hydrogen-Bonded 1:1 Charge Transfer Complex Composed of 1.6-Pyrenediamine and 7,7,8,8-Tetracyanoquinodimethane (DAP-YCNQ)$^+$", *Acta Chimica Hungaria-Models in Chemistry*, **130**, 537 (1993).

**Y. MARUYAMA**, "A Chessman Born from Science of Cosmic Space-$C_{60}$", *Kagaku to Kogyo* (in Japanese), **45**, 58 (1992).

**Y. MARUYAMA**, "Solid State Properties of $C_{60}$-Superconductivity", *Kotaibutsuri* (in Japanese), **27**, 231 (1992).

**Y. MARUYAMA**, "Solid State Properties of Fullerenes", *Gendaikagaku* (in Japanese), **1992**, 56.

**Y. MARUYAMA**, "Chemistry and Physics of Solid Fullerenes-Solid State Properties", in *$C_{60}$ · Fullerene Chemistry* (in Japanese), p.98 Kagakudohjin, Kyoto (1993).

**Y. MARUYAMA**, "Tunneling Spectroscopy", in Textbook of Experimental Chemistry, "Functionality of Materials," ed. by H. Inokuchi, Maruzen (in Japanese), p.67 (1993).

**S. MIYAJIMA**, "NMR and ESR" in Textbooks of Experimental Chemistry, vol.12 "Functionality of Materials" ed. by H. Inokuchi, Maruzen (in Japanese), p.396 (1993).

**K. ISOBE and A. YAGASAKI**, "Cubane-Type Clusters as Potential Models for Inorganic Solid Surfaces" *Acc. Chem. Res.*, **26**, 524 (1993).

**N. KOSUGI**, "XANES and Molecular Orbital Theory" (in Japanese), *Nippon Hoshako Gakkaishi* **6**, 73 (1993).

**K. KIMURA**, "Laser Photoelectron Spectroscopic Study of Gas-Phase Organometallic Molecules", in "Laser Chemistry of Organometallics", ed. by J. Chaiken, ACS Symposium Series 530, American Chemical Society, Washington, DC, pp.86–95 (1993).

**K. KIMURA**, "Photoelectron Spectroscopy" in "Spectroscopy III" (in Japanese), ed. by S. Tasumi and K. Yoshihara, Experimental Chemistry 4th Edition, Maruzen, Tokyo, pp.1–6, pp.16–23, pp.54–59, pp.69–78 (1993).

**K. SHOBATAKE**, "Recent Progress in State-to-State Chemistry", *Kagaku (Chemistry)* (in Japanese), **48**, 146 (1993).

**K. SHOBATAKE**, "Molecular Beams" in Experimental Chemistry 4th Edition No.11, Chemical Reactions and Reaction Rates (in Japanese), Ed. K. Obi, (Maruzen, Tokyo, 1993), pp.125–149.

**K. SHOBATAKE**, "Molecular Beams" in Experimental Chemistry 4th Edition, No.8, Spectroscopy III (in Japanese), Eds. M. Tasumi and K. Yoshihara (Maruzen, Tokyo, 1993), pp.107–130.

**M. KONO, Y. KUBO, S. HIRAYAMA, F. TANAKA, and K. SHOBATAKE**, "Solvent Effects on the Excited Dynamics of Substituted Anthracene Compounds" in "Recent Advances in Photosciences – Proceedings of Int. Symp. on Photochemistry, Photobiology, and Photomedicine" – Eds. M.-J. Yoon and P.-S. Song (Chungnam Natl. Univ., Taedok Science Town, Korea, 1993), pp.44–53.

**A. YOSHIDA**, "Fabrication and Characterization of InN and InAlN Crystalline Thin Films by Microwave-excited Metal-organic Vapor Phase Epitaxy", in "New Functionality Materials, Volume C", T. Tsuruta, M. Doyama and M. Seno Ed., Elsevier Science Pub. pp.183–188 (1993).

**S. SATO and N. KAKUTA**, "Preparation of Titanium Dioxide Films and Their Photocatalytic Properties", in "Preparation of Catalysts by Use of Metal Alkoxides" (in Japanese) ed. by A. Ueno, F. Mizukami, and T. Sodesawa, I.P.C., p.435 (1993).

**H. OHTAKI**, "Molecular Aspects on the Dissolution and Nucleation of Ionic Crystals in Water", *Adv. Inorg. Chem.* **39**, 401 (1992).

**H. OHTAKI, M. MIKAMI, and Y. TAGO**, "Molecular Dynamics Simulations for Dissolution and Nucleation Processes of Alkali Halide Crystals in Water", Computer Aided Innovation of New Materials II, M. Doyano, J. Kihara, M. Tanaka, and R. Yamamoto, Eds., Elsevier, p.265 (1993).

**H. OHTAKI and T. RADNAI**, "Structure and Dynamics of Hydrated Ions", *Chem. Rev.* **93**, 1157 (1993).

**H. OHTAKI**, "The Role of Electrolyte Solution Chemistry in Electrochemistry", *Denki Kagaku* **61**, 6 (1993) (in Japanese).

**Y. FUKUDA**, "Thermochromism of Transition Metal Complexes", *PetroTech(Sekiyu-gakkaishi, in Japanese)*, **16**, 786 (1993).

**A. NAKAMURA**, "Organometallic Polymers", *Shin Sozai.* **11**, 19 (1992).

**A. NAKAMURA**, "Multinuclear Metal Complexes with Sulfur Bridges", *Hyomen.* **30**, 575 (1992).

**T. TAKAHASHI**, "Organic Synthesis using Organozirconium Compounds", *Kagaku Sousetsu* (in Japanese) **17**, 99 (1993).

**K. FUKE**, "Physical and Chemical Properties of Gas-Phase Silicon Clusters", *Hyoumenkagaku* (in Japanese) **14**, 222 (1993).

## AUTHOR INDEX-RESEARCH ACTIVITIES AND SPECIAL RESEARCH PROJECTS

Institute for Molecular Science, Myodaiji, Okazaki 444, Japan